frontiers | Research Topics

Advances in plant-soil nitrogen management strategies

Edited by
Sumera Anwar, Shahbaz Khan
and Fahad Shafiq

Published in
Frontiers in Plant Science

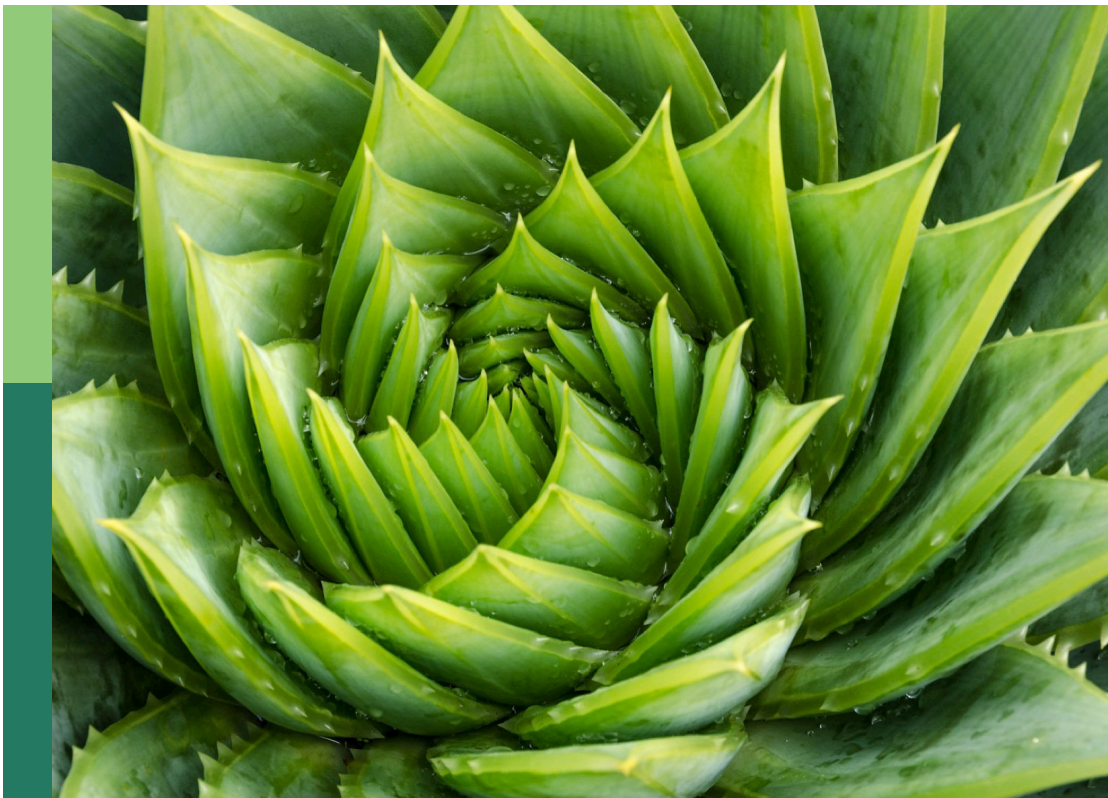

ISSN 1664-8714
ISBN 978-2-8325-4496-9
DOI 10.3389/978-2-8325-4496-9

About Frontiers

Frontiers is more than just an open access publisher of scholarly articles: it is a pioneering approach to the world of academia, radically improving the way scholarly research is managed. The grand vision of Frontiers is a world where all people have an equal opportunity to seek, share and generate knowledge. Frontiers provides immediate and permanent online open access to all its publications, but this alone is not enough to realize our grand goals.

Frontiers journal series

The Frontiers journal series is a multi-tier and interdisciplinary set of open-access, online journals, promising a paradigm shift from the current review, selection and dissemination processes in academic publishing. All Frontiers journals are driven by researchers for researchers; therefore, they constitute a service to the scholarly community. At the same time, the *Frontiers journal series* operates on a revolutionary invention, the tiered publishing system, initially addressing specific communities of scholars, and gradually climbing up to broader public understanding, thus serving the interests of the lay society, too.

Dedication to quality

Each Frontiers article is a landmark of the highest quality, thanks to genuinely collaborative interactions between authors and review editors, who include some of the world's best academicians. Research must be certified by peers before entering a stream of knowledge that may eventually reach the public - and shape society; therefore, Frontiers only applies the most rigorous and unbiased reviews. Frontiers revolutionizes research publishing by freely delivering the most outstanding research, evaluated with no bias from both the academic and social point of view. By applying the most advanced information technologies, Frontiers is catapulting scholarly publishing into a new generation.

What are Frontiers Research Topics?

Frontiers Research Topics are very popular trademarks of the *Frontiers journals series*: they are collections of at least ten articles, all centered on a particular subject. With their unique mix of varied contributions from Original Research to Review Articles, Frontiers Research Topics unify the most influential researchers, the latest key findings and historical advances in a hot research area.

Find out more on how to host your own Frontiers Research Topic or contribute to one as an author by contacting the Frontiers editorial office: frontiersin.org/about/contact

Advances in plant-soil nitrogen management strategies

Topic editors
Sumera Anwar — Durham University, United Kingdom
Shahbaz Khan — Huazhong Agricultural University, China
Fahad Shafiq — Government College University, Lahore, Pakistan

Citation
Anwar, S., Khan, S., Shafiq, F., eds. (2024). *Advances in plant-soil nitrogen management strategies*. Lausanne: Frontiers Media SA.
doi: 10.3389/978-2-8325-4496-9

Table of contents

frontiers | Frontiers in Plant Science

TYPE Editorial
PUBLISHED 09 February 2024
DOI 10.3389/fpls.2024.1380284

OPEN ACCESS

EDITED AND REVIEWED BY
Marta Wilton Vasconcelos,
Catholic University of Portugal, Portugal

*CORRESPONDENCE
Fahad Shafiq
fahadsheikh@gcu.edu.pk

RECEIVED 01 February 2024
ACCEPTED 02 February 2024
PUBLISHED 09 February 2024

CITATION
Shafiq F, Anwar S and Khan S (2024) Editorial: Advances in plant-soil nitrogen management strategies.
Front. Plant Sci. 15:1380284.
doi: 10.3389/fpls.2024.1380284

Editorial: Advances in plant-soil nitrogen management strategies

Fahad Shafiq[1]*, Sumera Anwar[2,3] and Shahbaz Khan[4]

[1]Department of Botany, Government College University Lahore, Lahore, Pakistan, [2]Department of Biosciences, Durham University, Durham, United Kingdom, [3]Department of Botany, Government College Women University Faisalabad, Faisalabad, Pakistan, [4]College of Tropical Crops, Hainan University, Haikou, China

KEYWORDS

nitrogen management, cropping patterns, soil health, sustainable agriculture, soil fertility

Editorial on the Research Topic
Advances in plant-soil nitrogen management strategies

Life on Earth is impossible without nitrogen (N). It is essentially required for all living organisms to synthesize amino acids, vitamins, proteins, enzymes, co-enzymes, and nucleic acids. This intensive dependence of living cells on N for almost all the metabolic and regulatory processes requires demands N uptake, its transport/mobilization and re-mobilization within plant parts, and synthesis of N storage proteins. The purpose of this focused Research Topic is to improve our understanding regarding different aspects of N mobilization/re-mobilization, influence of the cropping patterns and tillage practices on soil N transformations. Therefore, some key findings from different studies published in this Research Topic are summarized here.

Nitrogen is essentially required by plants for proper growth and development, whereas its deficiency triggers several metabolic and physiological changes in plants. In this context, Effah et al. studied the metabolomic profile of senescent wheat leaves and provided some key insights into N-remobilization. Widely untargeted metabolomic profile of the senescent wheat leaves under no, low, and high nitrogen (N) conditions across three phenological stages (anthesis, grain filling, and end grain filling stages) identified a total of 826 secondary metabolites; most of them were flavonoids and phenolic lipids. The authors concluded that lysine degradation and biosynthesis of alkaloids (primarily from lysine, ornithine, and nicotinic acid pathways) was primarily up-regulated under N deficiency growth conditions. Whereas, the high-N promoted the accumulation of flavones, flavonols, and anthocyanins. Similarly, Song et al. investigated nutrient stoichiometric ratios and resorption efficiency in fresh petals and petal litter of four tree species from the Rosaceae family. A lower nutrient resorption efficiency and stoichiometric ratio of petals compared to leaves was recorded. Moreover, the nutrient resorption efficiency was also strongly correlated with nutrition availability. These findings could provide key insights into N- management in tree species. By contrast, Chen et al. reported that the application of ammonium-nitrate mixtures improved N uptake and assimilation by pecan which substantially improved its growth characteristics. Pecan seedlings were exposed to different NH_4^+:NO_3^- sourced N regimes at 0:100; 25:75, 50:50; 75:25, and 100:0 respectively and the data was recorded after 45 days of experimental treatments. An improvement in the root proliferation, relative growth rate (RGR), biochemical traits, and enzymatic activities of N assimilating enzymes viz. nitrate

and nitrite reductases; glutamine and glutamate reductases; and glutamate dehydrogenase was recorded. In an overall assessment, these improvements in physio-biochemical traits were particularly evident in response to 75:25 and 100:0 NH_4^+:NO_3^-mixtures. Huang et al. proposed high-throughput root phenotyping (HTRP) as a tool to identify low-N-tolerant crops under waterlogged conditions. Several key root traits were highlighted in the review, including root length, surface area, and root architecture can be selected and analysed via imaging tools including MIFE, EMI, GPR, MRI, and other techniques including rhizotron imaging and X-ray CT to establish roots 3D structure. The authors also discussed experimental methods to study roto phenotypes and the limitations associated with them. In the final part of the mini-review, various image analysis tools are discussed which can be used to visualize root activity and HTRP and both the advantages and limitations associated with the imaging tools are provided. In summary, the analyses of root system architecture could provide key information in the context of N acquisition from the soil, and HTRP at the field scale could provide a better understanding of root NUE under field conditions.

It is well accepted that cropping patterns play a significant role in soil-N transformations and the soils with multiple cropping patterns improve N-recycling (Breza et al., 2023). Lesser crop rotation frequency ultimately leads to degradation of soil organic matter fraction and thereby contributes to N-losses (Khan et al., 2007). Alternatively, an increase in the number of rotational crops improved crop yields owing to better functional diversity (Bowles et al., 2020). Taken together, cropping patterns do influence N-mobilization and its availability in agricultural soils and studies focusing on cropping patterns will help us understand and enhance soil N status sustainably. By using a radiolabeled ^{15}N-isotope, Jia et al. determined the fate of N and its transport in soil under a wheat-rice rotation system. During this study, both N-utilization by crops and residual soil N were investigated in response to fertilizer, soil, and straw respectively. Interestingly, results revealed that a major fraction of crop N was derived from soil, followed by fertilizer and straw (averaging ~ 44.1, 35.9, and 19.0% respectively). However, N loss was prominent from soil, followed by fertilizer and straw application. In addition, soil N contributed to the highest N-utilization efficiency at 38.2%, followed by the contribution of fertilizer at 30.1% and contribution of straw was the least (around 13.9%). Post-seasonal N variations in the soil indicated an average loss of N by 7.3% from soil and 13.8% from fertilizer, whereas the straw contributed to soil N recovery by 4.38%. Above all, it is concluded that the grains exhibited maximum N translocation followed by stem and leaves. Likewise, Zhu et al. studied the influence of different N forms (ammonium and nitrate provided with and without dicyandiamide) on soil health and cucumber productivity during seven growing seasons in a monocropping system. The soil health index (SHI) calculations revealed improvements in soil health due to nitrates (SHI_{NN} and SHI_{NN+DCD}), whereas soil health was negatively correlated with plant productivity. It was concluded that the application of nitrate under monoculture could promote soil health. Wang et al. conducted a two-year field experiment to investigate the effects of biochar (0, 15, and 30 t ha^{-1}) and varying N levels (135, 180, and 225 kg ha^{-1}) on plant productivity under the maize-soybean intercropping system. The maize and soybean plants were cultivated in alternating rows (two rows each) and changes in growth, water use efficiency (WUE), and nitrogen recovery efficiency (NRE) were analyzed. Biochar soil amendment promoted maize starch contents during the second year. In addition, maximum grain yield was recorded in response to biochar application at 15 t ha^{-1}; whereas N was found beneficial at ~180 kg ha^{-1} respectively. Nonetheless, the biochar improved grain yield, WUE, and NRE, and combined application of biochar and N was most effective method which could reduce N inputs in an intercropping system. During another two-year experiment, Liu et al. investigated the influence of straw mulching on the growth, physiological, and agronomic characteristics of maize/sorghum intercropping system. Straw mulching was carried out at 0, 4.8, 7.2, and 9.6 t ha^{-1} doses. A significant increase in the photosynthesis rate (P_n rate) of maize by up to 15% was recorded when compared to no-mulching, whereas P_n rate of soybeans was enhanced by 24.5% on average. Moreover, prominent enhancements in N-uptake of both the crops was evident. Above all, the results indicated a 66.6% increase in maize crop yield in response to mulching, however, the mulching under inter-cropping caused a 15.4% yield improvement.

During a study by Yan et al., field experiments involving two cropping systems were performed. The first cropping system was the wheat-rice cropping system which utilized wheat straw mulching; whereas the second cropping system included an oilseed rape-rice cropping system which involved rapeseed straw mulching during the rice growing season. Rice cultivation without mulching served as control (N application at 135 and 48 kg ha^{-1}). Furthermore, in a parallel experiment in which ^{15}N-labelled urea and straw were applied to investigate N-dynamics and its utilization by plants. An increase in N-uptake especially by oil-seed straw mulching was + 45.1% whereas wheat straw mulching contributed to the enhancement of 9% N-uptake compared to control (fallow-rice rotation). The authors also reported improvement in NUE of crops in response to mulching however a significant amount of fertilizer remains un-utilized showing only 3-4% utilization by rice. It was concluded that straw mulching could effectively promote N-utilization in rice. A four-year field experimentation performed by Wang et al. investigated maize grain and nitrogen use efficiency (NUE) in response to different N-P fertilizer rates under a ridge-furrow rainfall harvesting system (RFRH). The fertilizer treatments included low, medium, and high inputs of fertilizers (N and P_2O_5 at 0-0, 150-75, 300-150, and 450-225 kg hm^{-2}) respectively. The results indicated a maximum N bioaccumulation in response to medium dose application whereas P uptake was linear and dose dependent. By contrast, both N and P use efficiencies were substantially reduced with an increase in fertilizer dose. The authors concluded that the medium fertilization dose of NP fertilizer at 300-150 kg hm^{-2} resulted in maximum biomass and grain yield. Above all, both NUE and PUE were maximum in response to a lower dose of fertilizer. da Silva et al. investigated residual N release from composted sewage sludge and its influence on crop growth under common bean-soybean-palisade grass crop rotation. The authors also studied changes in N-metabolism, biological N_2-fixation, and various physiological parameters. Experimentation was performed

over two years and results indicated an increase in the crop productivity and biological N_2-fixation which were linked with regulation of ureide metabolism and enzymatic activities of nitrate reductase, urease, and higher ammonium and nitrate N. Overall, it was concluded that the composted sewage sludge can be used as a residual source of N benefitting crop growth. Whereas Zhou et al. investigated the effects of positional application of N-fertilizer on the growth of maize and root proliferation under a wide-narrow row cropping system. The experimental treatments included both narrow-row and wide-row N applications under high and low N-fertilizer doses respectively. Narrow row combined with higher N rates contributed to increased root growth, surface area, and root density. Whereas wide-row cultivation in combination with high nitrogen significantly improved agronomic efficiency and partial factor productivity of N thereby contributing to improved yield. In short, wide row cropping of maize is suggested as a better approach to improve maize yield.

As per ecological viewpoint, modern agriculture practices have been reliant on intensive N-fertilizer inputs to main soil fertility (Galloway et al., 2008) and this practice has caused many problems and has altered soil-N and microbial dynamics. Huge inputs of N-fertilizers primarily contribute to N losses and pose a threat to terrestrial and aquatic life (Van Grinsven et al., 2013; Breza et al., 2023). Besides, very high levels suppress N mineralization (Mahal et al., 2019), affect soil microbial biodiversity by eutrophication (Liu et al., 2019; Wang et al., 2023), reduce NUE of crops (Sutton et al., 2011; Xu et al., 2020), ammonia volatilization, nitrate leaching, impairment of crop yields (Wang et al., 2015) and contributes of emission of greenhouse gasses (Velazquez et al., 2016). Therefore, understanding the soil N transformations and their recycling in terrestrial ecosystems is necessary (Robertson and Groffman, 2024). In this context, Tian et al. studied the effect of different irrigation levels (75-85%, 65-75%, 55-65%, and 45%-55%) and four N levels (0, 150, 300, and 450 kg ha^{-1}) on the distribution of soil nitrate nitrogen (NO_3^-N) and water in different soil layers and its effect on wolfberry (*Lycium barbarum* L.). Average soil moisture was maximum at full irrigation and likewise, the N levels were high in response to a high dose of 450 kg ha^{-1}. It is also reported that NO_3^-–N content in the 0-80 cm soil layer was more sensitive to irrigation. Maximum yield of wolfberry (2623.09 kg ha^{-1}) was recorded at 65-75% moisture and kg ha^{-1} N application rate (>18% higher than 75-85% combined with 450 kg ha^{-1}). Apart from that, the maximum water consumption was recorded at the flowering stage. The authors concluded that both WUE and NUE were optimum in the ranges of 315.4 to 374.3 mm combined with N at 300.0 to 308.3 kg·ha^{-1} respectively. Yang et al. investigated the influence of soil-applied biochar (0, 600, and 1200 kg ha^{-1}) and nitrogen fertilizer (105 and 126 kg ha^{-1}) on the enzymatic activities of sucrase, acid phosphatase, and urease enzymes were also determined from the tobacco plants. In addition, soil microbial dynamics including microbial C and N, SOC, soil nitrogen (NO_3^{2-} and NH_4^+), and the influence of biochar/fertilizer application on bacterial communities were also investigated by high throughput amplicon sequencing. The results revealed a dramatic shift in the microbial communities in response to BC and fertilizer application. The dominant bacterial communities included Proteobacteria, Bacteroidetes, Actinobacteria, Firmicutes, and Acidobacteria. Whereas changes in community structure were evident due to high rates of BC and fertilizer application. Apart from this, the application of BC and fertilizer, even at high concentrations benefitted tobacco plants and improved biomass. The authors concluded that the 1200 kg ha^{-1} + 126 kg ha^{-1} application was the best combination. Sarkis et al. quantified the N loss through volatilization when supplied to coffee plantations in the form of ammonia nitrogen (AN), urea (U), and urea with N- (n-butyl) thiophosphoric triamide (UNBPT) at five N doses (0, 150, 275, 400, and 525 kg ha^{-1} $year^{-1}$). Soil microbial biomass, respiration, microbial nitrogen, and enzyme activities of urease, and phosphatase were investigated as well and N levels in different coffee plant parts were also determined. The application of AN nitrogen fertilizer only contributed to 1% N loss whereas for urea fertilizer, losses of around 22%. Additionally, a major fraction of N was localized in the beans and husks of the harvested fruits. Above all, the study provided valuable insights into soil microbial dynamics under different N levels. Lastly, Saha et al. reviewed the mechanisms and factors that control fine root decomposition in forest ecosystems and their involvement in global C and N dynamics. There is a substantial contribution of biotic and abiotic factors to this phenomenon of root decomposition. These include precipitation rates, annual temperature, soil pH, soil salinity, and microbial diversity. Although it is very difficult to study the actual decomposition rates, the authors did report that this phenomenon contributes to the release of both N and P.

Author contributions

FS: Project administration, Writing – original draft, Writing – review & editing. SA: Project administration, Writing – review & editing, Conceptualization. SK: Project administration, Writing – review & editing, Conceptualization.

Conflict of interest

The authors declare that the research was conducted in the absence of any commercial or financial relationships that could be construed as a potential conflict of interest.

Publisher's note

References

Bowles, T. M., Mooshammer, M., Socolar, Y., Calderon, F., Cavigelli, M. A., Culman, S. W., et al. (2020). Long-term evidence shows that crop-rotation diversification increases agricultural resilience to adverse growing conditions in North America. *One Earth* 2, 284–293. doi: 10.1016/j.oneear.2020.02.007

Breza, L. C., Mooshammer, M., Bowles, T. M., Jin, V. L., Schmer, M. R., Thompson, B., et al. (2023). Complex crop rotations improve organic nitrogen cycling. *Soil Biol. Biochem.* 177, 108911. doi: 10.1016/j.soilbio.2022.108911

Galloway, J., Townsend, A., Erisman, J., Bekunda, M., Cai, Z., Freney, J., et al. (2008). Transformation of the nitrogen cycle: recent trends, questions, and potential solutions. *Science* 320, 889–892. doi: 10.1126/science.1136674

Khan, S. A., Mulvaney, R. L., Ellsworth, T. R., and Boast, C. W. (2007). The myth of nitrogen fertilization for soil carbon sequestration. *J. Env. Qual.* 36, 1821–1832. doi: 10.2134/jeq2007.0099

Liu, J., Li, X., Ma, Q., Zhang, X., Chen, Y., Isbell, F., et al. (2019). Nitrogen addition reduced ecosystem stability regardless of its impacts on plant diversity. *J. Ecol.* 107, 2427–2435. doi: 10.1111/1365-2745.13187

Mahal, N. K., Osterholz, W. R., Miguez, F. E., Poffenbarger, H. J., Sawyer, J. E., Olk, D. C., et al. (2019). Nitrogen fertilizer suppresses mineralization of soil organic matter in maize agroecosystems. *Fron. Ecol. Evol.* 7, 59. doi: 10.3389/fevo.2019.00059

Robertson, G. P., and Groffman, P. M. (2024). Nitrogen transformations. In *Soil microbiology, ecology and biochemistry*, pp. 407–438. Elsevier.

Sutton, M., Oenema, O., Erisman, J., Leip, A., Van Grinsven, H., and Winiwarter, W. (2011). Too much of a good thing: the nitrogen pollution problem. *Nature* 472, 159–161. doi: 10.1038/472159a

Van Grinsven, H. J., Holland, M., Jacobsen, B. H., Klimont, Z., Sutton, M. A., and Jaap Willems, W. (2013). Costs and benefits of nitrogen for Europe and implications for mitigation. *Environ. Sci. Technol.* 47, 3571–3579. doi: 10.1021/es303804g

Velazquez, E., Mueller, N. D., Billen, G., Lassaletta, L., Bouwman, L., Garnier, J., et al. (2016). Nitrogen use in the global food system: past trends and future trajectories of agronomic performance, pollution, trade, and dietary demand. *Environ. Res. Lett.* 11, 95007. doi: 10.1088/1748-9326/11/9/095007

Wang, C., Li, X., Hu, Y., Zheng, R., and Hou, Y. (2023). Nitrogen addition weakens the biodiversity multifunctionality relationships across soil profiles in a grassland assemblage. *Agric. Ecosys. Environ.* 342, 108241. doi: 10.1016/j.agee.2022.108241

Wang, J., Zhu, B., Zhang, J., Müller, C., and Cai, Z. (2020). Mechanisms of soil N dynamics following long-term application of organic fertilizers to subtropical rain-fed purple soil in China. *Soil Biology and Biochemistry* 91, 222–231. doi: 10.1016/j.agwat.2019.105904

Xu, J. T., Cai, H. J., Wang, X. Y., Ma, C. G., Lu, Y. J., Ding, Y. B., et al. (2020). Exploring optimal irrigation and nitrogen fertilization in a winter wheat-summer maize rotation system for improving crop yield and reducing water and nitrogen leaching. *Agric. Water Manage.* 228, 105904. doi: 10.1016/j.agwat.2019.105904

frontiers | Frontiers in Plant Science

TYPE Original Research
PUBLISHED 08 May 2023
DOI 10.3389/fpls.2023.1170739

OPEN ACCESS

EDITED BY
Shahbaz Khan,
Huazhong Agricultural University, China

REVIEWED BY
Lingling Li,
Gansu Agricultural University, China
Anil K. Choudhary,
ICAR–Central Potato Research Institute, India
Daocai Chi,
Shenyang Agricultural University, China
Mir Muhammad Nizamani,
Guizhou University, China

*CORRESPONDENCE
Yongjian Sun
yongjians1980@163.com
Jun Ma
majunp2002@163.com

†These authors have contributed equally to this work

RECEIVED 21 February 2023
ACCEPTED 07 April 2023
PUBLISHED 08 May 2023

CITATION
Yan F, Zhou W, Sun Y, Guo C, Xiang K, Li N, Yang Z, Wu Y, Zhang Q, Sun Y, Wang X and Ma J (2023) No-tillage with straw mulching promotes the utilization of soil nitrogen by rice under wheat–rice and oilseed rape–rice cropping systems. *Front. Plant Sci.* 14:1170739. doi: 10.3389/fpls.2023.1170739

No-tillage with straw mulching promotes the utilization of soil nitrogen by rice under wheat–rice and oilseed rape–rice cropping systems

Fengjun Yan[1,2,3†], Wei Zhou[2†], Yongjian Sun[1,2*], Changchun Guo[1,2], Kaihong Xiang[1], Na Li[1,2], Zhiyuan Yang[1], Yunxia Wu[1], Qiao Zhang[1], Yuanyuan Sun[4], Xiyao Wang[2] and Jun Ma[1,2*]

[1]Rice Research Institute of Sichuan Agricultural University, Wenjiang, Chengdu, China, [2]Crop Ecophysiology and Cultivation Key Laboratory of Sichuan Province, Wenjiang, China, [3]Institute of Plateau Meteorology, China Meteorological Administration, Chengdu, China, [4]The Rural Revitalization Research Institute of Sichuan Tianfu New Area, Chengdu, China

Introduction: To investigate the effects of no-tillage with straw mulching on the absorption and utilization of soil nitrogen (N), fertilizer N, and straw N by rice under paddy-upland rotations.

Methods: A field experiment with three cropping systems: fallow–rice rotation without straw mulching (FRN), wheat–rice rotation with wheat mulching in rice season (WRS), and oilseed rape–rice rotation with oilseed rape straw mulching in rice season (ORS) was conducted from 2015 to 2017, along with a mini-plot experiment with ^{15}N-labeled urea and straws, which was conducted in 2017.

Results: No-tillage with straw reduced rice N uptake up to 20 days after transplanting, the total amount of fertilizer N uptake of WRS and ORS rice plants was 46.33 and 61.67 kg/ha, respectively, which was 9.02 and 45.10% higher than that of FRN plants. Soil N was the main source for rice growth, followed by fertilizer N. Soil N uptake by WRS and ORS rice plants was 21.75 and 26.82% higher than that of FRN plants, accounting for 72.37 and 65.47%, respectively, of the total N accumulated in rice plants. Straw mulching increased the N utilization efficiency of tillering, panicle, and total fertilizer by 2.84–25.30%; however, base fertilizer was dependent on straw mulching. The total amount of N released from WRS and ORS straw mulching in the rice season was 34.97 and 24.82 kg/ha, respectively; however, only 3.04 and 4.82% of it was absorbed by the rice plants, accounting for only 0.62 and 0.66% of the total accumulated N.

Discussion: No-tillage with straw mulching under paddy-upland rotations increased the N utilization of rice, especially for the absorption of soil N. These results provide theoretical information for the effective utilization of straw and rational N application practices in rice-based cropping systems.

KEYWORDS

straw incorporation, conservation tillage, paddy-upland rotation, isotopic labeling, nitrogen uptake

1 Introduction

Rice is an important food crop and approximately 50% of the world's population depends on rice as a staple food. Alternating the rice crop with upland crops, known as paddy-upland rotation, is the most efficient cropping system for ensuring global food security, especially in Asia (Zheng et al., 2016). However, unreasonably intense cropping cultivation leads to a decrease in soil fertility and crop yield and an increase in the usage of chemical fertilizers (Srinivasan et al., 2012; Nishida, 2016; Nandan et al., 2019). For example, rice-wheat cropping systems, the most popular paddy-upland rotations, have shown a clear slowing or stagnation in crop yield, which is related to the cycling of soil N (Ram et al., 2016; Zhou et al., 2021). Moreover, the amount of N fertilizer (as pure N) applied worldwide in 2012 was nearly 186 times higher than that in 1961. China's N input generally exceeds 180 kg/ha for rice season; however, the N utilization rate in rice is only approximately 30% (Tian et al., 2001; Pan et al., 2017). Many inorganic fertilizers are lost into the atmosphere, surface water, and groundwater, leading to the pollution of the air and water environments and the wastage of nonrenewable resources (Wang et al., 2014). Therefore, stabilizing the rice yield with less N input or increasing the rice yield without increasing the N input is the focus of agricultural research.

No-tillage is a variant of conservation tillage that is generally used to improve soil properties and crop yield (Shakoor et al., 2020; Thapa et al., 2023). However, sustainable agricultural production cannot be achieved through an isolated practice of no-tillage; it must be combined with crop residue retention (Rafael et al., 2021). Crop straw is rich in N and other nutritional elements, but traditional straw disposition (directly burned or arbitrarily stacked) causes serious environmental pollution and leads to higher wastage of resources. By contrast, no-tillage with straw mulching increases soil quality and crop yield by regulating N cycling in the soil and N uptake by crops (Yang et al., 2020; Yang et al., 2022a; Yang et al., 2022b). However, straw mulching may lead to higher N consumption, increase its immobilization, and accumulate allelochemicals in the prior decomposition period, which causes N stress and inhibits root growth and N absorption during the initial growth period of crops (Liu et al., 2007; Yan et al., 2019; Singh et al., 2022). Over a larger 12-year rotation trial, Flower et al. (2022) revealed that whether straw mulching has a positive or negative impact on crop growth depends on the crop and straw types, and environmental conditions such as soil moisture. Therefore, we hypothesized that different crop types and the special water management alternating between wet and dry conditions will change soil properties, resulting in different responses to conservation tillage practices in paddy-upland rotations.

Previous studies on conservation tillage have mainly focused on dryland crops; however, studies on whether no-tillage in combination with straw mulching can promote N uptake by rice plants under paddy-upland rotations with less N input are scarce. Therefore, the present study set up a 3-year field experiment with three cropping systems under no-tillage in combination with low chemical N application. To determine the source of N absorbed by the rice, a mini-plot experiment using ^{15}N-labeled urea and straw was performed in 2017. The aim of this study was to elucidate the principles of N release from wheat and oilseed rape straw and its effects on N uptake by rice plants under paddy-upland rotation with no-tillage, which could provide theoretical support for the sustainable production of rice-based cropping systems with N reduction.

Abbreviations: FRN, fallow-rice rotation with no straw mulching; WRS, wheat-rice rotation with wheat straw mulching; ORS, oilseed rape-rice with oilseed rape straw mulching; DAT, days after rice transplanting; HS, heading stage; MS, mature stage.

2 Materials and methods

2.1 Experimental site

The experiment was performed at a farm of the Rice Research Institute of Sichuan Agricultural University Chengdu, China (30° 35′N, 103°45′E), during 2015–2017. The soil had a sandy loam texture with a total N of 1.96 g/kg, organic matter of 26.00 g/kg, available N of 29.13 mg/kg, available P of 81.60 mg/kg, and available K of 85.98 mg/kg at the time of experiment initiation. The region is classified as humid subtropical with a monsoon climate, and the meteorological data for the experimental years, which were measured at a weather station near the experimental site, are shown in Figure 1.

2.2 Experimental design and management

The experiment comprised three treatments in a single-factor randomized block design with three replicates during 2015–2017. The treatments were designed as follows: wheat–rice rotation with wheat straw mulching during the rice season (WRS), oilseed rape–rice rotation with oilseed rape straw mulching in the rice season (ORS), and fallow–rice rotation without straw mulching (FRN), which served as the control (Table 1). The plot size was 4.8 m × 3.3 m, and plots were separated by a 0.4 m wide alley with a plastic film inserted into the soil to form a barrier. Wide–narrow row spacing cultivation was used for rice plantation in the present study. Wheat and oilseed rape straws were cut into 5–10 cm long pieces and mulched on a wide row immediately after rice transplantation. Alternate dry/wet irrigation was applied, and the seedlings were transplanted in shallow water (1–2 cm). The field was submerged in a 2 cm water layer for 5–7 days after transplanting to ensure that the seedlings turned green and survived. Thereafter, the water was drained from the field until booting, and the soil water content accounted for 70–80% of the saturated water content. The field was dried during the ineffective tillering stage. The field was again submerged in a 1–3 cm water layer at the booting stage. Irrigation with 3 mm water was carried out in the bolting stage of wheat and oilseed rape, and rain-fed irrigation was applied in other growth periods. The total N applied in the rice and upland crop seasons was 135 and 48 kg/ha, respectively, which was much lower than the 180 and 120 kg/ha applied in conventional cultivation

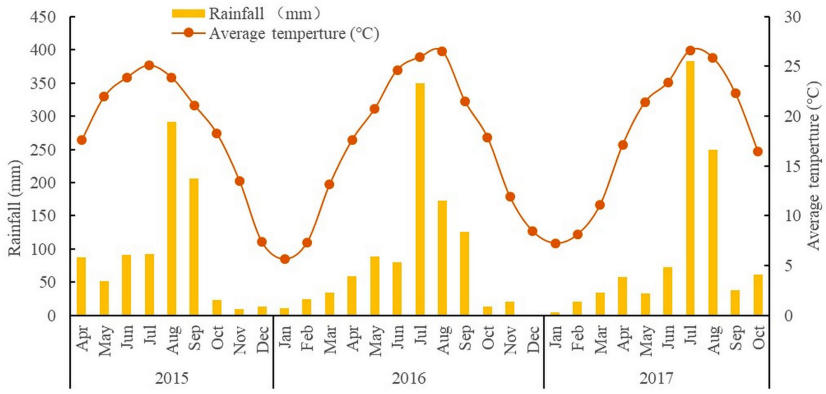

FIGURE 1
The average temperature (°C) and rainfall (mm) during 2015-2017.

reported by Peng et al. (2002). Details of other cultivation measures and fertilizer applications are shown in Tables 1, 2.

The ^{15}N mini-plot experiment was performed along with a field experiment in 2017. Four metal frames without bottoms (80 cm long × 70 cm wide × 50 cm high) were installed 30 cm deep in the soil and 20 cm above the soil surface around 10 adjacent rice plants in each field plot. The ^{15}N-labeled urea and straw were applied as described in Table 3. The ^{15}N abundance and total N content of labeled wheat and oilseed rape straw were 0.763 atom% and 0.749% and 0.634 atom% and 0.620%, respectively. The application times of fertilizers and other management practices were the same as those in the field experiment.

2.3 Indices and measurement methods

2.3.1 N release from straws

After rice transplanting, 4–6 bags of 0.4 mm mesh nylon filled with 30–40 g of straw was randomly mulched in each plot of WRS and ORS. The straw bags were collected on days 20 and 30 after the transplanting, heading, and mature stages (20 and 20 DAT, HS, and MS), and gently washed to remove the soil. All samples were oven-dried at 105 °C for 1 h, then at 70 °C until they reached a constant weight. Thereafter, the samples were crushed and sieved (mesh size = 0.178 mm). Total N content was determined using a FOSS-KJ8400 apparatus (FOSS, Sweden). The ^{15}N abundance values were determined using mass spectrometry at the Shanghai Research Institute of Chemical Industry (Arulmozhiselvan and Beeman, 2017).

2.3.2 N accumulation in plants

Three representative rice plants containing the average number of tillers in each plot were collected on day 30 DAT, HS, and MS of rice and at the MS of wheat and oilseed rape. The plants were separated into leaves, stems, sheaths, and panicles (at heading and maturity). The follow-up processing as described in section 2.3.1 was performed to determine the total N content and ^{15}N abundance values. The amount of ^{15}N originating from the labeled urea and straw was determined as described by Beeman and Arulmozhiselvan (Du et al., 2009).

2.4 Data analysis

The data were statistically analyzed to test the level of significance using a single-factor randomized block design. Analysis of variance was performed using SPSS Version 12.0 and Sigma Plot 12.0 to test the effects of treatments and interactions.

3 Results

3.1 N uptake by rice plants

N accumulation increased with the growth and development of rice plants, but the amount of N uptake at 30 DAT-HS was the highest, followed by HS-MS (Figure 2). Straw mulching promoted the absorption of N by rice plants, especially after 30 days of transplanting, and the effect of ORS was stronger than that of

TABLE 1 Field management for test crops.

Crop	Cultivar	Tillage	Planting method	Spacing (cm×cm)	Plants per hill	Crop season
Wheat	Sumai 375	No tillage	Hill-direct-seeding	20×10;	3-5	October- June
Oilseed rape	Chuanyou 58	No tillage	Hill-derect-seeding	30×20	3-5	October-June
Rice	Yixiang-3724	No tillage	Artificial transplanting	(40 + 26.5)×16.7	1	June-September

TABLE 2 Detailed application of fertilizers for test crops in field experiment (kg/ha).

Crop	Application amount			Base fertilizer				First top dressing		Second top dressing	
	N	P_2O_5	K_2O	CF	Urea	SSP	KCl	CF	Urea	CF	Urea
Wheat	48	48	48	64	–	–	–	128	–	128	–
Oilseed rape	48	48	48	64	–	–	–	128	–	128	–
Rice	135	67.5	135	–	88	562.5	225	–	88	–	117.4

CF, compound fertilizer (the content of N, P_2O_5, and K_2O all was 15%); SSP, calcium superphosphate; KCl, muriate of potash. Base fertilizer was applied before plant transplantation or sowing; first top dressing was applied at the early tillering stage for rice, at the jointing stage for wheat, and at the wintering stage for oilseed rape; second fertilizer top dressing was applied at the panicle initiation stage for rice, at the bolting stage for wheat and at oilseed rape.

TABLE 3 The usage of ^{15}N-labeled urea and straw in the mini-plots.

Mini-plot	Base N	Tillering N	Panicle N	Straws
1st	**^{15}N**	^{14}N	^{14}N	^{14}N
2nd	^{14}N	**^{15}N**	^{14}N	^{14}N
3rd	^{14}N	^{14}N	**^{15}N**	^{14}N
4th	^{14}N	^{14}N	^{14}N	**^{15}N**

WRS. In 2016, the rice N uptake of WRS at 20–30 DAT and 30 DAT-HS was significantly decreased by 27.56% and increased by 14.91%, respectively, compared to that of FRN, whereas the rice N uptake of ORS was 3.35–11.64% higher than that of FRN during the entire rice growth period. The rice N accumulation of ORS was 4.21% lower at 30 DAT-HS but 8.49, 54.12, and 9.32% higher at 0–20 DAT, 20–30 DAT, and HS-RS, respectively, compared to that of WRS. In 2017, except for 0–20 DAT, rice N uptake of WRS and ORS was 10.10–95.22% higher than that of FRN. Rice N uptake of ORS was 0.92 and 9.70% lower at 20–30 DAT and HS-RS, respectively, but 14.86 and 13.12% higher at 0–20 DAT and 30 DAT-HS, respectively, compared to that of WRS. Although the amount of N accumulation differed among the three treatments at different stages, the total amount of N accumulated at the mature stage was the highest for ORS, followed by that for WRS, which was 10.09–29.67% and 2.99–22.19% higher than that of FRN.

3.2 N sources of rice plants

Total N accumulation in rice plants increased in WRS mainly because of the increase in the uptake of soil N, whereas in ORS it was because of the synchronous increase in the uptake of soil N and fertilizer N (Figure 3). Straw mulching significantly promoted the uptake of N from the soil by rice plants from 30 DAT to MS. The amount of soil N uptake by rice plants with straw mulching was 11.68–12.01% lower than that of FRN at 20 DAT, but 14.79–29.43%, 40.11–40.64%, and 21.75–26.82% higher than that of FRN at 30 DAT, HS, and MS, respectively. The effects of oilseed rape and wheat straw mulching on N fertilizer uptake by rice plants were significantly different. The amount of fertilizer N uptake by WRS rice plants from 20 DAT to HS was lower than that of FRN, whereas ORS promoted fertilizer uptake by rice plants throughout the growth stages. As a result, the total amount of fertilizer N uptake

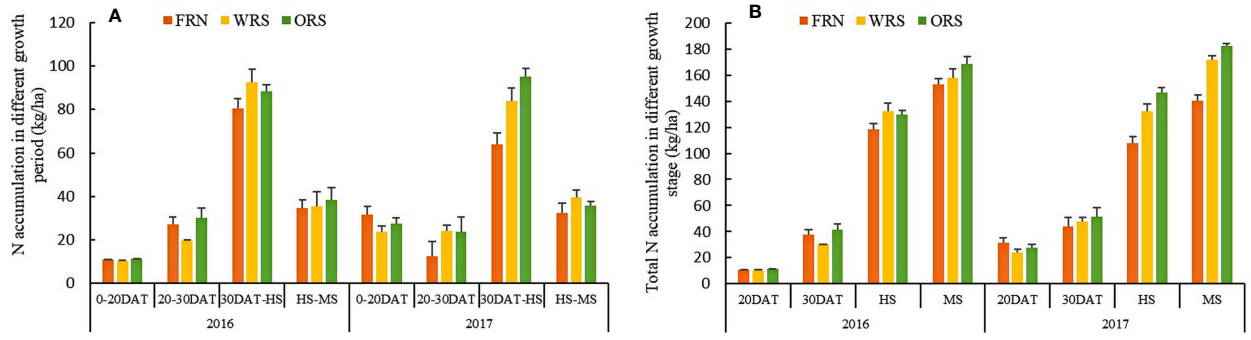

FIGURE 2
Rice nitrogen accumulation in rice growth **(A)** periods and total nitrogen accumulation in differenct growth stage **(B)**. FRN, fallow-rice rotation with no straw mulching; WRS, wheat-rice rotation with wheat straw mulching; ORS, oilseed rape-rice with oilseed rape straw mulching; DAT, days after rice transplanting; HS, heading stage; MS, mature stage.

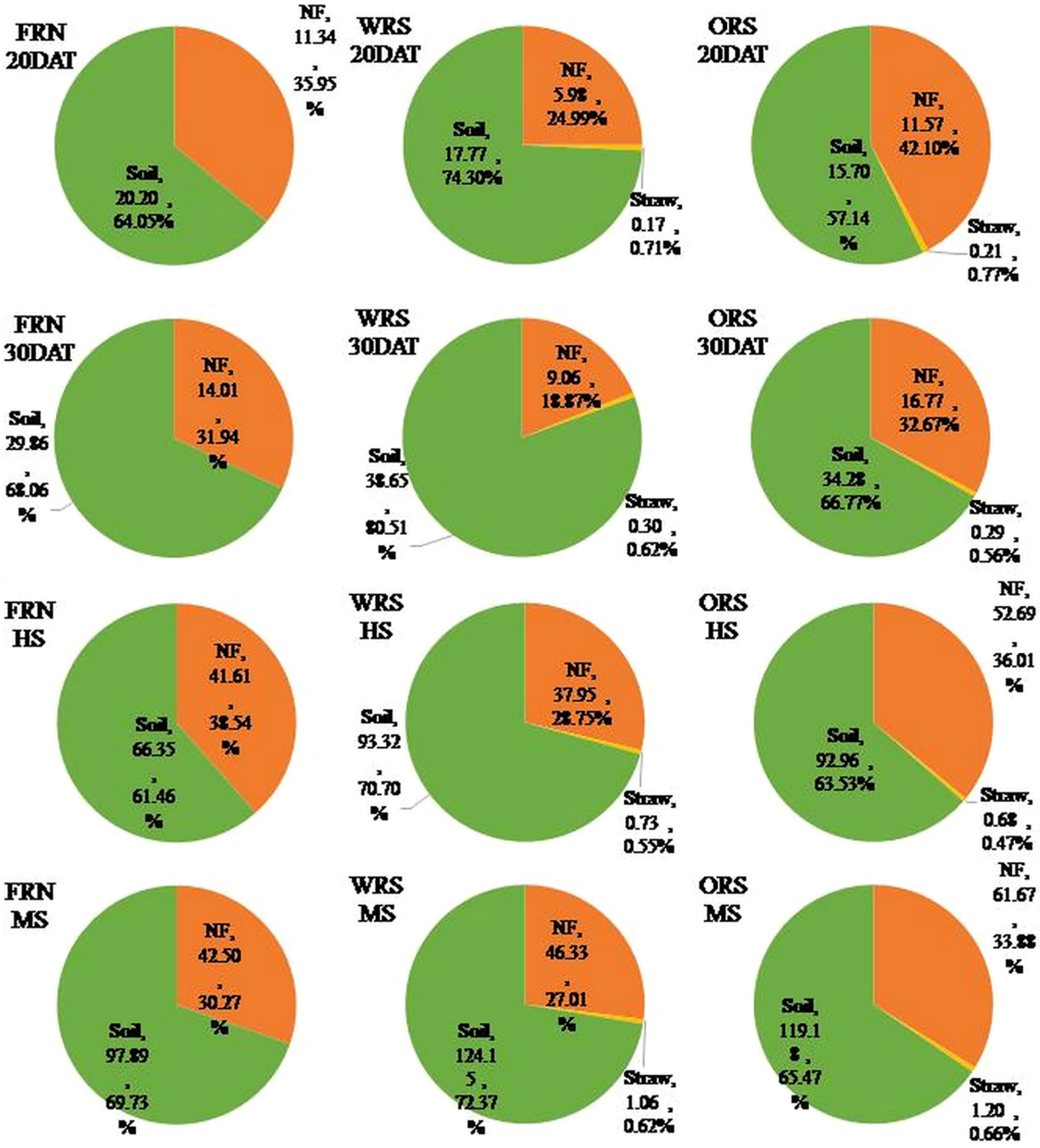

FIGURE 3
The source and its proportion of nitrogen in rice plants. FRN, fallow-rice rotation with no straw mulching; WRS, wheat-rice rotation with wheat straw mulching; ORS, oilseed rape-rice with oilseed rape straw mulching; DAT, days after rice transplanting; HS, heading stage; MS, mature stage; NF, fertilizer nitrogen.

by rice plants of WRS and ORS was 46.33 and 61.67 kg/ha, which was 9.02 and 45.10% higher than that of FRN, respectively. Although straw mulching promoted N absorption by rice plants, the amount of straw N absorbed by rice plants was 1.06–1.20 kg/ha, only accounting for 0.62–0.66% of the total N uptake.

3.3 Release and utilization of straw N

N release from straw increased gradually with the growth of rice plants (Figure 4). Except for the release rate at MS in 2016, the cumulative release amount and rate of WRS were higher than those

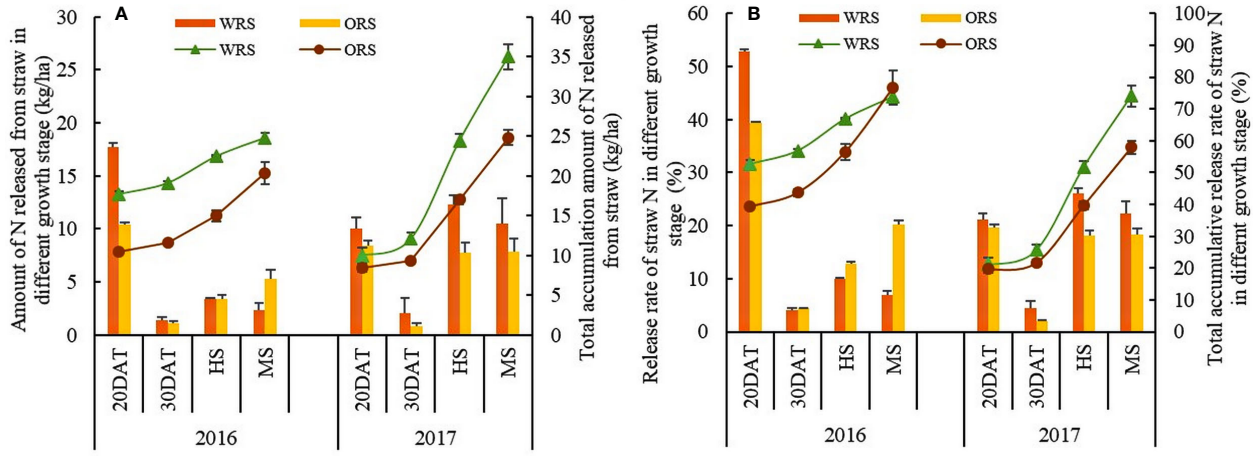

FIGURE 4
Straw nitrogen amount and accumulation amount of N release **(A)**, and straw release and accumulation release rate of straw **(B)** in rice growth stages. WRS, wheat-rice rotation with wheat straw mulching; ORS, oilseed rape-rice with oilseed rape straw mulching; DAT, days after rice transplanting; HS, heading stage; MS, mature stage.

of ORS at all stages. The total amount of N released from WRS was 24.76 and 34.97 kg/ha, which was 10.1 and 40.87% higher than that from ORS in 2016 and 2017, respectively. The N release amount and rate of WRS and ORS first decreased and then increased, and the release rate was the highest at 20 DAT, accounting for 21.20–52.77% and 19.68–39.41% of the total release in WRS and ORS, respectively. For different stages, the amount of straw N released from WRS at 0–20 DAT and 20–30 DAT was 69.70 and 19.54% higher than that from ORS in 2016, respectively, which significantly increased by 34.62–149.78% during the entire rice growth period in 2017. Only 3.04–4.82% was absorbed and utilized by rice plants out of the total 20.31–34.97 kg/ha of N released by straw mulching, and most of it remained in the soil (Figure 5). The amount of N released by WRS was higher than that released by ORS; however, the utilization rate was 1.78% lower than that of ORS.

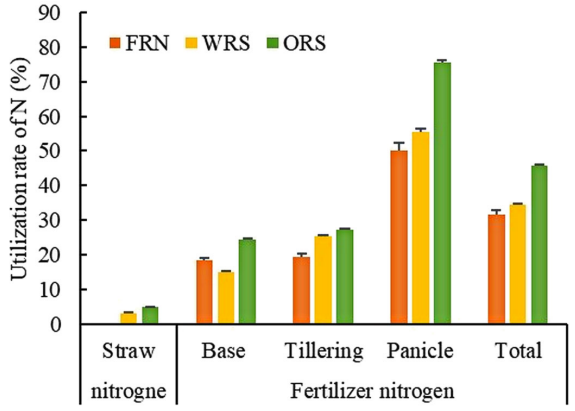

FIGURE 5
Utilization rate of nitrogen from straw and fertilizers. FRN, fallow-rice rotation with no straw mulching; WRS, wheat-rice rotation with wheat straw mulching; ORS, oilseed rape-rice with oilseed rape straw mulching.

3.4 Utilization of fertilizer N applied at different stages

N use efficiency increased with straw mulching; however, the absorption and utilization rates of N applied to rice at different growth stages were significantly different (Figure 6). N uptake of base fertilizer in WRS decreased by 19.03–68.48% at different growth stages, whereas that of tillering and panicle fertilizer in WRS first decreased and then increased, reaching 30.03 and 10.66% at MS, respectively, compared to that of FRN. N uptake of base, tillering, and panicle fertilizer in ORS increased at different growth stages (except for tillering fertilizer at 20 DAT), reaching 12.01–41.69%, 5.53–39.44%, and 22.94–50.39%, respectively, compared to that in FRN. Therefore, the N utilization rate of the base fertilizer of WRS and ORS decreased by 3.52% and increased by 5.91%, respectively, whereas that of tillering and panicles in WRS and ORS increased by 5.85 and 5.35%, and 7.68 and 25.30%, respectively, compared to that in FRN, which led to the increase in total N fertilizer utilization by 2.84 and 14.20%, respectively (Figure 5).

4 Discussion

4.1 N uptake by rice plants in different stages

The present study showed that the total N uptake by rice plants of WRS and ORS was higher than that by plants of FRN, but N uptake decreased at 0–20 DAT (Figure 1). In paddy systems, rapid straw decomposition may also lead to a high accumulation of allelochemicals during early straw incorporation and cause rapid changes in soil properties, inhibit root growth, and decrease N uptake (Liu et al., 2007; Yan et al., 2019). Except for the allelochemicals, the decrease in N uptake by rice plants in the

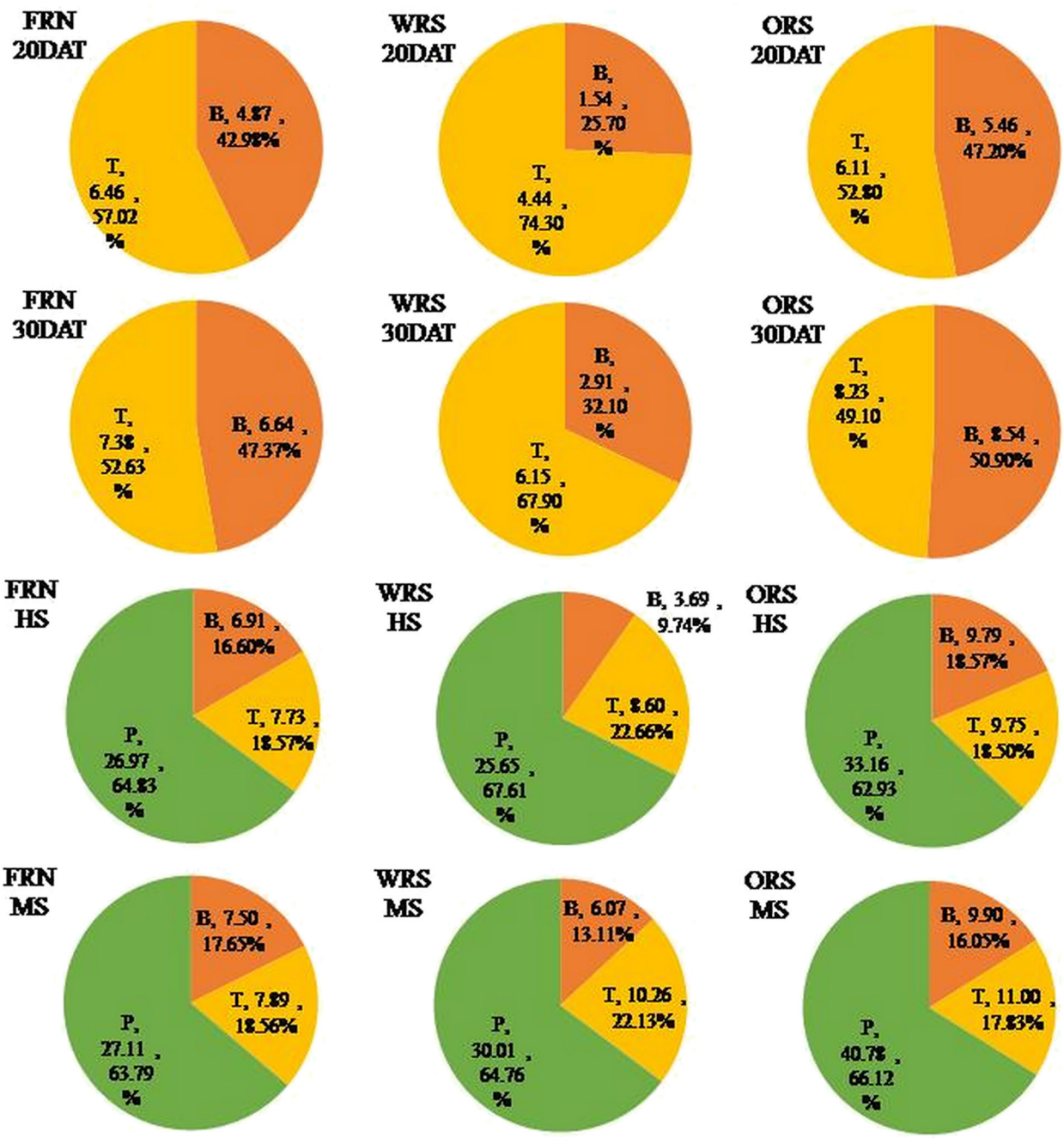

FIGURE 6
The amount and proportion of different N fertilizer uptake by rice plants. FRN, fallow-rice rotation with no straw mulching; WRS, wheat-rice rotation with wheat straw mulching; ORS, oilseed rape-rice with oilseed rape straw mulching; DAT, days after rice transplanting; HS, heading stage; MS, mature stage; B, base nitrogen fertilizer; T, tillering nitrogen fertilizer; P, panicle nitrogen fertilizer.

early growth stages may also be attributed to the following: i) Some amount of the N released by the base-tillering fertilizer was absorbed by the straw. Chen et al. (2022) found that the N content of mulched straw increases after fertilization, thus reducing the ammonia volatilization loss of fertilizer N. The results of the mini-plot experiment with ^{15}N-labeled urea showed that fertilizer N in the undecayed straw was 1.55–2.97 kg/ha at the mature stage of rice, which indicated that a large amount of fertilizer N was absorbed by the straw in the early stage, and part of fertilizer N was not released into the soil until rice maturity. ii) After returning to the field, straw decomposes rapidly in the early stage, which rapidly increases the soil C content, leading to an unbalanced soil C/N ratio and resulting in competition for N between microorganisms and rice plants (Zhang et al., 2010; Kuzyakov and Xu, 2013). However, no-tillage with straw mulching increases soil bacterial community diversity (Luo et al., 2020) and the activities of soil enzymes, including invertase, acid phosphatase, and urease (Iqbal et al., 2021); improves soil N retention capacity,

and reduces N loss risk (Yang et al., 2022b), all of which lead to more efficient N recycling in cropping systems (Yang et al., 2023). Therefore, WRS and ORS promoted N uptake by rice plants in the later growth stages (from HS to MS) and significantly increased the total N accumulation in rice plants under no-tillage with straw mulching conditions. This reveals that the straw mulching of dryland crops has the potential to reduce N input and increase rice yield under paddy-upland rotation with no-tillage.

4.2 N sources of rice plants with straw mulching

The results of this study showed that total N accumulation in rice plants increased in the WRS and ORS, which was mainly attributed to an increase in the uptake of soil N (Figure 3). Soil is the main N source for crop uptake, and approximately 50–80% of the N absorbed by rice during its entire growth period is sourced from the soil (Zhu, 2008). Additional N sources promote the absorption of soil N by plants, which was defined as the "priming effect" or "added N interaction" by Hamid and Ahmad (1993). Under the paddy-upland rotation, N application during the rice season increases the absorption of soil N from previous crops by rice plants (Zhou et al., 2020). In this study, the soil N uptake increased to 97.89, 124.15, and 119.18 kg/ha for FRN, WRS, and ORS, respectively. Straw mulching promotes the establishment of soil microbial colonies and increases fungal and enzyme activities (Bolinder et al., 2020; Dhaliwal et al., 2020), which significantly improves the mineralization and release of soil N, increases the transformation of ammonium and nitrate, and promotes the absorption of soil N by rice plants (Quan et al., 2018). In addition, although the straw released 20.31–34.97 kg/ha N in the rice season, there was little absorption by rice plants (Figure 5). Li et al. (2009) reported that more than 50% of the N in crop straw is refractory organic matter, which can only be absorbed by plants after transformation by microorganisms. Therefore, N released by straw is mainly retained in the soil during the short period of crop growth. This could explain why straw mulching not only increases N uptake by plants but also improves soil N content (Liu et al., 2021). The transformation and utilization of straw N require further study to reveal the mechanism of long-term straw return to improve soil fertility and crop yield.

5 Conclusion

The release, absorption, and utilization of straw N by rice under no-tillage and straw mulching conditions were investigated in the present study. It was revealed that wheat and oilseed rape straw mulching increased the total N uptake of rice by 2.99–29.67%. The amount of straw N absorbed by rice plants was 1.06–1.20 kg/ha, which is only 0.62–0.66% of the total N uptake; approximately 65.47–72.37% was from the soil indicating that straw mulching promotes the utilization of soil N to a higher degree than that of inorganic N fertilizer by rice plants under no-tillage wheat/oilseed rape–rice cropping systems. In addition, straw mulching increased the N utilization efficiency of tillering, panicle, and total fertilizer by 2.84–25.30%; however, base fertilizer was dependent on mulching straw. The results obtained in this study provide a theoretical basis for the effective utilization of straw and rational N application practices in paddy-upland rotations in the future. However, many aspects of straw mulching, in particular, how the microbial transformation process of straw N mediates the utilization of straw N, require further investigations.

Data availability statement

The original contributions presented in the study are included in the article/supplementary material. Further inquiries can be directed to the corresponding author.

Author contributions

FY and JM designed the research, FY performed the experiments. FY and WZ analyzed the data and wrote the manuscript. YjS, CG, KX, NL, ZY, YW and QZ provided assistance with sampling and investigation. YyS provided assistance with meteorological data collection. JM and XW revised the manuscript. All authors contributed to the article and approved the submitted version.

Funding

This work was supported by the National Key Research and Development Program Foundation of Ministry of Science and Technology of the People, s Republic of China [2018YFD0301202, 2022YFD1100204] and the Natural Science Foundation of Sichuan Province [Grant number 2022NSFSC1637].

Conflict of interest

The authors declare that the research was conducted in the absence of any commercial or financial relationships that could be construed as a potential conflict of interest.

Publisher's note

References

Arulmozhiselvan, K., and Beeman, K. (2017). Fate of ^{15}N labeled nitrogen in maize grown with nutriseed pack using tracer technique. *Int. J. Agric. Environ. Biotechnol.* 10, 39–44. doi: 10.5958/2230-732X.2017.00006.7

Bolinder, M. ,. A., Crotty, F., Elsen, A., Frac, M., and Ktterer, T. (2020). The effect of crop residues, cover crops, manures and nitrogen fertilization on soil organic carbon changes in agroecosystems: A synthesis of reviews. *Mitigation Adaptation Strategies Global Change.* 25, 929–952. doi: 10.1007/s11027-020-09916-3

Chen, Y. Q., Chen, J., Hu, Z. T., Zhang, Y. F., Yan, F. J., Ren, W. J., et al. (2022). Characteristics and influencing factors of ammonia volatilization in garlic field. *J. Sichuan Agric. Univ.* 40, 58–66. doi: 10.16036/j.issn.1000-2650.202109027

Dhaliwal, S., Naresh, K., Gupta, K., Panwar, S., Mahajan, C., Singh, R., et al. (2020). Effect of tillage and straw return on carbon footprints, soil organic carbon fractions and soil microbial community in different textured soils under rice–wheat rotation: A review. *Rev. Environ. Sci. Bio-Technology.* 19, 103–115. doi: 10.1007/s10705-020-10099-1

Du, X. N., Song, M. M., and Zhao, C. (2009). Treatment methods of isotope ^{15}N labeled sample for mass spectrometry. *Atomic Energy Sci. Technology.* 043, 59–63. doi: 10.7538/yzk.2009.43.suppl.0059

Flower, K. C., Ward, P. R., Passaris, N., and Cordingley, N. (2022). Uneven crop residue distribution influences soil chemical composition and crop yield under long-term no-tillage. *Soil Tillage Res.* 223, 105498. doi: 10.1016/j.still.2022.105498

Hamid, A., and Ahmad, M. (1993). Priming effects of 15N-labelled ammonium nitrate on uptake of soil n by wheat (Triticum aestivum l.) under field conditions. *Biol. Fertility Soils.* 15, 297–300. doi: 10.1007/BF00337216

Iqbal, A., Khan, A., Green, S. J., Ali, I., He, L., Zeeshan, M., et al. (2021). Long-term straw mulching in a no-till field improves soil functionality and rice yield by increasing soil enzymatic activity and chemical properties in paddy soils. *J. Plant Nutr. Soil Science.* 2021, 184. doi: 10.1002/jpln.202100089

Kuzyakov, Y., and Xu, X. (2013). Competition between roots and microorganisms for nitrogen: mechanisms and ecological relevance. *New Phytolog.* 198, 139–163. doi: 10.1111/nph.12235

Li, F. Y., Sun, X. F., Feng, W. Q., Qin, Y. S., Wang, C. Q., and Tu, S. H. (2009). Nutrient release patterns and decomposing rates of wheat and rapeseed straw. *Plant Nutr. Fertilizer Science.* 15, 374–380. doi: 10.11674/zwyf.2009.0218

Liu, S. P., Chen, W. L., Nien, X. T., Zhang, H. C., Dai, Q. G., Huo, Z. Y., et al. (2007). Effect of embedding depth on decomposition course of crop residues in rice-wheat system. *Plant Nutr. Fertilizer Science.* 13, 1049–1053. doi: 10.3321/j.issn:1008-505x.2007.06.010

Liu, N., Li, Y. Y., Cong, P., Wang, J., Guo, W., Pang, H. C., et al. (2021). Depth of straw incorporation significantly alters crop yield, soil organic carbon and total nitrogen in the north China plain. *Soil Tillage Res.* 205, 104772. doi: 10.1016/j.still.2020.104772

Luo, Y., Iqbal, A., He, L., Zhao, Q., and Jiang, L. (2020). Long-term no-tillage and straw retention management enhances soil bacterial community diversity and soil properties in southern China. *Agronomy.* 10.1233 doi: 10.3390/agronomy10091233

Nandan, R., Singh, V., Singh, S. S., Kumar, V., Hazra, K. K., Nath, C. P., et al. (2019). Impact of conservation tillage in rice–based cropping systems on soil aggregation, carbon pools and nutrients. *Geoderma.* 340, 104–114. doi: 10.1016/j.geoderma.2019.01.001

Nishida, M. (2016). Decline in fertility of paddy soils induced by paddy rice and upland soybean rotation, and measures against the decline. *Japan Agric. Res. Quarterly.* 50, 87–94. doi: 10.6090/jarq.50.87

Pan, F. F., Yu, W. T., Ma, Q., Zhou, H., Jiang, C. M., Xu, Y. G., et al. (2017). Influence of ^{15}N-labeled ammonium sulfate and straw on nitrogen retention and supply in different fertility soils. *Biol. Fertility Soils.* 53, 303–313. doi: 10.1007/s00374-017-1177-1

Peng, S. B., Huang, J. L., Zhong, X. H., Yang, J. C., Wang, G. H., Zou, Y. B., et al. (2002). Challenge and opportunity in improving fertilizer-nitrogen use efficiency of irrigated rice in China. *J. Integr. Agriculture.* 7, 776–785. doi: 10.1007/978-94-007-0394-0_42

Quan, Z., Li, S. L., Zhu, F. ,. F., Zhang, L. F., He, J. Z., Wei, W. X., et al. (2018). Fates of ^{15}N-labeled fertilizer in a black soil-maize system and the response to straw incorporation in northeast China. *J. Soils Sediments* 18, 1441–1452. doi: 10.1007/s11368-017-1857-3

Rafael, F. L., Tiago, S. T., Dimas., S. J., Thadeu, R. M., Theodor, F., and Amir, K. (2021). Expansion of no-tillage practice in conservation agriculture in Brazil. *Soil Tillage Res.* 208, 104877. doi: 10.1016/j.still.2020.104877

Ram, S., Singh, V., and Sirari, P. (2016). Effects of 41 years of application of inorganic fertilizers and farm yard manure on crop yields, soil quality, and sustainable yield index under a rice-wheat cropping system on mollisols of north India. *Commun. Soil Sci. Plant Analysis.* 47, 179–193. doi: 10.1080/00103624.2015.1109653

Shakoor, A., Shahbaz, M., Farooq, T. H., Sahar, N. E., Shahzad, S. M., Altaf, M. M., et al. (2020). A global meta-analysis of greenhouse gases emission and crop yield under no-tillage as compared to conventional tillage. *Sci. Total Environment.* 750, 142299. doi: 10.1016/j.scitotenv.2020.142299

Singh, J., Ale, S., DeLaune, P. B., Himanshu, S. K., and Barnes, E. M. (2022). Modeling the impacts of cover crops and no-tillage on soil health and cotton yield in an irrigated cropping system of the Texas rolling plains. *Field Crops Res.* 287, 108661. doi: 10.1016/j.fcr.2022.108661

Srinivasan, V., Maheswarappa, H. P., and Lal, R. (2012). Long term effects of topsoil depth and amendments on particulate and non-particulate carbon fractions in a miamian soil of central Ohio. *Soil Tillage Res.* 121, 10–17. doi: 10.1016/j.still.2012.01.014

Thapa, V. R., Ghimire., R., Paye, W., and Vanleeuwen, D. (2023). Soil organic carbon and nitrogen responses to occasional tillage in a continuous no-tillage system. *Soil Tillage Res.* 227, 105619. doi: 10.1016/j.still.2022.105619

Tian, G. M., Cai, Z. C., Cao, J. L., and Li, X. P. (2001). Ammonia volatilization from paddy field and its affection factors in zhengjiang hilly region. *Acta Pedologica Sinica.* 03, 324–332. doi: 10.11766/trxb200010140312

Wang, J., Wang, D. J., Zhang, G., Wang, Y., Wang, C., Teng, Y., et al. (2014). Nitrogen and phosphorus leaching losses from intensively managed paddy fields with straw retention. *Agric. Water Manage.* 141, 66–73. doi: 10.1016/j.agwat.2014.04.008

Yan, F. J., Sun, Y. J., Xu, H., Jiang, M. J., Xiang, K. H., Wu, Y. X., et al. (2019). The effect of straw mulch on nitrogen, phosphorus and potassium uptake and use in hybrid rice. *Paddy Water Environment.* 17, 23–33. doi: 10.1007/s10333-018-0680-9

Yang, H. K., Li, J. G., Wu, G., Huang, X. L., and Fan, G. Q. (2023). Maize straw mulching with no-tillage increases fertile spike and grain yield of dryland wheat by regulating root-soil interaction and nitrogen nutrition. *Soil Tillage Res.* 228, 105652. doi: 10.1016/j.still.2023.105652

Yang, H. K., Wu, G., Mo, P., Chen, S. H., Wang, S. Y., Xiao, Y., et al. (2020). The combined effects of maize straw mulch and no-tillage on grain yield and water and nitrogen use efficiency of dry-land winter wheat (Triticum aestivum l.). *Soil Tillage Res.* 197, 104485. doi: 10.1016/j.still.2019.104485

Yang, H. K., Xiao, Y., He, P., Ai, D. L., Zou, Q. S., Hu, J., et al. (2022a). Straw mulch-based no-tillage improves tillering capability of dryland wheat by reducing asymmetric competition between main stem and tillers. *Crop J.* 10, 864–878. doi: 10.1016/j.cj.2021.09.011

Yang, H. K., Xiao, Y., He, P., Ai, D., Zou, Q. S., Hu, J., et al. (2022b). Effects of long-term no-tillage and maize straw mulching on gross nitrogen transformations in mollisols of northeast China. *Geoderma.* 428, 116194. doi: 10.1016/j.geoderma.2022.116194

Zhang, S. Q., Zhong, X. H., Huang, N. R., and Lu, G. A. (2010). Effect of straw-mulch-incorporation on nitrogen uptake and n fertilizer use efficiency of rice (Oryza sativa l.). *Chin. J. Eco-Agriculture.* 18, 611–616. doi: 10.3724/SP.J.1011.2010.00611

Zheng, H. B., Huang, H., Zhang, C. M., and Li, J. Y. (2016). National-scale paddy-upland rotation in northern China promotes sustainable development of cultivated land. *Agric. Water Manage.* 170, 20–25. doi: 10.1016/j.agwat.2016.01.009

Zhou, W., Wang, T., Fu, Y., Yang, Z. P., and Ren, W. J. (2020). Residual nitrogen from preceding garlic crops is important for double-cropped rice. *Nutrient Cycling Agroecosyst.* 118, 311–324. doi: 10.1155/2016/2728391

Zhou, Y. J., Xu, L., Xu, Y. Z., Xi, M., Tu, D. B., Chen, J. H., et al. (2021). A meta-analysis of the effects of global warming on rice and wheat yields in a rice-wheat rotation system. *Food Energy Security.* 10, 1–12 doi: 10.1002/fes3.316

Zhu, Z. (2008). Advances in the research of nitrogen supply from soil and nitrogen use of chemical fertilizers in China. *Soil.* 05, 11–16.

frontiers | Frontiers in Plant Science

TYPE Original Research
PUBLISHED 08 May 2023
DOI 10.3389/fpls.2023.1171547

OPEN ACCESS

EDITED BY
Fahad Shafiq,
Government College University, Pakistan

REVIEWED BY
Linlin Wang,
Gansu Agricultural University, China
Muhammad Zahid Mumtaz,
The University of Lahore, Pakistan

*CORRESPONDENCE
Jianmei Ji
jjm1001@syau.edu.cn
Ismail Khan
ismailagronomist@gmail.com

†These authors have contributed equally to this work

RECEIVED 22 February 2023
ACCEPTED 07 April 2023
PUBLISHED 08 May 2023

CITATION
Wang L, Yu B, Ji J, Khan I, Li G, Rehman A, Liu D and Li S (2023) Assessing the impact of biochar and nitrogen application on yield, water-nitrogen use efficiency and quality of intercropped maize and soybean. *Front. Plant Sci.* 14:1171547. doi: 10.3389/fpls.2023.1171547

Assessing the impact of biochar and nitrogen application on yield, water-nitrogen use efficiency and quality of intercropped maize and soybean

Lixue Wang[1†], Binhang Yu[1†], Jianmei Ji[1*], Ismail Khan[2*], Guanlin Li[2], Abdul Rehman[3], Dan Liu[1] and Sheng Li[1]

[1]College of Water Conservancy, Shenyang Agricultural University, Shenyang, China, [2]School of the Environment and Safety Engineering, Jiangsu University, Zhenjiang, China, [3]Department of Agronomy, Faculty of Agriculture and Environment, The Islamia University of Bahawalpur, Bahawalpur, Pakistan

Introduction: Biochar (BC) and nitrogen (N) application have the potential to increase grain yield and resource use efficiency in intercropping systems. However, the effects of different levels of BC and N application in these systems remain unclear. To address this gap, the study is intended to ascertain the impact of various combinations of BC and N fertilizer on the performance of maize-soybean intercropping and determine the optimum application of BC and N for maximizing the effect of the intercropping system.

Methods: A two-year (2021-2022) field experiment was conducted in Northeast China to assess the impact of BC (0, 15, and 30 t ha^{-1}) and N application (135, 180, and 225 kg ha^{-1}) on plant growth, yield, water use efficiency (WUE), N recovery efficiency (NRE) and quality in an intercropping system. Maize and soybean were selected as materials in the experiment, where every 2 rows of maize were intercropped with 2 rows of soybean.

Results and discussion: The results showed that the combination of BC and N significantly affected the yield, WUE, NRE and quality of intercropped maize and soybean. The treatment of 15 t ha^{-1} BC and 180 kg ha^{-1} N increased grain yield and WUE, while that of 15 t ha^{-1} BC and 135 kg ha^{-1} N enhanced NRE in both years. Nitrogen promoted the protein and oil content of intercropped maize, but decreased the protein and oil content of intercropped soybean. BC did not enhance the protein and oil content of intercropped maize, especially in the first year, but increased maize starch content. BC was found to have no positive impact on soybean protein, but it unexpectedly increased soybean oil content. The TOPSIS method revealed that the comprehensive assessment value first increased and then declined with increasing BC and N application. BC improved the performance of maize-soybean intercropping system in terms of yield, WUE, NRE, and quality while N fertilizer input was reduced. The highest grain yield in two years was achieved for BC of 17.1-23.0 t ha^{-1} and N of 156-213 kg ha^{-1} in 2021, and 12.0-18.8 t ha^{-1} BC and 161-202 kg ha^{-1} N in 2022. These findings provide a comprehensive understanding of the growth of

maize-soybean intercropping system and its potential to enhance the production in northeast China.

KEYWORDS

maize-soybean intercropping, biochar, nitrogen application, yield, NRE, NUE

1 Introduction

Intercropping maize and soybean is considered as an effective method for improving land productivity in China (Zhang et al., 2008). This practice promotes farm biodiversity and resource efficiency, including land, nutrients, light and water (Ahmed et al., 2018; Feng et al., 2019; Iqbal et al., 2019; Raza et al., 2019a; Raza et al., 2019b). However, the spatial distributions of soil water and fertilizer vary greatly because of maize-soybean intercropping (Luan et al., 2021; Luo et al., 2022). Moreover, the nutrient supply of the system falls short of demand owing to such factors as interspecific competition in the middle and late crop growth stages (Raza et al., 2022), which may result in crop failure (Duchene et al., 2017). Because of this, it is generally considered for farmers that high fertilizer application improves crop growth and grain yield. But the fact is that the practice reduces the intercropped dominance, and negatively affects biological N fixation of intercropped legume (Zhou and Butterbach-Bahl, 2014), and also has an adverse effect on inter-specific competition between the intercropped crops. Therefore, it is important for the intercropping system to increase soil nutrient supply continuously during the critical period to balance resource competition and reach the aim of N fertilizer reduction and efficiency increase.

Biochar (BC) is a nutrient-rich solid and insoluble organic compound. It is produced by the thermal decomposition of organic matter at the temperature between 200 and 1200°C under the anaerobic condition (Weber and Quicker, 2018; Farhangi-Abriz et al., 2021). BC possesses high porosity, a large specific surface area, and a strong adsorption capacity (Alkharabsheh et al., 2021). Although it lacks effective N content, it plays a crucial role in influencing soil nitrogen's effectiveness by directly or indirectly impacting such process as nitrification, mineralization, and N fixation (Jindo et al., 2020). When the practice of combined BC and compound fertilizer application is conducted, it can improve nutrient use efficiency through achieving slow-release nutrients from BC (Mohammad et al., 2022). Previous researches (Seleiman et al., 2020; Solaiman et al., 2020; Wang et al., 2020) also indicate that BC combined with N fertilizer raises soil fertility, promotes soil aggregation, enhances plant N uptake and ultimately improve yield, water use efficiency (WUE), and N recovery efficiency (NRE). However, the optimal amounts of BC and N fertilizer vary depending on the crop's nutrient requirements and combination ratio. To maximize crop growth and yield, it is crucial to apply BC and N fertilizer at suitable rates based on crop nutrient requirements and soil properties. For example, the application of 5 t ha^{-1} of BC with 50 kg ha^{-1} of N fertilizer is recommended for achieving maximum N fertilizer use efficiency, while the application of 0 t ha^{-1} of BC and 100 kg ha^{-1} of N fertilizer is suggested to obtain the highest maize yield (Omara et al., 2020). Jin et al. (2019) found that 40 t ha^{-1} BC combined with 90 kg ha^{-1} N fertilizer resulted in the highest rapeseed yield, while 20 t ha^{-1} BC combined with 90 kg ha^{-1} N fertilizer to the utmost degree improved soil available phosphorus content in the rapeseed field. To improve efficiency, ensure crop yield, and save costs, it is essential to have scientific guidance on appropriate BC and N fertilizer applications (Sun et al., 2019). At present, mathematical models have been utilized to provide guidance for the application of water and fertilizer in agriculture (He et al., 2021a; He et al., 2021b), there has been limited research on mathematical models about BC and N fertilizer coupling. Additionally, current research on the combination of BC and N fertilizer mainly focuses on monoculture, with limited studies on intercropping systems, particularly regarding the comprehensive regulation and analysis of intercropping yield, water, and N utilization. Therefore, it is necessary to determine the optimum application of BC and N for maize-soybean intercropping systems. This will not only increase crop yield and enhance water and N utilization but also implement the synergistic effect of BC and N, leading to increased efficiency and cost savings.

The objective of this study is to address several important questions regarding the optimal use of BC and N fertilizer in maize-soybean intercropping systems in northeast China. Specifically, the study aims to investigate how various combinations of BC and N fertilizer impact crop yield, WUE, NRE, and quality. In addition, the study seeks to establish a systematic evaluation model for the intercropping system and determine the optimal application of BC and N for maximizing the benefits of the intercropping system.

2 Materials and methods

2.1 Experimental site

Two-year field experiments in the experimental station of Water Conservancy College, Shenyang Agricultural University, China (41°84′N, 123°57′E, and altitude of 44.7 m) were carried out from May to September 2021 and 2022. The experimental site is characterized as temperate continental semi-humid monsoon climate type, with simultaneous precipitation and heat. There is about 78% of annual precipitation occurring from June to September in the site. Figure 1 shows daily rainfall and daily average temperature during the growth period of intercropped

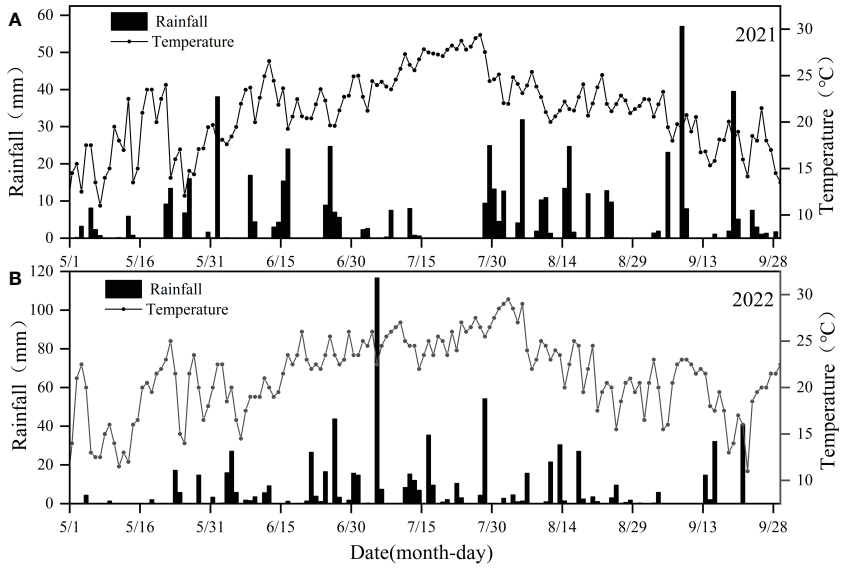

FIGURE 1
Rainfall and daily average temperature during the period of test. **(A)** stands for rainfall and daily average temperature during the period of test in 2021, **(B)** stands for rainfall and daily average temperature during the period of test in 2022.

crops, when total rainfall and average temperature were 596.2 mm and 9.0 °C in 2021 (Figure 1A), while they were 796.1 mm and 8.7 °C in 2022 (Figure 1B). The soil type of this site is brown soil, of which the physical and chemical properties are presented in Table 1.

2.2 Experimental design

Maize (*Zea mays* L., cv. Zhengdan 958) and soybean (*Glycine max* (Linn.) Merr., cv. Liaodou 32) were selected as materials in the experiment, where every 2 rows of maize were intercropped with 2 rows of soybean. The commercial BC, produced by pyrolyzing maize straw under the oxygen-free condition at a temperature of 450 °C, was purchased from Liaoning Jinhefu Agricultural Development Company. Its basic physical and chemical properties are given in Table 2. BC was mixed uniformly into the soil at a depth of 30 cm before sowing in 2021 but was not applied in the following year. BC application rates were 0 t ha^{-1} (C_0), 15 t ha^{-1} (C_1) and 30 t ha^{-1} (C_2), while N application rates were 135 kg ha^{-1} (N_1), 180 kg ha^{-1} (N_2), 225 kg ha^{-1} (N_3). Among them, N_3 is the conventional N application, which was used as control for N application, and the applications of 180 kg ha^{-1} and 135 kg ha^{-1} pointed at N reduction by 20% and 40% of N_3. The experiment in 2021 was laid out in an orthogonal design L9 (3^2) (Figure 2) by taking C_0N_3 as the control treatment with three replications, as was that in 2022.

There were 27 experimental plots, each of which was 18 m^2 (6 m × 3 m) in size. The distance between rows was 40 cm in maize or in soybean, and that between adjacent maize and soybean rows was 70 cm (Figure 2). The planting spacing in the maize row was 15 cm, while that in the soybean row was 20 cm. Besides, a 90 kg ha^{-1} of P_2O_5 and 120 kg ha^{-1} of K_2O were applied evenly with N to guarantee adequate nutrition in the experimental field fertilizer before sowing in the two years.. All treatments were under the normal field management and only natural rainfall was available without any irrigation during the two growing periods. Maize and soybean were simultaneously sown on 6 May, 2021 and on 2 May, 2022, and were harvested on 25 September, 2021 and 27 September, 2022.

TABLE 1 Basic physical and chemical properties of soil.

Total nitrogen (g·kg^{-1})	Total phosphorus (g·kg^{-1})	Total potassium (g·kg^{-1})	Soil organic matter (g·kg^{-1})	0~90cm volume weight of soil (g·cm^{-3})	Field water holding capacity (cm^3·cm^{-3})	wilting coef-ficient (cm^3·cm^{-3})
0.67	0.47	23.19	33.93	1.42	0.38	0.18

TABLE 2 Basic indicators of BC.

Total nitrogen (g·kg^{-1})	Total phosphorus (g·kg^{-1})	Total potassium (g·kg^{-1})	organic biochar (g·kg^{-1})	pH
10.2	8.1	15.7	515.0	8.5

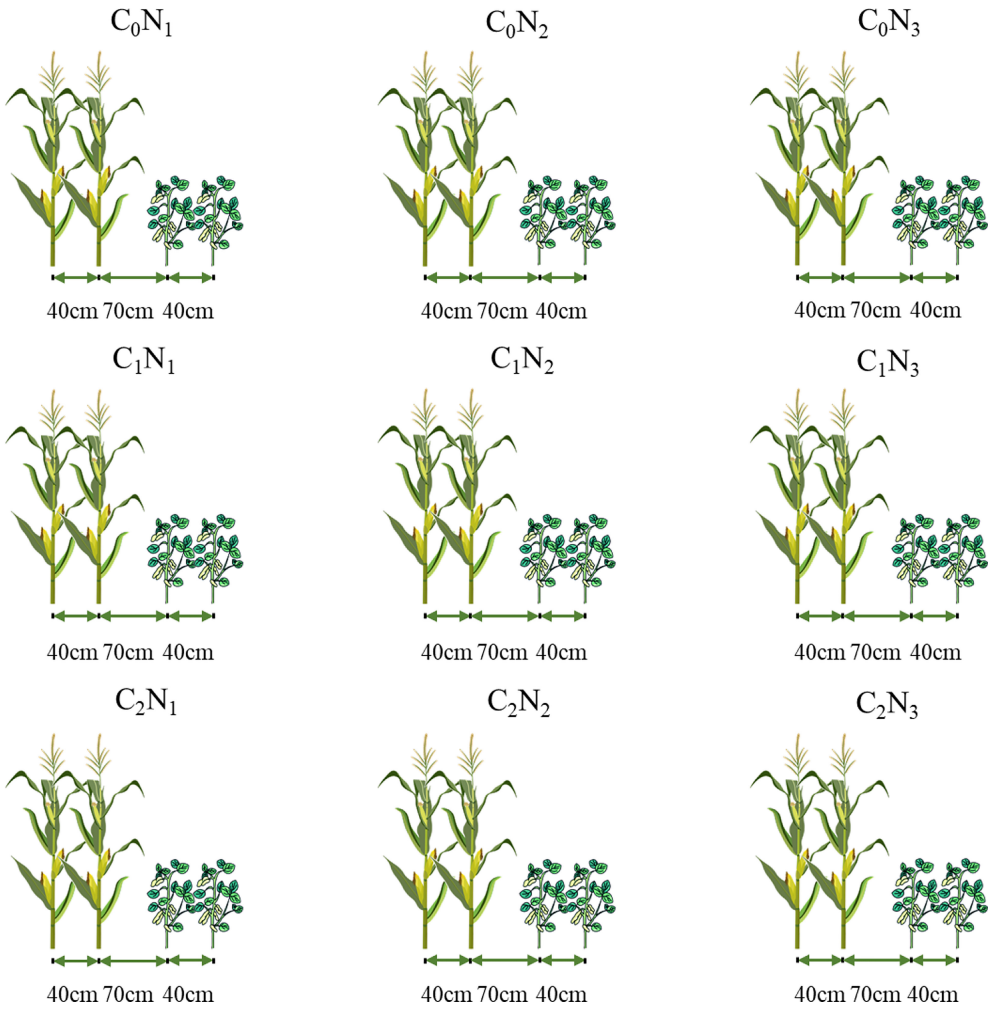

FIGURE 2
Schematic diagram of maize-soybean intercropping. BC application rates: 0 t ha^{-1} (C_0), 15 t ha^{-1} (C_1) and 30 t ha^{-1} (C_2); N application rates: 135 kg ha^{-1} (N_1), 180 kg ha^{-1} (N_2), 225 kg ha^{-1} (N_3). BC was mixed uniformly into the soil at a depth of 30 cm before sowing in 2021 but was not applied in the following year. N fertilizer was applied before sowing in the two years.

2.3 Measurements

2.3.1 Grain yield and quality

The grain yield of all maize and soybean plants in each plot was manually harvested at physiological maturity. Subsequently, their grain quality, including protein, oil content and starch, was analyzed using the FOSS near-infrared grain quality analyzer (Infratec 1241, Foss company, Denmark). It must be noted that all quality indicators except for soybean starch could be measured by the instrument, Despite this, soybean protein and oil content could also to some degree reflect its quality.

2.3.2 Water consumption and water use efficiency

Soil water content was measured to a depth of 100 cm at 10 cm increments by a soil auger using the oven-dried method before sowing and at harvest. A set of three probes was installed manually at a depth of 100 cm in the middle of the rows between maize and maize, maize and soybean, soybean and soybean in each plot.

Water consumption was calculated as follows:

$$ET = I + P - \Delta W - R - D + K \quad (1)$$

Where ET is water consumption; W_T is irrigation amount; P is effective rainfall in the growth stage; ΔW is the difference of water storage in the soil planned wetting layer between the beginning and end of the period; R is surface runoff; D is deep leakage; K is groundwater supply. W_T was zero because there was no irrigation in the experiment. Additionally, the experimental plot was flat, and hence there was no surface runoff loss, namely R=0. Soil moisture content at a depth of 90 cm to 100 cm did not vary significantly, which represented no deep leakage (D=0). Deeper groundwater depth was available, which means that there was no groundwater supply (K=0).

ΔW was calculated as follows:

$$\Delta W = \frac{\theta_m \rho_b h}{\rho_w} \quad (2)$$

Where θ_m is 0-100 cm soil mass moisture content (%); h is soil thickness (cm); ρ_b is average soil bulk density at the depth of 0 ~ 100 cm soil layer (g/cm^3), ρ_w is water density (g/cm^3).

WUE was calculated as follows:

$$WUE = \frac{Y}{ET} \tag{3}$$

Where Y is crop yield (kg ha^{-1}).

2.3.3 Nitrogen fertilizer recovery efficiency

N concentration of straw and grain was determined using Auto Kjeldahl Analysis Equipment (KJELTEC 2300, Foss company, Denmark) according to the Kjeldahl method. The aboveground N uptake was equal to straw N uptake and grain N uptake. NRE was defined as:

$$NRE = \frac{\text{Above ground N uptake(fertilizer)-Above ground N uptake(unfertilized)}}{\text{Total fertilizer N applied}} \times 100 \tag{4}$$

2.4 Comprehensive evaluation system framework

Two steps were involved to conduct the comprehensive evaluation. One was to categorize the factors and then establish a hierarchical structure of a system. Another was to analyze the relationships among the factors in the system in order to gain a better understanding of the system as a whole.

2.4.1 Evaluation factor set and its sub-factor set construction

(1) All indices of maize and soybean were divided into yield index (u_1), efficiency index (u_2) and quality index (u_3).

$$U_i = \{u_1, u_2, u_3\} \tag{5}$$

(2) All secondary indices were categorized and determined as sub-factors. Maize yield (u_{11}) and soybean yield (u_{12}) were categorized as yield indicators, WUE (u_{21}) and NRE (u_{22}) were categorized as efficiency indicators, Maize protein (u_{31}), maize starch (u_{32}), maize oil (u_{33}), soybean protein (u_{34}), soybean oil (u_{35}) were categorized as quality indicators.

$$u_{ij} \rightarrow \begin{pmatrix} u_1 = \{u_{11}, u_{12}\} \\ u_2 = \{u_{21}, u_{22}\} \\ u_3 = \{u_{31}, u_{32}, u_{33}, u_{34}, u_{35}\} \end{pmatrix} \tag{6}$$

The specific hierarchical model is shown in Figure 3.

2.4.2 Comprehensive evaluation of TOPSIS

2.4.2.1 Factor weight determination

An evaluation system is constructed to determine the subjective weight on basis of analytic hierarchy process (AHP). And the questionnaire is used to score each index (1-9 points) in pairs to compare the importance of the factors. Consistency ratio (C_R) is then used to check the acceptability of the matrix. When C_R is less than 0.10, the consistency test is considered to pass, and the judgment matrix is acceptable. The specific calculating procedure is in light of the literatures of Sahoo et al. (2018) and Kundu et al. (2017).

2.4.2.2 Sub factor weight determination

The entropy method is selected to calculate the objective weight. It is able to effectively reflect the information implied by the data and exhibit strong operability (Zhong et al., 2017). The detailed calculating procedure is according to the literatures of Wang et al. (2015); Hou et al. (2018) and Liu et al. (2013).

2.4.2.3 Combination weight determination

The combined weighting evaluation method is selected in order to better balance the subjective and objective demand and improve the reliability and scientific property of weight distribution based on the game theory. It is used to determine the comprehensive weight of a single index of maize-soybean intercropping, that is, a weight set is constructed based on the two weights of the subjective AHP and objective entropy,:u_k={u_{k1},u_{k2}, …, u_{kn}}(k=1,2).

$$u = \sum_{k=1}^{L} \alpha_k u_k{}^{T} (\alpha_k > 0, \sum_{k=1}^{L} \alpha_k = 1) \tag{7}$$

Where u is weight vector of weight set; α_k is linear combination coefficient.

The game theory method is used to get the combination weight.

$$W_j{}^{*} = \sum_{j=1}^{n} w_{1j} w_{2j}{}^{T}, j = 1, 2, \ldots, n \tag{8}$$

Where w_{1j} is subjective weight determined based on AHP; w_{2j} is objective weight determined based on entropy weight method

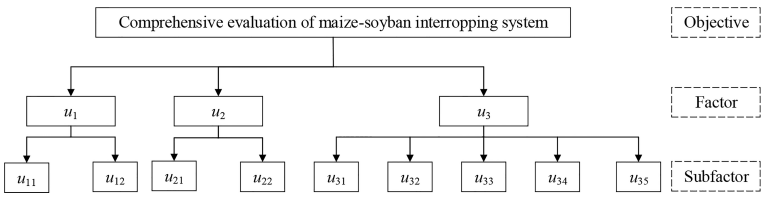

FIGURE 3
Maize-soybean intercropping system comprehensive evaluation hierarchical model.

2.4.2.4 Euclidean distance determination

The original data matrix of m evaluation indicators and an evaluation objects is as follows:

$$\begin{bmatrix} x_{11} & x_{12} & \cdots & x_{1n} \\ x_{21} & x_{22} & \cdots & x_{2n} \\ \vdots & \vdots & \ddots & \vdots \\ x_{m1} & x_{m2} & \cdots & x_{mn} \end{bmatrix} \quad (9)$$

The matrix is normalized as follows

$$Z = [z_{ij}]_{m\times n} \quad (10)$$

where

$$z_{ij} = x_{ij} / \sqrt{\sum_{i=1}^{n} x_{ij}^2} \quad (11)$$

The maximum value Z^+ is defined as $z_1^+, z_2^+, \cdots, z_m^+$ and the minimum value Z^- is defined as $z_1^-, z_2^-, \cdots, z_m^-$.

The weighted distance is calculated between the *ith* (i=1, 2,···, n) evaluation object and positive ideal solution Z_j^+ or negative ideal solution Z_j^- as follows:

$$D_i^+ = \sqrt{\sum_{j=1}^{m} w_j^* (Z_j^+ - z_{ij})^2} \quad (12)$$

$$D_i^- = \sqrt{\sum_{j=1}^{m} w_j^* (Z_j^- - z_{ij})^2} \quad (13)$$

D_i^+ is positive ideal solution distance;. D_i^- is negative ideal solution distance

The score S_i of the ith evaluation object is calculated as follows:

$$S_i = \frac{D_i^-}{D_i^- + D_i^+} \quad (14)$$

S_i is comprehensive evaluation score.

2.5 Data analysis

Microsoft Excel 2021 software was used to sort out data, and the plotting was performed by OriginPro 2023 software. All statistical analysis was conducted using SPSS (IBM, Chicago, USA). MATLAB 2021b software (MathWorks, MA, USA) was used to execute comprehensive evaluation.

3 Results

3.1 Yield

BC and N application significantly affected the yield of maize-soybean intercropping system in 2021 (Figure 4A) and 2022 (Figure 4B). The C_2 and C_1 treatments increased maize yield by 8.76%–23.3% and 3.23%–30.8%, respectively, compared with C_0. The soybean yield showed a declining trend with an increase in N addition in 2021, while in 2022, while soybean yield increased at first and then decreased with increasing application rate. Additionally, soybean yield in 2022 was higher than soybean yield in 2021. The highest total yield was for C_1N_2, 11.0 t ha^{-1} in 2021 and 12.1 t ha^{-1} in 2022. The application of BC increased the yield of the maize-soybean intercropping system, but the yield increase effect of C_2 was not as good as that of C_1.

3.2 Water use efficiency

BC and N application had a significant impact on ET, but their interaction had no significant effect on it (Table 3). The effect of BC in 2021 was slightly smaller than that of N fertilizer, on the contrary, its effect is much greater than that of N application in the next year. With increase in N application, ET showed an increasing trend, while it decreased at first and then increased as BC addition was raised. The maximum ET was noticed at C_0N_3 and the minimum one was for C_1N_1. It indicated that intercropped crops consumed more soil water under the condition of the conventional N addition. BC addition combined with reduced N decreased ET but BC was always negatively correlated with ET. BC and N application also had a significant impact on WUE, but the interaction between BC and N was not significant in the second year. WUE of C_1N_2 was significantly higher than that of other treatments. Thus, BC

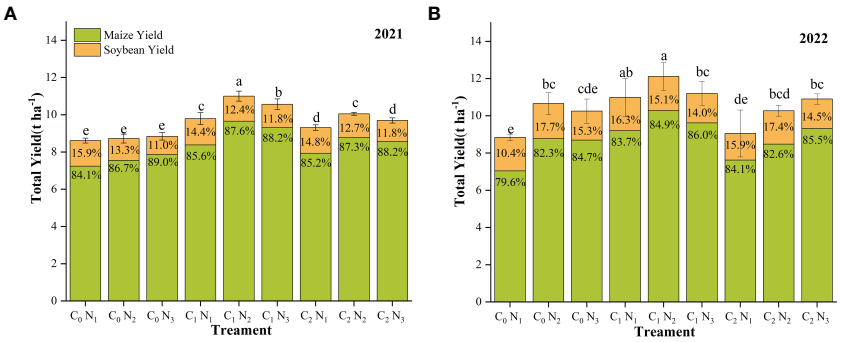

FIGURE 4
Yield of maize-soybean intercropping system in 2021 and 2022. **(A)** shows the yield in 2021 and **(B)** shows the yield in 2022. Different lowercase letters indicate significant differences among different treatments (P<0.05). The column bars and error bars represent the mean yield of three replicates and the standard deviation of the mean, respectively. BC application rates: 0 t ha^{-1} (C_0), 15 t ha^{-1} (C_1) and 30 t ha^{-1} (C_2); N application rates: 135 kg ha^{-1} (N_1), 180 kg ha^{-1} (N_2), 225 kg ha^{-1} (N_3). BC was mixed uniformly into the soil at a depth of 30 cm before sowing in 2021 but was not applied in the following year. N fertilizer was applied before sowing in the two years.

TABLE 3 ET and WUE under different combinations of BC and N levels.

Treatment	ET(mm)		WUE(kg·ha^{-1}·mm^{-1})	
	2021	2022	2021	2022
C_0N_1	664.37 ± 5.49c	830.32 ± 1.98ab	12.98 ± 0.27e	10.65 ± 0.27c
C_0N_2	670.42 ± 2.63ab	832.41 ± 2 08a	13.00 ± 0.40e	12.81 ± 0.40b
C_0N_3	672.73 ± 3.41a	834.65 ± 2.21a	13.13 ± 0.32e	12.28 ± 0.32b
C_1N_1	657.99 ± 2.22abc	812.24 ± 1.68e	14.88 ± 0.54c	13.53 ± 0.54ab
C_1N_2	664.37 ± 2.92bc	813.05 ± 3.43de	16.57 ± 0.38a	14.90 ± 0.38a
C_1N_3	665.68 ± 4.00abc	818.12 ± 3.17cde	15.86 ± 0.40b	13.68 ± 0.40ab
C_2N_1	662.68 ± 4.09bc	817.28 ± 2.82cde	14.05 ± 0.30d	11.09 ± 0.30c
C_2N_2	665.17 ± 4.26a	821.15 ± 5.58cd	15.12 ± 0.17c	12.51 ± 0.17b
C_2N_3	667.46 ± 6.41bc	822.25 ± 4.87bc	14.52 ± 0.88cd	13.26 ± 0.88b
C	3.69*	46.32*	144.71**	24.06**
N	4.37*	3.52*	16.64**	14.25**
C·N	0.16	0.22	4.70**	2.39

Values represent mean ± standard deviation of 3 replicates. * Indicates that the effect is significant at a level less than 0.05, and ** indicates that it is extremely significant at a level less than 0.01. BC application rates: 0 t ha^{-1} (C_0), 15 t ha^{-1} (C_1) and 30 t ha^{-1} (C_2); N application rates: 135 kg ha^{-1} (N_1), 180 kg ha^{-1} (N_2), 225 kg ha^{-1} (N_3). BC was mixed uniformly into the soil at a depth of 30 cm before sowing in 2021 but was not applied in the following year. N fertilizer was applied before sowing in the two years.

combined with reduced N fertilization led to reduction in ET and increase in WUE of maize-soybean intercropping system, but high BC addition could not keep the increasing trend of WUE.

3.3 Nitrogen uptake and nitrogen recovery efficiency

BC and N application had a significant impact on straw and grain N absorption, but the effect of BC application was greater than that of N application (Table 4). Maize straw and grain N uptake showed an overall increasing trend with increase in N application. However, total N uptake increased at first and then decreased with increasing BC application. Total N uptake of the C_1 treatments increased by approximately 4.03%~31.8% in 2021 and about 11.1%~19.5% in 2022 compared with that of the C_0 treatments. Among the treatments with the same BC level, the highest grain N uptake was observed for C_1 treatments while C_2 treatments had the maximum straw N uptake, indicating that excessive BC application was unhelpful for N

TABLE 4 N uptake and NRE under different combinations of BC and N levels.

Treatment	Straw N uptake (kg ha^{-1})		grain N uptake (kg ha^{-1})		total N uptake (kg ha^{-1})		NRE (%)	
	2021	2022	2021	2022	2021	2022	2021	2022
C_0N_1	55.87 ± 3.06d	56.41 ± 0.76cd	54.97 ± 1.50d	58.57 ± 3.78c	110.83 ± 2.56e	114.99 ± 4.54d	33.25 ± 0.57cd	34.40 ± 2.88bc
C_0N_2	53.98 ± 3.73d	58.75 ± 1.96cd	56.52 ± 0.88d	58.92 ± 2.51c	110.50 ± 3.51e	117.34 ± 4.14d	26.23 ± 1.95e	27.31 ± 2.103cd
C_0N_3	60.91 ± 4.05bcd	53.95 ± 1.38d	67.01 ± 3.94bc	68.42 ± 2.11b	127.92 ± 2.94d	122.37 ± 1.86d	28.73 ± 1.31de	23.67 ± 2.33cd
C_1N_1	67.76 ± 2.20ab	62.66 ± 1.68bcd	71.57 ± 3.28b	69.87 ± 1.52b	139.33 ± 5.47bc	132.53 ± 2.51c	50.68 ± 3.23a	47.65 ± 6.16a
C_1N_2	62.54 ± 1.94bc	58.19 ± 1.65cd	83.07 ± 2.27a	84.83 ± 4.26a	145.60 ± 4.11ab	143.03 ± 3.72b	45.74 ± 2.28a	41.45 ± 5.52ab
C_1N_3	71.38 ± 1.07a	60.98 ± 5.75bcd	80.60 ± 2.27a	84.39 ± 2.75a	151.98 ± 5.39a	145.37 ± 2.06ab	39.42 ± 2.40b	34.07 ± 2.59bc
C_2N_1	59.63 ± 3.85d	65.99 ± 1.91bc	55.66 ± 3.93d	56.46 ± 1.81c	115.30 ± 5.58e	122.44 ± 3.61d	38.53 ± 4.14bc	39.73 ± 4.49ab
C_2N_2	73.35 ± 2.50a	69.69 ± 2.65ab	61.30 ± 3.43cd	61.64 ± 2.78c	134.65 ± 4.20cd	131.33 ± 3.42c	39.65 ± 2.34b	34.81 ± 2.34bc
C_2N_3	74.97 ± 3.88a	80.13 ± 5.05a	64.21 ± 4.16c	71.27 ± 3.35b	139.18 ± 6.78bc	151.40 ± 6.25a	33.73 ± 3.56cd	36.82 ± 3.45b
C	27.45**	21.12**	78.53**	116.28**	80.16**	73.04**	81.80**	22.33**
N	10.64**	1.05	17.20**	50.06**	29.94**	37.08**	15.29**	11.57**
C·N	5.44**	2.99*	2.73*	6.51**	3.77*	7.19**	4.13**	1.63

Values represent mean ± standard deviation of 3 replicates. * Indicates that the effect is significant at a level less than 0.05, and ** indicates that it is extremely significant at a level less than 0.01. BC application rates: 0 t ha^{-1} (C_0), 15 t ha^{-1} (C_1) and 30 t ha^{-1} (C_2); N application rates: 135 kg ha^{-1} (N_1), 180 kg ha^{-1} (N_2), 225 kg ha^{-1} (N_3). BC was mixed uniformly into the soil at a depth of 30 cm before sowing in 2021 but was not applied in the following year. N fertilizer was applied before sowing in the two years.

transporting from straw to grain. NRE declined with increase in N application under C_0 and C_1 treatments, but this trend was not observed for C_2 treatments. Therefore, reduction in N fertilizer input was an effective way to improve NRE, but excessive BC application probably weakened the effect.

3.4 Maize and soybean quality

The impact of BC and N application on the quality of intercropped maize and soybean is presented in Figures 5 and 6. Maize protein (Figures 5A, B) and maize oil content (Figures 5C, D) decreased with an increase in BC application, although the variations in the two years were slightly different. The first year of BC application did not have a positive effect on protein and oil content of maize grain. However, BC had little effect on oil content in second year while protein content continued to decline. C_0N_3 resulted in the highest protein and oil content of maize. And maize starch content (Figures 5E, F) increased with the rising BC application. BC was found to have no positive impact on soybean protein (Figures 6A, B) but it unexpectedly increased soybean oil content (Figures 6C, D).

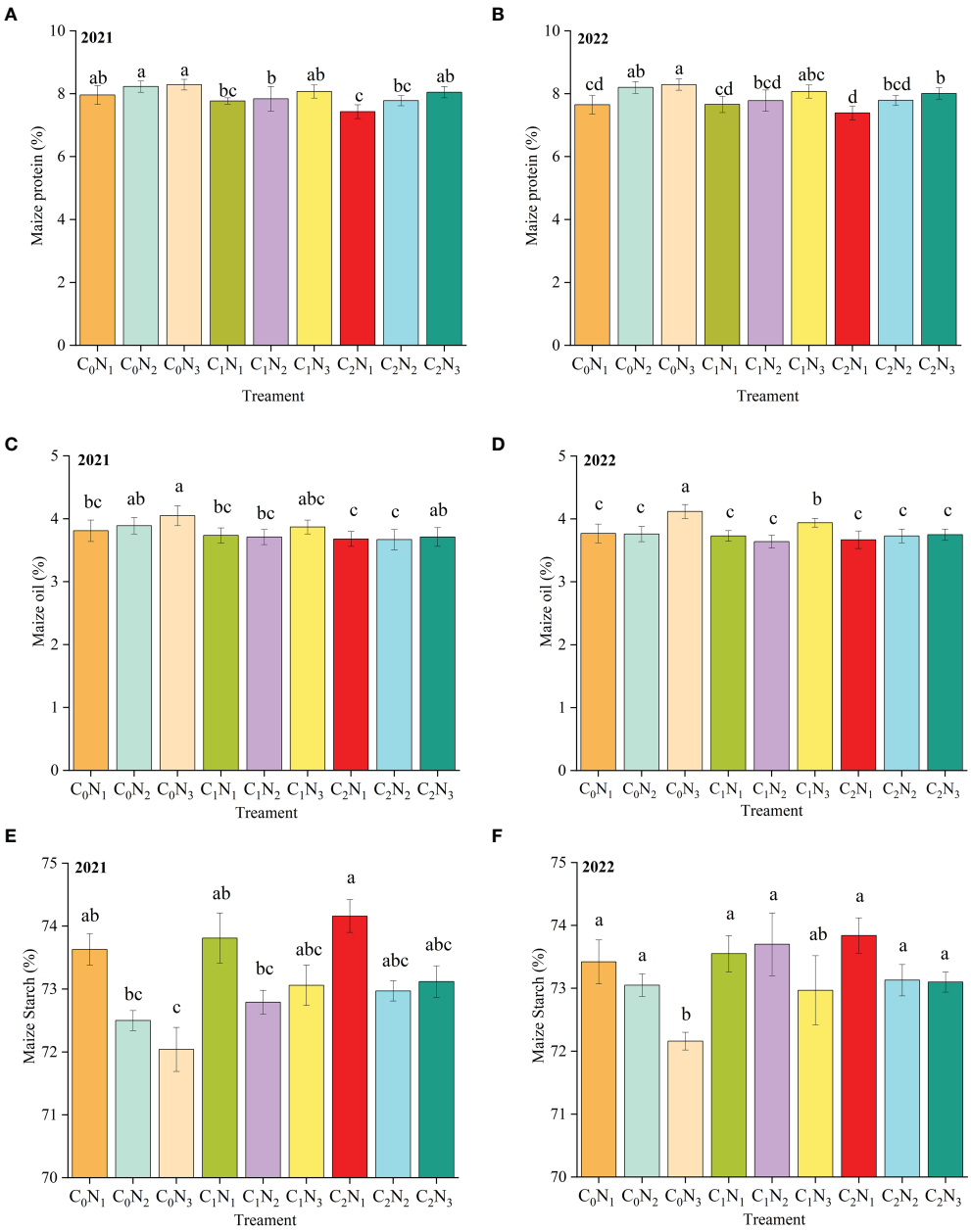

FIGURE 5
Maize quality in 2021 and 2022. **(A, B)** show maize protein content in 2021 and 2022, respectively. **(C, D)** show maize oil content in 2021 and 2022 respectively, and **(E, F)** show maize starch content in 2021 and 2022 respectively. Different lowercase letters in the same column mean significant differences among different treatments at 0.05 level. The column bars and error bars represent the mean maize quality of three replicates and the standard deviation of the mean, respectively. BC application rates: 0 t ha^{-1} (C_0), 15 t ha^{-1} (C_1) and 30 t ha^{-1} (C_2); N application rates: 135 kg ha^{-1} (N_1), 180 kg ha^{-1} (N_2), 225 kg ha^{-1} (N_3). BC was mixed uniformly into the soil at a depth of 30 cm before sowing in 2021 but was not applied in the following year. N fertilizer was applied before sowing in the two years.

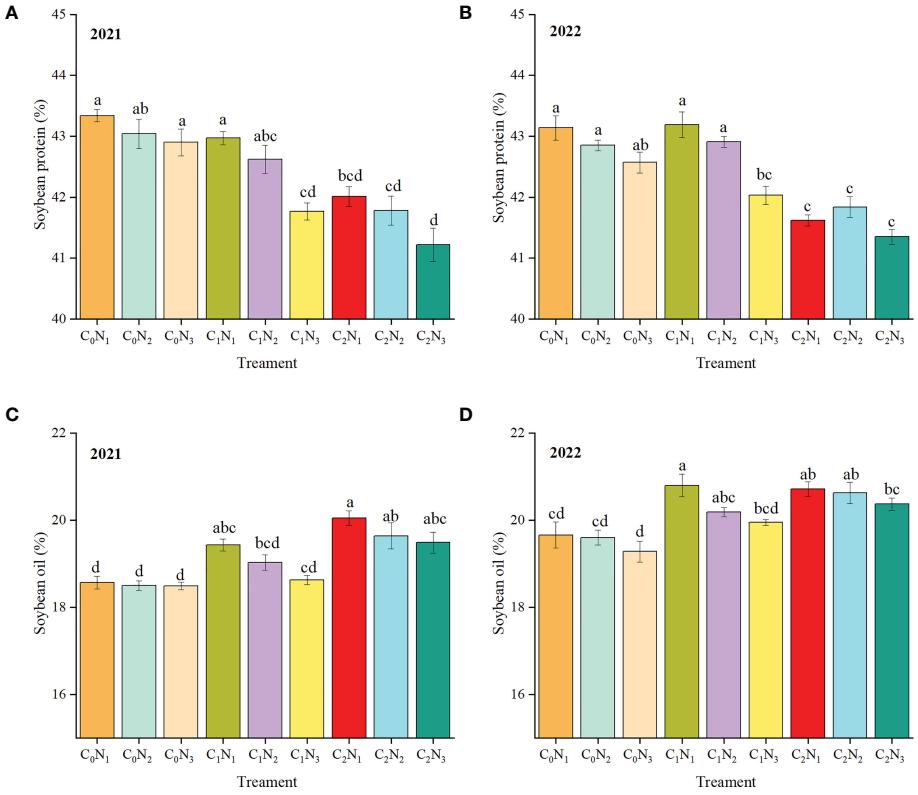

FIGURE 6
Soybean quality in 2021 and 2022. **(A, B)** show soybean protein content in 2021 and 2022, respectively. **(C, D)** show soybean oil content in 2021 and 2022, respectively. Different lowercase letters in the same column mean significant differences among different treatments at 0.05 level. The column bars and error bars represent the mean soybean quality of three replicates and the standard deviation of the mean, respectively. BC application rates: 0 t ha^{-1} (C_0), 15 t ha^{-1} (C_1) and 30 t ha^{-1} (C_2); N application rates: 135 kg ha^{-1} (N_1), 180 kg ha^{-1} (N_2), 225 kg ha^{-1} (N_3). BC was mixed uniformly into the soil at a depth of 30 cm before sowing in 2021 but was not applied in the following year. N fertilizer was applied before sowing in the two years.

3.5 Comprehensive growth evaluation

The weight of the model is determined by AHP method (Supplementary Table 1) and entropy weight method (Supplementary Table 2). respectively. The obtained two sets of weights are combined through the principle of game theory (Supplementary Table 3). The combined game theory weight was then utilized to calculate the ideal solution and comprehensive evaluation score by the TOPSIS comprehensive model (Table 5). The highest overall evaluation score was for C_1N_2, followed by C_1N_3

TABLE 5 Comprehensive growth evaluation based on TOPSIS.

Treatments	D^+		D^-		S		Rank	
	2021	2022	2021	2022	2021	2022	2021	2022
C_0N_1	0.498	0.446	0.232	0.231	0.318	0.341	8	9
C_0N_2	0.506	0.319	0.176	0.309	0.258	0.492	9	5
C_0N_3	0.490	0.366	0.235	0.305	0.324	0.454	7	7
C_1N_1	0.277	0.221	0.393	0.409	0.586	0.649	3	2
C_1N_2	0.234	0.223	0.489	0.472	0.676	0.679	1	1
C_1N_3	0.254	0.241	0.410	0.358	0.617	0.597	2	3
C_2N_1	0.381	0.440	0.296	0.235	0.437	0.348	6	8
C_2N_2	0.293	0.313	0.366	0.282	0.555	0.473	4	6
C_2N_3	0.341	0.279	0.297	0.324	0.465	0.537	5	4

BC application rates: 0 t ha^{-1} (C_0), 15 t ha^{-1} (C_1) and 30 t ha^{-1} (C_2); N application rates: 135 kg ha^{-1} (N_1), 180 kg ha^{-1} (N_2), 225 kg ha^{-1} (N_3). D_i^+ is the positive ideal solution distance; D_i^- is the negative ideal solution distance; S_i is the comprehensive evaluation score.

in 2021 and C_1N_1 in 2022. This meant that slight N fertilizer input in the second year was more beneficial for the overall growth of the intercropping system under the condition of C_1. The lowest scores were different over the two years, C_0N_2 in 2021 and C_0N_1 in 2022.

3.6 Mathematical model construction

The comprehensive evaluation scores obtained above were used to conduct the quadratic polynomial stepwise regression, and then got the regression equation between BC-N application amount and comprehensive evaluation indicator.

$$y_1 = 0.6600 - 0.2372x_1^{\ 2} + 0.0922x_1 - 0.0473x_2^{\ 2} + 0.0085x_2 + 0.0045x_1x_2 \quad (15)$$

$$y_2 = 0.6887 - 0.872x_1^{\ 2} + 0.0393x_1 - 0.2042x_2^{\ 2} + 0.0107x_2 + 0.0173x_1x_2 \quad (16)$$

Where x_1 and x_2 reflect the coding values of N and BC application BC; y_1 and y_2 are the comprehensive assessment scores for 2021 and 2022.

The combined BC and N had a highly significant impact on the comprehensive assessment scores with a coefficient of determination (R^2) of 0.944 for y_1 and 0.933 for y_2. Therefore, the regression model could be used to assess the impact of BC and N application on the overall growth of maize-soybean intercropping system. The positive and negative signs in front of x_1 and x_2 indicate promotion or inhibition, and the level of the coefficient indicates the strength of the influence. Both regression equations demonstrated that there was a positive role for BC or N application to promote the complete evaluation score, and the effect of BC was better. Additionally, the coefficient of x_1x_2 is positive. That is to say BC and N had a positive coupling effect and both improved the comprehensive evaluation score.

The reduced dimension was conducted to explore the impact of single factor-BC or N on the comprehensive evaluation score. Figure 7 showed the comprehensive assessment value firstly increased and subsequently decreased as BC or N increased. The comprehensive evaluation score was maximum when BC coding value was 0.19 and N coding value was 0.09 in 2021. In 2022, the maximum comprehensive evaluation score was achieved when BC was 0.02 and N was 0.03N. Besides, the comprehensive growth assessment score for 2021 varied slowly with rising BC and N compared to that for 2022, which indicated that the intercropping growth was more sensitive to the application of BC and N in 2022.

The quadratic polynomials (Formula 15 and 16) were simulated for the optimum using Matlab2020b software (Figure 8). The optimal application range was determined by 90% of the maximum comprehensive score with the consideration of BC cost. The ranges were 0.14~0.53 for BC and -0.53~0.71 for N in 2021, and -0.20~0.25 for BC and -0.43~0.49for N in 2022. This is to say, the ranges of BC were 17.1~22.95 t ha^{-1} in 2021 and 12~18.75 t ha^{-1} in 2022, and those of N were 156.15~211.95 kg·ha^{-1} in 2021 and 160.65~202.05 kg·ha^{-1} in 2022.Therefore, the optimum combination was BC of 17.10~22.95 t ha^{-1} and N of 156.15~211.95 kg ha^{-1} in 2021, and 12~18.75 t ha^{-1} and 160.65~202.05 kg ha^{-1} in 2022.

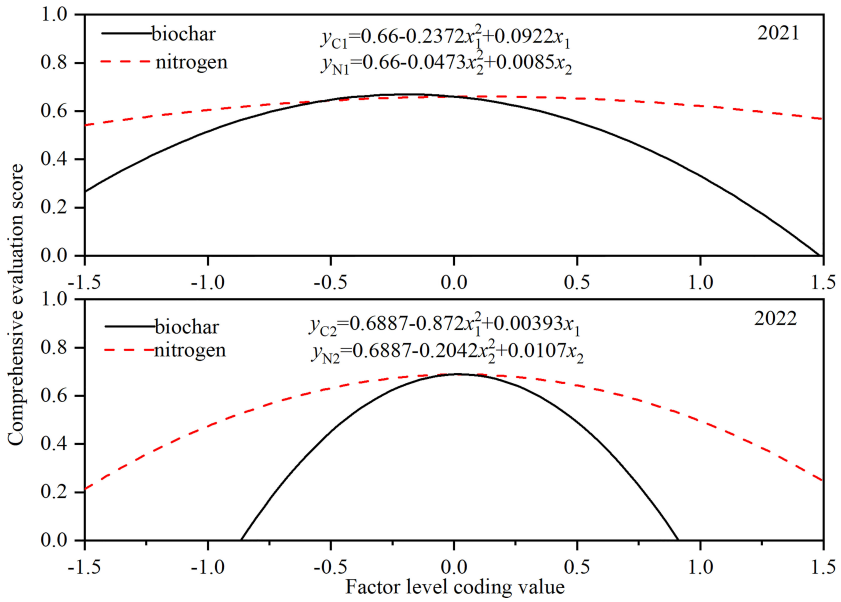

FIGURE 7
Effects of BC or N application on comprehensive evaluation score of maize-soybean intercropping system. y_{C1} and y_{N1} is the function of the single-factor effect function of on the comprehensive evaluation score in 2021, and y_{C2} and y_{N2} is single-factor effect function of comprehensive evaluation score in for 2022.

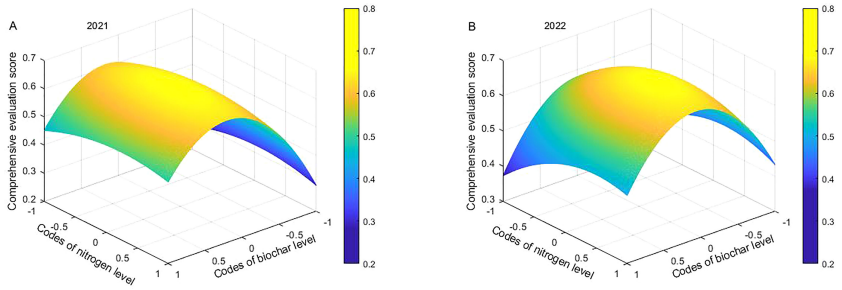

FIGURE 8
Coupling effect of BC and N on comprehensive evaluation score of Maize-Soybean intercropping system in 2021 and 2022.

4 Discussion

4.1 Combining BC with N fertilization increases crop yield

In this study, the combined application of BC and N resulted in increased yields in the maize-soybean intercropping system, to varying degrees compared to N application alone. This can be attributed to the ability of BC to absorb soil nutrients and release them slowly for crop absorption over an extended period (Purakayastha et al., 2019). In other words, N fertilizer supplements the nutrient deficiency of BC, while BC extends the retention time of fertilizer in the soil (Chen et al., 2018). However, the yield increase was higher in intercropping systems with lower BC compared to those with higher BC, as excessive BC increases soil C/N ratio, inhibiting soil microbial decomposition and N mineralization rate (Xia et al., 2022).

Intercropping, a traditional agricultural practice, offers several benefits including crop yield increase, resource utilization enhancement, pest and disease reduction, soil health improvement, and biodiversity increase (Mugi-Ngenga et al., 2022). However, intercropping systems also face challenges such as the negative impact of shade for intercropped soybean (Wu et al., 2016). Limited N fertilizer can restrict the growth of intercropped maize, thereby reducing the shading effect and significantly increasing soybean yield (Raza et al., 2019c). Moreover, reducing N fertilizer appropriately can increase maize's absorption and utilization of soil N, enhance soybean nodulation and N fixation ability (Li et al., 2016), and ensure that both maize and soybean have sufficient N for growth with less N application (Xu et al., 2020). This study highlights the significant interaction between BC and N, indicating that incorporating BC into the soil can increase crop yield in situations where N fertilizer is limited. The synergistic or complementary interaction between BC and N improves soil nutrient availability and enhances slow-release performance of fertilizer (Chen et al., 2018). These findings are consistent with previous studies conducted by Guo et al. (2021) and Omara et al. (2020), suggesting that combined appropriate BC application and reduced N fertilizer can enhance the productivity of maize-soybean intercropping system.

4.2 Combining BC with N fertilizer improves ET and WUE

Our results indicated that BC combined with N fertilizer improved ET and WUE. The improvement of ET may be due to that small BC particles fill larger soil pores and hence alter soil water flux, which further decreases soil water depletion caused by both BC and N fertilizer application (Faloye et al., 2019). The significant effect of combined BC and N fertilizer addition on WUE improvement may be attributed to the impact of BC on ET, soil hydro-physical and chemical properties (Ajayi and Horn, 2016; Faloye et al., 2017). BC application enhances the relative water content of crop leaves, which leads to increased photosynthetic activity (Akhtar et al., 2014; Kammann et al., 2011). It also promotes water consumption in the early and mid-term grain filling, which is possibly related to stronger water absorption capacity of roots (Chen et al., 2010). The increase in soil moisture content in the plow layer and soil moisture holding capacity induced by BC addition, is a main mechanism for increasing crop yield (Jeffery et al., 2011; Rogovska et al., 2014). However, our results showed that excessive BC reduced the amplification of WUE. High BC level increases soil porosity and excess hydrophobic compound, resulting in soil water loss (Jeffery et al., 2015). Castellini et al. (2015) found that BC application from 15 to 30 t ha^{-1} reduced soil water holding capacity by 23.5% and increased water consumption, thereby decreasing WUE, which is consistent with our findings. Additionally, high BC darkens soil color and then increases its surface temperature, which reduces water viscosity and surface tension, accelerates soil water evaporation through radiation absorption (Yang et al., 2020; Wu et al., 2022). Therefore, only an appropriate combination of BC and N fertilizer can improve WUE of th intercropping systems.

4.3 Combining BC with N fertilizer promotes N uptake and improve NRE

Our results found that BC-N interaction increased crop N absorption, consistent with the findings of Ibrahim et al. (2020) who reported that combined BC and N acted as a sustained-

release N fertilizer, providing sufficient N for crop growth. On the one hand, BC possesses a highly porous cellular structure and large specific surface area, enabling it to rapidly absorb N and other nutrients (Yao et al., 2017). This leads to the reduction in N leaching loss and improvement in mineral N, thereby increasing soil available N. BC application improves soil aeration by altering soil bulk density and porosity, and increases soil available water, which is beneficial for the alteration of soil N cycle and hence leads to greater soil mineralization and inorganic N availability (Xiao et al., 2016a; Xiao et al., 2016b). On the other hand, it is also helpful to promote maize roots growth and further improve N uptake through these roots. Additionally, higher N accumulation during the post-silking period under the BC-added conditions could not only reduce N remobilization from leaf to grain, but also maintain functional stay-green leaf, and thus promote dry matter accumulation and enhance grain yield (Lee and Tollenaar, 2007).

BC promotes plant N accumulation before and after silking, and high N transfer efficiency of BC treatment has the promotion of N transfer from vegetative organs to grains and increases grain N concentration (Xiao et al., 2017). Interestingly, under the treatments of C_2, N uptake of the straw was higher than that of the grain, possibly due to that the source-sink incoordination caused by high BC treatment, which disturbed N transport to the grain (He et al., 2021). This leads to that the redundant nutrient was kept in such vegetative organs as stems and leaves, which causes the "luxury uptake" of nutrients (Travis et al., 2017). N application can enhance soil colloid adsorption and cation exchange capacity, reducing ammonium N loss (Duan et al., 2018). Proper N application is therefore useful for increasing the NRE of maize. However, when excessive N is added, N release is too rapid to match crop absorption and even substantially consume soil fertility (Xia et al., 2022). Furthermore, excessive fertilization not only significantly reduces N use efficiency, but also is unable to improve maize yield (Zhang et al., 2022; Nasar et al., 2023). The previous studies also indicate that it is an effective way for reasonable N application to improve fertilizer utilization efficiency, and N utilization efficiency initially increases and then decreases as N application increases (Miah et al., 2016).

4.4 Combining BC with N fertilizer improves grain quality

Appropriate N application is able to improve maize quality traits such as grain protein and oil content (Amanullah et al., 2009). In particular, grain protein concentration is continuously rises with increase in N application (Correndo et al., 2021). It is noted that both of low and high N applications have the impact on maize quality, which indicates that it is of great importance for adequate N application to raise maize quality (Hammad et al., 2011). Our study revealed that maize protein and oil content had a positive correlation with N application, but was negatively related to BC application. The reason may be that soil organic N is converted into inorganic N, which is then absorbed and utilized by crops (Sharifi et al., 2008). High C/N ratio of BC we used reduces the mineralization of organic N (Shen et al., 2021). Nitrogen is a crucial component required for the synthesis of cereal protein and oil (Zhang et al., 2020; Hafiz et al., 2023), and after plants absorb nitrogen, it is transported to the growth center organs in large quantities. The nitrogen stored in the vegetative organs during the early stage of growth begins to move outward shortly after flowering and is transported to the developing ear or grain (Ren et al., 2021). However, the results of this study found that high BC treatment led to N transfer from grain to straw, which also reduced the protein and oil content of maize. This is due to that BC competes with the organic-inorganic composite colloidal cations in the soil to adsorb nutrients which is also absorbed by crops, resulting in a decrease in protein content (Keiblinger et al., 2015). Previous studies have found a trade-off relationship between protein and starch content under given conditions (Butts-Wilmseyer et al., 2019; Singh et al., 2002), which is consistent with our findings. High N fertilizer promotes the increase of starch content in the early stage of grain filling, but causes crop premature senescence in the later period, which results in lower starch content for the high N fertilizer treatment than the normal treatment at harvest (Ma et al., 2012). The problem may be solved by the BC-N combination because the slow-release fertilizer effect of BC reduces the content of available N fertilizer in the soil in the early stage. It can also be seen from the results of our study that BC increases maize starch content. Soybean quality is generally characterized by protein and oil content. Its oil content is strongly affected by environmental conditions, but its variation trend is usually contrary to that of protein (Mertz-Henning et al., 2018). For instance, when BC increases from 0 to 8 t ha^{-1}, soybean oil content shows an increased trend but protein content has the opposite one (Zahra et al., 2018), which is in accordance with our findings. One possible explanation for the result is that BC absorbs a large amount of nutrients in the prophase, which are then gradually released. The released nutrient rate may not coordinate with soybean protein formation but coordinate with fat formation (Liu et al., 2021). The other possible explanation for the result is that soybean protein and oil content may be mainly determined by the gene (Lin et al., 2022). In addition, soil microorganisms and environment also have an impact on crop quality (Studnicki et al., 2016; Kundel et al., 2020).

5 Conclusions

Appropriate BC and fertilizer application can have a positive impact on crop yield, N accumulation, WUE and NRE while also reducing ET. However, excessive BC can have negative effects on crop yield and quality by disturbing N translocation from grain to straw and reducing the benefits of intercropping. Based on our two-year experiment, we recommend a combination of 17.1-18.75 t ha^{-1} BC and 160.65-202.05 kg hac^{-1} N fertilizer to obtain high yields, water and N fertilizer use efficiency, and quality in the maize-soybean intercropping system. These findings have important implications for intercropping management and sustainable agricultural intensification.

Data availability statement

The original contributions presented in the study are included in the article/Supplementary Material. Further inquiries can be directed to the corresponding authors.

Author contributions

BY and IK conceptualized and wrote the main manuscript. BY, SL, and DL helped to perform lab analysis. IK and AR reviewed and edited the manuscript in the present form. JJ and LW helped with revisions and funding. All authors contributed to the article and approved the submitted version.

Funding

This research received funding from the Natural Science foundation of Liaoning province under grant Number 2019-ZD-0705.

Conflict of interest

The authors declare that the research was conducted in the absence of any commercial or financial relationships that could be construed as a potential conflict of interest.

Publisher's note

Supplementary material

The Supplementary Material for this article can be found online at: https://www.frontiersin.org/articles/10.3389/fpls.2023.1171547/full#supplementary-material

References

Ahmed, S., Raza, M. A., Zhou, T., Hussain, S., Khalid, M. H. B., Feng, L., et al. (2018). Responses of soybean dry matter production, phosphorus accumulation, and seed yield to sowing time under relay intercropping with maize. *Agronomy* 8, 282. doi: 10.3390/agronomy8120282

Ajayi, A. E., and Horn, R. (2016). Modification of chemical and hydro-physical properties of two texturally differentiated soils due to varying magnitudes of added biochar. *Soil Tillage Res.* 164, 34–44. doi: 10.1016/j.still.2016.01.011

Akhtar, S. S., Guitong, L., Mathias, N. A., and Fulai, L. (2014). Biochar enhances yield and quality of tomato under reduced irrigation. *Agric. Water Manage.* 138, 37–44. doi: 10.1016/j.agwat.2014.02.016

Alkharabsheh, H. M., Seleiman, M. F., Battaglia, L. B., Shami, A., Jalal, S. R., Bushra, A. A., et al. (2021). Biochar and its broad impacts in soil quality and Fertility,Nutrient leaching and crop productivity: a review. *Agronomy* 11, 5. doi: 10.3390/agronomy11050993

Amanullah,, Khattak, R. A., and Khalil, S. K. (2009). Plant density and nitrogen effects on maize phenologyand grain yield. *J. Plant Nutr.* 32 (2), 246–260. doi: 10.1080/01904160802592714

Butts-Wilmsmeyer, C. J., Seebauer, J. R., Singleton, L., and Below, F. E. (2019). Weather during key growth stages explains grain quality and yield of maize. *Agronomy*. 9, 16.

Castellini, M., Giglio, L., Niedda, M., Palumbo, A. D., and Ventrella, D. (2015). Impact of biochar addition on the physical and hydraulic properties of a clay soil. *Soil Tillage Res.* 154, 1–13. doi: 10.1016/j.still.2015.06.016

Chen, L., Chen, Q. C., Rao, P. H., Yan, L. L., Shakib, A., and Shen, G. Q. (2018). Formulating and optimizing a novel biochar-based fertilizer for simultaneous slow-release of nitrogen and immobilization of cadmium. *Sustainability* 10, 8. doi: 10.3390/su10082740

Chen, Y., Shinogi, Y., and Taira, M. (2010). Influence of biochar use on sugarcane growth, soil parameters, and groundwater quality. *Aust. J. Soil Res.* 48, 526–530. doi: 10.1071/SR10011

Correndo, A. A., Fernandez, J. A., Vara, P. V., and Ciampitti, I. A. (2021). Do water and nitrogenmanagement practices impact grain quality in maize? *Agronomy* 11 (9), 1851. doi: 10.3390/agronomy11091851

Duan, R., Long, X. E., Tang, Y. F., Wen, J., Su, S. M., Bai, L. Y., et al. (2018). Effects of different fertilizer application methods on the community of nitrifiers and denitrifiers in a paddy soil. *J. Soils Sediments* 18 (1), 24–38. doi: 10.1007/s11368-017-1738-9

Duchene, O., Vian, J.-F., and Celette, F. (2017). Intercropping with legume for agroecological cropping systems: complementarity andfacilitation processes and the importance of soil microorganisms. a review. *Agric. Ecosyst. Environ.* 240, 148–161. doi: 10.1016/j.agee.2017.02.019

Faloye, O. T., Alatise, M. O., Ajayi, A. E., and Ewulo, B. S. (2017). Synergistic effects of biochar and inorganic fertiliser on maize yield in an alfisol under drip irrigation. *Soil Tillage Res.* 174, 214–220. doi: 10.1016/j.still.2017.07.013

Faloye, O. T., Alatise, M. O., Ajayi, A. E., and Ewulo, B. S. (2019). Effects of biochar and inorganic fertilizer applications on growth, yield and water use efficiency of maize under deficit irrigation. *Agric. Water Manage.* 217, 165–178. doi: 10.1016/j.agwat.2019.02.044

Farhangi-Abriz, S., Torabian, S., Qin, R. J., Noulas, C., Lu, Y. Y., and Gao, S. D. (2021). Biochar effects on yield of cereal and legume crops using meta-analysis. *Sci. Total Environ.* 775, 145869. doi: 10.1016/j.scitotenv.2021.145869

Feng, L., Raza, M. A., Chen, Y., Khalid, M. H. B., Meraj, T. A., Ahsan, F., et al. (2019). Narrow-wide row planting pattern improves the light environment and seed yields of intercrop species in relay intercropping system. *PloS One* 14, 2. doi: 10.1371/journal.pone.0212885

Guo, L. L., Yu, H. W., Kharbach, M., and Wang, J. W. (2021). The response of nutrient uptake, photosynthesis and yield of tomato to biochar addition under reduced nitrogen application. *Agronomy* 11, 8. doi: 10.3390/agronomy11081598

Hafiz, M. H., Abbas, F., Ashfaq, A., Wajid, F., Carol, J. W., and Gerrit, H. (2023). Water and nitrogen management influence on oil and protein concentration in maize. *Agron. J.* 2023, 557–568. doi: 10.1002/agj2.21275

Hammad, H. M., Ahmad, A., Khaliq, T., Farhad, W., and Mubeen, M. (2011). Optimizing rate of nitrogen application for higher yield and quality in maize under semiarid environment. *Crop Environ.* 2 (1), 38–41. https://www.researchgate.net/publication/268422853

He, Z. H., Hong, T. T., Cai, Z. L., Yang, Z., Li, M., and Zhang, Z. (2021a). Determination of amount of irrigation and nitrogen for comprehensive growth of greenhouse cucumber based on multi-level fuzzy evaluation. *Int. J. Agric. Biol. Eng.* 14 (2), 35–42. doi: 10.25165/j.ijabe.20211402.5785

He, Z. H., Li, M., Cai, Z. L., Zhao, R. S., Hong, T. T., Yang, Z., et al. (2021b). Optimal irrigation and fertilizer amounts based on multi-level fuzzy comprehensive evaluation of yield, growth and fruit quality on cherry tomato. *Agric. Water Manage.* 243, 1–10. doi: 10.1016/j.agwat.2020.106360

He, D. W., Zhao., Y. Z., Gao, J. P., Sui, Y. H., Xin, W., Yi, J., et al. (2021). Effects of biochar application combined with nitrogen fertilizer on yield formation of japonica rice and the immediate and residual effects of nitrogen. *J. Plant Nutr. Fertilizers* 27 (12), 2114–2124. doi: 10.11674/zwyf.2021244

Hou, M. M., Lin, Z. Y., Chen, J. N., Zhai, Y. M., Jin, Q., and Zhong, F. L. (2018). Optimization on theburied depth of subsurface drainage under greenhouse condition based on entropy evaluation method. *Entropy* 20 (11), 10. doi: 10.3390/e20110859

Ibrahim, M. M., Tong, C. X., Hu, K., Zhou, B. Q., Xing, S. H., and Mao, Y. L. (2020). Biochar-fertilizer interaction modifies n-sorption, enzyme activities and microbial

functional abundance regulating nitrogen retention in rhizosphere soil. *Sci. Total Environmen* 739, 140065. doi: 10.1016/j.scitotenv.2020.140065

Iqbal, N., Hussain, S., Ahmed, Z., Yang, F., Wang, X., Liu, W., et al. (2019). Comparative analysis of maize–soybean strip intercropping systems: a review. *Plant Prod. Sci.* 22, 131–142. doi: 10.1080/1343943X.2018.1541137

Jeffery, S., Meinders, B. J. M., Stoof, R. C., Bezemer, T. M., Tess, F. J., Mommer, L., et al. (2015). Biochar application does not improve the soil hydrological function of a sandy soil. *Geoderma* 251/252, 47–54. doi: 10.1016/j.geoderma.2015.03.022

Jeffery, S., Verheijen, F. G. A., vanderVelde, M., and Bastos, A. C. (2011). A quantitative review of the effects of biochar application to soils on crop productivity using meta-analysis. *Agr. Ecosyst. Environ.* 144, 175–187. doi: 10.1016/j.agee.2011.08.015

Jin, Z. E., Chen, C., Chen, X. M., Jiang, F., Hopkins, I., Zhang, X. L., et al. (2019). Soil acidity, available phosphorus content, and optimal biochar and nitrogen ertilizer application rates: a five-year field trial in upland red soil, China. *Field Crops Res.* 232, 77–87. doi: 10.1016/j.fcr.2018.12.013

Jindo, K., Audette, Y., Higashikawa, F. S., Silva, C. A., Akashi, K., Mastrolonardo, G., et al. (2020). Role of biochar in promoting circular economy in the agriculture sector. part 1: a review of the biochar roles in soil n, p and K cycles. *Chem. Biol. Technol. Agric.* 7, 15. doi: 10.1186/s40538-020-00182-8

Kammann, C. I., Linsel, S., Gößling, J. W., and Koyro, H. W. (2011). Influence of biochar on drought tolerance of chenopodiumquinoa willd and on soil-plant relations. *Plant Soil* 345, 195–210. doi: 10.1007/s11104-011-0771-5

Keiblinger, K. M., Liu, D., Mentler, A., Zehetner, F., and Zechmeister-Boltenstern, S. (2015). Biochar application reduces protein sorption in soil. *Organic Geochemistry* 87, 21–24. doi: 10.1016/j.orggeochem.2015.06.005

Kundel, D., Bodenhausen, N., Jørgensen, H. B., Truu, J., Birkhofer, K., Hedlund, K., et al. (2020). A. effects of simulated drought on biological soil quality, microbial diversity and yields under long-term conventional and organic agriculture. *FEMS Microbiol. Ecol.* 96, 12. doi: 10.1093/femsec/fiaa205

Kundu, S., Khare, D., and Mondal, A. (2017). Landuse change impact on sub-watersheds prioritization by analytical hierarchy process (AHP). *Ecol. Inf.* 42, 100–113. doi: 10.1016/j.ecoinf.2017.10.007

Lee, E. A., and Tollenaar, M. (2007). Physiological basis of successful breeding strategies for maize grain yield. *Crop Sci.* 47, S-202–S-215. doi: 10.2135/cropsci2007.04.0010IPBS

Li, B., Wu, H. M., Zhang, F. F., Li, C. J., Li, X. X., Lambers, H., et al. (2016). Root exudates drive interspecific facilitation by enhancing nodulation and N2 fixation. *Proc. Natl. Acad. Sci. United States America* 113 (23), 6496–6501. doi: 10.1073/pnas.1523580113

Lin, S. F., Pi, Y. J., Long, D. Y., Duan, J. J., Zhu, X. T., Wang, X. L., et al. (2022). Impact of organic and chemical nitrogen fertilizers on the crop yield and fertilizer use efficiency of soybean–maize intercropping systems. *Agriculture* 12 (9). doi: 10.3390/agriculture12091428

Liu, B. J., Chen, X. H., Lian., Y. Q., and Wu, L. L. (2013). Entropy-based assessment and zoning of rainfall distribution. *J. Hydrology* 490, 32–40. doi: 10.1016/j.jhydrol.2013.03.020

Luan, C., He, W., Su, X., Wang, X. M., Bai, Y. K., and Wang, L. X. (2021). Effects of biochar on soil water and temperature, nutrients, and yield of maize/soybean and maize/peanut intercropping systems. *Int.Agroghys* 35, 365–373. doi: 10.31545/intagr/144133

Luo, K., Yuan, X. T., Xie, C., Liu, S. S., Chen, P., Du, Q., et al. (2022). Diethyl aminoethyl hexanoate increase relay strip intercropping soybean grain by optimizing photosynthesis aera and delaying leaf senescence. *Fontiers Plant Sci.* 12. doi: 10.3389/fpls.2021.818327

Ma, R. X., Wang, J. S., Li, X. Z., and Liu, W. C. (2012). Effect of different NPK fertilizers cooperating application on yield and quality of high starch maize. *Appl. Mechanics Materials* 214, 423–429. doi: 10.4028/www.scientific.net/AMM.214.423

Mertz-Henning, L. M., Ferreira, L. C., Henning, F. A. J., Mandarino, M. G., Santos, E. D., Oliveira, M. C. N. D., et al. (2018). Effect of water deficit-induced at vegetative and reproductive stages on protein and oil content in soybean grains. *Agron. J.* 8, 3. doi: 10.3390/agronomy8010003

Miah, M., Gaihre, Y. K., Hunter, G., Singh, U., and Hossain, S. A. (2016). Fertilizer deep placement increases rice production: evidence from 'farmers' fields in southern Bangladesh. *Agron. J.* 108 (2), 805–812. doi: 10.2134/agronj2015.0170

Mohammad, G., Petr, K., Reinhard, W. N., Marek, K., Elnaz, A., Daniel, B., et al. (2022). Interaction of biochar with chemical, green and biological nitrogen fertilizers on nitrogen use efficiency indices. *Agronomy* 12, 9. doi: 10.3390/agronomy12092106

Mugi-Ngenga, E., Bastiaans, L., Zingore, S., Anten, N. P. R., and Giller, K. E. (2022). The role of nitrogen fixation and crop n dynamics on performance and legacy effects of maize-grain legumes intercrops on smallholder farms in Tanzania. *Eur. J. Agron.* 141. doi: 10.1016/j.eja.2022.126617

Nasar, J., Zhai, J. C., Khan, R., Gul, H., Gitari, H., Shao, Z. Q., et al. (2023). Maize-soybean intercropping at optimal n fertilization increases the n uptake, n yield and n use efficiency of maize crop by regulating the n assimilatory enzymes. *Front. Plant Sci.*, 13. doi: 10.3389/fpls.2022.1077948

Omara, P., Aula, L., Oyebiyi, F. B., Eickhoff, E. M., Carpenter, J., and Raun, W. R. (2020). Biochar application in combination with inorganic nitrogen improves maize grain yield, nitrogen uptake, and use efficiency in temperate soils. *Agronomy* 10 (9). doi: 10.3390/agronomy10091241

Purakayastha, T. J., Bera, T., Bhaduri, D., Sarkar, B., Mandal, S., Wade, P., et al. (2019). A review on biochar modulated soil condition improvements and nutrient dynamics concerning crop yields: pathways to climate change mitigation and global food security. *Chemosphere* 227, 345–365. doi: 10.1016/j.chemosphere.2019.03.170

Raza, M. A., Feng, L. Y., Iqbal, N., Ahmed, M., Chen, Y. K., Bin Khalid, M. H., et al. (2019b). Growth and development of soybean under changing light environments in relay intercropping system. *Peerj* 7, e7262. doi: 10.7717/peerj.7262

Raza, M. A., Feng, L. Y., van der Werf, W., Cai, G. R., Khalid, M. H. B., Iqbal, N., et al. (2019a). Narrow-wide-row planting pattern increases the radiation use efficiency and seed yieldof intercrop species in relay-intercropping system. *Food Energy Secur* 8. doi: 10.1002/fes3.170

Raza, M. A., Feng, L. Y., van der Werf, W., Iqbal, N., Khan, I., Hassam, M. J., et al. (2019c). Optimum leaf defoliation: a new agronomic approach for increasing nutrient uptake and land equivalent ratio of maize soybean relay intercropping system. *Field Crops Res.* 244. doi: 10.1016/j.fcr.2019.107647

Raza, M. A., Yasin, H. S., Gul, H., Qin, R., Din, A. M. U., Khalid, M. H. B., et al. (2022). Maize/soybean strip intercropping produces higher crop yields and saves water under semi-arid conditions. *Front. Plant Sci.* 13. doi: 10.3389/fpls.2022.1006720

Ren, H., Jiang, Y., Zhao, M., Qi, H., and Li, C. F. (2021). Nitrogen supply regulates vascular bundle structure and matter transport characteristics of spring maize under high plant density. *Front. Plant Sci.* 11. doi: 10.3389/fpls.2020.602739

Rogovska, N., Laird, D. A., Rathke, S. J., and Karlen, D. L. (2014). Biochar impact on Midwestern mollisols and maize nutrient availability. *Geoderma* 230-231, 340–347. doi: 10.1016/j.geoderma.2014.04.009

Sahoo, S., Sil, I., Dhar, A., Debsarkar, A., Das, P., and Kar, A. (2018). Future scenarios of land-use suitability modeling for agricultural sustainability in a river basin. *J. Cleaner Production* 205, 313–328. doi: 10.1016/j.jclepro.2018.09.099

Seleiman, M. F., Alotaibi, M. A., Alhammad, B. A., Alharbi, B. M., Refay, Y., and Badawy, S. A. (2020). Effects of ZnO nanoparticles and biochar of rice straw and cow manure on characteristics of contaminated soil and sunflower productivity, oil quality, and heavy metals uptake. *Agronomy* 10, 790. doi: 10.3390/agronomy10060790

Sharifi, M., Zebarth, B. J., Burton, D. L., Grant, C. A., and Porter, G. A. (2008). Organic amendment history and crop rotation effects on soil nitrogen mineralization potential and soil nitrogen supply in a potato cropping system. *Agron. J.* 100, 1562–1572. doi: 10.2134/agronj2008.0053

Shen, S. Z., Wan, C., Ma, X. J., Hu, Y. K., Wang, F., and Zhang, K. Q. (2021). Nitrogen mineralization characteristics of organic fertilizer in livestock and poultry under the condition of flood-drought rotation. *J. Agric. Environ. Sci.* 40, 2513–2520. doi: 10.11654/jaes.2021-1032

Singh, M., Paulsen, M. R., Tian, L., and Yao, H. (2002). *Site-Specific Study of Corn Protein, Oil, and Extractable Starch Variability Using NIT Spectroscopy, ASAE Meeting Paper*, 02–1111. ASAE: St. Joseph, MI, USA.

Solaiman, Z. M., Shafi, M. I., Beamont, E., and Anawar, H. M. (2020). Poultry litter biochar increases mycorrhizal colonization, soil fertility and cucumber yield in a fertigation system on sandy soil. *Agriculture* 10, 480. doi: 10.3390/agriculture10100480

Studnicki, M., Wijata, M., Sobczy' nski, G., Samborski, S., Gozdowski, D., and Rozbicki, J. (2016). Effect of genotype, environment and crop management on yield and quality traits in spring wheat. *J. Cereal Sci.* 72, 30–37. doi: 10.1016/j.jcs.2016.09.012

Sun, H. J., Zhang, H. C., Shi, W. M., Zhou, M. Y., and Ma, X. F. (2019). Effect of biochar on nitrogen use efficiency, grain yield and amino acid content of wheat cultivated on saline soil. *Plant Soil Environ.* 65, 83–89. doi: 10.17221/525/2018-PSE

Travis, G., Jacob, N., Greg, S., Bill, D., and Manish., R. (2017). Mid-season leaf glutamine predicts end-season maize grain yield and nitrogen content in response to nitrogen fertilization under field conditions. *Agronomy* 7, 2. doi: 10.3390/agronomy7020041

Wang, D., Jiang, P., Zhang, H., and Yuan, W. (2020). Biochar production and applications in agro and forestry systems: a review. *Sci. Total Environ.* 723, 137775. doi: 10.1016/j.scitotenv.2020.137775

Wang, Q. S., Yuan, X. L., Zhang, J., Gao, Y., Hong, J. L., and Zuo, J. (2015). Assessment of the sustainable development capacity with the entropy weight coefficient method. *Sustainability* 7 (10), 13542–13563. doi: 10.3390/su71013542

Weber, K., and Quicker, P. (2018). Properties of biochar. *Fuel* 217, 240–261. doi: 10.1016/j.fuel.2017.12.054

Wu, Y. S., Gong, W. Z., Yang, F., Wang, X. C., Yong, T. W., and Yang, W. Y. (2016). Responses to shade and subsequent recovery of soya bean in maize-soya bean relay strip intercropping. *Plant Production Sci.* 19 (2), 206–214. doi: 10.1080/1343943X.2015.1128095

Wu, W. A., Han, J. Y., Gu, Y. N., Li, T., Xu, X. R., Jiang, Y. H., et al. (2022). Impact of biochar amendment on soil hydrological properties and crop water use efficiency: a global meta-analysis and structural equation model. *Global Change Biol. Bioenergy* 14 (6), 657–668. doi: 10.1111/gcbb.12933

Xia, H., Riaz, M., Zhang, M. Y., Liu, B., Li, Y. X., El-Desouki, Z., et al. (2022). Biochar-n fertilizer interaction increases n utilization efficiency by modifying soil C/N component under n fertilizer deep placement modes. *Chemospher* 286 (1). doi: 10.1016/j.chemosphere.2021.131594

Xiao, Q., Zhu, L. X., Shen, Y. F., and Li, S. Q. (2016b). Sensitivity of soil water retention and availability to biochar addition in rainfed semiarid farmland during a three-year field experiment. *Field Crop Res.* 196, 284–293. doi: 10.1016/j.fcr.2016.07.014

Xiao, Q., Zhu, L. X., Tang, L., Shen, Y. F., and Li, S. Q. (2017). Responses of crop nitrogen partitioning, translocation and soil nitrogen residue to biochar addition in a temperate dryland agricultural soil. *Plant Soil* 418 (1-2), 405–421. doi: 10.1007/s11104-017-3304-z

Xiao, Q., Zhu, L. X., Zhang, H. P., Li, X. Y., Shen, Y. F., and Li, S. Q. (2016a). Soil amendment with biochar increases maize yields in a semiarid region by improving soil quality and root growth. *Crop Pasture Sci.* 67 (5), 495–507. doi: 10.1071/CP15351

Xu, Z., Li, C. J., Zhang, C. C., Yu, Y., van der Werf, W., and Zhang, F. S. (2020). Intercropping maize and soybean increases efficiency of land and fertilizer nitrogen use, a meta-analysis. *Field Crops Res.* 246. doi: 10.1016/j.fcr.2019.107661

Yang, B. B., Xu, K., and Zhang, Z. (2020). Mitigating evaporation and desiccation cracks in soil with the sustainable material biochar. *Soil Sci. Soc. America J.* 84(2), 461–471. doi: 10.1002/saj2.20047

Yao, Q., Liu, J. J., Yu, Z. H., Li, Y. S., Jin, J., Liu, X. B., et al. (2017). Three years of biochar amendment alters soil physiochemical properties and fungal community composition in a black soil of northeast China. *Soil Biol. Biochem.* 110, 56–67. doi: 10.1016/j.soilbio.2017.03.005

Zahra, A., Hasan, E., Bahman, G., and Abolfazl, F. (2018). Effects of biochar and bio-fertilizer on yield and qualitative properties of soybean and some chemical properties of soil. *Arabian J. Geosciences* 11, 672. doi: 10.1007/s12517-018-4041-1

Zhang, L., Liang, Z. Y., He, X. M., Meng, Q. F., Hu, Y. C., Schmidhalter, U., et al. (2020). Improving grain yield and protein concentration of maize (Zea mays l.) simultaneously by appropriate hybrid selection and nitrogen management. *Field Crops Res.* 249. doi: 10.1016/j.fcr.2020.107754

Zhang, F. S., Wang, J. Q., Zhang, W. F., Cui, Z. L., Ma, W. Q., Chen, X. P., et al. (2008). Nutrient use efficiencies of major cereal crops in China and measures for improvement. *Acta Pedol. Sin.* 45, 915–924.

Zhang, Y. J., Ye, C., Su, Y. W., Peng, W. C., Lu, R., Liu, Y. X., et al. (2022). Soil acidification caused by excessive application of nitrogen fertilizer aggravates soil-borne diseases: evidence from literature review and field trials. *Agriculture Ecosyst. Environ.* 340. doi: 10.1016/j.agee.2022.108176

Zhong, F., Hou, M., He, B., and Chen, I. (2017). Assessment on the coupling effects of drip irrigation and organic fertilization based on entropy weight coefficient model. *Peer J.* 5, e3855. doi: 10.7717/peerj.3855

Zhou, M. H., and Butterbach-Bahl, K. (2014). Assessment of nitrate leaching loss on a yield-scaled basis from maize and wheat croppingsystems. *Plant Soil* 374, 977–991. doi: 10.1007/s11104-013-1876-9

frontiers | Frontiers in Plant Science

TYPE Original Research
PUBLISHED 16 May 2023
DOI 10.3389/fpls.2023.1166933

OPEN ACCESS

EDITED BY
Sumera Anwar,
Durham University, United Kingdom

REVIEWED BY
Farinaz Vafadar,
Isfahan University of Technology, Iran
Ivan Vasenev,
Moscow Timiryazev Agricultural Academy, Russia
Mir Muhammad Nizamani,
Guizhou University, China

*CORRESPONDENCE
Lingling Li
lill@gsau.edu.cn

RECEIVED 15 February 2023
ACCEPTED 24 March 2023
PUBLISHED 16 May 2023

CITATION
Effah Z, Li L, Xie J, Karikari B, Xu A, Wang L, Du C, Duku Boamah E, Adingo S and Zeng M (2023) Widely untargeted metabolomic profiling unearths metabolites and pathways involved in leaf senescence and N remobilization in spring-cultivated wheat under different N regimes. *Front. Plant Sci.* 14:1166933. doi: 10.3389/fpls.2023.1166933

Widely untargeted metabolomic profiling unearths metabolites and pathways involved in leaf senescence and N remobilization in spring-cultivated wheat under different N regimes

Zechariah Effah[1,2,3], Lingling Li[1,2]*, Junhong Xie[1,2], Benjamin Karikari[4], Aixia Xu[1,2], Linlin Wang[1,2], Changliang Du[1,2], Emmanuel Duku Boamah[3], Samuel Adingo[5] and Min Zeng[1,2]

[1]Department of Crop Science, State Key Laboratory of Arid Land Crop Science, Lanzhou, China, [2]College of Agronomy, Gansu Agricultural University, Lanzhou, China, [3]Department of Plant Genetic Diversity, Council for Scientific and Industrial Research (CSIR)-Plant Genetic Resources Research Institute, Bunso, Ghana, [4]Department of Agricultural Biotechnology, Faculty of Agriculture, Food and Consumer Sciences, University for Development Studies, Tamale, Ghana, [5]College of Forestry, Gansu Agricultural University, Lanzhou, China

Progression of leaf senescence consists of both degenerative and nutrient recycling processes in crops including wheat. However, the levels of metabolites in flag leaves in spring-cultivated wheat, as well as biosynthetic pathways involved under different nitrogen fertilization regimes, are largely unknown. Therefore, the present study employed a widely untargeted metabolomic profiling strategy to identify metabolites and biosynthetic pathways that could be used in a wheat improvement program aimed at manipulating the rate and onset of senescence by handling spring wheat (*Dingxi 38*) flag leaves sampled from no-, low-, and high-nitrogen (N) conditions (designated Groups 1, 2, and 3, respectively) across three sampling times: anthesis, grain filling, and end grain filling stages. Through ultrahigh-performance liquid chromatography–tandem mass spectrometry, a total of 826 metabolites comprising 107 flavonoids, 51 phenol lipids, 37 fatty acyls, 37 organooxygen compounds, 31 steroids and steroid derivatives, 18 phenols, and several unknown compounds were detected. Upon the application of the stringent screening criteria for differentially accumulated metabolites (DAMs), 28 and 23 metabolites were differentially accumulated in Group 1_vs_Group 2 and Group 1_vs_Group 3, respectively. From these, 1-O-Caffeoylglucose, Rhoifolin, Eurycomalactone;Ingenol, 4-Methoxyphenyl beta-D-glucopyranoside, and Baldrinal were detected as core conserved DAMs among the three groups with all accumulated higher in Group 1 than in the other two groups. Kyoto Encyclopedia of Genes and Genomes pathway analysis revealed that tropane, piperidine, and pyridine alkaloid biosynthesis; acarbose and validamycin biosynthesis; lysine degradation; and biosynthesis of alkaloids derived from ornithine, lysine, and nicotinic acid pathways were the most significantly ($p < 0.05$) enriched in Group 1_vs_Group 2, while flavone and flavonol as well as anthocyanins biosynthetic pathways were the most significantly ($p < 0.05$) enriched in Group 1_vs_Group 3.

The results from this study provide a foundation for the manipulation of the onset and rate of leaf senescence and N remobilization in wheat.

KEYWORDS

flavonoids, anthocyanins, grain yield, metabolite profile, nitrogen supply, postanthesis

Introduction

The world is challenged to increase food production to meet the needs of increasing population growth, and this has become a major goal of researchers in the plant science community (Grote et al., 2021a). Achieving this objective is threatened by climate change, abiotic and biotic stresses, reduction in soil fertility, and decline in arable lands (Shiferaw et al., 2011; Oshunsanya et al., 2019; Savary et al., 2019). Wheat (*Triticum aestivum* L.) is currently the world's most widely cultivated cereal and demand is expected to increase by 60% by 2050 (Vincent et al., 2022). It is the basic staple and food security crop accounting for over 60% of people's daily calorific and protein needs (Grote et al., 2021b). To sustain food production, the use of synthetic fertilizers like nitrogen (N) has greatly enhanced crop production, but their long-term use and overuse to meet the present food demand can result in heavy deposit of nitrate in soils (Zhang et al., 2013), ammonia emission (Xu et al., 2019), and soil salinity (David et al., 2009) with detrimental effects on soil fauna and flora (Anas et al., 2020).

In order to understand the molecular mechanism underlying plant response to stresses as well as their development under optimal conditions, a number of omics strategies such as genomics, transcriptomics, proteomics, and phenomics have been applied to deepen our knowledge (Palmer et al., 2014; Francki et al., 2016; Zhen et al., 2016; Vergara-Diaz et al., 2020; Bai et al., 2023; Kaur et al., 2021; Singh et al., 2021; Effah et al., 2022). Over the past century, yield has been the key factor influencing crop innovation. The main drivers of high yield are improved agronomic practices (Whitcomb et al., 2014), the use of chemical fertilizers, and the development of molecular tools supporting plant breeding (Fernie and Schauer, 2009), and mineral nutrient availability is a crucial factor for achieving optimal yield (Kant et al., 2011; Gastal et al., 2015). Domestication of cereals has a lengthy history, and wheat in particular exhibits a decline in genetic diversity (Chen et al., 2012b). Elite wheat varieties are typically developed with high nitrogen fertilizer levels, which reduces diversity and variation in N use and remobilization efficiency across related populations (Shewry and Hey, 2015).

A balanced nutrient supply is one of the abiotic factors necessary for plant growth and development. Insufficient nutrient supply has numerous effects on plant physiology, including having a negative impact on crop performance and yield (Marschner, 1995). Nitrogen availability is essential for crop systems, particularly wheat, to produce their best yields (Hawkesford, 2014). In order to improve plant performance at a given nutrient supply through fertilizers or to breed or engineer plants to improve crop ability to deal with low nutrient availability, systems biology should be useful. Our understanding of the intricate molecular mechanisms behind the physiology of such abiotic nutrients is insufficient, and any additional system-wide information will help to eventually fill in the gaps in this regard.

The phenotype of a plant is influenced by interactions between its genotype and external environmental elements such as humidity, temperature, and light, but it is also influenced by the biochemical changes that occur within its cells as part of its homeostasis. Finding the precise alterations in metabolite concentrations involved in any biochemical pathway that characterizes the phenotype of a plant's cells and tissues is exceedingly difficult in the case of plant metabolomics (Weckwerth, 2003). Metabolites are known to be the final products of cell activities that directly give a clue about the effect of environmental or physiological and pathogenic changes on plants (Shulaev et al., 2008). A total of 74 metabolites were reported during grain developmental stages in wheat with a correlation between metabolism of amino acids, carbohydrates, organic acids, amines, and lipids (Zhen et al., 2016). Metabolites such as organic acids (L-tartaric acid, a-hydroxyisobutyric acid, and 4-acetamidobutyric acid), sugars (melezitose, beta-D-lactose, D-sedheptulose 7-phosphate, 2-dexyribose 1-phosphate, and raffinose), and phenols (coniferin, curcumins, and feruloylputrescine) are reported to regulate post-harvest ripening of tomato fruit under low temperature (Bai et al., 2023), and these could be validated and used as biomarkers in practical crop improvement (Wen et al., 2014; Yan et al., 2021).

One of the physiological processes well known to affect grain yield/weight and quality is leaf senescence (Quirino et al., 2000; Watanabe et al., 2018; Paluch-Lubawa et al., 2021), which represents a phase of nutrient assimilation to remobilization to sink tissues (Masclaux et al., 2001; Li et al., 2017). Crops with delayed leaf senescence maintain leaf color and extend their photosynthetic competence, leading to a higher grain weight and yield (Spano et al., 2003; Borrell et al., 2014), while those with premature senescence of functional leaves at grain filling stages lead to reduced grain yield and quality (Spano et al., 2003). Applications of metabolomics in wheat study are highly valued and have great potential. To get more precise information from the wheat metabolome, however, a number of gaps and bottlenecks need to be resolved. With this in mind, the present study aimed to identify metabolites and biosynthetic pathways that could be used in a wheat improvement program targeted at manipulating the rate and onset of senescence in spring wheat by conducting metabolomic profiling of spring wheat (cultivar: *Dingxi 38*) flag leaves sampled from no-, low-, and high-N conditions in the semi-arid loess plateau of Gansu

Province, People's Republic of China. The flag leaves were sampled from three growth stages: anthesis, grain filling, and end of grain filling to give overall metabolic changes during these critical stages, which ultimately affect grain yield and quality (Djanaguiraman et al., 2020; Osman et al., 2021). The results of this study give an overview of metabolic changes involved in nutrient remobilization during the progression of leaf senescence in wheat, and lay a foundation in our attempt to manipulate leaf senescence and N remobilization *via* omics-assisted speed breeding for wheat improvement.

Materials and methods

Site description

This study was conducted in the Gansu Agricultural University's Rainfed Experimental Station in Dingxi, Gansu Province, China (35_280N, 104_440E, elevation 1,971 m above sea level) from 2003 to date (March to July each year). In crop season, the average minimum and maximum air temperatures at the research location were −22 and 38°C, respectively, while the average precipitation was 390.7 mm year^{-1}. With 2,480 h of sunshine for the crop season, the average crop season cumulative air temperature > 10°C was 2,240°C, and the average annual radiation was 5,930 MJ m^{-2}. The site experienced a rise in the amount of rainfall from May and peaked in August and declined in September. Evaporation was three to four times higher than precipitation, with an average of 1,531 mm (coefficient of variation: 24.3%) for the crop season. The soil type at the site is a Huangmian sandy loam (Hocking and Stapper, 2001) and is classified as a Calcaric Cambisol (Hu et al., 2013). Flax (*Linum usitatissimum L.*) had been the previous crop, and the field has a long history of traditional farming with wheat pea rotation system. The chemical characteristics of the soil (at 0–30 cm depth) were found to be 3.88 kg ha^{-1} of total nitrogen (TN), 24.92 kg ha^{-1} of NH_4-N, 12.72 kg ha^{-1} of NO_3-N, pH 8.33, 8.3 kg ha^{-1} of total phosphorus (P), 4.53 kg ha^{-1} of accessible P, and 82.68 kg ha^{-1} of total potassium (K).

Samples and sampling

Spring-cultivated wheat (*Dingxi 38*) was planted under five N fertilizer (urea) treatments, i.e., 0, 52.5, 105, 157.5, and 210 kg N ha^{-1} represented by N1, N2, N3, N4, and N5, respectively. Flag leaves were sampled from N1, N2, and N5 to represent no-, low-, and high-N conditions at anthesis and 14 and 28 days after anthesis (DAA). The three representative samples from no-N plots at the three stages were named WNR1, WNR7, and WNR13 for anthesis, 14 DAA, and 28 DAA. In the same order, samples from low-N plots were denoted WNR2, WNR8, and WNR11, while those from high-N plots were named WNR5, WNR9, and WNR14. At each sampling stage, the well-labeled tubes with each group sample were quickly placed in liquid nitrogen, stored on ice, and transported to the laboratory. Then, the samples were stored in a −80°C ultralow-temperature refrigerator until all the three sampling stages were done.

Measurement of leaf chlorophyll content

Using a soil-plant analysis development chlorophyll meter (SPAD-502, Konica Minolta Inc., Osaka, Japan), the amount of chlorophyll per unit area of flag leaves was calculated from anthesis to the soft dough stage at 3, 7, 10, 14, 18, 21, and 28 DAA from 22 June to 22 July 2020. The meter readings were taken on the second completely expanded leaf, halfway along the leaf blade, and halfway between the central vein and the leaf edge; the concentration of chlorophyll (Chl) content per unit area was calculated in attached leaves. On leaves that were later plucked for the metabolite analysis, measurements were also taken. An approved substitute for leaf nitrogen concentrations is leaf greenness (Lawlor, 2002; Foyer et al., 2003).

Sample and metabolite extraction process

Methanol/chloroform extraction, as previously described, was used to extract the metabolites (Erban et al., 2007). The leaves were first freeze-dried and then ground to powder using a grinder (MM 400; Retsch, Germany) with a zirconia bead for 1.5 min at 30 Hz. From 0.1 g of freeze-dried plant material, metabolites were extracted using 1 ml of 70% aqueous methanol at 4°C overnight, and vortexed three times during the period to enhance the extraction efficiency, 30 ml of nonadecanoic acid methylester (2 mg/ml stock in chloroform), and 30 ml of a pre-mixture of sorbitol (0.2 mg/ml methanol) and D-(−)-isoascorbic acid (0.5 mg/ml in H_2O) for quantitative internal standardization. Chloroform (200 µl) was added to the polar phase after the extract had been heated for 15 min at 70°C. After shaking the mixture at 37°C for an additional 5 min, 400 µl of water was added to it. The mixture was then vigorously vortexed before being centrifuged to separate the polar and non-polar phases. A speed-vac was used to dry 100-µl aliquots at a time. We assessed the amounts of primary metabolites and ions in dried extracts. Then, the extract was centrifuged at 10,000 *g* for 10 min, and finally, the supernatant was filtered through a microporous membrane (0.22 µm pore size; ANPEL, Shanghai, China) before ultrahigh-performance liquid chromatography–tandem mass spectrometry (UHPLC-MS/MS) analysis.

Identification and analyses of metabolites

Widely untargeted metabolomic profiling of samples was conducted by Gene pioneer Biotechnology Co., Ltd. (Su ICP No. 15038772-1; 9 Weidi Road, Xianlin University Town, Qixia District, Nanjing) following the protocol earlier published by Want et al. (2010) with minor modification. Briefly, the chromatographic separation was undertaken *via* an Accucore Hydrophilic interaction liquid chromatography column with dimensions 50 × 2.1 mm and 2.6 µm (Thermo Fisher ScientificTM, United States)

fitted to the Thermo Scientific UHPLC system. Metabolites were eluted from the column through a gradient mobile phase that comprised phase A (0.1% formic acid, 10 mM ammonium acetate, and 95% acetonitrile) and phase B (made up of 0.1% formic acid, 10 mM ammonium acetate, and 50% acetonitrile), at a flow rate of 0.3 ml min^{-1}. A volume of 5 µl per sample was added after equilibration. The temperature of the column was maintained at 40°C, while the auto-sampler was kept at 4°C. The linear gradient elution procedure followed 2% B for 0–1 min, from 2% B at 1 min to 50% B at 17 min until 17.5 min, thereafter returning to the initial gradient conditions (2% B) at 18 min, followed by maintaining at 2% B for a period of 18–20 min. In order to prevent the influence caused by the detected signal fluctuation of the apparatus, samples were randomly injected. A quality control (QC) sample followed by a blank sample was injected after every three experimental sample injections.

The electrospray ionization–mass spectrometry (ESI-MS) experiments were carried out on a Thermo Q ExactiveTM HF-X mass spectrometer with a spray voltage of 3.2 kV in both positive and negative modes. The sheath gas flow rate was set at 35 arbitrary units, while that of auxiliary was set at 10 arbitrary units. In addition, the capillary temperature was set at 320°C, and the MS analysis alternated between MS full scans and data-dependent MS/MS scans with dynamic exclusion. Finally, the mass scan range was selected from 100 to 1500 m/z at a scan rate of 40 Hz.

Data collection and processing

The total ion chromatograms of the nine samples were extracted after detection by UHPLC-MS/MS. The acquired raw MS files were processed via the Compound Discoverer (Thermo Fisher Scientific) software for data pretreatments covering peak identification, alignment, feature extraction, and area normalization, running separately under positive and negative ionization mode following the procedure outlined by Yu et al. (2018).

To begin with, screening for retention time (RT), mass-to-charge ratio (m/z), and other parameters as well as the peak alignment of different samples was carried out according to the RT deviation of 0.2 min and the mass deviation of 5 ppm in order to make the identification more accurate. Subsequently, the peak extraction was conducted according to the following criteria: mass deviation = 5 ppm, signal strength deviation = 30%, signal-to-noise ratio = 3, and minimum signal strength = 100,000. Moreover, the peak area was then quantified. The mass spectrometry matrix data containing sample names, m/z–RT pairs, and ion intensity information were generated and exported. The target ions were then integrated to predict the molecular formula and compared against the Japan Chemical Substance Dictionary (NIKKAJI) (Kimura and Kushida, 2015), Chemical Entities of Biological Interest (ChEBI) (Degtyarenko et al., 2007), PubChem (Kim et al., 2016), Kyoto Encyclopedia of Genes and Genomes (KEGG) both compound name and pathway (Kanehisa et al., 2016), and class assignment and ontology prediction using mass spectrometry (CANOPUS) (Dührkop et al., 2021) online databases for identification and confirmation of the compounds. The background ions were eliminated with blank samples, and the quantitative results were then normalized with QC samples. The identification and quantitative results from the data were obtained and used for further statistical analysis.

Statistical analyses

Multivariate statistical analyses: principal component analysis (PCA) and orthogonal projections to latent structures-discriminant analysis (OPLS-DA) of ion intensities of metabolites detected in the no, low, and high N renamed as Groups 1, 2, and 3, respectively, were performed with SIMCA-P software (v13.0, Umetrics, Umea, Sweden) after Pareto scaling in order to show the differences in the metabolic composition among the nine samples from the three groups. The reliability of the OPLS-DA model was verified by permutation test, which was used to assess whether the model was overfitted.

To determine the differentially accumulated metabolites (DAMs) between the Group 1 and either Group 2 or 3 samples, variable importance in the projection (VIP) > 1, p-value < 0.05, and fold change (FC) > 1.2 or FC < 0.83 were adopted for screening (Saccenti et al., 2014). The volcano and heatmap hierarchical clustering plots were generated with the *DESeq2* (Love et al., 2014) and *pheatmap* (Kolde, 2012) packages in R to visualize the metabolite profiles and reveal the relationship between the metabolites and samples. To determine the extent of relationship between metabolites in the pairwise group comparison, the *corrplot* package in R was used to generate and visualize Pearson correlation coefficients between metabolites (Wei et al., 2017).

Aside from the above, biosynthetic pathway enrichment was conducted according to KEGG *via* MetaboAnalyst based on the ion intensity of Group 2 or 3 relative to Group 1 with the threshold of $p < 0.05$ and finally bubble plots for two groups with the top 20 pathways were generated by *ggplot2* package in R (Wickham et al., 2016). A Venn diagram and a histogram of extent regulation of DAMs between the two pairwise groups were generated by TBtool (Chen et al., 2020) and GraphPadPrism (GraphPad Software, Inc., www.graphpad.com), respectively.

Results

Effect of N fertilization on chlorophyll content in leaves

The SPAD values of leaves were taken as an indicator of chlorophyll content from anthesis to the end of grain filling (28 DAA). The highest SPAD values were recorded at the anthesis stage and slowly declined towards maturity (Figure 1). At anthesis and post-anthesis, the SPAD value was the highest at the higher N rate (N4 and N5) and then declined with the decrease in N rate and was the lowest at control. The relative decline of the chlorophyll from anthesis to maturity was 52% under N5 treatment, while in the control and N2, the decline was 69% and 66.4%, respectively.

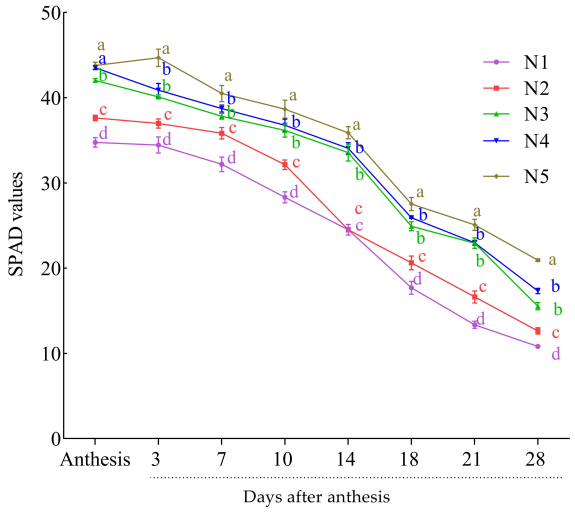

FIGURE 1
Effect of nitrogen rates on SPAD value at post-anthesis growth stages of the wheat cultivar (average of the 2 years: 2019 and 2020). Results are mean ± standard error (n = 3). Treatment comprised N at different rates: 0 kg ha^{-1} (N1), 52.5 kg ha^{-1} (N2), 105 kg ha^{-1} (N3), 157.5 kg ha^{-1} (N4), and 210 kg ha^{-1} (N5). Alphabets at each sampling time (days) indicate the level of difference among the five levels N used in this study. N level with the same or a common alphabet indicate no significant difference (P-vale >0.05), while those with different alphabet indicate significant difference (P-value<0.05).

However, no significant difference was observed between N4 and N3 in all the growth stages except at the end of grain filling.

Metabolites detected among the flag leaves from three N conditions at three different stages

In our earlier study, it was observed that N rate alters leaf senescence and N remobilization in spring-cultivated wheat, *Dingxi 38* (Effah et al., 2022); therefore, a UHPLC-MS/MS-based untargeted metabolomic approach was performed to profile the metabolites in flag leaves of spring-cultivated wheat, *Dingxi 38*, sampled from three N conditions (no, low, and high N) and three stages (anthesis, 14 DAA, and 28 DAA). The nine samples (3 N conditions × 3 stages) were grouped into Groups 1 (WNR1, WNR7, and WNR13), 2 (WNR2, WNR8, and WNR11), and 3 (WNR5, WNR9, and WNR14) under no, low, and high N, respectively. From these, we detected a total of 826 metabolites (Supplementary Table S1), of which 576, 495, 489, 365, 355, 335, and 291 were successfully confirmed in KEGG compound name (Kanehisa et al., 2016), the Human Metabolome Database (HMDB) (Wishart et al., 2018), CANOPUS (Dührkop et al., 2021), PubChem (Kim et al., 2016), NIKKAJI (Kimura and Kushida, 2015), ChEBI (Degtyarenko et al., 2007), and KEGG pathway (Supplementary Figure S1). The successful confirmation of detected compounds on these public databases gives credence to our results.

Among the classes of compounds, 107 are flavonoid and its associated compounds (2-arylbenzofuran flavonoids, flavonoid, and isoflavonoid), 51 are prenol lipids, 37 are fatty acyls, 37 are organooxygen compounds, 31 are steroids and steroid derivatives, 18 are phenols, and others such as carbohydrates and carbohydrate conjugates, phenylpropanoic acids, phenylpropanoids, and polyketides (Supplementary Figure S1). The dominance of some classes of compounds gives clues to their potential role in regulating spring wheat under different N regimes.

Based on the ion intensities of the 826 metabolites, we performed hierarchical heatmap clustering with the *pheatmap* package in R. The nine samples clustered into 2 clusters with Cluster 1 comprising samples from anthesis (WNR1, WNR2, and WNR5) and the grain filling stage (WNR7, WN8, and WNR9), while Cluster 2 consisted of only samples from the end of the grain filling stage (Figure 2A), suggesting that similar compounds are produced by wheat plants at either of the three stages (anthesis, grain filling, and end of grain filling) or three conditions (no, low, and high N rate), but differed in their intensity. In addition, PCA revealed that the first and second PC axes account for 95.30% variability among the nine samples (Figure 2B).

Taken together, the detected compounds, their confirmation on prominent public databases, and variability by cluster and PC analyses pinpoint the use of metabolites in regulating spring-cultivated wheat under different N rates. This called for the current study to discover and dissect the metabolites and pathways involved in regulating spring-cultivated wheat under different N rates.

Identification of differentially accumulated metabolites

The 826 metabolites detected in the nine flag leaf samples were subjected to differential accumulation analysis with Group 1 (no-N condition [WNR1, WNR7, and WNR13]) relative to either Group 2 (low-N condition [WNR2, WNR8, and WNR11]) or Group 3 (high-N condition [WNR5, WNR9, and WNR14]) samples *via* OPLS-DA, VIP > 1, p-value < 0.05, and FC > 1.2 or FC < 0.83 (Figures 2A, B). The goodness of prediction models of Group 1_vs_Group 2 and Group 1_vs_Group 3 samples caused 100% and 97.20% variability in the pairwise comparisons, respectively (Supplementary Figures S2A, B).

From the above stringent criteria, a total of 28 and 23 DAMs were detected in Group 1_vs_Group 2 (VIP = 1.50–1.71) and Group 1_vs_Group 3 (VIP = 1.49–1.76), respectively (Figures 3A–D; Supplementary Table S2A). Among those DAMs in Group 1_vs_Group 2, 17 and 11 accumulated higher and lower respectively (Figure 3C; Supplementary Table S2A). The up-accumulation of higher numbers of DAMs observed in Group 1 could be because of stressful conditions by the no-N treatment, which is responsible for influencing the number of metabolites for survival. The top three metabolites with the lowest FC between Group 1 and Group 2 include diethanolamine, 3-aminoisobutanoic acid, and 1-O-caffeoylglucose, while bergaptol, avenanthramide A, baptifoline, and (2E)-decenoyl-ACP;L-pipecolic acid;pipecolic acid accumulated at least 2.07-fold higher in Group 2 than in Group 1 (Supplementary Table S2A).

On the other hand, 17 metabolites accumulated higher under no-N conditions than under high-N conditions, while 6 metabolites

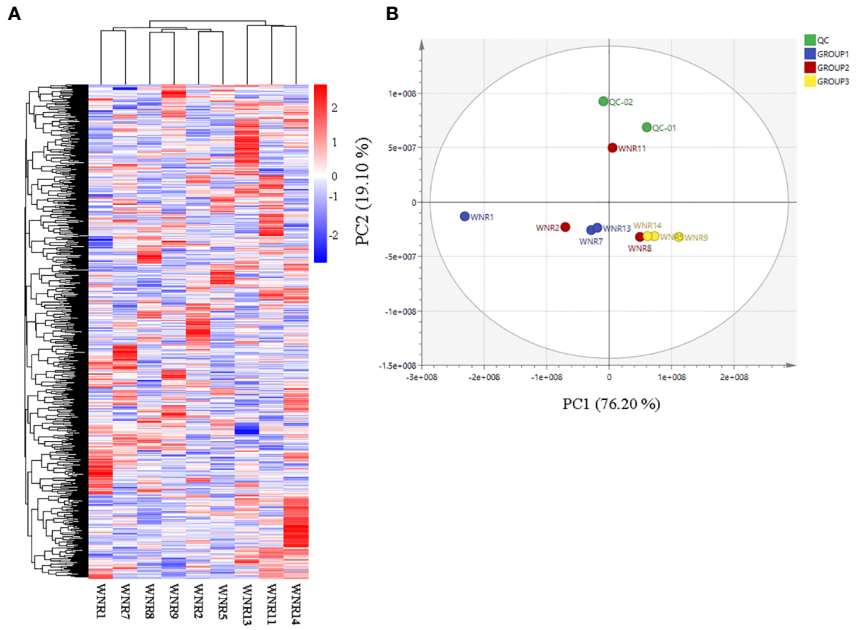

FIGURE 2
Quality assessment of metabolites based on their ion intensities from three nitrogen conditions. **(A)** Hierarchical heatmap clustering of all metabolites. **(B)** Principal component analysis. Three N conditions: no, low, and high nitrogen designated as Groups 1 (WNR1, WNR7, and WNR13), 2 (WNR2, WNR8, and WNR11), and 3 (WNR5, WNR9, and WNR14), respectively, and three stages [anthesis—WNR1, WNR2, and WNR5; grain filling period (14 days after anthesis)—WNR7, WNR8, and WNR9; and end of grain filling period—WNR11, WNR13 and WNR14]. QC represents quality control sample comprising the mixture of the three groups.

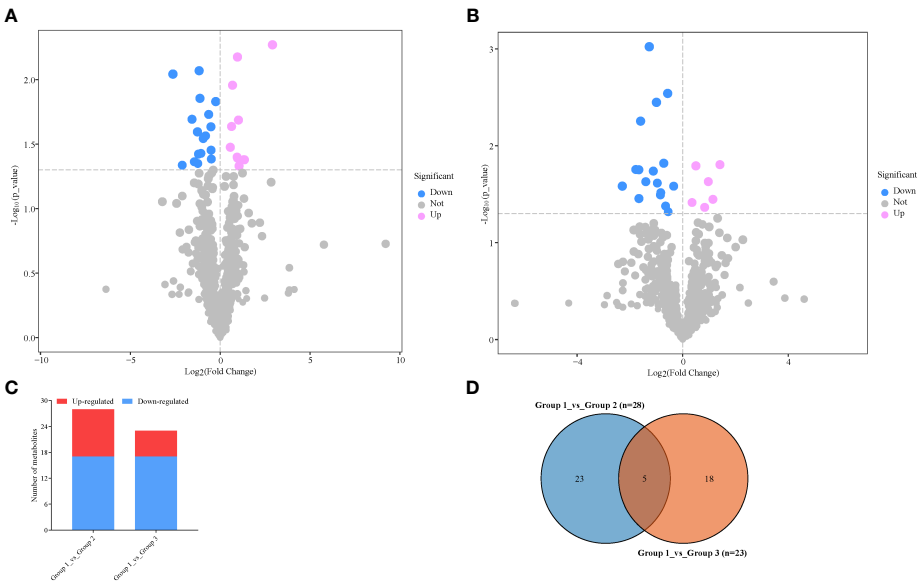

FIGURE 3
Differentially accumulated metabolites (DAMs) detected in samples from no nitrogen (Group 1) relative to either low nitrogen (Group 2) or high nitrogen (Group 3). **(A)** Volcano plot in Group 1_vs_Group 2. **(B)** Volcano plot in Group 1_vs_Group 3. Each point in the volcano plot represents a metabolite, the abscissa represents the fold change of each substance in the group compared to each other (take the logarithm with the base 2), and the ordinate represents the *p*-value of the Student's *t*-test (take 10 as the logarithm of the base). The size of the scatter represents the importance in projection (VIP) value of the orthogonal partial least squares discriminant analysis model; the larger the scatter, the greater the variable VIP value. Scattered colors represent the final screening results; significantly upregulated metabolites are shown in red, significantly downregulated metabolites are shown in blue, and non-significantly different metabolites are shown in gray. **(C)** Extent of regulation of DAMs. **(D)** Venn diagram of DAMs between the two pairwise comparisons.

10.3389/fpls.2023.1166933

had higher accumulation under high-N conditions than under low-N conditions (Figure 3C; Supplementary Table S2B). This highlights that N stress stimulates the accumulation of a number of metabolites essential to survival, hastens delay senescence, and reduces N remobilization. The top seven differentially accumulated metabolites with the least $-\log_2$FC values are as follows: 1-O-caffeoylglucose > anisatin > 6,7-dehydroferruginol > baldrinal > tricin > tetrahydrocurcumin > astragalin (Supplementary Table S2B). The six metabolites with the highest $-\log_2$FC are as follows: 1-(4-Hydroxyphenyl) propan-1-one < phendimetrazine < proline betaine < azithromycin < lupeol< sclareol (Supplementary Table S2B).

To identify conserved DAMs (CDAMs), five CDAMs (1-O-caffeoylglucose, rhoifolin, eurycomalactone;ingenol, 4-methoxyphenyl beta-D-glucopyranoside, and baldrinal) among the three conditions (no, low, and high N), all accumulated higher in the no-N condition than in either the low- or high-N condition (Table 1), suggesting that spring wheat increases the abundance of some of the metabolites to survive under the no-N condition (Law et al., 2018).

Functional analyses of differentially accumulated metabolites

The DAMs detected were annotated by the KEGG database, and the main enriched metabolic pathways of DAMs were analyzed. The results revealed that one compound—(2E)-decenoyl-ACP;L-pipecolic acid; pipecolic acid (carboxylic acids and derivatives; amino acid and derivative)—involved in amino acid metabolism was enriched on lysine degradation (map00310), tropane, piperidine, and pyridine alkaloid biosynthesis (map00960), and biosynthesis of alkaloids derived from ornithine, lysine, and nicotinic acid (map01064); these together with acarbose (carbohydrates and carbohydrate conjugates) involved in acarbose and validamycin biosynthesis (map00525) were significantly enriched in Group 1_vs_Group 2 (Supplementary Table S3A and Figure 5A). These two compounds, (2E)-decenoyl-ACP;L-pipecolic acid;pipecolic acid and acarbose, accumulated higher in Group 2 than in Group 1, suggesting their possible involvement in the delayed senescence and higher N remobilization observed in Group 2 (Figures 6A, B).

TABLE 1 Average ion intensities of the five common differentially accumulated metabolites detected among the three groups.

Metabolite	Class [a]	Group 1[b]	Group 2[c]	Group 3[d]
1-O-Caffeoylglucose	Carbohydrate	1.24E-04	4.19E-05	2.55E-05
Rhoifolin	Flavonoid	4.58E-03	3.20E-03	3.61E-03
Eurycomalactone;Ingenol	Diterpenoids	1.14E-04	6.45E-05	7.76E-05
4-Methoxyphenyl beta-D-glucopyranoside	Phenol	6.23E-05	2.59E-05	3.51E-05
Baldrinal	Miscellaneous	9.16E-05	3.86E-05	2.90E-05

[a] Assignment and ontology prediction using mass spectrometry (CANOPUS) (Dührkop et al., 2021). [b] Comprised WNR1, WNR2, and WNR5 samplings taken at anthesis. [c] Comprised WNR7, WNR8, and WNR9 samplings taken at the grain filling period [14 days after anthesis (DAA)]. [d] Comprised WNR11, WNR13, and WNR14 samplings taken at the end of the grain filling period (28 DAA).

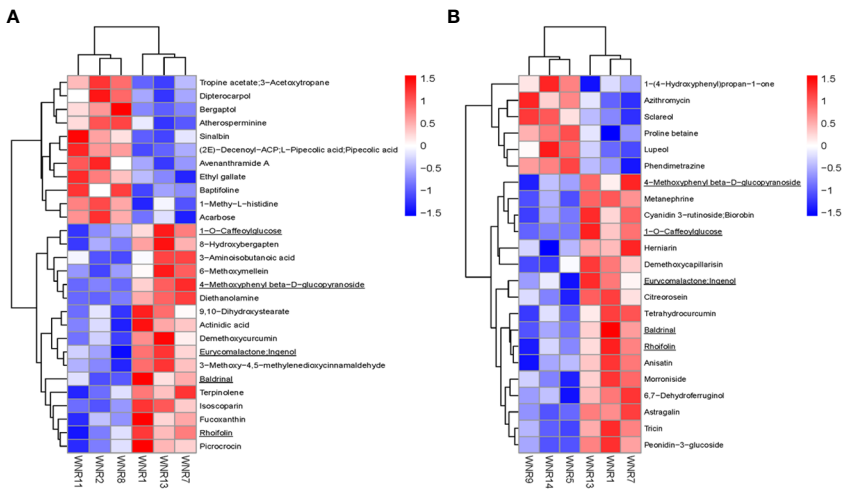

FIGURE 4
Heatmap clustering of differentially accumulated metabolites among the three groups based on their ion intensities. **(A)** Group 1_vs_Group 2. **(B)** Group 1_vs_Group 3. Five common DAMs are underlined. Three groups comprised no, low, and high nitrogen designated as Groups 1, 2, and 3, respectively. WNR1, WNR2, and WNR5 samplings were taken at anthesis; WNR7, WNR8, and WNR9 samplings were taken at the grain filling period [14 days after anthesis (DAA)]; and WNR11, WNR13, and WNR14 sampling were taken at the end of the grain filling period (28 DAA).

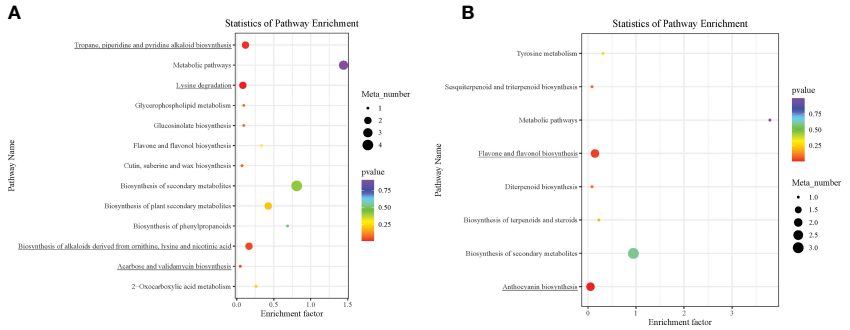

FIGURE 5
Kyoto Encyclopedia of Genes and Genomes (KEGG) pathway enrichment analysis bubble plot of differentially accumulated metabolites. **(A)** Group 1_vs_Group 2. **(B)** Group 1_vs_Group 3. Each row in the figure represents a KEGG pathway. The abscissa is the enrichment factor. The larger the enrichment factor, the more significant the enrichment level of differential metabolites in this pathway. The color of the dots represents the *p*-value, and the size of the bubbles represents the number of differential metabolites annotated in that pathway. Those underlined had $p < 0.05$.

Plants are sessile organisms and, as a result, develop different methods for protection against stressful conditions of the surroundings, including abiotic stress like limited/no-N condition. One prominent mechanism is the production of secondary metabolites such as flavonols, anthocyanins, and catechins (Gutierrez et al., 2017; Zandalinas et al., 2017). Interestingly, two anthocyanin biosynthetic-based metabolites (cyanidin 3-O-rutinoside and peonidin 3-O-glucoside) (Figures 6C, D) and two flavone and flavonol biosynthetic-based metabolites (map00944) (rhoifolin and astragalin, alternatively known as apigenin 7-O-neohesperidoside and Kaempferol 3-O-glucoside) (Figures 6E, F) accumulated higher in Group 1 than in Group 3, pointing out that the wheat plants under the no-N condition activate derivative pathways of phenylpropanoid biosynthesis. The number of metabolic pathways discovered could be targeted for metabolic engineering to delay leaf senescence while optimizing N remobilization in spring-cultivated wheat.

We further performed Pearson correlation analyses among the DAMs detected in each pairwise comparison, and the results of correlation coefficients (r) are shown in Figures 7A, B and Supplementary Tables S4A, B. It was observed that Acarbose negatively correlated with diethanolamine ($r = -0.902$, $p = 0.014$), 4-methoxyphenyl beta-D-glucopyranoside ($r = -0.860$, $p = 0.028$), and rhoifolin ($r = -0.9866$, $p = 0.026$) (Figure 7A; Supplementary Table S4A). The latter also negatively correlated with sinalbin ($r = -0.896$, $p = 0.016$). These strong negative correlated compounds could be targeted to manipulate acarbose and rhoifolin to increase yield under the no-N condition and regulate leaf senescence. rhoifolin, on the other hand, had a strong significant positive correlation with fucoxanthin ($r = 0.942$, $p = 0.005$), terpinolene ($r = 0.961$, $p = 0.002$), and picrocrocin ($r = 0.963$, $p = 0.002$), while acarbose and 1-methy-L-histidine had $r = 0.963$ at $p = 0.002$.

Under no N (Group 1) relative to high N (Group 3), astragalin/kaempferol 3-O-glucoside involved in flavone and flavonol biosynthesis increased significantly with 6,7-dehydroferruginol, herniarin, metanephrine, peonidin-3-glucoside, and tricin with $r = 0.912–0.930$ with $p < 0.05$, while astragalin/kaempferol 3-O-glucoside decreased in abundance as lupeol and phendimetrazine decreased significantly (Figure 7B; Supplementary Table S4B). In addition, cyanidin 3-rutinoside and biorobin implicated in anthocyanin biosynthesis significantly increased with the increase in 1-O-caffeoylglucose, 4-methoxyphenyl beta-D-glucopyranoside, and metanephrine (Figure 7B; Supplementary Table S4B). These give clues about the association between metabolites, which could be validated, and a few selected for biomarkers to aid omics-based wheat senescence and N remobilization improvement programs.

Effect of N fertilization on chlorophyll content in leaf

The primary objective of breeding is to increase yield, which is also necessary given the impending population growth, but this is only accomplished through small, gradual steps. The genetic makeup of the crop and the environmental factors, such as the availability of nutrient ions, both affect the yield in a multifactorial manner. A greater molecular understanding of the physiological and biochemical processes in agricultural plants holds the potential to bring a knowledge-based component to plant breeding in addition to the extremely efficient breeding and selection procedures. In order to find features or processes that are important under natural multifactorial situations, it is also vital to research such processes under field conditions. The goal of the experiment was to identify the metabolites of field-grown spring wheat under various N conditions targeted at manipulating the rate and onset of senescence by conducting metabolomic profiling of spring wheat leaf.

The results of the current study indicated that the highest N rate had the highest SPAD (chlorophyll) (Figure 1). In order to evaluate N level and N-use efficiency and to boost grain yield, chlorophyll content has been widely used in most cereal plants, including wheat (Singh and Ali, 2020; Ghosh et al., 2020). The chlorophyll content decreased from anthesis to maturity; in particular, more decrease was observed at the late grain filling stages (Figure 1). The first declines in chlorophyll content signaled the beginning of senescence and the transport of solutes to the growing grain simultaneously with the drop in nitrate content in the leaves at 7 DAA. The beginning of senescence usually leads to massive remobilization of phloem-mobile nutrients from the senescing plant parts to a developing sink, such as seeds and grains of monocarpic crops. Senescence is accelerated by low N levels, and this

10.3389/fpls.2023.1166933

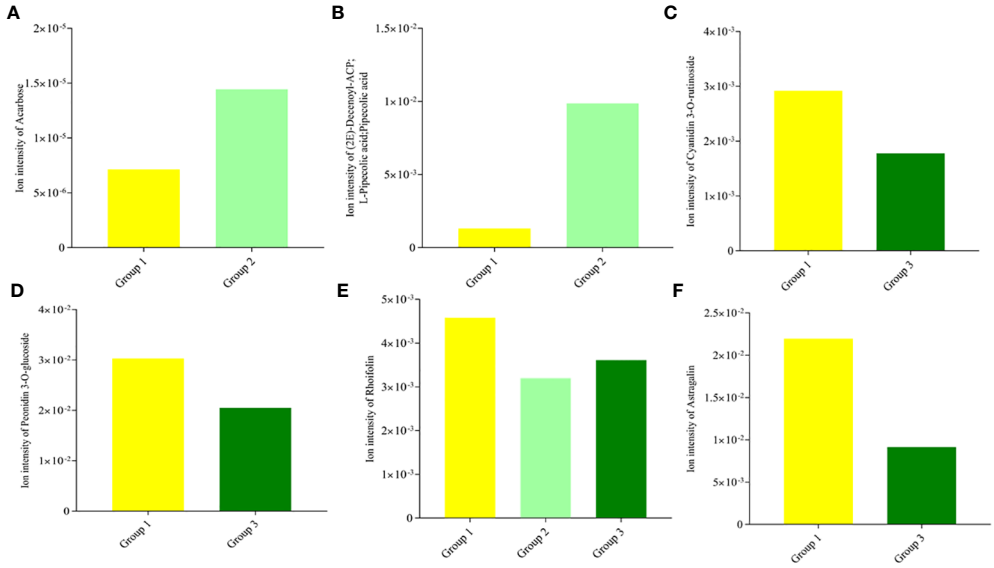

FIGURE 6
Ion intensities of differentially accumulated metabolites enriched in significantly ($p < 0.05$) associated Kyoto Encyclopedia of Gene and Genome pathway analyses. **(A)** Acarbose compound in acarbose and validamycin biosynthesis (map00525). **(B)** (2E)-decenoyl-ACP;L-pipecolic acid;pipecolic acid in amino acid metabolism [lysine degradation (map00310), tropane, piperidine, and pyridine alkaloid biosynthesis (map00960), and biosynthesis of alkaloids derived from ornithine, lysine, and nicotinic acid (map01064)]. **(C)** Cyanidin 3-O-rutinoside in anthocyanins biosynthesis (map00942). **(D)** peonidin 3-O-glucoside in anthocyanins biosynthesis (map00942). **(E)** Rhoifolin/apigenin 7-O-neohesperidoside in flavone and flavonol biosynthesis (map00944). **(F)** Astragalin/kaempferol 3-O-glucoside in flavone and flavonol biosynthesis (map00944).

is accompanied by earlier (plastidial) protein breakdown because of sink demand (Yoshida, 2003). According to Martre et al. (2006), high N levels can delay senescence because more stored inorganic or organic nitrogen can be used to meet sink demand, resulting in faster rates of continuous photosynthesis. The senescing organs of the parent plant provide a major portion of the transportable micro- and macronutrients that wheat grains need to grow, with root absorption providing a smaller portion (Kichey et al., 2007). Senescence and nutrient remobilization processes that occur during the reproductive stage are therefore more crucial for understanding the mechanisms that regulate plant productivity than organ senescence (sequence leaf senescence) activities that take place during vegetative plant growth and development (Martre et al., 2006).

The discovery of the genes responsible for no- or low-N tolerance in spring wheat will contribute to the understanding of the molecular mechanisms behind no- or low-N tolerance, as well as the genetic improvement of spring wheat through marker-assisted selection or gene transformation (Feller et al., 2008).

Differentially accumulated metabolites and their functional analysis relative to leaf senescence and N remobilization

Throughout breeding history, wheat genetic diversity endured a significant contraction (Zamir, 2001; Fu, 2015). Furthermore, plants

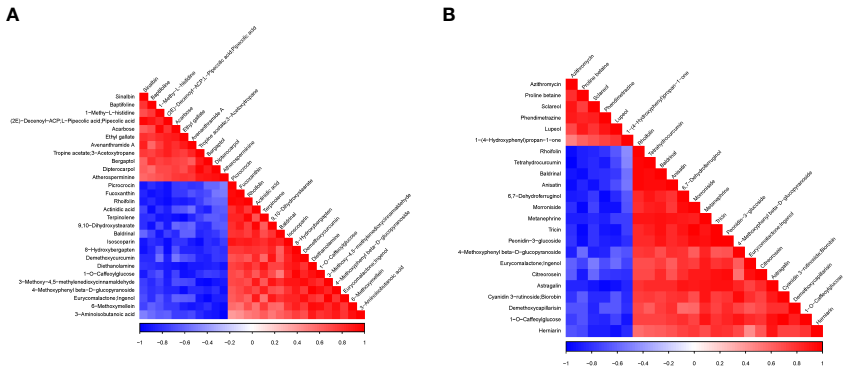

FIGURE 7
Association analysis heatmap of differentially accumulated metabolites detected in the pairwise comparisons. **(A)** Group 1_vs_Group 2. **(B)** Group 1_vs_Group 3. For the different metabolites represented vertically and diagonally in the figure, the color represents the level of correlation between different substances. The darker the color, the higher the correlation. at P-value < 0.05, while those with lighter color indicate no significant correlation (P-value>0.05).

tend to maintain nitrogen homeostasis for as long as possible through a variety of adaptation mechanisms, such as increased uptake of N, altered mobilization patterns, decreased growth, and the ability to maintain metabolite concentrations under abiotic stress conditions, as demonstrated for Arabidopsis under N-depletion (Heyneke et al., 2017). This makes studying leaf senescence after anthesis a prerequisite to understanding the physiological and genetic basis of photosynthesis, nutrient remobilization, and the rules of crop yield and quality of great value to the practice of crop improvement (Yuan et al., 2022). With the above in mind, the present study applied widely untargeted metabolomic profiling to uncover metabolites that may be involved in leaf senescence and N remobilization with three levels of N fertilization regimes (no, low, and high N). The use of untargeted metabolomics is well known to have a comparative advantage over targeted metabolomics. Briefly, untargeted metabolomics is a strategy that focuses on global detection and relative quantitation of small-molecule metabolites to dissect both known and unknown metabolic changes that accompany changes in the environment (Gomez-Gomez et al., 2019; Mehta et al., 2020). Using this strategy allows for simultaneous detection and quantification of a wide range of compounds that cover known and unknown classes of compounds, which make it ideal for the detection of unexpected changes or unknown information in metabolite levels (Gomez-Gomez et al., 2019; Li et al., 2019). By widely untargeted metabolomic profiling, we detected a total of 826 metabolites, of which larger portions were successfully mapped onto seven credible public databases (Supplementary Table S1; Supplementary Figure S1). The most prominent known class of compound detected was flavonoid and its associated compounds such as arylbenzofuran flavonoids, flavonoid, and isoflavonoid. It is not surprising as flavonoid accumulation is reported to increase in plants growing in soils with low N concentration (Bongue Bartelsman and Phillips, 1995; Aires et al., 2006; Ibrahim et al., 2012). One prominent mechanism adopted by stressful plants is the production of secondary metabolites such as flavonols, anthocyanins, and catechins (Dixon and Paiva, 1995; Zandalinas et al., 2017).

Upon application of the strict screening threshold of OPLS-DA, VIP > 1, $p < 0.05$, and FC > 1.2 or FC < 0.83, it was observed that the no-N condition (Group 1) induced and accumulated a higher number of metabolites as a survival mechanism. It has been reported that secondary metabolites such as phenylpropanoids and their derivatives, i.e., flavonoids, anthocyanins, coumarins, lignin building blocks, and tannins are an essential group of compounds necessary for plant acclimation and survival to varying environmental conditions including limited N conditions (Fraser and Chapple, 2011). For example, astragalin/kaempferol 3-O-glucoside, a flavonoid compound, accumulated nearly 60% higher in the no-N condition (Group 1) than in the high-N condition (Group 3) (Supplementary Table S2B). In addition, 1-O-caffeoylglucose, a well-known high-energy glucose ester potentially utilized as a donor molecule during the formation of diverse hydroxycinnamic acid O-esters in plants (Mock and Strack, 1993; Lim and Bowles, 2004; Le Roy et al., 2016), accumulated 79.50% and 387.91% higher in the no-N condition plants (Group 1) than in the low-N (Group 2) and high-N (Group 3) condition plants, respectively (Figure 4; Table 1). This suggests that stressed wheat plants under no N tend to spend a lot of energy for survival and maintenance of their physiological role. These compounds may be responsible for lower photosynthetic capacity observed under limited N conditions compared with Group 3. This corroborates with the reports of Chen et al. (2012a) and Hao et al. (2021) that higher accumulation of flavonoid compounds may affect the photosynthetic capacity of leaves.

In addition to the above, comparison of Group 1 to Group 2 presented compelling evidence for the possible basis for the higher grain yield and quality observed in Group 2 than in Group 1. One carbohydrate and its conjugate—acarbose—was implicated in acarbose and validamycin biosynthesis (map00525), and one carboxylic acid and derivative/amino acid and derivative—(2E)-decenoyl-ACP;L-pipecolic acid;pipecolic acid—were involved in amino acid metabolism-related biosynthetic pathways: lysine degradation (map00310); tropane, piperidine, and pyridine alkaloid biosynthesis (map00960); and biosynthesis of alkaloids derived from ornithine, lysine, and nicotinic acid (map01064) (Figures 6A, B) (Yang et al., 2021). Consistent with previous studies, amino acid metabolism is well documented to be involved in leaf senescence and N remobilization (Li et al., 2017). Acarbose and (2E)-decenoyl-ACP;L-pipecolic acid;pipecolic acid could be targeted to increase grain yield and quality as biomarkers for omics-based crop improvement program in wheat (Steinfath et al., 2010).

Plant pigment is one of the determinants of photosynthetic capacity and efficiency. Some flavonoids play an important role in plant development and defense. Flavonoids constitute one of the main pigments in plants, such as anthocyanins (red, orange, blue, and purple pigments); chalcones and aurones (yellow pigments); and flavonols and flavones (white and pale-yellow pigments), which impart on plants a wide variety of colors (Grotewold, 2006). This was evidenced in our current study as two anthocyanin biosynthetic-based metabolites (cyanidin 3-O-rutinoside and peonidin 3-O-glucoside) (Figures 6C, D) and two flavone and flavonol biosynthetic-based metabolites (rhoifolin/apigenin 7-O-neohesperidoside and astragalin/kaempferol 3-O-glucoside) (Figures 6E, F) accumulated higher in Group 1 than in Group 3, highlighting the role of flavonoid compounds in modulating leaf senescence under N-deficient conditions. The excess accumulation of flavonoid compounds under limited N conditions according to Moreland and Novitzky (1998) likely involves the interruption of the electron transport in the photosystem II reaction center through the disruption of the function of the secondary electron acceptor complex and the reduction of the effective quantum yield, which results in impairment of photosynthesis. This provides a clue for future flavonoid metabolic engineering to regulate leaf senescence in wheat (Naik et al., 2021). Our findings imply that opportunity exists to manipulate leaf senescence and N remobilization under different N fertilization rates with the identified metabolites, which could be validated and used as biomarkers to select wheat cultivars with optimum leaf senescence and N remobilization.

Conclusion

The present study was undertaken to profile metabolic changes in flag leaves sampled from spring-cultivated wheat under three regimes of N fertilization in our attempt to understand leaf senescence and N remobilization by UPLC-ESI-MS/MS. The no-N condition induced flavonoids (cyanidin 3-O-rutinoside, peonidin 3-O-glucoside, rhoifolin/apigenin 7-O-neohesperidoside, and astragalin/kaempferol 3-O-glucoside) and other secondary metabolites in an attempt to cope with the N-deficient condition. These compounds could be useful in metabolite-assisted breeding through their use as metabolic biomarkers to elucidate and regulate leaf senescence in wheat.

Data availability statement

The datasets presented in this study can be found in online repositories. The names of the repository/repositories and accession number(s) can be found in the article/Supplementary Material.

Author contributions

LL: funding acquisition, conceptualization, and supervision. CD: resources and project administration. ZE: investigation and writing—original draft. LW and JX: methodology. ZE, CD, MZ, and AX: data collection. ZE, SA, and BK: formal analysis. LL, BK, and EB: writing—review and editing. All authors read and approved the final manuscript.

Funding

This work was supported by the Major Special Research Projects in Gansu Province (22ZD6NA009), the National Natural Science Foundation of China (32260549), the State Key Laboratory of Aridland Crop Science, Gansu Agricultural University (GSCS-2022-Z02), and the Education Department of Gansu Province (2022QB-084).

Conflict of interest

The authors declare that the research was conducted in the absence of any commercial or financial relationships that could be construed as a potential conflict of interest.

Publisher's note

All claims expressed in this article are solely those of the authors and do not necessarily represent those of their affiliated organizations, or those of the publisher, the editors and the reviewers. Any product that may be evaluated in this article, or claim that may be made by its manufacturer, is not guaranteed or endorsed by the publisher.

Supplementary material

The Supplementary Material for this article can be found online at: https://www.frontiersin.org/articles/10.3389/fpls.2023.1166933/full#supplementary-material

References

Aires, A., Rosa, E., and Carvalho, R. (2006). Effect of nitrogen and sulfur fertilization on glucosinolates in the leaves and roots of broccoli sprouts *(Brassica oleracea* var. *italica). J. Sci. Food Agric.* 86, 1512–1516. doi: 10.1002/jsfa.2535

Anas, M., Liao, F., Verma, K. K., Sarwar, M. A., Mahmood, A., Chen, Z.-L., et al. (2020). Fate of nitrogen in agriculture and environment: agronomic, eco-physiological and molecular approaches to improve nitrogen use efficiency. *Biol. Res.* 53, 47. doi: 10.1186/s40659-020-00312-4

Bai, C., Wu, C., Ma, L., Fu, A., Zheng, Y., Han, J., et al. (2023). Transcriptomics and metabolomics analyses provide insights into postharvest ripening and senescence of tomato fruit under low temperature. *Hortic. Plant J.* 9 (1), 109–121. doi: 10.1016/j.hpj.2021.09.001

Bongue Bartelsman, M., and Phillips, D. A. (1995). Nitrogen stress regulates gene expression of enzymes in the flavonoid biosynthetic pathway of tomato [anthocyane]. *Plant Physiol. Biochem. (France).* 33.

Borrell, A. K., Van Oosterom, E. J., Mullet, J. E., George-Jaeggli, B., Jordan, D. R., Klein, P. E., et al. (2014). Stay-green alleles individually enhance grain yield in sorghum under drought by modifying canopy development and water uptake patterns. *New Phytol.* 203, 817–830. doi: 10.1111/nph.12869

Chen, C., Chen, H., Zhang, Y., Thomas, H. R., Frank, M. H., He, Y., et al. (2020). TBtools: an integrative toolkit developed for interactive analyses of big biological data. *Mol. Plant* 13, 1194–1202. doi: 10.1016/j.molp.2020.06.009

Chen, Y.-H., Guo, Q.-S., Zhu, Z.-B., and Zhang, L.-X. (2012a). Changes in bioactive components related to the harvested time from the spices of *Prunella vulgaris*. *Pharm. Biol.* 50, 1118–1122. doi: 10.3109/13880209.2012.658477

Chen, X., Min, D., Yasir, T. A., and Hu, Y.-G. (2012b). Genetic diversity, population structure and linkage disequilibrium in elite Chinese winter wheat investigated with SSR markers. *PLoS One* 7 (9), e44510. doi: 10.1371/journal.pone.0044510

David, M., Loubet, B., Cellier, P., Mattsson, M., Schjoerring, J. K., Nemitz, E., et al. (2009). Ammonia sources and sinks in an intensively managed grassland canopy. *Biogeosciences* 6, 1903–1915. doi: 10.5194/bg-6-1903-2009

Degtyarenko, K., De Matos, P., Ennis, M., Hastings, J., Zbinden, M., Mcnaught, A., et al. (2007). ChEBI: a database and ontology for chemical entities of biological interest. *Nucleic Acids Res.* 36, D344–D350. doi: 10.1093/nar/gkm791

Dixon, R. A., and Paiva, N. L. (1995). Stress-induced phenylpropanoid metabolism. *Plant Cell* 7, 1085–1097. doi: 10.2307/3870059

Djanaguiraman, M., Narayanan, S., Erdayani, E., and Prasad, P. V. V. (2020). Effects of high temperature stress during anthesis and grain filling periods on photosynthesis, lipids and grain yield in wheat. *BMC Plant Biol.* 20, 268. doi: 10.1186/s12870-020-02479-0

Dührkop, K., Nothias, L.-F., Fleischauer, M., Reher, R., Ludwig, M., Hoffmann, M. A., et al. (2021). Systematic classification of unknown metabolites using high-resolution fragmentation mass spectra. *Nat. Biotechnol.* 39, 462–471. doi: 10.1038/s41587-020-0740-8

Effah, Z., Li, L., Xie, J., Karikari, B., Liu, C., Xu, A., et al. (2022). Transcriptome profiling reveals major structural genes, transcription factors and biosynthetic pathways involved in leaf senescence and nitrogen remobilization in rainfed spring wheat under different nitrogen fertilization rates. *Genomics* 114, 110271. doi: 10.1016/j.ygeno.2022.110271

Erban, A., Schauer, N., Fernie, A. R., and Kopka, J. (2007). ""Nonsupervised construction and application of mass spectral and retention time index libraries from time-of-flight gas chromatography-mass spectrometry metabolite profiles,"," in *Metabolomics: methods and protocols*. Ed. W. Weckwerth (Totowa, NJ: Humana Press), 19–38.

Feller, U., Anders, I., and Mae, T. (2008). Rubiscolytics: fate of rubisco after its enzymatic function in a cell is terminated. *J. Exp. Bot.* 59, 1615–1624. doi: 10.1093/jxb/erm242

Fernie, A. R., and Schauer, N. (2009). Metabolomics-assisted breeding: a viable option for crop improvement? *Trends Genet.* 25, 39–48. doi: 10.1016/j.tig.2008.10.010

Foyer, C. H., Parry, M., and Noctor, G. (2003). Markers and signals associated with nitrogen assimilation in higher plants. *J. Exp. Bot.* 54, 585–593. doi: 10.1093/jxb/erg053

Francki, M. G., Hayton, S., Gummer, J. P. A., Rawlinson, C., and Trengove, R. D. (2016). Metabolomic profiling and genomic analysis of wheat aneuploid lines to identify genes controlling biochemical pathways in mature grain. *Plant Biotechnol. J.* 14, 649–660. doi: 10.1111/pbi.12410

Fraser, C. M., and Chapple, C. (2011). The phenylpropanoid pathway in arabidopsis. *Arabidopsis Book/American Soc. Plant Biologists* 9. doi: 10.1199/tab.0152

Fu, Y.-B. (2015). Understanding crop genetic diversity under modern plant breeding. *Theor. Appl. Genet.* 128, 2131–2142. doi: 10.1007/s00122-015-2585-y

Gastal, F., Lemaire, G., Durand, J.-L., and Louarn, G. (2015). "Quantifying crop responses to nitrogen and avenues to improve nitrogen-use efficiency," in V. O. Sadras and D. F. Calderini Eds. *Crop Physiology (Second Edition)* (San Diego: Academic Press) 2015, 161–206. doi: 10.1016/B978-0-12-417104-6.00008-X

Ghosh, M., Swain, D. K., Jha, M. K., Tewari, V. K., and Bohra, A. (2020). Optimizing chlorophyll meter (SPAD) reading to allow efficient nitrogen use in rice and wheat under rice-wheat cropping system in eastern India. *Plant Production Sci.* 23, 270–285. doi: 10.1080/1343943X.2020.1717970

Gomez-Gomez, A., Soldevila, A., Pizarro, N., Andreu-Fernandez, V., and Pozo, O. J. (2019). Improving liquid chromatography-tandem mass spectrometry determination of polycarboxylic acids in human urine by chemical derivatization. comparison of o-benzyl hydroxylamine and 2-picolyl amine. *J. Pharm. Biomed. Anal.* 164, 382–394. doi: 10.1016/j.jpba.2018.10.055

Grote, U., Fasse, A., Nguyen, T. T., and Erenstein, O. (2021). Food security and the dynamics of wheat and maize value chains in Africa and Asia. *Front. Sustain. Food Syst.* 4, 317. doi: 10.3389/fsufs.2020.617009

Grotewold, E. (2006). The genetics and biochemistry of floral pigments. *Annu. Rev. Plant Biol.* 57, 761–780. doi: 10.1146/annurev.arplant.57.032905.105248

Gutierrez, E., Velasco, A. G. V., Lucas, J. A., Gutierrez-Mañero, F. J., and Ramos-Solano, B. (2017). The flavonol-anthocyanin pathway in blackberry and arabidopsis: state of the art. In C. J. Goncalo Ed. *Flavonoids* (Rijeka: IntechOpen), 129–150. doi: 10.5772/67902

Hao, J., Li, Y., Jia, Y., Wang, Z., Rong, R., Bao, J., et al. (2021). Comparative analysis of major flavonoids among parts of *Lactuca indica* during different growth periods. *Molecules.* 26 (24), 7445. doi: 10.3390/molecules26247445

Hawkesford, M. J. (2014). Reducing the reliance on nitrogen fertilizer for wheat production. *J. Cereal Sci.* 59, 276–283. doi: 10.1016/j.jcs.2013.12.001

Heyneke, E., Watanabe, M., Erban, A., Duan, G., Buchner, P., Walther, D., et al. (2017). Characterization of the wheat leaf metabolome during grain filling and under varied n-supply. *Front. Plant Sci.* 8, 2048. doi: 10.3389/fpls.2017.02048

Hocking, P., and Stapper, M. (2001). Effects of sowing time and nitrogen fertiliser on canola and wheat, and nitrogen fertiliser on Indian mustard. i. dry matter production, grain yield, and yield components. *Aust. J. Agric. Res.* 52, 623–634. doi: 10.1071/ar00113

Hu, H., Ning, T., Li, Z., Han, H., Zhang, Z., Qin, S., et al. (2013). Coupling effects of urea types and subsoiling on nitrogen–water use and yield of different varieties of maize in northern China. *Field Crops Res.* 142, 85–94. doi: 10.1016/j.fcr.2012.12.001

Ibrahim, M. H., Jaafar, H. Z., Rahmat, A., and Rahman, Z. A. (2012). Involvement of nitrogen on flavonoids, glutathione, anthocyanin, ascorbic acid and antioxidant activities of Malaysian medicinal plant *Labisia pumila* blume (Kacip fatimah). *Int. J. Mol. Sci.* 13, 393–408. doi: 10.3390/ijms13010393

Kanehisa, M., Sato, Y., Kawashima, M., Furumichi, M., and Tanabe, M. (2016). KEGG as a reference resource for gene and protein annotation. *Nucleic Acids Res.* 44, D457–D462. doi: 10.1093/nar/gkv1070

Kant, S., Bi, Y.-M., and Rothstein, S. J. (2011). Understanding plant response to nitrogen limitation for the improvement of crop nitrogen use efficiency. *J. Exp. Bot.* 62, 1499–1509. doi: 10.1093/jxb/erq297

Kaur, B., Sandhu, K. S., Kamal, R., Kaur, K., Singh, J., Röder, M. S., et al. (2021). Omics for the improvement of abiotic, biotic, and agronomic traits in major cereal crops: applications, challenges, and prospects. *Plants* 10 (10), 1989. doi: 10.3390/plants10101989

Kichey, T., Hirel, B., Heumez, E., Dubois, F., and Le Gouis, J. (2007). In winter wheat (Triticum aestivum l.), post-anthesis nitrogen uptake and remobilisation to the grain correlates with agronomic traits and nitrogen physiological markers. *Field Crops Res.* 102, 22–32. doi: 10.1016/j.fcr.2007.01.002

Kim, S., Thiessen, P. A., Bolton, E. E., Chen, J., Fu, G., Gindulyte, A., et al. (2016). PubChem substance and compound databases. *Nucleic Acids Res.* 44, D1202–D1213. doi: 10.1093/nar/gkv951

Kimura, T., and Kushida, T. (2015). Openness of nikkaji RDF data and integration of chemical information by nikkaji acting as a hub. *J. Inf. Process. Manag* 58, 204–212. doi: 10.1241/johokanri.58.204

Kolde, R. (2012). *Pheatmap*: pretty heatmaps. *R Package version* 1, 747.

Law, S. R., Chrobok, D., Juvany, M., Delhomme, N., Lindén, P., Brouwer, B., et al. (2018). Darkened leaves use different metabolic strategies for senescence and survival. *Plant Physiol.* 177, 132–150. doi: 10.1104/pp.18.00062

Lawlor, D. W. (2002). Carbon and nitrogen assimilation in relation to yield: mechanisms are the key to understanding production systems. *J. Exp. Bot.* 53, 773–787. doi: 10.1093/jxb/53.370.773

Le Roy, J., Huss, B., Creach, A., Hawkins, S., and Neutelings, G. (2016). Glycosylation is a major regulator of phenylpropanoid availability and biological activity in plants. *Front. Plant Sci.* 7. doi: 10.3389/fpls.2016.00735

Li, W., Zhang, H., Li, X., Zhang, F., Liu, C., Du, Y., et al. (2017). Intergrative metabolomic and transcriptomic analyses unveil nutrient remobilization events in leaf senescence of tobacco. *Sci. Rep.* 7, 12126–12126. doi: 10.1038/s41598-017-11615-0

Li, X., Zhang, X., Ye, L., Kang, Z., Jia, D., Yang, L., et al. (2019). LC-MS-Based metabolomic approach revealed the significantly different metabolic profiles of five commercial truffle species. *Front. Microbiol.* 10. doi: 10.3389/fmicb.2019.02227

Lim, E. K., and Bowles, D. J. (2004). A class of plant glycosyltransferases involved in cellular homeostasis. *EMBO J.* 23, 2915–2922. doi: 10.1038/sj.emboj.7600295

Love, M., Anders, S., and Huber, W. (2014). Differential analysis of count data–the *DESeq2* package. *Genome Biol.* 15, 10–1186. doi: 10.1186/s13059-014-0550-8

Marschner, H. (1995). ""6-mineral nutrition and yield response,"," in *Mineral nutrition of higher plants*, vol. 2nd Edn. (London: Academic Press), 184–200.

Martre, P., Jamieson, P. D., Semenov, M. A., Zyskowski, R. F., Porter, J. R., and Triboi, E. (2006). Modelling protein content and composition in relation to crop nitrogen dynamics for wheat. *Eur. J. Agron.* 25, 138–154. doi: 10.1016/j.eja.2006.04.007

Masclaux, C., Quilléré, I., Gallais, A., and Hirel, B. (2001). The challenge of remobilisation in plant nitrogen economy. a survey of physio-agronomic and molecular approaches. *Ann. Appl. Biol.* 138, 69–81. doi: 10.1111/j.1744-7348.2001.tb00086.x

Mehta, A., Liu, C., Nayak, A., Tahhan, A. S., Ko, Y.-A., Dhindsa, D. S., et al. (2020). Untargeted high-resolution plasma metabolomic profiling predicts outcomes in patients with coronary artery disease. *PLoS One* 15, e0237579–e0237579. doi: 10.1371/journal.pone.0237579

Mock, H.-P., and Strack, D. (1993). Energetics of the uridine 5′-diphosphoglucose: hydroxycinnamic acid acyl-glucosyltransferase reaction. *Phytochemistry* 32, 575–579. doi: 10.1016/S0031-9422(00)95139-2

Moreland, D. E., and Novitzky, W. P. (1998). Interference by luteolin, quercetin, and taxifolin with chloroplast-mediated electron transport and phosphorylation. *Plant Soil.* 38, 145–159. doi: 10.1007/BF02381735

Naik, J., Rajput, R., Pucker, B., Stracke, R., and Pandey, A. (2021). The R2R3-MYB transcription factor MtMYB134 orchestrates flavonol biosynthesis in *medicago truncatula*. *Plant Mol. Biol.* 106, 157–172. doi: 10.1007/s11103-021-01135-x

Oshunsanya, S. O., Nwosu, N. J., and Li, Y. (2019). "Abiotic stress in agricultural crops under climatic conditions," in *Sustainable agriculture, forest and environmental management*. Eds. M. Jhariya, A. Banerjee, R. Meena and D. Yadav (Singapore: Springer), 71–100. doi: 10.1007/978-981-13-6830-1_3

Osman, R., Zhu, Y., Cao, W., Ding, Z., Wang, M., Liu, L., et al. (2021). Modeling the effects of extreme high-temperature stress at anthesis and grain filling on grain protein in winter wheat. *Crop J.* 9, 889–900. doi: 10.1016/j.cj.2020.10.001

Palmer, L. J., Dias, D. A., Boughton, B., Roessner, U., Graham, R. D., and Stangoulis, J. R. (2014). Metabolite profiling of wheat *(Triticum aestivum* L.) phloem exudate. *Plant Methods* 10, 27. doi: 10.1186/1746-4811-10-27

Paluch-Lubawa, E., Stolarska, E., and Sobieszczuk-Nowicka, E. (2021). Dark-induced barley leaf senescence–a crop system for studying senescence and autophagy mechanisms. *Front. Plant Sci.* 12, 425. doi: 10.3389/fpls.2021.635619

Quirino, B. F., Noh, Y.-S., Himelblau, E., and Amasino, R. M. (2000). Molecular aspects of leaf senescence. *Trends Plant Sci.* 5, 278–282. doi: 10.1016/S1360-1385(00)01655-1

Saccenti, E., Hoefsloot, H. C. J., Smilde, A. K., Westerhuis, J. A., and Hendriks, M. M. W. B. (2014). Reflections on univariate and multivariate analysis of metabolomics data. *Metabolomics* 10, 361–374. doi: 10.1007/s11306-013-0598-6

Savary, S., Willocquet, L., Pethybridge, S. J., Esker, P., Mcroberts, N., and Nelson, A. (2019). The global burden of pathogens and pests on major food crops. *Nat. Ecol. Evol.* 3, 430–439. doi: 10.1038/s41559-018-0793-y

Shewry, P. R., and Hey, S. J. (2015). The contribution of wheat to human diet and health. *Food Energy Secur.* 4, 178–202. doi: 10.1002/fes3.64

Shiferaw, B., Prasanna, B. M., Hellin, J., and Bänziger, M. (2011). Crops that feed the world 6. past successes and future challenges to the role played by maize in global food security. *Food Secur.* 3, 307. doi: 10.1007/s12571-011-0140-5

Shulaev, V., Cortes, D., Miller, G., and Mittler, R. (2008). Metabolomics for plant stress response. *Physiol. Plant* 132, 199–208. doi: 10.1111/j.1399-3054.2007.01025.x

Singh, B., and Ali, A. M. (2020). Using hand-held chlorophyll meters and canopy reflectance sensors for fertilizer nitrogen management in cereals in small farms in developing countries. *Sensors* 20, 1127. doi: 10.3390/s20041127

Singh, R. K., Sood, P., Prasad, A., and Prasad, M. (2021). Advances in omics technology for improving crop yield and stress resilience. *Plant Breed.* 140, 719–731. doi: 10.1111/pbr.12963

Spano, G., Di Fonzo, N., Perrotta, C., Platani, C., Ronga, G., Lawlor, D., et al. (2003). Physiological characterization of 'stay green' mutants in durum wheat journal of experimental botany 54(386):1415-1420. *J. Exp. Bot.* 54, 1415–1420. doi: 10.1093/jxb/erg150

Steinfath, M., Strehmel, N., Peters, R., Schauer, N., Groth, D., Hummel, J., et al. (2010). Discovering plant metabolic biomarkers for phenotype prediction using an untargeted approach. *Plant Biotechnol. J.* 8, 900–911. doi: 10.1111/j.1467-7652.2010.00516.x

Vergara-Diaz, O., Vatter, T., Vicente, R., Obata, T., Nieto-Taladriz, M. T., Aparicio, N., et al. (2020). Metabolome profiling supports the key role of the spike in wheat yield performance. *Cells* 9 (4), 1025. doi: 10.3390/cells9041025

Vincent, D., Bui, A., Ram, D., Ezernieks, V., Bedon, F., Panozzo, J., et al. (2022). Mining the wheat grain proteome. *Int. J. Mol. Sci.* 23 (2), 713. doi: 10.3390/ijms23020713

Want, E. J., Wilson, I. D., Gika, H., Theodoridis, G., Plumb, R. S., Shockcor, J., et al. (2010). Global metabolic profiling procedures for urine using UPLC–MS. *Nat. Protoc.* 5, 1005–1018. doi: 10.1038/nprot.2010.50

Watanabe, M., Tohge, T., Balazadeh, S., Erban, A., Giavalisco, P., Kopka, J., et al. (2018). ""Comprehensive metabolomics studies of plant developmental senescence,"," in *Plant senescence. methods in molecular biology*. Ed. Y. Guo (New York: Humana Press), 339–358.

Weckwerth, W. (2003). Metabolomics in systems biology. *Annu. Rev. Plant Biol.* 54, 669–689. doi: 10.1146/annurev.arplant.54.031902.135014

Wei, T., Simko, V., Levy, M., Xie, Y., Jin, Y., and Zemla, J. (2017). Package *corrplot*. *Statistician* 56, e24.

Wen, W., Li, D., Li, X., Gao, Y., Li, W., Li, H., et al. (2014). Metabolome-based genome-wide association study of maize kernel leads to novel biochemical insights. *Nat. Commun.* 5, 3438. doi: 10.1038/ncomms4438

Whitcomb, S. J., Heyneke, E., Aarabi, F., Watanabe, M., and Hoefgen, R. (2014). "Mineral nutrient depletion affects plant development and crop yield," in M. Hawkesford, S. Kopriva and L. De Kok Eds. *Nutrient Use Efficiency in Plants* (Cham: Plant Ecophysiology, Springer), 205–228. doi: 10.1007/978-3-319-10635-9_8

Wickham, H., Chang, W., and Wickham, M. H. (2016). Package *ggplot2. Create elegant data visualisations using the grammar of graphics. version* 2 1–189.

Wishart, D. S., Feunang, Y. D., Marcu, A., Guo, A. C., Liang, K., Vázquez-Fresno, R., et al. (2018). HMDB 4.0: the human metabolome database for 2018. *Nucleic Acids Res.* 46, D608–D617. doi: 10.1093/nar/gkx1089

Xu, R., Tian, H., Pan, S., Prior, S. A., Feng, Y., Batchelor, W. D., et al. (2019). Global ammonia emissions from synthetic nitrogen fertilizer applications in agricultural systems: empirical and process-based estimates and uncertainty. *Global Change Biol.* 25, 314–326. doi: 10.1111/gcb.14499

Yan, H., Pu, Z.-J., Zhang, Z.-Y., Zhou, G.-S., Zou, D.-Q., Guo, S., et al. (2021). Research on biomarkers of different growth periods and different drying processes of citrus wilsonii Tanaka based on plant metabolomics. *Front. Plant Sci.* 12. doi: 10.3389/fpls.2021.700367

Yang, Q., Zhao, D., Zhang, C., Sreenivasulu, N., Sun, S. S.-M., and Liu, Q. (2022). Lysine biofortification of crops to promote sustained human health in the 21st century. *J. Exp. Bot.* 73 (5), 1258–1267. doi: 10.1093/jxb/erab482

Yoshida, S. (2003). Molecular regulation of leaf senescence. *Curr. Opin. Plant Biol.* 6, 79–84. doi: 10.1016/S1369526602000092

Yu, C., Luo, X., Zhan, X., Hao, J., Zhang, L., L Song, Y.-B., et al. (2018). Comparative metabolomics reveals the metabolic variations between two endangered taxus species (T. fuana and t. yunnanensis) in the Himalayas. *BMC Plant Biol.* 18, 197. doi: 10.1186/s12870-018-1412-4

Yuan, J., Sadiq, M., Rahim, N., Li, G., Yan, L., Wu, J., et al. (2022). Tillage strategy and nitrogen fertilization methods influences on selected soil quality indicators and spring wheat yield under semi-arid environmental conditions of the loess plateau, China. *Appl. Sci.* 12 (3), 1101. doi: 10.3390/app12031101

Zamir, D. (2001). Improving plant breeding with exotic genetic libraries. *Nat. Rev. Genet.* 2, 983. doi: 10.1038/35103590

Zandalinas, S. I., Sales, C., Beltrán, J., Gómez-Cadenas, A., and Arbona, V. (2017). Activation of secondary metabolism in citrus plants is associated to sensitivity to combined drought and high temperatures. *Front. Plant Sci.* 7, 1954–1954. doi: 10.3389/fpls.2016.01954

Zhang, W.-F., Dou, Z.-X., He, P., Ju, X.-T., Powlson, D., Chadwick, D., et al. (2013). New technologies reduce greenhouse gas emissions from nitrogenous fertilizer in China. *Proc. Natl. Acad. Sci.* 110, 8375. doi: 10.1073/pnas.1210447110

Zhen, S., Dong, K., Deng, X., Zhou, J., Xu, X., Han, C., et al. (2016). Dynamic metabolome profiling reveals significant metabolic changes during grain development of bread wheat (*Triticum aestivum* L.). *J. Sci. Food Agric.* 96, 3731–3740. doi: 10.1002/jsfa.7561

frontiers | Frontiers in Plant Science

TYPE Original Research
PUBLISHED 29 May 2023
DOI 10.3389/fpls.2023.1186818

OPEN ACCESS

EDITED BY
Fahad Shafiq,
Government College University, Lahore, Pakistan

REVIEWED BY
Antonio Lupini,
Mediterranea University of Reggio Calabria, Italy
Shunfeng Ge,
Shandong Agricultural University, China
Hongmei Cai,
Huazhong Agricultural University, China

*CORRESPONDENCE
Fangren Peng
frpeng@njfu.edu.cn

RECEIVED 15 March 2023
ACCEPTED 27 April 2023
PUBLISHED 29 May 2023

CITATION
Chen M, Zhu K, Xie J, Liu J, Qiao Z, Tan P and Peng F (2023) Ammonium-nitrate mixtures dominated by NH_4^+-N promote the growth of pecan (*Carya illinoinensis*) through enhanced N uptake and assimilation. *Front. Plant Sci.* 14:1186818. doi: 10.3389/fpls.2023.1186818

Ammonium-nitrate mixtures dominated by NH_4^+-N promote the growth of pecan (*Carya illinoinensis*) through enhanced N uptake and assimilation

Mengyun Chen[1,2], Kaikai Zhu[1,2], Junyi Xie[1,3], Junping Liu[1,2], Zhenbing Qiao[1,2], Pengpeng Tan[1,2] and Fangren Peng[1,2]*

[1]College of Forestry, Nanjing Forestry University, Nanjing, China, [2]Co-Innovation Center for Sustainable Forestry in Southern China, College of Forestry, Nanjing Forestry University, Nanjing, China, [3]Department of Ecology, Nanjing Forestry University, Nanjing, China

Nitrogen (N) limits plant productivity, and its uptake and assimilation may be regulated by N sources, N assimilating enzymes, and N assimilation genes. Mastering the regulatory mechanisms of N uptake and assimilation is a key way to improve plant nitrogen use efficiency (NUE). However, it is poorly known how these factors interact to influence the growth process of pecans. In this study, the growth, nutrient uptake and N assimilation characteristics of pecan were analyzed by aeroponic cultivation at varying NH_4^+/NO_3^- ratios (0/0, 0/100,25/75, 50/50, 75/25,100/0 as CK, T1, T2, T3, T4, and T5). The results showed that T4 and T5 treatments optimally promoted the growth, nutrient uptake and N assimilating enzyme activities of pecan, which significantly increased aboveground biomass, average relative growth rate (RGR), root area, root activity, free amino acid (FAA) and total organic carbon (TOC) concentrations, nitrate reductase (NR), nitrite reductase (NiR), glutamine synthetase (GS), glutamate synthase (Fd-GOGAT and NADH-GOGAT), and glutamate dehydrogenase (GDH) activities. According to the qRT-PCR results, most of the N assimilation genes were expressed at higher levels in leaves and were mainly significantly up-regulated under T1 and T4 treatments. Correlation analysis showed that a correlation between N assimilating enzymes and N assimilating genes did not necessarily exist. The results of partial least squares path model (PLS-PM) analysis indicated that N assimilation genes could affect the growth of pecan by regulating N assimilation enzymes and nutrients. In summary, we suggested that the NH_4^+/NO_3^- ratio of 75:25 was more beneficial to improve the growth and NUE of pecan. Meanwhile, we believe that the determination of plant N assimilation capacity should be the result of a comprehensive analysis of N concentration, N assimilation enzymes and related genes.

KEYWORDS

pecan, nitrogen uptake and assimilation, NH_4^+–N, NO_3^-–N, gene expression

1 Introduction

Nitrogen (N) is the most important mineral nutrient required for plant growth and development (Guo et al., 2019). most nonlegume plants require their roots to take up 20-50 g N for every 1 kg of dry biomass produced (Xu et al., 2012). N fertilizer was the most widely used fertilizer in the world, and the suitable amount of N fertilizer can help improve crop yield and quality (Lu et al., 2021). However, the utilization efficiency of N fertilizer was very poor, with only about 30% (Guo et al., 2020). The loss of large amounts of N fertilizer has caused adverse effects such as land acidification, water pollution and greenhouse gas emissions (Qin et al., 2021). Therefore, improving N uptake and utilization by plants is important to promote better plant growth using less N fertilizer.

NH_4^+ and NO_3^- are the two main forms of N absorbed by plants, and studies have shown that the mixture of NH_4^+ and NO_3^- is more beneficial to promote plant growth and N uptake. The maximum biomass of C. *paliurus* (*Cyclocarya paliurus*) was reached when the NH_4^+: NO_3^- ratio was 50:50 (Qin et al., 2021, 2). And the mixed application of NH_4^+ and NO_3^- also increased the biomass, leaf area and TN concentration of black walnut (*Juglans nigra* L.) (Nicodemus et al., 2008). Zhang et al. (2007) showed that P, K^+, Ca^{2+}, and Mg^{2+} concentrations significantly varied under different N forms, while N forms affected the uptake of various mineral nutrients by plants in three main ways. Firstly, the N form can affect the absorption of mineral elements by regulating the balance of anions and cations (Egenolf et al., 2021), with antagonistic effects between NH_4^+ and cations and between NO_3^- and anions (M'rah Helali et al., 2010). Second, the intake of $NH_4^+$and NO_3^- by plants will change the pH of the medium, the absorption of NH_4^+ will acidify the medium, the absorption of NO_3^- will alkalize the medium, and the pH will directly affect the absorption of mineral elements (Zhao and Shen, 2018). Third, the uptake of NO_3^- by plants requires higher energy cost than the uptake of NH_4^+, which leads to slower absorption of other mineral elements (Tang et al., 2020).

Once NH_4^+ and NO_3^- enter the plant through root uptake, most NH_4^+ will be assimilated in the roots, while NO_3^- will be mainly assimilated in the leaves (Ruan et al., 2016). NO_3^- can be reduced to NO_2^- in the cytoplasm by nitrate reductase (NR), which is the rate-limiting and key enzyme of NO_3^- metabolism and is also involved in energy metabolism, water stress and photorespiration of plants (Polcyn and Garnczarska, 2009; Bloom, 2015). Subsequently, NO_2^- forms NH_4^+catalyzed by nitrite reductase (NiR). NR-related genes have two types, *Nia1*, which is specifically induced to be expressed by NADH, and *Nia2*, whose expression is based on NAD(P)H as a substrate (Harris et al., 2000). It was shown that deletion mutations in *AtNIA2* resulted in 90% reduction of NR activity in leaves, but *AtNIA1* and *AtNIA2* genes were overexpressed in the roots of NR-deficient mutants (Loqué et al., 2003). Loppes et al. (1999) found that *Nia* expression was down-regulated by the presence of NH_4^+, while NO_3^- and NO_2^- significantly up-regulated the expression of *Nia*. NiRs encoding genes include *nirS* and *nirK*, which encode heme *c* and heme d_1 (cd_1-Nir) and copper (Cu-Nir), respectively. *nirS* is more widely distributed than *nirK* (Priemé et al., 2002). At present, little research has been reported on the response of NiR to N morphology.

Glutamine synthetase (GS) is a key enzyme for N assimilation and reactivation, and it forms the GS-GOGAT cycle with glutamate synthase (GOGAT) (Li et al., 2017). NH_4^+ synthesizes a Glutamine (Gln) *via* GS with a glutamate (Glu), while Glu is synthesized by the action of Gln and two GOGAT. Meanwhile, glutamate dehydrogenase (GDH) located in mitochondria can also synthesize Glu directly using 2-ketoglutarate and NH_4^+ (Krapp, 2015). GS includes two isoforms, cytosolic GS1 and plastidic GS2, GS1 is the main enzyme in non-photosynthetic tissues or roots which is responsible for primary NH_4^+ assimilation in roots or for re-assimilation of NH_4^+ produced in leaves during protein turnover, while GS2 is mainly responsible for the assimilation of NH_4^+ produced by photorespiration in chloroplasts (Thomsen et al., 2014). GS-related genes in plants have two types, one is *Gln1* located in the cytoplasm and the other is *Gln2* in the chloroplast (Bernhard and Matile, 1994). *Gln1* was not induced by light and was mainly expressed in plant roots, while *Gln2* expression was induced by light and was majorly present in the aboveground of plants (Edwards and Coruzzi, 1989). In *Arabidopsis thaliana*, *GLN1;2* was significantly up-regulated in response to NH_4^+ induction (Guo et al., 2004), whereas *gln1;2* mutants exhibited lower GS activity and higher NH_4^+ concentrations in the presence of adequate NO_3^- supply (Lothier et al., 2011). Based on the electron donor, GOGAT can be divided into two types: ferredoxin-dependent (Fd-GOGAT) and NADH-dependent (NADH-GOGAT) enzymes (Li et al., 2017). *GLU1* and *GLU2* are two Fd-GOGATs identified in *Arabidopsis*, while *GLU1* plays a main role in photorespiration and N assimilation in leaves, *GLU2* may play a major role in primary N assimilation in roots (Coschigano et al., 1998). *GLT* is the only *NADH-GOGAT* gene in *Arabidopsis* that functions in non-photosynthetic NH_4^+ assimilation and Glu synthesis (Lancien et al., 2002).

The pecan [*Carya illnoinensis* (Wangenh.) K. Koch] is a member of the Juglandaceae family. Pecans have thin shells and full, sweet kernels, which makes them a world-renowned economic tree (Zhu et al., 2020). However, pecans have the same problem of low nitrogen use efficiency (NUE) in cultivation, and hardly any relevant reports are available. Therefore, in this experiment, pecan seedlings were used as materials to study the effects of different NH_4^+: NO_3^- ratios on their growth and development and N assimilation. Specifically, biomass, leaf area, root growth, mineral element content, N uptake, N assimilation enzymes, and expression of related genes were measured to address the following questions: (A) Which NH_4^+: NO_3^- ratio is more helpful to enhance the growth and NUE of pecan seedlings under certain N concentration? (B) How N assimilation genes, N assimilation enzymes, and N interact to affect the growth and development of pecan?

2 Material and methods

2.1 Plant material and experimental design

This experiment was conducted in the underground greenhouse of Nanjing Forestry University from April 18, 2021 to June 9, 2021. The seedlings of pecan "Pawnee" seeds were used as experimental materials. The seedlings with a height of about 25 cm were selected, and the roots were cleaned and disinfected for indoor aeroponic cultivation trials. Each treatment had 18 seedlings, arranged according to a randomized complete block design. Greenhouse conditions were as follows: natural light, 12h/12h day/night, day and night temperature of 30/25°C, relative humidity of 70% ± 5%. The nutrient solution was modified Hoagland nutrient solution. The formula was as follows: 1.25 mM $Ca(NO_3)_2$, 0.5 mM $Ca(H_2PO_4)_2$, 1.0 mM K_2SO_4, 0.5 mM $MgSO_4$, 1.0 μM $ZnSO_4$, 12.5 μM H_3BO_3, 1.0 μM $MnSO_4$, 0.25 μM $CuSO_4$, 0.1 μM $(NH_4)_6Mo_7O_{24}$, 10 μM EDTA-Fe. The pH was adjusted to approximately 6.0 every other day with 24 h aeration, and the nutrient solution was replaced every 7 days. The seedlings were precultured with 1/4 nutrient solution for one week, and then cultured in total nutrient solution for experimental treatment. The nitrogen concentration in the nutrient solution was 2 mM. Based on the same N supply, the five ammonium-nitrate ratios (NH_4^+: NO_3^-) were 0:100, 25:75, 50:50, 75:25, and 100:0, corresponding to T1, T2, T3, T4, and T5, respectively. The nutrient solution without N was used as the control (CK), and each treatment was repeated 3 times, each with 6 seedlings. $(NH_4)_6Mo_7O_{24}$ was replaced by $(Na)_6Mo_7O_{24}$, $(NH_4)_2SO_4$ was used as the ammonium source, and $Ca(NO_3)_2$ was used as the nitrate source. Samples were taken after 45 days of treatment for further determination.

2.2 Measurements

2.2.1 Growth parameters

To evaluate the effects of different N forms on the growth of pecans, pecan seedlings cultivated for 45 d under different treatments were used for the determination of growth indicators. Aboveground and underground biomass (g), which were measured by weighing. Leaf area (mm^2), which was measured by weighing method and LI-3000 leaf areometer. Pecan roots were scanned with a digital scanner (STDl600EpsonUSA) and root length, root surface area, and root volume were determined with winRhizo root analysis software. Root activity (mg g^{-1} h^{-1}) was determined by TTC redox method (Stūrīte et al., 2005). And the average relative growth rate (RGR) (g g^{-1} d^{-1}) calculation formula is as follows:

$$RGR = (\ln W2 - \ln W1)/\Delta t$$

Where W1 and W2 represent the total pecan biomass (g) of the same plant before and after treatment, respectively. Δt denotes the time interval (d) between the two measurements.

2.2.2 Biochemical traits

To evaluate the effects of different N forms on the biochemical traits of pecan seedlings, Total nitrogen (TN), total phosphorus (TP), and total potassium (TK) concentrations, which were determined by $HClO_4$-H_2SO_4 decoction method. The total organic carbon (TOC) concentrations were determined by $K_2Cr_2O_7$ volumetric and external heating method. And free amino acid (FAA) concentration measurements refer to GB/T 8312-87 to GB/T 8314-87.

2.2.3 Nitrogen assimilation

To evaluate the effect of different N forms on the nutrient absorption of pecans, the nitrate reductase (NR), nitrite reductase (NiR), glutamine synthetase (GS), glutamate synthase (Fd-GOGAT and NADH-GOGAT), and glutamate dehydrogenase (GDH) activity in roots and leaves were determined by enzyme activity kit (Jiancheng, Nanjing, China). NR catalyzes the reduction of NO_3^- to NO_2^- by NADH, and the NR activity was expressed by measuring the NADH reduction rate. NiR reduces NO_2^- to NO, and the NiR activity was calculated according to the reduction rate of NO_2^-. In the presence of ATP and Mg^{2+}, GS catalyzes NH_4^+ and glutamic acid to synthesize glutamine, which is further converted into γ-glutamyl hydroxamic acid. The complex formed under acidic conditions was measured to calculate GS activity. Fd-GOGAT catalyzes the transfer of the amino group of glutamine to α-ketoglutarate and forms glutamic acid. The dehydrogenation of glutamic acid produces NADH, which makes WST-8 orange-yellow. The absorbance value was measured to indicate Fd-GOGAT activity. NADH-GOGAT catalyzes the transfer of the amino group of glutamine to α-ketoglutarate to form glutamic acid, while NADH is oxidized to NAD^+. The NADH-GOGAT activity was reflected by measuring the NADH decline rate. GDH catalyzes NH_4^+, α-ketoglutarate and NADH to produce glutamic acid and NAD^+, and GDH activity was expressed by measuring the rate of NADH reduction.

2.2.4 Expression analysis

According to the manufacturer's protocol, the total RNA was extracted from the leaves and roots of pecan using a Universal Plant Total RNA Extraction Kit (Bioteke, Beijing, China) and stored at -80° C until further use. The purity and integrity of the isolated total RNA was analyzed by agarose gel electrophoresis and Nanodrop 2000 spectrophotometer (Thermo Scientific, Wilmington, NC, USA). First-strand cDNA was synthesized using a cDNA Synthesis Kit (HiScript ®RIII RT SuperMix for qPCR +gDNA wiper, Vazyme, Nanjing, China). The qRT-PCR was performed on a 7500 Real-Time PCR system (Applied BiosystemsTM, Foster City, CA, USA) using a Taq Pro Universal SYBR qPCR Master Mix (Vazyme, Nanjing, China). The specific primers were synthesized by Tsingke Biotechnology Ltd (Nanjing, China), the details of the primers were provided in Table 1, melting curve analyses were used to verify the efficiency of the primers (Supplementary Figure S1). The Actin gene was used as an internal reference gene (Zhu et al., 2022), and the relative expression levels of pecan Nia, NiR, Gln, GOGAT, and GDH genes were determined using the $2^{-\Delta\Delta Ct}$ method (Livak and Schmittgen, 2001). Values represent mean calculated from three biological replicates and three technological repeats. The pecan N assimilate genes were renamed according to the *Arabidopsis* gene name and the NCBI pblast results.

TABLE 1 The sequences of primers used for qPCR.

No.	Gene Name	Gene ID	Forward Primer Sequence(5′-3′)	Reverse Primer Sequence(5′-3′)
1	CiNia2a	CiPaw.05G228100	ACGCGTATTCGGTATTGCAG	CACGAGTCACTTTCCTCCCC
2	CiNia2b	CiPaw.06G025400	AAACTCGTGGACAACGCAGA	CACTTTTCTCCCACCTCCAGAA
3	CiNiR1a	CiPaw.05G006800	GGTCCAAGCAGACGACATGA	GCTCCACAATGAGCTGGAGT
4	CiNiR1b	CiPaw.06G172200	CCCAAAAGCAGCTGGAGAGA	TGCTTCTGTGGATGGACACC
5	CiGln2a	CiPaw.01G157900	CATCCGCCATTCCTGATCTGA	CCCCACATCTTTGCTGTCGT
6	CiGln2b	CiPaw.02G090300	TTGTAAGGGCTTCCCCCACC	CTGTGCCATTTTCACCTCGG
7	CiGln1.2	CiPaw.16G097000	CGCTAAAATCGCCTGTTGGG	ACCCGATCCACCGATCCATA
8	CiFd-GOGATa	CiPaw.09G047200	TGTGGCGTCGTGGAATGTAA	TGGCGTCTACGACCTTTCAC
9	CiFd-GOGATb	CiPaw.10G039900	GACGTCTTCGGCCGTCAA	CCAAGTTTGCAACCCTCGGTC
10	CiNADH-GOGAT	CiPaw.05G252100	CTCTGTCCGCAAGGACTGTT	TCAGGGCCATGTAGCTCGTA
11	CiGDHa	CiPaw.02G142100	AAGGAGTGTCCTGAAGCTTTG	GCACGGGCATTATTGTAAGAG
12	CiGDHb	CiPaw.01G227200	CTCAACGACCAGACGGAGAC	ACCTGCAGCACTCAACTCAAT
13	Actin	CiPaw.03G124400	ACAGGGAGAAGATGACTCAAATC	CACTGGCATACAGAGAGAGAAC

2.3 Data analysis

Before analysis of variance (ANOVA), data were checked for normality and homogeneity of variances. One-way ANOVA was performed to test the effects of different N forms on biomass, leaf area, root growth, N uptake rate, and N transport capacity of pecan. Two-way ANOVA was performed to test the effects of N form, organ and their interactions on the nutrients, enzyme activity and gene expression of pecan. Differences were considered significant at $p<0.05$. Correlation analysis was used to test the correlations between the growth and N assimilation indicators. Partial least squares path model (PLS-PM) was used to analyze the role between N assimilation genes, N assimilation enzymes, plant nutrients and growth. Finally, principal component analysis (PCA) was carried out on 20 indicators of N assimilation, determining the number of principal components according to characteristic values and cumulative contribution rates and calculating principal component scores based on factor scores (Rahmani and Atia, 2017).

All statistical analyses were performed with SPSS 23.0 software (Version 23.0, Chicago, IL, USA) and r4.2.1, the partial least squares path model was constructed using the "plspm" package (Latan and Noonan, 2017). All charts were drawn with r4.2.1 and SigmaPlot (Version 14.0, Barcelona, Spain).

3 Results

3.1 Growth analysis of pecan under different N forms

To explore the effect of different N forms on the growth characteristics of pecan, we analyzed pecan biomass, leaf area and root growth under different N forms (Figure 1, 2). The results showed that the leaf area of pecan was not significantly affected by different N form treatments (Figure 1A). T4 and T5 significantly increased aboveground biomass of pecan ($p< 0.05$), other treatments were not significantly different from CK (Figure 1B). However, there was no significant effect of N form on underground biomass of pecan (Figure 1C). T4 and T5 were significantly increased the RGR of pecan ($p< 0.05$), other treatments were not significantly different from CK (Figure 1D). T4 and T5 significantly increased the root length ($p< 0.05$), while the other treatments were not significantly different from CK (Figure 2A). Both T1-T5 treatments significantly increased root area and root activity compared to CK ($p< 0.05$) (Figures 2B, D). T2 and T4 significantly increased the root volume ($p< 0.05$), while the other treatments were not significantly different from CK (Figure 2C). T3 and T5 treatments significantly increased SRL ($p< 0.05$), and T1, T2, and T4 treatments were not significantly different from CK (Figure 2E). Different N forms had no significant effect on RMR of pecan (Figure 2F).

3.2 Analysis of N uptake and transport of pecan under different N forms

To study the effect of different N forms on the N uptake and assimilation of pecan, we analyzed the TN concentration in all organs of pecan under different N forms (Table 2, Figure 3). According to Table 2, we found that both N form and plant organ had a highly significant effect on TN ($p< 0.01$), but the interaction between them had no significant effect on TN. The TN concentrations in pecan leaves were greater than that in the stems and roots (Figure 3A). In leaves, T1, T3, and T4 treatments were not significantly different but significantly greater than CK ($p< 0.05$), and T2 and T5 were not significantly different from CK (Figure 3A). In the stems, the T4 was significantly higher than the other

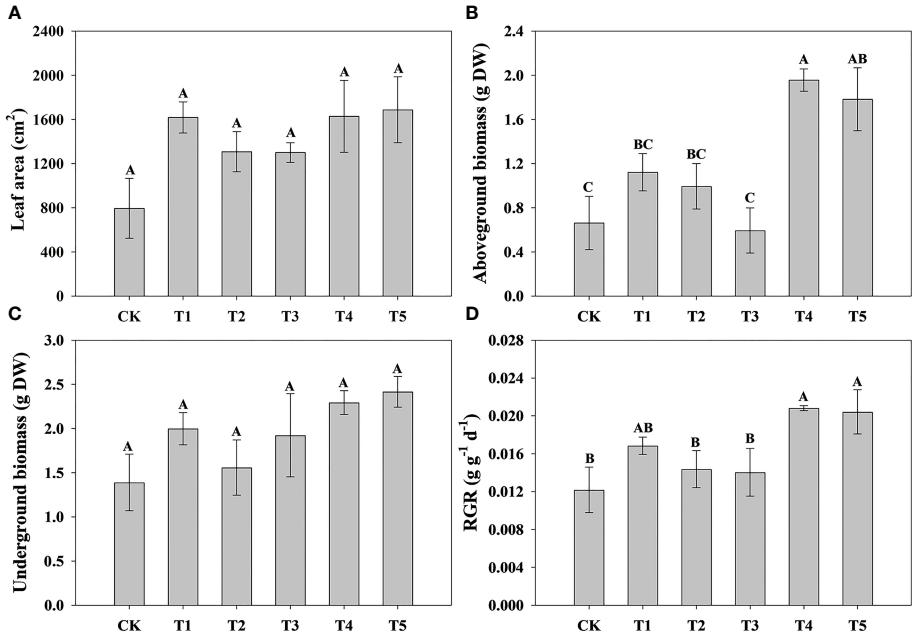

FIGURE 1
Analysis of leaf area and biomass of pecan under different N forms. Leaf area of pecan under different N forms **(A)**. Aboveground biomass of pecan under different N forms **(B)**. Underground biomass of pecan under different N forms **(C)**. RGR of pecan under different N forms **(D)**. Uppercase letters indicate differences between N form treatments, at $p< 0.05$. RGR, average relative growth rate; DW, dry weight.

treatments ($p< 0.05$), and there was no significant difference between other treatments (Figure 3A). In the roots, the difference between treatments was not significant (Figure 3A). According to the mean value of pecan leaf, stem, and root, the T4 was significantly higher than CK ($p< 0.05$), and they were not significantly different from the other treatments (Figure 3B). T4 treatment significantly increased the NUE of leaves and stems ($p< 0.05$), and the average NUE of leaves, stems, and roots also showed that T4 treatment was significantly higher than T1, T2, and T3 treatments ($p< 0.05$) (Figures 3C, D). Both N form treatments were significantly increased N uptake rate of pecan ($p< 0.05$), with the most significant being the T4 treatment (Figure 3E). surprisingly, the N uptake rate of pecan under CK was negative, indicating that the N efflux from pecan was greater than the influx under CK (Figure 3E). Both N forms and CK treatment had no significant effect on N transport capacity of pecan (Figure 3F).

3.3 Analysis of FAA, TP, TK, and TOC concentration of pecan under different N forms

To study the effect of different N forms on the FAA and nutrient elements of pecan, we analyzed the FAA, TP, TK, and TOC concentration in all organs of pecan under different N forms (Table 2, Figure 4). We found that N form had a highly significant effect on TK ($p< 0.01$) and a significant effect on FAA and TP ($p< 0.05$), plant organ had a strongly significant effect on FAA ($p< 0.01$), neither N form nor plant organ had a significant effect on TOC, and the interaction between them had no significant effect on FAA and all nutrient elements (Table 2). We found that FAA concentrations were highest in the leaves of pecan (Figure 4A). In the leaves, the FAA concentrations of pecan under T4 and T5 were significantly greater than CK ($p< 0.05$), and T1, T2, and T3 were not significantly different from other treatments (Figure 4A). In the stems, the FAA concentrations of pecan under T1, T3, and T5 were significantly greater than CK and T4 ($p< 0.05$), and T2 was significantly greater than CK ($p< 0.05$) and not significantly different from the other treatments (Figure 4A); The TP concentrations under T1, T2, and T4 were significantly greater than CK ($p< 0.05$), and T3 and T5 were not significantly different from the other treatments (Figure 4B). In the roots, the FAA concentrations were significantly greater under T3 and T4 than CK and T5 ($p< 0.05$), and T1 and T2 were not significantly different from the other treatments(Figure 4A); The TP concentrations under T4 were significantly greater than the other treatments ($p< 0.05$) (Figure 4B); The TK concentrations under T1 were significantly greater than CK and T5 ($p< 0.05$), and T2, T3, and T4 were not significantly different from the other treatments (Figure 4C); The TOC concentrations under T4 were significantly greater than CK ($p< 0.05$), and T1, T2, T3, and T5 were not significantly different from the other treatments (Figure 4D). According to the mean value of pecan leaf, stem, and root, the FAA concentrations of pecan under T1, T3, T4, and T5 were significantly greater than CK ($p< 0.05$), and T2 was not significantly different from the other treatments (Figure 4A); the TP concentrations of pecan under T3 and T5 were significantly greater than CK ($p< 0.05$), and T1, T2, and T4 were

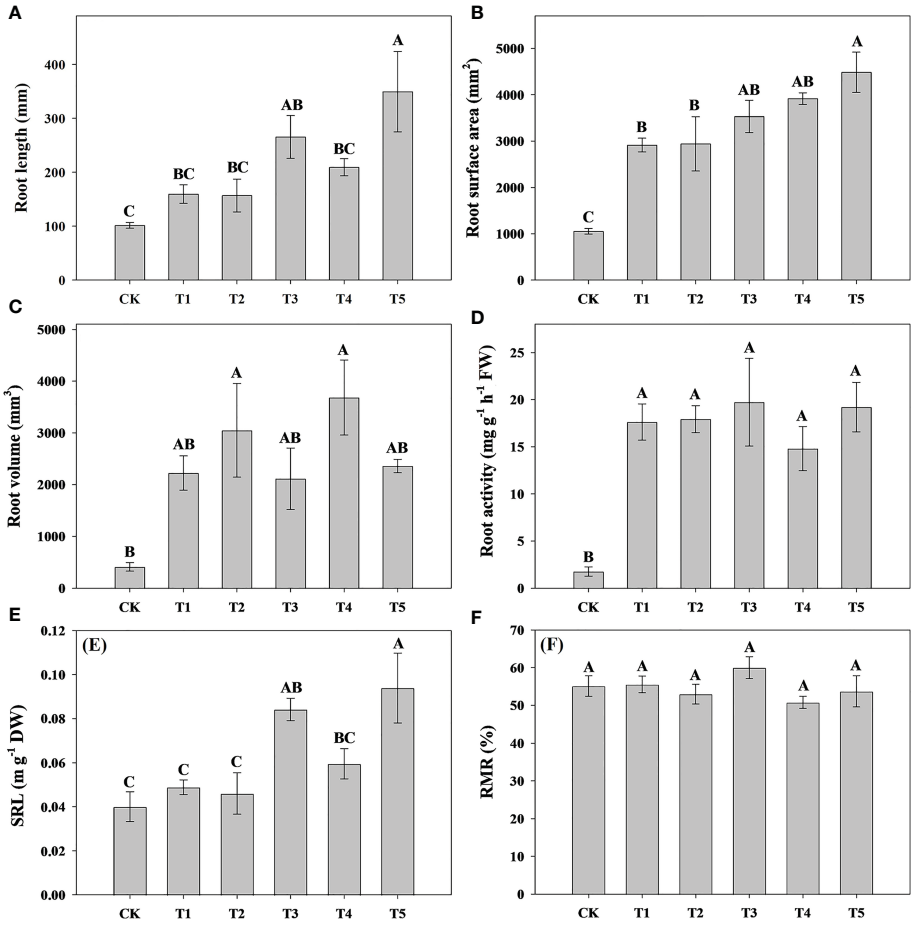

FIGURE 2
Analysis of root length, root surface area, root volume, and root activity of pecan under different N forms. Root length of pecan under different N forms **(A)**. Root surface area of pecan under different N forms **(B)**. Root volume of pecan under different N forms **(C)**. Root activity of pecan under different N forms **(D)**. SRL of pecan under different N forms **(E)**, SRL is the ratio of root length to root biomass. RMR of pecan under different N forms **(F)**, RMR is the ratio of root biomass to whole plant biomass. Uppercase letters indicate differences between N form treatments, at $p< 0.05$. SRL, specific root length; RMR, root mass ratio; FW, fresh weight; DW, dry weight.

not significantly different from the other treatments (Figure 4B); the TK concentrations of pecan under T2 and T3 were significantly greater than CK ($p< 0.05$), and T1 and T4 were not significantly different from the other treatments (Figure 4C); the TOC concentrations of pecan under T4 and T5 were significantly greater than CK ($p< 0.05$), and T1, T2, and T3 were not significantly different from the other treatments (Figure 4D).

3.4 Analysis of N assimilation-related enzyme activity of pecan under different N forms

To research the effect of N form on N assimilation in pecan, we analyzed the N assimilation-related enzyme activity in leaves and roots of pecan under different N forms (Figure 5). In the leaves, the NR activity under T4 and T5 was significantly greater than CK and

TABLE 2 ANOVAs on the effects of N form and organ on FAA and nutrient elements in pecan.

	TN		FAA		TP		TK		TOC	
Effects	F	*p*	F	*p*	F	*p*	F	*p*	F	*p*
N form	4.122	< **0.01**	3.122	**0.026**	2.664	**0.047**	5.852	< **0.01**	0.648	0.665
Organ	61.638	< **0.01**	42.687	< **0.01**	0.036	0.965	0.942	0.404	1.858	0.178
N form and Organ	1.478	0.208	1.583	0.172	2.090	0.068	0.923	0.529	0.463	0.897

The correlation reached a significant level ($p< 0.05$), and the correlation was extremely significant ($p< 0.01$). Significant results are shown in bold. TN, Total nitrogen; FAA, Free amino acid; TP, Total phosphorus; TK, Total potassium; TOC, Total organic carbon.

T2 ($p< 0.05$), and T1 and T3 were not significantly different from the other treatments (Figure 5A); the NiR activity under T1, T2, and T4 was significantly greater than CK and T5 ($p< 0.05$) (Figure 5B); the GS activity under all N form treatments was significantly greater than CK ($p< 0.05$) (Figure 5C); the F-GOGAT activity under T3, T4, and T5 was significantly greater than CK, T1, and T2 ($p< 0.05$), and CK, T1, and T2 treatments were not significantly different from each other, and T4 treatment was significantly greater than T3 and T5 ($p< 0.05$) (Figure 5D).The NADH-GOGAT activity under T1, T2, T4, and T5 was significantly greater than CK ($p< 0.05$), and T3 was not significantly different from the other treatments (Figure 5E); the GDH activity under T4 and T5 was significantly greater than CK, T1, T2, and T3 ($p< 0.05$) (Figure 5F). In the roots, the NR activity under T4 was significantly greater than CK, T1, T3, and T5 ($p< 0.05$), and T2 was not significantly different from the other treatments (Figure 5A); the NiR activity under T1, T2, T3, and T4 was significantly greater than CK and T5 ($p< 0.05$) (Figure 5B); the GS activity under T2, T4, and T5 was significantly greater than CK and T1 ($p< 0.05$), and CK, T1, and T3 were not significantly different from each other (Figure 5C); the Fd-GOGAT activity under T1, T3, and T4 treatments was significantly greater than CK, T2, and T5 ($p< 0.05$), and T1, T3, and T4 treatments were not significantly different from each other, and CK and T5 treatments had no significantly difference and less significantly than T2 ($p<$

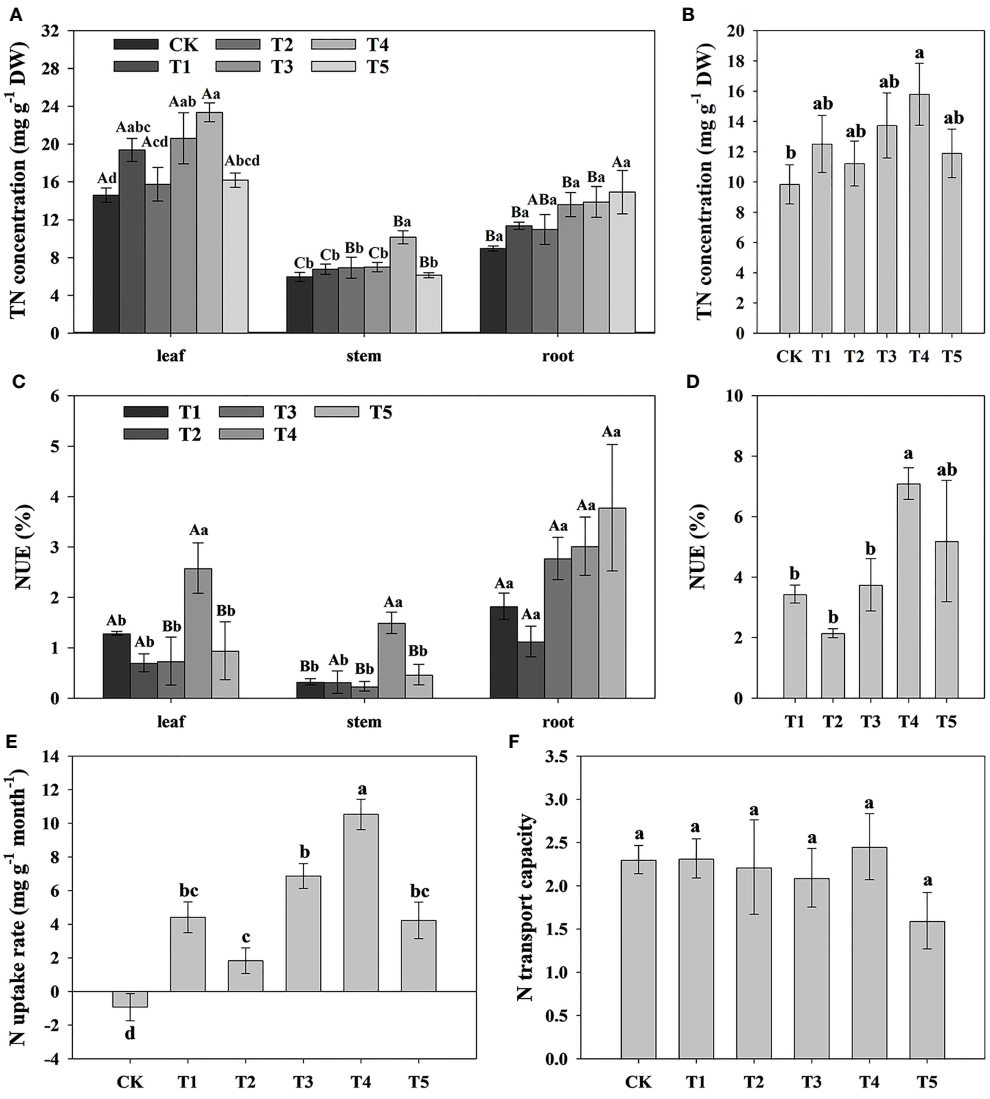

FIGURE 3
Analysis of N uptake rate and N transport capacity of pecan under different N forms. TN concentrations in leaves, stems and roots of pecan under different N forms **(A)**. The mean level of TN concentrations of pecan leaves, stems and roots under different N forms **(B)**. NUE of leaves, stems and roots of pecan under different N forms **(C)**, NUE was measured by the ratio of the difference between the TN accumulation of the N application treatment and the TN accumulation of the CK treatment to the total N application. The sum of NUE of pecan leaves, stems and roots under different N forms **(D)**. N uptake rate of pecan under different N forms **(E)**, N uptake rate was measured by the ratio of the differential of TN concentration before and after fertilization to the time. N transport capacity of pecan under different N forms **(F)**, N transport capacity was measured by the ratio of TN concentration in the aboveground and underground of the plant. Uppercase letters indicate differences between organs, and lowercase letters indicate differences between NH_4^+: NO_3^- treatments, at $p< 0.05$. TN, Total nitrogen; NUE, nitrogen use efficiency; DW, dry weight.

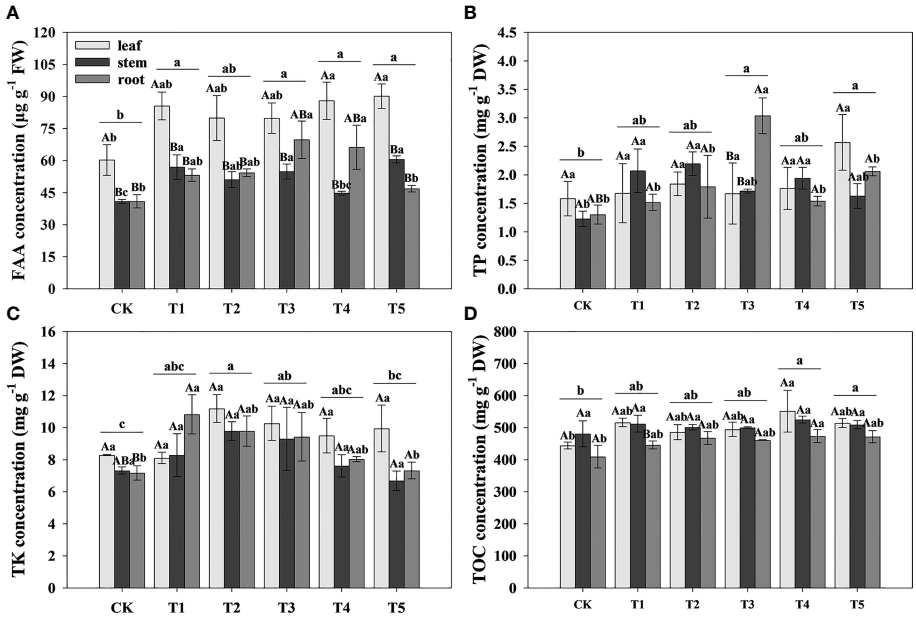

FIGURE 4
Analysis of FAA and nutrient elements concentration of pecan under different N forms. FAA concentrations in leaves, stems and roots of pecan under different N forms **(A)**. TP concentrations in leaves, stems and roots of pecan under different N forms **(B)**. TK concentrations in leaves, stems and roots of pecan under different N forms **(C)**. SOC concentrations in leaves, stems and roots of pecan under different N forms **(D)**. Uppercase letters indicate differences between organs, and lowercase letters indicate differences between NH_4^+: NO_3^- treatments, at $p< 0.05$. FAA, Free amino acid; TP, Total phosphorus; TK, Total potassium; TOC, Total organic carbon; FW, fresh weight; DW, dry weight.

0.05) (Figure 5D); the NADH-GOGAT activity under T4 was significantly greater than the other treatments ($p< 0.05$) (Figure 5E); the GDH activity under T1, T2, and T4 was significantly greater than CK ($p< 0.05$), and T3 and T5 were not significantly different from CK (Figure 5F).

3.5 Analysis of N assimilation genes expression of pecan under different N forms

To further investigate the effect of N form on N assimilation in pecan, we analyzed the N assimilation enzyme-related genes in leaves and roots of pecan under different N forms (Figure 6). In the leaves, the expression levels of *CiNia2a*, *CiGln1.2*, *CiGln2b*, *CiFd-GOGATb*, and *CiNADH-GOGAT* under T1 were significantly up-regulated ($p< 0.05$); the expression levels of *CiNia2b*, *CiNiR1a*, *CiNiR1b*, *CiGln2a*, *CiFd-GOGATb*, and *CiGDHa* under T4 were significantly up-regulated ($p< 0.05$); the expression levels of *CiFd-GOGATa* under T1, T4, and T5 were significantly up-regulated ($p< 0.05$); and the expression levels of *CiGDHb* under T1 and T4 were significantly up-regulated ($p< 0.05$). In the roots, the expression levels of *CiNia2a*, *CiNia2b*, *CiNiR1a*, *CiNiR1b*, *CiGln2a*, *CiFd-GOGATb*, *CiNADH-GOGAT*, and *CiGDHa* under T4 were significantly up-regulated ($p< 0.05$); the expression levels of *CiGln1.2*, *CiGln2b*, and *CiFd-GOGATa* under CK were significantly up-regulated ($p< 0.05$); and the expression levels of *CiGDHb* under T1 and T3 were significantly up-regulated ($p< 0.05$).

3.6 Correlation analysis of N assimilation genes with growth and N assimilation enzymes in pecan

Correlation analysis showed that most of the N assimilate enzyme genes were positively correlated with growth and N assimilate enzymes in pecan (Figure 7). Leaf area was significantly positively correlated with *CiNADH-GOGAT* ($p< 0.05$). Root length was significantly positively correlated with *CiNiR1b*, *CiFd-GOGATa*, and *CiGDHb* ($p< 0.05$), and highly significantly positively correlated with *CiGln2a*, *CiFd-GOGATb*, and *CiGDHa* ($p< 0.01$). Root surface area was significantly positively correlated with *CiNiR1b*, *CiGln2a*, and *CiGDHb* ($p< 0.05$), and highly significantly positively correlated with *CiGDHa* and *CiFd-GOGATb* ($p< 0.01$). SRL was significantly positively correlated with *CiNiR1b*, *CiGln2a*, and *CiGDHb* ($p< 0.05$), and highly significantly positively correlated with *CiFd-GOGATa*, *CiFd-GOGATb*, and *CiGDHa* ($p< 0.01$). TN was significantly positively correlated with *CiNiR1b*, *CiGln2a*, and *CiGDHb* ($p< 0.05$), and extremely significantly positively correlated with *CiFd-GOGATa*, *CiFd-GOGATb*, and *CiGDHa* ($p< 0.01$). NR was highly significantly positively correlated with *CiNiR1b*, *CiGln1.2*, *CiGln2a*, *CiGln2b*, *CiFd-GOGATa*, *CiFd-GOGATb*, *CiNADH-GOGAT*, *CiGDHa*, and *CiGDHb* ($p< 0.01$). NiR was significantly positively correlated with *CiNiR1b*, *CiFd-GOGATa*, and *CiGDHb* ($p< 0.05$), and extremely significantly positively correlated with *CiGln2a*, *CiFd-GOGATb*, and *CiGDHa* ($p< 0.01$). GS was significantly positively correlated with *CiGln2b* ($p< 0.05$), and extremely significantly positively

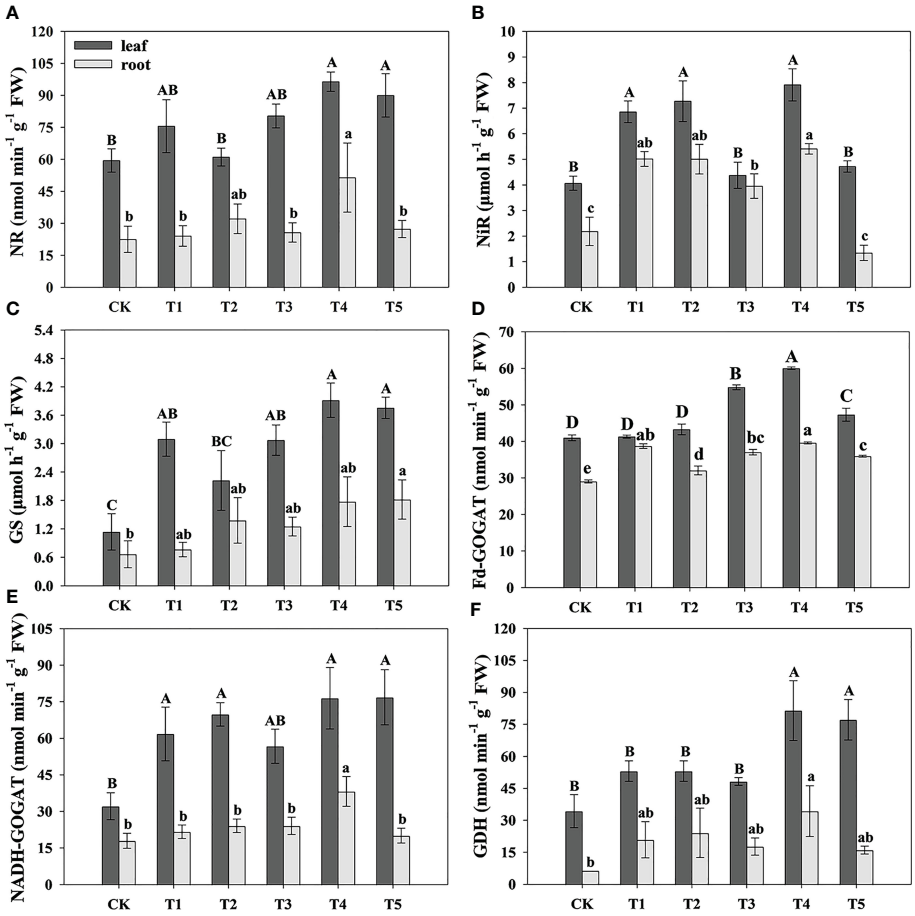

FIGURE 5
Analysis of N assimilation-related enzymes activity of pecan under different N forms. NR activity in leaves and roots of pecan under different N forms **(A)**. NiR activity in leaves and roots of pecan under different N forms **(B)**. GS activity in leaves and roots of pecan under different N forms **(C)**. GOGAT activity in leaves and roots of pecan under different N forms **(D)**. GDH activity in leaves and roots of pecan under different N forms **(E)**. Uppercase letters indicate differences between organs, and lowercase letters indicate differences between NH_4^+: NO_3^- treatments, at $p< 0.05$. NR, Nitrate reductase; NiR, Nitrite reductase; GS, Glutamine synthetase; GOGAT, Glutamate synthase; GDH, Glutamate dehydrogenase.

correlated with *CiNiR1b*, *CiGln2a*, *CiFd-GOGATa*, *CiFd-GOGATb*, *CiNADH-GOGAT*, *CiGDHa*, and *CiGDHb* ($p< 0.01$). Fd-GOGAT was significantly positively correlated with *CiNiR1b*, *CiGln2a*, and *CiFd-GOGATa* ($p< 0.05$), and highly significantly positively correlated with *CiGDHa* and *CiFd-GOGATb* ($p< 0.01$). GDH was significantly positively correlated with *CiNiR1b*, *CiGln2a*, and *CiGDHb* ($p< 0.05$), and highly significantly positively correlated with *CiFd-GOGATa*, *CiFd-GOGATb*, and *CiGDHa* ($p< 0.01$).

3.7 The partial least squares path model analysis

The partial least squares path model (PLS-PM), which has been widely used to study complex multivariate relationships among variables (Latan and Noonan, 2017), was performed to infer potential direct and indirect effects of N assimilation genes, N assimilation enzymes, and nutrients factors on growth of pecan (Figure 8). The PLS-PM differs from the conventional covariance-based path analysis, and does not impose any distributional assumptions on the data which is usually difficult to meet. According to the results of PLS-PM analysis, plant nutrients had the main direct contribution to pecan growth, with TN, FAA, and TOC having the largest contribution to plant nutrients (contribution ratio > 0.8). N assimilation genes had a direct contribution to N assimilatory enzyme activity, with *CiNiR1b*, *CiGln2a*, *CiGDHa*, *CiGDHb*, *CiFd-GOGATa*, *CiFd-GOGATb*, and *CiNADH-GOGAT* contributing more to N assimilation genes (contribution ratio >0.8). In addition, N assimilating enzymes were positively regulating pecan growth and nutrients, with GS, Fd-GOGAT, and NADH-GOGAT contributing more to N assimilating enzymes (contribution ratio >0.8). The main effect analysis showed that N assimilating enzymes had the greatest total effect on pecan growth.

3.8 Comprehensive evaluation of N assimilation of pecan

In order to objectively evaluate the effects of the NH_4^+:NO_3^- treatments on the N assimilation, a principal component analysis

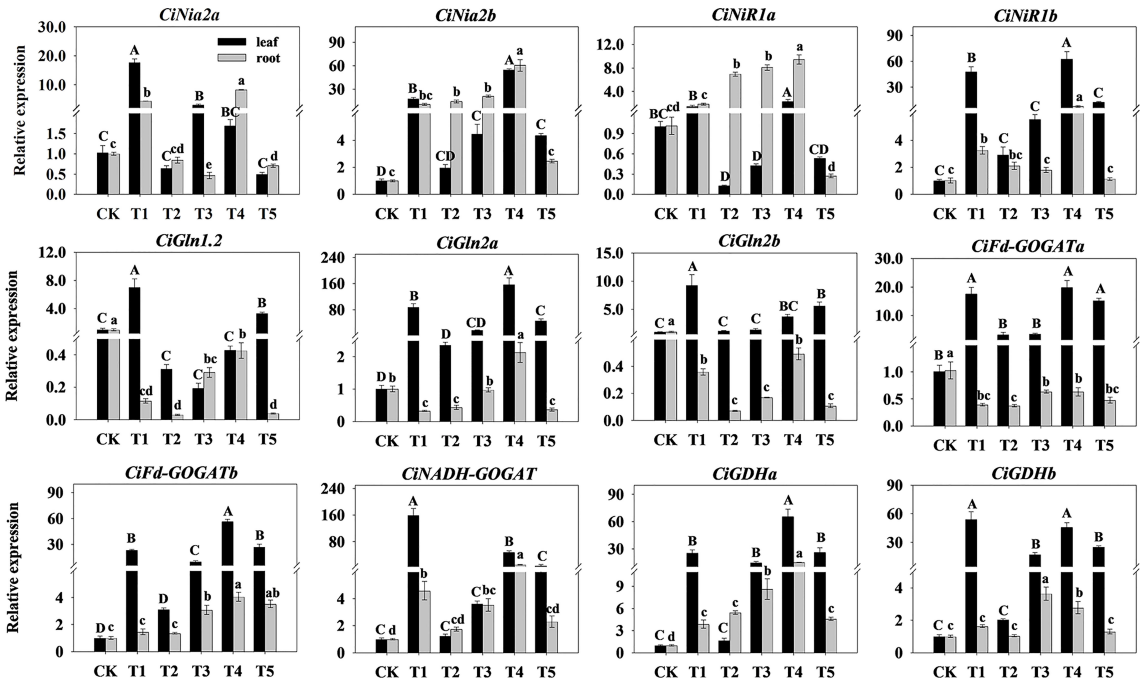

FIGURE 6
Relative expression of N assimilation-related enzymes genes in pecan under different N forms. The expression levels of *CiNia*, *CiNiR*, *CiGln*, *CiGOGAT*, and *CiGDH* genes in leaves and roots of pecan after varying NH_4^+: NO_3^- ratio treatments were quantified by qRT-PCR, with *Actin* as the reference gene. Different capital letters indicate significant differences in leaves ($p< 0.05$), and different lowercase letters indicate significant differences in roots ($p< 0.05$).

was performed on 20 N assimilation traits, and the two principal components with the largest eigenvalues were obtained. The eigenvalues of the first and second principal components were 11.261 and 4.194, respectively. The cumulative contribution of the two principal components was 77.276% (Table 3), suggesting that the common factor can contain 77.276% of the original data information without losing variables. The factor loadings of the first and second principal components were performed on the X-axis and Y-axis, respectively (Figure 9). In the first principal component, the indexes with higher load (> 0.7) were TN, N uptake rate, *CiNia2b*, *CiNiR1b*, *CiGln2a*, *CiFd-GOGATa*, *CiFd-GOGATb*, *CiGDH1a*, *CiGDH1b*, NR, and Fd-GOGAT, indicating that the main factors determining the first principal component. In the second principal component, the indicators with larger load (> 0.7) were *CiNia2a*, *CiGln1.2*, *CiGln2b*, and *CiNADH-GOGAT*, which were the main factors determining the second principal component. We weighted the contribution of the principal components to calculate the combined scores under different NH_4^+: NO_3^- treatments, and then ranked (Table 4). The results showed that the comprehensive scores of the different treatments were T4 > T1 > T5 > T3 > T2 > CK. Except for T1 and T4 treatments, the scores of all other treatments were negative, indicating that T4 had a better promoting effect on the N assimilation of pecan seedlings than did the other treatments.

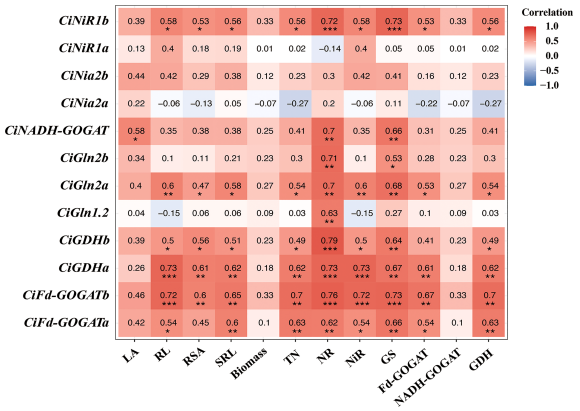

FIGURE 7
Correlation analysis of growth physiological indexes of pecan. *$p<$ 0.05; **$p<$ 0.01; ***$p<$ 0.001. LA, Leaf area; RL, Root length; RSA, Root surface area; SRL, specific root length; TN, Total nitrogen; NR, Nitrate reductase; NiR, Nitrite reductase; GS, Glutamine synthetase; GOGAT, Glutamate synthase; GDH, Glutamate dehydrogenase.

4 Discussion

4.1 Effects of N forms on the growth and nutrient accumulation of pecan

The application of N fertilizer is an important way to improve the productivity of cash crops (Negrini et al., 2020). However, the effect of different forms of N fertilizer on plant growth is different (Nicodemus et al., 2008; Lang et al., 2018; Qin et al., 2020). We found that the ammonium-nitrate mixture promoted the growth and nutrient

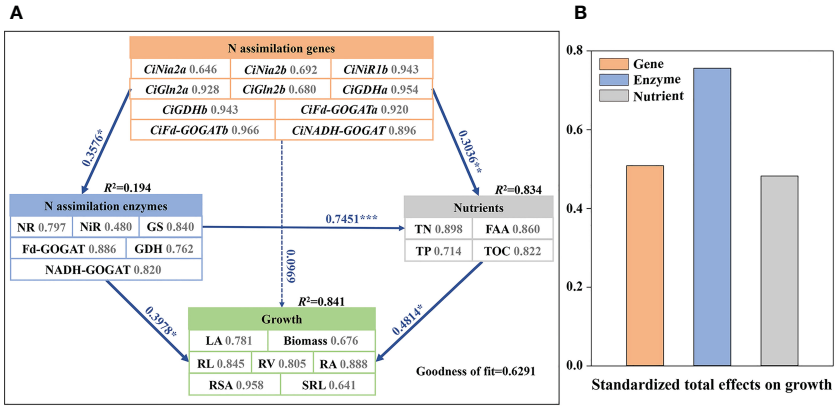

FIGURE 8
The partial least squares path models **(A)**. The partial least squares path models showing the effects of N assimilation genes, N assimilation enzymes, and nutrients on growth in pecan. The blue and red lines indicate positive and negative effects, respectively. Numbers adjacent to each arrow denote partial correlation coefficients (significance codes: ***p< 0.001, **p< 0.01, *p< 0.05). The number next to each indicator represents the contribution of each predictor variable to the latent variable. R^2 values display the proportion of variance explained for each factor. **(B)**. The bar chart showing the standardized total effect of each factor on the growth composition in pecan. NR, Nitrate reductase; NiR, Nitrite reductase; GS, Glutamine synthetase; GOGAT, Glutamate synthase; GDH, Glutamate dehydrogenase; TN, Total nitrogen; TP, Total phosphorus; FAA, Free amino acid; TOC, Total organic carbon; LA, Leaf area; SRL, specific root length; RL, Root length; RSA, Root surface area; RV, Root volume; RA, Root activity.

accumulation of pecan to different degree, Ammonia–Nitrate Mixture Dominated by NH_4^+–N had the best effect (Chen et al., 2021).

We found that T4 and T5 treatments significantly increased aboveground biomass and RGR by further study. However, Kim et al. (2002) found that biomass of pecan decreased instead when NH_4^+: NO_3^- ratio was 75:25, which might be caused by the different levels of N addition, and the high ammonium concentration could lead to plant toxicity. Both NH_4^+ and NO_3^- addition treatments increased but didn't have significant differences in the underground biomass of pecan compared to the N deficiency treatment, and a significant difference existed in root length, root area, root volume, SRL, and root activity of pecan. This suggests that the different NH_4^+: NO_3^- ratio treatments may only have a unilateral promotion effect on the horizontal or vertical growth of pecan roots. It has been suggested that NH_4^+ promotes the emergence of lateral roots to establish a highly branched root system (Meier et al., 2020), which may be one of the reasons why the T4 and T5 treatments significantly increased the root area of pecan. The accumulation of FAAs is the result of biosynthesis and catabolism, and Yang et al. (2020) showed that both single addition of NH_4^+ and ammonia-nitrate mixture significantly increased the total FAAs in tea (*Camellia sinensis* L.). The results of our study were generally agreed with them, as the T3, T4, and T5 treatments all significantly increased the FAA concentrations of pecan. Previous studies have suggested that N and P have interaction in plants, and the supply of N usually increases the efficiency of P acquisition and use by plants, which was consistent with our findings (Güsewell, 2004). In general, NH_4^+ uptake by plants decreases rhizosphere pH, while weak acid conditions are more favorable for P absorption (Barrow, 2017), and our study also found that TP concentrations significantly increased under the condition of single addition of NH_4^+. In addition, TK concentrations in roots increased significantly when NH_4^+: NO_3^- ratio was 50:50, which was consistent with the findings of Wang and Below (1998). The growth and development of plants are highly dependent on the interaction between C and N metabolism. Plants need to absorb a large amount of N into the photosynthesis mechanism, and also need a large amount of fixed C to provide C skeleton as a receptor in the assimilation process of inorganic N (Krapp and Traong, 2006). N can promote photosynthesis to produce more carbon substrates (Coruzzi and Bush, 2001). This study found that different forms of N addition increased the TOC concentration of plants, but with the decrease of NO_3^-, the TOC concentration was higher, which may be due to the assimilation of NO_3^- consumes more ATP and C skeleton (Nunes-Nesi et al., 2010). According to the results of PLS-PM analysis, TN and TOC were critical factors for plant growth, and T4 treatment significantly increased the FAA concentrations, TOC concentrations, TN concentrations, and NUE of pecan, indicating that ammonium-nitrate mixture dominated by NH_4^+ would be more beneficial to the growth of pecan, which was likewise confirmed by the results of principal component analysis.

TABLE 3 The rate of eigenvalue, contribution, and cumulative contribution in principal components.

Principal Components	Eigenvalues	Contribution Rate/%	Cumulative Contribution Rate/%
1	11.261	56.306	56.306
2	4.194	20.970	77.276

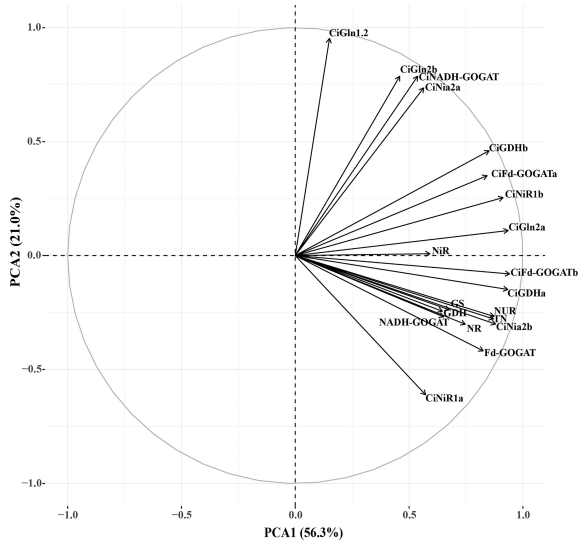

FIGURE 9
Factor loads of PCA. NUR, nitrogen uptake rate; NR, Nitrate reductase; NiR, Nitrite reductase; GS, Glutamine synthetase; GOGAT, Glutamate synthase; GDH, Glutamate dehydrogenase; TN, Total nitrogen.

4.2 Effects of N forms on the N uptake and assimilation of pecan

N assimilation of plants is the process by which they absorb NH_4^+ or NO_3^- to synthesize nitrogenous organic compounds such as amino acids and proteins. The main enzymes involved in the assimilation of NO_3^- are NR and NiR. In this study, both NR and NiR activities showed significantly greater in leaves than roots, which was attributed to the fact that most of the NO_3^- absorbed by the root would be transported to the shoot and reduced in the mesophyll cells (Liu et al., 2022). Nitrate is both a nutrient and a signal to initiate various processes that trigger the induction of NO_3^- assimilatory enzymes (Tischner and Kaiser, 2007). Therefore, NR and NiR activities in the leaves of pecan were significantly increased by a single addition of NO_3^-. It has been suggested that NH_4^+ stimulates NR activity (Ivashikina and Sokolov, 1997), but a negative feedback effect of NH_4^+ on the NO_3^- assimilation pathway has also been observed (Tischner, 2000), and the results of our study were the same as the former.

Regarding NH_4^+ assimilation of plant, the role of the GS/GOGAT cycle has been generally accepted (Zhao and Shi, 2006), while it still continues to be argued that the GDH shunt is also important and that it may be expected to play a deamination role in the tissue where amino acids are converted to transport compounds with low C/N ratios (Kant et al., 2007). Only a limited fraction of N is transferred in the organs after entering the plant, and a large fraction is released as NH_3 and reassimilated *via* GS (Miflin and Habash, 2002). It is generally believed that NH_4^+ is mainly assimilated in roots (Ruan et al., 2016), and GS, GOGAT, and GDH activities all showed higher in leaves in this study, which may be due to differences in species and N supply levels (Feng et al., 2020), or it may be that NH_4^+ assimilation genes were mainly expressed in leaves of pecan. Low concentrations of external NH_4^+ and NO_3^- had a positive effect on GS and GOGAT activity (Miflin and Habash, 2002; Balotf et al., 2016), which was consistent with the results of our study. Studies have shown that GDH activity increases under various stress conditions (Srivastava and Singh, 1987). GDH activity was significantly increased when NH_4^+ was added alone, which may be due to the role of GDH in relieving ammonium toxicity (Kant et al., 2007). Based on the results of the PLS-PM analysis, we suggested that pecan may enhance growth through increased N assimilation enzyme activity to accelerate NH_4^+ and. metabolism. The activities of all five N assimilating enzymes of pecan were significantly increased under T4 treatment, further indicating that ammonium-nitrate mixture dominated by NH_4^+ was more beneficial in promoting the growth of pecan.

4.3 Effects of N forms on the N assimilation-related genes expression of pecan

The PLS-PM results indicate that the N assimilate enzyme genes can influence nutrient uptake in pecan by regulating N assimilate enzyme activity, which ultimately affects growth of pecan, so the expression level of the N assimilate genes could indirectly reflect the growth status of pecan. In the assimilation of NO_3^-, *Nia2* was responsible for 90% of the total NR activity in seedlings, whereas *Nia1* accounts for the remaining 10% (Yu et al., 1998). Previous studies suggested that NO_3^- is a signal for NO_3^- assimilation genes (Wang et al., 2004), and it can up-regulate the expression of *Nia* and *NiR* genes (Loppes et al., 1999; Konishi and Yanagisawa, 2010), which was consistent with the results of our study, where the

TABLE 4 Scores of NH_4^+:NO_3^- ratio treatments in the principal component and comprehensive evaluation.

Treatments	Z1	Z2	Comprehensive Score	Ranking
CK	-4.5075	0.3975	-2.4525	6
T1	1.8075	4.0125	1.8600	2
T2	-2.3125	-1.2875	-1.5700	5
T3	-0.6900	-1.7475	-0.7550	4
T4	5.8825	-1.5850	2.9800	1
T5	-0.1900	0.2050	-0.0600	3

expression levels of pecan *CiNia2a*, *CiNia2b*, and *CiNiR1b* were significantly up-regulated under single application of NO_3^-. Loppes et al. (1999) also found that NH_4^+ down-regulated the expression level of *Nia* genes, but Kim et al. (2016) suggested that NH_4^+ up-regulated the expression level of *nia2*, and our study were consistent with the former, with *CiNia2a*, *CiNia2b*, and *CiNiR1b* expression levels significantly down-regulated under single application of NH_4^+. The response of critical NO_3^- NO_3^- assimilation genes to NO_3^- may be independent of NO_3^- reduction (Wang et al., 2004), and our study found no significant correlation between *CiNia2a* and NR, perhaps as *Nia2* gene was also involved in the regulation of chlorate resistance (Wilkinson and Crawford, 1991). Loqué et al. (2003) also showed that the *AtNIA2* gene was overexpressed in the roots of NR-deficient mutants.

In the *Arabidopsis* genome, one *Gln2* gene and five *Gln1* genes are encoded (Taira et al., 2004). *Gln1;2* is essential for N assimilation and ammonia detoxification, and *gln1;2* mutants exhibit lower GS activity (Lothier et al., 2011). Under high NH_4^+ treatment, the expression level of *AtGln1;2* in shoots was up-regulated, the expression level of *AtGln1;1*, *AtGln1;4*, and *AtGln1;5* was down-regulated, and the expression level of *AtGln1;3* was unchanged (Guan et al., 2016). The expression pattern of *CiGln1.2* was similar to that of *AtGln1;2*, and the expression level of *CiGln1.2* in leaves was significantly up-regulated by single treatment with NO_3^-, indicating that *CiGln1.2* also has an important role in NH_4^+ assimilation and ammonium detoxification in pecan leaves. Wang et al. (2021) found that *Gln2* was up-regulated in shoots when NH_4^+ was the only N source, which was consistent with the results of our study. However, recent studies have shown that *gln2* mutants do not exhibit an abnormal phenotype and that the isozyme encoded by the *GS1* genes, may mask the *gln2* mutation in *Arabidopsis* shoots (Lee et al., 2022). In case of NH_4^+ assimilation genes, NO_3^- is also a direct signal (Wang et al., 2004), and *CiGlns* were significantly up-regulated in leaves of pecan under T1 treatment. Additionally, *CiGln2s* were highly expressed in the leaves but very low levels in the roots, which agreed with the study of Guan et al. (2016).

GOGAT is mostly found in the plasmid, and Fd-GOGAT accounts for 96% of the total GOGAT activity (Bi et al., 2017). Studies have shown that the *Fd-GOGAT* gene acts primarily in leaves, while the *NADH-GOGAT* gene contributes more to root NH_4^+ assimilation (Konishi et al., 2014), which was also confirmed in poplar (*Populus* L.) (Cao et al., 2023). However, this was not entirely accordance with the results of our study, where *CiFd-GOGATs* were expressed at higher levels in leaves except for CK treatment, whereas *CiNADH-GOGAT* was expressed at higher levels in roots under CK, T2, and T3 treatments, which may be due to differences in species and N levels. (Balotf et al., 2016) found that high concentrations of NH_4^+ and NO_3^- could increase the expression level of GOGAT genes, sand the transcript level of GOGAT genes decreased under N-deficient conditions. This was the same with our findings that the expression level of pecan GOGAT gene was significantly up-regulated in leaves under the addition of NH_4^+ or NO_3^- alone, while *CiFd-GOGATb* and *CiNADH-GOGAT* were significantly down-regulated under CK treatment except for *CiFd-GOGATa*. Importantly, T4 treatment significantly up-regulated the pecan GOGAT gene, indicating that the addition of ammonium-nitrate mixtures dominated by NH_4^+ was more favorable for pecan NH_4^+ assimilation.

In the model plant *Arabidopsis*, besides the GS/GOGAT cycle, GDH has a complementary role in N assimilation under specific physiological conditions of high NH_4^+ concentrations (Glevarec et al., 2004). In this study, we found that not only T5 treatment up-regulated the expression level of *CiGDHs* in pecan leaves, but also T1, T3, and T4 treatments, suggesting that the expression level of *CiGDHs* can also be regulated by NO_3^-. Although the expression patterns of *CiGDHa* and *CiGDHb* were almost identical under different N form treatments, GDH was highly significantly positively correlated with *CiGDHa*, implying that *CiGDHa* may play a more important role in pecan NH_4^+ assimilation.

5 Conclusions

We analyzed the effects of different N form treatments on the growth, nutrient uptake, and N assimilation of pecan, and found that NH_4^+ was more beneficial to promote the growth, N uptake and assimilation of pecan, and the ammonium-nitrate mixture dominated by NH_4^+ had the best effect. The results of PLS-PM analysis also indicated that N uptake and assimilation would directly affect the growth of pecan. Furthermore, correlation analysis showed that N assimilate enzyme activity did not necessarily correlate positively with N assimilate gene expression level, partly because N assimilate enzymes are not only regulated by N assimilate genes, and partly because some N assimilate genes have other functions than regulating N assimilate enzymes. Therefore, we believe that the N assimilation ability of plants should not be judged only by N assimilation genes in future studies, which should be confirmed by a comprehensive analysis of N concentration, N assimilation enzymes, and related genes. The study provides a basis for further identification of the functions of N assimilation genes in the N assimilation process of pecan, and also provides a theoretical support for improving the yield of pecan by improving NUE, and promoting the scale development of pecan.

Data availability statement

The original contributions presented in the study are included in the article/Supplementary Material. Further inquiries can be directed to the corresponding author.

Author contributions

FP conceived and designed the study. MC collected experimental data, analyzed, and wrote the manuscript. MC and JL participated in the collection of samples. MC, ZQ, and JX performed the experiments. PT and KZ provided help in data

analysis and in improving the manuscript. All authors contributed to the article and approved the submitted version.

Funding

This research was funded by the Central Financial Forestry Science and Technology Extension Demonstration Funds Program (Su (2022) TG04) and a grant from the National Key R&D Program of China (2021YFD1000403).

Conflict of interest

The authors declare that the research was conducted in the absence of any commercial or financial relationships that could be construed as a potential conflict of interest.

Publisher's note

Supplementary material

The Supplementary Material for this article can be found online at: https://www.frontiersin.org/articles/10.3389/fpls.2023.1186818/full#supplementary-material

SUPPLEMENTARY FIGURE 1
Melt curves of 12 selected genes.

References

Balotf, S., Kavoosi, G., and Kholdebarin, B. (2016). Nitrate reductase, nitrite reductase, glutamine synthetase, and glutamate synthase expression and activity in response to different nitrogen sources in nitrogen-starved wheat seedlings. *Biotechnol. Appl. Biochem.* 63, 220–229. doi: 10.1002/bab.1362

Barrow, N. J. (2017). The effects of pH on phosphate uptake from the soil. *Plant Soil* 410, 401–410. doi: 10.1007/s11104-016-3008-9

Bernhard, W. R., and Matile, P. (1994). Differential expression of glutamine synthetase genes during the senescence of arabidopsis thaliana rosette leaves. *Plant Sci.* 98, 7–14. doi: 10.1016/0168-9452(94)90142-2

Bi, Z., Zhang, Y., Wu, W., Zhan, X., Yu, N., Xu, T., et al. (2017). ES7, encoding a ferredoxin-dependent glutamate synthase, functions in nitrogen metabolism and impacts leaf senescence in rice. *Plant Sci.* 259, 24–34. doi: 10.1016/j.plantsci.2017.03.003

Bloom, A. J. (2015). Photorespiration and nitrate assimilation: a major intersection between plant carbon and nitrogen. *Photosynth Res.* 123, 117–128. doi: 10.1007/s11120-014-0056-y

Cao, L., Xu, C., Sun, Y., Niu, C., Leng, X., Hao, B., et al. (2023). Genome-wide identification of glutamate synthase gene family and expression patterns analysis in response to carbon and nitrogen treatment in populus. *Gene* 851, 146996. doi: 10.1016/j.gene.2022.146996

Chen, M., Zhu, K., Tan, P., Liu, J., Xie, J., Yao, X., et al. (2021). Ammonia–nitrate mixture dominated by NH_4^+–N promoted growth, photosynthesis and nutrient accumulation in Pecan (*Carya illinoinensis*). *Forests* 12, 1808. doi: 10.3390/f12121808

Coruzzi, G., and Bush, D. R. (2001). Nitrogen and carbon nutrient and metabolite signaling in plants. *Plant Physiol.* 125, 61–64. doi: 10.1104/pp.125.1.61

Coschigano, K. T., Melo-Oliveira, R., Lim, J., and Coruzzi, G. M. (1998). *Arabidopsis* gls mutants and distinct fd-GOGAT genes. implications for photorespiration and primary nitrogen assimilation. *Plant Cell* 10, 741–752. doi: 10.1105/tpc.10.5.741

Edwards, J. W., and Coruzzi, G. M. (1989). Photorespiration and light act in concert to regulate the expression of the nuclear gene for chloroplast glutamine synthetase. *Plant Cell* 1, 241–248. doi: 10.1105/tpc.1.2.241

Egenolf, K., Verma, S., Schöne, J., Klaiber, I., Arango, J., Cadisch, G., et al. (2021). Rhizosphere pH and cation-anion balance determine the exudation of nitrification inhibitor 3-epi-brachialactone suggesting release *via* secondary transport. *Physiologia Plantarum* 172, 116–123. doi: 10.1111/ppl.13300

Feng, H., Fan, X., Miller, A., and xu, G. (2020). Plant nitrogen uptake and assimilation: regulation of cellular pH homeostasis. *J. Exp. Bot.* 71 (15), 4380–4392. doi: 10.1093/jxb/eraa150

Glevarec, G., Bouton, S., Jaspard, E., Riou, M.-T., Cliquet, J.-B., Suzuki, A., et al. (2004). Respective roles of the glutamine synthetase/glutamate synthase cycle and glutamate dehydrogenase in ammonium and amino acid metabolism during germination and post-germinative growth in the model legume medicago truncatula. *Planta* 219, 286–297. doi: 10.1007/s00425-004-1214-9

Guan, M., de Bang, T. C., Pedersen, C., and Schjoerring, J. K. (2016). Cytosolic glutamine synthetase Gln1;2 is the main isozyme contributing to GS1 activity and can be up-regulated to relieve ammonium toxicity. *Plant Physiol.* 171, 1921–1933. doi: 10.1104/pp.16.01195

Guo, Y., Cai, Z., and Gan, S. (2004). Transcriptome of arabidopsis leaf senescence. *Plant Cell Environ.* 27, 521–549. doi: 10.1111/j.1365-3040.2003.01158.x

Guo, Y., Chen, Y., Searchinger, T. D., Zhou, M., Pan, D., Yang, J., et al. (2020). Air quality, nitrogen use efficiency and food security in China are improved by cost-effective agricultural nitrogen management. *Nat. Food* 1, 648–658. doi: 10.1038/s43016-020-00162-z

Guo, J., Jia, Y., Chen, H., Zhang, L., Yang, J., Zhang, J., et al. (2019). Growth, photosynthesis, and nutrient uptake in wheat are affected by differences in nitrogen levels and forms and potassium supply. *Sci. Rep.* 9, 1248. doi: 10.1038/s41598-018-37838-3

Güsewell, S. (2004). N : p ratios in terrestrial plants: variation and functional significance. *New Phytol.* 164, 243–266. doi: 10.1111/j.1469-8137.2004.01192.x

Harris, N., Foster, J. M., Kumar, A., Davies, H. V., Gebhardt, C., and Wray, J. L. (2000). Two cDNAs representing alleles of the nitrate reductase gene of potato (*Solanum tuberosum* l. cv. desirée): sequence analysis, genomic organization and expression1. *J. Exp. Bot.* 51, 1017–1026. doi: 10.1093/jexbot/51.347.1017

Ivashikina, N. V., and Sokolov, O. A. (1997). Regulation of nitrate uptake and distribution in maize seedlings by nitrate, nitrite, ammonium and glutamate. *Plant Sci.* 123, 29–37. doi: 10.1016/S0168-9452(96)04566-9

Kant, S., Kant, P., Lips, H., and Barak, S. (2007). Partial substitution of NO_3^- by NH_4^+ fertilization increases ammonium assimilating enzyme activities and reduces the deleterious effects of salinity on the growth of barley. *J. Plant Physiol.* 164, 303–311. doi: 10.1016/j.jplph.2005.12.011

Kim, J. Y., Kwon, Y. J., Kim, S.-I., Kim, D. Y., Song, J. T., and Seo, H. S. (2016). Ammonium inhibits chromomethylase 3-mediated methylation of the *Arabidopsis* nitrate reductase gene NIA2. *Front. Plant Sci.* 6. doi: 10.3389/fpls.2015.01161

Kim, T., Mills, H. A., and Wetzstein, H. Y. (2002). Studies on effects of nitrogen form on growth, development, and nutrient uptake in pecan. *J. Plant Nutr.* 25, 497–508. doi: 10.1081/PLN-120003378

Konishi, N., Ishiyama, K., Matsuoka, K., Maru, I., Hayakawa, T., Yamaya, T., et al. (2014). NADH-dependent glutamate synthase plays a crucial role in assimilating ammonium in the *Arabidopsis* root. *Physiologia Plantarum* 152, 138–151. doi: 10.1111/ppl.12177

Konishi, M., and Yanagisawa, S. (2010). Identification of a nitrate-responsive cis-element in the *Arabidopsis* NIR1 promoter defines the presence of multiple cis-regulatory elements for nitrogen response. *Plant J.* 63, 269–282. doi: 10.1111/j.1365-313X.2010.04239.x

Krapp, A. (2015). Plant nitrogen assimilation and its regulation: a complex puzzle with missing pieces. *Curr. Opin. Plant Biol.* 25, 115–122. doi: 10.1016/j.pbi.2015.05.010

Krapp, A., and Traong, H.-N. (2006). Regulation of C/N interaction in model plant species. *J. Crop Improvement* 15, 127–173. doi: 10.1300/J411v15n02_05

Lancien, M., Martin, M., Hsieh, M.-H., Leustek, T., Goodman, H., and Coruzzi, G. M. (2002). Arabidopsis glt1-T mutant defines a role for NADH-GOGAT in the non-photorespiratory ammonium assimilatory pathway. *Plant J.* 29, 347–358. doi: 10.1046/j.1365-313x.2002.01218.x

Lang, C. P., Merkt, N., and Zörb, C. (2018). Different nitrogen (N) forms affect responses to n form and n supply of rootstocks and grafted grapevines. *Plant Sci.* 277, 311–321. doi: 10.1016/j.plantsci.2018.10.004

Latan, H., and Noonan, R. (2017). *Partial least squares path modeling* (Cham: Springer International Publishing). doi: 10.1007/978-3-319-64069-3

Lee, K.-T., Chung, Y.-H., and Hsieh, M.-H. (2022). The *Arabidopsis* glutamine synthetase2 mutants (gln2-1 and gln2-2) do not have abnormal phenotypes. *Plant Physiol.* 189, 1906–1910. doi: 10.1093/plphys/kiac224

Li, H., Hu, B., and Chu, C. (2017). Nitrogen use efficiency in crops: lessons from arabidopsis and rice. *J. Exp. Bot.* 68, 2477–2488. doi: 10.1093/jxb/erx101

Liu, X., Hu, B., and Chu, C. (2022). Nitrogen assimilation in plants: current status and future prospects. *J. Genet. Genomics* 49, 394–404. doi: 10.1016/j.jgg.2021.12.006

Livak, K. J., and Schmittgen, T. D. (2001). Analysis of relative gene expression data using real-time quantitative PCR and the $2^{-\Delta\Delta CT}$ method. *Methods* 25, 402–408. doi: 10.1006/meth.2001.1262

Loppes, R., Radoux, M., Ohresser, M. C. P., and Matagne, R. F. (1999). Transcriptional regulation of the *Nia1* gene encoding nitrate reductase in chlamydomonas reinhardtii: effects of various environmental factors on the expression of a reporter gene under the control of the Nia1 promoter. *Plant Mol. Biol.* 41, 701–711. doi: 10.1023/A:1006381527119

Loqué, D., Tillard, P., Gojon, A., and Lepetit, M. (2003). Gene expression of the NO_3^- transporter NRT1.1 and the nitrate reductase NIA1 is repressed in *Arabidopsis* roots by NO_2^-, the product of NO_3^- reduction. *Plant Physiol.* 132, 958–967. doi: 10.1104/pp.102.018523

Lothier, J., Gaufichon, L., Sormani, R., Lemaître, T., Azzopardi, M., Morin, H., et al. (2011). The cytosolic glutamine synthetase GLN1;2 plays a role in the control of plant growth and ammonium homeostasis in *Arabidopsis* rosettes when nitrate supply is not limiting. *J. Exp. Bot.* 62, 1375–1390. doi: 10.1093/jxb/erq299

Lu, J., Hu, T., Zhang, B., Wang, L., Yang, S., Fan, J., et al. (2021). Nitrogen fertilizer management effects on soil nitrate leaching, grain yield and economic benefit of summer maize in Northwest China. *Agric. Water Manage.* 247, 106739. doi: 10.1016/j.agwat.2021.106739

Meier, M., Liu, Y., Lay-Pruitt, K. S., Takahashi, H., and von Wirén, N. (2020). Auxin-mediated root branching is determined by the form of available nitrogen. *Nat. Plants* 6, 1136–1145. doi: 10.1038/s41477-020-00756-2

Miflin, B. J., and Habash, D. Z. (2002). The role of glutamine synthetase and glutamate dehydrogenase in nitrogen assimilation and possibilities for improvement in the nitrogen utilization of crops. *J. Exp. Bot.* 53, 979–987. doi: 10.1093/jexbot/53.370.979

M'rah Helali, S., Nebli, H., Kaddour, R., Mahmoudi, H., Lachaâl, M., and Ouerghi, Z. (2010). Influence of nitrate–ammonium ratio on growth and nutrition of *Arabidopsis thaliana*. *Plant Soil* 336, 65–74. doi: 10.1007/s11104-010-0445-8

Negrini, A. C. A., Evans, J. R., Kaiser, B. N., Millar, A. H., Kariyawasam, B. C., Atkin, O. K., et al. (2020). Effect of n supply on the carbon economy of barley when accounting for plant size. *Funct. Plant Biol.* 47, 368–381. doi: 10.1071/FP19025

Nicodemus, M. A., Salifu, F. K., and Jacobs, D. F. (2008). Growth, nutrition, and photosynthetic response of black walnut to varying nitrogen sources and rates. *J. Plant Nutr.* 31, 1917–1936. doi: 10.1080/01904160802402856

Nunes-Nesi, A., Fernie, A. R., and Stitt, M. (2010). Metabolic and signaling aspects underpinning the regulation of plant carbon nitrogen interactions. *Mol. Plant* 3, 973–996. doi: 10.1093/mp/ssq049

Polcyn, W., and Garnczarska, M. (2009). Short-term effect of nitrate or water stress on nitrate reduction and malate fermentation pathways in yellow lupine (*Lupinus luteus*) nodules. *Acta Physiol. Plant* 31, 1249. doi: 10.1007/s11738-009-0361-9

Priemé, A., Braker, G., and Tiedje, J. M. (2002). Diversity of nitrite reductase (nirK and nirS) gene fragments in forested upland and wetland soils. *Appl. Environ. Microbiol.* 68, 1893–1900. doi: 10.1128/AEM.68.4.1893-1900.2002

Qin, J., Yue, X., Ling, Y., Zhou, Y., Li, N., Shang, X., et al. (2021). Nitrogen form and ratio impact phenolic accumulation and relative gene expression in cyclocarya paliurus. *Trees* 35, 685–696. doi: 10.1007/s00468-020-02068-6

Qin, J., Yue, X., Shang, X., and Fang, S. (2020). Nitrogen forms alter triterpenoid accumulation and related gene expression in *Cyclocarya paliurus* (Batalin) iljinsk. seedlings. *Forests* 11, 631. doi: 10.3390/f11060631

Rahmani, M., and Atia, G. K. (2017). Coherence pursuit: fast, simple, and robust principal component analysis. *IEEE Trans. Signal Process.* 65, 6260–6275. doi: 10.1109/TSP.2017.2749215

Ruan, L., Wei, K., Wang, L., Cheng, H., Zhang, F., Wu, L., et al. (2016). Characteristics of NH_4^+ and NO_3^- fluxes in tea (*Camellia sinensis*) roots measured by scanning ion-selective electrode technique. *Sci. Rep.* 6, 38370. doi: 10.1038/srep38370

Srivastava, H. S., and Singh, R. P. (1987). Role and regulation of l-glutamate dehydrogenase activity in higher plants. *Phytochemistry* 26, 597–610. doi: 10.1016/S0031-9422(00)84749-4

Stūrīte, I., Henriksen, T. M., and Breland, T. A. (2005). Distinguishing between metabolically active and inactive roots by combined staining with 2,3,5-triphenyltetrazolium chloride and image colour analysis. *Plant Soil* 271, 75–82. doi: 10.1007/s11104-004-2027-0

Taira, M., Valtersson, U., Burkhardt, B., and Ludwig, R. A. (2004). *Arabidopsis thaliana* GLN2-encoded glutamine synthetase is dual targeted to leaf mitochondria and chloroplasts. *Plant Cell* 16, 2048–2058. doi: 10.1105/tpc.104.022046

Tang, D., Liu, M.-Y., Zhang, Q., Ma, L., Shi, Y., and Ruan, J. (2020). Preferential assimilation of NH_4^+ over NO_3^- in tea plant associated with genes involved in nitrogen transportation, utilization and catechins biosynthesis. *Plant Sci.* 291, 110369. doi: 10.1016/j.plantsci.2019.110369

Thomsen, H. C., Eriksson, D., Møller, I. S., and Schjoerring, J. K. (2014). Cytosolic glutamine synthetase: a target for improvement of crop nitrogen use efficiency? *Trends Plant Sci.* 19, 656–663. doi: 10.1016/j.tplants.2014.06.002

Tischner, R. (2000). Nitrate uptake and reduction in higher and lower plants. *Plant Cell Environ.* 23, 1005–1024. doi: 10.1046/j.1365-3040.2000.00595.x

Tischner, R., and Kaiser, W. (2007). "Chapter 18 - nitrate assimilation in plants," in *Biology of the nitrogen cycle*. Eds. H. Bothe, S. J. Ferguson and W. E. Newton (Amsterdam: Elsevier), 283–301. doi: 10.1016/B978-044452857-5.50019-9

Wang, X., and Below, F. E. (1998). Accumulation and partitioning of mineral nutrients in wheat as influenced by nitrogen form. *J. Plant Nutr.* 21, 49–61. doi: 10.1080/01904169809365382

Wang, Y., Hua, Y., Zhou, T., Huang, J., and Yue, C. (2021). Genomic identification of nitrogen assimilation-related genes and transcriptional characterization of their responses to nitrogen in allotetraploid rapeseed. *Mol. Biol. Rep.* 48, 5977–5992. doi: 10.1007/s11033-021-06599-0

Wang, R., Tischner, R., Gutiérrez, R. A., Hoffman, M., Xing, X., Chen, M., et al. (2004). Genomic analysis of the nitrate response using a nitrate reductase-null mutant of *Arabidopsis*. *Plant Physiol.* 136, 2512–2522. doi: 10.1104/pp.104.044610

Wilkinson, J. Q., and Crawford, N. M. (1991). Identification of the *Arabidopsis CHL3* gene as the nitrate reductase structural gene NIA2. *Plant Cell* 3, 461–471. doi: 10.1105/tpc.3.5.461

Xu, G., Fan, X., and Miller, A. J. (2012). Plant nitrogen assimilation and use efficiency. *Annu. Rev. Plant Biol.* 63, 153–182. doi: 10.1146/annurev-arplant-042811-105532

Yang, T., Li, H., Tai, Y., Dong, C., Cheng, X., Xia, E., et al. (2020). Transcriptional regulation of amino acid metabolism in response to nitrogen deficiency and nitrogen forms in tea plant root (*Camellia sinensis* l.). *Sci. Rep.* 10, 6868. doi: 10.1038/s41598-020-63835-6

Yu, X., Sukumaran, S., and Márton, L. (1998). Differential expression of the *Arabidopsis Nia1* and *Nia2* Genes1: cytokinin-induced nitrate reductase activity is correlated with increased Nia1 transcription and mRNA levels. *Plant Physiol.* 116, 1091–1096. doi: 10.1104/pp.116.3.1091

Zhang, F.-C., Kang, S.-Z., Li, F.-S., and Zhang, J.-H. (2007). Growth and major nutrient concentrations in brassica campestris supplied with different NH_4^+/NO_3^- ratios. *J. Integr. Plant Biol.* 49, 455–462. doi: 10.1111/j.1744-7909.2007.00373.x

Zhao, X. Q., and Shen, R. F. (2018). Aluminum–nitrogen interactions in the soil–plant system. *Front. Plant Sci.* 9. doi: 10.3389/fpls.2018.00807

Zhao, X.-Q., and Shi, W.-M. (2006). Expression analysis of the glutamine synthetase and glutamate synthase gene families in young rice (*Oryza sativa*) seedlings. *Plant Sci.* 170, 748–754. doi: 10.1016/j.plantsci.2005.11.006

Zhu, K., Fan, P., Liu, H., Tan, P., Ma, W., Mo, Z., et al. (2022). Insight into the CBL and CIPK gene families in pecan (*Carya illinoinensis*): identification, evolution and expression patterns in drought response. *BMC Plant Biol.* 22, 221. doi: 10.1186/s12870-022-03601-0

Zhu, K., Fan, P., Mo, Z., Tan, P., Feng, G., Li, F., et al. (2020). Identification, eexpression and co-expression analysis of R2R3-MYB family genes involved in graft union formation in pecan (*Carya illinoinensis*). *Forests* 11, 917. doi: 10.3390/f11090917

frontiers | Frontiers in Plant Science

TYPE Original Research
PUBLISHED 08 June 2023
DOI 10.3389/fpls.2023.1198366

OPEN ACCESS

EDITED BY
Sumera Anwar,
Durham University, United Kingdom

REVIEWED BY
Li Wang,
Shandong Academy of Agricultural Sciences, China
Linlin Wang,
Gansu Agricultural University, China
Sanjay Singh Rathore,
Indian Agricultural Research Institute (ICAR), India
Shuijin Hua,
Zhejiang Academy of Agricultural Sciences, China

*CORRESPONDENCE
Peng Zhang
pengzhang121@hotmail.com

RECEIVED 01 April 2023
ACCEPTED 23 May 2023
PUBLISHED 08 June 2023

CITATION
Wang J, Liu G, Cui N, Liu E, Zhang Y, Liu D, Ren X, Jia Z and Zhang P (2023) Suitable fertilization can improve maize growth and nutrient utilization in ridge-furrow rainfall harvesting cropland in semiarid area. *Front. Plant Sci.* 14:1198366. doi: 10.3389/fpls.2023.1198366

Suitable fertilization can improve maize growth and nutrient utilization in ridge-furrow rainfall harvesting cropland in semiarid area

Jiayi Wang[1,2], Gaoxiang Liu[1,2], Nan Cui[1,2], Enke Liu[3], Yan Zhang[4], Donghua Liu[1,2], Xiaolong Ren[1,2], Zhikuan Jia[1,2] and Peng Zhang[1,2]*

[1]College of Agronomy, Northwest A&F University, Yangling, Shaanxi, China, [2]Key Laboratory of Crop Physi-Ecology and Tillage Science in Northwestern Loess Plateau, Minister of Agriculture, Northwest A&F University, Yangling, Shaanxi, China, [3]Institute of Environment and Sustainable Development in Agriculture, Chinese Academy of Agricultural Sciences, Beijing, China, [4]Institute of Jiangxi Oil-tea Camellia, Jiujiang University, Jiujiang, Jiangxi, China

The ridge-furrow rainfall harvesting system (RFRH) improved the water shortages, and reasonable fertilization can promote nutrient uptake and utilization of crops, leading to better yield in semi-arid regions. This holds significant practical significance for improving fertilization strategies and reducing the application of chemical fertilizers in semi-arid areas. This field study was conducted to investigate the effects of different fertilization rates on maize growth, fertilizer use efficiency, and grain yield under the ridge-furrow rainfall harvesting system during 2013-2016 in semiarid region of China. Therefore, a four-year localization field experiment was conducted with four fertilizer treatments: RN (N 0 kg hm^{-2}, P_2O_5 0 kg hm^{-2}), RL (N 150 kg hm^{-2}, P_2O_5 75 kg hm^{-2}), RM (N 300 kg hm^{-2}, P_2O_5 150 kg hm^{-2}), and RH (N 450 kg hm^{-2}, P_2O_5 225 kg hm^{-2}). The results showed that the total dry matter accumulation of maize increased with the fertilizer application rate. The nitrogen accumulation was highest under the RM treatment after harvest, average increase by 1.41% and 22.02% ($P<0.05$) compared to the RH and RL, respectively, whereas the phosphorus accumulation was increased with the fertilizer application rate. The nitrogen and phosphorus use efficiency both decreased gradually with the fertilization rate increased, where the maximum efficiency was observed under the RL. With the increase of fertilizer application rate, the maize grain yield initially increased and then decreased. Under linear fitting, the grain yield, biomass yield, hundred-kernel weight, and ear-grain number all showed a parabolic trend with the increase of fertilization rate. Based on comprehensive consideration, the recommended moderate fertilization rate (N 300 kg hm^{-2}, P_2O_5 150 kg hm^{-2}) is suitable for the ridge furrow rainfall harvesting system in semiarid region, and the fertilization rate can be appropriately reduced according to the rainfall.

KEYWORDS

fertilizer rate, ridge-furrow rainfall harvesting system, maize yield, nutrient uptake and utilization, semi-arid area

1 Introduction

Drought and infertile soils are the major constraints to maize production in semiarid areas in China (Jia et al., 2020). Limited irrigation water and unstable rainfall in arid agriculture make it difficult to increase nutrient uptake, which may pose a threat to maize production in this regions (Gan et al., 2013; Wu and Ma, 2015). Over the past 20 years, the ridge-furrow rainfall harvesting planting (RFRH) system has been an effectively solution to alleviate issues of drought and water scarcity in dryland areas by reducing evaporation, conserving soil moisture, and increasing the utilization rate of precipitation to over 65%, and also resulted in nearly quadruple grain yields (Ren et al., 2017; Zhang et al., 2018). Fertilization is one of the primary method for improving soil infertile, as it enhances the soil water retention capacity and utilization efficiency, leading to improved photosynthesis and nutrient absorption and utilization by crops (Zhang et al., 2017). However, long-term excessive application of the chemical fertilizer has caused many negative effects, such as plant growth stunted, nutrient leaching, and declining soil quality, which can subsequently limit crop yields in these areas (Lian et al., 2016). Thus, it is necessary to scientifically determine the appropriate application rates of N and P fertilizers under RFRH system, to achieve the purpose of reducing fertilizer usage while increasing efficiency, and maintain the sustainable development In semiarid region.

The plastic film mulching is also beneficial for the dissolution and diffusion of soil nutrients, significantly increasing the concentration of nitrogen, phosphorus, potassium and organic matter in the soil, thus promoting the better efficient utilization of nutrients, growth and production of crops (Wang et al., 2022). Li et al. (2018) demonstrated that in the semi-arid western region of northeast China, application of fertilizer ranging from 70 to 210 kg hm^{-2} can maintain high level of yield, nutrient absorption and utilization, while the dry matter accumulation and yield are both negatively impacted with the increase of fertilizer application. In the arid region of northwest China, applying N at a rate of 265.0kg hm^{-2} and P_2O_5 at a rate of 132.5 kg hm^{-2} can maintain the yield and nutrient absorption and utilization at a high level, while the dry matter accumulation and yield are both affected with the continuous increase of fertilizer application.(Zhang et al., 2018). Ren et al. (2010) found that the RFRH system can promote the effectiveness of soil moisture for plant roots and enhance crop nutrient uptake. Xu et al. (2020) found that N 140 kg hm^{-2} for maize and N 240 kg hm^{-2} for wheat in the rotation of maize and winter wheat could achieve high production benefits in the North China Plain. In addition, Lian et al. (2016) also found that the application of N and P fertilizers at a ratio of 186:96 kg N:P hm^{-1} in RFRH system can significantly increase the height of foxtail millet, as well as the chlorophyll content and leaf area index, which can provide a foundation for the accumulation of dry matter and increased yield.

Previous studies on the RFRH system have focused mainly on water use efficiency, ridge-to-furrow ratio, irrigation, and covering materials (Ren et al., 2016a; Ren et al., 2016b; Zhang et al., 2019). However, there is still a lack of systematic evaluation of the effects of different rainfall patterns combined with N:P fertilization levels on nutrient accumulation, distribution, utilization, and yield. We hypothesized that: (1) As The maize yield could not increase with the fertilizer application rate increases under the RFRH system; (2) Different precipitation and fertilization would significantly affect the yield and nutrient uptake and utilization; (3) There would be differences in the effects of water-fertilizer relationship on yield an nutrient utilization. Thus, we conducted a four consecutive years of field positioning experiments with the aim of providing a theoretical basis and technical support for increasing yield and efficiency, and rational fertilizer management of dryland maize cultivation, and further tapping the potential for increasing production in arid areas. The objectives of our study were as follows: (1) Investigated the effects of different fertilizer application rates on crop growth; (2) Compared the improve effects on maize nutrient uptake and utilization with different fertilizer application rates; (3) Analyze the relationship between different water-fertilizer relationships and the yield as well as its components, develop a suitable fertilizer application model for the local area.

2 Materials and methods

2.1 Site description

The study was conducted during 2013-2016 at the Dry-land Agricultural Experiment Station of Northwest A&F University in Pengyang, Guyuan, Ningxia, China (35°51' E, 106°48' N), which is located in the Loess Plateau region, with a temperate semi-arid climate zone and an elevation of 1658 meters. The annual mean precipitation was 430 mm yr^{-1}(according to Figure 1), the annual mean temperature was 6.1°C, the total sunshine hours duration 2518.2 h yr^{-1}, the annual evaporation was 1753.2 mm, and the frost-free season was 140-160 days. The soil at the experimental site was loess soil, and the main physico-chemical properties of the plow layer (0-60 cm) are as follows: organic matter = g kg^{-1}, available nitrogen = 51.75 mg kg^{-1}, available phosphorus = 17.17 mg kg^{-1}, available potassium = 7.02 mg kg^{-1}, total nitrogen = 1.06 g kg^{-1}, soil pH = 8.5, and bulk density = 1.25 g cm^{-3}.

2.2 Experimental design and field management

The study was conducted using a completely randomized block design with three replicates and for a total of 12 plots. The field studies consisted of four fertilization treatments implemented in the ridge-furrow rainfall harvesting planting system (Figure 2): RFRH system with no fertilizer (RN, N 0 kg hm^{-2}, P_2O_5 0 kg hm^{-2}), RFRH system with low fertilizer (RL, N 150 kg hm^{-2}, P_2O_5 75 kg hm^{-2}), RFRH system with medium fertilizer (RM, N 300 kg hm^{-2}, P_2O_5 150 kg hm^{-2}), and RFRH system with high fertilizer (RH, N 450 kg hm^{-2}, P_2O_5 225 kg hm^{-2}). The plots were 90 cm apart, and each plot area measured 61.2 m^2 (17 × 3.6 m). The ridges and furrows were both 60 cm wide, with a ridge height of 15 cm, and the ridges were covered with polyethylene plastic film mulch (75 cm wide, 0.01 mm thick, produced by Gansu Tianbao Plastic Industry Co., Ltd.).

Maize (Dafeng 30) was planted at a rate of 75,000 plants hm^{-2}. The seeds were sown in mid to late April using a manual falcon beak

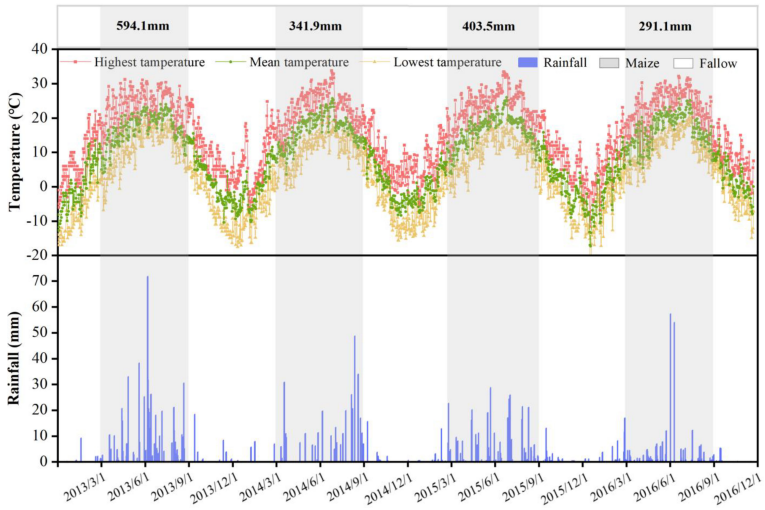

FIGURE 1
The daily precipitation, maximum, minimum, and average temperatures during the experimental period from 2013 to 2016.

planter. The maize was manually harvested in late September or early October and all straw was removed from the field. The plastic film was kept in field until 30 days before sowing, at which point it was removed, and the field was prepared for the next planting. Urea (N≥46%) and ammonium phosphate (P_2O_5≥46%) were used as fertilizers. Before sowing, uniformly applied all the phosphorus and 60% of the nitrogen as basal fertilizer to the plot. The other 40% of the nitrogen was applied during the early tasseling period of the maize (65-75 days after sowing). Throughout the maize growth period, no irrigation was applied, and weed control and pesticide application were carried out as commonly practiced by local farmers.

2.3 Sampling and measurements

2.3.1 Plant height and leaf area plant^{-1}

Five randomly selected plants were sampled from each plot to measure plant height and leaf area after 30, 60, 85, 105, and 129 days following maize sowing. The leaf area was calculated using Equation (1):

$$S = \sum_1^i L \times W \times 0.75 \quad (1)$$

where S is the total area (cm^2) of a fully expanded leaf, L is the leaf length (cm), W is the leaf maximum width (cm), *0.75* is the conversion coefficient, and i is the number of leaves.

2.3.2 Dry matter

Three randomly plants were selected from each plot at 30, 60, 85, 105, 129 and 170 days after maize sowing to measure the dry matter accumulation. The maize plants and different plant sections were weighed separately after oven dried at 105°C for 30 min, and then dried at 65°C until a constant weight was reached.

2.3.3 Yield and yield components

At harvest, three randomly rows of maize plants were selected from each plot to measure yield-related traits (ear grains and 100-kernel weight). After threshing and sun drying until the moisture content was less than 14%, then weighed to calculate the grain yield.

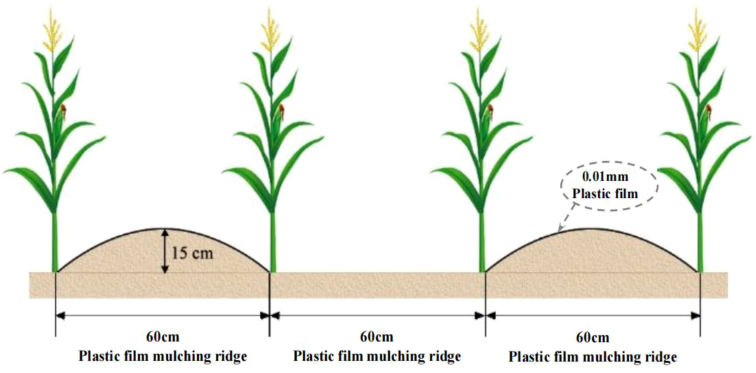

FIGURE 2
The ridge-furrow rainfall harvesting planting pattern diagram.

2.3.4 Plant nutrient

After the maturity stage of maize, three randomly plants were selected from each plot. Leaves, stalks, grains, husks, and the cob of each maize plant were collected, oven dried at 105°C for 30 minutes, and then dried at 65°C to a constant weight. Samples were finely ground and digested using H_2SO_4-H_2O_2. The N content in plant samples was analyzed using the Kjeldahl method, and the P content was determined using the molybdenum antimony anti-colorimetric method.

The NUE and PUE were calculated using Equation (2) and (3), respectively (Duan et al., 2014; Langholtz et al., 2021):

$$NUE = 100\,\% \times (N_F - N_0)/F_N \quad (2)$$

$$PUE = 100\,\% \times (P_F - P_0)/F_P \quad (3)$$

where NUE and PUE are the N and P use efficiency (kg kg^{-1}), N_F and P_F are the N and P uptake amounts (kg hm^{-2}) in the N and P fertilization treatments, N_0 and P_0 are the N and P uptake amounts (kg hm^{-2}) in the no N and P fertilization treatments, F_N and P_N are the N and P application rates (kg hm^{-2}).

The NPE and PPE were calculated using Equation (4) and (5), respectively (Rochester, 2011):

$$NPE = (GY_{NF} - GY_{N0})/(N_F - N_0) \quad (4)$$

$$PPE = (GY_{PF} - GY_{P0})/(P_F - P_0) \quad (5)$$

where NPE and PPE are N and P uptake efficiency (kg kg^{-1}), GY_{NF} and GY_{PF} are the grain yield under N and P fertilization treatments (kg hm^{-2}), GY_{N0} and GY_{P0} are the grain yield under no N and P fertilization treatments (kg hm^{-2}), N_F and P_F are the N and P uptake under N and P fertilization treatments (kg hm^{-2}), and N_0 and P_0 are the N and P uptake under no N and P fertilization treatments (kg hm^{-2}).

The NHI and PHI were calculated using Equation (6) and (7), respectively:

$$NHI = N_{GY}/N_{BY} \quad (6)$$

$$PHI = P_{GY}/P_{BY} \quad (7)$$

Where NHI and PHI are N and P harvest index (%), N_{GY} and P_{GY} are N and P uptake in the grains under N and P fertilization treatments (kg hm^{-2}), and N_{BY} and P_{BY} are the N and P uptake in the above-ground parts under no N and P fertilization treatments (kg hm^{-2}), respectively.

2.4 Data analysis

The experimental data were processed using Microsoft Excel. Single-factor analysis of variance was performed using SPSS Statistics 25, and multiple comparisons between different treatments were conducted using the Duncan's new multiple range test at a significance level of ($P< 0.05$). Origin 2022 was used for graphing.

3 Results

3.1 Growth of maize under different fertilizer rates

3.1.1 Plant height

During 2013-2016, the maize height showed an "S" shaped growth trend during the growth period, and reaching maximum in the R4 stage (Figure 3). The fertilization treatments were all significantly ($P<0.05$) higher than the unfertilized treatment RN, and the differences gradually increased with the fertilizer application years. Compared with RN, the plant height of RH, RM, and RL average increased by 22.67%, 22.40%, and 21.03%, respectively. In addition, due to the cumulative effects, the difference between the three fertilization treatments was gradually decreased with the fertilizer application years increase. In the early stage of experiment (2013-2014), the order of the fertilization treatments was RH>RM>RL, and the plant height of RH was significantly ($P<0.05$) higher than RM and RL by 16.65% and 20.61% in average in early growth stages (V2 and V8), respectively. In 2016, the order was changed to RL>RM>RH, and the plant height did not differ significantly between the treatments at each growth stages.

3.1.2 Plant leaf area

The leaf area of maize plants in response to fertilization showed an "S" shaped (Figure 4), and the maximum during the tasseling and flowering stage (R1). The difference between the fertilizer treatments was different with the increase of fertilizer application years. In 2013-2014, the order of leaf area throughout the growth period was RH>RM>RL>RN, the leaf area under RH and RM was higher than RL by 13.58% ($P<0.05$) and 6.45% in average, respectively. In 2015, the order of treatments was RM>RH>RL>RN at all growth stages (except V2), and there were no significant differences between the fertilization treatments during the vegetative period (V2-V14), whereas RH and RM were significantly ($P<0.05$) higher than RL during the R1 and R4 stages, by 15.68% and 18.20%, respectively. In 2016, the differences between fertilization treatments gradually decreased. During the V8 and V14 stages, compared with RH and RL, leaf area significantly ($P<0.05$) increased under RM by 19.99% and 9.91%, respectively, whereas during the R1 and R4 stages, RH and RM were higher than RL, but leaf area did not significant difference between these two treatments.

3.1.3 Dry matter

The dry matter accumulation was gradually decreased with the fertilizer application years (Figure 5). All fertilization treatments were significantly higher than unfertilized treatment at each growth stages, and the differences was gradually increased with the fertilization years. During 2013-2014, there was little difference among the fertilization treatments, only RH significantly increased by 11.47% ($P<0.05$) compared to RL. In 2015, the fertilization treatments at each growth stage (except V2 stage) followed the

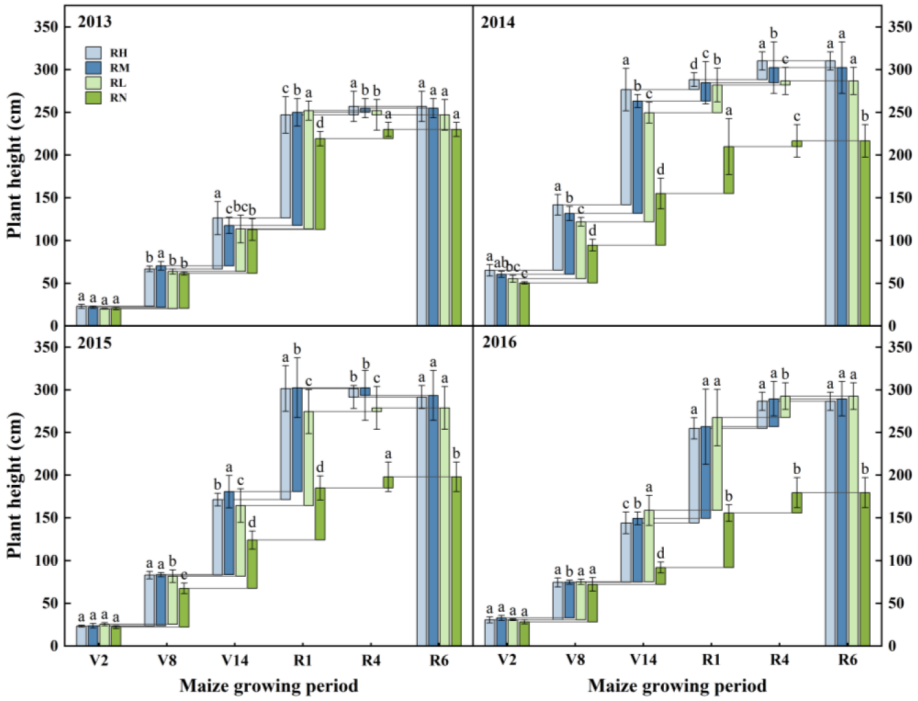

FIGURE 3
Growth rates of maize plant height under different fertilization levels during various growth periods from 2013 to 2016. Treatments RH, RM, RL, and RN represent applied N:P_2O_5 rates of 0:0, 150:75, 300:150, and 450:225 kg hm^{-1}, respectively. Data are means ± SD (n=3). Lower case letters indicate significant differences among treatments. Bars represent standard deviations (LSD test, P< 0.05). The period are as follows: V2, second leaf, about 30 days after sowing; V8, eighth leaf, about 60 days after sowing; V14, fourteenth leaf, about 85 days after sowing; R1, silking, about 105 days after sowing; R4, dough, about 129 days after sowing; R6, physiological maturity.

order as RH>RM>RL. Compared with RL, the dry matter accumulation under RH and RM average increased by 20.64% (*P<0.05*) and 12.10%, respectively. Due to the cumulative effects of fertilizer application, the dry matter in the late growth stages (R1-R6) decreased by 6.60% under RH than RM, and only increased by 17.12% under RH compared to RL.

3.1.4 Dry matter accumulation of different organs

The dry matter distribution of different organs under fertilization treatments was significantly (*P<0.05*) higher than the RN at harvest, and gradually decreased with the fertilization years (Figure 6). The dry matter mainly accumulated in the grains, which accounting for an average proportion of 46.13%. In 2014 and 2016, the dry matter of different organs significantly increased by 14.42% and 11.58% under RM and RH compared with RL. In 2015, compared with RH and RL, the average dry matter of different organs significantly (*P<0.05*) increased by 6.26% and 5.89% under the RM, respectively. Moreover, the dry matter accumulation of maize stem was highest in RM during 2013-2014, average increased by 19.62% and 6.66% under RM compared to RL and RH, respectively. In 2016, compared with RM and RL, the dry matter accumulation significantly (*P<0.05*) increased by 5.02% and 15.33% under RH. In addition, the leaves dry matter of RM and RH were 20.92% (*P<0.05*) and 22.08% (*P<0.05*) higher than RL in 2014, respectively. In 2016, the leaves dry matter accumulation of RM was 13.38% (*P<0.05*) higher than RL. Moreover, the dry matter proportion of maize husks and cobs was relatively low, with the similar trends among each experimental year. Compared with RL, the dry matter of husks average increased by 11.49% and 14.68% under RH and RM, and the cobs average increased by 16.70% and 14.14%, respectively.

3.2 Accumulation of N and P under different fertilizer rates

3.2.1 N and P accumulation

The total N uptake under fertilization treatments was higher than RN in each experimental year, and it was gradually decreased with the fertilization years (Table 1). In 2013, the order of N accumulation under fertilization treatments was RH>RM>RL, and only the accumulation of RH was 10.14% (*P<0.05*) higher than RL. As the years of fertilization increased, the differences among the fertilization treatments were increased. During 2014-2016, the order of total N accumulation changed to RM>RH>RL, and the N accumulation of RM and RH was 22.38% (*P<0.05*) and 19.77% (*P<0.05*) higher than RL, respectively. Moreover, compared with RH, the N accumulation of RM significantly (*P<0.05*) increased by 2.94% and 5.23% in 2014 and 2015, respectively.

Similar to the N uptake of maize, the P uptake of fertilization treatments was higher than RN (Table 1). Among the fertilization treatments, the P accumulation under RH and RM were significantly (*P<0.05*) higher than the RL, with average increased by 28.28% and 19.39% during 2013-2016, respectively. However, in

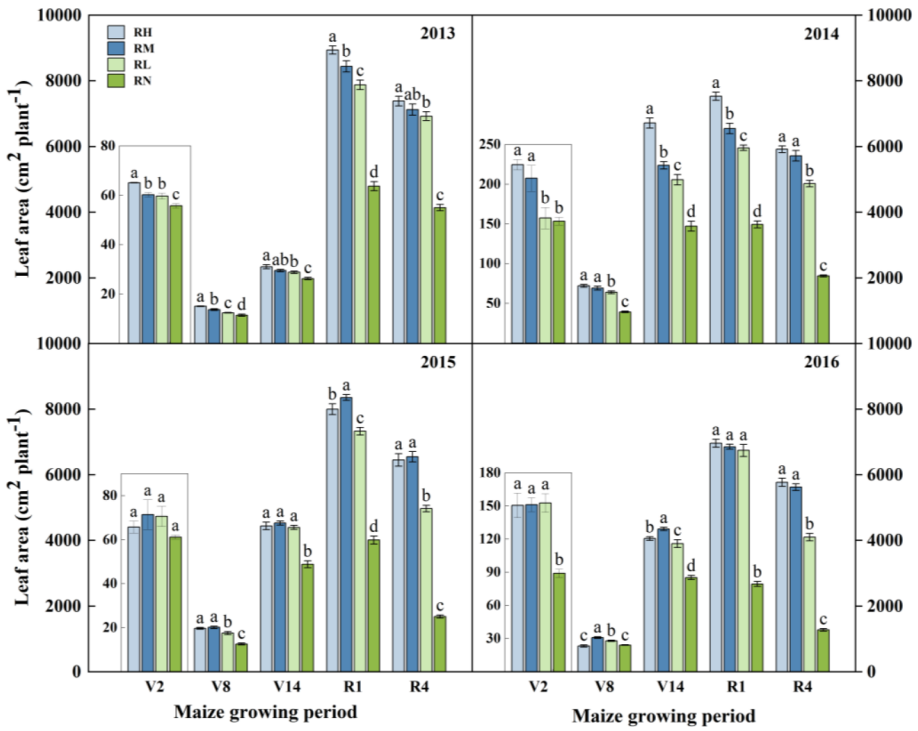

FIGURE 4
Leaf area of maize under different fertilization levels during various growth periods from 2013 to 2016. Treatments RH, RM, RL, and RN represent applied N:P_2O_5 rates of 0:0, 150:75, 300:150, and 450:225 kg hm^{-1}, respectively. Data are means ± SD (n=3). Lower case letters indicate significant differences among treatments. Bars represent standard deviations (LSD test, P< 0.05). The period are as follows: V2, second leaf, about 30 days after sowing; V8, eighth leaf, about 60 days after sowing; V14, fourteenth leaf, about 85 days after sowing; R1, silking, about 105 days after sowing; R4, dough, about 129 days after sowing; R6, physiological maturity.

2014 and 2015, the P accumulation was significantly (*P<0.05*) increased by 10.19% and 13.71% under RH compared to RM, respectively.

3.2.2 N and P accumulation in different organs

The order of N accumulation in different organs was grain > leaf > stalk > sheath > husk after harvest (Figure 7A). The N uptake of each organ under fertilization treatments was higher than RN, which was decreased gradually except for the stem with the fertilization years. In 2013-2014, the order of N accumulation in grain under fertilization treatments was RH > RM > RL > RN, and RH was average higher than RM, RL and RN by 3.82%, 9.38%, and 52.45% (*P<0.05*), respectively. The leaves have the similar trend in each year, the average N accumulation of RH and RM were all significantly higher than RL, average increased by 24.26% and 20.81%, respectively, but RH was 9.25% higher compared with RM in 2014. Furthermore, the stems N accumulation showed large differences among different years. In 2013, the RM significantly (*P< 0.05*) increased by 18.10% and 18.28% compared with RH and RL, respectively. In 2014, the RM and RH were 70.60% (*P< 0.05*) and 68.91% (*P< 0.05*) higher than RL. And no significant differences between the fertilization treatments in 2015. In 2016, the order of stems N accumulation was RH > RM > RL, the RH was 13.72% (*P<0.05*) and 46.99% (*P<0.05*) higher than that under RM and RL, respectively.

The phosphorus accumulation in different organs followed the order as grain > leaf > stalk > sheath > husk (Figure 7B). The P uptake under each fertilization treatment was higher than RN, and gradually decreased with the fertilization years. Analysis of P uptake in different organs showed that the grain P accumulation under each fertilization treatment first increased and then decreased with the fertilization years, reaching the maximum value in 2014. But the order changed to RH > RM > RL in 2013, and RH significantly (*P< 0.05*) increased by 11.44% and 29.87% compared to RM and RL, respectively. Besides, the leaf P accumulation under RH and RM in each year was significantly (*P< 0.05*) higher than RLby 34.33% and 28.24% in average, respectively. Except for 2014, RH was slightly higher than RM, but significantly increased (*P< 0.05*) by 16.28% and 3.87% in 2013 and 2016, respectively. Furthermore, stems P accumulation in each experimental year (except for 2013) followed the order of RH > RM > RL, RH significantly (*P< 0.05*) increased by 27.05% and 51.00% compared with RM and RL, respectively, and RM was only 57.83% (*P< 0.05*) and 24.65% (*P< 0.05*) significantly higher compared with RL in 2014 and 2016, respectively.

3.3 Yield effects of different fertilizer rates and rainfall

The effects of year and fertilization on grain and biomass yield were extremely significant (*P< 0.001*). The interaction of year and fertilization had an extremely significant effect on ear grains, 100-kernel weight, and grain yield (Table 2). As fertilizer application

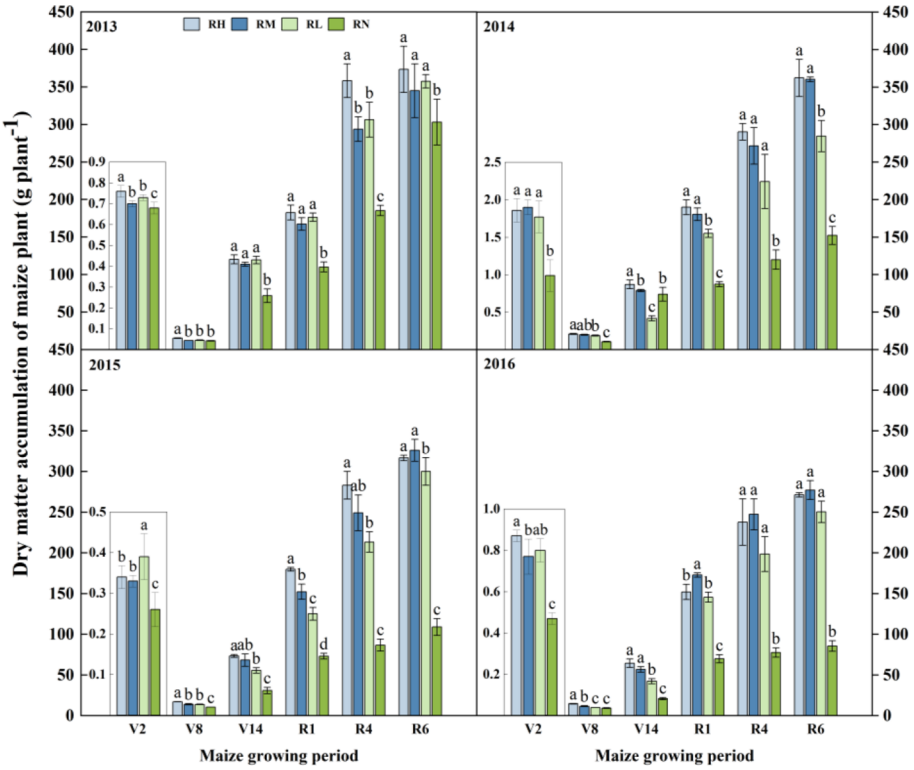

FIGURE 5
Dry matter of maize under different fertilization levels during various growth periods from 2013 to 2016. Treatments RH, RM, RL, and RN represent applied N:P_2O_5 rates of 0:0, 150:75, 300:150, and 450:225 kg hm^{-1}, respectively. Data are means ± SD (n=3). Lower case letters indicate significant differences among treatments. Bars represent standard deviations (LSD test, P< 0.05). The period are as follows: V2, second leaf, about 30 days after sowing; V8, eighth leaf, about 60 days after sowing; V14, fourteenth leaf, about 85 days after sowing; R1, silking, about 105 days after sowing; R4, dough, about 129 days after sowing; R6, physiological maturity.

rates increased, the ear grains and grain yield increased followed by a decreasing trend, reaching the maximum value under RM. Compared with the RH and RL, the ear grains increased by an average of 3.62% and 3.79% under RM, and the grain yield was increased by 2.93% and 3.27%, respectively.

All fertilization treatments significantly (*P<0.05*) increased the ear grain number by an average increase of 49.75% in each year. Also, differences in fertilization effects and rainfall produced differences among fertilization treatments. In 2013, the average ear grains significantly (*P<0.05*) increased under RH and RM by 2.83% and 4.73%, respectively. In 2015 and 2016, the order of fertilization treatments was RM>RL>RH with the fertilization years, and the RM and RL were 6.29% (*P<0.05*) and 2.39% higher compared with RH, respectively.

The 100-kernel weight was significantly affected by fertilization, which increased with the fertilizer application rate in the early stage, but the differences diminished gradually with the years of fertilization. Except for 2013, the order of three treatments was RH>RM>RL. In 2014, the average 100-kernel weight was 9.37% (*P<0.05*) and 7.95% (*P<0.05*) higher under RH and RM compared with RL, respectively, but there were no significant differences among the treatments in other years.

There was significant different in grain yield between different year, which increased significantly (*P<0.05*) by an average of 59.70% under all fertilization treatments compared to the RN (Figure 8). However, there was little variation among the fertilization treatments. Except for the 2013, in which RL yielded higher than RH and RM, the order of fertilization treatments was RM > RH > RL in the other years. Only in 2014, the yield significantly (*P< 0.05*) increased under RM by 8.34% compared with RL, while there were no significant differences among the other treatments.

The biomass yield followed a similar trend to the grain yield, with all fertilization treatments showing significant increase (*P< 0.05*) compared to RN, by 51.28%. However, the differences between the fertilization treatments decreased gradually with years of fertilization. In 2013, RH significantly (*P< 0.05*) increased by 4.07% and 4.29% compared with RM and RL, respectively, and RM was 20.98% (*P< 0.05*) and 9.69% (*P< 0.05*) higher compared with RL. No significant differences were observes among other treatments in each years.

3.4 N and P utilization under different fertilizer rates

The N fertilizer use efficiency, uptake efficiency, and harvest index of maize were significantly (*P< 0.001*) affected by the year and fertilization rate in each year (Figures 9, 10). The N fertilizer use efficiency of all treatments gradually decreased with fertilization rate increase, and the RL significantly (*P< 0.05*) increased by 54.47% and 30.80% compared to the RH and RM, respectively, whereas the RM increased by an average of 34.17% (*P< 0.05*) compared to the RH. In addition, the order of N fertilizer uptake efficiency was RL > RM >

FIGURE 6
Dry matter accumulation of different organs of maize under different fertilization levels during harvest period from 2013 to 2016. Treatments RH, RM, RL, and RN represent applied N:P_2O_5 rates of 0:0, 150:75, 300:150, and 450:225 kg hm^{-1}, respectively. Lower case letters indicate significant differences among treatments.

RH except for 2013 (RL > RH > RM), and the RL significantly ($P< 0.05$) increased by 22.05% and 23.39% compared to the RM and RH, respectively, but with no significant difference between RH and RM in 2014-2016. During the all experimental, the N fertilizer harvest index under RL was the highest, and the RL significantly ($P< 0.05$) increased by 6.71% and 10.51% compared to the RH and RM in 2013-2014. In 2015-2016, the order of N fertilizer harvest index of each fertilization treatments was RL > RM > RH, and the RL and RM increased by an average of 7.52% ($P< 0.05$) and 5.83%, respectively, compared to RH.

TABLE 1 Effects of years and fertilizer rate on accumulation of N and P for maize during harvest period from 2013 to 2016.

Treatment	N accumulation (kg hm^{-1})				P accumulation (kg hm^{-1})			
	2013	2014	2015	2016	2013	2014	2015	2016
RH	399.80a ± 30.31	315.38b ± 4.38	277.63b ± 6.81	291.17a ± 28.68	34.27a ± 2.57	38.07a ± 1.26	22.89a ± 1.00	15.41a ± 1.02
RM	389.81ab ± 15.26	324.92a ± 4.82	292.96a ± 3.46	294.41a ± 5.69	31.40ab ± 0.64	34.19b ± 0.72	19.75b ± 0.75	13.50ab ± 0.30
RL	359.28b ± 13.95	249.99c ± 6.29	249.22c ± 5.01	208.60b ± 20.16	29.32b ± 0.27	26.87c ± 0.27	16.37c ± 0.32	9.12b ± 0.27
RN	252.76c ± 12.92	93.89d ± 1.66	69.64d ± 5.33	45.48c ± 4.95	24.98c ± 1.74	11.15d ± 0.23	3.77d ± 0.99	2.47c ± 0.30
ANOVA								
Year(Y)	***<0.001				***<0.001			
Fertilization(F)	***<0.001				***<0.001			
Y×F	***<0.001				***<0.001			

Treatments RH, RM, RL, and RN represent applied N:P_2O_5 rates of 0:0, 150:75, 300:150, and 450:225 kg hm^{-1}, respectively. Data are means ± SD (n=3). Lower case letters indicate significant differences among treatments. Bars represent standard deviations (LSD test, P< 0.05). In Analysis of Variance, Y, F and Y×F represents the year, fertilizer and the interaction between the year and fertilizer. *** Significant differences at P < 0.001.

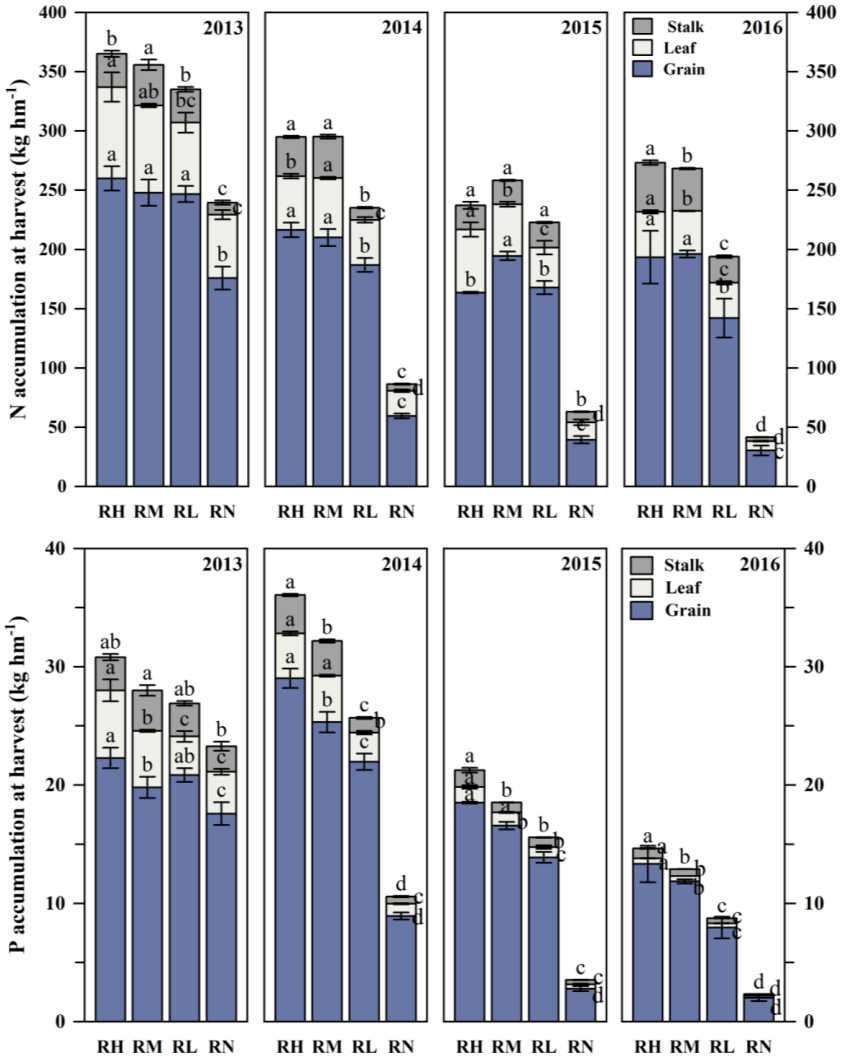

FIGURE 7
Accumulation of N and P in maize grains, leaves, and stalks under different fertilization levels during harvest period from 2013 to 2016. Treatments RH, RM, RL, and RN represent applied N:P_2O_5 rates of 0:0, 150:75, 300:150, and 450:225 kg hm^{-1}, respectively. Lower case letters indicate significant differences among treatments. Bars represent standard deviations (LSD test, P< 0.05).

The year and fertilization rate on P fertilizer use efficiency, uptake efficiency, and harvest index of maize were extremely significant (*P< 0.001*). The order of P fertilizer use efficiency for all treatment was RL>RM>RH, and RL significantly increased (*P<0.05*) by 39.05% and 26.63% compared to RH and RM, respectively, RM showed an average increase of 16.91% (*P<0.05*) compared to RH. Moreover, the P fertilizer uptake efficiency of all treatments gradually increased with the fertilization years, and the order was RL>RM>RH. The P uptake efficiency of RL and RM was 43.99% (*P<0.05*) and 18.48% higher than RH, respectively. Furthermore, there were differences in the phosphorus harvest index of each treatments among different years. In 2013-2014, the order of each treatments was RL>RN>RH>RM, the RL significantly (*P<0.05*) increased by 7.56% (*P<0.05*), 10.38% (*P<0.05*), and 1.54% compared to RH, RM, and RN, respectively, and the RH was 3.05% higher compared to RM. In 2015-2016, all fertilizer treatments were significantly higher (*P<0.05*) than RN, with average increases of 6.67% and 12.46%, respectively. Among the fertilization treatments, only RL and RM significantly increased (*P<0.05*) by 4.87% and 3.73% in 2015 compared to RH, respectively, but there were no significant differences between other treatments.

4 Discussion

4.1 Growth and yield effects of fertilizer rate in RFRH system

N and P are the essential nutrients for plant growth and development, and appropriate fertilization management has a positive impact on crop growth, yield formation, and ecological environment protection in farmland (Duan et al., 2011; Wu et al., 2018). In this study, the plant height and leaf area of maize were increased with fertilizer application rates increase during 2013-2014, this may be due to the abundant rainfall increased soil moisture and nutrient availability. Moreover, the cumulative effect

TABLE 2 Maize ear grains, 100-kernel weight, grain yield and biomass yield for different fertilization rates from 2013 to 2016, and the Analysis of Variance between years and fertilization rates.

Year	Treatment	Grains per ear	100-kemel weight (g)	Grain yield (Mg hm^{-1})	Biomass yield (Mg hm^{-1})
2013	RH	606.79a ± 12.65	29.13ab ± 0.80	12.36a ± 0.49	28.0la ± 3.26
	RM	618.9la ± 17.60	27.92b ± 0.49	12.0la ± 0.54	26.87b ± 1.36
	RL	589.63b ± 10.16	30.02a ± 1.28	12.77a ± 0.35	26.81b ± 1.95
	RN	499.18c ± 23.08	25.42c ± 1.25	9.75b ± 0.78	22.74c ± 7.66
2014	RH	486.29a ± 30.36	32.46a ± 0.73	10.79ab ± 0.12	27.17a ± 1.84
	RM	485.86a ± 20.47	31.96a ± 0.45	11.10a ± 0.59	27.03a ± 2.46
	RL	469.57a ± 43.88	29.42b ± 0.82	10.17b ± 0.43	21.36b ± 2.25
	RN	308.79b ± 113.60	21.05c ± 0.39	4.03c+0.39	10.76c ± 0.38
2015	RH	519.98b ± 27.07	27.85a ± 0.64	10.26a ± 0.46	22.75a ± 0.64
	RM	574.45a ± 14.47	27.72a ± 0.63	10.94a ± 0.57	23.45a ± 0.97
	RL	536.00b ± 28.53	27.07a ± 1.06	10.30a ± 1.31	22.17a ± 1.64
	RN	162.08c ± 13.98	21.12b ± 1.79	2.57b ± 0.34	8.17b ± 0.58
2016	RH	550.18a ± 25.20	23.36a ± 0.12	8.92a ± 0.55	20.35a ± 1.01
	RM	561.70a ± 8.41	23.15ab ± 0.25	9.37a ± 0.29	20.79a ± 0.40
	RL	559.55a ± 9.51	22.74ab ± 0.34	8.88a ± 0.23	18.78b ± 1.84
	RN	135.65b ± 3 29	22.12b ± 1 32	1.83b ± 0 36	6.43c ± 0 64
Analysis of Variance					
Year (Y)		**	*	***	***
Fertilization (F)		**	*	***	***
Y×F		***	***	***	**

Treatments RH, RM, RL, and RN represent applied N:P_2O_5 rates of 0:0, 150:75, 300:150, and 450:225 kg hm^{-1}, respectively. Lowercase letters indicate significant differences among treatments (LSD test, P<0.05). Data are means ± SD (n=3). Mean values within a column in each year followed by the same letter are not significantly different at p< 0.05. In Analysis of Variance, Y, F and Y×F represents the year, fertilizer and the interaction between the year and fertilizer. *** Significant differences at P < 0.001; ** significant differences at P < 0.01; * significant differences at P < 0.05.

of fertilizer decreased the maize plant height with high fertilization rates in 2016, whereas the height was highest under RL and leaf area was highest under RM in 2015-2016. The consecutive fertilizer application resulted in the gradual accumulation of N and P residues in the soil, and AE_{NP} (agronomic efficiency of fertilizer) was decreased with the increase of fertilizer rate (Figure 11). In addition, due to insufficient rainfall and dry conditions, the maize physiological growth processes was delayed, which could affect the crop water and fertilizer utilization, then weaken the water-fertilizer coupling effect even resulting in a negative effects (Lian et al., 2016; Li et al., 2018).

Under the RFRH system, the appropriation fertilizer application rate could coordinate the source-sink relationship of crops, and laying a foundation for high yield (Wu et al., 2022). Wei et al. (2019) suggested that the maize yield was determined by the sink capacity, which is affected by both ear grains and 100-kernel weight. This study indicate that fertilizer application had a significant effects on the dry matter accumulation and grain yield of maize, and the average value for four years was gradually increased with fertilizer rates increase (Figure 5). Because N and P fertilizers combined application could increase synthesis of active oxygen scavenging enzymes in crops, promote chlorophyll synthesis, transfer photosynthetic products to the grains, as well as increasing grain filling rates, thereby effectively improving maize sink capacity (ear grains) and filling degree (100-kernel weight) (Zhang X. D, et al., 2021; Fernandes et al., 2022; Nasar et al., 2022). Our study also showed that maize yield and dry matter accumulation generally increased and then decreased with fertilizer application rates increase, reaching a maximum value under RM, which is consistent with the results of Morell et al. (2011). The linear fitting also showed that grain yield, biomass, 100-kernel weight, and ear grains all followed a parabolic trend with increasing fertilizer application rates, reaching a peak value at RM, especially with the increase of fertilization years (Figure 8). This may be the results of both N and P fertilizer factors. Because the soil phosphorus was gradually accumulates with increasing years of fertilizer application, accelerating vegetative growth of crops, leading to premature development of reproductive organs, affecting the ear grains and grain weight of maize (Chen et al., 2015; Kong et al., 2017). Another, excessive N fertilizer application resulted in premature leaf senescence, reduced photosynthetic capacity, which affected the carbon assimilation process and

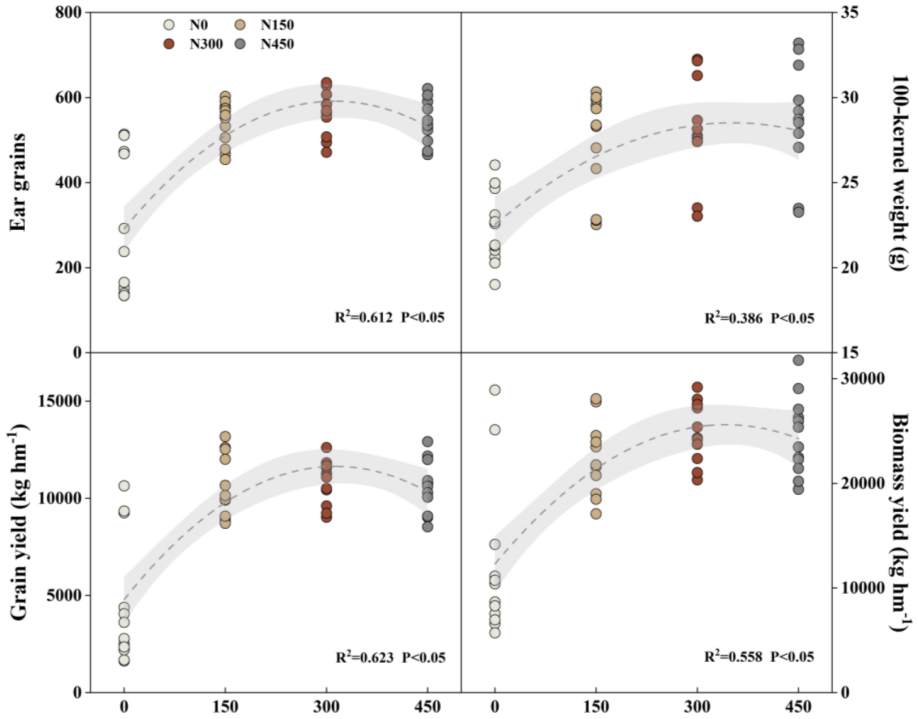

FIGURE 8
Linear regression relationships between different fertilization levels and maize ear grains, 100-kernel weight, grain yield, and biomass yield from 2013 to 2016. Treatments N450, N300, N150, and N0 represent applied N:P_2O_5 rates of 0:0, 150:75, 300:150, and 450:225 kg hm^{-1}, respectively.

decrease nitrogen proportion of maize grains, leading to the sterilization of maize grain (Liu et al., 2018; Loudari et al., 2022). Eventually, the combination of these two factors reduced maize yield.

4.2 Effects of nutrients uptake under fertilizer rates

The nutrients content and uptake in various plant organs were two important factors for assessing nutrient uptake and utilization in crops (Luo et al., 2016). In this study, fertilization treatments were significantly increased the accumulation of nitrogen and phosphorus, with an average increase by 260.53% and 264.74% compared to the RN, respectively. The above-ground biomass of maize significantly increased after fertilization under RFRH system. Because film mulching could effectively improve soil moisture and temperature conditions to promote the maize roots and canopy growth, thus increasing nutrient accumulation. Similar results was also obtained by Li et al. (2019) in the arid region of northwest China.

Li et al. (2021) found that crop plants nitrogen accumulation was initially increased and then followed by a decrease with fertilizer application rates. Similarly, our study also found that the increase in nitrogen accumulation was highest in RM treatments (Table 1). Because appropriate nitrogen application rate can effectively promote crop nitrogen accumulation, while excessive rate could alter soil structure, acidity, as well as soil moisture and temperature conditions, thereby affecting the survival environment of soil microorganisms and roots growth, resulting in negative effects and reduced nutrient uptake (Zhang et al., 2016; Wu et al., 2020). In contrast to the results of Zhang Y. M, et al. (2021) on maize phosphorus uptake in the Loess Plateau region, our results showed an upward trend in phosphorus accumulation with fertilizer application rates increase (Table 1). This may be related to different planting areas and soil nutrient contents, or it may be due to nitrogen application promotes aboveground growth and significant increases biomass yield. Another possibility was that the enzymes involved in nitrogen metabolism could also promote phosphorus absorption, thereby increasing the amount of phosphorus uptake, which did not reach the critical phosphorus uptake threshold (Jing et al., 2022). Additionally, differences between years was attributed to the influence of climates in different experimental years, and the N and P accumulation of maize during 2013-2014 was significantly higher than that during 2015-2016. This was likely due to abundant rainfall and favorable rainfall distribution for maize growth in 2013 and 2014, which could provide an ideal water-fertilizer coupling condition for crop growth, thus stimulating the growth-promoting effects on maize. Moreover, it also promoted the transformation of soil nitrate nitrogen and available phosphorus, thereby enhancing maize nutrient uptake (Dong et al., 2019).

The coordinated supply of nitrogen and phosphorus could promote the nutrient absorption and utilization of crop, and was

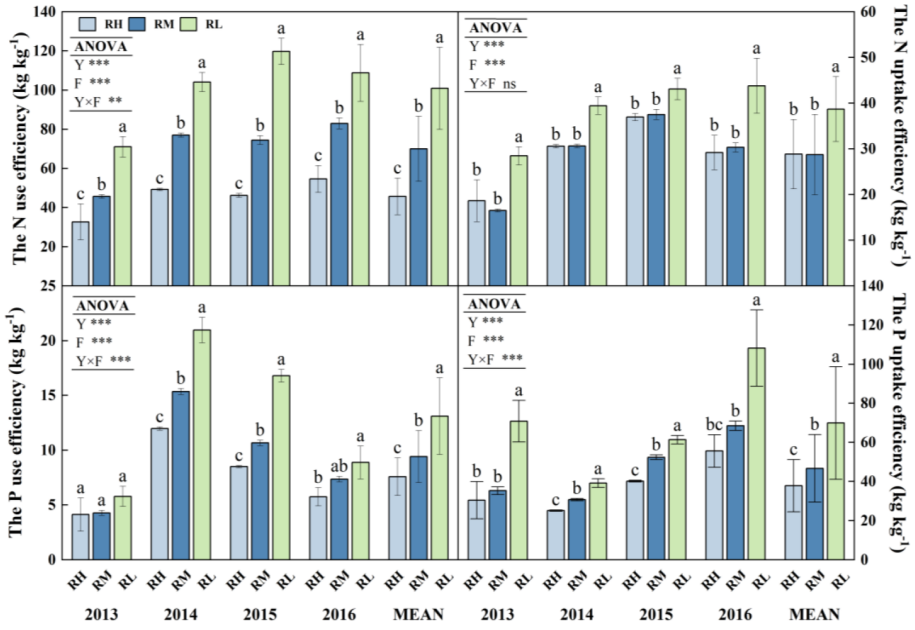

FIGURE 9
N and P use efficiency and uptake efficiency of maize under different fertilization levels from 2013 to 2016. Treatments RH, RM and RL represent applied N:P_2O_5 rates of 0:0, 150:75, 300:150, and 450:225 kg hm^{-1}, respectively. Data are means ± SD (n=3). Lower case letters indicate significant differences among treatments. Bars represent standard deviations (LSD test, P< 0.05). In Analysis of Variance, Y, F and Y×F represents the year, fertilizer and the interaction between the year and fertilizer. *** Significant differences at P < 0.001; ** significant differences at P < 0.01; ns indicates non−significant difference.

also beneficial to the growth and yield increase (Phares et al., 2022). This study found that the trends of nitrogen and phosphorus accumulation in different parts of maize plants in different fertilizer rates treatments was different in different experimental years (Figure 7). It indicates that the nutrient transfer from vegetative organs to reproductive organs under different precipitation patterns were different. Moreover, our results also showed that there was obvious threshold effect in fertilization promoting nutrient accumulation and yield increase. Because soil water participates in many growth processes, such as synthesis of biological macromolecules and enzymes, plant physiology and biochemical, thus the nutrient uptake and utilization depend on soil moisture effectiveness. Hu et al. (2009) found that soil moisture content determines the availability of soil nitrogen and its transport to the roots. Under dry conditions of the Loess Plateau, water stress limits both nitrogen mineralization and root nutrient uptake, thereby weakening the crop yield response to nitrogen input (Lian et al., 2017). The application of phosphorus fertilizer can promote rapid root development and branching, indirectly improving nitrogen uptake. When only phosphorus fertilizer is applied, it promotes the growth of a small amount of roots, whereas the impact of single nitrogen fertilizer application is relatively small, and it even increases the risk of nitrogen leaching (Wen et al., 2016). In addition, when sufficient water is available, leaf photosynthesis and root activity are enhanced, achieving more effective transportation and accumulation of nutrients (Qi et al., 2020). Alternation of wet and dry conditions can also change soil structure, affecting the adsorption and release of available nutrients by soil aggregates (Xiang et al., 2008).

4.3 Effect of N and P utilization under fertilizer rates

The RFRH systems can increase crop yield and fertilizer utilization efficiency. However, the utilization efficiency generally shows a downward trend as fertilizer application increased, and the highest yield does not always correspond to the highest utilization efficiency (Zhang et al., 2015; Wang et al., 2018). Similarly, in this study, compared with RL, the RM achieved higher N/P accumulation and maize yield, but with significantly lower nitrogen and phosphorus use efficiency, uptake efficiency, and harvest index. While the nitrogen and phosphorus fertilizer use efficiency, uptake efficiency, and grain yield of RM were moderately enhanced than RH. This study showed that the nitrogen use efficiency, uptake efficiency, and harvest index of maize decreased gradually with fertilizer application rates increase, and reaching the maximum value under RL (Figures 9, 10). This is consistent with the results of a long-term located field experiment by Yang et al. (2017). It may be due to the fact that the nitrogen fertilizer exists in the form of nitrate nitrogen in alkaline soils, and when the fertilizer application rate is too high and the inorganic nitrogen content exceeds the safe threshold, excessive nitrogen was leached, thus reduced nitrogen fertilizer use efficiency (Ju et al., 2004; Woli et al., 2016). Similarly, this study also showed that the phosphorus fertilizer use efficiency and uptake efficiency of maize decreased with fertilizer application rate increase, and the phosphorus fertilizer use efficiency was gradually decreased with the increasing of fertilizer application years (Figures 9, 10). This may be related to the fact that phosphorus was a fast-acting fertilizer, and it was easily strongly adsorbed and further mineralized by the soil

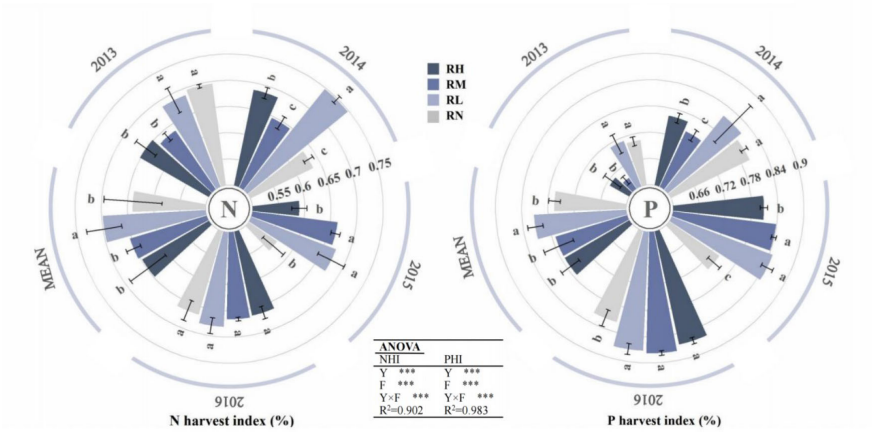

FIGURE 10
N and P harvest index of maize under different fertilization levels from 2013 to 2016. Treatments RH, RM, RL, and RN represent applied N:P_2O_5 rates of 0:0, 150:75, 300:150, and 450:225 kg hm^{-1}, respectively. Data are means ± SD (n=3). Lower case letters indicate significant differences among treatments. Bars represent standard deviations (LSD test, P< 0.05). In Analysis of Variance, Y, F and Y×F represents the year, fertilizer and the interaction between the year and fertilizer. *** Significant differences at P < 0.001.

(Yuan et al., 2022). Continuous fertilizer application leads to an increasing amount of unused phosphorus in the soil, which hinders its absorption and utilization. Moreover, the nitrogen and phosphorus use efficiency of each fertilization treatment have differences with the fertilizer application rate under different precipitation years. When rainfall is abundant (2013), it may have further exacerbated nitrogen and phosphorus nutrient leaching, while reducing soil cation exchange capacity. Meanwhile, excessive application of inorganic fertilizers also exacerbates soil nitrification, causing soil acidification and the soil phosphorus content may have been relatively low in the early stages of the experiment, resulting in lower nitrogen and phosphorus utilization efficiency in 2013 (Duan

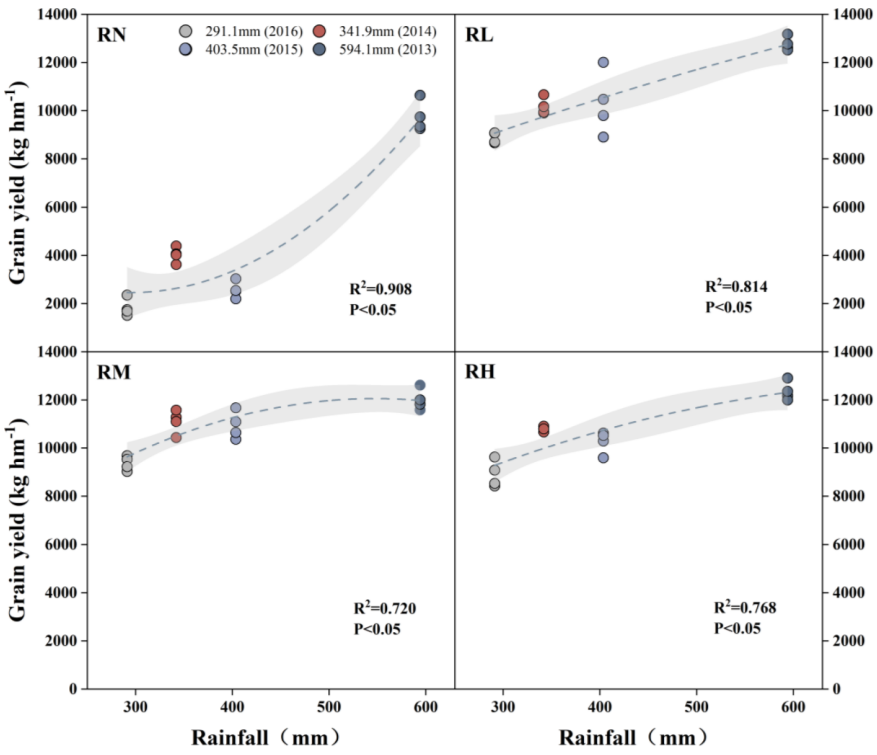

FIGURE 11
Linear regression relationship between maize grain yield and annual precipitation under different fertilization levels from 2013 to 2016. Treatments RH, RM, RL, and RN represent applied N:P_2O_5 rates of 0:0, 150:75, 300:150, and 450:225 kg hm^{-1}, respectively. The dots in the graph represent annual precipitation for different years: 594.1mm (2013), 341.9mm (2014), 403.5mm (2015), 291.1mm (2016).

et al., 2014; Guo et al., 2017). The appropriate alternation of dry and wet seasons (2014) promoted the release of phosphorus in soil and increased its solubility, greatly improving the effectiveness of phosphorus in soil (Bünemann et al., 2013; Suriyagoda et al., 2014). And good water-fertilizer effects resulted in high N and P fertilizer use efficiency with moderate rainfall in 2015. When rainfall is insufficient in 2016, the evapotranspiration was increased with fertilizer application, thereby exacerbating water stress, reducing water use efficiency and restricting root and rhizosphere growth, which was not conducive to the early growth and development, affects nutrient accumulation, and leads to a decrease in nitrogen use efficiency (Li et al., 2018; Zhang et al., 2022).

5 Conclusion

The RFRH system can effectively promote the water- fertilizer relationship of crops. The results of this study indicate that under sufficient precipitation, the RM treatment obtained the highest yield, while the RL treatment had the highest nitrogen and phosphorus utilization efficiency. Under less precipitation, the water-fertilizer relationship was somewhat inhibited and affected the yield, but the RM treatment still had highest dry matter, yield and nutrient accumulation, while the fertilizer utilization efficiency was little lower than the RL. Overall, the medium fertilizer rate (N 300 kg hm^{-2}, P_2O_5 150 kg hm^{-2}) was recommended as the suitable fertilizer rate for RFRH system in semi-arid regions, additionally, reduce the fertilization appropriately based on the precipitation amount.

Data availability statement

The original contributions presented in the study are included in the article/supplementary material. Further inquiries can be directed to the corresponding author.

Author contributions

The manuscript was reviewed and approved for publication by all authors. XR, ZJ and PZ conceived and designed the experiments. JW, GL, NC, YZ, and DL performed the experiments. JW, GL, NC, YZ, and DL analyzed the data. JW, YZ, and DL wrote the paper. EL, PZ, XR, and ZJ reviewed and revised the paper. PZ and EL corrected the English language for the paper.

Funding

This study was supported by the National key scientific research projects of China (2021YFE0101300, 2021YFD1901102), the Natural Science Basic Research Plan in Shaanxi Province (2023-JC-YB-185), the National Natural Science Foundation of China (31901475, 31801314), the Postdoctoral Science Foundation funded project (2019T120951).

Conflict of interest

The authors declare that the research was conducted in the absence of any commercial or financial relationships that could be construed as a potential conflict of interest.

Publisher's note

All claims expressed in this article are solely those of the authors and do not necessarily represent those of their affiliated organizations, or those of the publisher, the editors and the reviewers. Any product that may be evaluated in this article, or claim that may be made by its manufacturer, is not guaranteed or endorsed by the publisher.

References

Bünemann, E. K., Keller, B., Hoop, B., Jud, K., Boivin, P., and Frossard, E. (2013). Increased availability of phosphorus after drying and rewetting of a grassland soil. *Plant Soil* 370, 511–526. doi: 10.1007/s11104-013-1651-y

Chen, Y. L., Xiao, C. X., Wu, D. L., Xia, T. T., Chen, Q. W., Chen, F. J., et al. (2015). Effects of nitrogen application rate on grain yield and grain nitrogen concentration in two maize hybrids with contrasting nitrogen remobilization efficiency. *Eur. J. Agron.* 62, 79–89. doi: 10.1016/j.eja.2014.09.008

Dong, Z. Y., Zhang, X. D., Li, J., Zhang, C., Wei, T., Yang, Z., et al. (2019). Photosynthetic characteristics and grain yield of winter wheat (Triticum aestivum l.) in response to fertilizer, precipitation, and soil water storage before sowing under the ridge and furrow system: a path analysis. *Agric. For. Meteorol.* 272, 12–19. doi: 10.1016/j.agrformet.2019.03.015

Duan, Y. H., Xu, M. G., Gao, S. D., Yang, X. Y., Huang, S. M., Liu, H. B., et al. (2014). Nitrogen use efficiency in a wheat–corn cropping system from 15 years of manure and fertilizer applications. *Field Crops Res.* 157, 47–56. doi: 10.1016/j.fcr.2013.12.012

Duan, Y. H., Xu, M. G., Wang, B. R., Yang, X. Y., Huang, S. M., and Gao, S. D. (2011). Long-term evaluation of manure application on maize yield and nitrogen use efficiency in China. *Soil Sci. Soc. America J.* 75, 1562–1573. doi: 10.2136/sssaj2010.0315

Fernandes, A. P. G., Machado, J., Fernandes, T. R., Vasconcelos, M. W., and Carvalho, S. M. P. (2022). Water and nitrogen fertilization management in light of climate change: impacts on food security and product quality. *Plant Nutr. Food Secur. Era Climate Change* 5, 147–178. doi: 10.1016/B978-0-12-822916-3.00013-5

Gan, Y., Siddique, K. H. M., Turner, N. C., Li, X. G., Niu, J. Y., Yang, C., et al. (2013). Ridge-furrow mulching systems–an innovative technique for boosting crop productivity in semiarid rain-fed environments. *Adv. Agron.* 118, 429–476. doi: 10.1016/B978-0-12-405942-9.00007-4

Guo, J. M., Wang, Y. H., Blaylock, A. D., and Chen, X. P. (2017). Mixture of controlled release and normal urea to optimize nitrogen management for high-yielding (> 15 mg ha^{-1}) maize. *Field Crops Res.* 204, 23–30. doi: 10.1016/j.fcr.2016.12.021

Hu, T. T., Kang, S. J., Li, F. S., and Zhang, J. H. (2009). Effects of partial root-zone irrigation on the nitrogen absorption and utilization of maize. *Agric. Water Manag.* 96, 208–214. doi: 10.1016/j.agwat.2008.07.011

Jia, Q. M., Xu, R. R., Chang, S. H., Zhang, C., Liu, Y. J., Shi, W., et al (2020). Planting practices with nutrient strategies to improves productivity of rain-fed corn and resource use efficiency in semi-arid regions. *Agric. Water Manag.* 228, 105879. doi: 10.1016/j.agwat.2019.105879

Jing, J., Zhang, S., Yuan, L., Li, Y. T., Chen, C. R., and Zhao, B. Q. (2022). Humic acid modified by being incorporated into phosphate fertilizer increases its potency in stimulating maize growth and nutrient absorption. *Front. Plant Sci.* 13. doi: 10.3389/fpls.2022.885156

Ju, X. T., Liu, X. J., Zhang, F. S., and Roelcke, M. (2004). Nitrogen fertilization, soil nitrate accumulation, and policy recommendations in several agricultural regions of China. *Ambio.* 33, 300–305. doi: 10.1579/0044-7447-33.6.300

Kong, L., Xie, Y., Hu, L., Si, J., and Wang, Z. (2017). Excessive nitrogen application dampens antioxidant capacity and grain filling in wheat as revealed by metabolic and physiological analyses. *Sci. Rep.* 7, 43363. doi: 10.1038/srep43363

Langholtz, M., Davison, B. H., Jager, H. I., Eaton, L., Baskaran, L. M., Davis, M., et al. (2021). Increased nitrogen use efficiency in crop production can provide economic and environmental benefits. *Sci. Total Environ.* 758, 143602. doi: 10.1016/j.scitotenv.2020.143602

Li, G. H., Cheng, G. G., Lu, W. P., and Lu, D. L. (2021). Differences of yield and nitrogen use efficiency under different applications of slow release fertilizer in spring maize. *J. Integr. Agric.* 20, 554–564. doi: 10.1016/S2095-3119(20)63315-9

Li, C. X., Li, Y. Y., Li, Y. J., and Fu, G. Z. (2018). Cultivation techniques and nutrient management strategies to improve productivity of rain-fed maize in semi-arid regions. *Agric. Water Manag.* 210, 149–157. doi: 10.1016/j.agwat.2018.08.014

Li, Y., Yang, L. Y., Wang, H., Xu, R. R., Chang, S. H., Hou, F. J., et al. (2019). Nutrient and planting modes strategies improves water use efficiency, grain-filling and hormonal changes of maize in semi-arid regions of China. *Agric. Water Manag.* 223, 105723. doi: 10.1016/j.agwat.2019.105723

Lian, Y. H., Meng, X. P., Yang, Z., Wang, T. L., Ali, S., Yang, B. P., et al. (2017). Strategies for reducing the fertilizer application rate in the ridge and furrow rainfall harvesting system in semiarid regions. *Sci. Rep.* 7, 2644. doi: 10.1038/s41598-017-02731-y

Lian, Y. H., Shahzad, A., Zhang, X. D., Wang, T. L., Liu, Q., Jia, Q. M., et al. (2016). Nutrient and tillage strategies to increase grain yield and water use efficiency in semi-arid areas. *Agric. Water Manag.* 178, 137–147. doi: 10.1016/j.agwat.2016.09.021

Liu, Z., Gao, J., Gao, F., Liu, P., Zhao, B., and Zhang, J. W. (2018). Photosynthetic characteristics and chloroplast ultrastructure of summer maize response to different nitrogen supplies. *Front. Plant Sci.* 9. doi: 10.3389/fpls.2018.00576

Loudari, A., Mayane, A., Zeroual, Y., Colinet, G., and Oukarroum, A. (2022). Photosynthetic performance and nutrient uptake under salt stress: differential responses of wheat plants to contrasting phosphorus forms and rates. *Front. Plant Sci.* 13. doi: 10.3389/fpls.2022.1038672

Luo, H. H., Yong, H. H., Zhang, Y. L., and Zhang, W. F. (2016). Effects of water stress and rewatering on photosynthesis, root activity, and yield of cotton with drip irrigation under mulch. *Photosynthetica* 54, 65–73. doi: 10.1007/s11099-015-0165-7

Morell, F. J., Lampurlane, J., Alvaro, F. J., and Cantero, M. C. (2011). Yield and water use efficiency of barley in a semiarid Mediterranean agro-ecosystem: long-term effects of tillage and n fertilization. *Soil Tillage Res.* 117, 76–84. doi: 10.1016/j.still.2011.09.002

Nasar, J., Wang, G. Y., Ahmad, S., Muhammad, I., Zeeshan, M., Gitari, H., et al. (2022). Nitrogen fertilization coupled with iron foliar application improves the photosynthetic characteristics, photosynthetic nitrogen use efficiency, and the related enzymes of maize crops under different planting patterns. *Front. Plant Sci.* 13. doi: 10.3389/fpls.2022.988055

Phares, C. A., Amoakwah, E., Danquah, A., Afrifa, A., Beyaw, L. R., and Frimpong, K. A. (2022). Biochar and NPK fertilizer co-applied with plant growth promoting bacteria (PGPB) enhanced maize grain yield and nutrient use efficiency of inorganic fertilizer. *J. Agric. Food Res.* 10, 100434. doi: 10.1016/j.jafr.2022.100434

Qi, D. L., HU, T. T., and Xue, S. (2020). Effects of nitrogen application rates and irrigation regimes on grain yield and water use efficiency of maize under alternate partial root-zone irrigation. *J. Integr. Agric.* 19, 2792–2806. doi: 10.1016/S2095-3119 (20)63205-1

Ren, X. L., Cai, T., Chen, X. L., Zhang, P., and Jia, Z. K. (2016a). Effect of rainfall concentration with different ridge widths on winter wheat production under semiarid climate. *Eur. J. Agronomy.* 77, 20–27. doi: 10.1016/j.eja.2016.03.008

Ren, X. L., Chen, X. L., Cai, T., Wei, T., Wu, Y., Ali, S., et al. (2017). Effects of ridge-furrow system combined with different degradable mulching materials on soil water conservation and crop production in semi-humid areas of China. *Front. Plant Sci.* 8. doi: 10.3389/fpls.2017.01877

Ren, X. L., Chen, X. L., and Jia, Z. K. (2010). Effect of rainfall collecting with ridge and furrow on soil moisture and root growth of corn in semiarid northwest China. *J. Agron. Crop Science.* 196 (2), 109–122. doi: 10.1111/j.1439-037X.2009.00401.x

Ren, X. L., Zhang, P., Liu, X. L., Ali, S., Chen, X. L., and Jia, Z. K. (2016b). Impacts of different mulching patterns in rainfall-harvesting planting on soil water and spring corn growth development in semihumid regions of China. *Soil Res.* 55 (3), 285–295. doi: 10.1071/SR16127

Rochester, I. J. (2011). Assessing internal crop nitrogen use efficiency in high-yielding irrigated cotton. *Nutr. Cycling Agroecosyst.* 90 (1), 147–156. doi: 10.1007/s10705-010-9418-9

Suriyagoda, L. D. B., Ryan, M. H., Renton, M., and Lambers, H. (2014). Plant responses to limited moisture and phosphorus availability: a meta-analysis. *Adv. Agron.* 124, 143–200. doi: 10.1016/B978-0-12-800138-7.00004-8

Wang, D., Li, G. Y., Mo, Y., Cai, M. K., and Bian, X. Y. (2018). Evaluation of optimal nitrogen rate for corn production under mulched drip fertigation and economic benefits. *Field Crops Res.* 216, 225–233. doi: 10.1016/j.fcr.2017.10.002

Wang, J. B., Xie, J. H., Li, L. L., and Adingo, S. (2022). Review on the fully mulched ridge-furrow system for maize sustainable production on the semiarid Loess Plateau. *J. Integr. Agric.* 22, 1277–1290. doi: 10.1016/j.jia.2022.09.023

Wei, S. S., Wang, X. Y., Li, G. H., Jiang, D., and Dong, S. T. (2019). Maize canopy apparent photosynthesis and ^{13}C-photosynthate reallocation in response to different density and n rate combinations. *Front. Plant Sci.* 10. doi: 10.3389/fpls.2019.01113

Wen, Z. H., Shen, J. B., Blackwell, M., Li, H. G., Zhao, B. Q., Yuan, H. M., et al. (2016). Combined applications of nitrogen and phosphorus fertilizers with manure increase maize yield and nutrient uptake via stimulating root growth in a long-term experiment. *Pedosphere* 26 (1), 62–73. doi: 10.1016/S1002-0160(15)60023-6

Woli, P., Hoogenboom, G., and Alva, A. (2016). Simulation of potato yield, nitrate leaching, and profit margins as influenced by irrigation and nitrogen management in different soils and production regions. *Agric. Water Manag.* 171, 120–130. doi: 10.1016/j.agwat.2016.04.003

Wu, L. N., Jiang, Y., Zhao, F. Y., He, X. F., Liu, H. F., and Yu, K. (2020). Increased organic fertilizer application and reduced chemical fertilizer application affect the soil properties and bacterial communities of grape rhizosphere soil. *Sci. Rep.* 10, 1–10. doi: 10.1038/s41598-020-66648-9

Wu, W., and Ma, B. L. (2015). Integrated nutrient management (INM) for sustaining crop productivity and reducing environmental impact: a review. *Sci. Total Environ.* 512, 415–427. doi: 10.1016/j.scitotenv.2014.12.101

Wu, Q. H., Zhang, S. X., Ren, Y., Zhan, X. Y., Xu, M. G., and Feng, G. (2018). Soil phosphorus management based on the agronomic critical value of Olsen p. *Commun. Soil Sci. Plant Anal.* 49, 934–944. doi: 10.1080/00103624.2018.1448410

Wu, Y. W., Zhao, B., Li, X. L., Liu, Q. L., Feng, D. J., Lan, T. Q., et al. (2022). Nitrogen application affects maize grain filling by regulating grain water relations. *J. Integr. Agric.* 21, 977–994. doi: 10.1016/S2095-3119(20)63589-4

Xiang, S. R., Doyle, A., Holden, P. A., and Schimel, J. P. (2008). Drying and rewetting effects on c and n mineralization and microbial activity in surface and subsurface California grassland soils. *Soil Biol. Biochem.* 40, 2281–2289. doi: 10.1016/j.soilbio.2008.05.004

Xu, J. T., Cai, H. J., Wang, X. J., Ma, C. G., Lu, Y. J., Ding, Y. B., et al (2020). Exploring optimal irrigation and nitrogen fertilization in a winter wheat-summer maize rotation system for improving crop yield and reducing water and nitrogen leaching. *Agric. Water Manag.* 228, 105904. doi: 10.1016/j.agwat.2019.105904

Yang, X. L., Lu, Y. L., Ding, Y., Yin, X. F., Raza, S., and Tong, Y. A. (2017). Optimising nitrogen fertilisation: a key to improving nitrogen-use efficiency and minimising nitrate leaching losses in an intensive wheat/maize rotation, (2008–2014). *Field Crops Res.* 206, 1–10. doi: 10.1016/j.fcr.2017.02.016

Yuan, Y., Gai, S., Tang, C., Jin, Y. X., Cheng, K., Antonietti, M., et al. (2022). Artificial humic acid improves maize growth and soil phosphorus utilization efficiency. *Appl. Soil Ecology.* 179, 104587. doi: 10.1016/j.apsoil.2022.104587

Zhang, X., Davidson, E. A., Mauzerall, D. L., Searchinger, T. D., Dumas, P., and Shen, Y. (2015). Managing nitrogen for sustainable development. *Nature* 528, 51–59. doi: 10.1038/nature15743

Zhang, G. X., Hou, Y. T., Zhang, H. P., Fan, H. Z., Wen, X. X., Han, J., et al. (2022). Optimizing planting pattern and nitrogen application rate improves grain yield and water use efficiency for rain-fed spring maize by promoting root growth and reducing redundant root growth. *Soil Tillage Res.* 220, 105385. doi: 10.1016/j.still.2022.105385

Zhang, Y. L., Li, C. H., Wang, Y. W., Hu, Y. M., Christie, P., and Zhang, J. L. (2016). Maize yield and soil fertility with combined use of compost and inorganic fertilizers on a calcareous soil on the north China plain. *Soil Tillage Res.* 155, 85–94. doi: 10.1016/j.still.2015.08.006

Zhang, Y., Ma, Q., Liu, D. H., Sun, L. F., Ren, X. L., Ali, S., et al. (2018). Effects of different fertilizer strategies on soil water utilization and maize yield in the ridge and furrow rainfall harvesting system in semiarid regions of China. *Agric. Water Manag.* 208, 414–421. doi: 10.1016/j.agwat.2018.06.032

Zhang, X. D., Wang, R., Dong, Z. Y., Zhang, P., and Jia, Z. K. (2021). Nutritional quality degradation: a potential risk due to nutrient dilution effects in film-mulched maize. *Agric. Water Manag.* 257, 107133. doi: 10.1016/j.agwat.2021.107133

Zhang, Y. Q., Wang, J. D., Gong, S. L., Xu, D., and Sui, J. (2017). Nitrogen fertigation effect on photosynthesis, grain yield and water use efficiency of winter wheat. *Agric. Water Manag.* 179, 277–287. doi: 10.1016/j.agwat.2016.08.007

Zhang, P., Wei, T., Li, Y. L., Zhang, Y., Cai, T., Ren, X. L., et al. (2019). Effects of deficit irrigation combined with rainwater harvesting planting system on the water use efficiency and maize (Zea mays l.) yield in a semiarid area. *Irrigation Sci.* 37, 611–625. doi: 10.1007/s00271-019-00628-4

Zhang, Y. M., Xue, J., Zhai, J., Zhang, G. Q., Zhang, W. X., Wang, K. R., et al. (2021). Does nitrogen application rate affect the moisture content of corn grains? *J. Integr. Agric.* 20, 2627–2638. doi: 10.1016/S2095-3119(20)63401-3

frontiers | Frontiers in Plant Science

TYPE Original Research
PUBLISHED 15 June 2023
DOI 10.3389/fpls.2023.1201759

OPEN ACCESS

EDITED BY
Fahad Shafiq,
Government College University, Lahore, Pakistan

REVIEWED BY
Chenggang Liu,
Xishuangbanna Tropical Botanical Garden, Chinese Academy of Sciences (CAS), China
Gang Xu,
Southwest University of Science and Technology, China

*CORRESPONDENCE
Yuwu Li
liyuwu@qau.edu.cn

†These authors have contributed equally to this work and share first authorship

RECEIVED 07 April 2023
ACCEPTED 23 May 2023
PUBLISHED 15 June 2023

CITATION
Song D, Liu S, Fan L, Yang J, Li H, Xia Y and Li Y (2023) Nutrient stoichiometric and resorption characteristics of the petals of four common urban greening Rosaceae tree species. *Front. Plant Sci.* 14:1201759. doi: 10.3389/fpls.2023.1201759

Nutrient stoichiometric and resorption characteristics of the petals of four common urban greening Rosaceae tree species

Dan Song[1†], Shuting Liu[1†], Lide Fan[1], Jinyan Yang[1], Haifang Li[1,2], Yujie Xia[1] and Yuwu Li[1,2*]

[1]College of Landscape Architecture and Forestry, Qingdao Agricultural University, Qingdao, China, [2]Academy of Dongying Efficient Agricultural Technology and Industry on Saline and Alkaline Land in Collaboration with Qingdao Agricultural University, Dongying, China

Objective: Nutrient resorption efficiency and stoichiometric ratios are important strategies for understanding plants. The present study examined whether or not the nutrient resorption process of plant petals is similar to that of leaves and other vegetative organs, as well as the nutrient restriction status of the whole flowering process of plants in urban ecosystems.

Methods: Four Rosaceae tree species, *Prunus yedoensis* Matsum, *Prunus serrulata* var. *lannesiana, Malus micromalus* Makino, and *Prunus cerasifera* 'Atropurpurea', were selected as urban greening species to analyze the contents of C, N, P, and K elements in the petals and their stoichiometric ratios and nutrient resorption efficiencies.

Results: The results show interspecific differences in nutrient contents, stoichiometric ratios, and nutrient resorption efficiency of the fresh petals and petal litter of the four Rosaceae species. The nutrient resorption process was similar to that of the leaves before the petals fell. The nutrient contents of petals were higher than that of leaves at the global level, but the stoichiometric ratio and nutrient resorption efficiency of petals were lower. According to the "relative resorption hypothesis", N was limiting during the entire flowering period. The nutrient resorption efficiency of petals was positively correlated with nutrient variation. The correlation between the nutrient resorption efficiency of petals with nutrient content and stoichiometric ratio of petal litter was stronger.

Conclusion: The experimental results provide scientific basis and theoretical support for the selection, scientific maintenance and fertilization management of Rosaceae tree species in urban greening.

KEYWORDS

Rosaceae, fresh petals, petal litter, nutrient resorption, stoichiometry, Qingdao

1 Introduction

In the long-term evolution process, plants have formed a series of mechanisms and strategies to adapt to the changing environment. One of the important, nutrient resorption is important for nutrient recycling and reuse under the pressures of resource crisis caused by environmental changes and the need for a stable balance of nutrients to maintain the normal physiological activities of plants (Sterner and Elser, 2002; Fan et al., 2015; Xie et al., 2020; Li et al., 2021), thus increasing the chances of plant survival and species continuation (Zhao et al., 2006). Nutrient resorption is the transfer and transport of nutrients to other tissues of plants before senescence and litterfall (Killingbeck, 1986; Aerts, 1996; Lu et al., 2018); it provides energy and nutrients for new tissues and prolongs the retention time of nutrients in plants, thereby reducing the process of plant dependence on external nutrients (Covelo et al., 2008; Zhao et al., 2010; Vergutz et al., 2012). Nutrient resorption is a protective mechanism by which plants improve nutrient use efficiency in soil nutrient-poor environments (Yuan et al., 2006; Jiang et al., 2017). It also reduces the nutrient loss caused by litter decomposition and leaching (May and Killingbeck, 1992). Therefore, nutrient resorption plays an important role in plant adaptation to stress, nutrient preservation, enhancement of competitiveness and productivity, and maintenance of the stoichiometric balance of chemical elements in plants (Brant and Chen, 2015; Lu et al., 2018).

Carbon (C), nitrogen (N), phosphorus (P), and potassium (K), as essential life elements for the structure of plant somatic cells and growth and development, have a strong coupling effect (Ågren, 2004) and play an important role in various physiological functions of plant growth and adaptation to the environment. Reiners (1986) first proposed the theory of ecological stoichiometry, and many researchers have since studied and expanded the application of ecological stoichiometry theory in consumer-driven nutrient cycling (Sterner, 1990; Urabe et al., 1995), biological nutrient limitation (Koerselman and Meuleman, 1996; Aerts and Chapin, 1999), forest succession and decline (Wardle et al., 2004), and ecosystem nutrient supply and demand balance (Schade et al., 2005; Zeng and Chen, 2005). Among such applications, plant C, N, P, and K stoichiometry is an important means of studying the energy cycle and element balance of terrestrial ecosystems. C:N, C:P, and C:K can directly reflect the nutrient utilization characteristics of plants to a certain extent. N:P, N:K, and K:P can be used as indicators of the supply of soil nutrients to plant growth (Li et al., 2010; Yang et al., 2021). Recent years have seen many studies based on plant leaves. However, studies on nutrient content and element stoichiometric characteristics of flower organs, such as petals, during flowering are still rare. In particular, few reports have been done on whether there are similar nutrient resorption processes in plant petals and other organs accompanying this process. Studying the nutrient resorption and stoichiometric characteristics of plant petals is helpful for understanding the nutrient cycling process of urban ornamental flowering tree species.

There are approximately 124 genera and more than 3300 species of Rosaceae, which are widely distributed in the world but more common in the north temperate zone. China is the distribution center of Rosaceae, with about 50 genera and more than 1000 species (Su et al., 2015; Zou et al., 2019). Rosaceae, playing an important role in urban landscaping all over the world, are mostly ornamental flower plants, whose fruits, flowers, branches, and leaves have high ornamental value and strong ecological adaptability. Nutrient management of urban plants is the key to the management of urban green space and is also the basis for the selection, management, and ecological evaluation of urban landscaping plants (He, 2002).

Therefore, we chose four common Rosaceae species in northern China, *Prunus yedoensis* Matsum, *Prunus serrulata* var. *lannesiana*, *Malus micromalus* Makino, and *Prunus cerasifera* 'Atropurpurea', to clarify the C, N, P, and K nutrient contents, stoichiometric characteristics and their relationship with nutrient resorption of the fresh petals and petal litter of them, to study the petal nutrient resorption strategies during the flowering, and to judge whether there is an obvious nutrient resorption process in petals. The major scientific questions are as follows: (1) How did the nutrient content of the four Rosaceae species change during the short period of flowering and falling? (2) Is there a nutrient resorption process in petals similar to that in leaves? Do petals have greater nutrient resorption capacity than leaves? (3) What is the relationship between the nutrient content and stoichiometric ratio of the fresh petals and petal litter and nutrient resorption efficiency?

2 Materials and methods

2.1 Study site

The study was conducted in a green space at the Qingdao Agricultural University, Shandong Province, China (36°19'38 "N, 120°24'19" E), located in the north temperate zone and with a temperate oceanic monsoon climate (warm and humid). The site has a flat terrain and mainly brown loam soil. According to China Weather Network in, the annual average temperature of the area was 13.5°C in 2022, with August being the hottest month (25.5°C) and January the coldest (0°C). The annual average precipitation was 662.1 mm, with the most rainfall from June to August. The terrain of the test site is flat, and the soil is mainly brown loam.

2.2 Sample collection

Four Rosaceae species were commonly planted in the study site, including *Prunus yedoensis* Matsum, *Prunus serrulata* var. *lannesiana*, *Malus micromalus* Makino, and *Prunus cerasifera* 'Atropurpurea' were selected for the study. Three well-developed plants of each tree species were selected as the research objects. The basic information of the trees is shown in Table 1.

TABLE 1 Basic information of four Rosaceae tree species.

Species	Tree Age (year)	Tree Height (m)	Diameter at Breast Height (cm)	Tree Crown (m)
Prunus yedoensis Matsum	22	5.55 ± 0.43	17.40 ± 1.18	6.10 ± 0.65
Prunus serrulata var. *lannesiana*	22	5.75 ± 0.19	23.03 ± 2.43	6.72 ± 0.19
Malus micromalus Makino	20	5.73 ± 0.26	23.10 ± 1.40	7.19 ± 0.57
Prunus cerasifera 'Atropurpurea'	20	5.61 ± 0.20	24.67 ± 1.45	4.94 ± 0.32

Using herring-shaped escalators and high-branch shears, petals of the same weight were collected from branches in four directions, east, west, south and north of the crown of each sample tree, and mixed into a 100g samples of petals at the full bloom period (April 2022). These samples were immediately placed in Ziplock bags and brought to the laboratory, with three replicates collected per species.

Petal litter samples were collected during the whole flowering period (April to May 2022) of the selected tree species. Two 5 m × 2.5 m collection nets were set on both sides of the trunk of each tree species. Petals were collected from the nets at regular intervals until they fell completely. Each time, petal litters from the two collection nets of the same tree were mixed and placed in a Ziplock bag as a replicate (three replicates for each species).

2.3 Chemical analysis

After removing dust and impurities, the plant samples, including petals and petal litter, were dried to a constant weight in an oven at 60°C and ground to powder; this powder was passed through a 100-mesh sieve (0.149 mm) and stored until further analysis. The C and N contents in the plant samples were determined using an elemental analyzer (Primacs SNC 100-IC, Skalar Analytical B.V., Netherlands). The P and K were determined using an ICP-AES (iCAP6300, Thermo Fisher Scientific, USA) following HNO_3-$HClO_4$ digestion and leaching. Further, the nutrient resorption efficiency (NuRE) was calculated as follows (Lu et al., 2018):

$$NuRE = (1 - {}^{Nu_{litter}}\!/_{Nu_{fresh}}) \times 100\,\%$$

where Nu_{litter} indicates the nutrient content of petal litter ($g{\cdot}kg^{-1}$), and Nu_{fresh} means the nutrient content of fresh petals ($g{\cdot}kg^{-1}$).

Relative resorption efficiency (RR) was calculated as follows (Han et al., 2013):

$$RR = NRE - PRE$$

where NRE means the nitrogen resorption efficiency (%), and PRE means the phosphorus resorption efficiency (%). When RR≈0, plants are limited by N, P balance, or both. RR>0, plant growth was limited by N. RR<0, plant growth was limited by P.

Finally, the C, N, P, and K stoichiometric ratios of the fresh petals and petal litters were expressed as C:N, C:P, C:K, N:P, N:K, and K:P, and the element content ratio was adopted.

2.4 Statistical analyses

All data were represented as mean ± standard error. The independent sample *t*-test was used to compare the differences in N, P, and K contents, stoichiometric ratios, and nutrient resorption efficiencies between the fresh petals and petal litter of the same tree species. One-way analysis of variance (ANOVA) and Duncan's multiple range test ($\alpha = 0.05$) were used to compare between-species differences in each parameter. Origin 2021 was used to conduct linear fitting analysis on the relationships between nutrient resorption efficiencies of N, P, and K and the corresponding nutrient contents of the fresh petals and petal litter. Pearson correlation analysis (two-tailed) was used to analyze the correlation between nutrient resorption efficiency and the stoichiometric ratios of the fresh petals and petal litter, with Origin 2021 used to make correlation heat maps.

3 Results

3.1 C, N, P, and K contents of fresh petals and petal litter

The average C, N, P, and K contents of fresh petals of the four Rosaceae tree species were 465.67–482.33 $g{\cdot}kg^{-1}$, 20.84–36.93 $g{\cdot}kg^{-1}$, 3.47–4.63 $g{\cdot}kg^{-1}$, and 16.22–23.68$g{\cdot}kg^{-1}$, respectively (Figure 1). The content of C in fresh petals of *P. yedoensis* Matsum was significantly higher than that of *P. serrulata* var. *lannesiana* ($P< 0.05$), and that in *M. micromalus* Makino was significantly higher than that of *P. serrulata* var. *lannesiana* and *P. cerasifera 'Atropurpurea'* ($P< 0.05$) (Figure 1A). The contents of N in fresh petals of *P. yedoensis* Matsum and *P. serrulata* var. *lannesiana* were significantly higher than those of *M. micromalus* Makino and *P. cerasifera 'Atropurpurea'* ($P< 0.05$) (Figure 1B). Meanwhile, the P content in the fresh petals of *M. micromalus* Makino was significantly lower than those of the other three species ($P< 0.05$) (Figure 1C). The content of K in fresh petals of *P. serrulata* var. *lannesiana* was the highest, while that of *P. yedoensis* Matsum was the lowest ($P< 0.05$) (Figure 1D).

The C, N, P, and K content in fallen petal litter were 458.67–469.33 $g{\cdot}kg^{-1}$, 15.13–24.56 $g{\cdot}kg^{-1}$, 1.87–3.54 $g{\cdot}kg^{-1}$, and 12.08–20.93$g{\cdot}kg^{-1}$, respectively (Figure 1). No significant differences were found in C content in petal litter among the four Rosaceae species ($P > 0.05$) (Figure 1A). However, the N contents of the petal litter of *P. serrulata* var. *lannesiana* and *P. cerasifera 'Atropurpurea'* were significantly higher than that of *P. yedoensis* Matsum and *M.*

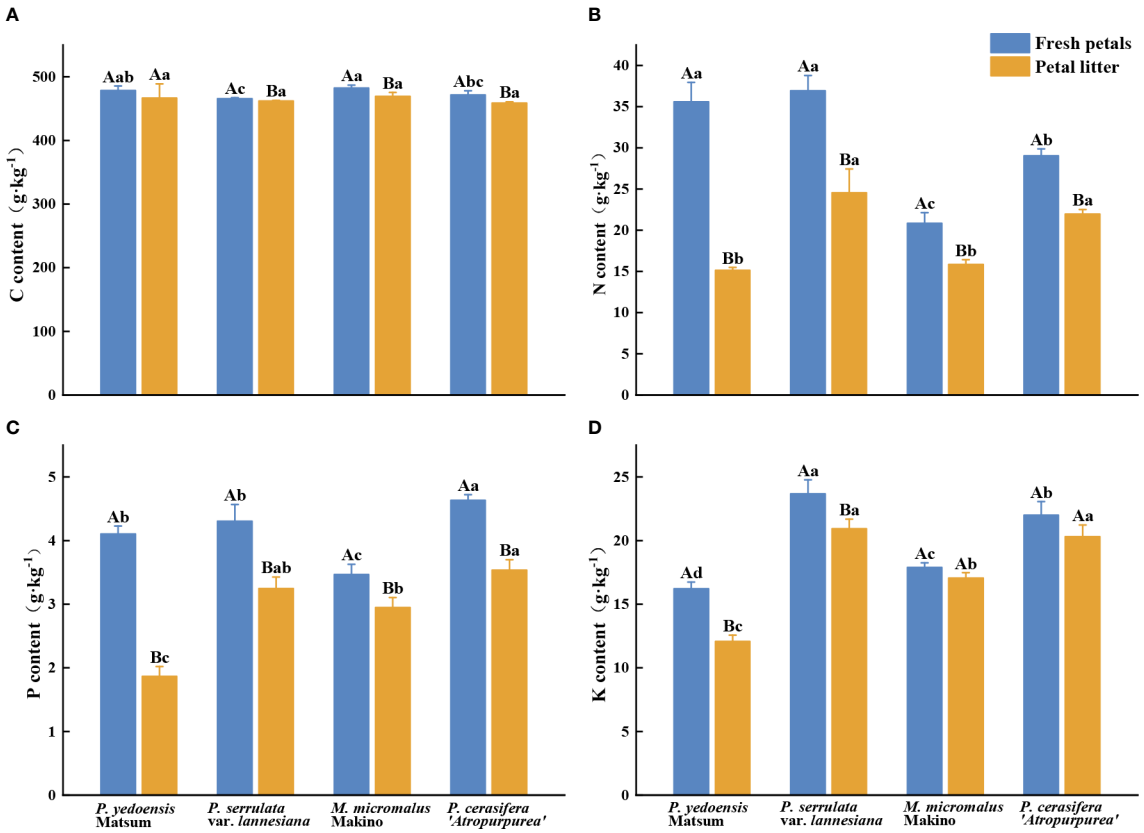

FIGURE 1
C, N, P, and K content of petals in fresh petals and petal litter of four Rosaceae species. Different uppercase letters indicate significant differences between fresh petals and petal litter of the same tree species ($P< 0.05$), and different lowercase letters indicate significant differences between different tree species of fresh petals or petal litter ($P< 0.05$).

micromalus Makino ($P< 0.05$) (Figure 1B). The P content of the petal litter of *P. yedoensis* Matsum was considerably lower than that of the other three species ($P< 0.05$) (Figure 1C). The K content of the petal litter of *P. serrulata* var. *lannesiana* and *P. cerasifera* '*Atropurpurea*' was the highest, while that of *P. yedoensis* Matsum was the lowest ($P< 0.05$) (Figure 1D).

The analysis also showed that the nutrient contents were higher in the fresh petals than in the petal litter for the four Rosaceae species. Except for *P. yedoensis* Matsum, the other three species had significantly higher C contents in the fresh petals than that in petal litter ($P< 0.05$) (Figure 1A). Similarly, the contents of N and P in the petal litter of the four Rosaceae species were significantly lower than those in the fresh petals ($P< 0.05$) (Figures 1B, C). The contents of K in the fresh petals were markedly higher than those in the petal litters of *P. yedoensis* Matsum and *P. serrulata* var. *lannesiana* ($P< 0.05$) (Figure 1D).

3.2 C, N, P, and K stoichiometric ratios in fresh petals and petal litter

The average C:N, C:P, C:K, N:P, N:K, and K:P ratios in the fresh petals of the four Rosaceae species were 12.63–23.19, 101.74–139.30, 19.70–29.51, 6.01–8.67, 1.17–2.20, and 3.96–5.5, respectively (Figure 2). The C:N and C:P of fresh petals of *M. micromalus* Makino were significantly the highest among the four species (Figures 2A, B), and the C:K and N:K of *P. yedoensis* Matsum were statistically significantly the highest ($P< 0.05$) (Figures 2C, E). The N:P of *P. yedoensis* Matsum and *P. serrulata* var. *lannesiana* was markedly higher than that of *M. micromalus* Makino and *P. cerasifera* '*Atropurpurea*' (Figure 2D), while the K:P of *P. yedoensis* Matsum was significantly lower than that of the other three species ($P< 0.05$) (Figure 2F).

Meanwhile, the C:N, C:P, C:K, N:P, N:P, N:K, and K:P of the petal litters of the four Rosaceae species were 19.00–30.84, 129.86–251.22, 22.09–38.68, 5.39–8.14, 0.93–1.25, and 5.75–6.49, respectively (Figure 2). The C:N of the petal litters of *P. yedoensis* Matsum and *M. micromalus* Makino were significantly higher than those of *P. serrulata* var. *Lannesiana* and *P. cerasifera* '*Atropurpurea*' (Figure 2A), and the C:P and C:K of *P. yedoensis* Matsum were the highest ($P< 0.05$) (Figures 2B, C). The N:P and K:P of the petal litter of *P. yedoensis* Matsum and *P. serrulata* var. *Lannesiana* were significantly higher than those of *M. micromalus* Makino and *P. cerasifera* '*Atropurpurea*' (Figures 2D, F), while the N:K of *M. micromalus* Makino was substantially lower than that of *P. yedoensis* Matsum and *P. serrulata* var. *Lannesiana* ($P< 0.05$) (Figure 2E).

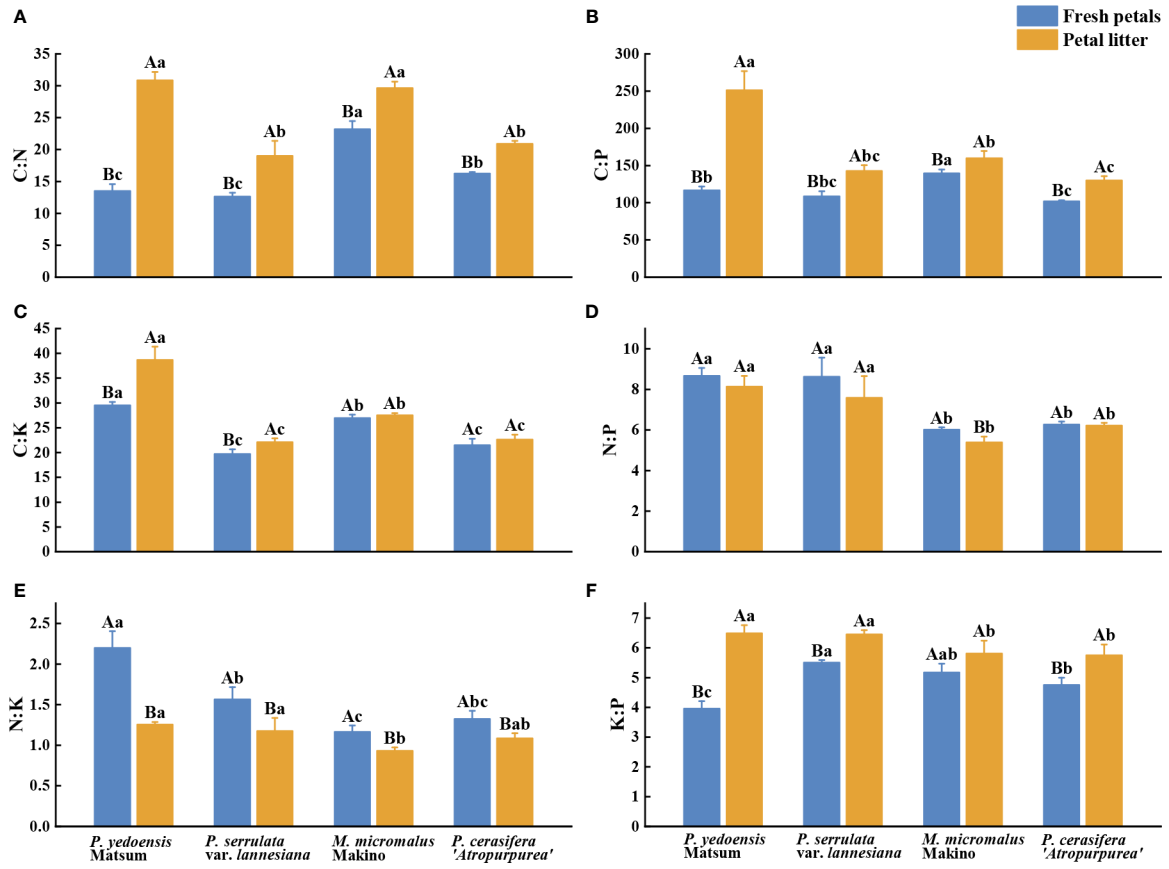

FIGURE 2
C, N, P, and K stoichiometric ratios of petals in fresh petals and petal litter of four Rosaceae species. Different uppercase letters indicate significant differences between fresh petals and petal litter of the same tree species ($P< 0.05$), and different lowercase letters indicate significant differences between different tree species of fresh petals or petal litter ($P< 0.05$).

Comparative analysis of the two sample types revealed that the C:N, C:P, C:K, and K:P of the petal litters of the four Rosaceae species were higher than those of the fresh petals, as well as significant differences between the fresh petals and petal litter of *P. yedoensis* Matsum and *P. serrulata* var. *lannesiana* ($P< 0.05$) (Figures 2A–C, F). Meanwhile, the N:P of the petal litters of the four Rosaceae species appeared slightly lower than that of the fresh petals, with a significant difference only in *M. micromalus* Makino ($P< 0.05$) (Figure 2D). Besides, the N:K ratios of petal litters was significantly lower than that of the fresh petals for all four tree species ($P< 0.05$) (Figure 2E).

3.3 Nutrient resorption characteristics in the petals of four tree species

The N, P, and K resorption efficiencies of the four Rosaceae tree species were 23.87%–57.35%, 14.95%–54.55%, and 4.66%–25.40%, respectively (Table 2). The efficiencies in the four species were in the decreasing order of *P. yedoensis* Matsum > *P. serrulata* var. *lannesiana* > *P. cerasifera* 'Atropurpurea' > *M. micromalus* Makino; the efficiencies of *P. yedoensis* Matsum were significantly the highest, and that of *M. micromalus* Makino was the lowest ($P< 0.05$). The N, P, and K

TABLE 2 N, P, and K resorption efficiencies of petals of four Rosaceae species.

Species	NRE%	PRE%	KRE%
Prunus yedoensis Matsum	57.35 ± 1.73Aa	54.55 ± 1.56Aa	25.40 ± 3.01Ba
Prunus serrulata var. *lannesiana*	33.62 ± 3.21Ab	24.49 ± 1.99Bb	11.56 ± 1.10Cb
Malus micromalus Makino	23.87 ± 1.16Ac	14.95 ± 2.37Bc	4.66 ± 0.25Cc
Prunus cerasifera 'Atropurpurea'	24.34 ± 1.09Ac	23.69 ± 1.21Ab	7.72 ± 0.24Bbc
Average	34.80 ± 4.18	29.42 ± 4.58	12.34 ± 2.49

Uppercase letters indicate significant differences among the resorption efficiencies of different elements in the same tree species ($P< 0.05$), and lowercase letters indicate significant differences in the resorption efficiency of the same element among different species ($P< 0.05$).

resorption efficiencies of *P. yedoensis* Matsum were 2.40, 3.65, and 5.45 times those of *M. micromalus* Makino, respectively. Besides, the resorption efficiencies of different elements differed within the same tree species. In *P. yedoensis* Matsum and *P. cerasifera 'Atropurpurea'*, the N and P resorption efficiencies were significantly higher than the K resorption efficiency (KRE). Besides, there were significant differences in N, P and K resorption efficiencies between *P. serrulata* var. *lannesiana* and *M. micromalus* Makino ($P< 0.05$). The order of these four tree species was NRE>PRE>KRE.

3.4 Correlation between nutrient resorption efficiencies and nutrient contents in petals

Linear regression analysis of the nutrient resorption efficiencies of the petals and the nutrient contents of the fresh petals and petal litter was performed. The nutrient resorption efficiencies of N, P, and K of petals increased with the increase of N content in fresh petals, showing significant positive correlations (Figures 3A, 4A, 5A). NRE, PRE, and KRE were positively correlated with P content in fresh petals (Figures 3C, 4C, 5C) and negatively correlated with K content in fresh petals (Figures 3E, 4E, 5E). However, their linear regression relationships were not significant. The nutrient resorption efficiencies of N, P, and K in petals decreased with the increase of P and K contents in petal litter, showing significant negative correlations (Figures 3D, 4D, 5D, 3F, 4F, 5F). However, NRE, PRE, and KRE were negatively correlated with the N content in petal litter, and the linear regression relationships between each were not significant (Figures 3B, 4B, 5B).

Linear regression analysis was conducted on the nutrient resorption efficiency and the nutrient variation of plants from fresh petals to petal litter, and the nutrient resorption efficiency of petal N, P, and K showed an extremely significant positive correlation with the corresponding nutrient variation (Figure 6). The regression equation, R^2, r, and P values are as follow: y =

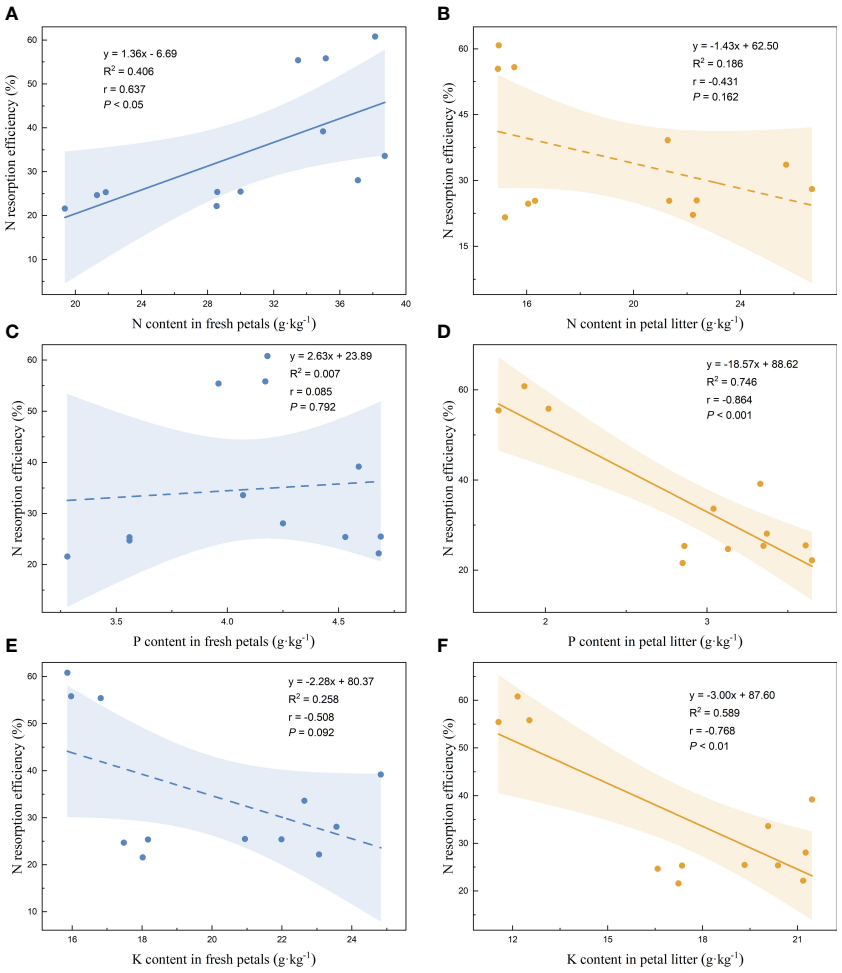

FIGURE 3
Linear fitting of N resorption efficiency of petals to the content in fresh petals and petal litter. The solid line is the significant correlation of linear regression between the two variables ($P< 0.05$), while the dashed line is the insignificant correlation ($P > 0.05$). The colored areas are 95% confidence bands.

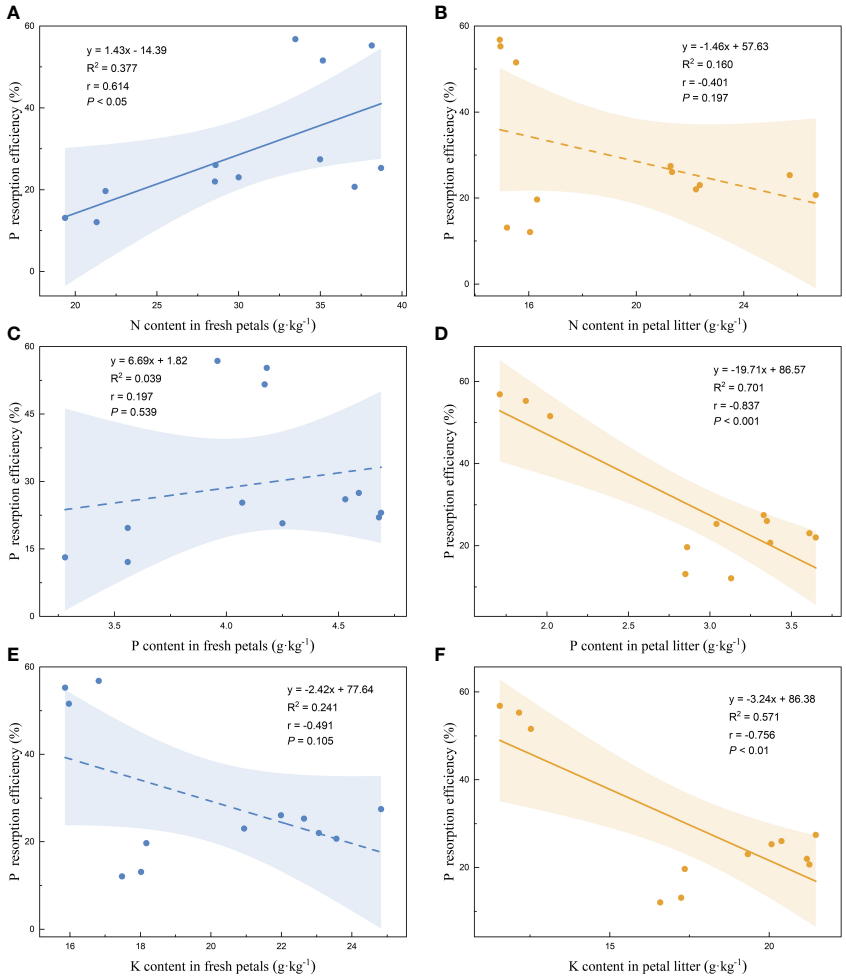

FIGURE 4
Linear fitting of P resorption efficiency of petals to the content in fresh petals and petal litter. The solid line is the significant correlation of linear regression between the two variables ($P< 0.05$), while the dashed line is the insignificant correlation ($P > 0.05$). The colored areas are 95% confidence bands.

2.22x + 9.89, R^2 = 0.953, r = 0.976, $p< 0.001$ (Figure 6A). y = 23.69x + 0.34, R^2 = 0.980, r = 0.990, $p< 0.001$ (Figure 6B); y = 6.02x - 1.84, R^2 = 0.926, r = 0.962, $p< 0.001$ (Figure 6C).

3.5 Correlation between nutrient resorption efficiency and stoichiometric ratio of petals

The correlation analysis between the stoichiometric ratio of the fresh petals and petal litter with the nutrient resorption efficiency of petals showed that the N resorption efficiency (NRE) of petals was significantly negatively correlated with the C:N of the fresh petals ($P< 0.05$). There was a significant positive correlation with the N:P and N:K of the fresh petals ($P< 0.01$, $P< 0.001$). The P resorption efficiency (PRE) of petals was positively correlated with the N:P of the fresh petals ($P< 0.05$) and negatively correlated with the K:P of the fresh petals ($P< 0.01$), but not significantly correlated with the C:P of the fresh petals ($P > 0.05$). The KRE of petals was positively correlated with the N:K of the fresh petals ($P< 0.001$), and it was negatively correlated with K:P of the fresh petals ($P< 0.05$) (Figure 7).

The NRE, PRE, and KRE of petals were positively correlated with the stoichiometric ratio of petal litter. NRE of petals was significantly positively correlated with the N:P and N:K of petal litter ($P< 0.01$, $P< 0.05$), and there was no significant relationship with the C:N of petal litter ($P > 0.05$). The PRE of petals was positively correlated with the C:P, N:P, and K:P of petal litter ($P< 0.001$, $P< 0.01$, $P< 0.05$). The KRE of petals was positively correlated with the C:K, N:K, and K:P of petal litter ($P< 0.01$, $P< 0.05$, $P< 0.05$) (Figure 8).

4 Discussion

4.1 Nutrient content of petals of Rosaceae species

The contents of C, N, P, and K in the fresh petals of the four Rosaceae species were higher than the average C (464.00 g·kg^{-1}) content of mature leaves of terrestrial plants in the world and than

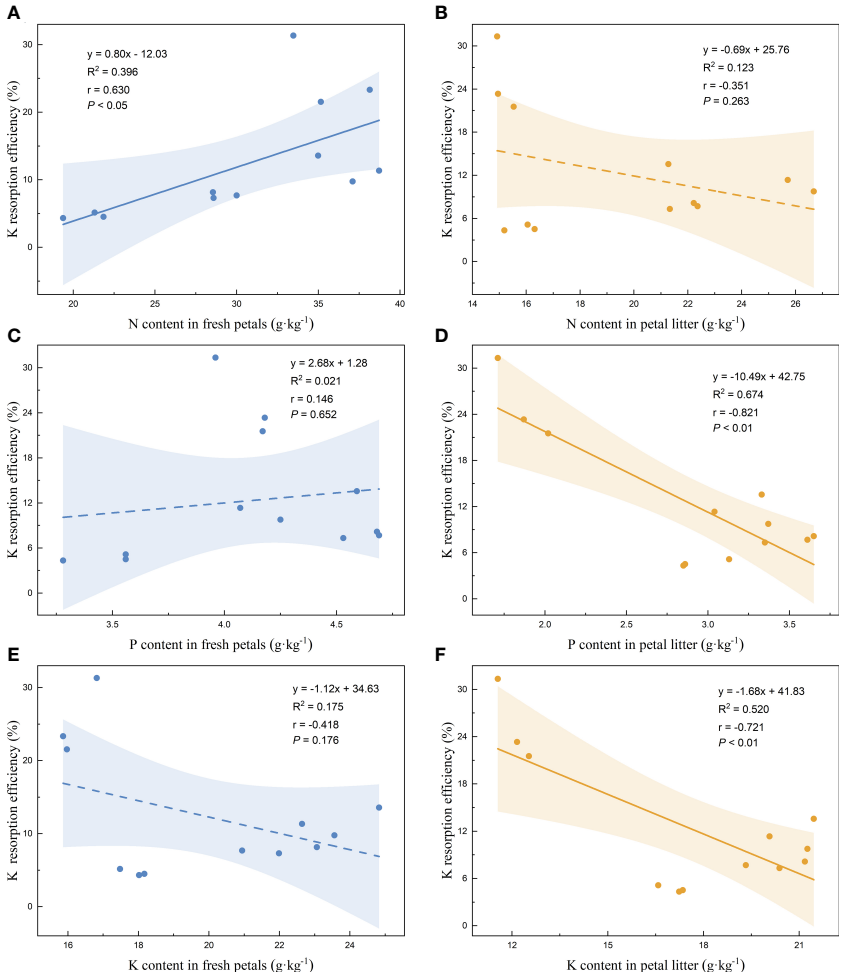

FIGURE 5
Linear fitting of K resorption efficiency of petals to the content in fresh petals and petal litter. The solid line is the significant correlation of linear regression between the two variables ($P < 0.05$), while the dashed line is the insignificant correlation ($P > 0.05$). The colored areas are 95% confidence bands.

average contents of N (20.20 g·kg^{-1}), P (1.46 g·kg^{-1}) and K (15.09 g·kg^{-1}) of terrestrial plants in China (Elser et al., 2000; Han et al., 2005; Qin et al., 2010) (Figure 1). Except for *Malus micromalus* Makino, the contents of C in the petal litter of the other three plants were lower than the average value of C (467.0 g·kg^{-1}) in the litter leaves of global terrestrial plants. The N and P contents of the petal litter were higher than the global average value of N (10.0 g· kg^{-1}) and P (0.7 g·kg^{-1}) in the litter leaves (Yuan and Chen, 2009) and than the N (10.1 g·kg^{-1}) and P (0.65 g· kg^{-1}) contents of the litter leaves in eastern China (Tang et al., 2013). The K content of petal litter was also higher than that of litter leaves of woody plants in northern China (Zhang, 2018) (Figure 1). The physiological functions of plants, as well as the distribution of nutrient elements of different organs, are different. Usually, large amounts of nutrient elements are invested in the parts with the strongest physiological functions (Liu et al., 2008; Jiang, 2016). It has been found that the C content of plant reproductive organs is higher than other organs (Zheng et al., 2007). In a study of *Ceratocephalus orthoceras*, it was found that a large amount of P was transferred from other organs to floral organs before flowering (Jia et al., 2013). Ma et al. (2009) found K distribution of wild *Cerasus humilis* floral organs to be greater than that of other tissues and organs. In the present study, the contents of C, N, P, and K of the fresh petals were higher than those in mature leaves of terrestrial plants in the world and China. This may be due to the selected tree species all growing leaves after flowering plants and flowers were the reproductive organs of plants. The good development of flowers and fruits is the material basis for the growth of leaves and other vegetative organs, and plants may have the principle of priority of reproductive organs in nutrient supply strategies. In order to meet the needs of reproduction, plants tend to prioritize nutrient needs of reproductive organs such as flowers in nutrient absorption and distribution strategies. The contents of N, P, and K in the four Rosaceae species were higher in fresh petals than in petal litter, indicating that the petals transferred some nutrients to other tissues before falling, resulting in the nutrient content in the petal litter was lower than that in the fresh petals, which verified that the petals had a similar leaf resorption process. Nutrient resorption mechanism is a survival strategy for plants to cope with nutrient poor soil. There was a nutrient resorption process in the petals of small trees of Rosaceae, but whether the petals of herbaceous plants, vines and shrubs have the same process require further studies.

10.3389/fpls.2023.1201759

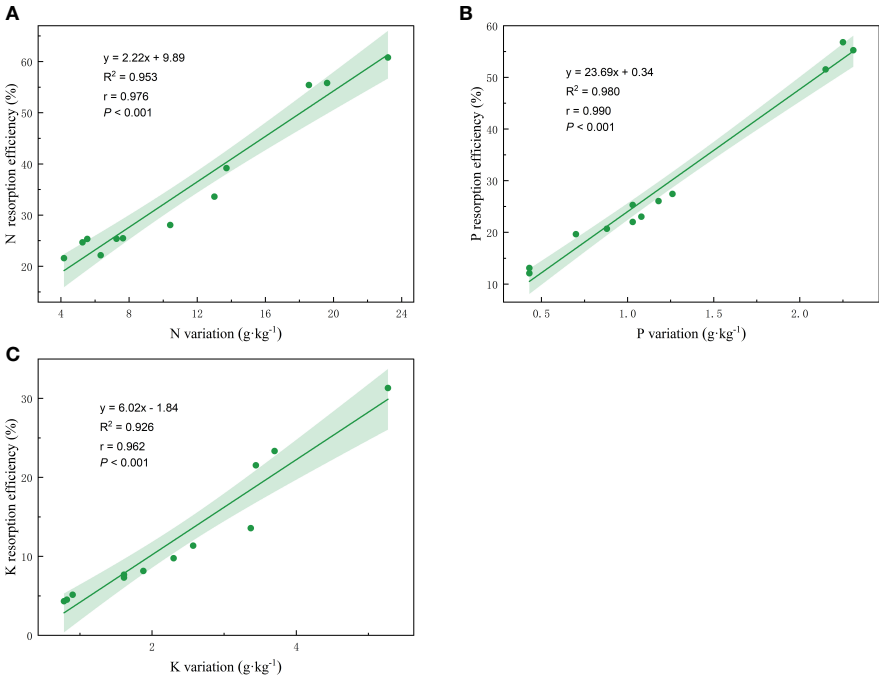

FIGURE 6
Linear fitting of N, P, K resorption efficiency and petal nutrient variation. The solid line is the significant correlation of linear regression between the two variables ($P< 0.05$). The colored areas are 95% confidence bands.

4.2 Stoichiometric characteristics of petals of Rosaceae species

The stoichiometric ratio of plants can reflect their nutrient utilization efficiency, C assimilation efficiency, and nutrient limitation, which has important ecological significance (Aerts and Chapin, 1999; Güsewell, 2004; Yan et al., 2010). The C:N, C:P, and N:P of the fresh petals of the four Rosaceae species were significantly lower than the average values of C:N (30.9), C:P (374.7) and N:P (12.6) of mature leaves of terrestrial plants at

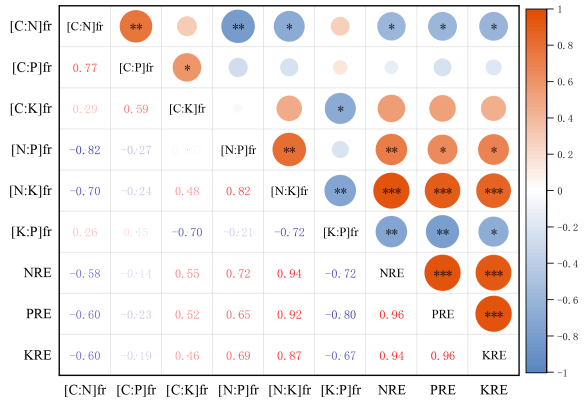

FIGURE 7
Correlation heat map of N, P, K resorption efficiency of petals with stoichiometric ratios of fresh petals. NRE is the nitrogen resorption efficiency of petal, PRE is the phosphorus resorption efficiency of petal, KRE is the potassium resorption efficiency of petal. [C:N]fr is carbon to nitrogen ratio of fresh petals, [C:P]fr is carbon to phosphorus ratio of fresh petals, [C:K]fr is carbon to potassium ratio of fresh petals, [N:P]fr is nitrogen to phosphorus ratio of fresh petals, [N:K]fr is nitrogen to potassium ratio of fresh petals, [K:P]fr is potassium to phosphorus ratio of fresh petals. *P <0.05, **P <0.01, ***P <0.001.

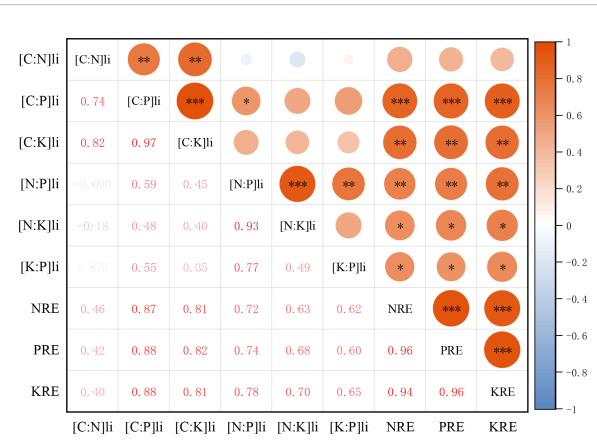

FIGURE 8
Correlation heat map of N, P, K resorption efficiency of petals with stoichiometric ratios of petal litter. NRE is the nitrogen resorption efficiency of petal, PRE is the phosphorus resorption efficiency of petal, KRE is the potassium resorption efficiency of petal. [C:N]li is carbon to nitrogen ratio of petal litter, [C:P]li is carbon to phosphorus ratio of petal litter, [C:K]li is carbon to potassium ratio of petal litter, [N:P]li is nitrogen to phosphorus ratio of petal litter, [N:K]li is nitrogen to potassium ratio of petal litter, [K:P]li is potassium to phosphorus ratio of petal litter. *P <0.05, **P <0.01, ***P <0.001.

global scale (Elser et al., 2000; Zeng et al., 2013), and the N:P ratio of the fresh petals was also lower than that of terrestrial plants in China (14.4) (Ren et al., 2007; Zeng et al., 2013) (Figure 2). The C:N, C:P and N:P of petal litter of the four Rosaceae species were significantly lower than the mean values of C:N (50.1), C:P (659.0) and N:P (13.1) of leaf litter in the global temperate broad-leaved forest (McGroddy et al., 2004). It was also significantly lower than the average C:N (44.8), C:P (1132.5) and N:P (25.0) of leaf litter in Chinese forest ecosystems (Wang et al., 2011) (Figure 2). Some researchers have proposed that the C:N and C:P of fresh leaves could be used to characterize the ability of plants to absorb N and P nutrient elements while assimilating C, reflecting the C fixation efficiency and N and P utilization efficiency of plants (He and Dijkstra, 2014). The C:N and C:P of the four Rosaceae species were lower than those of the global and Chinese horizontal leaves, indicating that the nutrient utilization efficiency of plant petals was lower than that of leaves. Among the four Rosaceae plants, the C:N and C:P of *Malus micromalus* Makino of the fresh petals were significantly higher, indicating that it had higher N, P utilization efficiency and carbon assimilation efficiency than the other three species. Generally, the C:N of leaf litter was negatively correlated with the decomposition rate of litters and that lower C:N ratio and higher initial N concentration were usually associated with a faster decomposition rate. Some scholars have also found that the initial N content in leaf litter can indicate the mass loss of litter. The decomposition rate of leaf litter is negatively correlated with the initial C content and has no significant correlation with litter C:N but has significant positive correlation with the initial N concentration (Chen et al., 2005). Ma et al. (2021) found the decomposition rate of petal litter to be positively correlated with the content of N, P, and K, and negatively correlated with N:P in the decomposition efficiency of fallen flowers of common trees in northern cities of China. There are some differences in the research results, which may be related to different species and different litter properties. Compared with the other three plants, the petal litter of *Prunus cerasifera* 'Atropurpurea' contain higher N, P, K content and lower N:P, so the petal litter of *Prunus cerasifera* 'Atropurpurea' are relatively easier to decompose. The N:P of fresh leaf has often been used to determine the element limitation during plant growth and reproduction (Dijkstra et al., 2012). It is generally believed that when the N:P of fresh leaf<14, plant growth is mainly restricted by N. When the N:P of fresh leaves >16, plant growth was mainly limited by P. When fresh leaves 14<N:P<16, plants are restricted by both N and P (Koerselman and Meuleman, 1996). In addition, Güsewell (2004) proposed that when the N:P<10 or N:P >20, the leaves can be determined N limitation or P limitation. Some researchers also proposed that when the leaves were N:P<14.5 and N:K<2.1, plant growth was limited by N; when N:P>14.5 and K:P>3.4, plant growth was limited by P or P and K; when N:K>2.1 and K:P<3.4, growth was limited by K or K and N (Venterink et al., 2003; Wang et al., 2019). However, there is a lack of research on the threshold of nutrient restriction in flower petals, which needs further exploration in the future.

4.3 Nutrient resorption characteristics of petals of Rosaceae species

Vergutz et al. (2012) studied terrestrial plant leaves at the global scale and found that approximately 62.1% N, 64.9% P, and 70.0% K were reabsorbed and transferred to other tissues (Lu and Yang, 2020). The NRE, PRE, and KRE of the petals of the four Rosaceae species were significantly lower than the nutrient resorption efficiency of the leaf at the global level (Table 2). It indicates that the proportion of nutrients transferred from petals to other tissues of plants during falling is smaller than that of leaves. The contents of N, P, and K in the petal litter of *Prunus yedoensis* Matsum were significantly lower than those of the other three tree species, so the nutrient resorption potential of *Prunus yedoensis* Matsum was higher. At the same time, the study on the resorption efficiency of N, P, and K in the petals of the four plants also found that *Prunus yedoensis* Matsum > *Prunus serrulata* var. *lannesiana* > *Prunus cerasifera* 'Atropurpurea' > *Malus micromalus* Makino, indicating that *Prunus yedoensis* Matsum can better adapt to the harsh and barren environment. Tang (2012) and Han et al. (2013) believed that plants tend to absorb more nutrient that limits their growth. In other word, plants tend to absorb more restricted elements that is "relative nutrient resorption". When RR≈0, plants are limited by N, P balance or common restrictions; when RR>0, the plant NRE was greater than PRE, and the plant recovered a larger proportion of N, so the plant growth was limited by N; when RR<0, plants recovered a greater proportion of P, and plant growth was limited by P. In this study, the resorption efficiency of N, P, and K elements of petals in four Rosaceae species was NRE>PRE>KRE (RR>0), indicating that compared with P and K elements, petals recovered a larger proportion of N element before falling, and the growth of plants during the flowering process was mainly limited by N element. Therefore, more nitrogen fertilizer should be applied to the maintenance and management of the four Rosaceae plants throughout the flowering period to ensure the growth and development of the plants. However, efficient NRE may be a strategy for the four Rosaceae plants to adapt to a low N environment.

4.4 Effects of petal nutrient content and stoichiometry on nutrient resorption efficiency

Nutrient resorption efficiency is affected by multiple factors, including leaf and soil nutrients, growth environment and climatic conditions (Zhou et al., 2020). We found that the resorption efficiencies of N, P, and K in Rosaceae were positively correlated with the content of N in fresh petals. It was contrary to the finding of Kobe et al. (2005). They found that the nutrient resorption efficiency of N and P in leaves was significantly negatively correlated with the content of N and P in mature leaves. However, some other studies have shown that nutrient resorption efficiency had no or very weak relationship with the corresponding element content in mature leaves (Chapin and Kedrowski, 1983; Escudero et al., 1992; Aerts, 1996). According to the mechanism of plant nutrient resorption, the smaller the nutrient

content of the plant itself, the more nutrients need to be reabsorbed to redress the deficiency of its own nutrients. Therefore, the negative correlation between nutrient resorption efficiency and nutrient content of fresh petals is the most consistent result of this mechanism.

We found that the resorption efficiencies of N, P, and K in petals were negatively correlated with the contents of P and K in litter of petals. Killingbeck (1996) proposed using nutrient concentration of leaf litter to characterize the nutrient resorption capacity of plants. The lower the nutrient concentration of leaf litter, the higher the proportion of plant nutrient resorption. There was a significant positive correlation between the nutrient resorption efficiency of petals and the amount of nutrient variation, which indicated that the nutrient resorption of petals before falling down was one of the important factors determining the nutrient resorption efficiency.

The NRE of petals was negatively correlated with the C:N of fresh petals and positively correlated with the N:P and N:K of fresh petals. The PRE was positively correlated with N:P and negatively correlated with K:P of fresh petals. The KRE of petals was positively correlated with N:K and negatively correlated with K:P of fresh petals. The nutrient resorption efficiency of petal N, P, and K was positively correlated with the stoichiometric ratios of petal litter. Overall, the correlation between the nutrient resorption efficiency of petals and the stoichiometric ratio of petal litter was more obvious. Similar to results of Wang et al. (2019) on the relationship between nutrient resorption and stoichiometric ratio in alfalfa leaves, the nutrient resorption efficiency of leaves was basically positively correlated with the stoichiometric ratio of senescent leaves. However, unlike in the study of nutrient resorption and C:N:P stoichiometric characteristics of *Eucalyptus grandis* × *urophylla* at different ages by Qiu et al. (2017), they found that NRE was significantly positively correlated with C:N of senescent leaves and that PRE was significantly negatively correlated with C:P of fresh leaves. This also differs from the results in Lu and Yang (2020) on forage grass in the Loess Plateau, which found that PRE had a good correlation with N, P, and K stoichiometric characteristics of leaves, while NRE and KRE had a poor correlation with stoichiometric ratios. N:P and N:K of petals were closely correlated with nutrient resorption efficiency, while C:N, C:P and C:K were negatively correlated or not correlated with carbon participation, indicating poor carbon reuse and that nitrogen was significantly recovered. This may be related to structural or organic materials produced by carbon and nitrogen in the petals.

The different correlation conclusions between plant nutrient resorption and stoichiometric ratio are mainly due to differences in species, experimental area conditions, and measurement methods (Kobe et al., 2005). At present, no clear conclusion has been drawn on the internal relationship between plant nutrient resorption and C:N:P stoichiometry, and there is a need for more quantitative research on the internal relationship between the two (Kobe et al., 2005; Qin et al., 2017).

5 Conclusions

There were interspecific differences in C, N, P, and K elements content, stoichiometric ratio and nutrient resorption efficiency of the fresh petals and petal litter of the four Rosaceae species. The nutrient contents of petal litter were lower than those of the fresh petals; thus, petals had transferred nutrients to other tissues of the plant before fall, and the nutrient resorption process of petals was similar to that of leaves. The nutrient content of petals was higher than that of leaves at global level, but the stoichiometric ratio and nutrient resorption efficiency of petals were lower than those of leaves at the global level. The N and P utilization efficiencies and carbon assimilation efficiency of *Malus micromalus* Makino were higher. The petal litter of *Prunus cerasifera* 'Atropurpurea' contains higher contents of N, P, and K and lower N:P, so its petal litter was relatively easier to decompose. *Prunus yedoensis* Matsum has higher N, P, and K resorption efficiencies and better adaptability to the environment. NRE was all higher than PRE and KRE in each of the four plants, and petals recovered a larger proportion of N element before falling. The growth of plants during flowering was mainly restricted by N element. Therefore, N fertilizer could be applied before flowering to ensure good growth and development. The resorption efficiency of N, P, and K in petals was positively correlated with the content of N in fresh petals, and negatively correlated with the content of P and K in petal litter. In addition, the nutrient resorption efficiency of petals was positively correlated with nutrient variation. The correlation between the nutrient resorption efficiency of petals with nutrient content and stoichiometric ratio of petal litter was stronger.

This work is the first on plant nutrient resorption and stoichiometric ratio in reproductive organs such as petals, which defines the nutrient requirements and nutrient limitations of the growth and development of flowering trees in urban green space, as well as providing a scientific basis and theoretical support for the utilization and nutrient management of urban landscaping trees. However, only the effects of plant nutrient status on plant nutrient resorption, and soil nutrient were considered; moisture content, plant functional traits, temperature, light, and other environmental factors are also important factors affecting plant nutrient resorption, requiring further studies. The regulation mechanism of petal nutrient resorption characteristics and stoichiometric characteristics, such as the threshold range of limiting elements, remain unclear, and a large number of experiments are needed for further verification.

Data availability statement

The original contributions presented in the study are included in the article/supplementary material. Further inquiries can be directed to the corresponding author.

Author contributions

YL and DS designed experiments and initiated research projects. YL, DS, SL, LF, JY, and YX performed experiments and analyzed data. All authors contributed to the writing of the manuscript. All authors contributed to the article and approved the submitted version.

Funding

This study was supported by the Project of the Natural Science Foundation of China (31870428), the Science & Technology Specific Projects in Agricultural High-tech Industrial Demonstration Area of the Yellow River Delta (2022SZX16), the Project of Qingdao Science and Technology Foundation for Public Wellbeing (23-2-8-cspz-10-nsh), the Fund of High-level Talents of Qingdao Agricultural University (663/1120089), the Natural Science Fund of Yunnan Province (2019FB033).

Acknowledgments

The authors thank staff members of the Biogeochemistry Lab of Xishuangbanna Tropical Botanical Garden, Chinese Academy of Sciences (CAS) for their assistance in fresh petals and petal litter analysis. We also thank Prof. Kuiling Wang, Prof. Shaoxia Guo, Prof. Qinglin Li, Dr. Xiao Guo, Dr. Huicui Lu, Dr. Peng Meng, Dr. Shimei Li, Dr. Tong Wang, Dr. Jing Li, Dr. Jinming Yang, and Dr. Lina Xu for their suggestions and revisions on the manuscript. We are grateful to WORDVICE for the English language editing services on the manuscript. We appreciate the detailed suggestions and comments from the editor, the typesetter and two reviewers.

Conflict of interest

The authors declare that the research was conducted in the absence of any commercial or financial relationships that could be construed as a potential conflict of interest.

Publisher's note

All claims expressed in this article are solely those of the authors and do not necessarily represent those of their affiliated organizations, or those of the publisher, the editors and the reviewers. Any product that may be evaluated in this article, or claim that may be made by its manufacturer, is not guaranteed or endorsed by the publisher.

References

Aerts, R. (1996). Nutrient resorption from senescing leaves of perennials: are there general patterns? *J. Ecol.* 84, 597–608. doi: 10.2307/2261481

Aerts, R., and Chapin, F. S. (1999). The mineral nutrition of wild plants revisited: a re-evaluation of processes and patterns. *Adv. Ecol. Res.* 30, 1–67. doi: 10.1016/S0065-2504(08)60016-1

Ågren, G. I. (2004). The c: n: p stoichiometry of autotrophs-theory and observations. *Ecol. Lett.* 7, 185–191. doi: 10.1111/J.1461-0248.2004.00567.X

Brant, A. N., and Chen, H. Y. H. (2015). Patterns and mechanisms of nutrient resorption in plants. *Crit. Rev. Plant Sci.* 34, 471–486. doi: 10.1080/07352689.2015.1078611

Chapin, III. F. S., and Kedrowski, R. A. (1983). Seasonal changes in nitrogen and phosphorus fractions and autumn retranslocation in evergreen and deciduous taiga trees. *Ecology* 64, 376–391. doi: 10.2307/1937083

Chen, Y. P., Pan, K. W., Wu, N., Luo, P., Wang, J. C., and Xiao, J. S. (2005). Effect of litter quality and decompositoin on n mineralization in soil of castanopsis platyacanth aschima sinensis forest. *Chin. J. Appl. Environ. Biol.* 11, 146–151. doi: 10.3321/j.issn:1006-687X.2005.02.005

Covelo, F., Rodriguez, A., and Gallardo, A. (2008). Spatial pattern and scale of leaf n and p resorption efficiency and proficiency in a *Quercus robur* population. *Plant Soil.* 311, 109–119. doi: 10.1007/s11104-008-9662-9

Dijkstra, F. A., Pendall, E., Morgan, J. A., Blumenthal, D. M., Carrillo, Y., LeCain, D. R., et al. (2012). Climate change alters stoichiometry of phosphorus and nitrogen in a semiarid grassland. *New Phytol.* 196, 807–815. doi: 10.1111/j.1469-8137.2012.04349.x

Elser, J. J., Fagan, W. F., Denno, R. F., Dobberfuhl, D. R., Folarin, A., Huberty, A., et al. (2000). Nutritional constraints in terrestrial and freshwater food webs. *Nature* 408, 578–580. doi: 10.1038/35046058

Escudero, A., del Arco, J. M., Sanz, I. C., and Ayala, J. (1992). Effects of leaf longevity and retranslocation efficiency on the retention time of nutrients in the leaf biomass of different woody species. *Oecologia* 90, 80–87. doi: 10.1007/BF00317812

Fan, H. B., Wu, J. P., Liu, W. F., Yuan, Y. H., Hu, L., and Cai, Q. ,. K. (2015). Linkages of plant and soil C:N:P stoichiometry and their relationships to forest growth in subtropical plantations. *Plant Soil* 392, 127–138. doi: 10.1007/s11104-015-2444-2

Güsewell, S. (2004). N:P ratios in terrestrial plants: variation and functional significance. *New Phytol.* 164, 243–266. doi: 10.1111/J.1469-8137.2004.01192.x

Han, W. X., Fang, J. Y., Guo, D. L., and Zhang, Y. (2005). Leaf nitrogen and phosphorus stoichiometry across 753 terrestrial plant species in china. new. *Phytologist* 168, 377–385. doi: 10.1111/j.1469-8137.2005.01530.x

Han, W. X., Tang, L. Y., Chen, Y. H., and Fang, J. Y. (2013). Relationship between the relative limitation and resorption efficiency of nitrogen vs phosphorus in woody plants. *PLoS One* 8, 1932–6203. doi: 10.1371/journal.pone.0083366

He, X. Y. (2002). *Advances in urban forest ecology research* (Beijing: China Forestry Publishing House).

He, M., and Dijkstra, F. A. (2014). Drought effect on plant nitrogen and phosphorus: a meta-analysis. *New Phytol.* 204, 924–931. doi: 10.1111/nph.12952

Jia, F. Q., Naseng, B. T., Zhang, N., and Gao, S. (2013). Mineral element content and its seasonal dynamic in ceratocephalus testiculatu. *Pratacultural Sci.* 30, 759–762.

Jiang, Y. L. (2016). Characteristics of elements contents in trees from nonggang karst forest and their associations with habitats. *Master Thesis Guangxi Normal University.* doi: 10.7666/d.Y3081122

Jiang, D. L., Xv, X., and Ruan, H. H. (2017). Review of nutrient resorption and its regulating in plants. *J. Nanjing Forestry Univ.* 41, 183–188. doi: 10.3969/j.issn.1000-2006.2017.01.028

Killingbeck, K. T. (1986). The terminological jungle revisited: making a case for use of the term resorption. *Oikos* 46, 263–264. doi: 10.2307/3565477

Killingbeck, K. T. (1996). Nutrients in senesced leaves: keys to the search for potential resorption and resorption proficiency. *Ecology* 77, 1716–1727. doi: 10.2307/2265777

Kobe, R. K., Lepczyk, C. A., and Iyer, M. (2005). Resorption efficiency decreases with increasing green leaf nutrients in a global date set. *Ecology* 86, 2780–2792. doi: 10.1890/04-1830

Koerselman, W., and Meuleman, A. F. M. (1996). The vegetation N:P ratio: a new tool to detect the nature of nutrient limitation. *J. Appl. Ecol.* 33, 1441–1450. doi: 10.2307/2404783

Li, Y. L., Mao, W., Zhao, X. Y., and Zhang, T. H. (2010). Leaf nitrogen and phosphorus stoichiometry in typical desert and desertified regions, north China. *Environ. Sci.* 31, 1716–1725. doi: 10.13227/j.hjkx.2010.08.001

Li, F. F., Sun, B. D., Shi, Z. W., and Pei, N. C. (2021). Changes in ecological stoichiometry and nutrient resorption in *Castanopsis hystrix* plantations along an urbanization gradient in the lower subtropics. *J. Forestry Res.* 32, 2323–2331. doi: 10.1007/s11676-021-01293-0

Liu, P., Hao, C. Y., Chen, Z. L., Zhang, Z. X., Wei, F. M., and Xu, S. Z. (2008). Nutrient element distribution in organs of *Heptacodium mconioides* in different communties and its relationship with soil nutrients. *Acta Pedologica Sin.* 45, 304–312. doi: 10.3321/j.issn:0564-3929.2008.02.016

Lu, J. Y., Duan, B. H., Ynag, M., Yang, H., and Yang, H. M. (2018). Research progress in nitrogen and phosphorus resorption form senesced leaves and the influence of ontogenetic and environmental factors. *Acta Prataculturae Sin.* 27, 178–188. doi: 10.11686/cyxb2017223

Lu, Y. X., and Yang, H. M. (2020). Leaf n, p and K resorption and stoichiometry of forages in the legume-grass mixture in the loess plateau of east gansu. *J. Lanzhou Univ. (Natural Sciences)* 56, 285–293. doi: 10.13885/j.issn.0455-2059.2020.03.001

Ma, Y., Fan, X. H., Liu, Z. W., Zhu, F., and Lin, Y. Y. (2021). Decomposition and nutrient release characteristics of falling flowers of 12 common tree species in northern cities. *Acta Ecologica Sin.* 41, 48–56. doi: 10.5846/stxb201910292275

Ma, J. J., Yu, F. M., Du, B., Zhang, L. B., Ren, Y. J., and Xiao, X. (2009). Study on distribution laws of several mineral elements during flowering stage in fruiting basal branch of wild *Cerasus humilis*. *Nonwood For. Res.* 27, 1216. doi: 10.14067/j.cnki.1003-8981.2009.04.006

May, J. D., and Killingbeck, K. T. (1992). Effects of preventing nutrient resorption on plant fitness and foliar nutrient dynamics. *Ecology* 73, 1868–1878. doi: 10.2307/1940038

McGroddy, M. E., Daufresne, T., and Hedin, L. O. (2004). Scaling of C:N:P stoichiometry in forests worldwide: implications of terrestrial redfield-type ratios. *Ecology* 85, 2390–2401. doi: 10.1890/03-0351

Qin, Y. Y., Feng, Q., Zhu, M., Li, H. Y., and Zhao, Y. (2017). Influence of slope aspect on ecological stoichiometry of grassland plant leaves in dayekou basin of qilian mountains. *J. Lanzhou Univ. (Natural Sciences)* 53, 362–367. doi: 10.13885/j.issn.0455-2059.2017.03.011

Qin, H., Li, J. X., Gao, S. P., Li, C., Li, R., and Shen, X. H. (2010). Characteristics of leaf element contents for eight nutrients across 660 terrestrial plant species in China. *Acta Ecologica Sin.* 30, 1247–1257. doi: CNKI:SUN:STXB.0.2010-05-017

Qiu, L. J., Hu, H. T., Lin, Y., Ge, L. L., Wang, K. Y., He, Z. M., et al. (2017). Nutrient resorption efficiency and C:N:P stoichiometry of eucalyptus urophylla×E. grandis of different ages in a sandy coastal plain area. *Chin. J. Appl. Environ. Biol.* 23, 739–744. doi: 10.3724/SP.J.1145.2016.11028

Reiners, W. A. (1986). Complementary models for ecosystems. *Am. Nat.* 127, 59–73. doi: 10.1086/284467

Ren, S. J., Yu, G. R., Tao, B., and Wang, S. Q. (2007). Leaf nitrogen and phosphorus stoichiometry across 654 terrestrial plant species in NSTEC. *Environ. Sci.* 28, 2665–2673. doi: 10.3321/j.issn:0250-3301.2007.12.001

Schade, J. D., Espeleta, J. F., Klausmeier, C. A., McGroddy, M. E., Thomas, S. A., and Zhang, L. X. (2005). A conceptual framework for ecosystem stoichiometry: balancing resource supply and demand. *Oikos* 109, 40–51. doi: 10.1111/j.0030-1299.2005.14050.x

Sterner, R. W. (1990). The ratio of nitrogen to phosphorus resupplied by herbivores: zooplankton and the algal competitive arena. *Am. Nat.* 136, 209–229. doi: 10.1086/285092

Sterner, R. W., and Elser, J. J. (2002). Ecological stoichiometry: biology of elements from molecules to the biosphere. *Princeton Univ. Press*. doi: 10.1515/9781400885695

Su, B. L., Fan, Y. Z., Yang, M., Tang, Q., and Wang, J. G. (2015). Application and arrangement of rosaceae trees in urban green land: a case study of shenyang city. *J. Shenyang Univ. (Natural Science).* 27, 355–362. doi: 10.16103/j.cnki.21-1583/n.2015.05.004

Tang, L. Y. (2012). Nutrient resorption proficiency and efficiency of woody plants. the. *Doctoral dissertation Peking University*.

Tang, L. Y., Han, W. X., Chen, Y. H., and Feng, J. Y. (2013). Resorption proficiency and efficiency of leaf nutrients in woody plants in eastern China. *J. Plant Ecol.* 6, 408–417. doi: 10.1093/jpe/rtt013

Urabe, J., Nakanishi, M., and Kawabata, K. (1995). Contribution of metazoan plankton to the cycling of n and p in lake biwa. *Limnology Oceanogr.* 40, 232–242. doi: 10.4319/lo.1995.40.2.0232

Venterink, H. O., Wassen, M. J., Verkroost, W. M., and De Ruiter, P. C. (2003). Species richness-productivity patterns differ between n-, p-, and K-limited wetlands. *Ecology* 84, 2191–2199. doi: 10.1890/01-0639

Vergutz, L., Manzoni, S., Porporato, A., Novais, R. F., and Jackson, R. B. (2012). Global resorption efficieneies and concentrations of carbon and nutrients in leaves of terrestrial plants. *Ecol. Monogr.* 82, 205–220. doi: 10.1890/11-0416.1

Wang, J. Y., Wang, S. Q., Li, R. L., Yan, J. H., Sha, L. Q., and Han, S. J. (2011). C:N:P stoichiometric characteristics of four forest types' dominant tree species in China. *Chin. J. Plant Ecol.* 35, 587–595. doi: 10.3724/SP.J.1258.2011.00587

Wang, Z. N., Zhao, M., Yang, Y., Li, F. K., Wang, H., and Lü, S. J. (2019). Relationship between alfalfa leaf nutrient resorption and stoichiometric ratios of nitrofen, phosphorus, and potassium. *Acta Prataculturae Sinic* 28, 177–183. doi: 10.11686/cyxb2018750

Wardle, D. A., Walker, L. R., and Bardgett, R. D. (2004). Ecosystem properties and forest decline in contrasting long-term chronosequences. *Science* 305, 509–513. doi: 10.1126/science.1098778

Xie, J., Yan, Q. L., Yuan, J. F., Li, R., Lü, X. T., Liu, S. L., et al. (2020). Temporal effects of thinning on the leaf C:N:P stoichiometry of regenerated broadleaved trees in larch plantations. *Forests* 11, 54. doi: 10.3390/f11010054

Yan, E. R., Wang, X. H., Guo, M., Zhong, Q., and Zhou, W. (2010). C:N:P stoichiometry across evergreen broad-leaved forests, evergreen coniferous forests and deciduous broad-leaved forests in the tiantong region, zhejiang province, eastern China. *Chin. J. Plant Ecol.* 34, 48–57. doi: 10.3773/j.issn.1005-264x.2010.01.008

Yang, H., Liu, W. J., Liu, H. M., and Cao, L. H. (2021). Nutrient contents and stoichiometric characteristics of plant leaf-litter-soil in alpine forest. *J. Zhejiang Univ.* 47, 607–618. doi: 10.3785/j.issn.1008-9209.2020.10.261

Yuan, Z., and Chen, H. Y. H. (2009). Global trends in senesced-leaf nitrogen and phosphorus. *Global Ecol. Biogeogr.* 18, 532–542. doi: 10.1111/j.1466-8238.2009.00474.x

Yuan, Z. Y., Li, L. H., Han, X. G., Chen, S. P., Wang, Z. W., Chen, Q. S., et al. (2006). Nitrogen response efficiency increased monotonically with decreasing soil resource availability: a case study from a semiarid grassland in northern China. *Oecologia* 148, 564–572. doi: 10.1007/s00442-006-0409-0

Zeng, D. H., and Chen, G. S. (2005). Ecological stoichiometry: a science to explore the complexity of living systems. *Acta Phytoecologica Sin.* 29, 1007–1019. doi: 10.17521/cjpe.2005.0120

Zeng, D. P., Jiang, L. L., Zeng, C. S., Wang, W. Q., and Wang, C. (2013). Reviews on the ecological stoichiometry characteristics and its applications. *Acta Ecologica Sin.* 33, 5484–5492. doi: 10.5846/stxb201304070628

Zhang, M. X. (2018). Resorption patterns of 10 nutrient elements in leaves of woody plants in northern China. *China Agric. University*.

Zhao, H. B., Liu, G. B., and Hou, X. L. (2006). Characteristics of nutrient cycling of different vegetation types in the zhifanggou watershed on the loess hilly region. *Acta Prataculturae Sin.* 15, 63–69.

Zhao, Q., Liu, X. Y., Hu, Y. L., and Zeng, D. H. (2010). Effects of nitrogen addition on nutrient allocation and nutrient resorpiton efficiency in *Larix gmelinii*. *Scientia Silvae Sinicae* 46, 14–19. doi: CNKI:SUN:LYKE.0.2010-05-005

Zheng, W. J., Bao, W. K., Gu, B., He, X., and Leng, L. (2007). Carbon concentration and its characteristics in terrestrial higher plants. *Chin. J. Ecol.* 26, 307–313. doi: 10.13292/j.1000-4890.2007.0055

Zhou, L. L., Li, S. B., Wang, W. P., Yan, X. Y., Chen, Z., and Pan, H. (2020). Leaf c, n, p stoichiometry and nutrient resorption characteristics among four mangrove tree species in the zhangjiangkou wetland, fujian province. *Chin. J. Appl. Environ. Biol.* 26, 674–680. doi: 10.19675/j.cnki.1006-687x.2019.07057

Zou, D. T., Wang, Q. G., Luo, A., and Wang, Z. H. (2019). Species richness patterns and resource plant conservation assessments of rosaceae in China. *Chin. J. Plant Ecol.* 43, 1–15. doi: 10.17521/cjpe.2018.0091

frontiers | Frontiers in Plant Science

TYPE Original Research
PUBLISHED 17 July 2023
DOI 10.3389/fpls.2023.1190929

OPEN ACCESS

EDITED BY
Fahad Shafiq,
Government College University, Lahore, Pakistan

REVIEWED BY
Fayong Li,
Tarim University, China
Ping He,
Chinese Academy of Agricultural Sciences, China
Muhammad Zahid Mumtaz,
The University of Lahore, Pakistan

*CORRESPONDENCE
Min Wang
minwang@njau.edu.cn

RECEIVED 21 March 2023
ACCEPTED 16 June 2023
PUBLISHED 17 July 2023

CITATION
Zhu L, Liang A, Wang R, Shi Y, Li J, Wang RR, Wang M and Guo S (2023) Harnessing nitrate over ammonium to sustain soil health during monocropping. *Front. Plant Sci.* 14:1190929. doi: 10.3389/fpls.2023.1190929

Harnessing nitrate over ammonium to sustain soil health during monocropping

Linxing Zhu, Aichen Liang, Rongfeng Wang, Yaman Shi, Jia Li, RuiRui Wang, Min Wang* and Shiwei Guo

Jiangsu Provincial Key Lab for Organic Solid Waste Utilization, National Engineering Research Center for Organic-based Fertilizers, Jiangsu Collaborative Innovation Center for Solid Organic Waste Resource Utilization, Nanjing Agricultural University, Nanjing, China

Introduction: In achieving food security and sustainable agricultural development, improving and maintaining soil health is considered as a key driving factor. The improvement based on different forms of nitrogen fertilization has aroused great public interest in improving and restoring monocropping obstacles for specific soil problems.

Methods: For this, a short-term cucumber cropping field experiment was conducted in the subtropical region of China under four fertilization treatments: ammonium (AN), nitrate (NN), ammonium with dicyandiamide (AN +DCD), nitrate with dicyandiamide (NN+DCD). In this study, we measured the effects of nitrogen forms addition on plant productivity and soil health in a monocropping system over seven seasons.

Results: To systematically evaluate soil health, a wide range of soil environmental factors were measured and incorporated into the soil health index (SHI) by entropy method. Compared with ammonium treatment (SHI_{AN} = 0.059, SHI_{AN+DCD} = 0.081), the positive effect of nitrate was mainly reflected in improving soil health (SHI_{NN} = 0.097, SHI_{NN+DCD} = 0.094), which was positively correlated with the increase in plant productivity of cucumber after seven seasons of monocropping. The most critical factor affecting SHI is soil ammonium nitrogen content, which was negatively correlated with plant productivity.

Discussion: Nitrate promotes soil health and plant productivity by optimizing soil environmental factors. The study thus emphasized the necessity of nitrate input for the sustenance of soil-crop ecosystems, with the consequent possibility of application of the results in planning monoculture obstacle prevention and management measures.

KEYWORDS

cucumber, monocropping, nitrogen forms, soil health, plant productivity

Introduction

As the foundation of sustainable agricultural development, soil health plays a pivotal role in ensuring food security and maintaining the functioning of terrestrial ecosystems (Yang T et al., 2020). Environmental, economic, and social benefits such as healthy food and beautiful landscapes require a steady energy supply from healthy soils. In China, more than 95% of cultivated land soil resources have suffered from monocropping obstacles by the end of 2013 (Yang T et al., 2020). As the main culprit of unsustainable agriculture, monocropping not only causes severe land nutrient depletion and accelerates soil degradation, but also makes the single agricultural ecosystem more vulnerable to the threat of pests and diseases. Previous studies revealed that continuous cropping of watermelon, banana, ginseng, and potato increased the abundance of pathogenic microbes (Shen et al., 2018; Gao et al., 2019; Zhang et al., 2020; Gu et al., 2022). In addition, microorganisms involved with nutrient element cycling and the decomposition of harmful allopathic substances, such as *Pseudomonas* spp. and *Bacillus* spp., showed an inhibitory effect (Huang et al., 2019; Luo et al., 2019). Hence, cultivated land protection and management measures are proposed by researchers, including planting systems and fertilization systems.

Fertilizer plays an indispensable role in the soil health and ecosystem function, and it is a critical limiting factor for plant productivity (Baer et al., 2003). Over the past decade, substantial addition of atmospheric nitrogen deposition has been observed by Jia et al. (2014). However, the response of soil health to increase nitrogen levels is not always clear and consistent. The view that a large amount of nitrogen addition damages soil health has been repeatedly proposed to support the argument against fertilization, while other studies have demonstrated otherwise (Treseder, 2008; Zhang et al., 2018). A reasonable fertilization system is an important way to maintain soil health. According to the needs of crops, balanced nitrogen fertilizer application promoted the enhancement of soil health, such as increased plant litter and root biomass and accumulated soil organic matter and microbial biomass. Most studies have examined the effect of the nitrogen application rate on soil health, overlooking on the nitrogen forms (ammonium and nitrate).

Ammonium and nitrate are the main inorganic nitrogen forms absorbed by plants, playing a crucial role in the growth and development of plants. It is important to study the effects of two forms of nitrogen (ammonium and nitrate) on soil properties to support the prediction of improved ecosystems under increased nitrogen deposition. Several studies have reported that microbes and plants preferentially absorb ammonium, as ammonium is more energy-advantageous than nitrate, and the energy costs are lower (Zhang et al., 2017). Another essential feature of ammonium is that it leads to rhizosphere acidification compared to nitrate (Treseder, 2008; Zhang et al., 2017). More specifically, H^+ offsetting excessive cation uptake by roots was proved to account for the decrease in rhizosphere pH during ammonium fertilization. Hence, many plants are directly inhibited when they absorb ammonium alone due to its special action. In brief, the principal indications of ammonium toxicity include the plant's overall growth yield, significant leaf chlorosis, decreased root-to-shoot ratio, yield reduction, and even mortality (Britto and Kronzucker, 2002; Li et al., 2010).

Ammonium and nitrate can easily produce a variable effect on soil microbial community biomass excitation and decomposition (Tao et al., 2018; Jia et al., 2019). For instance, the respiration of peat substrate increased with ammonium, but did not change with nitrate (Currey et al., 2009). However, from laboratory incubation trials, the researchers concluded that nitrogen inhibited soil microbial respiration regardless of the form of applied nitrogen based on the results observed (Ramirez et al., 2010; Yang et al., 2022). Based on a long-term forest experiment, ammonium significantly reduces the organic carbon content of the organic layer. In contrast, nitrate affects both the organic carbon content and density fractions of the mineral layer (Geng et al., 2021). Such phenomenon might be more closely related to more inputs from plant sources, rather than to a slower breakdown of organic matter. However, another study suggested that the promoting effect of ammonium on soil organic carbon accumulation is significantly higher than that of nitrate, likely as a result of their different soil pH and microbial enzyme activity (Lu et al., 2011). In the past, there have been a large number of studies on the effects of nitrogen forms on the soil single properties (Treseder, 2008; Zhong et al., 2017). However, there remains a knowledge gap on how nitrogen forms impact comprehensive indexes of soil health, which hampers the efforts to predict soil health in the context of global changes.

To better understand the association between nitrogen forms and soil health in monocropping, we investigated the impacts of ammonium and nitrate on the composition of the microbial community, soil resources (such as nutrient retention and availability), overall soil health, and plant productivity (related to element accumulation and yield). Understanding those complex relationships, two main hypotheses were addressed: (1) soil resources and microbial community properties vary with nitrogen form, and each contributes distinctively to soil health; (2) nitrate would boost the soil health by enhancing the soil resources (e.g., soil enzyme activity) and environmental allocation (e.g., pH and EC) and thereby plant productivity.

Materials and methods

Experiment design and sampling

This trial was set up at Changzhou city, Jiangsu Province, China (31°27′ N, 119°19′ E) in 2017 for the monocropping of spring and autumn cucumber (Jin Chun 4). The trials in the spring and autumn seasons were initiated in early March and late July, respectively. The area has a typical subtropical monsoon climate, with an average annual precipitation of 1,033 mm and an average annual temperature of 15.5°C. At the beginning of the experiment, the soil properties were pH 6.8, 25.2 g kg^{-1} organic matter, 1.5 g kg^{-1} total nitrogen, and 40.3 mg kg^{-1} and 182 mg kg^{-1} of available P and K, respectively. The 12 sampling plots (6 m × 2.5 m each) were designed within the greenhouse and assigned to four treatments:

ammonium fertilizer (AN), nitrate fertilizer (NN), ammonium fertilizer with dicyandiamide (AN+DCD), and nitrate fertilizer with dicyandiamide (NN+DCD), with three replicates arranged in a completely randomized block design. Dicyandiamide is implemented as a nitrification suppressant in soil.

The chemical fertilizer was applied at the rates of 350 kg N hm^{-2}, 150 kg P_2O_5 hm^{-2}, 210 kg K_2O hm^{-2}, and 10.5 kg DCD hm^{-2} to a depth of 0–20 cm. Calcium nitrate (17.07% N) and ammonium sulfate (21.21% N) were used as sources of nitrate and ammonium, respectively. The P and K fertilizers were prepared from calcium superphosphate (12% P_2O_5) and potassium sulfate (34% K_2O), respectively. Chicken manure containing 31.7% water, 1.3% N, 2.9% P_2O_5, and 1.3% K_2O was applied as an organic fertilizer at the rate of 15,000 kg hm^{-2}. Additionally, all of the fertilizer application rates were used for a single growing season (Figure 1).

Samples of three cucumber plants selected randomly from each plot were harvested at maturity, and dissected into leaves, stems, and fruits. These components of cucumber were washed with deionized water and oven dried to a constant weight at 70°C to determine the dry-matter biomass. Moreover, dry samples are ground into powder for the analysis of nitrogen, phosphorus, and potassium.

The sustainability yield index (SYI) was used to describe the fluctuating crop yield under different fertilization regimes. A system's sustainability is increased when its SYI is higher (Reddy and Babu, 2003). The formula is as follows:

$$SYI = \frac{x - \sigma}{Y_{max}}$$

In the formula, σ (kg hm^{-2}) is the standard deviation; x (kg hm^{-2}) is the average annual yield of the same fertilization treatment in spring; Y_{max} (kg hm^{-2}) is the maximum yield of in all treatments in spring.

Ten soil subsamples were taken from the cultivated layer (0–20 cm depth) during the cucumber harvest in June 2020 and mixed as a composite sample per plot. For each soil samples, three subsamples were taken: one subsample was dried and stored until physicochemical properties are tested, one subsample was stored at 4°C for biochemical analysis, and the remaining subsample was frozen at −80°C for PLFA analyses.

Plant nutrient assays

Dried plant samples were digested with H_2SO_4-H_2O_2 at 260–270°C (Li et al., 2022), after which N concentration was measured using an Auto Analyzer 3 digital colorimeter (BRAN + Lu-EBBE) (Guo et al., 2007). The determination of phosphorus (P) in the digested solution was carried out by the molybdenum-blue method (Xu et al., 2020). The determination of potassium (K) in the digested solution was conducted using a flame photometer (Xu et al., 2019).

Soil properties assays

Soil pH and EC were determined with a soil-to-water ratio of 1:2.5 by a pH meter (FE28-Meter) and a conductivity meter (DDSJ-308F), respectively. Soil total nitrogen (TN) and organic matter (SOC) were determined using an Elemental Analyzer (Vario MAX; Elementar, Germany). Soil mineral nitrogen (nitrate and ammonium) (NO_3^- and NH_4^+) was extracted with 0.01 M $CaCl_2$ and was quantified by Bran + Luebbe GmbH-AutoAnalyzer 3 (Norderstedt, Germany), while soil available P (AP) was extracted using $NaHCO_3$ and then measured by the molybdenum-blue method. Soil available K (AK) was extracted with NH_4OAc and determined using a flame photometer.

Soil extracellular enzyme activities and respiration assays

Urease was determined by the method of May and Douglas (1976). Soil samples were treated with toluene for 15 min and then incubated with urea in citrate buffer at 37°C for 24 h. After filtration, sodium phenol and sodium hypochlorite were added. After 20 min, the color was determined by spectrophotometer at 578 nm. Acid phosphatase was determined according to the description of Sun et al. (2017). The mixed solution of 0.2 ml of toluene, 4 ml of buffer solution, and 1 ml of a disodium p-nitrophenyl phosphate solution was added with 1 g of soil, and then incubated at 37°C for 1 h. The catalase activity was determined by ultraviolet spectrophotometry (Yang R et al., 2020). Hydrogen peroxide solution was added to the soil as a substrate, and saturated aluminum potassium jarosite was quickly added after sealing oscillation for 20 min, and quickly filtered into a triangular flask containing sulfuric acid. The filtrate was subjected to colorimetric analysis using a quartz cuvette at 240 nm. Finally, the sucrase activity was determined by the 5-dinitrosalicylic acid colorimetric method (Wang et al., 2020). The sample was treated with toluene and incubated in water at 37°C for 15 min. Then, sucrose solution and phosphate buffer were added and cultured at 37°C for 24 h. The filtrate was removed after filtration and DNS reagent was added to a boiling water bath for 5 min. After cooling and constant volume, the sample was colorimetric at 540 nm. An enzyme activity unit of urease and invertase was defined by the production of 1 μg of NH_3-N and 1 mg of reducing sugar per gram of soil sample within 24 h. Catalase was expressed as milligram of hydrogen peroxide decomposed per gram of soil within 20 min. The results of acid phosphatase were expressed as μg of pNP g^{-1} of dry soil h^{-1}.

The CO_2 evolution from the samples that had been precultured at 25°C for 24 h in darkness was measured by a gas chromatograph and then incubated at 25°C in tight containers for 6 h, to evaluate soil basal respiration (Hofman et al., 2003). Soil metabolic entropy (qCO_2) was calculated as the ratio between soil basal respiration and soil microbial biomass carbon.

Soil microbial assays

The soil microbial biomass carbon (MBC) and microbial biomass nitrogen (MBN) were quantified using the chloroform fumigation extraction and a 0.5 M K_2SO_4 solution extraction method. To calculate MBC or MBN contents, the difference in soil soluble carbon or nitrogen between unfumigated and fumigated samples was determined (Gregorich and Kachanoski, 1991). Soil soluble carbon in the extracts was quantified using a TOC analyzer (Elementar, Germany), and soil soluble nitrogen was detected using the Kjeldahl method. Conversion factors of 0.45 (KE_C) and 0.54 (KE_N) were used to calculate average MBC and MBN values (Brookes et al., 1985; Wu et al., 1990).

The composition of the soil microbial community was evaluated by PLFA analysis according to Frostegård and Bååth (1996). Qualitative and quantitative PLFA analysis was performed by GC-MS (a gas chromatograph combined with a mass spectrometer, Thermo Scientific, Bremen, Germany). The PLFAs i14:0, i15:0, a15:0, i16:0, i17:0, and a17:0 were used as indicators of Gram-positive bacteria (G^+); 16:1ω7c, 17:1ω8c, 18:1ω7c, cy17:0, and cy19:0 were used as indicators of Gram-negative bacteria (G^-); the PLFAs 10Me16:0, 10Me17:0, and 10Me18:0 were used as indicators of actinomycetes; the PLFAs 16:1ω5c and 18:2ω6,9c were used as indicators of fungi. The total bacterial PLFAs are represented by the combined count of G^+ PLFAs and G^- PLFAs. The PLFAs for soil microbes were expressed as nmol g^{-1} dry soil.

Soil health index

The soil health index is calculated using the entropy method (Geng et al., 2018; Wu et al., 2018). According to the attribute of the index j (e.g., TN and SOC), it is divided into three categories: positive (except EC, qCO_2, and pH), negative (EC and qCO_2), and moderate (pH). Among them, the greater the index value, the better the role of the index, which is a positive index (X). The smaller the index value, the better the effect of the index. It is a negative index. The moderate index means that when the value of the index is in the middle, the index performs best. Before the soil health index evaluation of the monocropping of cucumber, all the selected evaluation indexes were uniformly processed to unify them into positive index (X). The formula is as follows:

Reverse indicator transformation

If the index j is a negative index, it can be transformed into a positive index (X).

$$X = \frac{1}{j}$$

Moderate indicator conversion

If the index j is a moderate index, it can be transformed into a positive index (X) by the following formula:

$$X = \begin{cases} \frac{2*(j-m)}{M-m}, & m \le j < \frac{m+M}{2} \\ \frac{2*(M-j)}{M-m}, & \frac{m+M}{2} \le j \le M \end{cases}$$

where M and m are the maximum and minimum values in the range of index j, respectively.

Data standardization processing ($X`_{ij}$)

Different evaluation index units are changeable. All indexes are dimensionless before calculation, which makes the data comparable. The extreme value method is used for dimensionless treatment of indicators, and all the indicators are transformed into interval of 0–1. Then, $X`_{ij}$ was calculated as below:

$$X`_{ij} = \frac{X_{ij} - m_j}{M_j - m_j}$$

where X_{ij} is the sample i of the index j, and m_j and M_j are the minimum and maximum values among all the evaluation objects under the same index, respectively.

Weighting

1. Calculate the contribution of the sample i of the index j. In order to make the data operation meaningful, it is necessary to eliminate the zero and negative values. Dimensionless data are translated as a whole, namely, $X`_{ij} = X`_{ij} + \alpha$. At the same time, in order to maximize the retention of the original data, α takes the minimum value closest to $X`_{ij}$, and $\alpha = 0.0001$.

2. Calculate the characteristic weight of the ith evaluated object under the jth index:

$$p_{ij} = \frac{X`_{ij}}{\sum_{i=1}^{n} X`_{ij}}, \quad n = 1, 2, 3, \ldots 12$$

where p_{ij} is the proportion of the standard value of the sample i of the index j, and n is the number of samples involved in the calculation.

3. Calculate the entropy value e_j of the jth index, with the expression:

$$e_j = -\frac{1}{ln\ n} \sum_{i=1}^{n} p_{ij} ln(p_{ij}), \quad n = 1, 2, 3, \ldots 12$$

4. Calculate the difference coefficient (g_j):

$$g_j = 1 - e_j$$

5. Determine the weight of the evaluation index:

$$W_j = \frac{g_j}{\sum_{j=1}^{z} g_j}, \quad j = 1, 2, 3 \ldots z$$

where W_j is the importance of the index j among all indicators, and z refers to the total number of indexes that participate in the calculation.

Calculation of soil health (S)

$$S = \sum_{j=1}^{z} w_j * p_{ij}, \quad j = 1, 2, 3 \ldots z$$

10.3389/fpls.2023.1190929

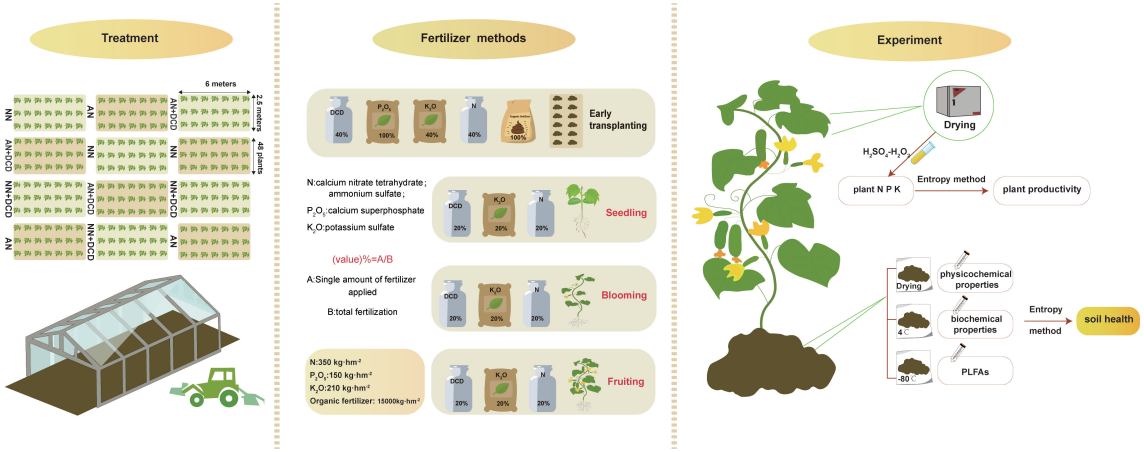

FIGURE 1
The concept map shows the key experimental arrangements in the current study, including experimental treatment, fertilization methods, and experimental processes. The application of DCD, nitrogen fertilizer, and potassium fertilizer was done four times: 40% of the fertilizer amount was used for applying base fertilizer while the remaining 60% was used for top dressing. Phosphate fertilizer and organic fertilizer were applied once as the base fertilizer.

Statistical analysis

Data were compared using one-way analysis of variance (ANOVA) at the end of each bioassay in the IBM SPSS 19.0 software program (SPSS Inc., USA). The ggcor package in R was used to test the correlation between soil physicochemical and biological properties, and its relationship with the plant quality index. Based on the Bray–Curtis distance matrix, the effects of nitrogen forms on microbial composition were analyzed by principal coordinate analysis (PCoA). Permutational multivariate analysis of variance (PEROMOVA with 999 permutations) was executed by utilizing the "adoni" function within the "vegan" R package. Causal relationships between soil properties and plant productivity were tested by partial least squares path modeling (PLS-PM) using "plspm". Statistical significance was deemed to be achieved when the alpha level was equal to or less than 0.05.

Results

Plant productivity

After seven seasons, all of the plant productivity-related parameters were significantly affected by nitrogen forms. Overall, the productivity of plants significantly increased by approximately 140% on nitrate treatment (NN) compared to ammonium treatment (AN) (Figure 2). Additionally, in terms of nutrient accumulation (Figure S1), nitrate treatment (NN) provides more nutrients to the plant, whether it is nitrogen, phosphorus, or potassium. Likewise, we observed a similar pattern in the DCD treatment, wherein plant productivity was significantly higher with nitrate treatment (NN+DCD) than with ammonium treatment (AN +DCD). Furthermore, the present results revealed that neither DCD nor the interactions of nitrogen forms and DCD could affect the plant productivity-related parameters (Figure S1).

Soil physicochemical and biological properties

The physicochemical properties of the soil were significantly influenced by the fertilization regime, with the exception of TN and SOC (Table 1). Different nitrogen forms directly affected the nitrate-to-ammonium ratio (NO_3^-/NH_4^+), and nitrate treatment (NN) was significantly higher than the ammonium treatment (AN). All the treatments were acidic in pH, but ammonium treatment (AN, pH = 4.14) had lower acidity than nitrate treatment (NN, pH = 5.99). However, soil AP (131 mg kg^{-1}) and AK (346 mg kg^{-1}) with ammonium treatment (AN) added were both elevated. With respect to EC, application of nitrate treatment (NN) significantly decreased the electrical conductivity (EC) by approximately 150 μS cm^{-1} compared to ammonium treatment (AN). Overall, the addition of DCD did not alter the trend of physicochemical properties between the nitrate and ammonium nitrogen treatments. Nevertheless, our findings revealed that DCD application caused a notable increase in soil pH while decreasing soil EC (AN vs. AN+DCD or NN vs. NN+DCD).

Soil effective nutrient content, biological activity, and energy circulation are mainly dominated by soil microorganisms. Soil microbial nutrient content differed notably under different fertilization treatments. Nitrate (NN)-treated MBC increased by 150 mg kg^{-1} compared with ammonium treatment (AN) (Table 2). Unexpectedly, for MBN content, the administration of nitrogen in different forms was ineffective, and the difference between treatments was not significant. It was noted that similar to MBC, both the ratio of MBN and TN (MBN/TN) and the ratio of MBC and SOC (MBC/SOC) were prominently impacted by fertilization regimes. Compared with ammonium treatment (AN), both MBN/TN and MBC/SOC were significantly increased (by 50%) in nitrate treatment (NN). Basal respiration in soil was determined, and there were no significant differences in different nitrogen forms. In contrast, the soil metabolic entropy (qCO_2) of nitrate (NN) was

10.3389/fpls.2023.1190929

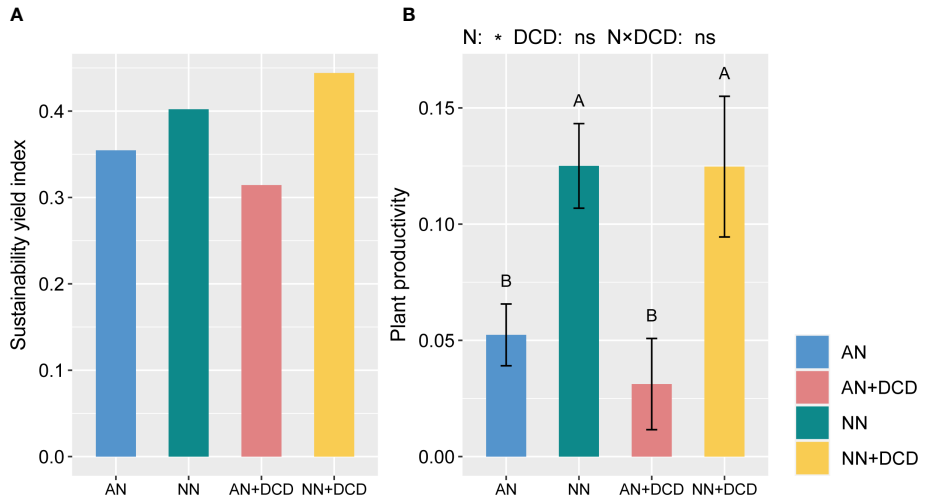

FIGURE 2
Sustainability yield index **(A)** and plant productivity **(B)** under different fertilization treatments. Data points represent the means and standard deviations of three replicates. Different capital letters denote significant differences ($p < 0.05$) with Duncan's multiple range test. The plant productivity is calculated in the same way as the soil health index, which includes aboveground biomass, yield, and nutrient accumulation. AN, ammonium fertilizer; NN, nitrate fertilizer; AN+DCD, ammonium fertilizer with dicyandiamide; NN+DCD, nitrate fertilizer with dicyandiamide. N, Nitrogen form; *$p < 0.05$; ns, $p > 0.05$.

significantly lower than that of ammonium treatment (AN) (Table 2), by approximately 50%.

Nutrient and redox-related microbial enzyme activities were directly affected by soil nitrogen forms. There was an overall increase in soil enzyme activity upon nitrate addition. Specifically, in soils (Figure 3), nitrate treatment (NN) obviously increased the activities of sucrase, catalase, and urease. In contrast, significant reductions in acidic phosphatase

TABLE 1 Effect of different forms of nitrogen on soil physical and chemical properties.

Treatment	TN (g kg^{-1})	SOC (g kg^{-1})	NH_4^+ (mg kg^{-1})	NO_3^- (mg kg^{-1})	NO_3^-/NH_4^+	AP (mg kg^{-1})	AK (mg kg^{-1})	pH	EC (µS cm^{-1})
AN	1.67 ± 0.07 a	16.8 ± 0.58 a	29.2 ± 4.63 a	119 ± 7.69 b	4.15 ± 0.59 b	131 ± 1 6.8 a	346 ± 5.29 a	4.14 ± 0.15 c	2,500 ± 166 a
NN	1.65 ± 0.09 a	17.1 ± 0.94 a	2.24 ± 0.52 b	208 ± 1.68 a	96.2 ± 20.5 a	93.4 ± 18.0 b	255 ± 27.7 bc	5.99 ± 0.11 a	2,026 ± 89.5 b
AN+DCD	1.64 ± 0.08 a	17.1 ± 0.71 a	37.7 ± 8.29 a	120 ± 42.1 b	3.23 ± 0.98 b	115 ± 18.6 ab	332 ± 32.6 ab	4.55 ± 0.23 b	2,269 ± 55.0 ab
NN+DCD	1.61 ± 0.11 a	17.1 ± 0.76 a	3.25 ± 1.77 b	235 ± 30.9 a	96.8 ± 68.1 a	88.3 ± 13.9 b	264 ± 79.3 c	6.09 ± 0.16 a	1,549 ± 155 c

TN, soil total nitrogen; SOC, soil organic carbon; NH_4^+, soil ammonium nitrogen; NO_3^-, soil nitrate nitrogen; AP, soil available phosphorus; AK, soil available potassium; EC, soil electrical conductivity. Values are means of three replicates ± standard deviations. Means followed by the same letter for a given factor are not significantly different ($p < 0.05$; Duncan test). AN, ammonium fertilizer; NN, nitrate fertilizer; AN+DCD, ammonium fertilizer with dicyandiamide; NN+DCD, nitrate fertilizer with dicyandiamide.

TABLE 2 Effects of different nitrogen forms on soil microbial biomass.

Treatment	MBC (mg·kg^{-1})	MBN (mg·kg^{-1})	MBC/SOC	MBN/TN	SBR (µg·g^{-1}·h^{-1})	qCO_2
AN	198 ± 79.6 c	80.2 ± 21.6 b	0.01± 0.00 b	0.05 ± 0.01 b	3.22 ± 0.23 a	18.4 ± 8.41 a
NN	384 ± 20.5 b	114 ± 10.9 a	0.02 ± 0.00 a	0.07 ± 0.00 a	3.53 ± 0.39 a	9.18 ± 0.66 b
AN+DCD	278 ± 44.0 c	102 ± 10.9 ab	0.02 ± 0.00 b	0.06 ± 0.00 ab	3.51 ± 0.21 a	12.8 ± 1.72 ab
NN+DCD	490 ± 26.5 a	125 ± 20.0 a	0.03 ± 0.00 a	0.08 ± 0.01 a	3.69 ± 0.51 a	7.55 ± 1.33 b

MBC, soil microbial biomass carbon; MBN, soil microbial biomass nitrogen; SBR, soil base respiration; qCO_2, soil metabolic entropy. Values are means of three replicates ± standard deviations. Means followed by the same letter for a given factor are not significantly different ($p < 0.05$; Duncan test). AN, ammonium fertilizer; NN, nitrate fertilizer; AN+DCD, ammonium fertilizer with dicyandiamide; NN+DCD, nitrate fertilizer with dicyandiamide.

10.3389/fpls.2023.1190929

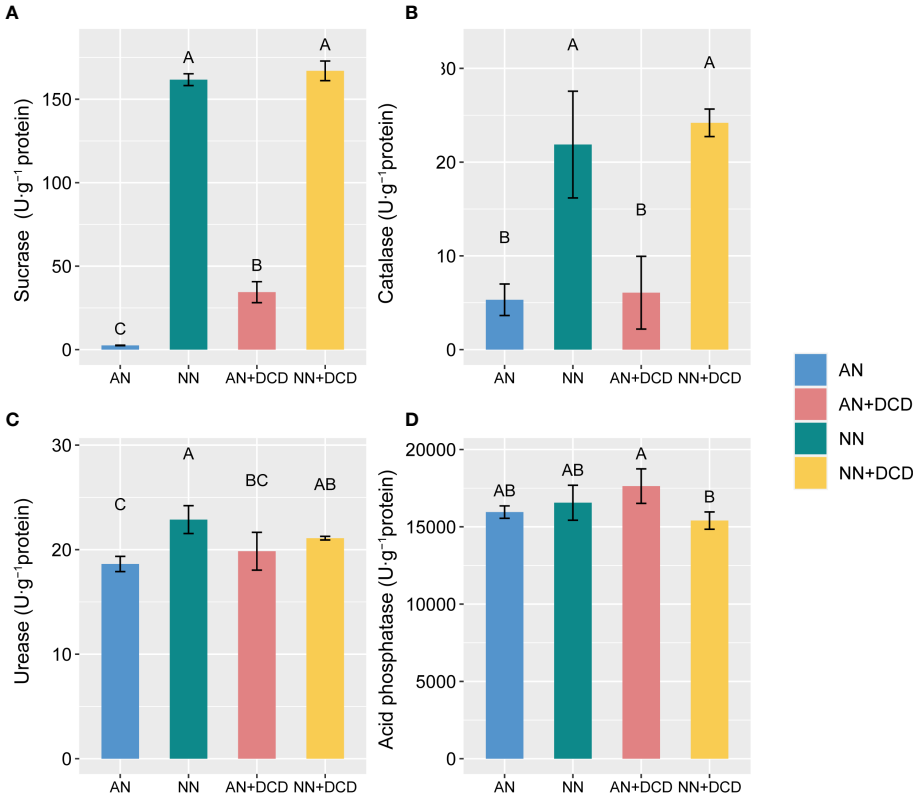

FIGURE 3
Response of soil enzyme activity to different forms of nitrogen after monocropping for the seven seasons. **(A)** Sucrase; **(B)** catalase; **(C)** urease; **(D)** acid phosphatase. Data points represent the means and standard deviations of three replicates. Different capital letters denote significant differences ($p < 0.05$) with Duncan's multiple range test. AN, ammonium fertilizer; NN, nitrate fertilizer; AN+DCD, ammonium fertilizer with dicyandiamide; NN+DCD, nitrate fertilizer with dicyandiamide.

activity were observed with the nitrate treatment, as compared with the ammonium treatment (AN). Furthermore, regarding soil biological properties, we observed that DCD supplementation had no significant impact, except for the notable increase in MBC (AN vs. AN+DCD or NN vs. NN +DCD) and sucrase (AN vs. AN+DCD).

Microbial community structure

Soil microbial community composition (based on PLFAs) varied with fertilization regimes, with PC1 explaining 49.67% of the variation and PC2 explaining 28.79% (Figure S2A). Across all fertilization treatments (Table 3), the total amount of PLFAs in soil hardly

TABLE 3 Effects of different nitrogen forms on soil PLFAs.

Treatment	Total PLFAs (nmol·g^{-1})	Bacterial PLFAs (nmol·g^{-1})				Actinomycetic PLFAs (nmol·g^{-1})	Fungal PLFAs (nmol·g^{-1})	B/F
		Total PLFAs	G^+ PLFAs	G^- PLFAs	G^+/G^-			
AN	21.2 ± 2.46 a	16.6 ± 2.23 a	10.8 ± 1.62 a	5.80 ± 0.65 ab	1.85 ± 0.13 b	0.21 ± 0.02 a	4.41 ± 0.34 ab	3.76 ± 0.41 ab
NN	20.5 ± 2.02 a	16.6 ± 2.12 a	9.55 ± 0.87 a	7.07 ± 1.41 a	1.37 ± 0.20 c	0.17 ± 0.03 a	3.73 ± 0.47 bc	4.51 ± 0.90 ab
AN+DCD	21.2 ± 3.75 a	16.0 ± 3.54 a	10.9 ± 2.31 a	5.04 ± 1.24 b	2.18 ± 0.09 a	0.22 ± 0.09 a	4.99 ± 0.14 a	3.19 ± 0.64 b
NN+DCD	17.8 ± 2.39 a	14.6 ± 1.57 a	9.34 ± 1.36 a	5.26 ± 0.30 ab	1.77 ± 0.20 b	0.15 ± 0.04 a	3.08 ± 0.83 c	4.88 ± 0.79 a

G^+ PLFAs, soil Gram-positive bacterial; G^- PLFAs, soil Gram-negative bacteria; B/F, the ratio of bacteria to fungi; G^+/G^-, the ratio of Gram-positive bacteria to Gram-negative bacteria. Values are means of three replicates ± standard deviations. Means followed by the same letter for a given factor are not significantly different ($p < 0.05$; Duncan test). AN, ammonium fertilizer; NN, nitrate fertilizer; AN+DCD, ammonium fertilizer with dicyandiamide; NN+DCD, nitrate fertilizer with dicyandiamide.

changed, with bacterial PLFA concentration being the highest (76%–82%), followed by fungi (17%–24%) and actinomycetes (1%). The concentrations of bacteria and actinomycete PLFAs did not differ significantly among the treatments. However, ammonium treatment (AN) increases soil fungal biomass, which is more pronounced in DCD treatment. At the same time, nitrate treatment (NN) decreased the ratio of G^+ to G^- (G^+/G^-) and increased the ratio of bacteria to fungi (B/F) in rhizosphere soil, compared with ammonium treatment (AN). In line with the majority of other soil properties, our results revealed no significant effect arising from the addition of DCD on soil microorganisms.

As a visual analysis, we mapped a heat map (Figure 4) of the correlation between the physicochemical and biological properties of the soil and calculated the correlation coefficients. Figure 4 showed a significant negative correlation of soil NH_4^+, AP, AK, and EC with soil enzyme activity, MBC, and MBC/SOC, and a significant positive correlation with soil respiration entropy. In addition, NH_4^+ and EC were negatively correlated with the ratio of fungi to bacteria, and NH_4^+ was positively correlated with the fungi and G^+/G^- alone. Regarding the correlation with other soil properties, soil NO_3^- and NH_4^+ exhibited opposite trends. The soil's NO_3^- is positively correlated with MBN and MBN/TN, and there is no significant relationship between pH and G^+/G^-. Although the physical and chemical properties have a greater impact on biological properties, the importance of the total amount of microorganisms cannot be ignored. Total PLFAs, G^+, and soil fungi were significantly and negatively correlated with MBN and MBN/TN. In addition, MBC and MBC/SOC were also negatively correlated with fungi.

Quantitative examination of the effects of fertilization

The partial least squares path model was used to reveal the possible ways of nitrogen addition affecting plant productivity (Figure 5). This analysis provides the most appropriate exponential model based on our data (GOF = 0.83). Our findings indicate that available nitrogen (NH_4^+ and NO_3^-) and biological properties significantly and negatively influenced plant productivity (−0.89 and −0.75, respectively), whereas soil physicochemical properties (except NH_4^+ and NO_3^-) had a significant positive impact (0.34) (Figure 5B). Together, these factors explained 90% (R^2 = 0.9) of the variation in plant productivity of cucumbers (Figure 5B).

Further analysis of soil factors and plant productivity showed that NH_4^+, EC, fungi, and G^+/G^- were significantly negatively correlated with plant productivity (Figure 4). Soil nitrate nitrogen, pH, sucrase, catalase, MBC, MBN, MBN/TN, MBC/SOC, and the ratio of bacteria and fungi (B/F) were significantly positively correlated (Figure 4). It also has the same trend for a single plant productivity index (such as yield, biomass, etc.) (Figure S2B). The comprehensive score of soil health was calculated by entropy method. As shown in Figure 6C, in the soil health evaluation system, NH_4^+ and sucrase have higher weight (0.100 and 0.083,

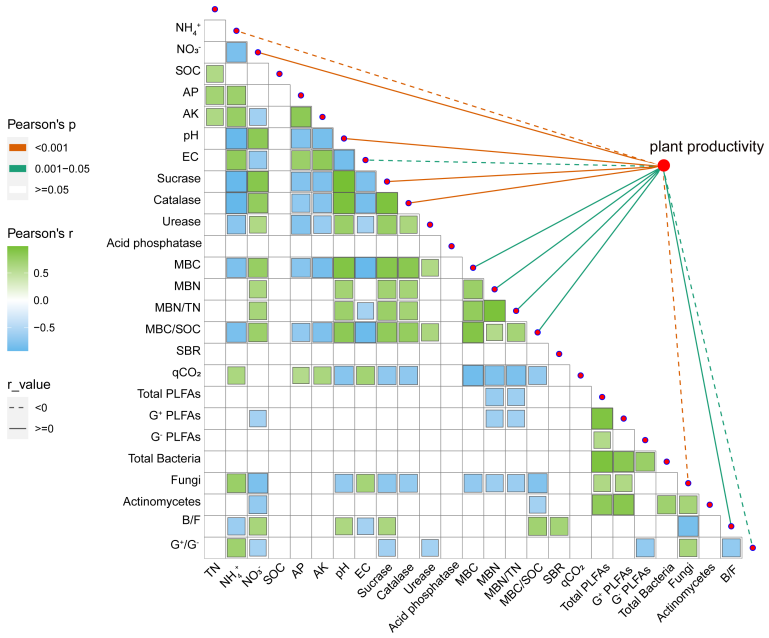

FIGURE 4
Correlation between soil physicochemical properties and biological properties, and the relationship between various factors and plant productivity. SOC, soil organic carbon (g kg^{-1}); TN, soil total nitrogen (g kg^{-1}); AP, soil available phosphorus (mg kg^{-1}); AP, soil available potassium (mg kg^{-1}); NO_3^-, soil nitrate nitrogen (mg kg^{-1}); NH_4^+, soil ammonium nitrogen (mg kg^{-1}); EC, soil electrical conductivity(μS cm^{-1}); MBC, soil microbial biomass carbon content (mg kg^{-1}); MBN, soil microbial biomass nitrogen content (mg kg^{-1}); MBN/TN, the ratio of soil microbial biomass nitrogen content to total nitrogen; MBC/SOC, the ratio of soil microbial biomass carbon content to soil organic carbon; SBR, soil basal respiration (μg g^{-1} h^{-1}); qCO_2, soil metabolic entropy; G^+ PLFAs, Gram-positive bacteria (nmol g^{-1}); G^- PLFAs, Gram-negative bacteria (nmol g^{-1}); B/F, the ratio of bacteria to fungi; G^+/G^-, the ratio of Gram-positive bacteria to Gram-negative bacteria. All correlation analysis use Pearson's correlation. Correlation coefficient *r* value is shown in the figure.

10.3389/fpls.2023.1190929

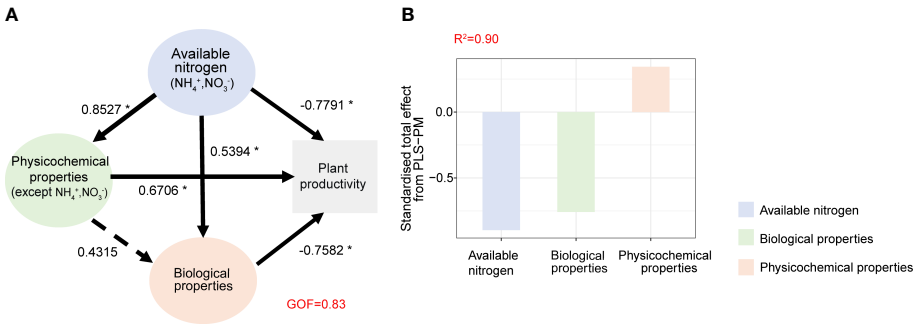

FIGURE 5
The partial least squares path models (PLS-PM) illustrating the direct and indirect effects of available nitrogen, physical–chemical properties (except NH_4^+, NO_3^-) and biological properties on cucumber plant productivity **(A)** and standardized total effects on plant health from PLS-PM **(B)**. Numbers on the arrowed lines indicate normalized path coefficient. The dotted arrows represent non-significant path relationships. The GOF index represents the goodness of fit. Asterisks represent significant effects: *p< 0.05; **p< 0.01; ***p< 0.001.

respectively) while MBC, MBN, and AK have smaller weight (0.031, 0.025, and 0.0225, respectively). The comprehensive score of soil health treated with nitrate treatment (NN and NN+DCD) was significantly higher than ammonium treatment (AN and AN +DCD), and the specific ranking from high to low was NN+DCD (0.098), NN (0.094), AN+DCD (0.082), and AN (0.060) (Figure 6A). Nevertheless, no discernible impact of DCD addition on soil health was observed in our study (AN vs. AN+DCD or NN vs. NN+DCD) (Figure 6A). Finally, we performed a correlation analysis between the comprehensive score of soil health and plant

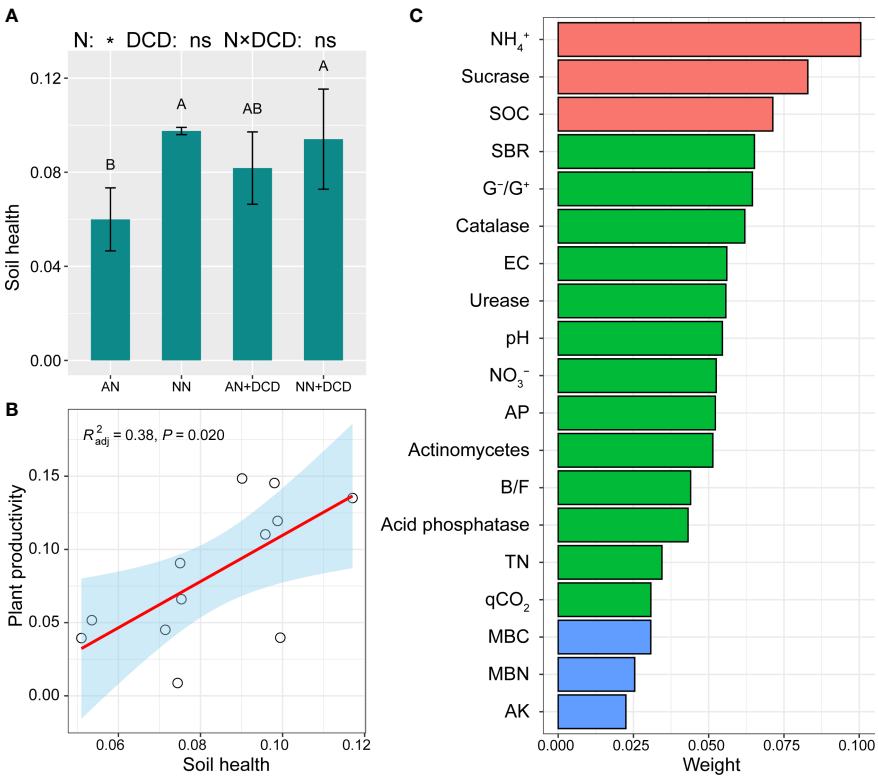

FIGURE 6
The entropy method determined the response of soil health index **(A)** and plant productivity to different nitrogen forms **(B)**, and calculated the weight **(C)** of soil physicochemical and biological indexes in soil health. SOC, soil organic carbon (g kg^{-1}); TN, soil total nitrogen (g kg^{-1}); AP, soil available phosphorus (mg kg^{-1}); AK, soil available potassium (mg kg^{-1}); NO_3^-, soil nitrate nitrogen (mg kg^{-1}); NH_4^+, soil ammonium nitrogen (mg kg^{-1}); EC, soil electrical conductivity (μS cm^{-1}); MBC, soil microbial biomass carbon content (mg kg^{-1}); MBN, soil microbial biomass nitrogen content (mg kg^{-1}); MBN/TN, the ratio of soil microbial biomass nitrogen content to total nitrogen; SBR, soil basal respiration (μg g^{-1} h^{-1}); qCO_2, soil metabolic entropy; B/F, the ratio of bacteria to fungi; G^-/G^+, the ratio of Gram-negative bacteria to Gram-positive bacteria. Data points represent the means and standard deviations of three replicates. Different capital letters denote significant differences (p< 0.05) with Duncan's multiple range test. AN, ammonium fertilizer; NN, nitrate fertilizer; AN+DCD, ammonium fertilizer with dicyandiamide; NN+DCD, nitrate fertilizer with dicyandiamide. N, Nitrogen form; *p< 0.05; ns, p > 0.05.

productivity, which showed a positive correlation between these two factors (Figure 6B, Figure S2C).

Discussion

Nitrate increased plant productivity

The physiological metabolic processes of plants are controlled by nitrogen, such as nitrogen metabolism, photosynthesis, respiration, and absorption of mineral elements, which determine the different growth effects of plants. Since nitrate addition increased plant productivity over time in our test site, compared to ammonium addition (Figure 2, Figure S1), this, to some extent, resembles previous findings indicating that the absorption of K^+ is reduced with the rise of NH_4^+ concentration in watermelon, foxtail algae, and tobacco, respectively, when ammonium serves as the exclusive source of nitrogen. This inhibition is probably caused by the ions' competition taking place within nonselective cation channels and potassium-specific channels (Lu et al., 2015). Furthermore, our previous findings showed that nitrate treatment promoted the increase of root length, which might also be one of the reasons for the weak nutrient absorption capacity of ammonium treatment (Figure 2, Figure S1) (Wang et al., 2016).

Interestingly, the sustainability yield index under nitrate treatment (NN and NN+DCD) was higher than that of ammonium treatment (AN and AN+DCD) (Figure 2). This phenomenon could be explained by the fact that nitrate is more conducive to maintaining the stability of microbial flora, thereby alleviating monocropping obstacles (Gu et al., 2020). Thus, it is reasonable to speculate that the effect of different forms of nitrogen on monoculture obstacles is not a simple factor, but a combination of multiple factors, such as soil health, and plant characteristics. Unexpectedly, in this study, the effects of dicyandiamide on cucumber yield and nutrient uptake were not signified under different nitrogen forms. Table 4 (PERMANOVA) shows that variations in plant productivity, soil microbial community, and soil nutrients were all best explained (R^2) by nitrogen form (73.3%, 34.5%, and 63.7%, respectively) and, to a lesser extent, by DCD (0.9%, 11.9%, and 12.7%, respectively) and the interaction between nitrogen form and DCD (0.3%, 9.12%, and 2.79%, respectively). This unknown phenomenon is likely to be affected by soil temperature, soil texture, microbial activity, and other factors, which needs further study (Guiraud and Marol, 1992; Grundmann et al., 1995).

Optimizing soil physicochemical properties by nitrate

It is generally believed that the NH_4^+ is easily converted to NO_3^- when NH_4^+ is used as the substrate for nitrification under oxygen-rich conditions. In contrast, the high ammonium (29.2 mg kg^{-1}, 37.7 mg kg^{-1}) that still exists under ammonium treatment (AN and AN+DCD) in our study was presumably attributed to the large reduction in nitrification rate under ammonium treatment (AN and AN+DCD) by the low pH (Table 1). Other studies observed that the rate of nitrification increased with the increase in pH, when the pH value was 3.7–8.6. This could be due to pH that increases the growth of nitrifying microorganisms in soil (Jiang et al., 2015). On the other hand, according to previous reports, another important reason for low pH inhibition of nitrification rate is the direct inhibition of nitrification enzyme activity (Jia et al., 2014). Notably, characteristics of ion release from roots during the nutrient uptake period of plants under ammonium treatment (AN and AN+DCD) might expose more H^+, capable of reducing soil pH (Telles-Pupulin et al., 1996; Evans et al., 2008; Ghorbani et al., 2008). In addition, we found a response to different nitrogen forms by root exudates of cucumber, which may eventually result in citric acid accumulation in ammonium treatment (Wang et al., 2016). Accordingly, the changes in carbon and nitrogen metabolism in plants are regarded as one of the reasons for the regulation of soil pH when exposed to different nitrogen forms. The results showed that the soil pH was more stable during nitrate treatment (NN and NN+DCD) and that there was a significant positive correlation between pH and plant productivity in all treatments (Figure 4, Table 1). These findings indicated that nitrate treatment (NN and NN+DCD) effectively reduced soil acidification and promoted soil health, thus creating a suitable environment for monocrop growth. The study findings displayed no notable influence on soil total nitrogen and organic matter among treatments. This observation could possibly be associated with the shorter duration of continuous cropping. However, significant deviations in soil available potassium and phosphorus were visible among treatments. These variations probably arose from the growth differences of cucumbers under different nitrogen forms. Notably, the nitrate nitrogen treatment expedited cucumber growth and yield formation, leading to greater nutrient absorption from the soil during the crop harvest stage.

TABLE 4 Results from PERMANOVA testing the effects of nitrogen versus DCD on plant productivity, soil nutrients, and soil microbial community.

	Df	Pseudo-*F*	*p*-value	R^2 (%)	Pseudo-*F*	*p*-value	R^2 (%)	Pseudo-*F*	*p*-value	R^2 (%)
		Plant productivity			Soil microbial community			Soil nutrients		
Nitrogen form	1	23.0	0.003	73.3	6.23	0.001	34.5	31.5	0.001	67.3
DCD	1	0.280	0.638	0.9	2.13	0.126	11.9	5.97	0.036	12.7
Nitrogen form × DCD	8	0.111	0.839	0.3	1.64	0.187	9.12	1.30	0.249	2.79
Residuals	11			25.5			44.4			17.1

Nitrate improves soil biological properties

Understanding the mechanisms of soil microbial carbon and nitrogen content, and how they respond to nutrient enrichment, is essential for accurate predictions and management of ecosystem health and related functions. Given that the result of our study is not in line with earlier reports on the significant positive correlation between soil organic carbon and microbial carbon, it is also therefore likely that carbon components are the dominant drivers of this relationship (Figure 4). We speculated that this phenomenon was caused by higher active carbon components produced by nitrate treatment (NN and NN+DCD). Previous research, based on preferential utilization of unstable active carbon sources by soil microorganisms, has also highlighted the potential importance of roots and aboveground parts of plants in unstable carbon source turnover through litter production (Wang and Wang, 2006; Geng et al., 2021). Therefore, our results, together with previous studies, emphasized the objectivity of higher microbial biomass carbon and nitrogen under nitrate treatment (NN and NN+DCD) (Table 2). In fact, soil available nitrogen supply potential and organic carbon turnover rate were controlled by MBN/TN and MBC/SOC, respectively. The soils treated with nitrate (NN and NN+DCD), especially those fertilized with DCD, showed higher magnitudes of MBC/SOC and MBN/TN compared to the soils treated with ammonium (AN and AN+DCD). This suggests that microbial immobilization under nitrate treatment (NN and NN+DCD) is beneficial for the enrichment of soil nutrient sources, which provides indispensable support for soil health (Table 2).

After further analysis (Figure 3), we found that carbon-gaining enzymes and nitrogen-gaining enzymes showed high activity in nitrate treatment (NN and NN+DCD), most likely due to an elevated strong unstable carbon input ability by nitrate additions, given that rich energy sources stimulate microbial secretion of soil enzymes related to carbon and nitrogen cycling (Paz-Ferreiro et al., 2011). The inhibitory effect of ammonium treatment (AN and AN+DCD) on soil enzyme activity may be more closely related to abiotic factors (soil pH and NH_4^+) than biotic factors (microbial biomass). On the other hand, the authors believe that this is partly due to the direct toxicity of NH_4^+ and acidic soil to microorganisms and enzymes (Luo et al., 2016). Consistent with our results, NH_4^+ and pH were negatively and positively correlated with soil enzyme activities, respectively (Figure 4). In addition, it is well known that the increase of catalase is conducive to soil remediation of monocropping. Therefore, under monocropping conditions, long-term application of nitrate can make the soil more mature, result in less toxic substances, and better maintain soil health. However, soil acid phosphatase activity was higher in AN+DCD, which is probably related to lower pH and higher fungal PLFAs in AN+DCD.

Regardless of nitrogen forms, exogenous nitrogen input might not cause changes in the total number of soil microorganisms, at the current deposition rate, because microbes living in high nitrogen soils can adapt to nitrogen-rich environments (Table 3). Here, it does not mean that nitrogen forms have no significant effect on soil microbial community composition at other levels (such as species composition) (Figure S2A). After ammonium application, we found that soil microbial community changed from "bacteria" to "fungi", and fungi were negatively *($p< 0.01$)* correlated with the overall plant productivity (Figure 4 and Table 3). We speculate that the decline in plant productivity under ammonium treatment (AN and AN +DCD) was caused by fungal accumulation. This is in line with earlier reports on the directional transformation of rhizosphere microorganisms in monocropping crops (Wei et al., 2017). In a similar study, ammonium input changed the microbial community structure with fungal biomass experiencing greater change than bacterial biomass, resulting in a decreased ratio of B to F and a more saprophytic fungal dominance of microbial populations (Geng et al., 2021). In fact, other studies also reported that nitrate addition reduced soil fungal biomass by gradually inhibiting the growth of white rot fungi or the activity of ligninase (Pregitzer et al., 2008; Frey et al., 2014). Otherwise, the evaluation of root exudates and soil microorganisms showed that the diversity of root exudates (heterogeneity of soil microbial resources) was also an important factor driving the composition of the soil microbial community.

With regard to the ratio of G^+ to G^-, there was a widely held assumption that it can be used to characterize soil nutrient status. G^- had been grown rapidly in nutrient-rich soil relative to other nutrient-poor soil, which was opposite to G^+. Results from our study showed that nitrate amendment decreased the ratio of G^+ to G^- (Table 3), consistent with previous studies on the subtropical field soil, and indicating that the nutritional stress of nitrate treatment (NN and NN+DCD) was weaker than that of ammonium treatment (AN and AN+DCD) (Kramer and Gerd, 2008), which directly affected plant productivity. The qCO_2 value reflects the intensity of soil microbial respiration and, hence, serves as a direct measure of the microbial community's stability (Anderson and Domsch, 2010). Nitrate treatment (NN and NN +DCD) showed a significant reduction in qCO_2 levels (Table 2), indicating its strong potential in preserving the soil microbial community and high substrate utilization rate. Finally, monocropping drove soil microorganisms to an unfavorable environmental state, but nitrate gave soil microorganisms a stronger ability to resist disturbance and maintain stability, thus providing quality assurance for soil health.

Healthy soil promotes crop production

A long-term positive correlation between soil health and field plant productivity has been reported in grain crop systems (Nunes et al., 2018). This is similar to the result in Figure 6B, where there was a significant positive correlation between soil health and aboveground productivity (R^2 = 0.38, p = 0.02). As shown in Figure 6, the comprehensive score of soil treated with nitrate treatment (NN and NN+DCD) was higher (NN = 0.097 and NN +DCD = 0.094), which was related to the richer nutrient content and higher biological activity of soil treated with nitrate treatment (NN and NN+DCD). In addition, it may be related to the direct effect of ammonium on soil degradation. pH, soil enzyme activity, and microbial biomass significantly decreased with the addition of

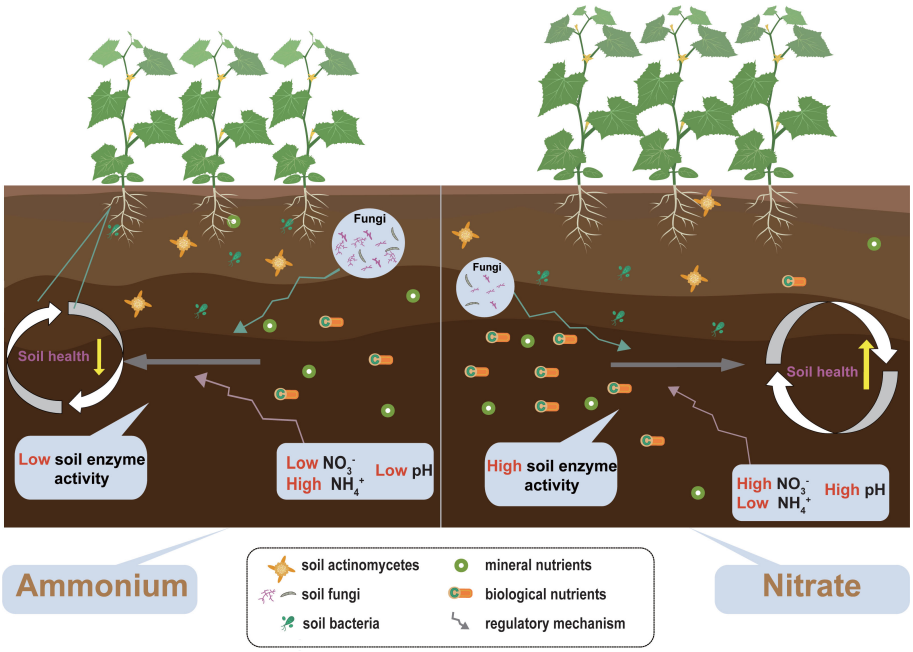

FIGURE 7
The concept map shows the effects of different nitrogen forms on soil health and plant productivity. The yellow vertical arrows correspond to the soil health and soil stability change intensity. Plant size corresponds to plant productivity.

ammonium nitrogen. Therefore, this study supports the second hypothesis that nitrate fertilization is one of the important ways to promote soil sustainable function by improving soil health.

Conclusions

Nitrate fertilization is more conducive to the absorption and utilization of nutrients, yields formation of monocropping, and delays soil acidification and salinization (Figure 7). Furthermore, nitrate fertilization helps to maintain the nutrient structure of soil microbial communities, increases their stability, and promotes soil nutrient transformation and utilization, leading to an improvement in soil health. Hence, nitrate fertilizer application is preferred in the monocropping system of cucumbers. The current findings advance the knowledge of different forms of nitrogen fertilization effects on plant productivity and its role in shaping soil health. Overall, we suggest that agricultural sustainable management by integrating amendments of nitrogen form could enhance regulation of soil ecosystem processes, sustaining the synergies between soil health and crop productivity.

Data availability statement

The original contributions presented in the study are included in the article/Supplementary Material. Further inquiries can be directed to the corresponding author.

Author contributions

MW conceived the ideas and designed the study; LZ and AL were used in field and laboratory experiments, respectively. LZ analyzed the data and wrote the manuscript with substantial contributions from RFW, YS, JL, RRW, SG, and MW. All authors contributed to the article and approved the submitted version.

Funding

This study was supported by the National Natural Science Foundation of China (32072673) and the Fundamental Research Funds for the Central Universities (XUEKEN2022006).

Conflict of interest

The authors declare that the research was conducted in the absence of any commercial or financial relationships that could be construed as a potential conflict of interest.

Publisher's note

Supplementary material

The Supplementary Material for this article can be found online at: https://www.frontiersin.org/articles/10.3389/fpls.2023.1190929/full#supplementary-material

References

Anderson, T.-H., and Domsch, K. H. (2010). Soil microbial biomass: the eco-physiological approach. *Soil Biology and Biochemistry* 42 (12), 2039–2043. doi: 10.1016/j.soilbio.2010.06.026

Baer, S., Blair, J., Collins, S., and Knapp, A. J. E. (2003). Soil resources regulate productivity and diversity in newly established tallgrass prairie. *Ecology* 84, 724–735. doi: 10.2307/3107866

Britto, D. T., and Kronzucker, H. J. (2002). NH_4^+ toxicity in higher plants: a critical review. *Journal of Plant Physiology* 159 (6), 567–584. doi: 10.1078/0176-1617-0774

Brookes, P. C., Landman, A., Pruden, G., and Jenkinson, D. S. (1985). Chloroform fumigation and the release of soil nitrogen: a rapid direct extraction method to measure microbial biomass nitrogen in soil. *Soil Bid. Biocfre* 17 (6), 837–842. doi: 10.1016/(85)90144-0

Currey, P. M., Johnson, D., Sheppard, L. J., Leith, I. D., Toberman, H., van der Wal, R., et al. (2009). Turnover of labile and recalcitrant soil carbon differ in response to nitrate and ammonium deposition in an ombrotrophic peatland. *Glob. Chang. Biol.* 16 (8), 2307–2321. doi: 10.1111/j.1365-2486.2009.02082.x

Evans, C. D., Goodale, C. L., Caporn, S. J. M., Dise, N. B., Emmett, B. A., Fernandez, I. J., et al. (2008). Does elevated nitrogen deposition or ecosystem recovery from acidification drive increased dissolved organic carbon loss from upland soil? a review of evidence from field nitrogen addition experiments. . *Biogeochemistry* 91 (1), 13–35. doi: 10.1007/s10533-008-9256-x

Frey, S. D., Ollinger, S., Nadelhoffer, K., Bowden, R., Brzostek, E., Burton, A., et al. (2014). Chronic nitrogen additions suppress decomposition and sequester soil carbon in temperate forests. *Biogeochemistry* 121 (2), 305–316. doi: 10.1007/s10533-014-0004-0

Frostegård, A. B., and Bååth, E. (1996). The use of phospholipid fatty acid analysis to estimate bacterial and fungal biomass in soil. *Biol Fertil Soils* 22 (1-2), 59–65. doi: 10.1007/BF00384433

Gao, Z., Han, M., Hu, Y., Li, Z., Liu, C., Wang, X., et al. (2019). Effects of continuous cropping of sweet potato on the fungal community structure in rhizospheric soil. *Front Microbiol* 10, 2269. doi: 10.3389/fmicb.2019.02269

Geng, J., Fang, H., Cheng, S., and Pei., J. (2021). Effects of n deposition on the quality and quantity of soil organic matter in a boreal forest: contrasting roles of ammonium and nitrate. *Catena* 198, 104996. doi: 10.1016/j.catena.2020.104996

Geng, S., Shi, P., Zong, N., and Zhu, W. (2018). Using soil survey database to assess soil quality in the heterogeneous taihang mountains, north China. *Sustainability* 10 (10), 3443. doi: 10.3390/su10103443

Ghorbani, R., Wilcockson, S., Koocheki, A., and Leifert, C. (2008). Soil management for sustainable crop disease control: a review. *Environmental Chemistry Letters* 6 (3), 149–162. doi: 10.1007/s10311-008-0147-0

Gregorich, R. P. V. E.G., and Kachanoski, R. G. (1991). Turnover of carbon through the microbial biomass in soils with different texture. *Soil Biology and Biochemistry* 23, 799–805. doi: 10.1016/0038-0717(91)90152-a

Grundmann, G. L., Renault, P., Rosso, L., and Bardin, R. (1995). Differential effects of soil water content and temperature on nitrification and aeration. *Soil Sci Soc Am J* 59, 1342–1349. doi: sssaj1995.03615995005900050021x

Gu, Z., Wang, M., Wang, Y., Zhu, L., Mur, L. A. J., Hu, J., et al. (2020). Nitrate stabilizes the rhizospheric fungal community to suppress fusarium wilt disease in cucumber. *Mol Plant Microbe Interact* 33 (4), 590–599. doi: 10.1094/MPMI-07-19-0198-R

Gu, X., Yang, N., Zhao, Y., Liu, W., and Li., T. (2022). Long-term watermelon continuous cropping leads to drastic shifts in soil bacterial and fungal community composition across gravel mulch fields. *BMC Microbiol* 22 (1), 189. doi: 10.1186/s12866-022-02601-2

Guiraud, G., and Marol, C. (1992). Influence of temperature on mineralization kinetics with a nitrification inhibitor (mixture of dicyandiamide and ammonium thiosulphate). *Biol Fertil Soils* 13, 1–5. doi: 10.1007/bf00337229

Guo, S., Chen, G., Zhou, Y., and Shen, Q. (2007). Ammonium nutrition increases photosynthesis rate under water stress at early development stage of rice (Oryza sativa l.). *Plant and Soil* 296 (1-2), 115–124. doi: 10.1007/s11104-007-9302-9

Hofman, J., Bezchlebová, J., Dušek, L., Doležal, L. K., Holoubek, I., Anděl, P., et al. (2003). Novel approach to monitoring of the soil biological quality. *Environment International* 28 (8), 771–778. doi: 10.1016/s0160-4120(02)00068-5

Huang, W., Sun, D., Fu, J., Zhao, H., Wang, R., and An., Y. (2019). Effects of continuous sugar beet cropping on rhizospheric microbial communities. *Genes (Basel)* 11 (1), 13. doi: 10.3390/genes11010013

Jia, Z., Hu, X., Xia, W., Fornara, D., Nannipieri, P., and Tiedje., J. (2019). Community shift of microbial ammonia oxidizers in air-dried rice soils after 22 years of nitrogen fertilization. *Biology and Fertility of Soils* 55 (4), 419–424. doi: 10.1007/s00374-019-01352-z

Jia, Y., Yu, G., He, N., Zhan, X., Fang, H., Sheng, W., et al. (2014). Spatial and decadal variations in inorganic nitrogen wet deposition in China induced by human activity. *Sci Rep.* 4, 3763. doi: 10.1038/srep03763

Jiang, X., Hou, X., Zhou, X., Xin, X., Wright, A., and Jia, Z. (2015). pH regulates key players of nitrification in paddy soils. secondary pH regulates key players of nitrification in paddy soils. *Soil Biology and Biochemistry* 81, 9–16. doi: 10.1016/j.soilbio.2014.10.025

Kramer, C., and Gerd, G. (2008). Soil organic matter in soil depth profiles: distinct carbon preferences of microbial groups during carbon transformation. *Soil Biology and Biochemistry* 40 (2), 425–433. doi: 10.1016/j.soilbio.2007.09.016

Li, Q., Li, B. H., Kronzucker, H. J., and Shi., W. M. (2010). Root growth inhibition by NH_4^+ in arabidopsis is mediated by the root tip and is linked to NH_4^+ efflux and GMPase activity. *Plant Cell Environ* 33 (9), 1529–1542. doi: 10.1111/j.1365-3040.2010.02162.x

Li, C., Wang, X., Guo, Z., Huang, N., Hou, S., He, G., et al. (2022). Optimizing nitrogen fertilizer inputs and plant populations for greener wheat production with high yields and high efficiency in dryland areas. *Field Crops Research* 276, 108374. doi: 10.1016/j.fcr.2021.108374

Lu, D., Lu, F., Pan, J., Cui, Z., Zou, C., Chen, X., et al. (2015). The effects of cultivar and nitrogen management on wheat yield and nitrogen use efficiency in the north China plain. *Field Crops Research* 171, 157–164. doi: 10.1016/j.fcr.2014.10.012

Lu, M., Zhou, X., Luo, Y., Yang, Y., Fang, C., Chen, J., et al. (2011). Minor stimulation of soil carbon storage by nitrogen addition: a meta-analysis. *Agriculture, Ecosystems & Environment* 140 (1-2), 234–244. doi: 10.1016/j.agee.2010.12.010

Luo, X., Fu, X., Yang, Y., Cai, P., Peng, S., Chen, W., et al. (2016). Microbial communities play important roles in modulating paddy soil fertility. *Sci Rep.* 6, 20326. doi: 10.1038/srep20326

Luo, L., Guo, C., Wang, L., Zhang, J., Deng, L., Luo, K., et al. (2019). Negative plant-soil feedback driven by re-assemblage of the rhizosphere microbiome with the growth of panax notoginseng. *Front Microbiol.* 10, 1597. doi: 10.3389/fmicb.2019.01597

May, P. B., and Douglas, L. A. (1976). Assay for soil urease activity. secondary assay for soil urease activity. *Plant and Soil.* 45 (1), 301–305. doi: 10.1007/bf00011156

Nunes, M. R., van Es, H. M., Schindelbeck, R., Ristow, A. J., and Ryan, M. (2018). No-till and cropping system diversification improve soil health and crop yield. *Geoderma.* 328, 30–43. doi: 10.1016/j.geoderma.2018.04.031

Paz-Ferreiro, J., Trasar-Cepeda, C., Leirós, M., Seoane, S., and Gil-Sotres, F. (2011). Intra-annual variation in biochemical properties and the biochemical equilibrium of different grassland soils under contrasting management and climate. *Biology and Fertility of Soils* 47 (6), 633–645. doi: 10.1007/s00374-011-0570-4

Pregitzer, K. S., Burton, A. J., Zak, D. R., and Talhelm, A. F. (2008). Simulated chronic nitrogen deposition increases carbon storage in northern temperate forests. *Global Change Biology* 14 (1), 142–153. doi: 10.1111/j.1365-2486.2007.01465.x

Ramirez, K. S., Craine, J. M., and Fierer, N. (2010). Nitrogen fertilization inhibits soil microbial respiration regardless of the form of nitrogen applied. *Soil Biology and Biochemistry* 42 (12), 2336–2338. doi: 10.1016/j.soilbio.2010.08.032

Reddy, B. N., and Babu, S. N. S. (2003). Sustainability of sunflower-based crop sequences in rainfed alfisols. *Helia* 26 (39), 117–124. doi: 10.2298/HEL0339117R

Shen, Z., Penton, C. R., Lv, N., Xue, C., Yuan, X., Ruan, Y., et al. (2018). Banana fusarium wilt disease incidence is influenced by shifts of soil microbial communities under different monoculture spans. *Microb Ecol* 75 (3), 739–750. doi: 10.1007/s00248-017-1052-5

Sun, X., Zhu, L., Wang, J., Wang, J., Su, B., Liu, T., et al. (2017). Toxic effects of ionic liquid 1-octyl-3-methylimidazolium tetrafluoroborate on soil enzyme activity and soil microbial community diversity. *Ecotoxicol Environ Saf* 135, 201–208. doi: 10.1016/j.ecoenv.2016.09.026

Tao, B., Wang, Y., Yu, Y., Li, Q., Luo, C., and Zhang, B. (2018). Interactive effects of nitrogen forms and temperature on soil organic carbon decomposition in the coastal wetland of the yellow river delta, China. *Catena* 165, 408–413. doi: 10.1016/j.catena.2018.02.025

Telles-Pupulin, A. R., Diniz, S. P. S. S., Bracht, A., and Ishii-Iwamoto, E. L. (1996). Effects of fusarie acid on respiration in maize root mitochondria. *Biologia Plantarum* 38, 421. doi: 10.1007/BF02896673

Treseder, K. K. (2008). Nitrogen additions and microbial biomass: a meta-analysis of ecosystem studies. *Ecol Lett* 11 (10), 1111–1120. doi: 10.1111/j.1461-0248.2008.01230.x

Wang, M., Sun, Y., Gu, Z., Wang, R., Sun, G., Zhu, C., et al. (2016). Nitrate protects cucumber plants against fusarium oxysporum by regulating citrate exudation. *Plant Cell Physiol Plant Cell Physiol* 57 (9), 2001–2012. doi: 10.1093/pcp/pcw124

Wang, Q. K., and Wang, S. L. (2006). Microbial biomass in subtropical forest soils: effect of conversion of natural secondary broad-leaved forest to cunninghamia lanceolata plantation. *Journal of Forestry Research* 17 (3), 197–200. doi: 10.1007/s11676-006-0046-9

Wang, H., Wu, J., Li, G., and Yan, L. (2020). Changes in soil carbon fractions and enzyme activities under different vegetation types of the northern loess plateau. *Ecol Evol.* 10 (21), 12211–12223. doi: 10.1002/ece3.6852

Wei, H., Chen, X., He, J., Zhang, J., and Shen, W. (2017). Exogenous nitrogen addition reduced the temperature sensitivity of microbial respiration without altering the microbial community composition *Front Microbiol.* 8, 2382. doi: 10.3389/fmicb.2017.02382

Wu, J., Joergensen, R. G., Pommerening, B., Chaussod, R., and Brookes, P. C. (1990). Measurement of soil microbial biomass c by fumigation-extraction-an automated procedure. *Sod Ed. Biochrm* 22.I 167-l, 169. doi: 10.1016/0038-0717(90)90046-3

Wu, C., Wu, X., Zhu, G., Qian, C., Mu, W.-P., and Zhang, Y.-z. (2018). Influence of a power plant in ezhou city on the groundwater environment in the nearby area. *Environmental Earth Sciences* 77, 1–13. doi: 10.1007/s12665-018-7674-1

Xu, M., Gao, P., Yang, Z., Su, L., Wu, J., Yang, G., et al. (2019). Biochar impacts on phosphorus cycling in rice ecosystem. *Chemosphere* 225, 311–319. doi: 10.1016/j.chemosphere.2019.03.069

Xu, R., Li, T., Shen, M., Yang, Z. L., and Zhao., Z.-W. (2020). Evidence for a dark septate endophyte (Exophiala pisciphila, H93) enhancing phosphorus absorption by maize seedlings. *Plant and Soil.* 452 (1), 249–266. doi: 10.1007/s11104-020-04538-9

Yang, Y., Li, T., Pokharel, P., Liu, L., Qiao, J., Wang, Y., et al. (2022). Global effects on soil respiration and its temperature sensitivity depend on nitrogen addition rate. *Soil Biology and Biochemistry* 174, 108814. doi: 10.1016/j.soilbio.2022.108814

Yang, T., Liu, K., and Siddique, K. H. M. (2020). Cropping systems in agriculture and their impact on soil health-a review. *Global Ecology and Conservation* 23, e01118. doi: 10.1016/j.gecco.2020.e01118

Yang, R., Xia, X., Wang, J., Zhu, L., Wang, J., Ahmad, Z., et al. (2020). Dose and time-dependent response of single and combined artificial contamination of sulfamethazine and copper on soil enzymatic activities. *Chemosphere* 250, 126161. doi: 10.1016/j.chemosphere.2020.126161

Zhang, T., Chen, H. Y. H., and Ruan, H. (2018). Global negative effects of nitrogen deposition on soil microbes. *ISME Journal* 12 (7), 1817–1825. doi: 10.1038/s41396-018-0096-y

Zhang, J., Fan, S., Qin, J., Dai, J., Zhao, F., Gao, L., et al. (2020). Changes in the microbiome in the soil of an American ginseng continuous plantation. *Front Plant Sci.* 11, 572199. doi: 10.3389/fpls.2020.572199

Zhang, X.-Y., Zhang, C., Zou, H.-T., Kou, L., Yang, Y., Wen, X., et al. (2017). Contrasting effects of ammonium and nitrate additions on the biomass of soil microbial communities and enzyme activities in subtropical China. *Biogeosciences* 14 (20), 4815–4827. doi: 10.5194/bg-14-4815-2017

Zhong, X.-l., Li, J.-t., Li, X.-j., Ye, Y.-c., Liu, S.-s., Hallett, P. D., et al. (2017). Physical protection by soil aggregates stabilizes soil organic carbon under simulated n deposition in a subtropical forest of China. *Geoderma* 285, 323–332. doi: 10.1016/j.geoderma.2016.09.026

frontiers | Frontiers in Plant Science

TYPE Opinion
PUBLISHED 13 September 2023
DOI 10.3389/fpls.2023.1271539

OPEN ACCESS

EDITED BY
Fahad Shafiq,
Government College University, Lahore, Pakistan

REVIEWED BY
Chao Wang,
Shanxi Agricultural University, China

*CORRESPONDENCE
Yongjun Guo
1695533623@qq.com

†These authors share first authorship

RECEIVED 02 August 2023
ACCEPTED 29 August 2023
PUBLISHED 13 September 2023

CITATION
Huang L, Zhang Y, Guo J, Peng Q, Zhou Z, Duan X, Tanveer M and Guo Y (2023) High-throughput root phenotyping of crop cultivars tolerant to low N in waterlogged soils.
Front. Plant Sci. 14:1271539.
doi: 10.3389/fpls.2023.1271539

High-throughput root phenotyping of crop cultivars tolerant to low N in waterlogged soils

Liping Huang[1,2†], Yujing Zhang[1,2†], Jieru Guo[1,2], Qianlan Peng[1], Zhaoyang Zhou[1], Xiaosong Duan[1], Mohsin Tanveer[3] and Yongjun Guo[1,2*]

[1]International Research Center for Environmental Membrane Biology, College of Food Science and Engineering, Foshan University, Foshan, China, [2]Foshan ZhiBao Ecological Technology Co. Ltd., Foshan, China, [3]Tasmanian Institute of Agriculture, University of Tasmania, Hobart, TAS, Australia

KEYWORDS

root phenotyping, root traits, NUE, imaging sensors, waterlogging

Introduction

Waterlogging (WL) is one of the most damaging abiotic stresses, affecting 1,700 million hectares of land surface annually (Kaur et al., 2020). Under WL, saturation of soil pores with excessive water results in the development of anaerobic conditions with a subsequent reduction in root growth (Figure 1A; Pais et al., 2022). WL induces nutrient imbalances in soil by inducing chemical reduction of some nutrients, including nitrogen (N) (Steffens et al., 2005), thus leading to both nutrient deficiency and/or toxic buildups in soil. N is a very important mineral nutrient and plays a critical role in plant physiology; thus, nitrogen fertilization is adopted as one of the most essential principles for efficient crop production systems (Shah et al., 2021). Nitrogen application boosts crop yield (Shah et al., 2017; Shah et al., 2022); however, excessive application of N comes with several environmental issues. WL promotes soil N losses via runoff, leaching, and denitrification with a concomitant reduction in crop productivity, thus imposing economic and environmental implications. Thus, it is important to understand and improve nitrogen use efficiency (NUE) in plants under WL.

Roots uptake N from the soil in various forms, including amino acids, nitrate (NO_3^-), and ammonium (NH_4^+); however, NO_3^- is a major source of N in plants (Arduini et al., 2019). WL reduces root N uptake by altering root development (RD), root system architecture (RSA), and N availability in soil. The adoption of advanced agronomic N management techniques, including slow-release fertilizer, biochar application, or inoculation, plays a significant role in improving NUE under WL; however, the efficacy of any agronomic technique greatly depends on soil type and plant species. Moreover, recent development in genetics and breeding techniques have also shown tremendous potential in the development of crop cultivars with higher NUE under low N availability;

however, the development of such cultivars is very complex due to genotype and environmental interactions. Moreover, a bottleneck has arisen in the collection of quality phenotypic data to advance crop breeding programs compared with genetic analysis. In this context, adoption of high-throughput root-phenotyping (HTRP) can provide blueprints for breeders to enhance N acquisition in roots under WL.

Several HTRP techniques enable us to phenotype and visualize the root performance under different growth conditions (Figure 1B); however, contemporary aboveground canopy-based crop phenotyping (GCCP) techniques account for N-deficiency-induced changes in vegetation index (VI) by measuring photosynthesis, chlorophyll contents, leaf temperature, and stay greenness. However, such GCCP data can be easily camouflaged by the multiple environmental factors that can directly or indirectly influence VI traits. Contrarily, roots being the first line of contact with N and WL, focusing on the establishment of HTRP at least at the early growth stage would be beneficial in determining the genetic basis of NUE in plants under WL.

Correlation between root traits and NUE

Root system (RS) is very important in the context of N acquisition from soil, and several root traits such as root size, root length (RL), root density (Rd), and root distribution determine N acquisition from soil (Figure 1C; Garnett et al., 2009). Crop cultivars with larger RL and Rd uptake more N from soil (Ju et al., 2015), thus reducing N losses under WL. RSA is closely related to N uptake, and crop plants with steeper roots uptake more N from the soil (Zhan & Lynch, 2015). The duration of WL also influences the RS and N uptake (Malik et al., 2001); e.g., short-term WL reduced N uptake only in the bottom layer of the soil-filled pot, while long-term WL resulted in reduced N uptake in both the bottom and top layers of the pot (Dresbøll and Thorup-Kristensen, 2012). Root N uptake was more quickly recovered after short exposure to WL than after long exposure to WL, probably due to the production of new roots (Dresbøll and Thorup-Kristensen, 2012). However, even though N uptake was resumed after recovery from WL, oat roots exhibited reduced root biomass under WL, most likely due to the separation of dead root fragments (Brisson et al., 2002), advanced growth stage during recovery (Arduini et al., 2019), continuous N leakage from root tissues, or other detrimental effects of WL on RS (De San Celedonio et al., 2017). Nonetheless, a cultivar-specific relationship between RS and NUE was observed among two Chinese and one American variety of maize (Ju et al., 2015). The insufficient N uptake by roots under WL could also be due to low availability of N in soil (Nguyen et al., 2018), higher N losses, reduced RD (Brisson et al., 2002), and impaired NO_3^- uptake by roots (Pang et al., 2007). Thus, it is not practically easy to ascertain whether lower N availability to roots is the primary cause of reduced root growth under WL or *vice versa*. Therefore, it is important to consider factors such as cultivars, WL duration, WL method, and plant growth stage when performing HTRP.

Application of HTRP under waterlogging

Labeling the variations among genotypes and species that uphold improved root traits and integrating them into breeding programs for the development of N-efficient cultivars is a very demanding method. However, studying RSA is very challenging due to the complexity of accurately and precisely phenotyping RS under WL. Several HTRP techniques are being used to understand the relationship between RS and NUE under WL (Figure 1B); however, under field conditions, root phenotyping is still handled using a medium- to low-throughput platform (Araus et al., 2022). Different WL methods can also influence root phenotyping (Figure 1D). Under controlled conditions, growing plants in hydroponics or gel-based media provides an easy approach to monitoring root morphology; however, this is applicable only in early growth conditions (Langan et al., 2022). Sand culture is another HTRP technique to study RS for improved NUE and performance of root traits using scanners (Paez-Garcia et al., 2015). The pH level of soil and soilless cultures needs to be well monitored, as systems with pH instability and low buffer capacity affect N uptake and RD (Lager et al., 2010). Noninvasive measurements of RS for improved NUE under WL can also be examined using image technology, enabling 2D root growth accompanied by real-time gene expression relating to NUE in roots (Rellán-Álvarez et al., 2015). Other noninvasive techniques, including magnetic resonance imaging (MRI) and X-ray computed tomography (CT) (see glossary in Figure 1B), assist in visualizing the physiological properties of roots (Mairhofer et al., 2013; Metzner et al., 2015). Nonetheless, technical complexities and high operation costs make these techniques less useful for large-scale phenotyping. The noninvasive microelectrode ion flux measurements (MIFE) technique was used to perform cell-based phenotyping for revealing QTL associated with hypoxia tolerance in barley (Gill et al., 2017) and understanding the N uptake by measuring the kinetics of NO_3^- and NH_4^+ fluxes (Garnett et al., 2003).

At field conditions, several techniques have been applied for performing root phenotyping, such as shovelomics and soil coring (SC). Shovelomics also known as root crown phenotyping, consists of the manual digging and excavation of roots and up to 30 cm of rhizosphere (Wasson et al., 2020). SC also works as shovel omics does to some extent; however, SC consists of the extraction of cores from deeper soil using a corer, with a betting examination of RS (Wasson et al., 2014). For a better view of RS, SC is supplemented with a portable fluorescence imaging system known as BlueBox, which provides automatic root counting using image analysis software (Wasson et al., 2016). Geophysical platforms such as electrical resistance tomography and electromagnetic inductance are used to infer root growth under changes in soil water (Srayeddin & Doussan, 2009; Whalley et al., 2017). Moreover, ground-penetrating radar performs mapping of subsurface soil using radio wave pulses and detects RS under field conditions (Liu et al., 2017; Atkinson et al., 2019).

These HTRP techniques can be ineffective, laborious, and subject to soil conditions (soil types, WL duration, N in soil). Moreover, root

extraction under WL is also very difficult due to the breakage of root fragments during extraction; thus, alternate approaches supplement HTRP, including phenotyping of aboveground traits. However, measuring aboveground traits can only infer root growth indirectly (Reynolds et al., 2012; Tracy et al., 2020). To understand root response, examination of the stable isotope composition of N in roots under WL can improve our understanding of the physiological basis of roots and NUE under WL. Having said that, isotopic signatures of oxygen in stem water were used as an indicator of water status in water-stressed roots

A

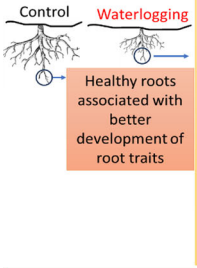

B

Glossary of different HTRP techniques

- *MIFE*-measures the kinetics of net ion transport across cell membrane based on the electrochemical gradient near root surfaces. *EMI* — imaging and mapping of spatial soil and root electrical conductivity *GPR* — mapping of sub-surface structure by measuring reflection, refraction, and scattering of pulses of high-frequency radio waves. *MRI*— detecting the radio waves and magnetic signals from roots and then visualizing the physiological properties of roots *Rhizotron* — a growth chamber with transparent or removable observation windows through which roots can be imaged. *X-ray CT* — examining the root growth by measuring the attenuation of radiation when passes through roots into a 3D model.

C

Root traits and their roles for improving NUE and crop growth under waterlogging (WL)	
Rdia and Rd	Regulates root length, provides more root surface area to increase N uptake under WL.
Rhs	Assist in maintaining contact between root and soil for uptake of water and nutrients under WL
RSA	Comprises a collection of root phones, determines the temporal and spatial distribution of roots in soil, and regulates the ability of crop roots to obtain mobile and immobile resources from soil.
RL	Determines the root depth-longer roots enable crops to increase N uptake under WL.
RA	Promotes deeper root growth, rhizosphere area, and nutrient acquisition.
Roots	Support crop anchorage under WL, constitute RSA, control depth of root system and enhances crop's ability to acquire more nutrients.
RB	Aids in the foraging for nutrients particularly in nitrate deficient soil patch or layer.

D

Comparison of different WL methods; advantages and challenges associated with them		
Root phenotyping method	**Advantages**	**Challenges**
Hydroponics	• Homogenous growth conditions • Easy root handling and harvesting • Year-round experiment	• pH-sensitive • Requires continuous monitoring. • No substrate for typical root development
Pot (sand/soil culture)	• Easy to harvest • Mobile system • Easy management of WL	• Limited space for root development. • Water levels must be maintained throughout experiment. • Root breakage during root sampling. • Difficult to remove soil particles from root surface, thus affects image analysis.
Field	• Agronomic relevant conditions • Large sample size	• Resources intensive • Cost ineffective • Subject to growing season and environmental conditions.

E

Overview of currently available root image analysis software for visualizing root activity and HTRP		
Software	**Advantage**	**Challenges**
EZ-Rhizo*; GiA Roots*; GLO-RIA*; GrowScreen-Root*; Growth Explorer*; MYROOT*; RootNav*; RootReader2D*; RootScape*; RootTip Trace*; RooTrak* * Represents semi-automated	• Suitable for investigating a wide range of biological questions • Add on new algorithms and trait estimation steps using plugins • Quantify complex root systems and local root growth zones at a high throughput • Assist in visualizing root morphology at different development stage and in overlapped root system • Minimal user interaction/Adapt to changing root density estimates	• Subject to different WL methods, WL exposure time, and crop growth stage • Partially require statistical models • Semi-automated thus obtained results can partially be influenced by human errors • Require trained personal to operate
Aria**; ARTT**; BRAT**; DIRT**; ElonSim**; EZ-Root-VIS**; faRIA**; GROW Map-Root**; RootGraph**; Root System Analyzer**; RootFlowRT**; RootFly**; RootReader3D**; RootTrace**; RhizoVision Explorer** ** Represents fully automated	• Fast/Batch analysis/Ability to analyze 3D images • Robust, fully automatic examination of root traits in high spatial and temporal resolution • Processing of 3D images • Capture RSA features of many individual plants/Visualize averaged RSAs for different genotypes under various environments or at different time points • Least rely on any statistical learning • Distinguish root overlaps from branches • Combination of optical flow methods • Time savings, and default broken roots mode	• Subject to different WL methods, WL exposure time, and crop growth stage • Subject to climatic conditions at field conditions

FIGURE 1
Application of HTRP for studying root systems and improving NUE under WL: **(A)** effects of WL on root growth, **(B)** glossary of different HTRP techniques used for root phenotyping, **(C)** role of different root traits for improving NUE under WL, **(D)** comparison of different WL methods, and **(E)** application of different image analysis software to quantify and visualize root system. Rd, root development; Rdia, root diameter; RL, root length; Rhs, root hairs; RA, root activity; Root*, fine and coarse roots; Lp, root hydraulic conductivity; RB, root branching; MIFE, microelectrode ion flux estimation; EMI, electromagnetic induction; GPR, ground-penetrating radar; MRI, magnetic resonance imaging; X-ray-CT, X-ray computed tomography.

(Kale Celik et al., 2018). Thus, this approach should be used along with other HTRP techniques.

Can image-based HTRP be used to phenotype under WL?

Performing HTRP using imaging sensors (IS) and platforms goes on to grow exponentially, easing the bottleneck of root phenotypic data collection (Roitsch et al., 2019). IS such as red, green, and blue (RGB) sensors that take images within the wavelength range of 400–700 nm are termed visible IS, while IS that go beyond the visible wavelength are known as spectral IS (SIS) (Beisel et al., 2018; Bruning et al., 2020). In controlled conditions such as glasshouses or growth chambers, IS range from low-cost cameras to costly custom-made imaging setups (Tovar et al., 2018). Recently, Xia et al. (2019) used hyperspectral and RGB to phenotype WL in rape plants and found promising results. Nonetheless, the use of low-cost cameras may result in image noise; thus, to reduce image noise, image fragmentation must performed (Agata et al., 2007). Imaging plants under WL face other challenges due to the presence of extra water in a pot, which reflects the lights of IS and is due to unwanted algal growth. On the other hand, in field conditions, the use of unmanned ariel vehicles (UAV) and satellite-based imaging are the most popular imaging techniques (Li et al., 2014; Langan et al., 2022). Nonetheless, these imaging techniques also face challenges associated with soil heterogeneity and water drainage, so the use of machine learning (ML) has been suggested along with these imaging techniques to study WL in plants (Zhou et al., 2021). For 2D root images, tip locations have been identified using a deep network-based classifier scanned over an image to produce a location map (Pound et al., 2017). For 3D images, deep learning has been applied to the root–soil segmentation problem, where deep-learned features are used to drive a support vector machine classifying root/soil pixels (Douarre et al., 2016).

As mentioned before, RS plays a very important role in N uptake under WL, and using growth pouches to study root performance under WL or performing root phenotyping using the classical 2D imaging technique (Nagel et al., 2012) does not provide a clear understanding of the root development under WL. Thus, the use of tomographic techniques including CT scanning, MRI, or positron emission tomography has been successfully reported in the study of root phenotyping (Atkinson et al., 2019; Wasson et al., 2020). For instance, X-ray CT scanning was used to visualize the formation of aerenchyma under WL in the roots of barley (Kehoe et al., 2022). Therefore, the application of tomographic techniques can assist in root phenotyping under WL, thereby opening new opportunities for future studies. Though several other methods have been designed for root phenotyping by studying different root traits, including root surface area, crown roots, root length, and root density in soil core (Koyama et al., 2021), there is not any standard root phenotyping method to study different aspects of RSA under WL; therefore, the field of IS exhibits much to extend to the research community. Having said that, several image analysis software are available to quantify and visualize root systems (Figure 1E). A new initiative has been established to attempt to harness crop-management synergies using phenotyping, robotics, and computational technologies (http://www.phenorob.de/).

Conclusion

N fertilization has become the necessity of almost every intensive cropping system, and under WL conditions, crops face N deficiency. Thus, it is imperative to improve the ability of crops to improve NUE under limited N availability. Roots play a critical role in acquiring N from soil; thus, it is important to phenotype RS to highlight the root traits and their relationship with NUE under WL. Given that, the application of HTRP is intensifying due to the technical development and measurement of RS. The utilization of IS and noninvasive measurements of RS can facilitate improving NUE in roots under WL. Advances in ML further benefit analyzing root phenotyping data; however, under field conditions, high-throughput analysis of root phenotyping remains subtle.

Author contributions

LH: Conceptualization, Writing – review & editing. YZ: Writing – original draft. JG: Writing – original draft. QP: Writing – original draft. ZZ: Writing – original draft. XD: Writing – review & editing. MT: Conceptualization, Writing – review & editing. YG: Conceptualization, Methodology, Writing – review & editing.

Funding

The authors declare financial support was received for the research, authorship, and/or publication of this article. This work was supported by the National Natural Science Foundation of China (Grant No. 31901202).

Conflict of interest

Author YG is employed by Foshan ZhiBao Ecological Technology Co. Ltd., Foshan, China.

The remaining authors declare that the research was conducted in the absence of any commercial or financial relationships that could be construed as a potential conflict of interest.

The author(s) declared that they were an editorial board member of Frontiers, at the time of submission. This had no impact on the peer review process and the final decision

Publisher's note

References

Agata, H., Yamashita, A., and Kaneko, T. (2007). Chroma key using a checker pattern background. *IEICE Trans. Inf. Syst.* 90 (1), 242–249. doi: 10.1093/ietisy/e90-1.1.242

Araus, J. L., Kefauver, S. C., Vergara-Díaz, O., Gracia-Romero, A., Rezzouk, F. Z., Segarra, J., et al. (2022). Crop phenotyping in a context of global change: What to measure and how to do it. *J. Integr. Plant Biol.* 64 (2), 592–618. doi: 10.1111/jipb.13191

Arduini, I., Baldanzi, M., and Pampana, S. (2019). Reduced growth and nitrogen uptake during waterlogging at tillering permanently affect yield components in late sown oats. *Front. Plant Sci.* 10, 1087. doi: 10.3389/fpls.2019.01087

Atkinson, J. A., Pound, M. P., Bennett, M. J., and Wells, D. M. (2019). Uncovering the hidden half of plants using new advances in root phenotyping. *Current. Opin. Biotechnol.* 55, 1–8. doi: 10.1016/j.copbio.2018.06.002

Beisel, N. S., Callaham, J. B., Sng, N. J., Taylor, D. J., Paul, A.-L., and Ferl, R. J. (2018). Utilization of single-image norMalized difference vegetation index (SI-NDVI) for early plant stress detection. *App. Plant Sci.* 6, e01186. doi: 10.1002/aps3.1186

Brisson, N., Rebiere, B., Zimmer, D., and Renault, P. (2002). Response of the root system of a winter wheat crop to waterlogging. *Plant Soil* 243, 43–55. doi: 10.1023/A:1019947903041

Bruning, B., Berger, B., Lewis, M., Liu, H., and Garnett, T. (2020). Approaches, applications, and future directions for hyperspectral vegetation studies: An emphasis on yield-limiting factors in wheat. *Plant Phenome J.* 3, e20007. doi: 10.1002/ppj2.20007

De San Celedonio, R. P., Abeledo, L. G., Mantese, A. I., and Miralles, D. J. (2017). Differential root and shoot biomass recovery in wheat and barley with transient waterlogging during pre-flowering. *Plant Soil* 417, 481–498. doi: 10.1007/s11104-017-3274-1

Douarre, C., Schielein, R., Frindel, C., Gerth, S., and Rousseau, D. (2016). Deep learning based root-soil segmentation from X-ray tomography images. *BioRxiv*, 071662. doi: 10.1101/071662

Dresbøll, D. B., and Thorup-Kristensen, K. (2012). Spatial variation in root system activity of tomato (*Solanum lycopersicum* L.) in response to short and long-term waterlogging as determined by 15 N uptake. *Plant Soil.* 357, 161–172. doi: 10.1007/s11104-012-1135-5

Garnett, T., Conn, V., and Kaiser, B. N. (2009). Root based approaches to improving nitrogen use efficiency in plants. *Plant Cell Environ.* 32, 1272–1283. doi: 10.1111/j.1365-3040.2009.02011.x

Garnett, T. P., Shabala, S. N., Smethurst, P. J., and Newman, I. A. (2003). Kinetics of ammonium and nitrate uptake by eucalypt roots and associated proton fluxes measured using ion selective microelectrodes. *Func. Plant Biol.* 30, 1165–1176. doi: 10.1071/FP03087

Gill, M. B., Zeng, F., Shabala, L., Zhang, G., Fan, Y., Shabala, S., et al. (2017). Cell-based phenotyping reveals QTL for membrane potential maintenance associated with hypoxia and salinity stress tolerance in barley. *Front. Plant Sci.* 8, 1941. doi: 10.3389/fpls.2017.01941

Ju, C., Buresh, R. J., Wang, Z., Zhang, H., Liu, L., Yang, J., et al. (2015). Root and shoot traitsforrice varieties with higher grain yield and higher nitrogen use efficiency at lower nitrogen rates application. *Field Crops Res.* 175, 47–55. doi: 10.1016/j.fcr.2015.02.007

Kale Çelik, S., Madenoğlu, S., Sönmez, B., Avağ, K., Türker, U., Çayci, G., et al. (2018). Oxygen isotope discrimination of wheat and its relationship with yield and stomatal conductance under irrigated conditions. *Turk. J. Agric. For.* 42, 22–28. doi: 10.3906/tar-1709-31

Kaur, G., Singh, G., Motavalli, P. P., Nelson, K. A., Orlowski, J. M., and Golden, B. R. (2020). Impacts and management strategies for crop production in waterlogged or flooded soils: A review. *Agron. J.* 112, 1475–1501. doi: 10.1002/agj2.20093

Kehoe, S., Byrne, T., Spink, J., Barth, S., Ng, CYK., and Tracy, S. (2022). A novel 3D X-ray computed tomography (CT) method for spatio-temporal evaluation of waterlogging-induced aerenchyma formation in barley. *Plant Phenome J.* 5 (1), e20035. doi: 10.1002/ppj2.20035

Koyama, T., Murakami, S., Karasawa, T., Ejiri, M., and Shiono, K. (2021). Complete root specimen of plants grown in soil-filled root box: sampling, measuring, and staining method. *Plant Methods* 17, 1-13. doi: 10.1186/s13007-021-00798-3

Lager, I., Andréasson, O., Dunbar, T. L., Andreasson, E., Escobar, M. A., and Rasmusson, A. G. (2010). Changes in external pH rapidly alter plant gene expression and modulate auxin and elicitor responses. *Plant Cell Environ.* 33, 1513–1528. doi: 10.1111/j.1365-3040.2010.02161.x

Langan, P., Bernád, V., Walsh, J., Henchy, J., Khodaeiaminjan, M., Mangina, E., et al. (2022). Phenotyping for waterlogging tolerance in crops: current trends and future prospects. *J. Exp. Bot.* 73, 5149–5169. doi: 10.1093/jxb/erac243

Li, L., Zhang, Q., and Huang, D. (2014). A review of imaging techniques for plant phenotyping. *Sensors* 14, 20078–20111. doi: 10.3390/s141120078

Liu, X., Dong, X., Xue, Q., Leskovar, D. I., Jifon, J., Butnor, J. R., et al. (2017). Ground penetrating radar (GPR) detects fine roots of agricultural crops in the field. *Plant Soil* 423, 517–531. doi: 10.1007/s11104-017-3531-3

Mairhofer, S., Zappala, S., Tracy, S., Sturrock, C., Bennett, M. J., Mooney, S. J., et al. (2013). Recovering complete plant root system architectures from soil via X-ray m-computed tomography. *Plant Methods* 9, 8. doi: 10.1186/1746-4811-9-8

Malik, A. I., Colmer, T. D., Lambers, H., and Schortemeyer, M. (2001). Changes in physiological and morphological traits of roots and shoots of wheat in response to different depths of waterlogging. *Fun. Plant Biol.* 28, 1121–1131. doi: 10.1071/PP01089

Metzner, R., Eggert, A., Van Dusschoten, D., Pflugfelder, D., Gerth, S., Schurr, U., et al. (2015). Direct comparison of MRI and X-ray CT technologies for 3D imaging of root systems in soil: potential and challenges for root trait quantification. *Plant Methods* 11, 17. doi: 10.1186/s13007-015-0060-z

Nagel, K. A., Putz, A., Gilmer, F., Heinz, K., Fischbach, A., Pfeifer, J., et al. (2012). GROWSCREEN-Rhizo is a novel phenotyping robot enabling simultaneous measurements of root and shoot growth for plants grown in soil-filled rhizotrons. *Fun. Plant Biol.* 39, 891–904. doi: 10.1071/FP12023

Nguyen, L. T., Osanai, Y., Anderson, I. C., Bange, M. P., Braunack, M., Tissue, D. T., et al. (2018). Impacts of waterlogging on soil nitrification and ammonia-oxidizing communities in farming system. *Plant Soil* 426, 299–311. doi: 10.1007/s11104-018-3584-y

Paez-Garcia, A., Motes, C., Scheible, W.-R., Chen, R., Blancaflor, E., and Monteros, M. (2015). Root traits and phenotyping strategies for plant improvement. *Plants* 4, 334–355. doi: 10.3390/plants4020334

Pais, I. P., Moreira, R., Semedo, J. N., Ramalho, J. C., Lidon, F. C., Coutinho, J., et al. (2022). Wheat crop under waterlogging: potential soil and plant effects. *Plants* 12, 149. doi: 10.3390/plants12010149

Pang, J., Ross, J., Zhou, M., Mendham, N., and Shabala, S. (2007). Amelioration of detrimental effects of waterlogging by foliar nutrient sprays in barley. *Fun. Plant Biol.* 34, 221–227. doi: 10.1071/FP06158

Pound, M. P., Atkinson, J. A., Townsend, A. J., Wilson, M. H., Griffiths, M., Jackson, A. S., et al. (2017). Deep machine learning provides state-of-the-art performance in image-based plant phenotyping. *Gigascience* 6 (10), gix083. doi: 10.1093/gigascience/gix083

Rellán-Álvarez, R., Lobet, G., Lindner, H., Pradier, P.-L., Sebastian, J., Yee, M.-C., et al. (2015). GLO-Roots: an imaging platform enabling multidimensional characterization of soil-grown root systems. *eLife* 4, e07597. doi: 10.7554/eLife.07597

Reynolds, M., Pask, A., and Mullan, D. (2012). *Physiological Breeding, I: interdisciplinary approaches to improve crop adaptation* (Mexico: CIMMYT).

Roitsch, T., Cabrera-Bosquet, L., Fournier, A., Ghamkhar, K., JimenezBerni, J., Pinto, F., et al. (2019). Review: New sensors and data-driven approaches—A path to next generation phenomics. *Plant Sci.* 282, 2–10. doi: 10.1016/j.plantsci.2019.01.011

Shah, A. N., Iqbal, J., Tanveer, M., Yang, G., Hassan, W., Fahad, S., et al. (2017). Nitrogen fertilization and conservation tillage: a review on growth, yield, and greenhouse gas emissions in cotton. *Environ. Sci. Poll. Res.* 24, 2261–2272. doi: 10.1007/s11356-016-7894-4

Shah, A. N., Javed, T., Singhal, R. K., Shabbir, R., Wang, D., Hussain, S., et al. (2022). Nitrogen use efficiency in cotton: Challenges and opportunities against environmental constraints. *Front. Plant Sci.* 13, 970339. doi: 10.3389/fpls.2022.970339

Shah, A. N., Wu, Y., Iqbal, J., Tanveer, M., Bashir, S., Rahman, S. U., et al. (2021). Nitrogen and plant density effects on growth, yield performance of two different cotton cultivars from different origin. *J. King Saud Uni-Sci.* 33, 101512. doi: 10.1016/j.jksus.2021.101512

Srayeddin, I., and Doussan, C. (2009). Estimation of the spatial variability of root water uptake of maize and sorghum at the field scale by electrical resistivity tomography. *Plant Soil.* 319, 185–207. doi: 10.1007/s11104-008-9860-5

Steffens, D., Hutsch, B. W., Eschholz, T., Losak, T., and Schubert, S. (2005). Water logging may inhibit plant growth primarily by nutrient deficiency rather than nutrient toxicity. *Plant Soil Environ.* 51, 545. doi: 10.17221/3630-PSE

Tovar, J. C., Hoyer, J. S., Lin, A., Tielking, A., Callen, S. T., Castillo, E., et al. (2018). Raspberry Pi-powered imaging for plant phenotyping. *App. Plant Sci.* 6, e1031. doi: 10.1002/aps3.1031

Tracy, S. R., Nagel, K. A., Postma, J. A., Fassbender, H., Wasson, A., and Watt, M. (2020). Crop improvement phenotyping roots: highlights reveal expanding opportunities. *Trends Plant Sci.* 25, 105–118. doi: 10.1016/j.tplants.2019.10.015

Wasson, A., Bischof, L., Zwart, A., and Watt, M. (2016). A portable fluorescence spectroscopy imaging system for automated root phenotyping in soil cores in the field. *J. Exp. Bot.* 67, 1033–1043. doi: 10.1093/jxb/erv570

Wasson, A. P., Nagel, K. A., Tracy, S., and Watt, M. (2020). Beyond digging: non-invasive root and rhizosphere phenotyping. *Trends Plant Sci.* 25, 119–120. doi: 10.1016/j.tplants.2019.10.011

Wasson, A. P., Rebetzke, G. J., Kirkegaard, J. A., Christopher, J., Richards, R. A., and Watt, M. (2014). Soil coring at multiple field environments can directly quantify variation in deep root traits to select wheat genotypes for breeding. *J. Exp. Bot.* 65, 6231–6249. doi: 10.1093/jxb/eru250

Whalley, W. R., Binley, A., Watts, C. W., Shanahan, P., Dodd, I. C., Ober, E. S., et al. (2017). Methods to estimate changes in soil water for phenotyping root activity in the field. *Plant Soil.* 415, 407–422. doi: 10.1007/s11104-016-3161-1

Xia, J.A., Cao, H., Yang, Y., Zhang, W., Wan, Q., Xu, L., et al. (19). Detection of waterlogging stress based on hyperspectral images of oilseed rape leaves (Brassica napus L.). *Com. Electron. Agric.* 59–68. doi: 10.1016/j.compag.2019.02.022

Zhan, A., and Lynch, J. P. (2015). Reduced frequency of lateral root branching improves N capture from low-N soils in maize. *J. Exp. Bot.* 66, 2055–2065. doi: 10.1093/jxb/erv007

Zhou, J., Mou, H., Zhou, J., Ali, M. L., Ye, H., Chen, P., et al. (2021). Qualification of soybean responses to flooding stress using UAV-based imagery and deep learning. *Plant Phenomics* 2021, 1–13. doi: 10.34133/2021/9892570

frontiers | Frontiers in Plant Science

TYPE Original Research
PUBLISHED 15 September 2023
DOI 10.3389/fpls.2023.1250669

OPEN ACCESS

EDITED BY
Shahbaz Khan,
Huazhong Agricultural University, China

REVIEWED BY
Ismail Khan,
Jiangsu University, China
Xiangwei You,
Tobacco Research Institute (CAAS), China
Manan Abdul,
University of Balochistan, Pakistan

*CORRESPONDENCE
Waqar Ahmed
ahmed.waqar1083@yahoo.com
Zhengxiong Zhao
zhaozx0801@163.com

RECEIVED 30 June 2023
ACCEPTED 10 August 2023
PUBLISHED 15 September 2023

CITATION
Yang Y, Ye C, Zhang W, Zhu X, Li H, Yang D, Ahmed W and Zhao Z (2023) Elucidating the impact of biochar with different carbon/nitrogen ratios on soil biochemical properties and rhizosphere bacterial communities of flue-cured tobacco plants.
Front. Plant Sci. 14:1250669.
doi: 10.3389/fpls.2023.1250669

Elucidating the impact of biochar with different carbon/nitrogen ratios on soil biochemical properties and rhizosphere bacterial communities of flue-cured tobacco plants

Yingfen Yang[1], Chenghu Ye[2], Wei Zhang[1], Xiaohong Zhu[1], Haohao Li[3], Dehai Yang[4], Waqar Ahmed[1]* and Zhengxiong Zhao[1]*

[1]Yunnan Agricultural University, Kunming, Yunnan, China, [2]Yunnan Revert Medical and Biotechnology Co., Ltd., Kunming, Yunnan, China, [3]Kunming Branch of Yunnan Tobacco Company, Kunming, Yunnan, China, [4]Hongta Tobacco Group Limited Company, Dali, Yunnan, China

Background and aims: In agriculture, biochar (BC) and nitrogen (N) fertilizers are commonly used for improving soil fertility and crop productivity. However, it remains unclear how different levels of BC and N fertilizer affect soil fertility and crop productivity.

Methods: This study elucidates the impact of different application rates of BC (0, 600, and 1200 kg/ha) and N fertilizer (105 and 126 kg/ha) on biomass accumulation, soil microbial biomass of carbon (SMC) and nitrogen (SMN), and soil biochemical properties, including soil organic carbon (SOC), total nitrogen (TN), soil nitrate nitrogen (NO_3^-–N), ammonium nitrogen (NH_4^+–N), urease (UE), acid phosphatase (ACP), catalase (CAT), and sucrase (SC) of tobacco plants. In addition, a high throughput amplicon sequencing technique was adopted to investigate the effect of different application rates of BC/N on rhizosphere bacterial communities of tobacco plants.

Results: The results confirm that high dosages of BC and N fertilizer (B1200N126) significantly enhance dry matter accumulation by 31.56% and 23.97% compared with control B0N105 and B0N126 under field conditions and 23.94% and 24.52% under pot experiment, respectively. The soil biochemical properties, SMC, and SMN significantly improved under the high application rate of BC and N fertilizer (B1200N126), while it negatively influenced the soil carbon/nitrogen ratio. Analysis of rhizosphere bacteriome through amplicon sequencing of 16S rRNA revealed that the structure, diversity, and composition of rhizosphere bacterial communities dramatically changed under different BC/N ratios. Proteobacteria, Bacteroidetes, Actinobacteria, Firmicutes, and Acidobacteria were highly abundant bacterial phyla in the rhizosphere of tobacco plants under different treatments. Co-occurrence network analysis displayed fewer negative correlations among rhizosphere bacterial communities under high dosages of biochar and nitrogen (B1200N126) than other treatments, which showed less competition for resources among microbes. In

addition, a redundancy analysis further proved a significant positive correlation among SMC, SMN, soil biochemical properties, and high dosage of biochar and nitrogen (B1200N126).

Conclusions: Thus, we conclude that a high dosage of BC (1200 kg/ha) under a high application rate of N fertilizer (126 kg/ha) enhances the biomass accumulation of tobacco plants by improving the soil biochemical properties and activities of rhizosphere bacterial communities.

KEYWORDS

biochar, soil biochemical properties, nitrogen fertilizer, rhizosphere bacterial communities, biomass accumulation

1 Introduction

Biochar, which is produced through the incomplete combustion or geothermal carbonization of diverse biomass, such as animal manures, sewage sludge, and woody biomass, has beneficial impact on plant growth, soil enrichment, and climate change (Chen et al., 2021). Generally, pyrolysis and hydrothermal carbonization (HTC) techniques are used for biochar production. Pyrolysis is a conventional process which thermally transforms biomass into a solid product (pyrochar) under anaerobic conditions and at moderate temperature (350-700°C) (Akhtar et al., 2018; Li et al., 2022). HTC, however, transforms biomass into a solid product (hydrochar) utilizing water as the reaction medium at considerably gentler temperature (130-250°C) and self-generated pressure (2-6 MPa) (Qin et al., 2017). The various HTC and pyrolysis processes endow hydrochar and pyrochar with distinct properties (e.g., surface area, element content, and surface functionalization). For example, biochar contains a huge quantity of micro-/macro-nutrients and carbon contents (70–80%) and a large surface area, while hydrochar contains higher oxygen contents (Liu et al., 2010; Ronsse et al., 2013; Wiedner et al., 2013).

In recent years, biochar application has been gaining much attention of researchers due to its potential role in waste mitigation, lessening of greenhouse gas emissions, carbon sequestration, ecological restoration, soil amendment, and disease suppression (Lehmann and Joseph, 2015; Li et al., 2022; Wang et al., 2022). Soil amendments with biochar increase soil fertility and crop productivity under different agroecosystems by improving soil organic matter contents, nutrient retention, acquisition ability, and plant growth despite repeated cultivations (Pandey et al., 2016; Khan et al., 2021a). Various agricultural waste materials are used to produce diverse types of biochar that modulate soil health and physicochemical properties (Streubel et al., 2011). For example, regarding improvement in soil nutrients, cedar leaf biochar was shown to be superior to sawdust biochar but reduced the soil's total carbon contents (Hu et al., 2019). However, a high dosage of biochar negatively influences soil fertility, plant growth and yield, short-term reduction in the availability of soil mineral nutrients, and soil microbial activities (Tammeorg et al., 2014; Khan et al., 2022).

Thus, an appropriate biochar application rate is essential for increase crop yield, soil fertility, and soil adsorption capacity (Peng et al., 2021). For instance, it is reported that biochar application at a certain range (1–4%) improves soil fertility, nutrient uptake ability of plants, and crop yield. While application of biochar >5% reduces soil fertility and inhibits plant growth (Pokovai et al., 2020; Zheng et al., 2020). Excessive biochar applications (more than 12 t ha^{-1}) negatively influenced chlorophyll contents, the photosynthesis rate of maize crops, and soil total nitrogen contents (Khan et al., 2023). Furthermore, the application of biochar improves the systemic resistance of plants against a variety of plant pathogens, such as in strawberries, against *Colletotrichum acutatum* and *Botrytis cinerea* (Meller Harel et al., 2012) and in tobacco, against *Ralstonia solanacearum*, the causative agent of tobacco bacterial wilt (Li et al., 2022). However, the efficacy of biochar in disease suppression is varied according to biochar type, dosage, nature of phytopathogen, and host (Graber et al., 2014; De Tender et al., 2016).

The plant rhizosphere is one of the most intricate ecosystems on the planet and a hotspot habitat for various microorganisms (Raaijmakers, 2015). The addition of biochar has a substantial effect on the diversity and structure of rhizosphere microorganisms (Chen et al., 2013), such as *Pseudomonas*, *Bacillus*, and *Lysobacter* Spp., which play a vital role in the decomposition of organic matter, nutrients cycle, maintaining soil carbon/nitrogen (C/N) ratio, nitrogen fixation, and mineralization of soil nutrients (Fuke et al., 2021). Thus, the effectiveness of rhizosphere microbial diversity and soil nutrients are the key factors for healthy plant growth (Ren et al., 2022). Previous studies have reported that soil amendment with biochar can change the soil physicochemical properties and structure and the composition of rhizosphere microbial communities (Prayogo et al., 2014; Xu et al., 2014). Therefore, it is suggested that applying biochar at a specific range is essential for improving soil health, diversity of rhizosphere microbial community, and metabolic activities of rhizospheric microorganisms (Ren et al., 2022).

For instance, the soil C/N ratio and microbial biomass carbon significantly increased under biochar dose < 40 t/hm^2, while application of biochar > 40 t/hm^2 decreased the functional diversity, metabolic activity, and richness indexes of rhizosphere microorganisms (Zhou and Chen-yang, 2019). Nitrogen (N) is a critical macronutrient for plant growth, development, and high yield (Song et al., 2022). The unnecessary use of N fertilizers limits economic benefits and cause environmental hazards, such as water contamination, air pollution, and soil acidification (Xia et al., 2020). It has been reported that soil amendment with biochar improves plants' nitrogen use efficiency and reduced nitrogen loss, thus enhanced plant growth and yield (Seyedghasemi et al., 2021; Wang et al., 2023). Therefore, the combined application of biochar and N fertilizer is recommended to mitigate the environmental hazards caused by N fertilizer and to improve plants' nitrogen use efficiency (Xia et al., 2022). However, the impact of the high application rate of biochar and N fertilizer on crop productivity, soil biochemical properties, and rhizosphere bacterial communities remains unclear.

Tobacco is an important industrial crop in China, broadly cultivated in the south-central regions of China (Ahmed et al., 2022). Thus, farmers use a massive volume of N fertilizers yearly to obtain a high yield of flue-cured tobacco leaves. In addition, tobacco stems that comprise 25–30% of the weight of the tobacco leaves are left over after leaf collection. Nowadays, burning tobacco stems is the most common approach, which causes environmental pollution and wastage of natural resources. In this study, tobacco stem biochar was used as a soil amendment in pot and field experiments to develop a system for the better utilization of natural resources. The objective of this study is to address several important questions regarding the optimal use of biochar and N fertilizer in tobacco crops. Specifically, the study aims to investigate how various combinations of biochar and N fertilizer influence soil biochemical properties, biomass accumulation, and rhizosphere bacterial communities of tobacco plants. We hypothesized that different application rates of C/N ratio would have a distinct influence on soil enzymatic activities, soil nutrients, and rhizosphere bacterial community compared with non-treated, which may affect tobacco plants' growth and biomass accumulation. Overall, this study provides experimental-based knowledge to better utilize agricultural resources for the high-yield and quality production of tobacco leaves.

2 Materials and methods

2.1 Experimental site and material description

Pot and field experiments were conducted during the two growing seasons from April to September in 2021 and April to September in 2022 in Kunming City (25° 02′ 11″ N, 102° 42′ 31″ E) and Malong County, Qujing City (25° 29′ 27.6″ N, 103° 47′ 45.6″ E) Yunnan Province, China, respectively. The greenhouse conditions were maintained at a 28°C day temperature and a 22°C night temperature, with 14 h light and 10 h dark photoperiods. At the field conditions, the climatic conditions were recorded as follows: annual rainfall of 927.1 mm, average yearly temperature of 14.3°C, and 2158 sunshine hours per year with an average of 234 frost-free days. Tobacco stem biochar was used as a soil amendment, prepared by pyrolysis at 450°C from Kunming Canghui Co. Ltd. Yunnan, China, and passed through a 3 mm sieve before application. The basic physicochemical properties of biochar and soil used in these experiments are listed in Tables S1, S2.

2.2 Pot experiment

The pot experiment was conducted using the flue-cured tobacco cultivar "Yun87" in the greenhouse from April to September 2021 in Kunming City, Yunnan. The experiment was performed under different carbon/nitrogen (C/N) ratios according to 0, 600, and 1200 kg/ha biochar and 0, 105, and 126 kg/ha pure nitrogen. The experiment was performed under six different treatments as follows: 0 g/pot of biochar + 7 g/pot of pure nitrogen (B0N105), 40 g/pot of biochar + 7 g/pot of pure nitrogen (B600N105), 80 g/pot of biochar + 7 g/pot of pure nitrogen (B1200N105), 0 g/pot of biochar + 8.4 g/pot of pure nitrogen (B0N126), 40 g/pot of biochar + 8.4 g/pot of pure nitrogen (B600N126), and 80 g/pot of biochar + 8.4 g/pot of pure nitrogen (B1200N126). Seedlings (50 days old) of tobacco cultivar "Yun87" were transferred into pots (40 × 37 cm) comprising 20 kg of paddy soil and biochar dosage and irrigated three times a week (1000 mL/pot). To overcome the nutrient shortage, fertilizer was applied as a base and top fertilizer (70:30) in the form of tobacco-specific compound fertilizer (N: P_2O_5: K_2O = 10: 10: 20) as a 1:1:3 ratio (Cai et al., 2021). Whole biochar and 70% of the base fertilizer were applied before transplanting the seedlings, while 30% of the top fertilizer was applied at 25 days of post-transplantation. The experiment was performed three times using 180 plants (30 plants per treatment and 10 plants per replicate) under a complete block design.

2.3 Field experiment

The field experiment was conducted using the flue-cured tobacco cultivar "Yun121" from April to September 2022 in Qujing City, Yunnan. Tobacco field preparations such as ridge raising, biochar amendment, and farm fertilizer applications were conducted in April 2022. The experiment was conducted under different C/N ratios of 0, 600, and 1200 kg/ha biochar and 105 and 126 kg/ha pure nitrogen. Tobacco-specific compound fertilizer (N: P_2O_5: K_2O) was used as a 1:1:3 ratio in the form of base and top fertilizer (70:30) (Cai et al., 2021). After the ridge preparations, holes were made on the ridges with plant × plant (60×60 cm) and row × row (120×120 cm) distance, and whole biochar and 70% of the base fertilizer were applied in the holes and mixed thoroughly with the soil. Tobacco seedlings (50 days old) of the cultivar "Yun121" were transplanted on the ridges in the holes and the experiment was executed under six different conditions as follows: 0 kg/ha of biochar + 105 kg/ha of pure nitrogen (B0N105), 600 kg/ha of biochar + 105 kg/ha of pure nitrogen (B600N105), 1200 kg/ha of biochar + 105 kg/ha of pure nitrogen (B1200N105), 0 kg/ha of biochar

+ 126 kg/ha of pure nitrogen (B0N126), 600 kg/ha of biochar + 126 kg/ha of pure nitrogen (B600N126), and 1200 kg/ha of biochar + 126 kg/ha of pure nitrogen (B1200N126). The remaining 30% of the top fertilizer was applied with irrigation water at 25 days of post-transplantation. The integrated field management approaches were adopted according to China's National Standards of the Tobacco Industry (Cai et al., 2021). The experiment was repeated three times under a randomized complete block design with 18 plots (3 plots per treatment), each containing 80 tobacco plants.

2.4 Samples collection and analysis of different indexes

To assess biomass accumulation in different plant parts (leaf, stem, and root) and soil biochemical properties, tobacco plant and soil samples were collected in replicates from pot and field experiments under different treatments after 85 (at the early baking stage) days post-transplantation. Briefly, three cores of plant and soil samples from the pot experiment/replicate and five cores from the field experiment/plot were taken and mixed thoroughly to make one composite sample per replication.

2.4.1 Assessment of soil biochemical properties

Bulk soil samples were collected at a depth of 10-20 cm with a shovel (5 cm in diameter) by following the zig-zag sampling method and sieved through a 2-mm mesh and air-dried naturally to analyze soil physicochemical properties and enzymatic activity. The contents of soil organic carbon (SOC; g/kg) and total nitrogen (TN; g/kg) were determined by using the $K_2Cr_2O_7$ oxidation external heating method and elemental analyzer (Elementar Analysensysteme GmbH, Germany), respectively (Khan et al., 2021b). Soil nitrate-nitrogen (NO_3^-–N; mg/kg) and ammonium nitrogen (NH_4^+–N; mg/kg) were extracted with indophenol-blue colorimetric and 1 M KCl methods, and their concentrations were measured at OD_{275} and OD_{220} nm using a spectrophotometer (UV-6000, China), respectively (Singh and Mavi, 2018). The chloroform fumigation method was used to determine the amount of soil microbial biomass of carbon (SMC) and soil microbial biomass of nitrogen (SMN). The activity of soil urease (S-UE) was determined by the indophenol blue colorimetric method. Whereas the activities of soil acid phosphatase (S-ACP), soil catalase (S-CAT), and soil sucrase (S-SC) were determined by the colorimetric method (Guan et al., 2022).

2.4.2 Determination of biomass accumulation

The biomass accumulation in different parts of tobacco plants was determined through incubation (Li et al., 2022). Tobacco plant parts, including leaf, stem, and root, were incubated for 30 min at 105 °C and immediately dried for 48 h at 80 °C. The biomass accumulation in each part (leaf, stem, and root) was recorded to calculate whole plant biomass accumulation (g/plant).

Whole plant biomass accumulation (g/plant) = Σ (biomass accumulation in leaves + stems + roots)

2.5 Investigation of rhizosphere bacterial community composition

2.5.1 Rhizosphere soil samples collection and DNA extraction

In total, 18 rhizosphere soil samples (three samples/treatment) were collected to analyze rhizosphere bacterial community composition from the flue-cured tobacco plants at 85 days of post-transplantation from the field experiment, as described by Zhang et al. (2022). Five plants/plot from each treatment were uprooted, and soil particles attached to the root surface were collected using a brush and mixed to make one composite sample. According to the manufacturer's instructions, 0.5 g of soil per sample was used to extract soil DNA using HiPure® Soil DNA Kits (Magen, Guangzhou, China). The extracted DNA was stored at −80°C to analyze rhizosphere bacterial community composition and diversity.

2.5.2 PCR amplification and library preparation

The V3-V4 region of the 16S gene of bacteria was amplified using primer pair 341F (5′- CCTAYGGGRBGCASCAG -3′) and 806R (5′- GGACTACNNGGGTATCTAAT-3′) (Ahmed et al., 2022) and sequenced on an Illumina MiSeq platform at Genedenovo Biotechnology Co., Ltd (Guangzhou, China). Raw data obtained from 16S *rRNA* amplicon sequencing were processed through Trimmomatic software (Version 0.33) and UCHIME (Version 8.1) for quality control (score < 20) and Chimera's removal, respectively, to generate clean reads (Edgar et al., 2011; Bolger et al., 2014). The obtained clean reads were clustered into operational taxonomic units (OTUs) at a 97% similarity level using the UPARSE pipeline (Edgar, 2013). The taxonomic annotation of bacterial OTUs was done at a 70% threshold level using the SILVA database (Quast et al., 2012).

2.5.3 Bioinformatics analysis

Quantitative insights in the microbial ecology pipeline (QIIME 2) were used to compute alpha diversity metrics and beta diversity based on Bray–Curti's dissimilarity matrix for bacterial communities. The results of alpha and beta diversity metrics were visualized by boxplots and principal coordinate analysis (PCoA) using the R packages "ggplot2" and "Vegan", respectively (Ahmed et al., 2022). Permutational multivariate analysis of variance (PERMANOVA) was performed according to "Adonis" using the vegan package in R (v.4.2.1). The interaction between common and unique OTUs within a group was visualized by "UpSet plots" in the UpSetR package in R (v.4.2.1). A Venn diagram was used to calculate the common and unique OTUs among the treatments and the result was visualized by "ggplot2" in R (v.4.2.1). The relative abundance (RA) of most abundant bacterial phylum, and genus was determined based on the OTU classified reads and plotted using R scripts in R package "ggplot2". Redundancy analysis (RDA) was performed in the "Vegan package" in R (v.4.2.1) under different application rates of C/N ratio to confirm the relationship between rhizosphere bacterial communities, soil physicochemical properties

and enzymatic activities, SMC, and SMN. Network analysis was performed at the phylum level within phylum ($p < 0.05$ and correlation coefficient > 0.9) using the "sparcc package" and visualized by the "psych package" in R (v.4.2.1).

2.6 Statistical analysis

The analysis of variance (ANOVA) in IBM SPSS V.20.0 (SPSS Inc., USA) was used to statistically assess the data about soil physicochemical parameters, enzymatic activities, biomass accumulation, and bacterial diversity in the rhizosphere. The results are shown as the standard error of means (± SEM), and the least significant difference (LSD) test was performed to identify differences among groups and was considered significant at $p < 0.05$. All figures were processed and combined using Adobe Illustrator 2019.

3 Results

3.1 Impact of varying C/N ratios on contents of SOC, TN, C/N ratio, NO_3^-–N, and NH_4^+–N

The levels of soil organic carbon (SOC), total nitrogen (TN), carbon/nitrogen (C/N) ratio, and nitrate nitrogen (NO_3^-–N) of flue-cured tobacco plants significantly changed (LSD; $p < 0.05$) with the increased application rate of biochar (0, 600, and 1200 kg/ha) under two nitrogen levels (105 and 126 kg/ha) in pot and field experiments, while no significant difference (LSD; $p > 0.05$) was observed for the contents of ammonium nitrogen (NH_4^+–N) among the treatments (Table 1). The level of SOC increased with the increased application rates of the C/N ratio in both the pot and field experiments. The contents of SOC were found to be significantly higher under treatment B1200N105 (30.04 g/kg) and B1200N126 (29.11 g/kg) in the pot experiment and under treatments B1200N105 (24.07 g/kg) and B1200N126 (23.57 g/kg) in the field experiment compared with B0N105 and B0N126 treatments and increased by 63.53%, 62.72%, 68.44%, and 69.32%, respectively (LSD, $p < 0.05$; Table 1). The contents of soil TN increased with the increased application rate of carbon and nitrogen and were found to be significantly higher under treatment B1200N126 (2.43 and 1.58 g/kg) in both the pot and field experiments, respectively, compared to other treatments (LSD, $p < 0.05$; Table 1). In both experiments (pot and field), the soil C/N ratio of flue-cured tobacco plants increased with the increased biochar and nitrogen fertilizer application rate. However, the soil C/N ratio of flue-cured tobacco plants was found to be significantly higher under treatment B1200N105 in the pot (13.39) and field (17.44) experiments compared with other treatments (LSD, $p < 0.05$; Table 1). In both experiments (pot and field), contents of NO_3^-–N first increased then decreased with the increased application rate of biochar under 105 kg/ha application of nitrogen fertilizer and were found to be significantly higher under treatment B600N105 (29.82 and 18.27 mg/kg) than B0N105 (LSD, $p < 0.05$; Table 1). Whereas, under 126 kg/ha application of nitrogen fertilizer, the level of NO_3^-–N increased with the increased application rate of biochar and was observed to be significantly higher under treatment B1200N126 (29.82 and 18.37 mg/kg) compared to B0N126, in both the pot and field experiments, respectively (LSD, $p < 0.05$; Table 1). These results suggested that the contents of NO_3^-–N

TABLE 1 Effects of various combinations of biochar and nitrogen fertilizer on contents of soil organic carbon (SOC), total nitrogen (TN), carbon/nitrogen ratio (C/N), soil nitrate nitrogen (NO_3^-–N), and ammonium nitrogen (NH_4^+–N) of tobacco soil.

Experimental site	Treatments	SOC(g/kg)	TN(g/kg)	C/N	NO_3^--N(mg/kg)	NH_4^+-N(mg/kg)
Pot experiment	B0N105	18.37 ± 0.09d	2.04 ± 0.04d	9.02 ± 0.15e	19.78 ± 1.00c	12.67 ± 1.72a
	B600N105	22.63 ± 0.55c	2.25 ± 0.04c	10.08 ± 0.34c	29.82 ± 1.45a	13.59 ± 0.9a
	B1200N105	30.04 ± 0.26a	2.24 ± 0.02c	13.39 ± 0.05a	22.46 ± 1.19b	14.05 ± 0.82a
	B0N126	17.89 ± 0.59d	2.06 ± 0.03d	8.69 ± 0.39e	20.66 ± 1.38bc	13.23 ± 0.67a
	B600N126	22.46 ± 0.45c	2.35 ± 0.01b	9.57 ± 0.15d	31.46 ± 0.97a	13.29 ± 0.74a
	B1200N126	29.11 ± 0.31b	2.43 ± 0.03a	12 ± 0.17b	29.82 ± 1.03a	13.22 ± 0.81a
Field experiment	B0N105	14.29 ± 0.23d	1.24 ± 0.03c	11.52 ± 0.24e	12.66 ± 0.34c	2.79 ± 0.05a
	B600N105	18.8 ± 0.68c	1.35 ± 0.02b	13.93 ± 0.71c	18.27 ± 0.34a	2.75 ± 0.03a
	B1200N105	24.07 ± 0.63a	1.38 ± 0.04b	17.44 ± 0.23a	11.37 ± 0.54d	2.73 ± 0.05a
	B0N126	13.92 ± 0.15d	1.3 ± 0.03d	10.71 ± 0.11f	13.22 ± 0.6c	2.77 ± 0.03a
	B600N126	20.75 ± 0.5b	1.57 ± 0.02a	13.25 ± 0.45d	16.87 ± 0.53b	2.75 ± 0.04a
	B1200N126	23.57 ± 0.34a	1.58 ± 0.04a	14.88 ± 0.13b	18.37 ± 0.26a	2.74 ± 0.03a

B0, B600, and B1200 represent 0, 600, and 1800 kg/ha biochar application rates, respectively. N105 and N126 represent 105 and 126 kg/ha application rates of pure nitrogen, respectively. The significant difference among treatments after specific days of post-transplantation is shown by different lowercase letters within a column according to the least significant difference test (LSD; $p < 0.05$).

decreased under the high application rate of biochar and low nitrogen level but increased with the increased application rate of biochar and nitrogen fertilizer.

3.2 Effect of different C/N ratios on SMC, SMN, and SMC/SMN ratios

The application of biochar (0, 600, and 1200 kg/ha) under two different levels (105 and 126 kg/ha) of nitrogen fertilizer had a significant impact on the contents of SMC, SMN, and SMC/SMN ratio (LSD, $p < 0.05$; Table 2). In both experiments (pot and field), the SMC and SMN first increased and then decreased with the increased application rate of biochar under 105 kg/ha application of nitrogen fertilizer but increased with the increased application rate of biochar under 126 kg/ha application of nitrogen fertilizer. The SMC (140.87 and 128.15 mg/kg) and SMN (18.67 and 14.57 mg/kg) were found significantly higher under treatment B1200N126 compared with B0N105 and B0N126, in both the pot and field experiments, respectively (LSD, $p < 0.05$; Table 2). The SMC under treatment B1200N126 increased by 61.92% and 70.38% in the pot experiment and increased by 78.93% and 75.40% in the field experiment compared with B0N105 and B0N126, respectively. The SMC/SMN ratio of flue-cured tobacco plants was found to be significantly higher under treatment B1200N105 (8.38 and 9.35) compared with B0N105 and B0N126, in both the pot and field experiments, respectively (LSD, $p < 0.05$; Table 2). The SMC/SMN ratio of flue-cured tobacco plants decreased under treatment B1200N126 with the increased biochar and nitrogen fertilizer application rate compared with B1200N105 (LSD, $p > 0.05$; Table 2).

3.3 Influence of different C/N ratios on soil enzymatic activities

Soil enzymatic activities, including S-UE, S-SC, S-CAT, and S-ACP, significantly changed under the different C/N ratios in both the pot and field experiments (LSD, $p < 0.05$; Table 3). In both the pot and field experiments, the activities of S-UE, S-SC, S-CAT, and S-ACP first increased and then decreased with the increased biochar application rate under 105 kg/ha of nitrogen fertilizer. However, soil enzymatic activities increased with the increased biochar application rate under 126 kg/ha application of nitrogen fertilizer (Table 3). The activities of S-UE, S-SC, and S-CAT were found to be significantly higher under treatment B1200N126 than B0N105 and B0N126 in both experiments (LSD, $p < 0.05$; Table 3), except for S-CAT in the field experiment in which no significant difference was observed among the treatments (LSD, $p > 0.05$; Table 3). The activity of S-UE, S-SC, and S-CAT under treatment B1200N126 were increased by 53.33%, 64.82%, and 20.79%, respectively, compared with B0N105 and increased by 43.75%, 58.83%, and 22.54%, respectively, compared with B0N126 in the pot experiment. In the field experiment, the activity of S-UE and S-SC under treatment B1200N126 were increased by 86.44% and 53.37%, respectively, relative to B0N105 and increased by 77.41% and 41.51%, respectively, compared to B0N126. The activity of S-ACP was found to be significantly higher under treatment B1200N126 compared with B0N105 and B0N126 in pot and field experiments (LSD, $p < 0.05$; Table 3). The activity of S-ACP under treatment B1200N126 was increased by 42.05%, 132.25%, and 36.94%, 60% as compared with B0N105 and B0N126 in pot and field experiments, respectively.

TABLE 2 Effects of different biochar and nitrogen fertilizer ratios on contents of soil microbial biomass of carbon (SMC), soil microbial biomass of nitrogen (SMN), and SMC/SMN ratio of tobacco soil.

Experimental site	Treatments	SMC (mg/kg)	SMN (mg/kg)	SMC/SMN
Pot experiment	B0N105	87.00 ± 9.95c	13.63 ± 0.47b	6.40 ± 0.87c
	B600N105	126.46 ± 3.15b	17.70 ± 0.60d	7.15 ± 0.39b
	B1200N105	117.26 ± 1.08b	14.00 ± 0.33c	8.38 ± 0.27a
	B0N126	82.68 ± 3.83c	15.04 ± 0.49c	5.51 ± 0.44c
	B600N126	138.74 ± 6.09a	18.91 ± 0.83a	7.35 ± 0.56b
	B1200N126	140.87 ± 9.48a	18.67 ± 0.21a	7.54 ± 0.45ab
Field experiment	B0N105	71.62 ± 6.42d	9.72 ± 0.86c	7.37 ± 0.23c
	B600N105	109.61 ± 2.48b	13.15 ± 0.34b	8.34 ± 0.27b
	B1200N105	92.14 ± 3.68c	9.86 ± 0.32c	9.35 ± 0.26a
	B0N126	73.06 ± 4.07d	10.23 ± 0.55c	7.15 ± 0.49c
	B600N126	126.18 ± 4.14a	14.46 ± 0.28a	8.73 ± 0.13b
	B1200N126	128.15 ± 3.95a	14.57 ± 0.47a	8.79 ± 0.09b

B0, B600, and B1200 represent 0, 600, and 1800 kg/ha biochar application rates, respectively. N105 and N126 represent 105 and 126 kg/ha application rates of pure nitrogen, respectively. The significant difference among treatments after specific days of post-transplantation is shown by different lowercase letters within a column according to the least significant difference test (LSD; $p < 0.05$).

10.3389/fpls.2023.1250669

TABLE 3 Impact of various combinations of biochar and nitrogen fertilizer on soil enzymatic activities.

Experimental site	Treatments	S-UE [mg/(d·g)]	S-ACP [umol/(d·g)]	S-CAT [umol/(min·g)]	S-SC [mg/(d·g)]
Pot experiment	B0N105	0.90 ± 0.03c	1.07 ± 0.04c	14.00 ± 0.68c	7.42 ± 0.47d
	B600N105	1.16 ± 0.04b	1.50 ± 0.04a	15.59 ± 0.72b	10.33 ± 0.47c
	B1200N105	0.88 ± 0.04c	1.28 ± 0.05b	12.02 ± 0.75d	5.85 ± 0.46e
	B0N126	0.96 ± 0.05c	1.11 ± 0.02c	13.80 ± 0.21c	7.70 ± 0.55d
	B600N126	1.23 ± 0.06b	1.54 ± 0.05a	16.78 ± 0.43a	11.10 ± 0.13b
	B1200N126	1.38 ± 0.08a	1.52 ± 0.06a	16.91 ± 0.51a	12.23 ± 0.34a
Field experiment	B0N105	0.59 ± 0.03d	0.31 ± 0.06c	11.56 ± 0.31a	4.89 ± 0.38b
	B600N105	0.82 ± 0.04c	0.67 ± 0.01a	11.90 ± 0.73a	7.64 ± 0.57a
	B1200N105	0.64 ± 0.05d	0.44 ± 0.05b	11.66 ± 0.32a	3.44 ± 0.20c
	B0N126	0.62 ± 0.04d	0.45 ± 0.03b	11.89 ± 0.48a	5.30 ± 0.81b
	B600N126	0.94 ± 0.02b	0.70 ± 0.07a	12.15 ± 0.36a	7.32 ± 0.31a
	B1200N126	1.10 ± 0.03a	0.72 ± 0.09a	11.96 ± 0.79a	7.50 ± 0.48a

Urease (UE), Acid phosphatase (ACP), Catalase (CAT), and Sucrase (SC). B0, B600, and B1200 represent 0, 600, and 1800 kg/ha biochar application rates, respectively. N105 and N126 represent 105 and 126 kg/ha application rates of pure nitrogen, respectively. The significant difference among treatments after specific days of post-transplantation is shown by different lowercase letters within a column according to the least significant difference test (LSD; $p < 0.05$).

3.4 Dry matter accumulation under different application rates of C/N ratio

The effect of different C/N ratios on the accumulation of dry matter in the whole and various parts (root, stem, and leaf) of tobacco plants was assessed in both experiments (Table 4). In both the pot and field experiments, the dry matter accumulation (g/plant) in whole and different parts (root, stem, and leaf) of flue-cured tobacco plants under 105 kg/ha of nitrogen fertilizer first increased and then decreased with the increased biochar application rate. While under 126 kg/ha application of nitrogen fertilizer, dry matter accumulation (g/plant) of flue-cured tobacco plants increased with the increased biochar application rate (Table 4). The accumulation of dry matter in the whole plant and different parts (root, stem, and leaf) of flue-cured tobacco plants was found to be significantly higher under treatment B1200N126 compared with B0N105 and B0N126 in the pot and field experiments (LSD, $p < 0.05$; Table 4). The whole plant dry matter accumulation under treatment B1200N126 was increased by 23.94% and 24.53% in the pot experiment and 31.57% and 23.97% in the field experiment, compared with B0N105 and B0N126. The accumulation of dry matter in different parts, such as the root, stem, and leaf, under

TABLE 4 Effects of different application ratios biochar and nitrogen fertilizer on dry matter accumulation and distribution of tobacco plants.

Experimental site	Treatments	Dry matter accumulation(g/plant)	Dry matter accumulation (g/plant)			Dry matter distribution ratio (%)		
			Root	Stem	Leaf	Root	Stem	Leaf
Pot experiment	B0N105	104.26 ± 1.67c	17.91 ± 0.74c	34.73 ± 0.37c	51.62 ± 1.05c	17.18 ± 0.43a	33.32 ± 0.68a	49.50 ± 0.40a
	B600N105	117.22 ± 1.00b	21.31 ± 1.56b	38.32 ± 0.61b	57.59 ± 1.21b	18.18 ± 1.31a	32.69 ± 0.66a	49.13 ± 0.83a
	B1200N105	101.04 ± 2.14c	18.92 ± 0.84c	34.54 ± 0.87c	47.58 ± 1.06c	18.73 ± 0.71a	34.18 ± 0.58a	47.09 ± 0.15b
	B0N126	103.77 ± 2.03c	18.01 ± 0.07c	34.40 ± 1.20c	51.36 ± 1.23c	17.36 ± 0.39a	33.14 ± 0.68a	49.49 ± 0.63a
	B600N126	129.02 ± 6.92a	22.65 ± 1.48ab	42.55 ± 1.40a	63.82 ± 3.41a	17.58 ± 1.20a	33.01 ± 1.26a	49.41 ± 1.59a
	B1200N126	129.22 ± 5.91a	23.63 ± 0.99a	41.73 ± 1.07a	63.85 ± 3.49a	18.27 ± 0.76a	32.33 ± 1.34a	49.40 ± 0.59a
Field experiment	B0N105	451.25 ± 23.65d	44.91 ± 3.77d	123.02 ± 12.15b	283.32 ± 11.30cd	9.94 ± 0.41c	27.23 ± 1.47bc	62.83 ± 1.88a
	B600N105	511.66 ± 17.17b	59.06 ± 6.48b	130.43 ± 10.16b	322.17 ± 2.13b	11.53 ± 0.95ab	25.47 ± 1.23c	63.01 ± 1.71a
	B1200N105	458.47 ± 2.78cd	55.99 ± 1.76c	131.64 ± 6.21b	270.84 ± 6.47d	12.21 ± 0.33a	29.22 ± 1.43ab	60.12 ± 1.35b
	B0N126	478.89 ± 8.04c	48.45 ± 2.34b	135.38 ± 1.04b	295.06 ± 6.85c	10.11 ± 0.37c	28.28 ± 0.58ab	61.61 ± 0.57a
	B600N126	590.80 ± 6.32a	66.40 ± 3.00a	180.80 ± 5.11a	343.61 ± 8.06a	11.24 ± 0.40b	30.61 ± 1.06a	58.16 ± 1.00b
	B1200N126	593.69 ± 9.14a	66.43 ± 0.56a	178.29 ± 4.65a	348.96 ± 9.05a	11.19 ± 0.26b	30.03 ± 0.76a	58.77 ± 0.82b

B0, B600, and B1200 represent 0, 600, and 1800 kg/ha biochar application rates, respectively. N105 and N126 represent 105 and 126 kg/ha application rates of pure nitrogen, respectively. The significant difference among treatments after specific days of post-transplantation is shown by different lowercase letters within a column according to the least significant difference test (LSD; $p < 0.05$).

treatment B1200N126 was increased by 31.94%, 20.16% and 23.69%, respectively, compared with B0N105, and 31.20%, 21.31%, and 24.32%, respectively, compared with B0N126 in the pot experiment. However, in the field experiment, the accumulation of dry matter in different parts (root, stem, and leaf) under treatment B1200N126 increased by 47.91%, 44.93%, and 23.17%, respectively, compared to B0N105, and 37.11%, 31.70%, and 18.26%, respectively, compared with B0N126. This suggests that the accumulation of dry matter in whole and different parts (root, stem, and leaf) of flue-cured tobacco plants increases under high application of nitrogen fertilizer (126 kg/ha) and biochar (1200 kg/ha), while it decreased under the excessive application of biochar (≧1200 kg/ha) and low nitrogen levels (105 kg/ha).

3.5 Effect of different C/N ratios on bacterial community assembly of tobacco plants

A total of 18 rhizosphere samples from six different treatments (three biological replicates per treatment) were processed on an Illumina MiSeq platform for high-throughput amplicons sequencing of the 16S *rRNA* V3-V4 variable region of bacteria. The amplicons sequencing resulted in a total of 2,235,225 raw reads, with an average of 124,179 reads per sample (Table S3). After Chimera's removal and quality control, 1,936,376 effective reads (107,576 reads per sample) were obtained with an average length of 461 bp/sample (Table S3). These effective reads were clustered into 55,469 OTUs, averaging 3,082 OTUs per sample (Table S3).

3.6 Bacterial community diversity, structure, and OTUs distribution under different application rates of C/N ratio

Firstly the alpha diversity indices and beta diversity of bacterial communities were calculated under different application rates of C/N ratio (Figure 1). The alpha diversity indices (Shannon, Simpson, Pielou, and Chao1) of bacterial communities were significantly changed under different application rates of C/N ratio (Figure 1 and Table S4). Shannon and Pielou indexes had substantially higher values under treatments B0N126 and B1200N126 compared with B0N125, B600N126, B1200N125, and B600N126 (LSD, $p < 0.05$; Figure 1A). Compared to B0N125, B600N125, and B600N126, treatments B1200N125, B0N126, and B1200N126 had significantly higher Simpson index values (LSD, $p < 0.05$), while no significant difference was observed among B1200N125, B0N126, and B1200N126 (LSD, $p > 0.05$; Figure 1A). The values of the Chao 1 index were increased significantly under treatments B0N126 and B1200N126 compared to B0N125 and B600N125 (LSD, $p < 0.05$), whereas no significant difference was found compared to B1200N125 and B600N126 (LSD, $p > 0.05$; Figure 1A). Bray–Curti's dissimilarity matrix was used to calculate the variations in the structure of bacterial communities (beta diversity) under treatments, and results were visualized by PCoA. PCoA results showed a clear separation among the treatments, where PCoA-1 and PCoA-2 showed a total of 33.01% and 24.65% variations in the structure of bacterial community (Figure 1B). Furthermore, PERMANOVA analysis based on pairwise interactions between bacterial communities demonstrated that the overall structure of rhizosphere bacterial communities significantly changed under different treatments ($R^2 = 0.7296$, $p = 0.001$, Table S5).

An OTUs distribution analysis confirmed the shared and unique OTUs among the treatments (Figure 2). UpSet plots displayed the interaction between shared and unique OTUs at different application rates of biochar (0, 600, and 1200 kg/ha) under two levels of nitrogen fertilizer 105 kg/ha (Figure 2A) and 126 kg/ha (Figure 2B). According to the results of UpSet plots, a significant difference was observed for shared and unique OTUs among the treatments under different application rates of biochar (0, 600, and 1200 kg/ha) at the same level of nitrogen fertilizer (105 and 126 kg/ha). The maximum number of unique OTUs was recorded under treatments B1200N105 (685 OTUs) and B1200N126 (723 OTUs) (Figures 2A, B). A Venn diagram further confirmed that the difference in the alpha and beta diversity indices of bacterial communities among the treatments might be due to common and unique OTUs (Figure 2C). These results suggest that alpha-beta diversity indices and OTUs distribution of bacterial communities significantly changed under different application rates of C/N ratio and were found to be significantly higher in treatment B1200N126 under high application of biochar (1200 kg/ha) and nitrogen fertilizer (126 kg/ha).

3.7 Bacterial community composition under different application rates of C/N ratio

The bacterial community composition at the phylum and genus level significantly changed under different application rates of C/N ratio (Figure 3 and Tables S6, S7). The relative abundance (RA) of the top 10 bacterial communities at the phylum and genus level is shown in the river map (Figure 3A and Table S6) and chord diagram (Figure 3B and Table S7). The phyla Actinobacteria, Acidobacteria, Bacteroidetes, Firmicutes, Proteobacteria, and Patescibacteria were present in high RA in all rhizosphere soil samples, dominated the rhizosphere soil bacterial communities, and accounted for around 85.40% of total soil bacteriome. Furthermore, RA bar plots were constructed to confirm the significant difference in the RA of specific phylum and genera among the treatments (Figures 3C, D). The RA of Actinobacteria, Bacteroidetes, and Proteobacteria were significantly increased, and the RA of Acidobacteria and Firmicutes significantly decreased in the rhizosphere soil of flue-cured tobacco plants under treatment B1200N125 (LSD, $p < 0.05$; Figure 3C). Furthermore, RA analysis at the genus level revealed that the RA of *Bacillus* was significantly increased under treatments B0N105, B600N105, and B600N126 (LSD, $p < 0.05$), and the RA of *Sphingomonas* was decreased considerably under B600N105 and B1200N105 (LSD, $p < 0.05$; Figure 3D). The RA of *RB41* and *Flavisolibacter* was significantly increased under B0N126, while the RA of *Ochrobactrum* was increased dramatically under B600N106 (LSD, $p < 0.05$; Figure 3D).

10.3389/fpls.2023.1250669

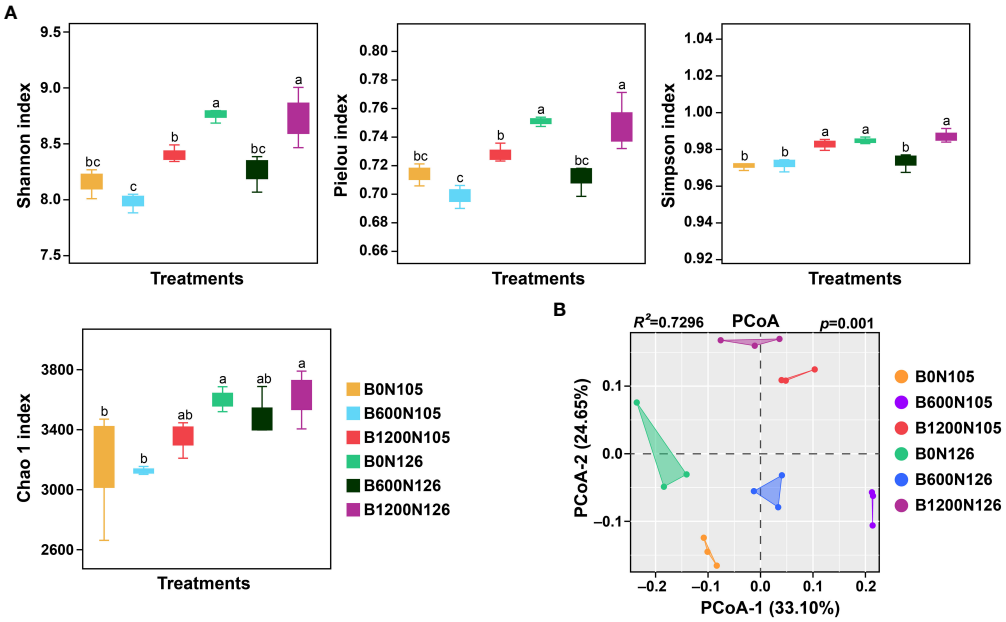

FIGURE 1
Impact of different application rates of carbon/nitrogen on diversity and structure of tobacco plant rhizosphere bacterial communities. **(A)** alpha diversity indices of rhizosphere bacterial communities under different treatments. **(B)** Principal coordinate analysis based on Bray–Curti's dissimilarity matrix shows the changes in bacterial community structure under different treatments. The lowercase letters on the error bars represent the significant difference among treatments according to the least significant difference test at $p < 0.05$. B0, B600, and B1200 represent 0, 600, and 1800 kg/ha biochar application rates, respectively. N105 and N126 represent 105 and 126 kg/ha application rates of pure nitrogen, respectively.

3.8 Characteristics of bacterial co-occurrence network and redundancy analysis

Bacterial co-occurrence network analysis was performed according to "spearmen correlation ($p < 0.05$ and correlation coefficient > 0.9) for most abundant bacterial genera within phylum under different treatments (Figure 4). Nodes represent the specific bacterial phylum and edges display a pairwise correlation (positive; red lines and negative; blue lines) between the nodes. Together, nodes and edges show a biochemical interaction among the bacterial communities within the network. The number of nodes (30) was

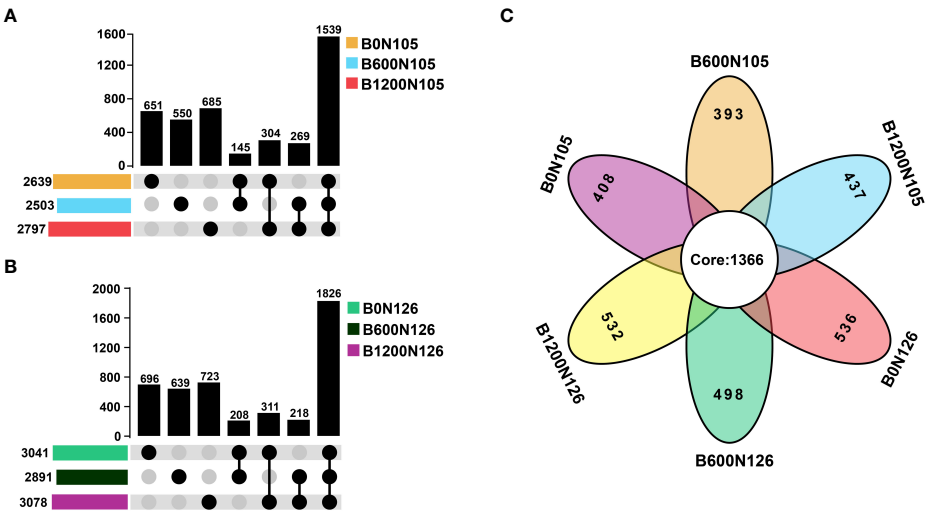

FIGURE 2
UpSet plots and Venn diagrams show the distribution of operational taxonomic units (OTUs) under different application rates of carbon/nitrogen ratios. **(A, B)** UpSet plots display the interaction between shared and unique OTUs under different treatments. **(C)** The Venn diagram illustrates the core and unique OTUs among the treatments. B0, B600, and B1200 represent 0, 600, and 1800 kg/ha biochar application rates, respectively. N105 and N126 represent 105 and 126 kg/ha application rates of pure nitrogen, respectively.

found to be the same under different treatments, and no significant difference was observed among the treatments. The number of edges decreased in the order B0N105 (174) > B1200N105 (162) > B1200N126 (160) > B600N105 (156) > B600N126 (142) > B0N126 (138). Analysis of pairwise correlation among the bacterial communities within a treatment showed the highest positive (106) and fewest negative (54) correlations among the bacterial communities under treatment B1200N126 compared with other treatments (Figure 4). No significant difference was observed for positive 88, 82, 79, 63, and 76 edges and negative 86, 74, 83, 75, and 66 edges among the nodes under treatments B0N105, B600N105, B1200N105, B0N126, and B600N126 (Figure 4).

An RDA further confirmed that rhizosphere soil bacterial communities, soil physicochemical properties, enzymatic activity, SMC, and SMN were affected by different application rates of the C/N ratio. RDA displayed a total of 42.93% variation in rhizosphere soil bacterial communities, soil physicochemical properties, enzymatic activity, SMC, and SMN under different treatments (Figure 5). RDA results revealed that TN, SOC, S-UE, S-SC, S-CAT, S-ACP, NO_3^--N, SMN, and SMN had a strong positive correlation with treatment B1200N126, while NH_4^+-N had a negative correlation with B1200N126 (Figure 5).

4 Discussion

This study aimed to evaluate the impact of the combined application of biochar and nitrogen fertilizer on soil properties, rhizosphere bacterial community, and biomass accumulation of flue-cured tobacco plants, which might be related to the biochar and nitrogen fertilizer dose and their interaction. The results showed that the appropriate application of biochar and nitrogen fertilizer significantly affected the accumulation of tobacco biomass. A proper biochar dose (600 kg/ha and 1200 kg/ha) under high nitrogen (N) fertilizer (126 kg/ha) was beneficial to the dry matter accumulation of tobacco plants and soil biochemical and microbial activities. However, a high dose of biochar (1200 kg/ha) under a low N fertilizer rate (105 kg/ha) was not conducive to the dry matter accumulation in tobacco plant and soil biochemical and microbial activities, which is in the agreement with previous studies (Ali et al., 2020; Sun et al., 2022). Biochar can improve soil's physicochemical properties, nutrient availability, and utilization rate and promotes tobacco plants' growth and dry matter accumulation (Ding et al., 2016; Zheng et al., 2021). This study shows that combining biochar and nitrogen fertilizer significantly increases the contents of soil organic carbon, soil total nitrogen, and

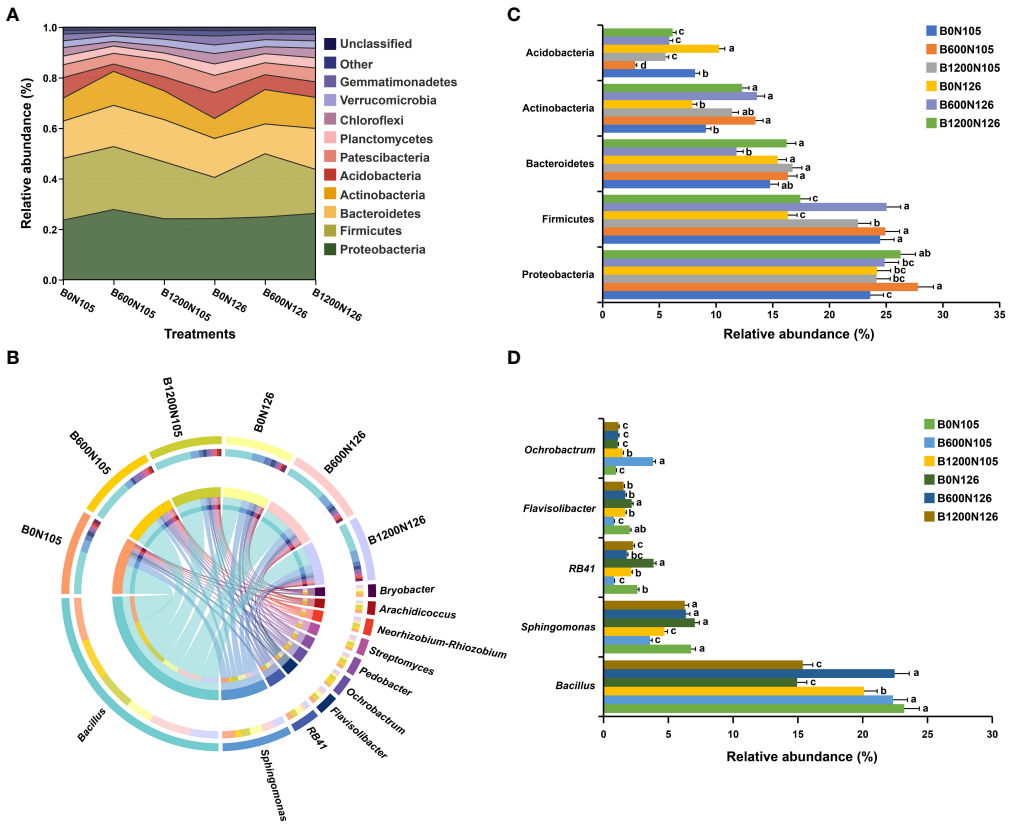

FIGURE 3
Relative abundance analysis of most abundant bacterial phylum and genus under different biochar and nitrogen fertilizer application ratios. River map **(A)** and chord diagram **(B)** showing the relative abundance of the top 10 bacterial phyla and genera under different treatments. Bar plots representing the significant difference among the most abundant bacterial phylum **(C)** and genus **(D)** among the treatments. According to the least significant difference test at $p < 0.05$, different small letters on the error bars show the difference among treatments. B0, B600, and B1200 represent 0, 600, and 1800 kg/ha biochar application rates, respectively. N105 and N126 represent 105 and 126 kg/ha application rates of pure nitrogen, respectively.

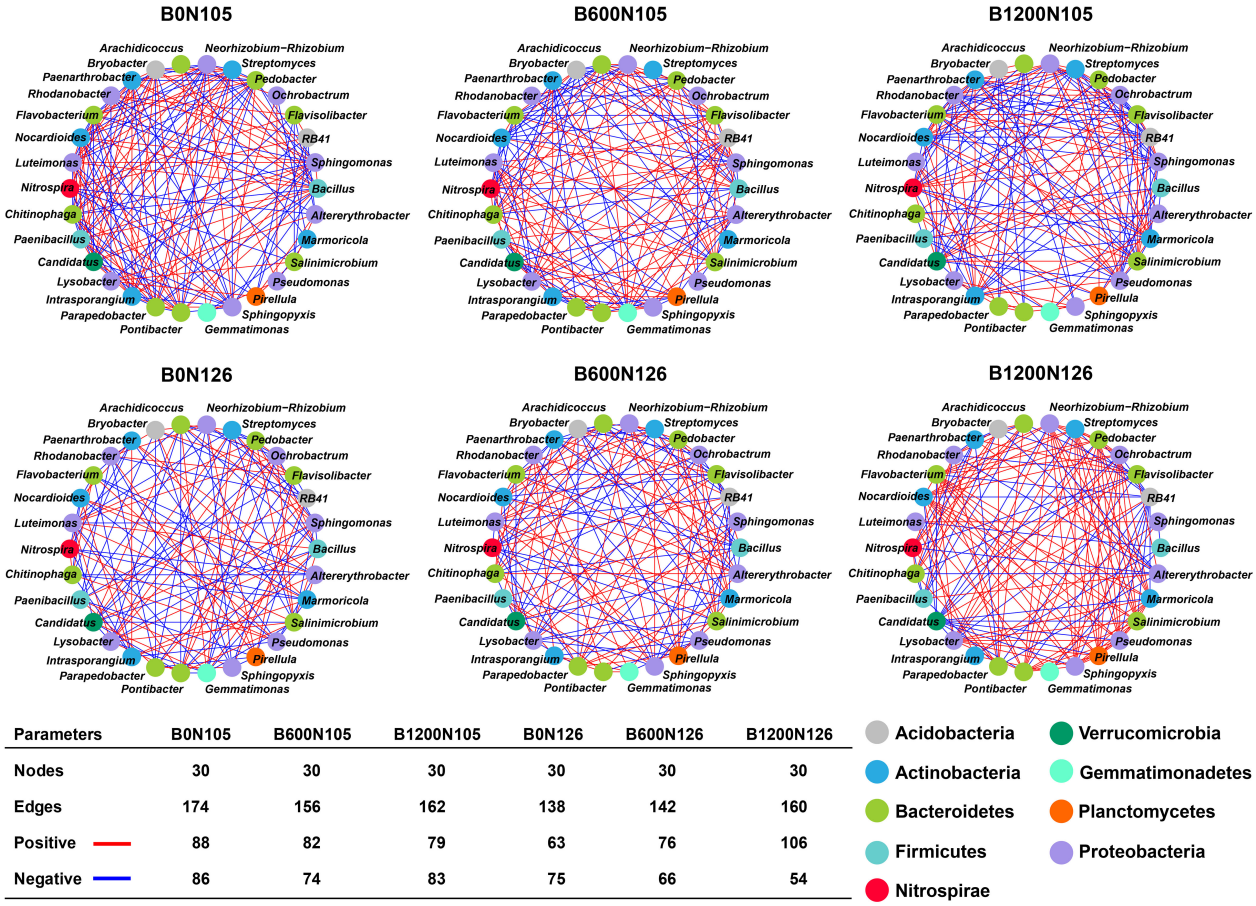

Parameters	B0N105	B600N105	B1200N105	B0N126	B600N126	B1200N126
Nodes	30	30	30	30	30	30
Edges	174	156	162	138	142	160
Positive	88	82	79	63	76	106
Negative	86	74	83	75	66	54

Acidobacteria
Actinobacteria
Bacteroidetes
Firmicutes
Nitrospirae
Verrucomicrobia
Gemmatimonadetes
Planctomycetes
Proteobacteria

FIGURE 4
Co-occurrence network analysis of rhizosphere bacterial communities at phylum level under different treatments. Nodes represent the bacterial phylum, and edges show the positive (red line) and negative (red lines) correlations among the bacterial phyla within a treatment. B0, B600, and B1200 represent 0, 600, and 1800 kg/ha biochar application rates, respectively. N105 and N126 represent 105 and 126 kg/ha application rates of pure nitrogen, respectively.

soil carbon-nitrogen ratio. Our findings are consistent with the previous studies reporting that using biochar and mineral fertilizers simulate crop growth (Schulz and Glaser, 2012). We found that the soil NO_3^-–N concentration was higher under the combined application of biochar and nitrogen than that of single nitrogen fertilizer treatment. This indicates that the combined application of biochar and nitrogen fertilizer had a synergistic effect on soil nitrification, and it might be related to the adsorption of nitrification inhibitors (phenol and terpene) by biochar (Ball et al., 2010). In addition, biochar can significantly increase soil organic carbon, resulting in a higher carbon-nitrogen ratio, thereby enhancing soil nitrification and improving nitrogen bioavailability, increasing plants' overall biomass accumulation (Zhao et al., 2020).

It was found that the high biochar dosage (1200 kg/ha) and low nitrogen levels (105 kg/ha) were not conducive to the dry matter accumulation in tobacco leaves and whole plants. Some reports have shown adverse or insignificant effects of biochar on crop growth and yield. For example, Li et al. (2022) found that when the concentration of tobacco stem biochar reached more than 4%, the soil nitrate-nitrogen content began to decline rapidly, and the dry matter accumulation of tobacco plants also reduced significantly than that of the control. Excessive biochar can inhibit crop growth due to nitrogen fixation caused by the high content of volatile components and toxic or harmful substances, reducing nutrient absorption and crop growth (Zhang et al., 2018; Song et al., 2020). The heavy metals in biochar are all below the threshold level of heavy metals which are considered damaging for plant growth, as reported by the International Biochar Initiative (IBI) and the European Biochar Certificate (EBC) (IBI, 2016). Therefore, nitrogen fixation may be a factor in limiting tobacco growth under higher biochar doses. Zheng et al. (2020) reported that high amounts of biochar may inhibit the growth of tobacco because at high C/N ratios, microbial biomass fixes nitrogen, thereby reducing nitrogen availability, which is in concurrence with our study. However, we found that high doses of biochar (1200 kg/ha) and nitrogen (126 kg/ha) treatments increased the biomass of tobacco plants, which was related to increasing the amount of nitrogen fertilizer and reducing the C/N ratio (Xia et al., 2022).

Soil enzyme activity can sensitively and accurately reflect the changes in soil quality and is closely related to soil physicochemical properties, nutrient contents, and fertilization methods (Datta et al.,

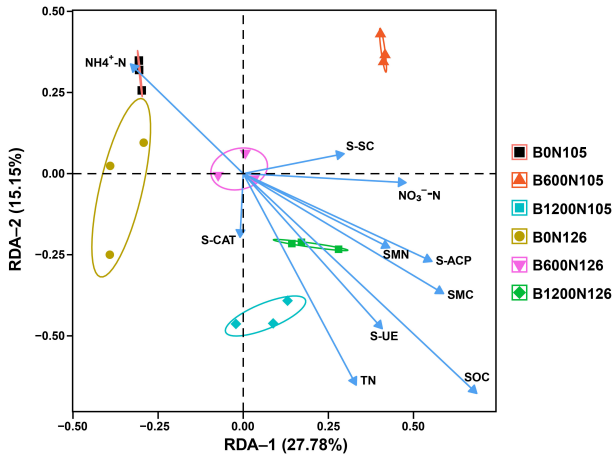

FIGURE 5
Redundancy analysis shows the correlation between rhizosphere bacterial communities, soil physicochemical properties, soil enzymatic activities, and soil microbial biomass of carbon and nitrogen under different treatments. B0, B600, and B1200 represent 0, 600, and 1800 kg/ha biochar application rates, respectively. N105 and N126 represent 105, and 126 kg/ha application rates of pure nitrogen, respectively.

2017; Zhou et al., 2020). We found that the rational combination of biochar and nitrogen fertilizer significantly increased the enzyme activities of soil urease, soil invertase, soil acid phosphatase, and hydrogen peroxide, which is in accordance with the results of previous studies (Wang et al., 2015; Elzobair et al., 2016). Similarly, biochar stimulates soil enzyme activity and affects bacterial community abundance by increasing soil organic carbon and available nitrogen, which is consistent with previous reports (Li et al., 2016). Applying biochar (600 kg/ha) and nitrogen (105 kg/ha and 126 kg/ha) significantly increased soil organic carbon and available nitrogen contents, which may be partly due to the increase in urease activity. Previous studies reported that biochar application may inhibit enzymatic reactions by occupying binding sites (Liu et al., 2018; Ali et al., 2021), which is also related to biochar and soil types. However, further in-depth analysis is needed for different situations. A suitable nitrogen fertilizer application rate should be maintained when biochar and nitrogen fertilizer are applied together. This experiment showed that the soil enzyme activity was decreased when the amount of biochar was too high (1200 kg/ha), and the amount of nitrogen fertilizer was too low (105 kg/ha). This might be due to excessive biochar and low nitrogen fertilizer increased the C/N ratio, inhibiting the soil microbial activity and reducing the number of rhizosphere microorganisms (Zheng et al., 2020). However, under high dosages of biochar (1200 kg/ha) and nitrogen fertilizer (126 kg/ha), the soil C/N ratio decreased, which enhanced the soil enzyme activity. These findings suggest that the key reason for the reduced enzyme activity might be related to the soil's high C/N ratio.

Biochar can significantly increase the contents of microbial biomass carbon in the soil, mainly when applied with NPK fertilizer (Khan et al., 2021b). This study found that the appropriate amount of biochar (600 kg/ha) combined with nitrogen fertilizer significantly increased the contents of microbial biomass carbon and nitrogen. One possible explanation is that biochar has a porous structure and a large specific surface area, which can maintain and balance soil moisture, air, and nutrients, thereby improving the living conditions for microorganisms (Li et al., 2020). In addition, biochar may become a new carbon source for microorganisms after degradation in soil and promote microbial growth (Ullah et al., 2020). More importantly, the combination of biochar (600 kg/ha) and nitrogen fertilizer (105 kg/ha and 126 kg/ha) significantly increased the contents of soil microbial biomass carbon and nitrogen compared with the control (biochar 0 kg/ha and N fertilizer 105 kg/ha and 126 kg/ha). This can be attributed to the synergistic effect of biochar and fertilizer and may also be because biochar can adsorb nitrogen and other nutrients, creating a nutrient-rich microenvironment and providing ideal conditions for microbial growth (Ullah et al., 2020; Zhao et al., 2022). However, in this study, the content of soil microbial biomass carbon and nitrogen under the combined application of high biochar (1200 kg/ha) and low nitrogen fertilizer (105 kg/ha) was significantly lower than that in the combined application of high biochar (1200 kg/ha) and high nitrogen fertilizer (126 kg/ha), which may be related to the soil C/N ratio and needs further in-depth study.

Soil microorganisms are an integral part of the soil's ecosystem (Dai et al., 2023). The abundance and composition of soil microbes affect the soil structure and nutrient cycle, thus affecting plant growth, development, yield, and quality (Zheng et al., 2021). This study found that applying biochar and nitrogen fertilizer increased the diversity and abundance of rhizosphere bacteriomes to a certain extent. This might be because the porous structure of biochar and its ability to adsorb water and fertilizer make it a suitable habitat for soil microorganisms, which enhances the abundance of the rhizosphere microbiome, and increased application of nitrogen fertilizer promotes the reproduction of microorganisms in the soil (Ali et al., 2020). In this study, compared with high biochar (1200 kg/ha) and low nitrogen (105 kg/ha) treatments, the high biochar (1200 kg/ha) and high nitrogen (126 kg/ha) significantly increased the diversity of rhizosphere bacterial communities. This shows that

the appropriate application of biochar and nitrogen fertilizer has a more positive effect on promoting the diversity of rhizosphere bacteriome, which is mainly favorable to the species richness of rhizosphere microorganisms.

The changes in the structure and composition of microbial communities depend on the source of the biochar and soil type (Adams et al., 2021). It has been reported that biochar can significantly affect the abundance of soil bacterial communities, but different soil types and microbial species have different responses to biochar (Adams et al., 2021). This study found that after applying biochar and nitrogen fertilizer, Acidobacteria, Bacteroidetes, Firmicutes, Proteobacteria, and Patescibacteria were the dominant phylum. The relative abundance of Actinobacteria, Bacteroidetes, and Proteobacteria in the rhizosphere soil of flue-cured tobacco was significantly increased by a high amount of biochar (1200 kg/ha) and high nitrogen (126 kg/ha), while that of Acidobacteria and Firmicutes decreased. These results are in accordance with previous reports that soil amendment with biochar enhanced the relative abundance of Proteobacteria, Bacteroidetes, and Actinobacteria but reduces the relative abundance of Acidobacteria, Chloroflexi, and Gemmatimonadetes (Xu et al., 2016). A co-occurrence network analysis showed a lower negative correlation among the rhizosphere bacterial communities under higher biochar and nitrogen fertilizer application rates than other treatments.

Further, RDA analysis proved that soil physicochemical and enzymatic properties were positively correlated with higher biochar and nitrogen fertilizer application rates. This may be affected by synergistic effects, such as the co-metabolism or synthesis of these bacteria or their similar reaction patterns to biological, chemical, or physical variables and common niches (Ullah et al., 2020). However, the effect of biochar and nitrogen fertilizer on the rhizosphere bacterial community is a complex process, and the internal mechanism of microorganisms needs to be elucidated through long-term experiments.

5 Conclusions

In summary, we conclude that the combined application of biochar and nitrogen significantly increase the soil carbon-nitrogen pool and change the soil carbon/nitrogen ratio, influencing the abundance and composition of rhizosphere bacteriome. The appropriate application of biochar combined with nitrogen could significantly increase the soil microbial biomass carbon and nitrogen, soil enzymatic activities, and biomass of flue-cured tobacco plants. The combined application of high biochar (1200 kg/ha) and low nitrogen (105 kg/ha) increased the soil C/N ratio, reducing the soil enzymatic activity, bacterial diversity, and biomass accumulation. In contrast, higher application of biochar (1200 kg/ha) and high nitrogen (126 kg/ha) reduced the soil C/N ratio and enhanced soil enzymatic activity, soil physicochemical properties, and relative abundance of rhizosphere bacteriome, which increased the biomass accumulation of flue-cured tobacco plants. Future studies will focus on elucidating the effect of high biochar and nitrogen fertilizer application on dry matter accumulation and the rhizosphere bacteriome of tobacco plants under a long-term mono-cropping system.

Data availability statement

The raw data related to 16S rRNA sequencing is deposited in the sequence read archive (SRA) in NCBI public database with BioProject No. PRJNA975294.

Author contributions

ZZ conceived and designed the experiments. YY, CY, WZ, XZ, HL, and DY performed the experiments. YY, WA, and XZ collected and analyzed the data. YY and WA wrote the manuscript. WA and ZZ revised the manuscript. All authors contributed to the final draft of the manuscript. All authors have read and agreed to the published version of the manuscript.

Funding

This study was financially supported by the National Key Research Plan of China (2022YFD1901504).

Conflict of interest

Author CY is employed by Yunnan Revert Medical and Biotechnology Co., Ltd., HL is employed by the Kunming Branch of Yunnan Tobacco Company, DY is employed by Hongta Tobacco Group Limited Company, Dali which are members of tobacco industry.

The remaining authors declare that the research was conducted in the absence of any commercial or financial relationships that could be construed as a potential conflict of interest.

Publisher's note

Supplementary material

The Supplementary Material for this article can be found online at: https://www.frontiersin.org/articles/10.3389/fpls.2023.1250669/full#supplementary-material

References

Adams, M., Xie, J., Chang, Y., Kabore, A. W. J., and Chen, C. (2021). Start-up of Anammox systems with different biochar amendment: Process characteristics and microbial community. *Sci. Total Environ.* 790, 148242. doi: 10.1016/j.scitotenv.2021.148242

Ahmed, W., Dai, Z., Zhang, J., Li, S., Ahmed, A., Munir, S., et al. (2022). Plant-microbe interaction: mining the impact of native bacillus amyloliquefaciens WS-10 on tobacco bacterial wilt disease and rhizosphere microbial communities. *Microbiol. Spectr.* 10, e01471–e01422. doi: 10.1128/spectrum.01471-22

Akhtar, A., Krepl, V., and Ivanova, T. J. E. (2018). A combined overview of combustion, pyrolysis, and gasification of biomass. *Energy Fuels* 32, 7294–7318. doi: 10.1021/acs.energyfuels.8b01678

Ali, I., Ullah, S., He, L., Zhao, Q., Iqbal, A., Wei, S., et al. (2020). Combined application of biochar and nitrogen fertilizer improves rice yield, microbial activity and N-metabolism in a pot experiment. *PeerJ* 8, e10311. doi: 10.7717/peerj.10311

Ali, I., Zhao, Q., Wu, K., Ullah, S., Iqbal, A., Liang, H., et al. (2021). Biochar in combination with nitrogen fertilizer is a technique: to enhance physiological and morphological traits of rice (Oryza sativa L.) by improving soil physio-biochemical properties. *J. Plant Growth Regul.* 41, 2406–2420. doi: 10.1007/s00344-021-10454-8

Ball, P. N., MacKenzie, M. D., DeLuca, T. H., and Holben, W. E. (2010). Wildfire and charcoal enhance nitrification and ammonium-oxidizing bacterial abundance in dry montane forest soils. *J. Environ. Qual* 39, 1243–1253. doi: 10.2134/jeq2009.0082

Bolger, A. M., Lohse, M., and Usadel, B. (2014). Trimmomatic: a flexible trimmer for Illumina sequence data. *Bioinformatics* 30, 2114–2120. doi: 10.1093/bioinformatics/btu170

Cai, Q., Zhou, G., Ahmed, W., Cao, Y., Zhao, M., Li, Z., et al. (2021). Study on the relationship between bacterial wilt and rhizospheric microbial diversity of flue-cured tobacco cultivars. *Eur. J. Plant Pathol.* 160, 265–276. doi: 10.1007/s10658-021-02237-4

Chen, N., Cao, S., Zhang, L., Peng, X., Wang, X., Ai, Z., et al. (2021). Structural dependent Cr (VI) adsorption and reduction of biochar: hydrochar versus pyrochar. *Sci. Total Environ.* 783, 147084. doi: 10.1016/j.scitotenv.2021.147084

Chen, J., Liu, X., Zheng, J., Zhang, B., Lu, H., Chi, Z., et al. (2013). Biochar soil amendment increased bacterial but decreased fungal gene abundance with shifts in community structure in a slightly acid rice paddy from Southwest China. *Appl. Soil Ecol.* 71, 33–44. doi: 10.1016/j.apsoil.2013.05.003

Dai, Z., Ahmed, W., Yang, J., Yao, X., Zhang, J., Wei, L., et al. (2023). Seed coat treatment by plant-growth-promoting rhizobacteria Lysobacter antibioticus 13–6 enhances maize yield and changes rhizosphere bacterial communities. *Biol. Fertil. Soil* 59, 317–331. doi: 10.1007/s00374-023-01703-x

Datta, R., Anand, S., Moulick, A., Baraniya, D., Pathan, S. I., Rejsek, K., et al. (2017). How enzymes are adsorbed on soil solid phase and factors limiting its activity: A Review. *Int. Agrophysics* 31, 287–302. doi: 10.1515/intag-2016-0049

De Tender, C., Haegeman, A., Vandecasteele, B., Clement, L., Cremelie, P., Dawyndt, P., et al. (2016). Dynamics in the strawberry rhizosphere microbiome in response to biochar and Botrytis cinerea leaf infection. *Front. Microbiol.* 7, 2062. doi: 10.3389/fmicb.2016.02062

Ding, Y., Liu, Y., Liu, S., Li, Z., Tan, X., Huang, X., et al. (2016). Biochar to improve soil fertility. A review. *Agron. Sustain. Dev.* 36. doi: 10.1007/s13593-016-0372-z

Edgar, R. C. (2013). UPARSE: highly accurate OTU sequences from microbial amplicon reads. *Nat. Methods* 10, 996–998. doi: 10.1038/nmeth.2604

Edgar, R. C., Haas, B. J., Clemente, J. C., Quince, C., and Knight, R. (2011). UCHIME improves sensitivity and speed of chimera detection. *Bioinformatics* 27, 2194–2200. doi: 10.1093/bioinformatics/btr381

Elzobair, K. A., Stromberger, M. E., Ippolito, J. A., and Lentz, R. D. (2016). Contrasting effects of biochar versus manure on soil microbial communities and enzyme activities in an Aridisol. *Chemosphere* 142, 145–152. doi: 10.1016/j.chemosphere.2015.06.044

Fuke, P., Kumar, M., Sawarkar, A. D., Pandey, A., and Singh, L. (2021). Role of microbial diversity to influence the growth and environmental remediation capacity of bamboo: A review. *Ind. Crops Products* 167, 113567. doi: 10.1016/j.indcrop.2021.113567

Graber, E., Frenkel, O., Jaiswal, A., and Elad, Y. (2014). How may biochar influence severity of diseases caused by soilborne pathogens? *Carbon Manage.* 5, 169–183. doi: 10.1080/17583004.2014.913360

Guan, Z., Lin, D., Chen, D., Guo, Y., Lu, Y., Han, Q., et al. (2022). Soil microbial communities response to different fertilization regimes in young Catalpa bungei plantation. *Front. Microbiol.* 13. doi: 10.3389/fmicb.2022.948875

Hu, H., Yin, D., Cao, S., Zhang, H., Zhou, C., and He, Z. (2019). Effects of biochar on soil nutrient, enzyme activity, and bacterial properties of Chinese fir plantation. *Acta Ecologica Sin.* 39, 4138–4148.

IBI (2016). *Standardized Product Definition and Product Testing Guidelines for Biochar That Is Used in Soil, IBI, 2016* (accessed 26.08.16). Available at: http://www.biochar-international.org/sites/default/files/IBI Biochar Standards V2.1 Final. pdf.

Khan, I., Chen, T., Farooq, M., Luan, C., Wu, Q., Wanning, D., et al. (2021a). The residual impact of straw mulch and biochar amendments on soil physiochemical properties and yield of maize under rainfed system. *Agron. J.* 113, 1102–1120. doi: 10.1002/agj2.20540

Khan, I., Iqbal, B., Khan, A. A., Inamullah,, Rehman, A., Fayyaz, A., et al. (2022). The interactive impact of straw mulch and biochar application positively enhanced the growth indexes of maize (Zea mays L.) crop. *Agronomy* 12, 2584. doi: 10.3390/agronomy12102584

Khan, I., Luan, C., Qi, W., Wang, X., Yu, B., Rehman, A., et al. (2023). The residual impact of straw mulch and biochar amendments on grain quality and amino acid contents of rainfed maize crop. *J. Plant Nutr.* 46, 1283–1295. doi: 10.1080/01904167.2022.2056483

Khan, Z., Nauman Khan, M., Luo, T., Zhang, K., Zhu, K., Rana, M. S., et al. (2021b). Compensation of high nitrogen toxicity and nitrogen deficiency with biochar amendment through enhancement of soil fertility and nitrogen use efficiency promoted rice growth and yield. *GCB Bioenergy* 13, 1765–1784. doi: 10.1111/gcbb.12884

Lehmann, J., and Joseph, S. (2015). *Biochar for environmental management: an introduction* (Routledge: Biochar for environmental management).

Li, C., Ahmed, W., Li, D., Yu, L., Xu, L., Xu, T., et al. (2022). Biochar suppresses bacterial wilt disease of flue-cured tobacco by improving soil health and functional diversity of rhizosphere microorganisms. *Appl. Soil Ecol.* 171, 104314. doi: 10.1016/j.apsoil.2021.104314

Li, M., Liu, M., Z-p, Li, Jiang, C.-y., and Wu, M. (2016). Soil N transformation and microbial community structure as affected by adding biochar to a paddy soil of subtropical China. *J. Integr. Agric.* 15, 209–219. doi: 10.1016/s2095-3119(15)61136-4

Li, S., Wang, S., Fan, M., Wu, Y., and Shangguan, Z. (2020). Interactions between biochar and nitrogen impact soil carbon mineralization and the microbial community. *Soil Tillage Res.* 196, 104437. doi: 10.1016/j.still.2019.104437

Liu, Y., Dai, Q., Jin, X., Dong, X., Peng, J., Wu, M., et al. (2018). Negative impacts of biochars on urease activity: high pH, heavy metals, polycyclic aromatic hydrocarbons, or free radicals? *Environ. Sci. Technol.* 52, 12740–12747. doi: 10.1021/acs.est.8b00672

Liu, Z., Zhang, F.-S., and Wu, J. J. F. (2010). Characterization and application of chars produced from pinewood pyrolysis and hydrothermal treatment. *Fuel* 89, 510–514. doi: 10.1016/j.fuel.2009.08.042

Meller Harel, Y., Elad, Y., Rav-David, D., Borenstein, M., Shulchani, R., Lew, B., et al. (2012). Biochar mediates systemic response of strawberry to foliar fungal pathogens. *Plant Soil* 357, 245–257. doi: 10.1007/s11104-012-1129-3

Pandey, V., Patel, A., and Patra, D. (2016). Biochar ameliorates crop productivity, soil fertility, essential oil yield and aroma profiling in basil (Ocimum basilicum L.). *Ecol. Eng.* 90, 361–366. doi: 10.1016/j.ecoleng.2016.01.020

Peng, Y., Sun, Y., Fan, B., Zhang, S., Bolan, N. S., Chen, Q., et al. (2021). Fe/Al (hydr) oxides engineered biochar for reducing phosphorus leaching from a fertile calcareous soil. *J. Cleaner Production* 279, 123877. doi: 10.1016/j.jclepro.2020.123877

Pokovai, K., Tóth, E., and Horel, Á (2020). Growth and photosynthetic response of Capsicum annuum L. @ in biochar amended soil. *Appl. Sci.* 10, 4111. doi: 10.3390/app10124111

Prayogo, C., Jones, J. E., Baeyens, J., and Bending, G. D. (2014). Impact of biochar on mineralisation of C and N from soil and willow litter and its relationship with microbial community biomass and structure. *Biol. Fertility Soils* 50, 695–702. doi: 10.1007/s00374-013-0884-5

Qin, Y., Zhang, L., and An, T. (2017). Hydrothermal carbon-mediated Fenton-like reaction mechanism in the degradation of alachlor: direct electron transfer from hydrothermal carbon to Fe (III). *ACS Appl. Materials Interfaces* 9, 17115–17124. doi: 10.1021/acsami.7b03310

Quast, C., Pruesse, E., Yilmaz, P., Gerken, J., Schweer, T., Yarza, P., et al. (2012). The SILVA ribosomal RNA gene database project: improved data processing and web-based tools. *Nucleic Acids Res.* 41, D590–D596. doi: 10.1093/nar/gks1219

Raaijmakers, J. M. (2015). *The minimal rhizosphere microbiome. In Principles of Plant-Microbe Interactions: Microbes for Sustainable Agriculture* (pp. 411–417) (Cham: Springer International Publishing).

Ren, T., Feng, H., Xu, C., Xu, Q., Fu, B., Azwar, E., et al. (2022). Exogenous application and interaction of biochar with environmental factors for improving functional diversity of rhizosphere's microbial community and health. *Chemosphere* 294, 133710. doi: 10.1016/j.chemosphere.2022.133710

Ronsse, F., Van Hecke, S., Dickinson, D., and Prins, W. (2013). Production and characterization of slow pyrolysis biochar: influence of feedstock type and pyrolysis conditions. *Gcb Bioenergy* 5, 104–115. doi: 10.1111/gcbb.12018

Schulz, H., and Glaser, B. (2012). Effects of biochar compared to organic and inorganic fertilizers on soil quality and plant growth in a greenhouse experiment. *J. Plant Nutr. Soil Sci.* 175, 410–422. doi: 10.1002/jpln.201100143

Seyedghasemi, S. M., Rezvani Moghaddam, P., and Esfahani, M. (2021). Optimization of biochar and nitrogen fertilizer in rice cultivation. *J. Plant Nutr.* 44, 1705–1718. doi: 10.1080/01904167.2021.1881542

Singh, G., and Mavi, M. S. (2018). Impact of addition of different rates of rice-residue biochar on C and N dynamics in texturally diverse soils. *Arch. Agron. Soil Sci.* 64, 1419–1431. doi: 10.1080/03650340.2018.1439161

Song, R., Ahmed, W., Tan, Y., and Zhao, Z. (2022). Different levels of nitrogen fertilizer in nursery stage positively affect the activity of defense-related enzymes and

resistance of tobacco plant to phytophthora nicotianae. *Chiang Mai J. Sci.* 49, 551–564. doi: 10.12982/CMJS.2022.046

Song, X., Razavi, B. S., Ludwig, B., Zamanian, K., Zang, H., Kuzyakov, Y., et al. (2020). Combined biochar and nitrogen application stimulates enzyme activity and root plasticity. *Sci. Total Environ.* 735, 139393. doi: 10.1016/j.scitotenv.2020.139393

Streubel, J., Collins, H., Garcia-Perez, M., Tarara, J., Granatstein, D., and Kruger, C. (2011). Influence of contrasting biochar types on five soils at increasing rates of application. *Soil Sci. Soc. America J.* 75, 1402–1413. doi: 10.2136/sssaj2010.0325

Sun, C., Sun, J., Gao, J., Liu, J., Yu, X., Wang, Z., et al. (2022). Comprehensive application of bio-char and nitrogen fertilizer in dry-land maize cultivation. *Sci. Rep.* 12, 13478. doi: 10.1038/s41598-022-16971-0

Tammeorg, P., Simojoki, A., Mäkelä, P., Stoddard, F. L., Alakukku, L., and Helenius, J. (2014). Short-term effects of biochar on soil properties and wheat yield formation with meat bone meal and inorganic fertiliser on a boreal loamy sand. *Agricult. Ecosyst. Environ.* 191, 108–116. doi: 10.1016/j.agee.2014.01.007

Ullah, S., Liang, H., Ali, I., Zhao, Q., Iqbal, A., Wei, S., et al. (2020). Biochar coupled with contrasting nitrogen sources mediated changes in carbon and nitrogen pools, microbial and enzymatic activity in paddy soil. *J. Saudi Chem. Soc.* 24, 835–849. doi: 10.1016/j.jscs.2020.08.008

Wang, X., Song, D., Liang, G., Zhang, Q., Ai, C., and Zhou, W. (2015). Maize biochar addition rate influences soil enzyme activity and microbial community composition in a fluvo-aquic soil. *Appl. Soil Ecol.* 96, 265–272. doi: 10.1016/j.apsoil.2015.08.018

Wang, L., Yu, B., Ji, J., Khan, I., Li, G., Rehman, A., et al. (2023). Assessing the impact of biochar and nitrogen application on yield, water-nitrogen use efficiency and quality of intercropped maize and soybean. *Front. Plant Sci.* 14, 1171547. doi: 10.3389/fpls.2023.1171547

Wang, H., Zhang, R., Zhao, Y., Shi, H., and Liu, G. (2022). Effect of biochar on rhizosphere soil microbial diversity and metabolism in tobacco-growing soil. *Ecologies* 3, 539–556. doi: 10.3390/ecologies3040040

Wiedner, K., Naisse, C., Rumpel, C., Pozzi, A., Wieczorek, P., and Glaser, B. (2013). Chemical modification of biomass residues during hydrothermal carbonization–What makes the difference, temperature or feedstock? *Organic Geochem.* 54, 91–100. doi: 10.1016/j.orggeochem.2012.10.006

Xia, H., Riaz, M., Zhang, M., Liu, B., Li, Y., El-Desouki, Z., et al. (2022). Biochar-N fertilizer interaction increases N utilization efficiency by modifying soil C/N component under N fertilizer deep placement modes. *Chemosphere* 286, 131594. doi: 10.1016/j.chemosphere.2021.131594

Xia, Y., Zhang, M., Tsang, D. C., Geng, N., Lu, D., Zhu, L., et al. (2020). Recent advances in control technologies for non-point source pollution with nitrogen and phosphorous from agricultural runoff: current practices and future prospects. *Appl. Biol. Chem.* 63, 1–13. doi: 10.1186/s13765-020-0493-6

Xu, N., Tan, G., Wang, H., and Gai, X. (2016). Effect of biochar additions to soil on nitrogen leaching, microbial biomass and bacterial community structure. *Eur. J. Soil Biol.* 74, 1–8. doi: 10.1016/j.ejsobi.2016.02.004

Xu, H.-J., Wang, X.-H., Li, H., Yao, H.-Y., Su, J.-Q., and Zhu, Y.-G. (2014). Biochar impacts soil microbial community composition and nitrogen cycling in an acidic soil planted with rape. *Environ. Sci. Technol.* 48, 9391–9399. doi: 10.1021/es5021058

Zhang, J., Ahmed, W., Dai, Z., Zhou, X., He, Z., Wei, L., et al. (2022). Microbial consortia: An engineering tool to suppress clubroot of Chinese cabbage by changing the rhizosphere bacterial community composition. *Biology* 11, 918. doi: 10.3390/biology11060918

Zhang, G., Guo, X., Zhu, Y., Liu, X., Han, Z., Sun, K., et al. (2018). The effects of different biochars on microbial quantity, microbial community shift, enzyme activity, and biodegradation of polycyclic aromatic hydrocarbons in soil. *Geoderma* 328, 100–108. doi: 10.1016/j.geoderma.2018.05.009

Zhao, Y., Wang, X., Yao, G., Lin, Z., Xu, L., Jiang, Y., et al. (2022). Advances in the effects of biochar on microbial ecological function in soil and crop quality. *Sustainability* 14 (16), 10411. doi: 10.3390/su141610411

Zhao, H., Yu, L., Yu, M., Afzal, M., Dai, Z., Brookes, P., et al. (2020). Nitrogen combined with biochar changed the feedback mechanism between soil nitrification and Cd availability in an acidic soil. *J. Hazard Mater* 390, 121631. doi: 10.1016/j.jhazmat.2019.121631

Zheng, X., Song, W., Guan, E., Wang, Y., Hu, X., Liang, H., et al. (2020). Response in physicochemical properties of tobacco-growing soils and N/P/K accumulation in tobacco plant to tobacco straw biochar. *J. Soil Sci. Plant Nutr.* 20, 293–305. doi: 10.1007/s42729-019-00108-w

Zheng, J., Zhang, J., Gao, L., Wang, R., Gao, J., Dai, Y., et al. (2021). Effect of straw biochar amendment on tobacco growth, soil properties, and rhizosphere bacterial communities. *Sci. Rep.* 11, 20727. doi: 10.1038/s41598-021-00168-y

Zhou, F., and Chen-yang, X. (2019). Effect of biochar dosage on soil microbial biomass and carbon source metabolic activity. *J. Plant Nutr. Fertilizer* 25, 1277–1289.

Zhou, B., Zhao, L., Wang, Y., Sun, Y., Li, X., Xu, H., et al. (2020). Spatial distribution of phthalate esters and the associated response of enzyme activities and microbial community composition in typical plastic-shed vegetable soils in China. *Ecotoxicol Environ. Saf.* 195, 110495. doi: 10.1016/j.ecoenv.2020.110495

frontiers | Frontiers in Plant Science

TYPE Original Research
PUBLISHED 13 October 2023
DOI 10.3389/fpls.2023.1280382

OPEN ACCESS

EDITED BY
Shahbaz Khan,
Huazhong Agricultural University, China

REVIEWED BY
Naveed Ahmad,
Shanghai Jiao Tong University, China
Muhammad Noman,
University of Florida, United States
Hafeez Noor,
Shanxi Agricultural University, China

*CORRESPONDENCE
Lixue Wang
wlx1964@163.com
Ismail Khan
ismailagronomist@gmail.com

RECEIVED 20 August 2023
ACCEPTED 25 September 2023
PUBLISHED 13 October 2023

CITATION
Liu S, Wang L, Chang L, Khan I, Nadeem F, Rehman A and Suo R (2023) Evaluating the influence of straw mulching and intercropping on nitrogen uptake, crop growth, and yield performance in maize and soybean.
Front. Plant Sci. 14:1280382.
doi: 10.3389/fpls.2023.1280382

Evaluating the influence of straw mulching and intercropping on nitrogen uptake, crop growth, and yield performance in maize and soybean

Siping Liu[1], Lixue Wang[1]*, Liang Chang[1], Ismail Khan[2]*, Faisal Nadeem[3], Abdul Rehman[4] and Ran Suo[5]

[1]College of Water Conservancy, Shenyang Agricultural University, Shenyang, China, [2]School of the Environment and Safety Engineering, Jiangsu University, Zhenjiang, China, [3]Department of Agronomy, The University of Agriculture, DI Khan, KP, Pakistan, [4]Department of Agronomy, Faculty of Agriculture and Environment, The Islamia University of Bahawalpur, Bahawalpur, Pakistan, [5]Quality Supervision Department, Chaoyang City Water Engineering Quality and Safety Supervision Station, Chaoyang, China

Introduction: Intercropping and straw mulching are sustainable agricultural practices that can positively affect crop growth and development, especially together.

Methods: A split-plot experimental design was used to investigate the effects of intercropping and straw mulching on crop growth, crop yield, nitrogen uptake, and photosynthetic characteristics. The main plot focused on three planting patterns: soybean monoculture (S), maize monoculture (M), and maize/soybean intercropping (I). The subplot structure consisted of four levels of straw mulching (0, 4.8, 7.2, 9.6 t ha^{-1}).

Results: Interaction and variance analyses showed that straw mulching, intercropping, and their interaction had significant effects on plant height, stem diameter, leaf area index, chlorophyll content, nitrogen uptake, photosynthetic characteristics, and crop yield. Based on two-year averages for maize and soybean, the net photosynthetic rate (Pn) was up to 51.6% higher, stomatal conductance (Sc) was up to 44.0% higher, transpiration rate (Tr) was up to 46.6% higher, and intercellular carbon dioxide concentration (Ci) was up to 25.7% lower relative to no mulching. The maximum increases of Pn, Sc, and Tr of intercropped maize were 15.48%, 17.28%, and 23.94%, respectively, and the maximum Ci was 17.75% lower than that of monoculture maize. The maximum increase of Pn, Sc, and Tr of monoculture soybean was 24.58%, 16.90%, and 17.91%, respectively, and the maximum Ci was 13.85% lower than that of intercropped soybean. The nitrogen uptake of maize and soybean in the mulching treatment was 24.3% higher than that in the non-mulching treatment; the nitrogen uptake of intercropped maize was 34.2% higher than that of monoculture maize, and the nitrogen uptake of monoculture soybean was 15.0% higher than that of intercropped soybean. The yield of maize and soybean in the mulching treatment was 66.6% higher than that in the non-mulching treatment, the maize yield under intercropping was 15.4% higher than

that under monoculture, and the yield of monoculture soybean was 9.03% higher than that of intercropped soybean.

Discussion: The growth index and photosynthesis of crops are important parts of yield formation. The results of this study confirmed that straw mulching, intercropping, and their interaction can ultimately increase crop yield by improving crop growth, nitrogen uptake, and photosynthesis. This result can be used as the theoretical basis for the combined application of these measures in agriculture.

KEYWORDS

maize/soybean intercropping, straw mulch, crop growth, photosynthesis, N uptake, yield

1 Introduction

Agricultural production is facing increasing pressure to meet growing food demand while minimizing negative environmental impacts. The gap between grain production and food demand has widened owing to the increases in population in recent decades (Godfray et al., 2010). Therefore, identification of promising and sustainable methods to produce more grain to meet food needs is urgently required. Increasing crop yield per unit area has become an inevitable objective of agricultural production. Thus, straw mulching, a resource utilization measure that can increase crop productivity (Yin et al., 2018), and intercropping, a planting mode that can increase the land equivalent ratio (Wang L. et al., 2023), have becomes critical focuses of agricultural researchers. Intercropping is a profitable strategy that efficiently uses inputs (e.g., nutrients and water), expands agricultural diversity, and increases grain yield significantly (Qin et al., 2013). Moreover, intercropping plays a crucial role in China's grain production (Malézieux et al., 2009) and in ensuring biodiversity in a sustainable and eco-friendly manner (Lithourgidis et al., 2011). Appropriate intercropping patterns can more fully utilize agricultural resources, such as light, temperature, water, and nutrients (Hinsinger et al., 2011), and help effectively control pests and diseases. Furthermore, intercropping reduces the dependence on chemical fertilizers and pesticides in crop production, thereby lowering production costs and environmental pollution (Zhang et al., 2013).

The advantages of intercropping may depend on niche differentiation (Hector et al., 1999; Teste et al., 2014) owing to interspecific interactions (Qiao et al., 2016; Liu et al., 2022), such as nutrient complementary utilization (Li et al., 2014), and different utilization rates of light energy by different crops (Liu et al., 2017), among other factors. Under intercropping, when two crops are planted together, the competition and beneficial effects between adjacent plants will affect the growth of crops (Teste et al., 2014; Zhang et al., 2014). Positive interactions between crops increase the balance among cropping systems and enhance the economic and ecological benefits (Li et al., 2007; Ahmad et al., 2019; Hong et al., 2023). Under China's limited cultivated land resources, intercropping is a suitable method to improve land resource utilization efficiency and attain higher crop yield (Li R. et al., 2020). Therefore, intercropping of the cereal maize (*Zea mays* L.) with the legume soybean (*Glycine max* L.) offers multiple advantages, such as high land productivity, improved resource use, and decreased disease incidence, ultimately leading to higher grain yield (Iqbal et al., 2019; Chang et al., 2020). This intercropping system is enabled by the growing seasons and growth periods of maize and soybean being the same, which permits them to be harvested simultaneously, reducing the number of field operations and thereby improving production efficiency (Liu et al., 2022). When grown together, maize and soybean have a long period of overlap, a high rate of light capture, and a large photosynthetic area that can sustainably improve the light energy utilization rate of the system (Xia et al., 2013).

Straw mulching, another sustainable method of increasing agricultural effificiency, is a way of straw returning to the fifield, and it includes whole straw mulching, deep plowing, and broken mixed mulching (Khan et al., 2022a). Studies have shown that straw mulching can increase the content of organic carbon and nutrients in topsoil, improve the stability of soil aggregates (Kumar et al., 2012; Zuber et al., 2015), improve soil temperature, and enhance the suitability of the environment for crop growth (Khan et al., 2022b). Straw mulching has positive effects, including reducing soil water evaporation, increasing soil water retention and crop yield, and high-water use efficiency. It is also a widely promoted cultivation technique in arid and semi-arid areas (Liy et al., 2021). Crop residues maintain soil temperature balance, lower the maximum soil temperature, and increase soil microbial biomass and enzymatic activities (Masciandaro et al., 2004; Chen et al., 2007; Guo et al., 2013). Straw mulch application in maize cultivation decreases water evapotranspiration and soil water consumption and increases water use efficiency, resulting in higher yield and overall economic benefit (Wang L. et al., 2023). Plants perform a variety of essential functions that are critical to their survival and growth. These functions include photosynthesis, gas exchange, water transpiration, and the production of nutrients, all of which take place primarily in the leaves (Bucher et al., 2021). The crop grain yield and dry matter is derived mainly from the assimilation products of photosynthesis that occur in plant leaves (Makino & Amane, 2021), and an increase of total leaf area will prolong the functional period of leaves, which is

beneficial to the accumulation of photosynthetic products and ultimately affects crop yield (Zhang et al., 2014).

The present study investigates the effects of straw mulching and intercropping on the leaf traits, physiological characteristics, and yield of maize and soybean in Northeast China. While previous studies have examined these agronomic methods separately (Chen et al., 2007; Ahmed et al., 2018), this study focuses on the combined effects of straw mulching and intercropping on agricultural production systems. Given the close relationship between leaf traits, physiological characteristics, and crop yield, this study explores the impact of different straw mulching levels on leaf area index, plant nitrogen uptake, chlorophyll content, leaf photosynthetic characteristics, and crop yield under intercropping. The objective is to determine the optimal straw mulching amount and planting pattern to maximize yield and photosynthetic performance under combined straw mulching and intercropping. Through this investigation, the study seeks to provide technical and theoretical support for the effective combination of intercropping and straw mulching in China's agricultural production and contribute to developing the effectiveness of these practices. Ultimately, the findings of this study are intended to enhance crop productivity and grain yield in China.

2 Materials and methods

2.1 Experimental site

This experiment was carried out at the comprehensive experiment base of the College of Water Conservancy of Shenyang Agricultural University (123.57°E, 41.83°N, average altitude 44.7 m) from May to September in 2017 and 2018. The experiment base is located in the eastern part of Shenyang, which has a temperate continental monsoon climate, and the average annual rainfall is 703.4 mm. During the growth period of soybean and maize crops (May to September), the precipitation was relatively concentrated. In 2017, the precipitation during the growth period was 420.5 mm, and the total annual rainfall was 463.8 mm. In 2018, the precipitation during the growth period was 594.6 mm, and the total annual rainfall was 665.9 mm. The soil in the test area is tidal brown soil.

The key nutrient contents of the soil were as follows: total nitrogen 1.24 g kg^{-1}, available phosphorus 62.4 mg kg^{-1}, total potassium content 130.2 mg kg^{-1}, and organic matter content 33.9 g kg^{-1}. The pH was 7.14, and the electrical conductivity (EC) was 1.38 mS cm^{-1}. The soil bulk density of the 20-cm soil layer was 1.36 g cm^{-3}, and that of the 40-cm soil layer was 1.41 g cm^{-3}. The soil was evenly distributed and was a typical representative soil in this area. The field water holding rate was 30.28%, and the wilting coefficient was 18%.

2.2 Experimental design

In this experiment, a split-plot experimental design was used across three planting patterns, which were soybean monoculture (S), maize monoculture (M), and maize/soybean intercropping (I). Thesubplots had four different levels of straw mulching: 0 t ha^{-1} (M0), 4.8 t ha^{-1} (M1), 7.2 t ha^{-1} (M2), 9.6 t ha^{-1} (M3). Thus there were a total of 12 treatments, as presented in Table 1. Each treatment was set up with three replicates, for a total of 36 test plots; each test plot area was 18 m^2 (3 m × 6 m). The maize variety planted in the experiment was Dongdan 80, and the soybean variety was Dongdou 1, which both have high seed yield and great yield potential and are widely used in this area, making them particularly suitable for this study. The intercropping treatment of maize and soybean involved their seeds being planted at a ratio of 1:1, and the row spacing of maize and soybean was 0.4 m. For monoculture maize, the row spacing was 0.4 m, and the plant spacing was 0.3 m. For monoculture soybean, the row spacing was 0.4 m, and the hole spacing was 0.2 m, with two plants per hole. No additional irrigation was applied during the experiment. The only supplementary water source for the crops came from rainfall. The mulching maize straw of the previous season's crop was cut into 2- to 3-cm pieces and kept in dark and ventilated storage. During sowing, this mulching straw was shallowly buried in the 0–15 cm plough layer soil. The growth period of maize and soybean were basically the same. Soybean and maize were sown at the same time on both May 8, 2017 and May 5, 2018.

The amount of fertilizer applied was based on the specific intercropping treatment. The amount of fertilizer used in intercropping should be limited to the amount of nitrogen required by soybeans, not more than 60 kg ha^{-1} pure nitrogen (Central Agricultural Broadcasting School, 2022). Therefore, each treatment involved the application of compound fertilizer (N-P_2O_5-K_2O contents of 13%, 17%, and 15%, respectively) as base fertilizer at one-time according to the standard application of 450 kg ha^{-1}. No additional fertilizer was applied during each growth stage, and unified management measures were adopted for field crops.

TABLE 1 Experimental Treatment numbers.

Straw mulching level (t·ha^{-1})		Planting pattern		Treatment numbers
0	M0	Soybean monoculture	S	M0S
4.8	M1			M1S
7.2	M2			M2S
9.6	M3			M3S
0	M0	Maize monoculture	M	M0M
4.8	M1			M1M
7.2	M2			M2M
9.6	M3			M3M
0	M0	Maize/soybean intercropping	I	M0I
4.8	M1			M1I
7.2	M2			M2I
9.6	M3			M3I

2.3 Experimental data determination

2.3.1 Rainfall and monthly mean temperature

Precipitation and temperature data were obtained from the meteorological data observed by the Dongling hydrological station, which is 3.8 km from the experiment site. The rainfall and temperature data during the growth period of maize and soybean (May–October) are shown in Figure 1.

2.3.2 Crop growth dynamics

Three maize and soybean plants with uniform growth were selected for each plot. The height from the ground to the top of each plant was measured, and the plants were chosen to be labeled and observed every ten days. The average stem diameter was measured with a vernier caliper at each growth stage. The measurement site was the third internode of the stem base from the bottom of the plant. The plants were marked and observed every ten days.

2.3.3 Leaf area index

Three maize and soybean plants with consistent growth were selected during each growth stage. A ruler was used to measure the length and width of maize ear leaves and soybean leaves, and the width was measured at the widest part of the leaf. The leaf area per unit area in the plot was calculated, and the single leaf area and leaf area index (LAI) were calculated using equations (1) and (2).

$$S_n = \frac{L_n \times W_n \times 0.75}{10000} \quad (1)$$

where S_n is single leaf area, in m^2; l_n and W_n are the length and width of a single leaf, in cm.

$$LAI = \frac{S \bullet n}{S_L}, \quad (2)$$

where S is leaf area per plant; N is the number of plants in the plot area; S_L is the plot land area, in m^2.

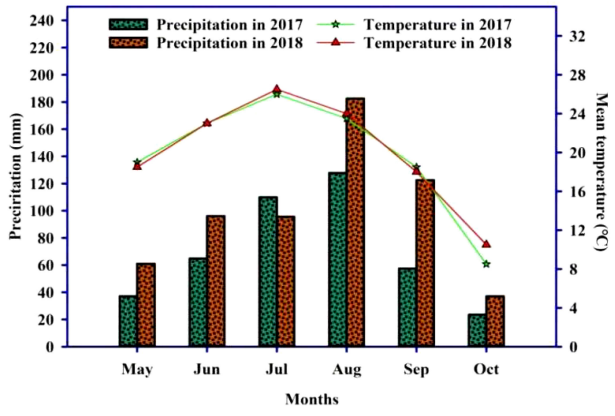

FIGURE 1
Rainfall and monthly mean temperature during maize and soybean growth period (May to October) in 2017 and 2018.

2.3.4 Chlorophyll content

The leaf chlorophyll content of crops was measured by a CCM-300 chlorophyll content measuring instrument (Opti-Sciences, Inc., Hudson, NH, USA). Three representative plants were selected in each maize and soybean monoculture plot, and three maize and three soybean plants were selected in the intercropping plot. The measurement sites were fully expanded functional leaves in the middle and upper parts of each selected plant. The average value was recorded, and the measurement time was the growth period of the crop.

2.3.5 Determination of photosynthetic parameters

In each growth stage, three maize and soybean plants with uniform growth were selected in each treatment, and the photosynthetic parameters of maize and soybean plants were measured. The photosynthetic parameters, including net photosynthetic rate (Pn), stomatal conductance (Sc), intercellular carbon dioxide concentration (Ci), and transpiration rate (Tr), were measured using the LI-6400 (LI-COR Company, Lincoln, NE, USA) portable photosynthetic instrument. To avoid any potential edge effect, in the intercropping treatment, plants were selection from among the middle row of plants for measurement. The measurement site was the ear leaf of maize plants and the third leaf of soybean plants, which were fully expanded functional leaves in the middle and upper parts of the crops, and measurements were recorded from 9:00 to 12:00 a.m. during sunny weather.

2.3.6 Crop nitrogen uptake

The crop samples for each period were collected, and a grinderfilled with maize and soybean stems, leaves, and grains was used to crush the dried plant samples. After samples were thoroughly mixed, they were transferred into a plastic sealed bag for the measurement of crop nitrogen uptake, and the N nutrient content of the plant was measured using a Kjeldahl nitrogen analyzer (KDN-520; Sayas Technology Co., Ltd., Jilin, China).

2.3.7 Yield and yield components

The two crops were harvested manually when maize and soybean had matured, and crop samples were collected from a random 2 × 2 m area for threshing and yield measurement in the monoculture area. To avoid any potential edge effect of the plot, maize and soybean crop samples were collected from the inner rows with a length of more than 2 m in the intercropping plot, and maize and soybean plants were selected for threshing and yield measurement. The grain moisture content of maize and soybean was measured using a moisture meter. The dry weight was measured after artificial threshing, and the yield per unit area was calculated. The yield of maize was finally converted to the grain yield based on 14% moisture content (dry weight), and the soybean yield was transformed based on a moisture content of 13% (dry weight). The calculation formula is dry weight = original weight × (1 - original moisture content %)/(1 - moisture content after drying %), and the yield per unit area is expressed as t ha^{-1}.

Five maize and soybean plants with consistent development were selected from each plot to measure the yield traits, including ear length, ear diameter, grain number per ear, and 100-grain weight, of maize at the end of the growing season. The yield traits, including pod number per plant, grain number per plant, grain weight per plant, and 100-grain weight, of soybean plants were also determined.

2.4 Data analysis

The data for all collected parameters were processed using Excel 2021 (Microsoft Corp., Redmond, WA, USA) and analyzed by analysis of variance (ANOVA) using the statistical software package SPSS 24 (IBM Corp., Armonk, NY, USA). To test differences among groups based on both growing seasons, the *post-hoc* least significant difference (LSD) test was applied at the $P< 0.05$ probability level. SigmaPlot (Ver.12.5, Systat Software Inc., Palo Alto, CA, USA) was used for graphing.

3 Results

3.1 Effects of straw mulching and intercropping on plant height and stem diameter of crops

The plant height of maize reached its maximum at the filling stage, and the effect of the combined treatment decreased slightly compared with the filling stage from one year to the next (Figure 2). The interaction between straw mulching and planting pattern significantly affected maize plant height at each growth stage (Table 2).

Under the same mulching level, the plant height of intercropped and monoculture maize was significantly different ($P< 0.05$). Under the M0, M1, M2, and M3 mulching levels, the plant height of intercropped maize was 6.57%, 7.76%, 9.38%, and 14.3% higher than that of monoculture maize (based on a two-year average during the whole growing season, as indicated for the results presented below unless otherwise noted), indicating that intercropping had a significant effect on maize plant height (Figure 2). The plant height of maize under M1, M2, and M3 levels was significantly higher than under M0 ($P< 0.05$). Under monoculture conditions, the plant height of M1, M2, and M3 increased by 6.29%, 10.6%, and 13.2%, respectively, compared with that of M0. Under intercropping, maize plant height increased by 7.48%, 13.6%, and 21.4%, respectively (Figure 2).

Soybean plant height reached its maximum at the filling stage, andheight at maturity decreased slightly compared with the filling stage during the two years (Figure 3). The interaction between straw mulching and planting patterns significantly affected soybean plant height at each growth stage (Table 3).

Under the same mulching level, the plant height of intercropped and monoculture soybean was significantly different ($P< 0.05$). Under the M0, M1, M2, and M3 mulching levels, the plant height of intercropped soybean decreased by 7.48%, 8.22%, 10.1%, and 17.1%, respectively, indicating that intercropping inhibited soybean plant height (Figure 3). As shown in Figure 3, the soybean plant height under M1, M2, and M3 was significantly ($P< 0.05$) higher than that under M0. Under monoculture conditions, the soybean plant height under M1, M2, and M3 increased by 6.94%, 14.7%, and 25.8%, respectively, compared with M0. Under intercropping, soybean plant height increased by 6.20%, 12.1%, and 15.5%, respectively (Figure 3).

The stem diameter of maize reachedits maximum at the filling stage, and the diameter at maturity decreased slightly compared with the fillingstage during the two years (Figure 4). Except for the seedling stage in 2018, the interaction between straw mulching and planting patterns significantly affected the stem diameter of maize at each growth stage (Table 4).

Under the same mulching level, maize's stem diameter significantly differed between intercropping and monoculture ($P<0.05$). Under the M0, M1, M2, and M3 mulching levels, the stem diameter of intercropped maize was 6.31%, 8.78%, 10.9%, and 11.7% higher than that of monoculture maize, respectively. The two-year average shows that intercropping significantly increases maize stem diameter (Figure 4). It can also be seen from the figure that the stem diameter of M1, M2, and M3 was significantly ($P< 0.05$) higher than that of M0. Under monoculture conditions, the stem diameter of maize in M1, M2, and M3 increased by 3.86%, 9.18%, and 15.9%, respectively, compared with M0. Under intercropping, stem diameter of maize increased by 6.28%, 13.9%, and 21.7%, respectively (Figure 4).

The stem diameter of soybean reachedits maximum at the filling stage, anddiameter at maturity decreased slightly compared with the filling stage during the two years (Figure 5). In addition to the seedling stage in 2018, the interaction between straw mulching and planting patterns significantly affected soybean stem diameter at each growth stage (Table 5).

The intercropped and monoculture soybean plant height significantly differed under the same mulching level ($P< 0.05$). Similar to the plant height of soybean, the stem diameter of monoculture soybean increased by 3.19%, 6.31%, 11.4%, and 12.3%, respectively, under M0, M1, M2, and M3 mulching levels, indicating that intercropping inhibited the soybean stem diameter (Figure 5). As also seen in Figure 5, the soybean stem diameter of M1, M2, and M3 was significantly ($P< 0.05$) higher than that of M0. Under monoculture conditions, the stem diameter of M1, M2, and M3 increased by 9.60%, 27.4%, and 46.1%, respectively, compared with M0. Under intercropping conditionssoybean stem diameter increased in these mulching treatments by 6.39%, 18.1%, and 34.4%, respectively, based on the two-year average (Figure 5).

3.2 Effects of straw mulching and planting patterns on crop LAI

The changes in LAI during the growth period of maize under different planting patterns and straw mulching levels are shown in Table 6; straw mulching amount, planting pattern, and their interaction significantly affected maize LAI ($P< 0.05$). The LAI of maize was significantly affected by the amount of straw mulching at

10.3389/fpls.2023.1280382

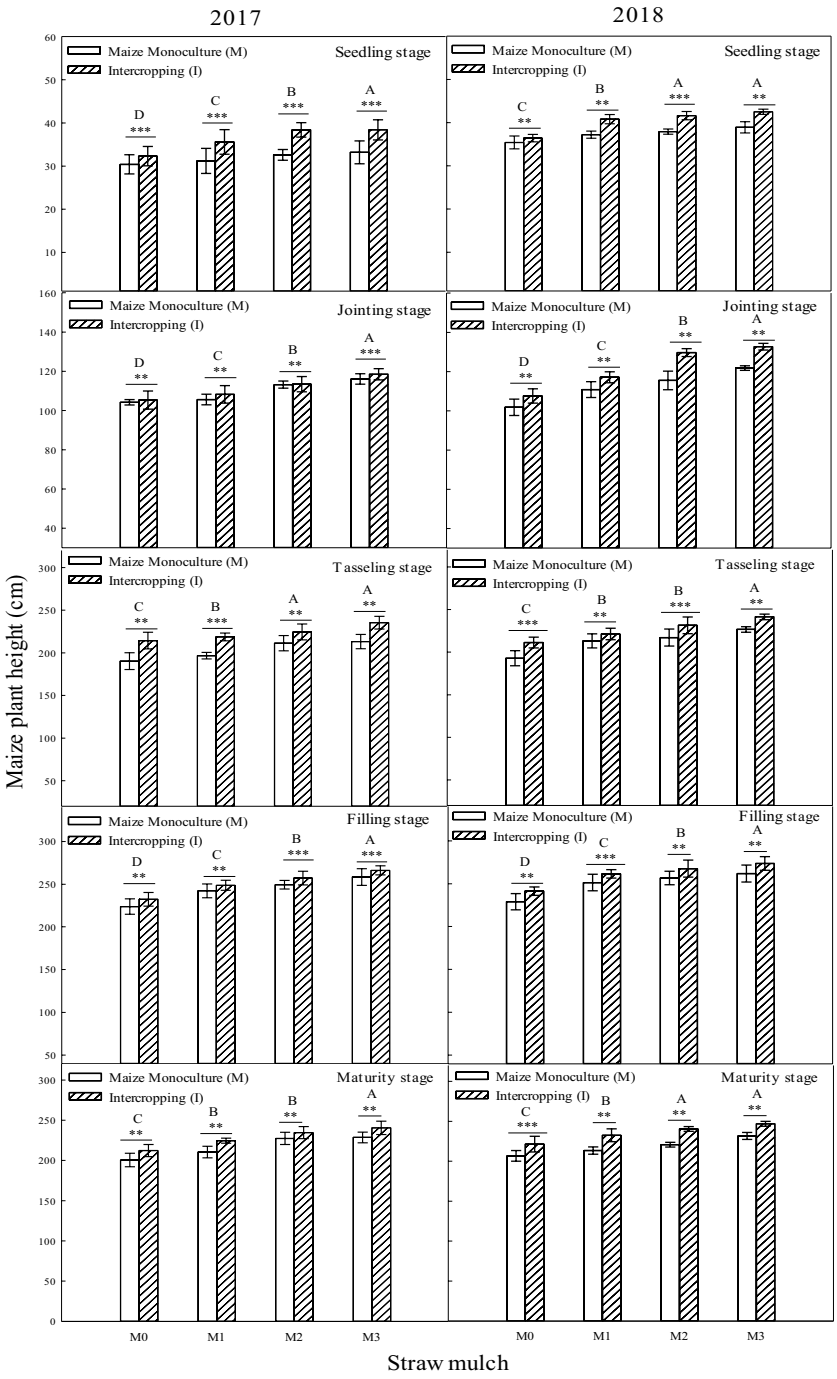

FIGURE 2
Effect of planting pattern and straw mulch on maize plant height. Values labelled with different capital letters indicate significant differences between straw mulch treatments (p< 0.05). Straw mulching levels: 0 t ha^{-1} (M0), 4.8 t ha^{-1} (M1), 7.2 t ha^{-1} (M2), 9.6 t ha^{-1} (M3). ** and *** indicate significant differences at the P < 0.01, and P < 0.001 levels, respectively.

TABLE 2 Variance analysis of planting pattern and straw mulch on maize plant height.

Year	Source of variation	Seedling stage	Jointing stage	Tasseling stage	Filling stage	Maturity stage
2017	P	315***	121**	52**	254**	134**
	M	246***	98**	122**	222**	25**
	P×M	14.6**	125.2*	84.3**	26.4**	26.4**

(Continued)

TABLE 2 Continued

Year	Source of variation	Seedling stage	Jointing stage	Tasseling stage	Filling stage	Maturity stage
2018	P	114***	56**	26**	112**	141**
	M	86***	38**	67**	64**	36**
	P×M	137**	235**	5.32**	10.6**	22.4**

The values in the table represent the F-values of the main effect and interaction term in an analysis of variance; ns means not significant; *, * *, and * * * indicate significant differences at the P< 0.05, P< 0.01, and P< 0.001 levels, respectively; P, planting pattern; M, straw mulch.

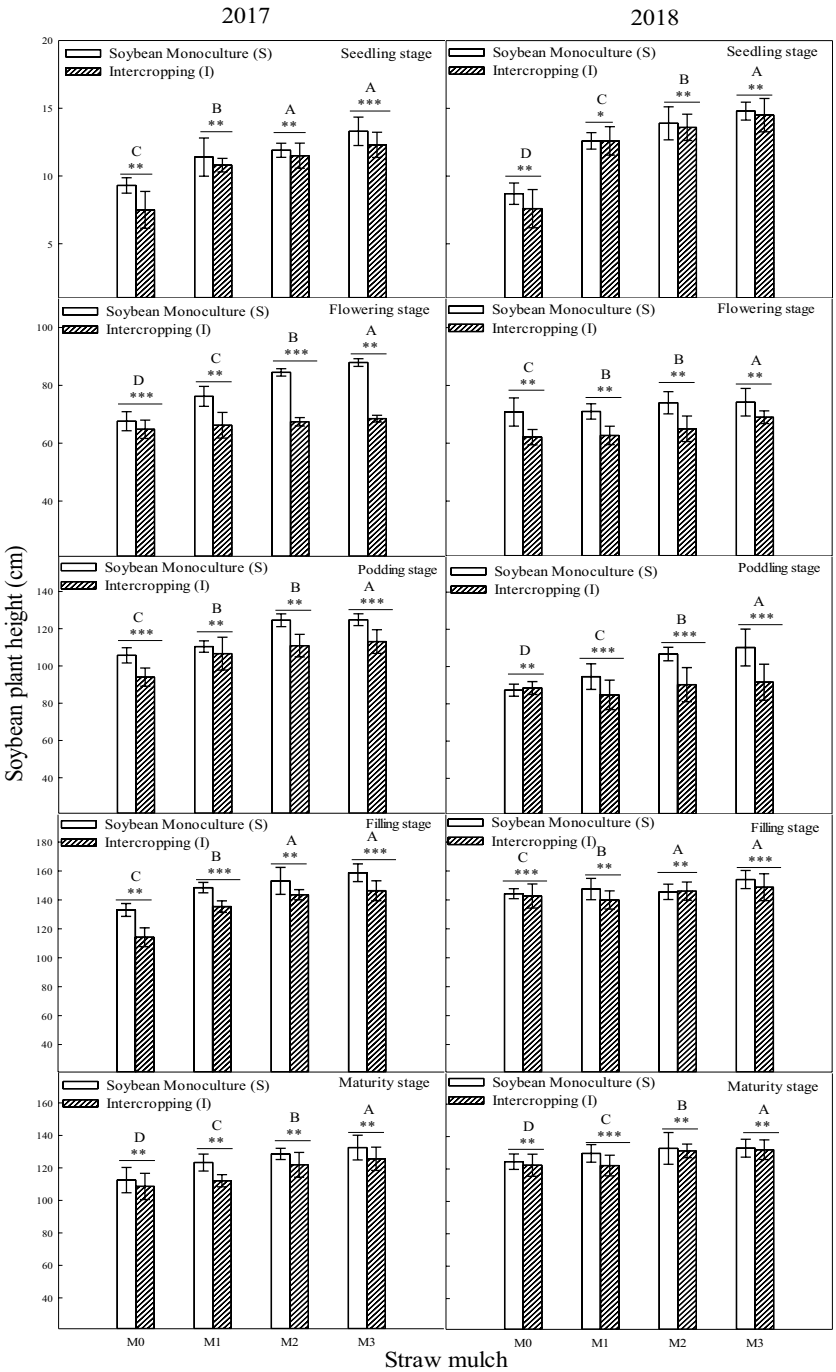

FIGURE 3
Effect of planting pattern and straw mulching on soybean plant height. Values labeled with different letters indicate significant differences between straw mulch treatments (*P*< 0.05). Straw mulching levels: 0 t ha^{-1} (M0), 4.8 t ha^{-1} (M1), 7.2 t ha^{-1} (M2), 9.6 t ha^{-1} (M3); *, ** and *** indicate significant differences at the *P* < 0.05, *P* < 0.01, and *P* < 0.001 levels, respectively.

TABLE 3 Variance analysis of straw mulch and planting pattern on soybean plant height.

Year	Source of variation	Seedling stage	Flowering stage	Podding stage	Filling stage	Maturity stage
2017	P	78**	64**	65**	31*	35**
	M	113**	121**	19*	95**	62**
	P×M	15.2**	25.5**	24.3**	16.6**	26.4**
2018	P	56**	133**	224**	112**	99**
	M	8.9**	214**	366**	98**	76**
	P×M	11.5**	12.3**	15.2*	5.68*	32.6**

The values in the table represent the F-value of the interaction term in an analysis of variance; ns means not significant; *, * *, and * * * indicate significant differences at the P< 0.05, P< 0.01, and P< 0.001 levels, respectively; P, planting pattern; M, straw mulch.

each growth stage, with higher mulching levels consistently associated with higher LAI (Table 6). The LAI of maize increased significantly under intercropping. The LAI of maize increased by 5.73%, 5.99%, 7.95%, and 10.5%across the four straw mulching levels from M0 to M3, respectively, throughout the whole growth periodbased on two-year averages. The increasein LAI of intercropped maize was the greatest compared with that of monoculture maize under M3 treatment.

As shown in Table 7, straw mulching amount, planting pattern, and their interaction significantly affected soybean LAI ($P< 0.05$). The LAI of soybean was significantly affected by the amount of straw mulching at each growth stage, with LAI consistently increasing with mulching amount. The soybean LAIunder mulching treatments M1, M2, and M3 were 10.8%, 21.8%, and 38.7% higher than that under non-mulching treatment M0, respectively, under intercroppingbased on the two-year averagethroughout the whole growth period; the LAI of soybean under mulching treatments M1, M2, and M3 was 11.7%, 23.2% and 41.6% higher than M0 in monoculture, respectively. The planting pattern significantly affected soybean LAI ($P< 0.05$). Under the four straw mulching levels from M0 to M3, the LAI of monoculture soybean was 6.00%, 6.87%, 7.21%, and 8.24% higher than that of intercropped soybean, respectively. The increase of LAI in intercropped soybean relative to monoculture soybean was the largest under M3 treatment.

3.3 Effects of straw mulching and planting patterns on crop chlorophyll content

It can be seen from Figure 6 that the chlorophyll content during the growth period of maize was significantly affected by straw mulching and planting pattern ($P< 0.05$). As mulching level increased from M0 to M3, chlorophyll content of maize also increased. Under intercropping, the chlorophyll content of maize under mulching treatments M1 to M3 was 3.18%, 6.27%, and 9.59% higher thanM0, respectively. The chlorophyll content of maize under mulching treatments M1, M2, and M3 were 3.00%, 5.88% and 8.71% higher than M0 in monoculture, respectively. The planting pattern significantly affected the chlorophyll content of maize ($P< 0.05$). Under the four straw mulching levels from M0 to M3, the chlorophyll content of monoculture maize was 9.26%, 9.45%, 9.66%, and 10.2% higher than that of intercropped maize. The chlorophyll content of intercropped maize increased the most compared with monoculture maize under M3 treatment.

It can be seen from Figure 7 that the chlorophyll content during the growth period of soybean was significantly affected by both straw mulching amount and planting pattern ($P< 0.05$). As the mulching amount increased from M0 to M3, the chlorophyl content of soybean consistently increased. Under intercropping, the chlorophyll content of soybean under mulching treatments M1 to M3 was 7.61%, 17.3%, and 24.0% higher than M0, respectively (based on two-year averages during the whole growth period). The chlorophyll content of soybean under mulching treatments M1, M2, and M3 was 7.19%, 14.7%, and 18.7% higher than M0 in monoculture. The planting pattern significantly affected the chlorophyll content of soybean ($P< 0.05$). Under the four straw mulching levels from M0 to M3, the chlorophyll content of monoculture soybean was 12.7%, 13.1%, 15.3%, and 17.7% higher than that of intercropped soybean. The chlorophyll content of intercropped soybean increased the most compared with that of monoculture soybean under M3 treatment.

3.4 Effects of straw mulching and intercropping on crop photosynthesis

As shown in Figures 8, 9, straw mulching and planting patterns significantly affect maize photosynthetic parameters. The two years of results showed that intercropping significantly affected the photosynthetic characteristics of maize ($P< 0.05$).

Based on the average results from the two years of intercropped maize, under mulching treatments M1, M2, and M3. Pn was 3.64%, 11.3%, and 16.4% higher, Sc was 7.58%, 27.3%, and 43.9% higher, Tr was 14.8%, 27.6%, and 44.5% higher, and Ci was 10.9%, 18.7%, and 25.7% lower, respectively, relative to the M0 treatment. For maize monoculture, under mulching treatments M1, M2, and M3, Pn was 3.23%, 7.83%, and 11.4% higher, Sc was 6.72%, 22.7%, and 36.1% higher, Tr was 8.81%, 19.1%, and 28.8% higher, and Ci was 8.64%, 15.5%, and 20.6% lower, respectively, relative to the M0 treatment.

Straw mulching significantly affected the photosynthetic characteristics of maize ($P< 0.05$). Under the four straw mulching levels from M0 to M3 for intercropped maize, Pn was 10.6%, 11.0%, 14.1%, and 15.5% higher, Sc was 10.9%, 11.8%, 15.1%, and 17.3% higher, Tr was 10.5%, 16.6%, 18.3%, and 23.9% higher, and Ci was

10.3389/fpls.2023.1280382

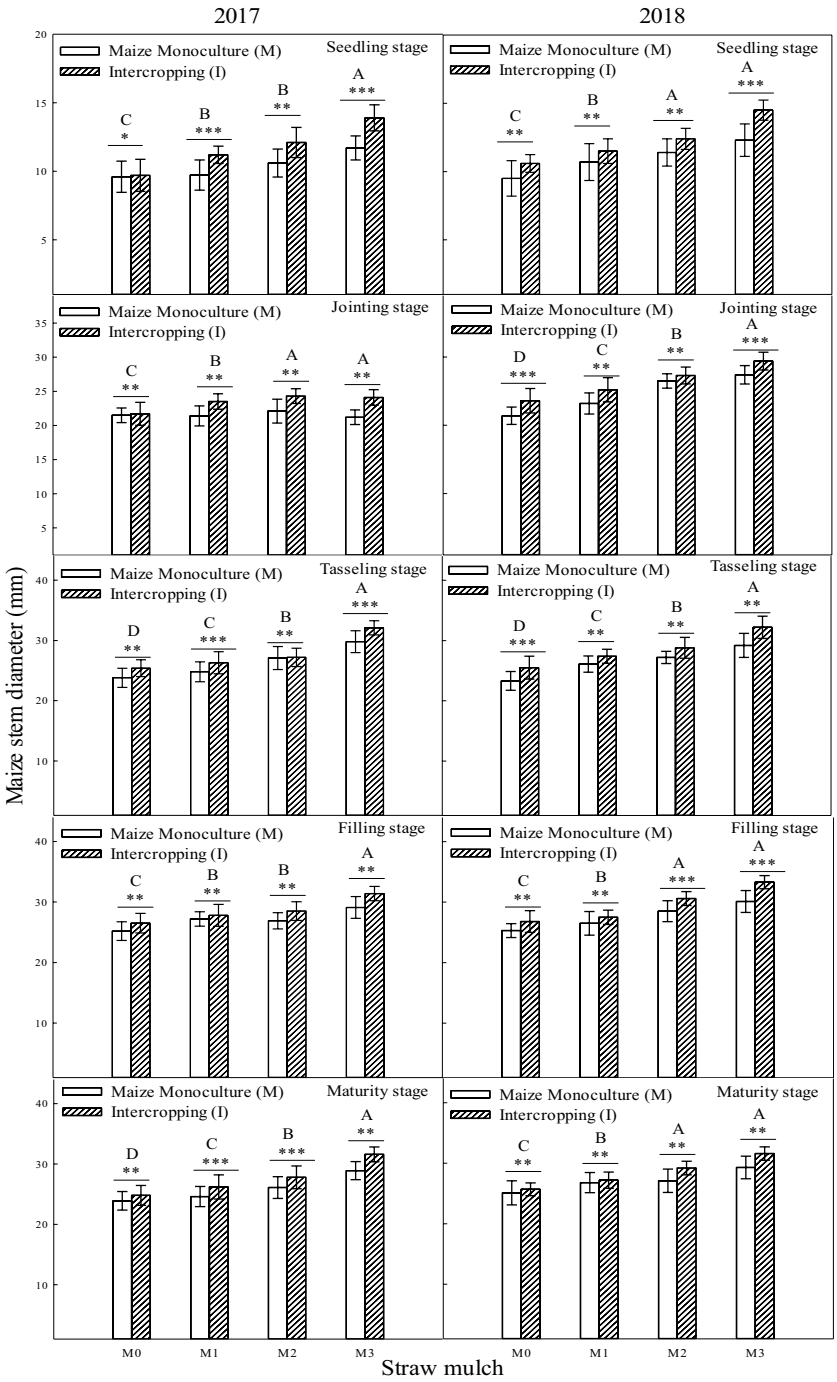

FIGURE 4
Effect of straw mulch and planting pattern on stem diameter of maize. Bars labeled with different capital letters indicate significant differences between straw mulch treatments ($P< 0.05$). Straw mulching levels: 0 t ha^{-1} (M0), 4.8 t ha^{-1} (M1), 7.2 t ha^{-1} (M2), 9.6 t ha^{-1} (M3). *, **, and *** indicate significant differences at the $P< 0.05$, $P< 0.01$, and $P< 0.001$ levels, respectively.

TABLE 4 Variance analysis of straw mulch and planting pattern on stem diameter of maize.

Year	Source of variation	Seedling stage	Jointing stage	Tasseling stage	Filling stage	Maturity stage
2017	P	115**	253**	241**	67**	200**
	M	10*	178**	312**	86**	142**
	P×M	11.2**	13.7**	7.26*	6.18*	8.35*

(Continued)

TABLE 4 Continued

Year	Source of variation	Seedling stage	Jointing stage	Tasseling stage	Filling stage	Maturity stage
2018	P	35**	266**	25**	122**	162**
	M	96**	232**	48**	97**	213**
	P×M	0.27ns	1044***	12.4**	6.8*	14.2**

The values in the table represent the F-values of the interaction term in an analysis of variance; ns means not significant; *, * *, and * * * indicate significant differences at the P< 0.05, P< 0.01, and P< 0.001 levels, respectively; P, planting pattern; M, straw mulch.

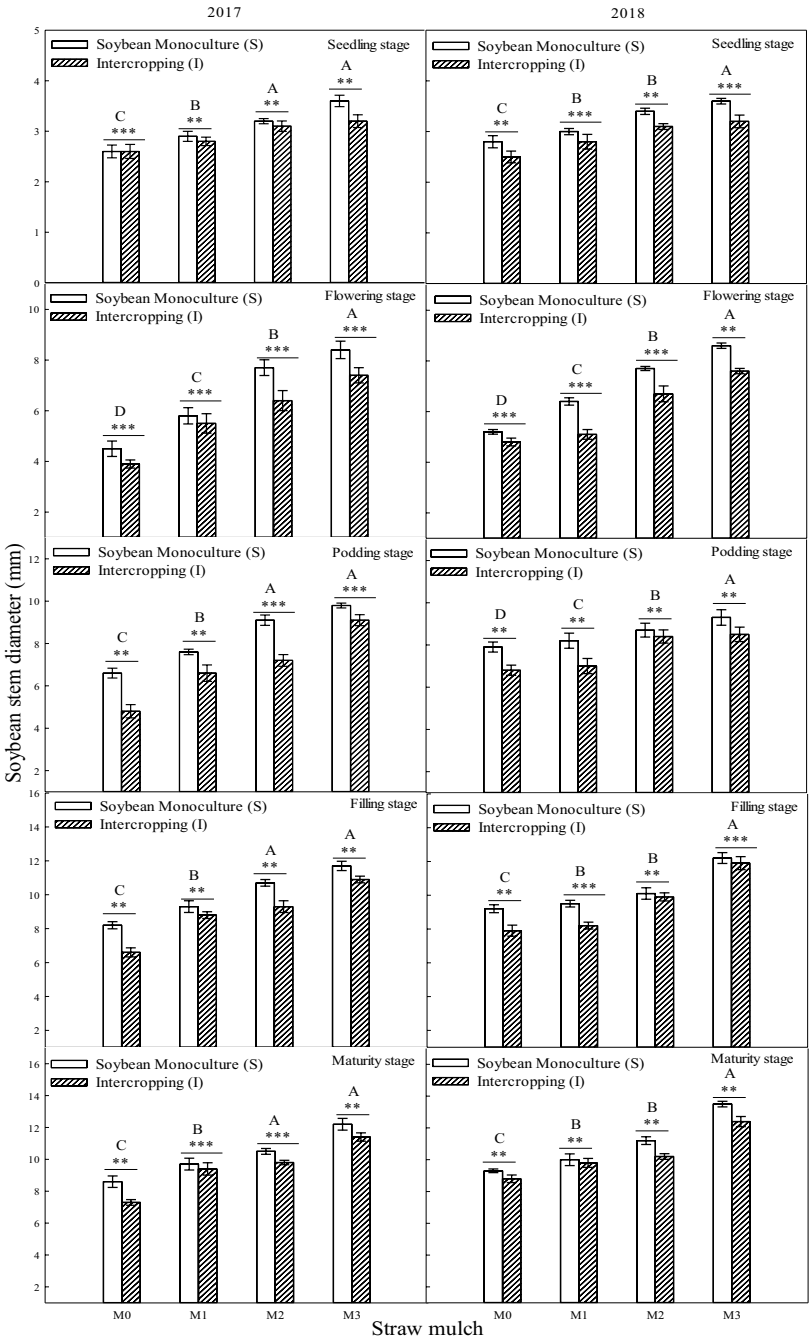

FIGURE 5
Effect of straw mulch and planting pattern on stem diameter of soybean. Bars labeled with different capital letters indicate significant differences between straw mulch treatments (*P*< 0.05). Straw mulching levels: 0 t ha^{-1} (M0), 4.8 t ha^{-1} (M1), 7.2 t ha^{-1} (M2), 9.6 t ha^{-1} (M3). ** and *** indicate significant differences at the *P* < 0.01, and *P* < 0.001 levels, respectively.

TABLE 5 Variance analysis of straw mulch and planting pattern on steam diameter of soybean.

Year	Source of variation	Seedling stage	Flowering stage	Podding stage	Filling stage	Maturity stage
2017	P	108**	332***	86**	122**	35**
	M	34**	278***	154**	57**	61**
	P×M	12.3**	8.77**	5.69*	5.22*	9.28**
2018	P	132**	52	95**	276**	43**
	M	69**	168	37**	164**	251**
	P×M	0.46ns	351**	2.31*	4.6*	13.2**

The values in the table represent the F-values of the interaction term in an analysis of variance; ns means not significant; *, * *, and * * * indicate significant differences at the P< 0.05, P< 0.01, and P< 0.001 levels, respectively; P, planting pattern; M, straw mulch.

12.0%, 14.2%, 15.3%, and 17.8% lower, respectively relative to monoculture maize.

As shown in Figures 10, 11, straw mulching and planting patterns significantly affected soybean photosynthetic parameters. The two years of results showed that intercropping had a significant effect on the photosynthetic characteristics of soybean ($P< 0.05$). For intercropped soybean, under mulching treatments M1, M2, and M3, Pn was 11.9%, 22.5%, and 35.0% higher, Sc was 7.96%, 15.9%, and 25.7% higher, Tr was 8.54%, 23.0%, and 35.1% higher, and Ci was 3.13%, 6.38%, and 10.8 lower, respectively relative to M0. For

TABLE 6 Effect of planting pattern and straw mulch treatments on maize leaf area index (LAI).

Growth stage	Treatment	2017			2018		
		Monoculture	Intercropping	Mean	Monoculture	Intercropping	Mean
Seedling	M0	0.49 ± 0.06b	0.51 ± 0.04a	0.50D	0.52 ± 0.07b	0.53 ± 0.08a	0.53D
	M1	0.53 ± 0.03b	0.54 ± 0.06a	0.54C	0.56 ± 0.03b	0.60 ± 0.08a	0.58C
	M2	0.56 ± 0.04b	0.58 ± 0.12a	0.57B	0.59 ± 0.04b	0.62 ± 0.04a	0.61B
	M3	0.63 ± 0.02b	0.65 ± 0.07a	0.64A	0.63 ± 0.07b	0.65 ± 0.01a	0.64A
Jointing	M0	0.93 ± 0.09b	1.18 ± 0.16a	1.06D	1.13 ± 0.13b	1.27 ± 0.08a	1.20C
	M1	1.13 ± 0.32b	1.63 ± 0.04a	1.38C	1.93 ± 0.18b	1.52 ± 0.33a	1.73B
	M2	1.38 ± 0.16b	1.82 ± 0.06a	1.60B	1.87 ± 0.12b	1.71 ± 0.23a	1.79B
	M3	1.75 ± 0.08b	1.86 ± 0.10a	1.81A	2.11 ± 0.13b	1.97 ± 0.17a	2.04A
Tasseling	M0	4.61 ± 0.13b	4.83 ± 0.08a	4.72D	4.43 ± 0.03b	4.59 ± 0.13a	4.51D
	M1	4.76 ± 0.24b	5.22 ± 0.21a	4.99C	4.92 ± 0.28b	5.29 ± 0.18a	5.11C
	M2	5.12 ± 0.15b	5.52 ± 0.24a	5.32B	5.00 ± 0.18b	5.48 ± 0.27a	5.24B
	M3	5.39 ± 0.38b	6.09 ± 0.16a	5.74A	5.69 ± 0.54b	6.38 ± 0.13a	6.04A
Filling	M0	4.15 ± 0.19b	4.30 ± 0.08a	4.23C	4.09 ± 0.40b	4.18 ± 0.11a	4.14D
	M1	4.48 ± 0.28b	4.55 ± 0.35a	4.52B	4.47 ± 0.31b	4.68 ± 0.31a	4.58C
	M2	4.60 ± 0.13b	4.81 ± 0.12a	4.71A	4.77 ± 0.23b	4.87 ± 0.10a	4.82B
	M3	4.61 ± 0.22b	5.32 ± 0.33a	4.97A	5.15 ± 0.20b	5.61 ± 0.25a	5.38A
Maturity	M0	2.43 ± 0.21b	2.68 ± 0.08a	2.56D	2.53 ± 0.12b	2.69 ± 0.04a	2.61C
	M1	2.75 ± 0.03b	2.9 ± 0.05a	2.83C	2.83 ± 0.12b	3.13 ± 0.05a	2.98C
	M2	3.18 ± 0.29b	3.42 ± 0.05a	3.30B	3.12 ± 0.18b	3.76 ± 0.17a	3.44B
	M3	3.37 ± 0.09b	3.86 ± 0.08a	3.62A	3.80 ± 0.26b	4.21 ± 0.06a	4.01A
ANOVA	P	329.8**	244.8**		58.8**	122**	
	M	422.3**	115.8**		124**	16.8**	
	P×M	38.8**	24.3**		575.3**	174.5**	

Values labeled with different capital letters indicate significant differences in maize LAI between different amounts of straw mulching (P< 0.05), while different lowercase letters indicate significant differences in maize LAI between intercropping and monoculture (P< 0.05). Straw mulching levels: 0 t ha^{-1} (M0), 4.8 t ha^{-1} (M1), 7.2 t ha^{-1} (M2), 9.6 t ha^{-1} (M3). * * indicate significant differences at the P< 0.01 level.

10.3389/fpls.2023.1280382

TABLE 7 Effect of planting pattern and straw mulch treatments on soybean leaf area index (LAI).

Growth stage	Treatment	2017			2018		
		Monoculture	Intercropping	Mean	Monoculture	Intercropping	Mean
Seedling	M0	0.48 ± 0.09a	0.46 ± 0.11b	0.47C	0.52 ± 0.07a	0.48 ± 0.08b	0.50D
	M1	0.55 ± 0.13a	0.50 ± 0.05b	0.53C	0.58 ± 0.06a	0.53 ± 0.08b	0.56C
	M2	0.60 ± 0.01a	0.56 ± 0.12b	0.58B	0.64 ± 0.05a	0.58 ± 0.07b	0.61B
	M3	0.72 ± 0.03a	0.62 ± 0.06b	0.67A	0.78 ± 0.04a	0.65 ± 0.09b	0.72A
Flowering	M0	0.72 ± 0.22a	0.70 ± 0.02b	0.71D	0.82 ± 0.15a	0.78 ± 0.12b	0.80D
	M1	0.81 ± 0.42a	0.78 ± 0.04b	0.80C	0.98 ± 0.22a	0.88 ± 0.29b	0.93C
	M2	0.89 ± 0.33a	0.84 ± 0.23b	0.87B	1.06 ± 0.14a	0.97 ± 0.19b	1.02B
	M3	0.97 ± 0.19a	0.94 ± 0.21b	0.96A	1.15 ± 0.16a	1.07 ± 0.15b	1.11A
Podding	M0	0.88 ± 0.21a	0.80 ± 0.18b	0.84D	0.91 ± 0.07a	0.88 ± 0.14b	0.90D
	M1	0.93 ± 0.28a	0.91 ± 0.15b	0.92C	0.99 ± 0.05a	0.93 ± 0.18b	0.96C
	M2	1.02 ± 0.28a	0.99 ± 0.18b	1.01B	1.16 ± 0.05a	1.08 ± 0.25b	1.12B
	M3	1.34 ± 0.23a	1.23 ± 0.15b	1.29A	1.38 ± 0.21a	1.29 ± 0.17b	1.34A
Filling	M0	0.80 ± 0.18a	0.75 ± 0.11b	0.78D	0.92 ± 0.15a	0.88 ± 0.05b	0.90C
	M1	0.85 ± 0.28a	0.80 ± 0.22b	0.83C	0.99 ± 0.18a	0.96 ± 0.36b	0.98B
	M2	0.90 ± 0.18a	0.88 ± 0.25b	0.89B	1.11 ± 0.29a	1.00 ± 0.16b	1.06A
	M3	1.00 ± 0.23a	0.96 ± 0.28b	0.98A	1.18 ± 0.16a	1.11 ± 0.52b	1.15A
Maturity	M0	0.56 ± 0.17a	0.52 ± 0.09b	0.54C	0.63 ± 0.18a	0.58 ± 0.37b	0.61D
	M1	0.69 ± 0.31a	0.61 ± 0.27b	0.65B	0.72 ± 0.19a	0.67 ± 0.28b	0.70C
	M2	0.75 ± 0.11a	0.69 ± 0.15b	0.72B	0.79 ± 0.15a	0.73 ± 0.19b	0.76B
	M3	0.85 ± 0.18a	0.78 ± 0.28b	0.82A	0.88 ± 0.26a	0.82 ± 0.18b	0.85A
ANOVA	P	228.01**	421.35**		526.8**	172.36**	
	M	1132.42**	1243.2**		1128.3**	520.65**	
	P×M	35.96**	543.9**		135.64**	70.25**	

Values labeled with different capital letters indicate significant differences in soybean LAI between different amounts of straw mulching (P< 0.05), while different lowercase letters indicate significant differences in soybean LAI between intercropping and monoculture (P< 0.05). Straw mulching levels: 0 t ha^{-1} (M0), 4.8 t ha^{-1} (M1), 7.2 t ha^{-1} (M2), 9.6 t ha^{-1} (M3). * * indicate significant differences at the P < 0.01 level.

monoculture soybean, under these same mulching treatments, Pn was 18.0%, 32.4%, and 51.6% higher, Sc was 12.0%, 25.6%, and 41.9% higher, Tr was 9.17%, 26.0%, and 46.6% higher, and Ci was 6.73%, 12.4%, and 19.8% lower, respectively, relative to M0.

Straw mulching had a significant effect on the photosynthetic characteristics of soybean ($P< 0.05$). Under the four straw mulching levels from M0 to M3 in soybean monoculture, Pn was 11.0%, 17.0%, 19.9%, and 24.6% higher, Sc was 3.54%, 7.38%, 12.2%, and 16.9% higher, Tr was 8.66%, 9.29%, 11.3%, and 17.9% higher, and Ci was 4.14%, 7.71%, 10.3%, and 13.9% lower, respectively, relative to intercropped soybean.

3.5 Effects of straw mulching on nitrogen uptake in maize/soybean intercropping

This study investigated and analyzed the impact of straw mulching amount, planting pattern, and their interaction on the nitrogen uptake of maize. As shown in Table 8, all three factors had significant effects on the nitrogen uptake of maize ($P< 0.05$). Notably, the amount of straw mulching significantly impacted the nitrogen uptake of maize.Under intercropping, the nitrogen uptake of soybean under mulching treatments M1, M2, and M3 were 10.8%, 20.4%, and 24.3% higher than M0. In monoculture, the nitrogen uptake of soybean under these mulching treatments was 4.81%, 9.84%, and 22.0% higher than M0, respectively (Figure 12). Additionally, intercropping conditions positively influenced the nitrogen uptake of maize, leading to a significant increase of 22.4%, 29.5%, 34.2%, and 24.8% across all four straw mulching levels (M0 to M3, respectively) compared to monoculture maize over the two years. Notably, the highest nitrogen uptake was observed for intercropped maize under the M2 treatment.

As shown in Figure 13, the nitrogen uptake of soybean was significantly affected by both straw mulching and planting patterns ($P< 0.05$). The amount of straw mulching significantly affected the nitrogen uptake of soybean plants, and the nitrogen uptake

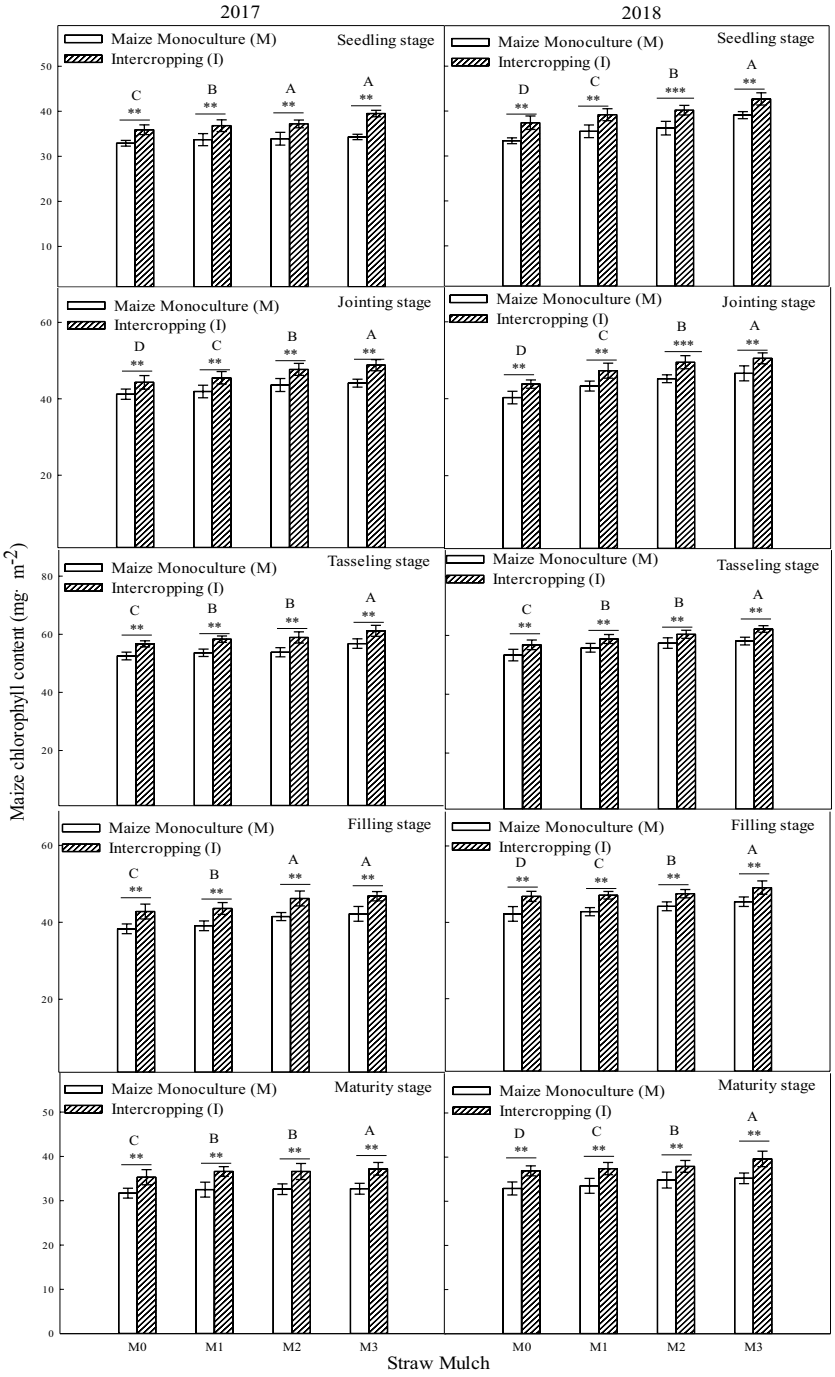

FIGURE 6
Effects of straw mulching and planting patterns on chlorophyll content of maize at different growth stages. Bars labeled with different capital letters indicate significant differences between straw mulch treatments ($P< 0.05$). Straw mulching levels: 0 t ha^{-1} (M0), 4.8 t ha^{-1} (M1), 7.2 t ha^{-1} (M2), 9.6 t ha^{-1} (M3). ** and *** indicate significant differences at the $P < 0.01$, and $P < 0.001$ levels, respectively.

consistently increased with increased mulching. The nitrogen uptake of soybean under mulching treatments M1, M2, and M3 was 10.7%, 12.9%, and 21.0% higher, respectively, thanM0 in intercropping based on two-year averages. The nitrogen uptake of soybean under these mulching treatments was 11.1%, 18.1%, and 23.2% higher, respectively, thanM0, based on the two-year averages in monoculture. The planting pattern significantly affected the nitrogen uptake of soybean ($P< 0.05$). Under the four straw mulching levels from M0 to M3, the nitrogen uptake of monoculture soybean was 9.96%, 10.3%, 15.0%, and 11.9% higher than under intercropping based on two-year averages, respectively.

As seen in Figure 14, the total nitrogen uptake of the entire intercropping system consistently increased with thestraw mulching amount, reaching its maximum value under M3 treatment, which

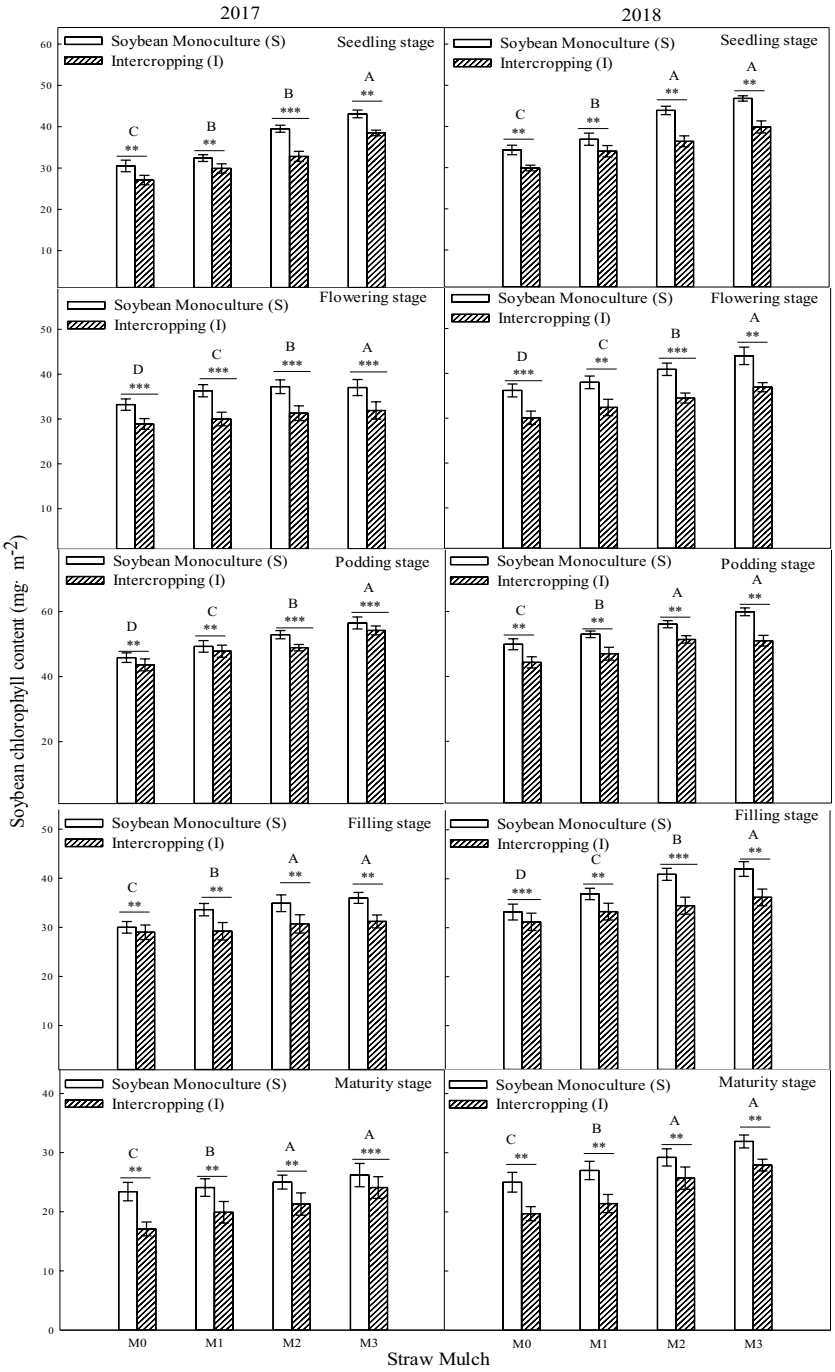

FIGURE 7
Effects of straw mulching and planting patterns on chlorophyll content of soybean at different growth stages. Bars labeled with different capital letters indicate significant differences between straw mulch treatments ($P< 0.05$). Straw mulching levels: 0 t ha^{-1} (M0), 4.8 t ha^{-1} (M1), 7.2 t ha^{-1} (M2), 9.6 t ha^{-1} (M3). ** and *** indicate significant differences at the $P < 0.01$, and $P < 0.001$ levels, respectively.

was significantly higher than that of the other three treatments. Under the four straw mulching treatments M0–M3, intercropping significantly increased nitrogen uptake by 9.66%, 13.2%, 14.2%, and 10.3%, respectively, compared with monoculture based on two-year averages. Under M2 treatment, the difference between monoculture and intercropping was the largest. As seen in Table 8, the straw mulching amount and planting pattern had a significant effect on the total nitrogen absorption of the system ($P< 0.05$).

3.6 Effects of straw mulching and intercropping on crop yield and yield-related traits

As shown in Figure 15, maize yield and its components were significantly affected by straw mulching and planting patterns ($P< 0.05$). Under the four straw mulching levels, the yield components of intercropped maize were significantly higher than those of

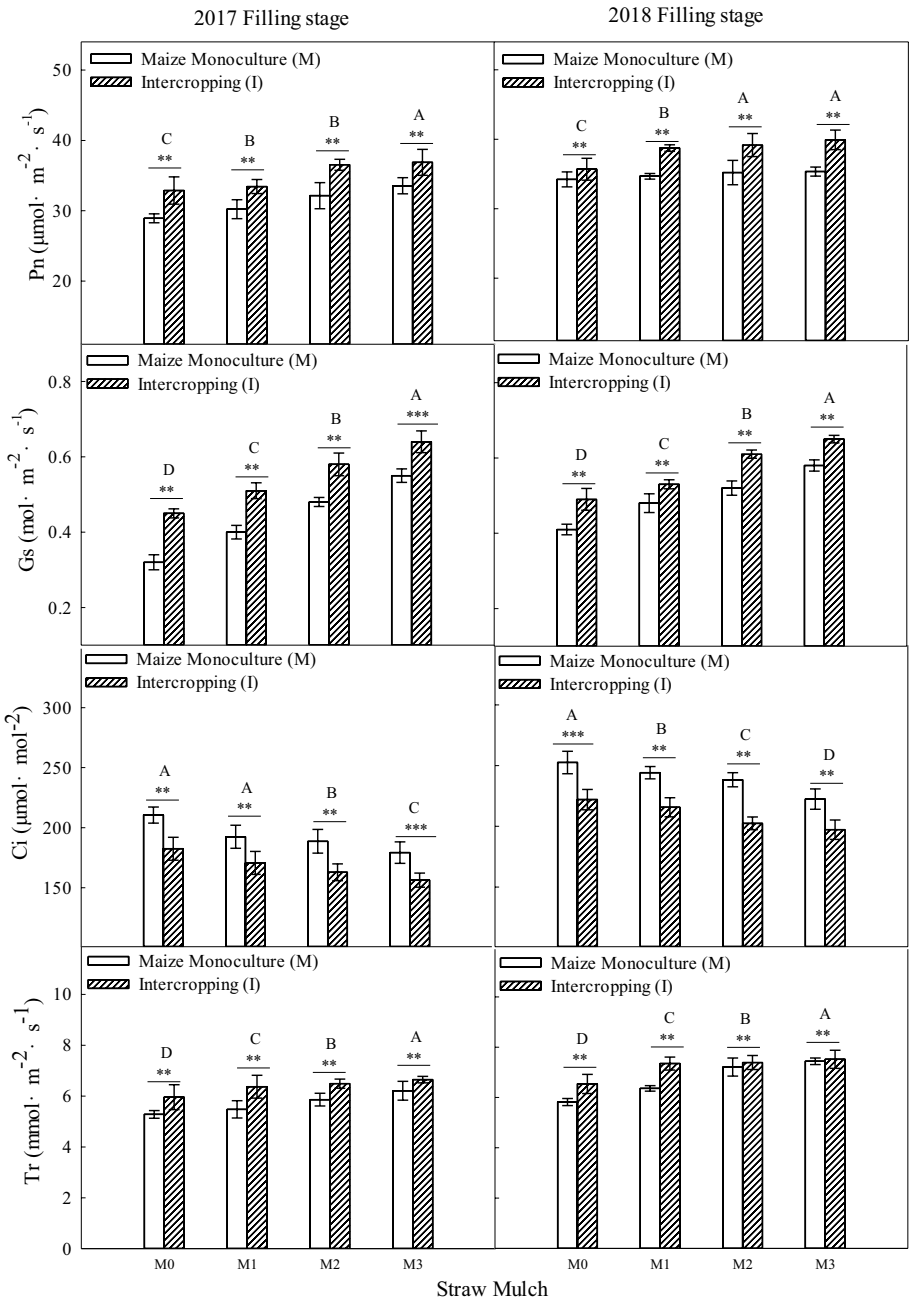

FIGURE 8
Effects of straw mulching and intercropping on maize photosynthesis at the filling stage. Bars labeled with different capital letters indicate significant differences in each photosynthetic parameter between straw mulch treatments ($P< 0.05$). Straw mulching levels: 0 t ha^{-1} (M0), 4.8 t ha^{-1} (M1), 7.2 t ha^{-1} (M2), 9.6 t ha^{-1} (M3). **, and *** indicate significant differences at the $P < 0.01$, and $P < 0.001$ levels, respectively. Pn, net photosynthetic rate; Sc, stomatal conductance; Tr, transpiration rate; Ci, intercellular carbon dioxide concentration.

monoculture maize ($P< 0.05$). For intercropped maize, under the four straw mulching levels from M0 to M3, tassel length was 8.50%, 11.2%, 13.8%, and 14.1% higher, tassel diameter was 5.16%, 10.0%, 12.7%, and 19.7% higher, tassel grain number was 6.65%, 7.27%, 10.6%, and 14.90% higher, 100-grain weight was 6.02%, 9.93%, 11.8%, and 16.3% higher, and yield was 10.1%, 10.7%, 13.0% and 15.4% higher, respectively, than that of monoculture maize based on two-year averages.

Straw mulching significantly affected maize yield and its components ($P< 0.05$). Based on the results of the two years, the tassel length, tassel diameter, tassel grain number, 100-grain weight, and yield of maize each consistently increased with the increase of straw mulching under intercropping and monoculture.

It can be seen from Figure 16 that soybean yield and its components were significantly affected by straw mulching and planting patterns ($P< 0.05$). Under the four straw mulching levels,

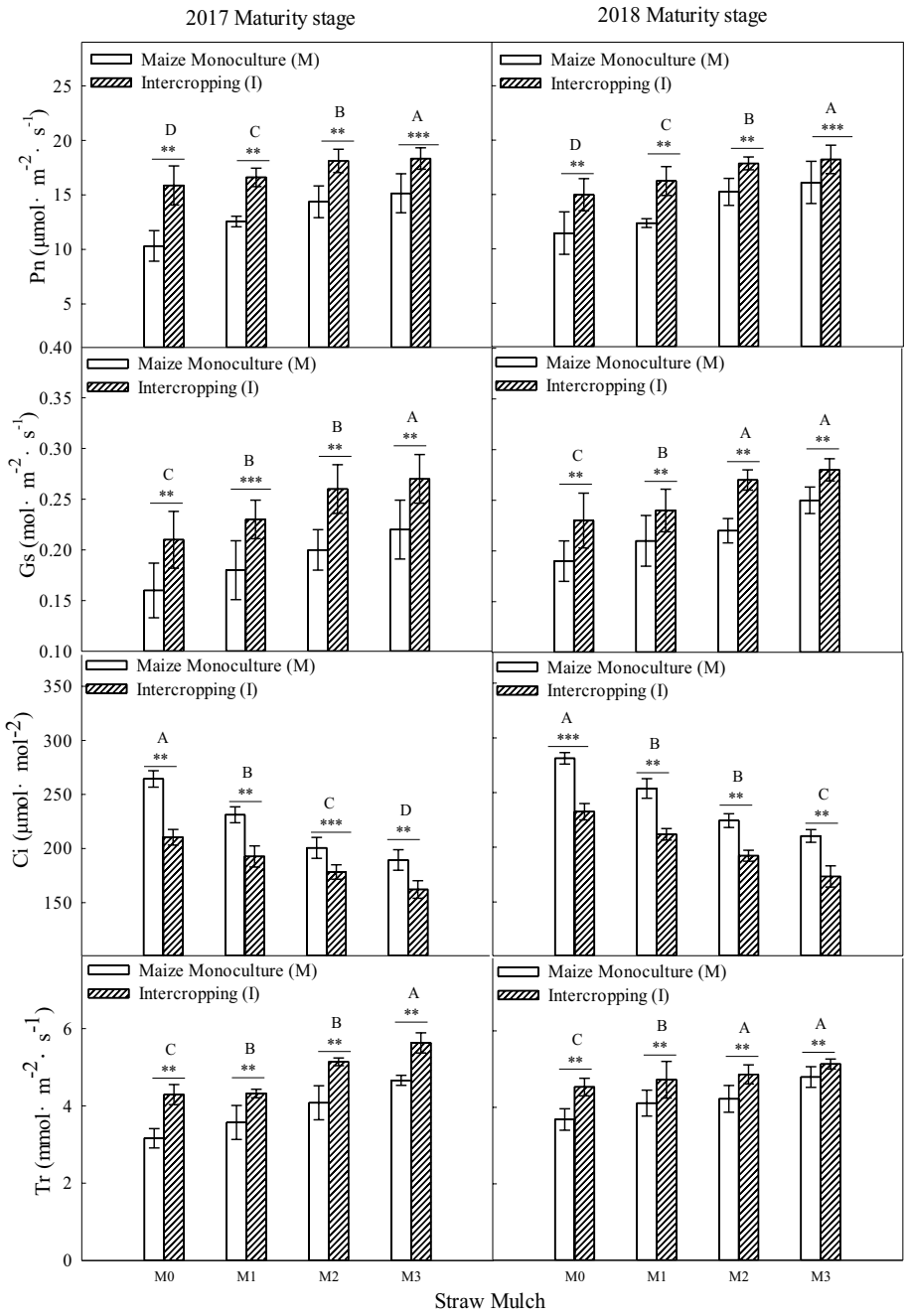

FIGURE 9
Effects of straw mulching and intercropping on maize photosynthesis at maturity. Bars labeled with different capital letters indicate significant differences in each photosynthetic parameter between straw mulch treatments ($P< 0.05$). Straw mulching levels: 0 t ha^{-1} (M0), 4.8 t ha^{-1} (M1), 7.2 t ha^{-1} (M2), 9.6 t ha^{-1} (M3). ** and *** indicate significant differences at the $P < 0.01$, and $P < 0.001$ levels, respectively. Pn, net photosynthetic rate; Sc, stomatal conductance; Tr, transpiration rate; Ci, intercellular carbon dioxide concentration.

the yield components of monoculture soybean were considerably higher than those of intercropped soybean ($P< 0.05$). For monoculture soybean, under the four straw mulching levels from M0 to M3, per plant pod number was 6.45%, 8.50%, 10.1%, and 15.9% higher, per plant grain number was 4.05%, 8.48%, 9.09%, and 10.2% higher, per plant grain weight was 9.06%, 9.59%, 11.5%, and 12.8% higher, 100-grain weight was 3.37%, 8.84%, 9.59%, and 15.8% higher, and yield was 5.26%, 6.19%, 8.77%, and 9.03%higher, respectively, than that of intercropped soybean based on two-year averages.

Straw mulching significantly affected soybean yield and its components ($P< 0.05$). Based on the results of the two years, per plant pod number, per plant grain number, per plant grain weight, 100-grain weight, and yield of soybean increasedconsistently with the straw mulching amount under both intercropping and monoculture.

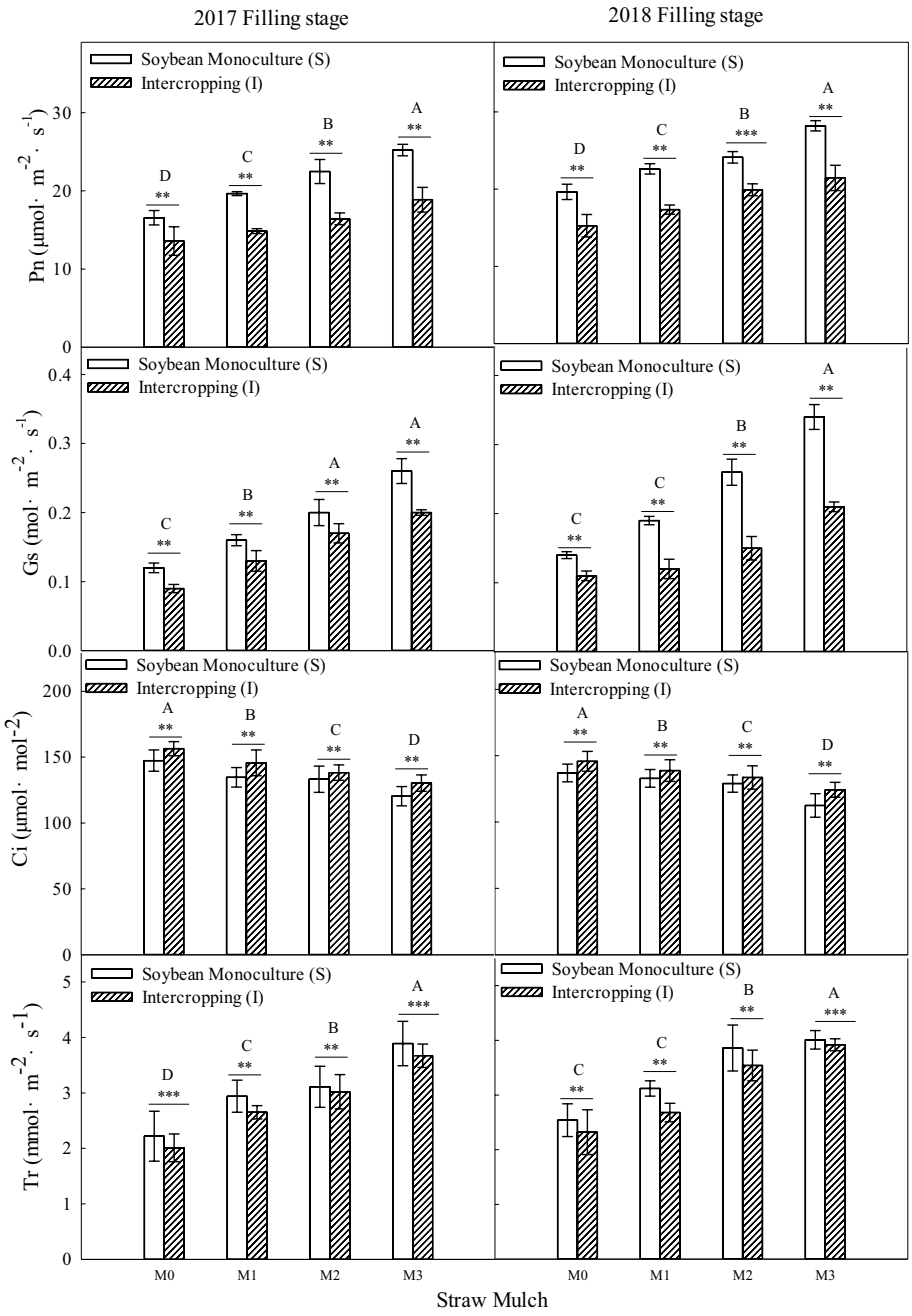

FIGURE 10
Effects of straw mulching and intercropping on soybean photosynthesis at the filling stage. Bars labeled with different capital letters indicate significant differences in each photosynthetic parameter between straw mulch treatments (P< 0.05). Straw mulching levels: 0 t ha^{-1} (M0), 4.8 t ha^{-1} (M1), 7.2 t ha^{-1} (M2), 9.6 t ha^{-1} (M3). ** and *** indicate significant differences at the P < 0.01, and P < 0.001 levels, respectively. Pn, net photosynthetic rate; Sc, stomatal conductance; Tr, transpiration rate; Ci, intercellular carbon dioxide concentration.

4 Discussion

The present two-year field study in Northeast China showed that intercropping maize and soybean with straw mulching improved the growth performance and grain yield of both crops (maize and soybean) compared withno mulching. Moreover, the performance of maize was improved by intercropping relative to monoculture conditions. This is consistent with previous studies investigating intercropping of various crops and finding better combined growth indices and yields of cereals and legumes. Many studies have shown intercropping advantages in different intercropping systems (Li et al., 2009; Fang et al., 2010). Intercropping often results in better crop performance and grain yield relative to monocropping systems by utilizing available resources moreeffectively (Raza et al., 2021). Maize/soybean intercropping enhanced the capture and utilization ofresources overall compared with mono-croppingowing to the complementary resource use of both crops in the intercrop system (Liu et al., 2018; Li C. et al., 2020). One crop can improve the growth

10.3389/fpls.2023.1280382

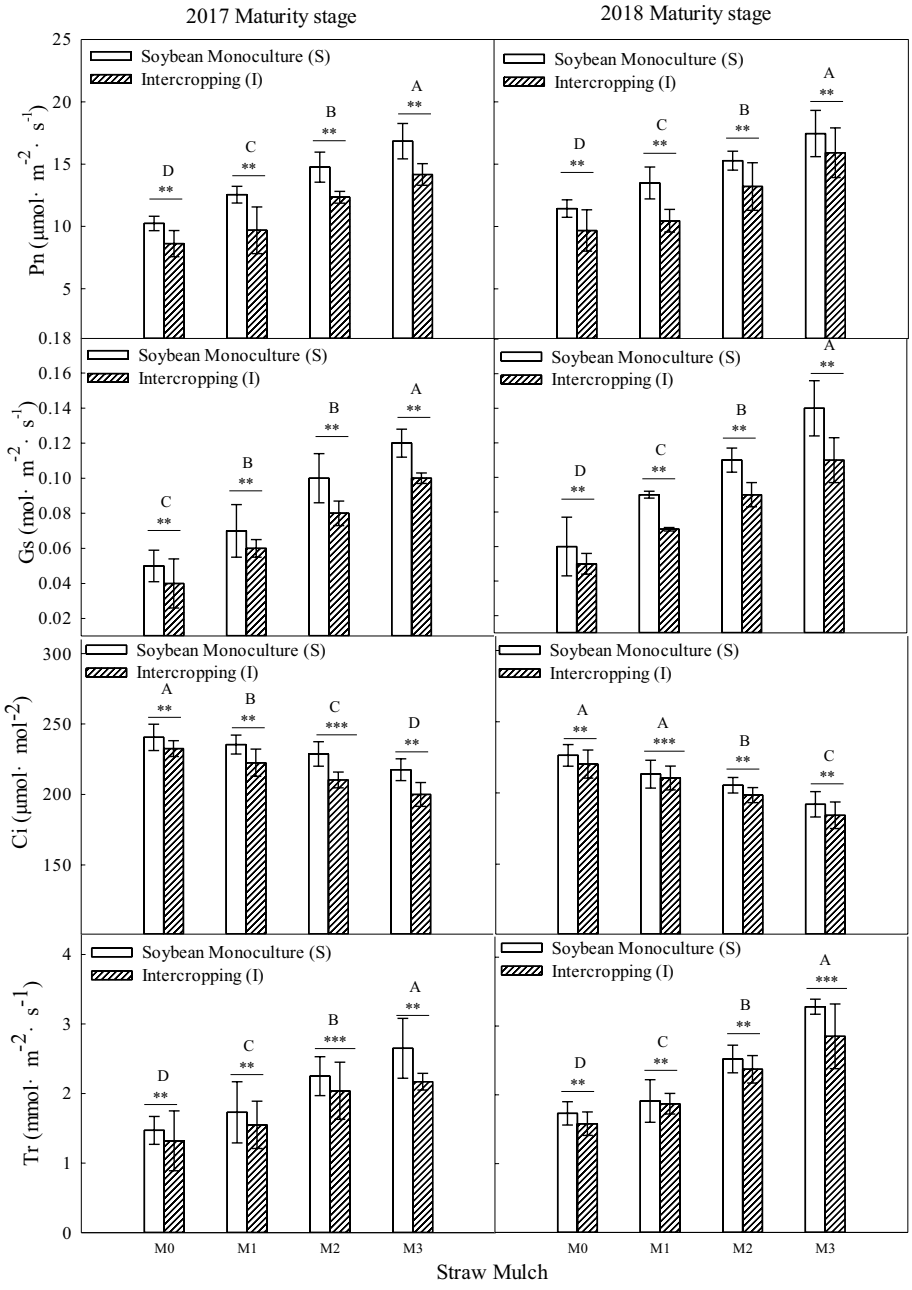

FIGURE 11
Effects of straw mulching and intercropping on soybean photosynthesis parameters at maturity. Bars labeled with different capital letters indicate significant differences in photosynthetic parameters between straw mulch treatments ($P< 0.05$). Straw mulching levels: 0 t ha^{-1} (M0), 4.8 t ha^{-1} (M1), 7.2 t ha^{-1} (M2), 9.6 t ha^{-1} (M3). ** and *** indicate significant differences at the $P < 0.01$, and $P < 0.001$ levels, respectively. Pn, net photosynthetic rate; Sc, stomatal conductance; Tr, transpiration rate; Ci, intercellular carbon dioxide concentration.

TABLE 8 Analysis of variance of the effects of straw mulching amount and planting pattern on crop nitrogen uptake.

Source of variation	N					
	Maize		Soybean		Intercropping system	
	F	*P*	*F*	*P*	*F*	*P*
Planting pattern (P)	313.25	0.000	58.21	0.000	400.75	0.000
Straw mulch (M)	200.10	0.000	90.34	0.000	86.34	0.000
P×M	5.36	0.028	0.19	0.883	5.64	0.057

The values in the table represent the F- and P-values of the analysis of variance of the effects of straw mulching amount and planting pattern on crop nitrogen uptake. P, planting pattern; M, straw mulch.

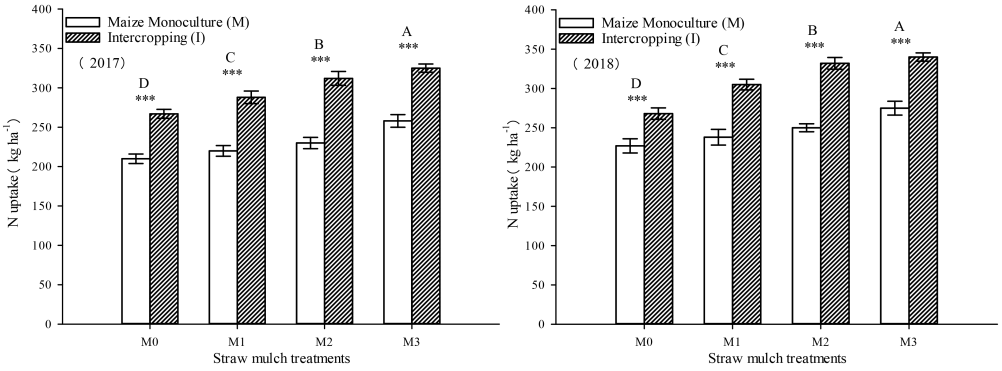

FIGURE 12
Effects of different straw mulching amounts on nitrogen uptake of maize in maize/soybean intercropping system in 2017 and 2018. Bars labeled with different capital letters indicate significant differences in nitrogen uptake between straw mulching treatments (P< 0.05). Straw mulching levels: 0 t ha^{-1} (M0), 4.8 t ha^{-1} (M1), 7.2 t ha^{-1} (M2), 9.6 t ha^{-1} (M3). *** indicate significant differences at the P < 0.001 levels, respectively.

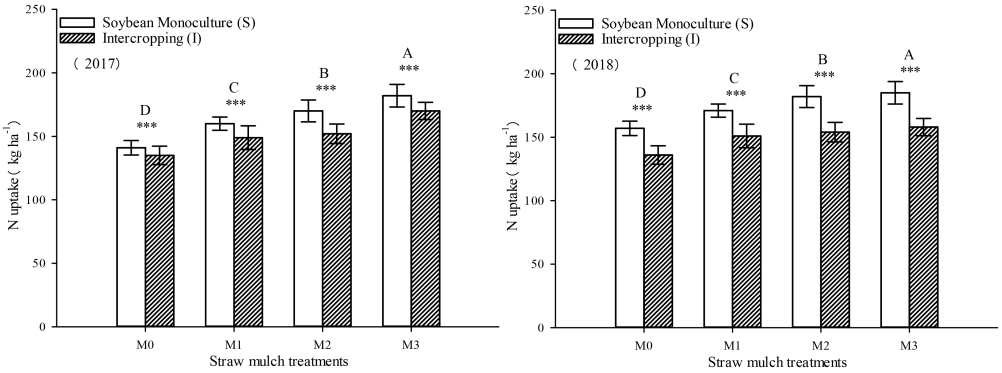

FIGURE 13
Effects of different straw mulching amounts on nitrogen uptake of soybean in maize/soybean intercropping system in 2017 and 2018. Bars labeled with different capital letters indicate significant differences in nitrogen uptake between straw mulch treatments (P< 0.05). Straw mulching levels: 0 t ha^{-1} (M0), 4.8 t ha^{-1} (M1), 7.2 t ha^{-1} (M2), 9.6 t ha^{-1} (M3). *** indicate significant differences at the P < 0.001 levels, respectively.

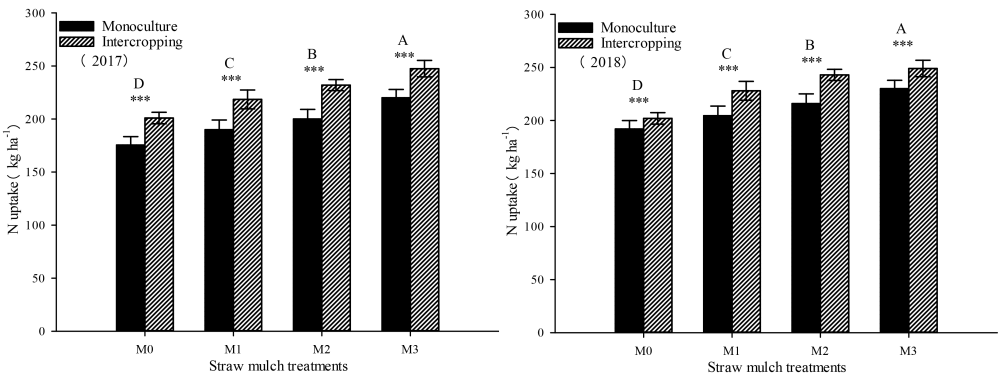

FIGURE 14
Effects of different straw mulching amounts on nitrogen uptake in the maize/soybean intercropping system in 2017 and 2018. Bars labeled with different capital letters indicate significant differences between straw mulch treatments (P< 0.05). Straw mulching levels: 0 t ha^{-1} (M0), 4.8 t ha^{-1} (M1), 7.2 t ha^{-1} (M2), 9.6 t ha^{-1} (M3). *** indicate significant differences at the P < 0.001 levels, respectively.

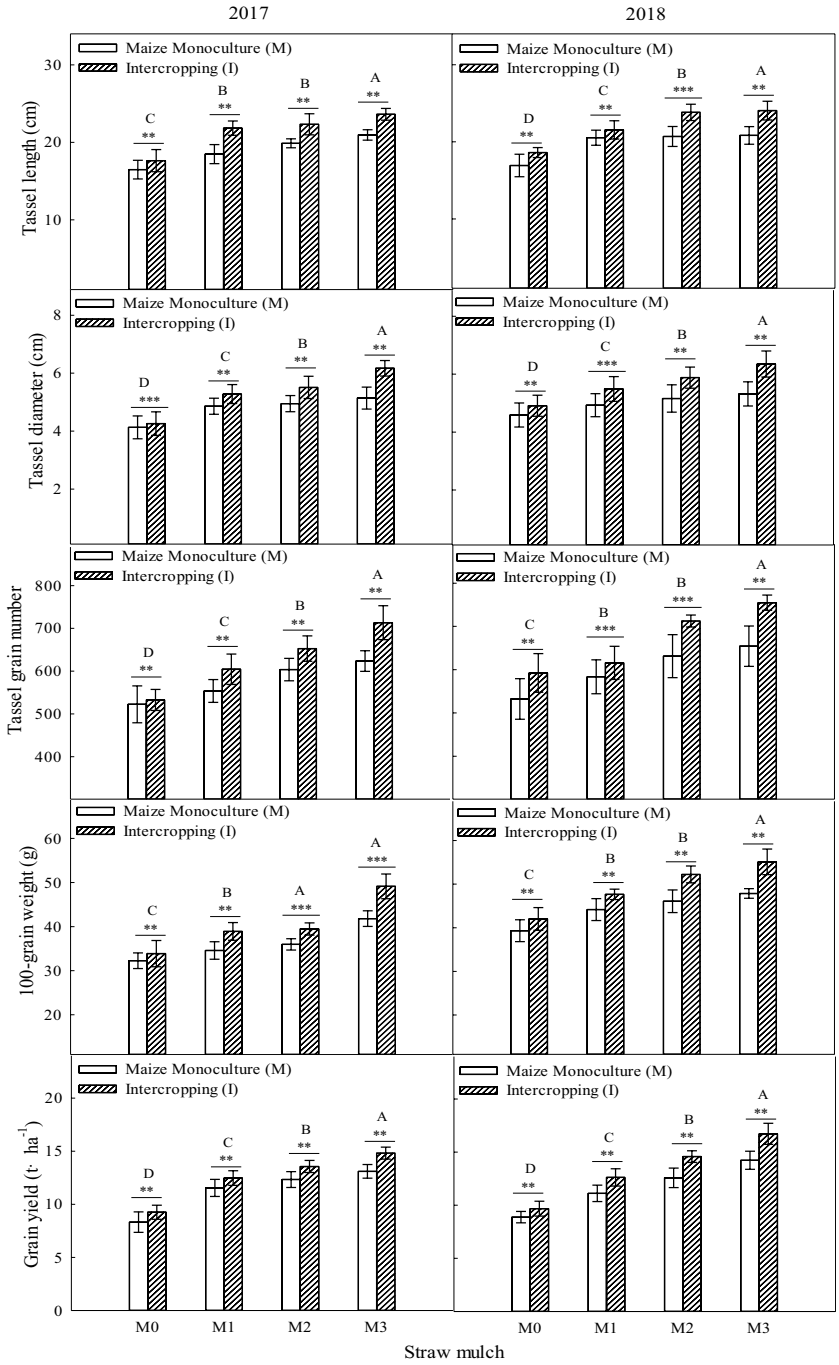

FIGURE 15
Effects of straw mulching and intercropping on maize yield and yield-related traits. Bars labeled with different capital letters indicate significant differences between straw mulch treatments ($P< 0.05$). Straw mulching levels: 0 t ha^{-1} (M0), 4.8 t ha^{-1} (M1), 7.2 t ha^{-1} (M2), 9.6 t ha^{-1} (M3). ** and *** indicate significant differences at the $P < 0.01$, and $P < 0.001$ levels, respectively.

and development of another crop and increase the activity of individual plants through the reciprocity between species in the intercropping systemsuch that the economic benefits of the intercropping systemare higher than that of crop monocultures (Hauggaard-Nielsen and Jensen, 2005).

A global analysis of the many advantages of intercropping showed that the land equivalent ratio of intercropping worldwide is around 1.3 (Martin et al., 2018). A maize/soybean intercropping system increases the total energy output value by 38% (Martin et al., 2018), and the land equivalent ratios of oat/maize intercropping, oat/sunflower intercropping, and oat/mung bean intercropping have been estimated at 1.10–1.4, 1.23–1.38, and 1.05–1.08, respectively (Qian et al., 2018). Intercropping has advantages in fertilizer and land use, mainly because intercropping concentrates production on less land under the same nitrogen fertilizer input per unit area. The present study found that maize intercropping had a

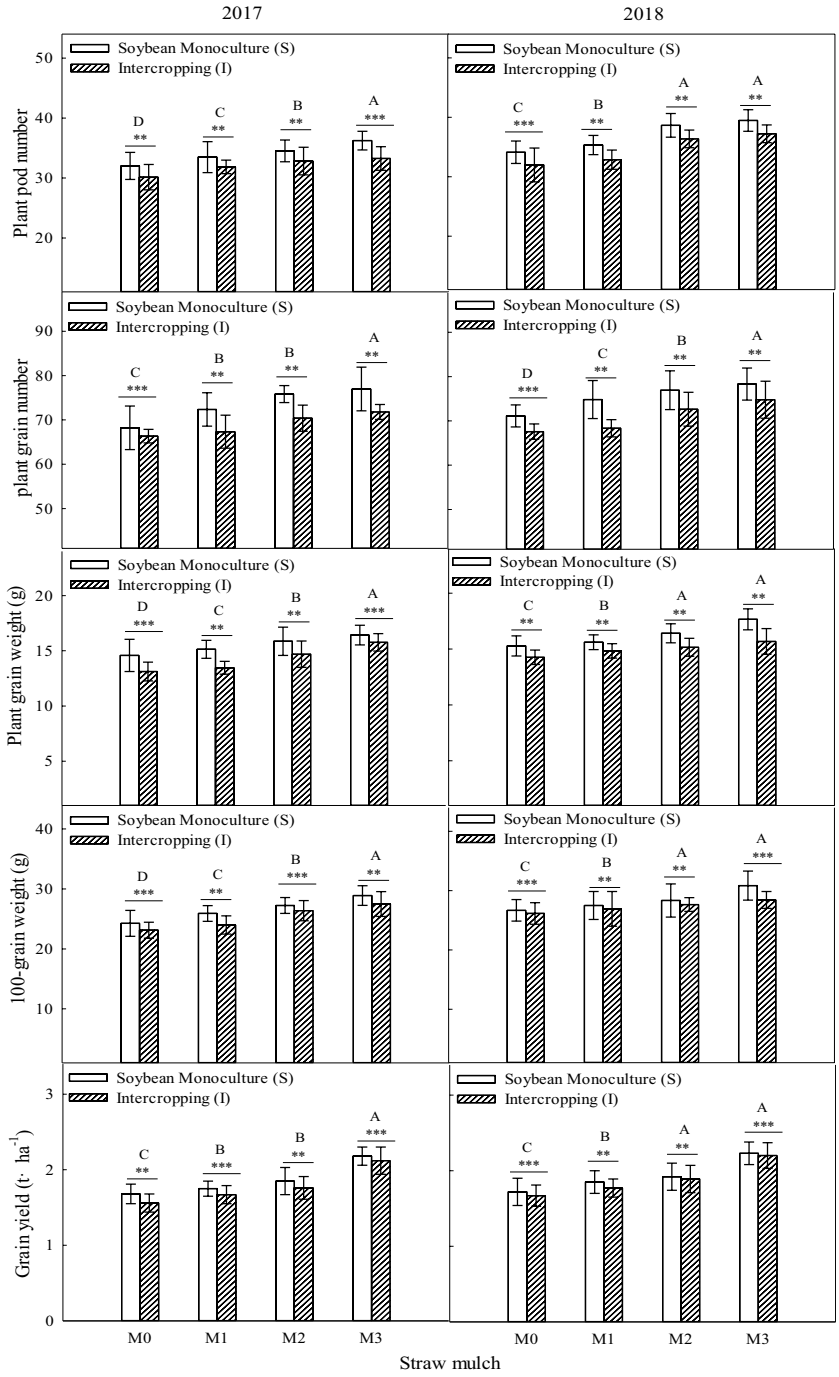

FIGURE 16
Effects of straw mulching and intercropping on soybean yield and yield-related traits. Bars labeled with different capital letters indicate significant differences between straw mulch treatments ($P< 0.05$). Straw mulching levels: 0 t ha^{-1} (M0), 4.8 t ha^{-1} (M1), 7.2 t ha^{-1} (M2), 9.6 t ha^{-1} (M3). ** and *** indicate significant differences at the $P < 0.01$, and $P < 0.001$ levels, respectively.

noticeable advantage compared with monoculture. Under the same straw mulching level, the plant height (Figure 2), stem diameter (Figures 4, 5), andLAI (Table 7) of intercropped maize were significantly higher than those of monoculture maize ($P< 0.05$). The improved growth of both crops in the intercropping system (measured as increased leaf area index and dry matter accumulation) is most likely associated with higher water use efficiency, improved light use efficiency, and nutrient accumulation (Rahman et al., 2017; Ahmed et al., 2018; Liu et al., 2018). Moreover, efficient uptake and utilization of nutrients and soil waterenhance root system proliferation and lead to improved crop growth by promoting crop plant height, stem diameter, leaf area, and other growth indicators (Mao et al., 2012; Chen et al., 2017; Li et al., 2020). Soybean in a maize/soybean intercropping system exhibits an inhibition of growth, so the intercropped soybean plant height (Figure 3), stem diameter (Figure 5), and

leaf area index (Table 6) were significantly less than those of monoculture soybean ($P< 0.05$).

Straw mulching can promote crop growth and development, increase leaf area index and leaf chlorophyll content, and improve aboveground dry matter quality (Qin et al., 2010; Khan et al., 2022a). The leaf area index is a positive indicatorof improved yield and lower evaporation and is critical to maintaining higher intercropping yield (Kamara et al., 2017). Studies in soybean have shown that straw mulching can enhance the growth and development of plants, increase nodule weight, nodule number, LAI, and chlorophyll content, increase growth indexes (such as plant height and stem diameter), and, ultimately, increase the biomass and economic yield (Sekhon et al., 2005; Khan et al., 2022a). The present study showed that maize straw mulching could increase plant height (Figures 2, 3), stem diameter (Figures 4, 5), LAI (Tables 7, 6), and chlorophyll content (Figures 6, 7) of rain-fed maize and soybean crops, supporting previous research results (Khan et al., 2022a).

Two years of experimental data have shown that intercropping has a positive effect on the photosynthetic performance of crops (Figures 8–11). Additionally, intercropping of tall and short plants creates an umbrella canopy structure during the overlapping growth period, which increases the incident radiation on both sides of crop rows and allows for full exposure of the leaves in the middle of the canopy to light, thus promoting photosynthesis (Lin et al., 2020). The improved photosynthetic characteristics of maize in intercropping are also owing to the ventilation and light conditions being optimized by intercropping soybean, which is a short crop, with maize, a tall crop (Xiangqian, et al., 2014). This increases the photosynthetic performance parameters of maize in the maize/soybean intercropping system, while simultaneously weakening the photosynthetic performance parameters of soybean (Figures 8–11). Furthermore, straw mulchingwas also found to improve the photosynthetic characteristics of maize and soybean. The level of improvement increased with increasing levels of mulching, with the improvement mainlyconsistent with enhanced water use, growth, and development of maize (Liu et al., 2019) (Figures 8–11). Overall, these findings suggest that intercropping and straw mulching have the potential to significantly improve crop productivity and sustainability, thereby contributing to sustainable food production.

It has been shown that straw mulching can improve the net photosynthetic rate (Pn) of functional leaves of winter wheat (Zhai et al., 2021). In addition, studies have found that the effects of straw mulching on crop photosynthetic parameters, including Pn, Sc, Tr, and Ci, are indirect (Liu et al., 2019). Mulching improves the soil environment, increases the absorption and utilization of nutrients and water by crops, and promotes the growth of roots (He et al., 2017), thereby increasing the morphological indicators of crops, such as leaf area, and internal physiological indicators, which ultimately improves the light interception and growth of crops (Retta et al., 2016). The present study also confirmed that under mulching, the nitrogen uptake of maize and soybean crops increased with the increase of straw mulching (Figures 12–14), which would also explain the ultimate rise in crop yield (Yu et al., 2010). Intercropping has obvious yield advantages, whichare based on the effective use of nutrient resources (Willey, 1979; Wang Z. et al., 2023), and is the result of the combined effect of nutrient uptake and utilization efficiency of intercropped crops (Chowdhury and Rosario, 1994).Regarding the yield-increasing effect of straw mulching, although there are some differences in the yield results of each test treatmentowing to different study regions, years, and mulching amounts, overall, within a given coverage range, crop yield increases withincreasing coverage. Inthe present study, a crop yield advantage in the intercropping system was found under all straw mulching levels. Straw mulching significantly increased crop yield (Figures 15, 16), which is similar to the results of previous studies (Khan et al., 2021; Runzhi et al., 2021; Du et al., 2022). Crop yield and dry matter quality are closely related to crop photosynthetic characteristics. Under straw mulching, crop photosynthetic performance is improved, and as crop yield and dry matter quality are the accumulation of photosynthetic products, they also increase (Monti et al., 2005).

5 Conclusions

The two years of results showed that straw mulching and intercropping can promote the growth of crops, significantly increase the plant height and stem diameter of crops, increase the leaf area and chlorophyll content of crops, and thus promote the photosynthesis of crops, increase the nitrogen absorption of crops, and ultimately increase the yield of crops. The strongest effect was observed under a coverage of 9.6 t ha^{-1} maize straw under maize/soybean intercropping. Thus, in the actual agricultural production process, agricultural measures combining straw mulching and crop intercropping can be adopted to improve the leaf traits and photosynthetic physiological characteristics of crops, so as to achieve the goal of optimizing crop growth and development status while increasing crop yield.

Data availability statement

The original contributions presented in the study are included in the article/supplementary material. Further inquiries can be directed to the corresponding authors.

Author contributions

SL: Conceptualization, Data curation, Formal Analysis, Methodology, Software, Writing – original draft. IK: Writing – review & editing. FN: Data curation, Visualization, Writing – review & editing. AR: Conceptualization, Data curation, Writing – review & editing. RS: Conceptualization, Writing – review & editing. LC: Conceptualization, Data curation, Writing – review & editing. LW: Funding acquisition, Investigation, Project administration, Resources, Supervision, Validation, Writing – original draft.

Funding

The author(s) declare financial support was received for the research, authorship, and/or publication of this article. This research received funding from the Natural Science foundation of Liaoning province under grant Number 2019-ZD-0705.

Conflict of interest

The authors declare that the research was conducted in the absence of any commercial or financial relationships that could be construed as a potential conflict of interest.

The author(s) declared that they were an editorial board member of Frontiers, at the time of submission. This had no impact on the peer review process and the final decision.

Publisher's note

References

Ahmad, N., Jianyu, L., Xu, T., Noman, M., Jameel, A., Na, Y., et al. (2019). Overexpression of a novel cytochrome P450 promotes flavonoid biosynthesis and osmotic stress tolerance in transgenic arabidopsis. *Genes* 10 (10), 756. doi: 10.3390/genes10100756

Ahmed, S., Raza, M., Zhou, T., Hussain, S., Khalid, M., and Feng, L. (2018). Responses of soybean dry matter production, phosphorus accumulation, and seed yield to sowing time under relay intercropping with maize. *Agronomy* 8, 282. doi: 10.3390/agronomy8120282

Amane, M. (2021). Photosynthesis improvement for enhancing productivity in rice. *Soil Sci. Plant Nutr.* 67 (5), 513–519. doi: 10.1080/00380768.2021.1966290

Bucher, S.F., Auerswald, K., Grun-Wenzel, C., Higgins, S. I., and Romermann, C. (2021). Abiotic site conditions affect photosynthesis rates by changing leaf functional traits. *Basic Appl. ecol.* 57, 54–64. doi: 10.1016/j.baae.2021.09.003

Central Agricultural Broadcasting School (2022). Fertilization technology of soybean-maize strip composite planting. *China Rural Netw*. Available at: https://www.ngx.net.cn/ztzl/ddym/jszd/202201/t20220121_227880.html.

Chang, X., Yan, L., Naeem, M., Khaskheli, M. I., Zhang, H., Gong, G., et al. (2020). Maize/soybean relay strip intercropping reduces the occurrence of Fusarium root rot and changes the diversity of the pathogenic Fusarium species. *Pathogens* 9 (3), 211. doi: 10.3390/pathogens9030211

Chen, P., Du, Q., Liu, X., Li, Z., Sajad, H., Lu, L., et al. (2017). Effects of reduced nitrogen inputs on crop yield and nitrogen use efficiency in a long-term maize- soybean relay strip intercropping system. *PloS One* 12, 1–19. doi: 10.1371/journal.pone.0184503

Chen, S., Zhang, X., Pei, D., Sun, H., and Chen, S. (2007). Effects of straw mulching on soil temperature, evaporation and yield of winter wheat: Field experiments on the North China Plain. *Ann. Appl. Biol.* 150, 261–268. doi: 10.1111/j.1744-7348.2007.00144.x

Chowdhury, M. K., and Rosario, E. L. (1994). Comparison of nitrogen, phosphorus and potassium utilization efficiency in maize/mungbean intercropping. *J. Agric. Sci.* 122 (4), 193–199. doi: 10.1017/S0021859600087360

Du, C., Li, L., and Effah, Z. (2022). Effects of straw mulching and reduced tillage on crop production and environment: A review. *Water* 14, 2471. doi: 10.3390/w14162471

Fang, S. Z., Li, H. L., Sun, Q. X., and Chen, L. B.. (2010). Biomass production and carbon stocks in poplar-crop intercropping systems: A case study in northwestern Jiangsu, China. *Agroforestry Sys.* 79 (2), 213–222. doi: 10.1007/s10457-010-9307-x

Godfray, H. C. J., Beddington, J. R., Crute, I. R., Haddad, L., Lawrence, D., Muir, J. F., et al. (2010). Food security: the challenge of feeding 9 billion people. *Science* 327, 812–818. doi: 10.1126/science.1185383

Guo, D., Li, X., Li, X., Wang, J., and Fu, H. (2013). Conventional tillage increases soil microbial biomass and activity in the Loess Plateau, China. *Acta Agric. Scand. Sect. B Soil Plant Sci.* 63, 489–496. doi: 10.1080/09064710.2013.807356

Hauggaard-Nielsen, H., and Jensen, E. S. (2005). Facilitative root interactions in intercrops. *Plant Soil* 274 (1/2), 237–250. doi: 10.1007/1-4020-4099-7_13

He, H. H., Peng, Q., Wang, X., Fan, C. B., Pang, J. Y., Lambers, H., et al. (2017). Growth,morphological and physiological responses of alfalfa (Medicago sativa) to phosphorus supply in two alkaline soils. *Plant Soil* 416 (1/2), 565–584. doi: 10.1007/s11104-017-3242-9

Hector, A., Schmid, B., and Beierkuhnlein, C. (1999). Plant diversity and productivity experiments in European grasslands. *Science* 286 (5442), 1123–11277. doi: 10.1126/science.286.5442.1123

Hinsinger, P., Betencourt, E., Bernard, L., Brauman, A., Plassard, C., Shen, J., et al. (2011). P for two, sharing a scarce resource: Soil Phosphorus acquisition in the rhizosphere of intercropped species. *Plant Physiol.* 156 (3), 1078–1086. doi: 10.1104/pp.111.175331

Hong, Y., Lv, Y., Zhang, J., Ahmad, N., Li, X., Yao, N., et al. (2023). The safflower MBW complex regulates HYSA accumulation through degradation by the E3 ligase CtBB1. *J. Integr. Plant Biol.* 65, 1277–1296. doi: 10.1111/jipb.13444

Iqbal, N., Hussain, S., Ahmed, Z., Yang, F., Wang, X., Liu, W., et al. (2019). Comparative analysis of maize-soybean strip intercropping systems: a review. *Plant Prod. Sci.* 22 (2), 131–142. doi: 10.1080/1343943X.2018.1541137

Kamara, A., Tofa, A., Ademulegun, T., Solomon, R., Shehu, H., Kamai, N., et al. (2017). Maize–soybean intercropping for sustainable intensification of cereal–legume cropping systems in Northern Nigeria. *Exp. Agricult.* 55 (1), 1–15. doi: 10.1017/S0014479717000564

Khan, I., Chen, T., Farooq, M., Luan, C., Wu, Q., Wanning, D., et al. (2021). The residual impact of straw mulch and biochar amendments on soil physiochemical properties and yield of maize under rainfed system. *Agron. J.* 113, 1102–1120. doi: 10.1002/agj2.20540

Khan, I., Iqbal, B., Khan, A. A., Inamullah,, Rehman, A., Fayyaz, A., et al. (2022a). The interactive impact of straw mulch and biochar application positively enhanced the growth indexes of maize (Zea mays L.) crop. *Agronomy* 12, 2584. doi: 10.3390/agronomy12102584

Khan, I., Luan, C., Qi, W., Wang, X., Yu, B., Rehman, A., et al. (2022b). The residual impact of straw mulch and biochar amendments on grain quality and amino acid contents of rainfed maize crop. *J. Plant Nutr.* 46 (7), 1283–1295. doi: 10.1080/01904167.2022.2056483

Kumar, S., Kadono, A., Lal, R., and Dick, W. (2012). Long-term no-till impacts on organic carbon and properties of two contrasting soils and corn yields in ohio. *Soil Sci. Soc. America J.* 76, 1798–1809. doi: 10.2136/sssaj2012.0055

Li, C., Hoffland, E., Kuyper, T. W., Yu, Y., Zhang, C., Li, H., et al. (2020). Syndromes of production in intercropping impact yield gains. *Nat. Plants* 6, 1–8. doi: 10.1038/s41477-020-0680-9

Li, L., Li, S. M., Sun, J. H., Zhou, L. L., Bao, X. G., Zhang, H. G., et al. (2007). Diversity enhances agricultural productivity *via* rhizosphere phosphorus facilitation on phosphorus-deficient soils. *Proc. Natl. Acad. Sci. United States America.* 104 (27), 11192–11196. doi: 10.1073/pnas.0704591104

Li, Y. F., Ran, W., Zhang, R. P., Sun, S., and Xu, G. (2009). Facilitated legume nodulation, phosphate uptake and nitrogen transfer by arbuscular inoculation in an upland rice and mung bean intercropping system. *Plant Soil* 315 (1/2), 285–296. doi: 10.1007/s11104-008-9751-9

Li, L., Tilmanm, D., Lambers, H., and Zhang, F.. (2014). Plant diversity and overyielding_ insights from below ground facilitation of intercropping in agriculture. *New Phytol.* 203, 63–69. doi: 10.1111/nph.12778

Li, R., Zhang, Z., Tang, W., Huang, Y., Coulter, J. A., and Nan, Z. (2020). Common vetch cultivars improve yield of oat row intercropping on the Qinghai-Tibetan plateau by optimizing photosynthetic performance. *Eur. J. Agro.* 117, 1–13. doi: 10.1016/j.eja.2020.126088

Lin, F., Liu, X. J., Tong, C. C., and Wu, Y. (2020). Characteristics of light energy utilization of intercropping alfalfa/Gramineae forage based on yield effect. *Chin. J. Appl. Ecol.* 31 (9), 2963–2976. doi: 10.13287/j.1001-9332.202009.026

Lithourgidis, A. S., Dordas, C. A., Damalasc, A., and Vlachostergios, D. N. (2011). Annual intercrops: an alternative pathway for sustainable agriculture. *Aust. J. Crop Sci.* 5, 396–410. doi: 10.1016/j.agwat.2011.01.017

Liu, J., Ahmad, N., Hong, Y., Zhu, M., Zaman, S., Wang, N., et al. (2022). Molecular characterization of an isoflavone 2'-hydroxylase gene revealed positive insights into

flavonoid accumulation and abiotic stress tolerance in safflower. *Molecules* 27 (22), 8001. doi: 10.3390/molecules27228001

Liu, J., Liu, L., Fu, Q., Zhang, L., and Xu, Q. (2019). Effects of straw mulching and tillage measures on the photosynthetic characteristics of maize leaves. *Trans. ASABE.* 62 (3), 851–858. doi: 10.13031/trans.13235

Liu, X., Rahman, T., Song, C., Su, B. Y., Yang, F., Yong, T. W., et al. (2017). Changes in light environment, morphology, growth and yield of soybean in maize-soybean intercropping systems. *Field Crops Res.* 200, 38–46. doi: 10.1016/j.fcr.2016.10.003

Liu, X., Rahman, T., Song, C., Yang, F., Su, B., Cui, L., et al. (2018). Relationships among light distribution, radiation use efficiency and land equivalent ratio in maize-soybean strip intercropping. *Field Crop Res.* 224, 91–101. doi: 10.1016/j.fcr.2018.05.010

Li, Y. W., Chai, S. X., Chai, Y. W., Li, R., Lan, X. M., Ma, J. T., et al. (2021). Effects of mulching on soil temperature and yield of winter wheat in the semiarid rainfed area. *Field Crops Res.* 271, 108244. doi: 10.1016/j.fcr.2021.108244

Malézieux, E., Crozat, Y., Dupraz, C., Laurans, M., Makowski, D., Ozier-Lafontaine, H., et al. (2009). Mixing plant species in cropping systems: Concepts, tools and models. A review. *Agron. Sustain. Dev.* 29 (1), 43–62. doi: 10.1051/agro:2007057

Mao, L., Zhang, L., Li, W., Werf, W., Sun, J., Spiertz, H., et al. (2012). Yield advantage and water saving in maize/pea intercrop. *Field Crops Res.* 138, 11–20. doi: 10.1016/j.fcr.2012.09.019

Martin, M. O., Paquette, A., Dupras, J., Rivest, D., et al. (2018). The new Green Revolution: Sustainable intensification of agriculture by intercropping. *Sci. Total Environ.* 615, 767–772. doi: 10.1016/j.scitotenv.2017.10.024

Masciandaro, G., Ceccanti, B., Benedicto, S., Lee, H. C., and Cook, H. F. (2004). Enzyme activity and C and N pools in soil following application of mulches. *Can. J. Soil Sci.* 84, 19–30. doi: 10.4141/S03-045

Monti, A., Amducci, M. T., Pritoni, G., and Venturi, G. (2005). Growth,fructan yield, and quality of chicory (Cichorium intybus L.) as related to photosynthetic capacity, harvest time,and water regime. *J. Exp. Bot.* 56 (415), 1389–1395. doi: 10.1093/jxb/eri140

Qian, X., Zang, H., Xu, H., Hu, Y., Ren, C., Guo, L., et al. (2018). Relay strip intercropping of oat with maize, sunflower and mung bean in semi-arid regions of Northeast China: Yield advantages and economic benefits. *Field Crops Res.* 223, 33–40. doi: 10.1016/j.fcr.2018.04.004

Qiao, X., Bei, S., Li, H., Christie, P., Zhang, F. S., Zhang, J L., et al. (2016). Arbuscular mycorrhizal fungi contribute to overyielding by enhancing crop biomass while suppressing weed biomass in intercropping systems. *Plant Soil.* 406 (1-2), 173–185. doi: 10.1007/s11104-016-2863-8

Qin, A., Huang, G., Chai, Q., Yu, A., and Huang, P. (2013). Grain yield and soil respiratory response to intercropping systems on arid land. *Field Crops Res.* 144, 1–10. doi: 10.1016/j.fcr.2012.12.005

Qin, J., Wang, X. M., Hu, F. M., and Li, H.. (2010). Growth and physiological performance responses to drought stress under non-flooded rice cultivation with straw mulching. *Plant Soil Environ.* 56 (2), 51–59. doi: 10.17221/157/2009-PSE

Rahman, T., Liu, X., Hussain, S., Ahmed, S., Chen, G., Yang, F., et al. (2017). Water use efficiency and evapotranspiration in maize-soybean relay strip intercrop systems as affected by planting geometries. *PloS One* 12 (6), e0178332. doi: 10.1371/journal.pone.0178332

Raza, M. A., Cui, L., Khan, I., Din, A. M. U., Chen, G., Ansar, M., et al. (2021). Compact maize canopy improves radiation use efficiency and grain yield of maize/soybean relay intercropping system. *Environ. Sci. pollut. Res.* 28 (30), 41135–41148. doi: 10.1007/s11356-021-13541-1

Retta, M., Yin, X. Y., Van Der Putten, P. E. L., Cantre, D., Berghuijs, H. N.C., Ho, Q. T., et al. (2016). Impact of anatomical traits of maize (Zea mays L.) leaf as affected by nitrogen supply and leaf age on bundle sheath conductance. *Plant Sci.* 252, 205–214. doi: 10.1016/j.plantsci.2016.07.013

Runzhi, Z., Lingbo, M., Ying, L., Xuerong, W., Ogundeji, A. O., Xinrui, L., et al. (2021). Yield and nutrient uptake dissected through complementarity and selection effects in the maize/soybean intercropping. *Food Energy Secur.* 10 (2), 379–393. doi: 10.1002/fes3.282

Sekhon, N. K., Hira, G. S., Sidhu, A. S., and Thind, S. S. .(2005). Response of soybean (Glycine max Mer.) to wheat straw mulching in different cropping seasons. *Soil Use Manage.* 21 (4), 422–426. doi: 10.1079/SUM2005356

Teste, F. P., Veneklaas, E. J., Dixon, K. W., and Lambers, H.. (2014). Complementary plant nutrient-acquisition strategies promote growth of neighbour species. *Funct. Ecol.* 28, 819–828. doi: 10.1111/1365-2435.12270

Wang, Z., Dong, B., Stomph, T. J., Evers, J. B., van der Putten, P. E. L., Ma, H., et al. (2023). Temporal complementarity drives species combinability in strip intercropping in the Netherlands. *Field Crops Res.* 291, 108157. doi: 10.1016/j.fcr.2022.108757

Wang, L., Yu., B., Ji, J., Khan, I., Li, G., Rehman, A., et al. (2023). Assessing the impact of biochar and nitrogen application on yield, water-nitrogen use efficiency and quality of intercropped maize and soybean. *Front. Plant Sci.* 14, 1171547. doi: 10.3389/fpls.2023.1171547

Willey, R. W. (1979). Intercropping-its importance and research needs: Part 1. Competition and yield advantages. *Field Crop Abst.* 32, 1–10. Available at: https://ci.nii.ac.jp/naid/10024068486/.

Xia, H. Y., Zhao, J. H., Sun, J. H., Bao, X. G., Christie, P., Zhang, F. S., et al. (2013). Dynamics of root length and distribution and shoot biomass of maize as affected by intercropping with different companion crops and phosphorus application rates. *Field Crops Res.* 150, 52–62. doi: 10.1016/j.fcr.2013.05.027

Xiangqian, Z., Guoqin, H., and Qiguo, Z. (2014). Effects of straw mulching on photosynthetic characteristics and yield of intercropped maize (In Chinese). *Chin. J. Eco-Agricult.* 22 (4), 414–421. doi: 10.3724/SP.J.1011.2014.31037

Yin, H., Zhao, W., Li, T., Cheng, X., and Liu, Q. (2018). Balancing straw returning and chemical fertilizers in China: Role of straw nutrient resources. *Renewable Sustain. Energy Rev.* 81 (2), 2695–2702. doi: 10.1016/j.rser.2017.06.076

Yu, C. B., Li, Y. Y., Li, C., Sun, J. H., He, X. H., Zhang, F. S., et al. (2010). An improved nitrogen difference method for estimating biological nitrogen fixation in legume-based intercropping systems. *Biol. Fertil. Soils.* 46 (3), 227–235. doi: 10.1007/s00374-009-0418-3

Zhai, L., Wang, Z., Song, S., Zhang, L., Zhang, Z., and Jia., X. (2021). Tillage practices affects the grain filling of inferior kernel of summer maize by regulating soil water content and photosynthetic capacity. *Agric. Water Manage.* 245, 106600. doi: 10.1016/j.agwat.2020.106600

Zhang, W., Ahanbieke, P., Wang, B. J., Gan, Y. W., Li, L. H., Christie, P., et al. (2014). Temporal and spatial distribution of roots as affected by interspecific interactions in a young walnut/wheat alley cropping system in northwest China. *Agroforestry Sys.* 89 (2), 327–343. doi: 10.1007/s10457-014-9770-x

Zhang, X. Q., Huang, G. Q., Bian, X. M., and Zhao, Q. G. (2013). Effects of nitrogen fertilization and root interaction on the agronomic traits of intercropped maize, and the quantity of microorganisms and activity of enzymes in the rhizosphere. *Plant Soil* 368 (1/2), 407–417. doi: 10.1007/s11104-012-1528-5

Zuber, S. M., Behnke, G. D., Nafziger, E. D., and Villamil, M. B. (2015). Crop rotation and tillage effects on soil physical and chemical properties in Illinois. *Agron. J.* 107, 971–978. doi: 10.2134/agronj14.0465

frontiers | Frontiers in Plant Science

TYPE Original Research
PUBLISHED 19 October 2023
DOI 10.3389/fpls.2023.1271325

OPEN ACCESS

EDITED BY
Shahbaz Khan,
Huazhong Agricultural University, China

REVIEWED BY
Ismail Khan,
Jiangsu University, China
Huabin Zheng,
Hunan Agricultural University, China
Wen Lin,
Shanxi Agricultural University, China

*CORRESPONDENCE
Xinkai Zhu
xkzhu@yzu.edu.cn

RECEIVED 02 August 2023
ACCEPTED 25 September 2023
PUBLISHED 19 October 2023

CITATION
Jia W, Ma Q, Li L, Dai C, Zhu M, Li C, Ding J, Guo W and Zhu X (2023) The fate of nitrogen from different sources in a rice-wheat rotation system – A ^{15}N labeling study.
Front. Plant Sci. 14:1271325.
doi: 10.3389/fpls.2023.1271325

The fate of nitrogen from different sources in a rice-wheat rotation system – A ^{15}N labeling study

Wenxin Jia[1], Quan Ma[1], Li Li[1], Cunhu Dai[1], Min Zhu[1,2], Chunyan Li[1,2], Jinfeng Ding[1,2], Wenshan Guo[1,2] and Xinkai Zhu[1,2,3]*

[1]Jiangsu Key Laboratory of Crop Genetics and Physiology, Agricultural College of Yangzhou University, Yangzhou, Jiangsu, China, [2]Co-Innovation Center for Modern Production Technology of Grain Crops, Yangzhou University, Yangzhou, Jiangsu, China, [3]Joint International Research Laboratory of Agriculture and Agri-Product Safety, the Ministry of Education of China, Yangzhou University, Yangzhou, Jiangsu, China

High loss and low nitrogen (N) efficiency in agricultural production is severe. Also, ammonia volatilization and N leaching aggravated environmental pollution. The eutrophication of surface water and the emissions of N_2O increased, hence green fertilization management urgently needs to be rationalized. Coordinating N supply from different sources has been shown to reduce environmental pollution. Therefore, this study was dedicated to clarifying the transport of N sources in the rice-wheat rotation system. The stable isotope tracer technology was used to label fertilizer (F), soil (T), and straw (J) with ^{15}N, respectively. The utilization of N by crops (the N ratio in organs), as well as the residual N in soil and loss status, were measured. According to the potential of response to N, all the wheat cultivars were divided into groups with high (HNV) and low efficiency (LNV). The N contribution ratio showed that 43.28%~45.70% of total N accumulation was from T, while 30.11%~41.73% and 13.82%~24.19% came from F and J. The trend in soil N residue (T > F > J) was consistent with the above, while it was the opposite in N loss (T< F< J). The seasonal effectiveness showed that T achieved the highest N utilization efficiency (31.83% ~44.69%), followed by F (21.05%~39.18%) and J (11.02%~16.91%). The post-season sustainability showed that T decreased the most in soil N residue (2.08%~12.53%), and F decreased the most in N accumulation (9.64%~18.13%). However, J showed an increase in N recovery rate (2.87%~5.89%). N translocation and distribution showed that N from different sources in grains was significantly higher than that in stems, glumes, and leaves. The ratio of HNV (75.14%~79.62%) was higher than that of LNV (71.90%~74.59%) in grain, while it was the opposite in other organs. Plant N accumulation, soil N supply, and straw N transformation were determined jointly by the three N sources, thus reducing N loss and N_2O production. Therefore, the results will highlight the insights for constructing local N and emission reduction models.

KEYWORDS

N sources, rice-wheat rotation system, plant utilization efficiency, soil N residual rate, N loss rate, contribution ratio

1 Introduction

Wheat (*Triticum aestivum* L.) is the second largest food crop in China, occupying an important position in modern agricultural production due to its numerous elite varieties (Cui et al., 2023). With the increase in population density and the lack of natural resources, the demand for food has improved steadily. The linear increase in wheat yield has gradually become a crucial guarantee to solve the problem of food security (FAO, 2020; Tan et al., 2021). In agricultural production, N plays a dominant role in the growth and development of wheat (González-Cencerrado et al., 2020). In the rice-wheat rotation cultivation system, proper nitrogen application could improve the photosynthetic physiological potential of wheat by enhancing the synthesis of chlorophyll in leaves, which was conducive to photosynthesis and nutrient accumulation of crops (Falcinelli et al., 2022; Sharma et al, 2022). In addition, nitrogen has the potential to promote tillering and earing of wheat (Benincasa et al., 2017; Zörb et al., 2018). The first nitrogen absorption peak of wheat appeared in the tillering stage before winter, contributing to the formation of tillering and the improvement of the vitality index. The second peak was from the jointing to the booting stage when sufficient nitrogen could promote the differentiation of young spikes and the development of reproductive organs.

At present, the paddy rice-wheat double cropping area in China is mainly distributed in the middle and lower reaches of the Yangtze River, which is characterized by a humid climate and a shallow water table. The excessive application of nitrogen fertilizer was frequent, aggravating problems such as the excessive nitrate nitrogen content in groundwater and the increase of greenhouse gas (GHG) emissions (Sharma and Bali, 2018; Bhattacharya, 2019; Bhattarai et al., 2021). On the one hand, excessive application of nitrogen fertilizer could lead to the decline of ecological environment quality and economic yield of crops (Liu et al., 2018; Guo et al., 2021; Wan, 2021). On the other hand, nitrogen deficiency reduced the effective tillers at the seedling stage and spikes at maturity. The grain number per spike decreased in a later period due to the increase in floret degradation. Then, the nitrogen transferred to grains was reduced, which affected grain filling and 1000-grain weight, and ultimately led to a decrease in grain yield (Rivera-Amado et al., 2019; Pareja-Sánchez et al., 2020; Mahmood et al., 2022). Hence, rationally applying nitrogen fertilizer and improving its utilization efficiency is the prerequisite for the green and sustainable development of wheat (Cui et al., 2023).

After anthesis, nitrogen was mainly transferred from vegetative organs to reproductive organs, contributing to grain filling and nitrogen accumulation. Therefore, studies have been carried out on the rule of nitrogen translocation after anthesis under the high-yield system of crops. The tracer technique of ^{15}N isotope labeling has been widely and accurately used in plant-soil systems, especially in the case of straw mulching (Xu et al., 2021). It is well known that there is a significant interaction between soil and residual straw in the rice-wheat rotation system (Rhymes et al., 2016; Wang et al., 2019). After the straw is returned to the field, it then returns nutrients to the soil through decomposition (Tan and Liu, 2015; Yang, 2023). Compared with traditional methods, nitrogen budget and straw nutrient decomposition rate were more accurately mastered under the combination of the two technologies. The dual goals of increasing crop internal nitrogen supply and reducing fertilizer input were achieved (Huddell et al., 2023). Soil nitrogen availability was improved and a stable high yield was obtained (Kaur et al., 2021).

At present, there are numerous studies on the source and fate of nitrogen, but the transfer principle of different nitrogen sources in the rice-wheat cultivation system for many consecutive seasons remains unclear. Therefore, a two-factor test based on the isotope tracing technology and straw returning technology was used to study nitrogen uptake, transport, and distribution in crops post-anthesis. According to the control variable method, the nitrogen utilization rate and seasonal change rate of crops were investigated. Both the external (temperature, humidity, etc.) and internal environments (pH, soil organic matter content, etc.) of crops have been considered in the experiment. Actually, we attempted to design a reasonable nitrogen management strategy for rice-wheat rotation fields, which may contribute to the sustainable development of agriculture and the gradual recovery of the ecological environment in the future.

2 Materials and methods

2.1 Description of the experiment site

The experiment was conducted at the Experimental Pot Farm of Jiangsu Provincial Key Laboratory of Crop Genetics and Physiology of Yangzhou University (119°25′E, 32°39′N) from 2021 to 2022. This area experiences a transition from a subtropical monsoon humid climate to a temperate monsoon climate. The average high temperature of the crop cultivation year was 22°CC, the average low temperature was 12°CC and the total precipitation was 638.1 mm. The typical soil in the test was sandy loam, which has been used for local conventional planting patterns in recent years. The soil's basic fertility is described in Table 1. The tested rice variety Nanjing9108 was the main cultivar in Jiangsu Province, and the tested wheat varieties (Yangmai25, Yangfumai4, Shengxuan6, and Yangmai22) were bred by the Institute of Agricultural Sciences of Lixiahe District, Jiangsu Province.

2.2 Experimental design

2.2.1 Design of pot experiment in the first rice season

Sandy loam soil was used with approximately 55 kg per pot, totaling four pots. Nanjing9108 was transplanted in late June 2021 (Table 1). The planting specification was three rows per pot, five holes per row, and three plants per hole. The ratio of basal fertilizer : tillering fertilizer : spikelet-promoting fertilizer : flowering-preserving fertilizer was 5:1:2:2. Before transplanting, urea was applied at the N rate of 3 g pot^{-1}. Phosphate fertilizer (P_2O_5) and potassium fertilizer (K_2O) were applied as one-off basal fertilizer at

TABLE 1 The soil properties before sowing at the rice experimental site.

Rice variety	pH	Organic matter (g kg^{-1})	alkali-Hydrolysable N(mg kg^{-1})	Available P(mg kg^{-1})	Available K (mg kg^{-1})
Nanjing9108	7.26	22.3	118.65	63.72	123.75

25 g pot^{-1} and 7.5 g pot^{-1}, respectively. Urea was applied to approximately 1.7 g pot^{-1} at the 4~5 leaf stage; urea of 2.65 g pot^{-1} was applied at the penultimate one leaf stage. The ^{15}N isotope was applied twice, with 56% as basal fertilizer and 44% as topdressing, a total of 36 g, and the isotope abundance was 60%. ^{15}N topdressing was applied at the penultimate 2.5 leaf stage. A manual shelter was set up in the cultivation process. The other cultivation measures were referred to as the management measures of local experimental farmland. Immediately after maturity of 9108, the straw was taken and dried by natural light in the greenhouse. This step was to simulate the state of the straw from the harvest of rice to the sowing of wheat in the field trial. Also, the sample (only stems and leaves) was cut into approximately 10 cm for sealing. It was necessary to collect the soil in the growth stage of rice, sieve, and dry, and they were weighed at the same weight for standby. As two material factors before the second season of wheat planting, sieving was to ensure that the soil did not have excessive plate stubble, which had an unnecessary impact on the growth and development of wheat in the later stage.

Rice was planted in the first season. The transfer and distribution ratio of the labeled nitrogen in the rice-soil system was studied in order to provide details of labeled straw and labeled soil for wheat (Figure 1). The transport of ^{15}N isotope in the whole growth of rice was roughly divided into three directions: nitrogen loss rate (NLO), soil nitrogen residual rate (NSR), and nitrogen plant utilization rate (NPU). The final result was NPU > NSR > NLO. Among them, the ratio of isotopes absorbed by shoots from the application of nitrogen fertilizer was 29.48%, and NPU was 45.44%, which meant nitrogen accumulation in the spike was higher than that in the straw. The spike accounted for 57.61% of the total plant utilization, and the straw accounted for 42.39%. The proportion of soil residual nitrogen from nitrogen fertilizer was 19.5%, and NSR was 29.73%. The loss part was approximately 51.02%, and NLO was 24.83%. According to the principle of simulated field straw returning directly, the spike did not participate in further tests. The remaining straw stubble and residual fertilizer were treated as J and T for the next season, respectively. In addition, ^{15}N in rice roots was calculated in the soil in order to improve test accuracy.

The conventional planting pattern of straw returning was simulated in the field. Three different nitrogen sources contained the same weight and type of straw, soil, and fertilizer, which ensured the accuracy of the control variables in the study. First, all the remaining soil from the first season was mixed evenly and set aside for subsequent experiments, and the dry humidity of each pot was equal to that of ^{15}N-labeled soil. Secondly, the amount of straw required for each pot was converted according to the field ratio, and the same amount was weighed as a backup for ^{15}N-labeled straw (fully mixed with the soil when used). Finally, in order to reduce the loss of isotopes in the experiment, a bottom-closed pot was used, which was also a prerequisite for achieving ^{15}N-labeled fertilizer. The whole growth period of the experimental crop was ensured to be carried out under the rain shelter. This measure reduced the loss of consumables caused by extreme weather such as heavy rainfall and aimed to avoid large errors caused by surface runoff of ^{15}N in the results.

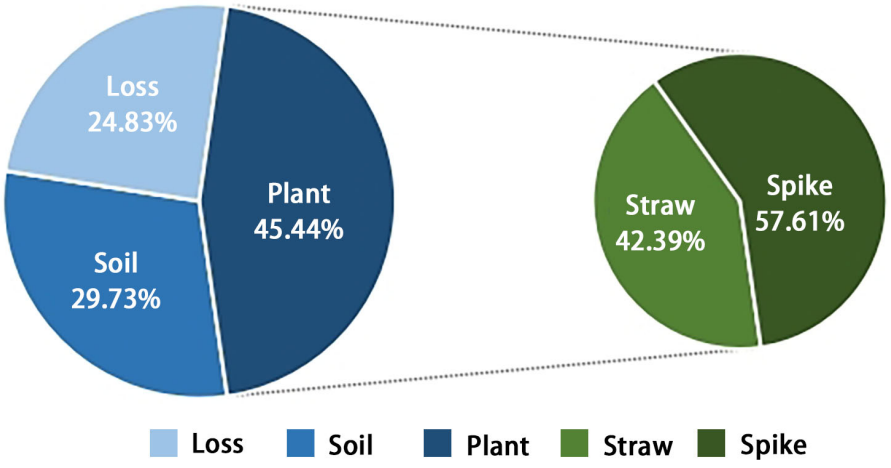

FIGURE 1
The comprehensive performance of ^{15}N fertilizer nitrogen at maturity of rice. The soil represents the residual nitrogen that can be utilized in the next season, while the plant represents the nitrogen absorbed and utilized in the current season. It was divided into spike and straw. The percentage on the left represents the proportion of different nitrogen directions, while the right side represents the ratio of each component to the total absorption of the plant.

2.2.2 Design of pot experiment in wheat season

The previous crop was rice and the soil was sandy loam. A two-factor design was used. The main area was two high nitrogen-efficient wheat varieties: Yangmai25 and Yangfumai4, and two low nitrogen-efficient varieties: Shengxuan6 and Yangmai22 (Table 2). The sub-area was three different nitrogen sources (T, F, and J), with a total of 12 treatments (Table 3). Since there were some studies of related varieties in our research group, we cited their conclusions to continue the experiment (Ding et al., 2022). In early November 2021, artificial spot sowing was carried out in pots, with a sowing depth of 2 cm, 12 seeds per pot, 8 seedlings left, and 1 cm soil covered after sowing.

Phosphorus (P_2O_5) and potassium (K_2O) fertilizers were a one-time basal application for 6.15 g pot^{-1} and 1.33 g pot^{-1}, respectively. The nitrogen fertilizer application was basal fertilizer : tillering fertilizer : jointing fertilizer : booting fertilizer = 5:1:2:2, which was applied to 1.74 g pot^{-1}, 0.35 g pot^{-1}, 0.7 g pot^{-1}, and 0.7 g pot^{-1}, respectively. Basal fertilizer was mixed with water into the soil before sowing; tillering fertilizer was applied at the 4~5 leaf stage; jointing fertilizer was applied at the penultimate 2.5 leaf age, and booting fertilizer was applied at the penultimate 1 leaf age. All nitrogen fertilizers in F were replaced by ^{15}N, and the same amount of urea was applied to T and J. In the cultivation process, a manual rain shelter was still set up. Except that the fertilizer was directly poured into the soil, other measures were based on the management measures of the local experimental field.

TABLE 2 The abbreviations of different nitrogen efficiency types, variety names, and treatments that will be repeatedly mentioned in the full text.

Species	Defined terms	Abbreviations
Wheat varieties	Shengxuan6	SX6
	Yangmai22	YM22
	Yangfumai4	YFM4
	Yangmai25	YM25
N variety classification	High nitrogen-efficient varieties	HNV
	Low nitrogen-efficient varieties	LNV
Treatments	^{15}N labeled fertilizer	F
	^{15}N labeled soil	T
	^{15}N labeled straw	J
Nitrogen indicators	Plant Nitrogen Utilization Efficiency	NPU
	Soil Nitrogen Residual Rate	NSR
	Nitrogen Loss Rate	NLO
	Nitrogen Transport Efficiency (pre-anthesis)	NTE
	Nitrogen Contribution Rate to Grains (pre-anthesis)	NCR
	Nitrogen Harvest Index	NHI
Rice variety	Nanjing9108	NJ9108

2.2.3 Design of pot experiment in the second rice season

The previous crop was wheat and the soil was sandy loam. A single-factor randomized-block experimental design was adopted, and three treatments (T, F, and J) were set as before. Nanjing 9108 was still adopted, and the closed barrel remained unchanged. Phosphorous potash complex fertilizer (KH_2PO_4) was applied as basal fertilizer at one time for 1 g pot^{-1}. The ratio of basal fertilizer : tillering fertilizer : spikelet-promoting fertilizer : flowering-preserving fertilizer was 5:1:2:2, which was applied to 1g pot^{-1}, 0.2 g pot^{-1}, 0.4 g pot^{-1}, and 0.4 g pot^{-1}, respectively. In addition, basal fertilizer was applied before transplanting; tillering fertilizer was applied at 4~5 leaf stage; spikelet-promoting fertilizer was applied at the penultimate 2.5 leaf age, and flowering-preserving fertilizer was applied at the penultimate 1 leaf age. The plants were transplanted in June 2022, and equidistant point insertion was used, with four points per pot and four plants per hole. Water replenishment and prevention of diseases were necessary according to the seedling situation later. Other management measures were the same as high-yield cultivation in the field.

2.2.4 Systematic sampling and ^{15}N determination

Ten shoots of rice with similar growth were taken in the frame at maturity. After 1 hour of deactivation at 105°CC, they were dried to constant weight at 80°CC. The shoots were divided into straw and spike for powder samples and then passed through 100 mesh (0.15 mm) for later use. At anthesis and maturity of wheat, four shoots with uniform growth were taken from three treatments respectively. After the shoots were separated, the same method as rice was used for the standby experiment. Meanwhile, the depth in 0~20 cm of soil was removed vertically from rice (maturity) and wheat (anthesis and maturity), repeating the process three times. The samples were mixed evenly and passed through 100 mesh (0.15 mm) after being dried and ground; 3~4 mg of each sample was weighed to be determined and wrapped into a regular rectangle (side length less than 5 mm) with tin paper. Then, the ^{15}N abundance was measured with Isoprime 100 stable isotope mass spectrometer by putting them into the machine.

2.3 Statistical analysis

The ratio of nitrogen in each fate was determined and analyzed. NPU, NSR, and NLO represented plant utilization efficiency (%), soil residual rate (%), and loss rate (%) of nitrogen, respectively. The letters in parentheses were used to distinguish three nitrogen sources (Table 2). The $^{15}N_{uptake}$, $^{15}N_{soil\ residue}$, and $^{15}N_{total}$ represented the total accumulation of ^{15}N (g pot^{-1}) in shoots, the residual amount of ^{15}N (g pot^{-1}) in soil, and the total input of ^{15}N (g pot^{-1}), respectively.

$$N\ (F)\ PU\ (\%) = {}^{15N}\ (F)_{uptake} \,/\, {}^{15N}\ (F)_{total}$$

$$N\ (F)\ SR\ (\%) = {}^{15N}\ (F)_{soil\ residue} \,/\, {}^{15N}\ (F)_{total}$$

TABLE 3 The soil properties before sowing at the wheat experimental site.

Treatment	pH	Organic matter(g kg^{-1})	alkali-Hydrolysable N (mg kg^{-1})	Available P (mg kg^{-1})	Available K (mg kg^{-1})
^{15}N-labeled soil	8.07	14.75	84.8	63.02	82.68
^{15}N-labeled straw and fertilizer	7.66	15.19	83.72	74.88	89.96

$$N\,(F)\,LO\,(\%) = 100 - N\,(F)\,PU\,(\%) - N\,(F)\,SR\,(\%)$$

$$N\,(T)\,PU\,(\%) = {}^{15N}\,(T)_{uptake} \,/\, {}^{15N}\,(T)_{total}$$

$$N\,(T)\,SR\,(\%) = {}^{15N}\,(T)_{soil\ residue} \,/\, {}^{15N}\,(T)_{total}$$

$$N\,(T)\,LO\,(\%) = 100 - N\,(T)\,PU\,(\%) - N\,(T)\,SR\,(\%)$$

$$N\,(J)\,PU\,(\%) = {}^{15N}\,(J)_{uptake} \,/\, {}^{15N}\,(J)_{total}$$

$$N\,(J)\,SR\,(\%) = {}^{15N}\,(J)_{soil\ residue} \,/\, {}^{15N}\,(J)_{total}$$

$$N\,(J)\,LO\,(\%) = 100 - N\,(J)\,PU\,(\%) - N\,(J)\,SR\,(\%)$$

Nitrogen-related physiological indicators were also mentioned here. NHI, NTE, and NCR were used to represent the nitrogen harvest index, nitrogen transfer rate before anthesis (%), and the contribution rate of pre-anthesis transferred nitrogen to grains (%), respectively. N_{grains}, $N_{anthesis}$, $N_{maturity}$, and $N_{maturity,\ veg}$ were selected to represent nitrogen accumulation of grains (g pot^{-1}), nitrogen accumulation of shoots at anthesis (g pot^{-1}), nitrogen accumulation of shoots at maturity (g pot^{-1}), and nitrogen accumulation of vegetative organs (g pot^{-1}), respectively

$$NHI = N_{grains} \,/\, N_{maturity}$$

$$NTE\,(\%) = (N_{anthesis} - N_{maturity,\ veg}) \,/\, N_{anthesis}$$

$$NCR\,(\%) = (N_{anthesis} - N_{maturity,\ veg}) \,/\, N_{grains}$$

Excel 2016 and Origin 2022 were used to process data and draw pictures. DPS7.05 (Zhejiang University, Hangzhou, China) was used for statistical analysis, and the LSD method was used for dominance analysis.

3 Results

3.1 The flow direction of ^{15}N isotopes during wheat maturity

As can be seen from Figure 2A, when the nitrogen source was ^{15}N-labeled straw, the nitrogen utilization efficiency of wheat at maturity was in the order of NLO > NSR > NPU (nitrification, denitrification, ammonia volatilization, and surface runoff were included in the losses, which was not mentioned below). It was speculated that because the straw was decomposed in the soil without adding a decomposition agent, the decomposition effect was terrible. Due to the slow release and decomposition of nutrients, most of the nitrogen in the straw still remained in itself, so the loss rate was higher in the current season. However, when the speed was accelerated in the later stage, a large amount of nitrogen could enter the soil, resulting in an increase in soil residual nitrogen.

Figure 2B shows that the nitrogen utilization efficiency of wheat at maturity was NSR > NPU > NLO under the treatment of ^{15}N-labeled fertilizer. Since fertilizer nitrogen could be directly absorbed by crops or enter the soil as a supplement to the soil nitrogen pool without undergoing complex forms of transformation, its loss rate was relatively low.

According to Figure 2C, when the nitrogen source was ^{15}N-labeled soil, the nitrogen fate of wheat with different nitrogen efficiency at maturity was NPU > NSR > NLO. The nitrogen supply capacity of the soil was affected by the C/N ratio, microbial activity, temperature, and humidity, but it did not prevent soil nitrogen from being the main source of nitrogen utilization for shoots.

By comparing three nitrogen sources, the plant utilization efficiency was found to be T > F > J. T was 1.14%~5.51% and 20.81%~30.65% higher than F and J, respectively. The soil residual rate was also T > F > J, with T being 2.72%~6.05% and 10.52% ~15.42% higher than F and J, respectively. The loss rate was T< F< J, with T being 5.80%~11.53% and 36.23%~41.20% lower than F and J, respectively. The result of F may be due to the barrier of the fertilizer leaching downward so that most nitrogen was retained in the soil layer of 0~20 cm. Then, the utilization of fertilizer nitrogen was increased and the loss was declined. Meanwhile, the trend of the three treatments among the four varieties was basically the same. The utilization rate and loss rate were HNV > LNV, and the residual rate was HNV< LNV. A few data that did not meet this result appeared in T, which may be due to the fact that the nitrogen supply capacity of the soil was affected by the nitrogen pool and external environment compared to F and J.

The nitrogen distribution ratio of shoots at maturity was in the order of spike > stem > leaf (Figure 2). The trend of nitrogen absorption efficiency in different organs of wheat was identical in these three graphs. After anthesis, countless nitrogen flowed to the grains, while the leaves gradually turned yellow, or even partially withered. Ineffective tillers gradually died and decreased. Thus, the spike received the most nitrogen from the shoots.

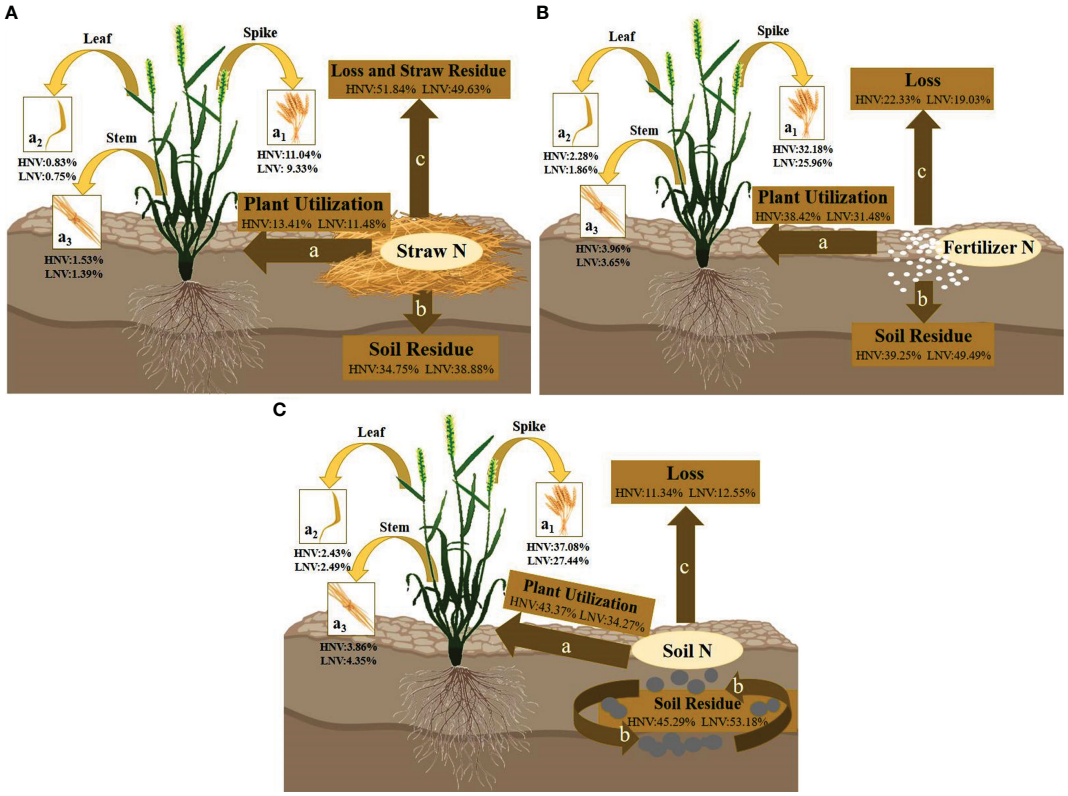

FIGURE 2
(A–C) Showed the overall nitrogen transport patterns of wheat at maturity when ^{15}N-labeled with straw, fertilizer, and soil. a, b, and c represent three broad transport directions, (for ^{15}N-labeled straw, the losses included residual nitrogen and losses of the straw itself); a_1, a_2, and a_3 represent three narrowly defined transport flows to the plant, namely, to the spike, leaf, and stem. The percentage represents the relative numerical range of nitrogen loss rate, plant utilization rate, and soil residual rate in wheat with different nitrogen efficiency.

3.2 Distribution of ^{15}N in different organs of wheat

Isotope tracing technology was conducted to detect ^{15}N in various organs of wheat at maturity (Figure 3). The ratio of ^{15}N in grain, stem, glume, and leaf of wheat were 71.90%~79.92%, 8.63%~13.04%, 5.93%~9.53%, and 4.50%~7.39%, respectively (Figure 3A). There was no significant difference among the three nitrogen sources, indicating that nitrogen transport post-anthesis was regulated by the plant itself and was not affected by nitrogen sources.

The distribution ratio of nitrogen in ^{15}N-labeled fertilizer, soil, and straw treatments was in the order of grain > stem > glume > leaf, and the proportion of grain was all higher than two-thirds of the total application of ^{15}N (Figure 3A). The proportion of glume and leaf was basically lower than one-tenth of the total application of ^{15}N (Figure 3A). Different nitrogen efficiency varieties had no difference in this rule, indicating that the nitrogen accumulated by shoots was mainly supplied to grain filling post-anthesis.

In addition, the nitrogen utilization efficiency of various organs in different varieties showed significant differences, basically being HNV > LNV and YFM4 > YM25 > YM22 > SX6 (Figure 3B). In terms of distribution ratio, different nitrogen efficiency varieties basically showed HNV< LNV among stems, leaves, and glumes, and HNV > LNV between grains (Figure 3A). It was indicated that different organs had different response abilities to nitrogen, and the nitrogen sensitivity of grains was higher. There was no significant difference under the same treatment in F and J for HNV, while the difference was significant in T, and the trend of LNV was consistent with HNV (Figure 3B). The effect of soil nitrogen on the utilization ability of different varieties was significantly higher than that of fertilizer and straw nitrogen.

3.3 Correlation analysis of different nitrogen indicators

Spearman correlation analysis was used to compare the correlation between different nitrogen physiological indicators (Figure 4), including NTE, NCR, NHI, NPU, NSR, and NLO (Table 2). There was a highly significant positive correlation among NTE, NCR, and NHI, indicating that nitrogen accumulation in the vegetative organs before anthesis was necessary due to the great significance for grain-filling, transport, and distribution of nitrogen after anthesis. More nitrogen accumulation before anthesis was beneficial for grains at the filling stage to fully absorb nutrients, and the three are interrelated and complementary. NPU showed no significant

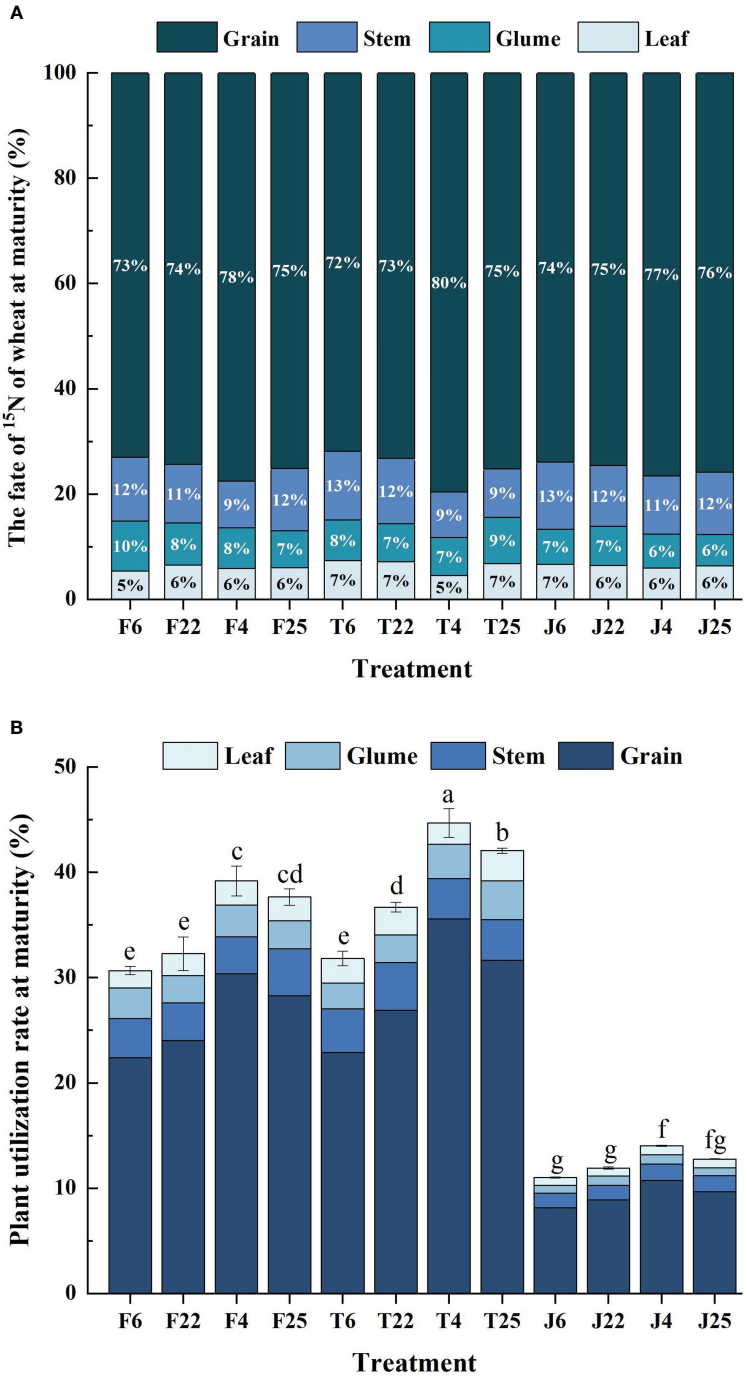

FIGURE 3
(A) Reveals the distribution ratio of nitrogen in the plant organs of wheat under all treatments in the study, including stem, leaf, grain, and glume. It represents the proportion of nitrogen in different organs in the shoots in order to compare the response potential of different organs to nitrogen. **(B)** Puts the proportion of organs into the nitrogen utilization efficiency of plants at maturity for overall comparison, which had advantages in observing the organ allocation of different nitrogen efficiency. Different lowercase letters indicate significant differences among the three cultivar groups at $P< 0.05$ **(B)**.

positive correlation with the above three factors, while NSR showed no significant negative correlation with them. Also, there was no clear pattern for the correlation analysis of NLO with them. There was no significant positive correlation between NSR and NPU, while NLO showed a highly significant negative correlation with NSR and NPU. The effect of plant nitrogen uptake and soil residue nitrogen were simultaneously responsive under the condition of equal nitrogen fertilizer application. It meant higher nitrogen accumulation determined higher accumulation and transport and they synergistically improved grain protein content at maturity.

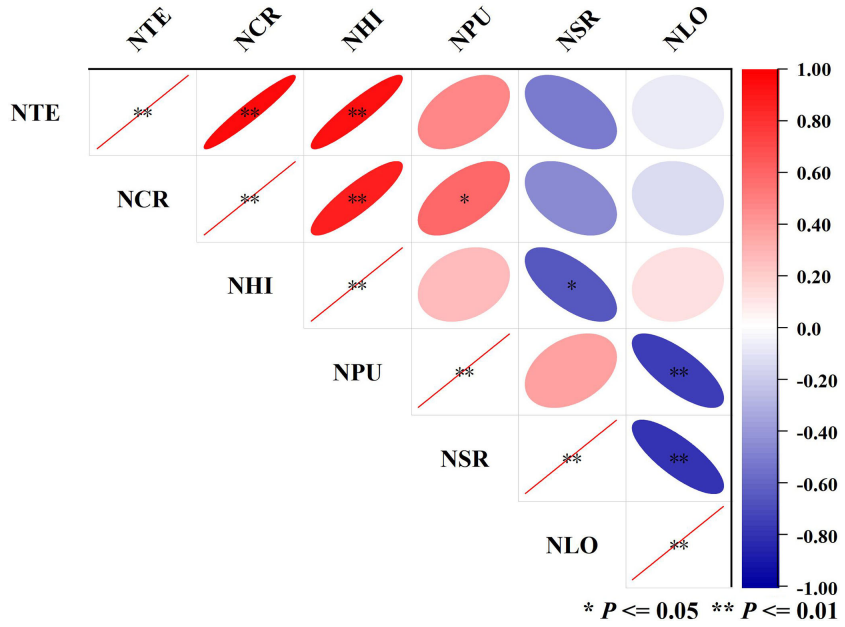

FIGURE 4
Summary of correlation of important nitrogen efficiency indicators. Blue at different depths represents a positive correlation, while red at different depths represents a negative correlation. The size of the ellipse reflects the size of the p-value. The larger the ellipse, the larger the absolute value of *P*, and the smaller the ellipse, the smaller the absolute value of *P*. * (*P*<= 0.05) represents a significant correlation, and ** (*P*<= 0.01) represents a very significant correlation.

3.4 The flow direction of ^{15}N isotopes during rice maturity

The transport relationship of residual nitrogen between the third crop (rice) and the previous crop (wheat) is shown in Figure 5. The specific performance first appeared between different treatments. F and J showed NLO > NSR > NPU (Figures 5A, B), while T showed NSR > NPU > NLO (Figure 5C). Secondly, the different destinations of nitrogen were summarized as follows: plant utilization efficiency and soil residual rate were T > F > J, while loss rate was J > F > T (Figure 5). These patterns were consistent with the second season. Compared to F and J, T was 10.90% and 15.03% higher in plant utilization rate, 4.97% and 10.98% higher in soil residual rate, and 15.86% and 26.01% lower in loss rate, respectively (Figure 5). The distribution proportion of nitrogen among various organs of shoots showed spike > stem > leaf, which was also an inevitable result of multiyear crops (Figure 5).

Compared to the second season, the share of the three nitrogen destinations changed (Figures 2, 5). For F and T, the utilization rate decreased by 13.90% and 6.88%, but the loss rate increased by 20.63% and 13.50%, respectively (Figures 2, 5B, C). However, the plant utilization rate of J increased by 4.46%, and the loss rate remained basically unchanged, indicating that straw decomposition was more significant in the long term than in the short term (Figures 2, 5A). All the nitrogen sources showed a small decrease in soil residual rate (5.19%~6.73%), which indicated that the nitrogen utilization rate could be greater than the recovery rate in the current season (Figures 2, 5). During the two seasons, fertilizer nitrogen exhibited the greatest changes in nitrogen recovery rate while soil nitrogen showed the smallest. The results could be inferred that fertilizer nitrogen was unstable in the process of recycling and susceptible to the external environment, while straw nitrogen was suitable to provide reserve nitrogen for crops.

3.5 Different contributions of nitrogen sources among three nitrogen transport directions

The contribution rate for plant nitrogen accumulation and soil residual nitrogen from different sources were both T > F > J, while it was T< F< J of nitrogen losses (Figure 6). There were significant differences between different treatments (Table 4). The contribution rates for the nitrogen accumulation of shoots from soil nitrogen, fertilizer nitrogen, and straw nitrogen were 43.28%~45.70%, 30.11%~41.73%, and 13.82%~24.19%, respectively (Figure 6A). Also, soil residual nitrogen accounted for 37.18%~38.08%, 32.90%~35.20%, and 27.33%~29.21%, respectively (Figure 6B). Without special management, 12.56%~21.53% of lost nitrogen came from soil nitrogen, of which 23.21%~34.94% came from fertilizer nitrogen, and 43.53%~61.50% came from straw nitrogen (Figure 6C).

There were different impacts on nitrogen flow among the three nitrogen sources in rice and wheat. The contribution rate of fertilizer nitrogen in plant utilization efficiency was 9.77%~11.62% lower than that in wheat, while that of soil nitrogen and straw nitrogen were 0.06%~2.42% and 9.20%~10.37% higher than that in wheat, respectively (Figure 6A). The ratio of straw nitrogen of rice in nitrogen loss decreased by 16.47%~17.97% compared with wheat, while soil nitrogen and fertilizer nitrogen increased by

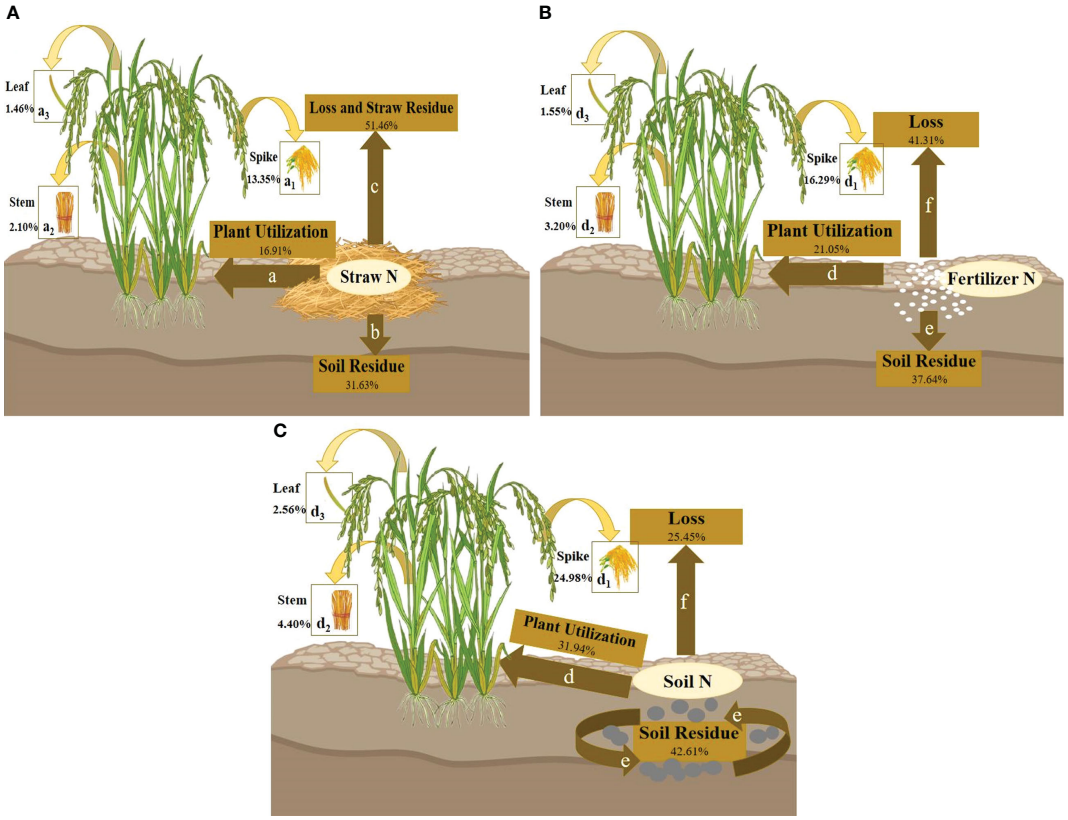

FIGURE 5
(A–C) Show the overall transport pattern of nitrogen from different sources (where nitrogen was the nitrogen remaining in the soil of wheat in the previous season, and the three sources were consistent with the above) for the third crop (rice) at maturity. Where d, e, and f represent three broad transport directions (for ^{15}N-labeled straw, the loss included residual nitrogen and losses of the straw itself); d_1, d_2, and d_3 represent three narrowly defined transport flows to the plant, namely, to the spike, leaf, and stem. The percentage represents the average value of nitrogen loss rate, utilization rate, and soil residual rate in wheat with different nitrogen efficiency.

5.47%~8.97% and 8.75%~11.73%, respectively (Figure 6C). There was no obvious trend in the distribution ratio of residual nitrogen in soil among different crops (Figure 6B).

3.6 Different contributions of nitrogen sources among three organs

As shown in Figure 7, there existed differences in the contribution of various organs among different nitrogen sources in the two crops. The organs of wheat showed a uniform trend of T > F > J. However, the rule for rice was quite opposite to the former. Nitrogen accumulation in stems of rice showed F > T > J, which showed J > T > F in leaves and spikes. The proportion of nitrogen accumulation in leaves, stems, and spikes of wheat from soil nitrogen was 39.01%~49.88%, 39.30%~47.82%, and 42.56%~46.28%, respectively. Similarly, the ratio of fertilizer nitrogen was 34.72%~44.74%, 37.72%~45.29%, and 39.83%~42.53%, respectively. There were differences in straw nitrogen, accounting for only 13.79%~16.24%, 14.46%~17.45%, and 13.60%~14.91%, respectively. Compared with that of wheat, the contribution rate of straw nitrogen for nitrogen accumulation in rice increased by 14.39%~1.99%, which was reduced by 0.49%~13.84% and 5.69%~16.56% for fertilizer nitrogen and soil nitrogen, respectively. Overall, the contribution rate of soil nitrogen in shoots was the highest, while the potential of straw nitrogen in the after-effect was significantly higher than that of soil and fertilizer nitrogen.

3.7 Comparison of trends in the second and third seasons

In view of the nitrogen distribution patterns in the second and third quarters, a dumbbell chart was created (Figure 8). The results showed that the soil nitrogen of rice was in the order of S2 > S3, with 20.63%, 13.50%, and 0.73% less than that in wheat, respectively. In terms of loss rate, it showed that $S_2 < S_3$, and the previous season of F, T, and J was 6.73%, 6.62%, and 5.19% lower than the subsequent season, respectively. However, there are differences in plant utilization efficiency among the three. F and T showed $S_2 > S_3$, with the previous season being 13.90% and 6.88% higher than the latter, while J showed $S_2 < S_3$, with the previous season being 4.46% lower than the latter. The decomposition ability of straw was better in paddy fields than in wheat (paddy fields had sufficient water). In that way, nitrogen could be continuously released from the supplied

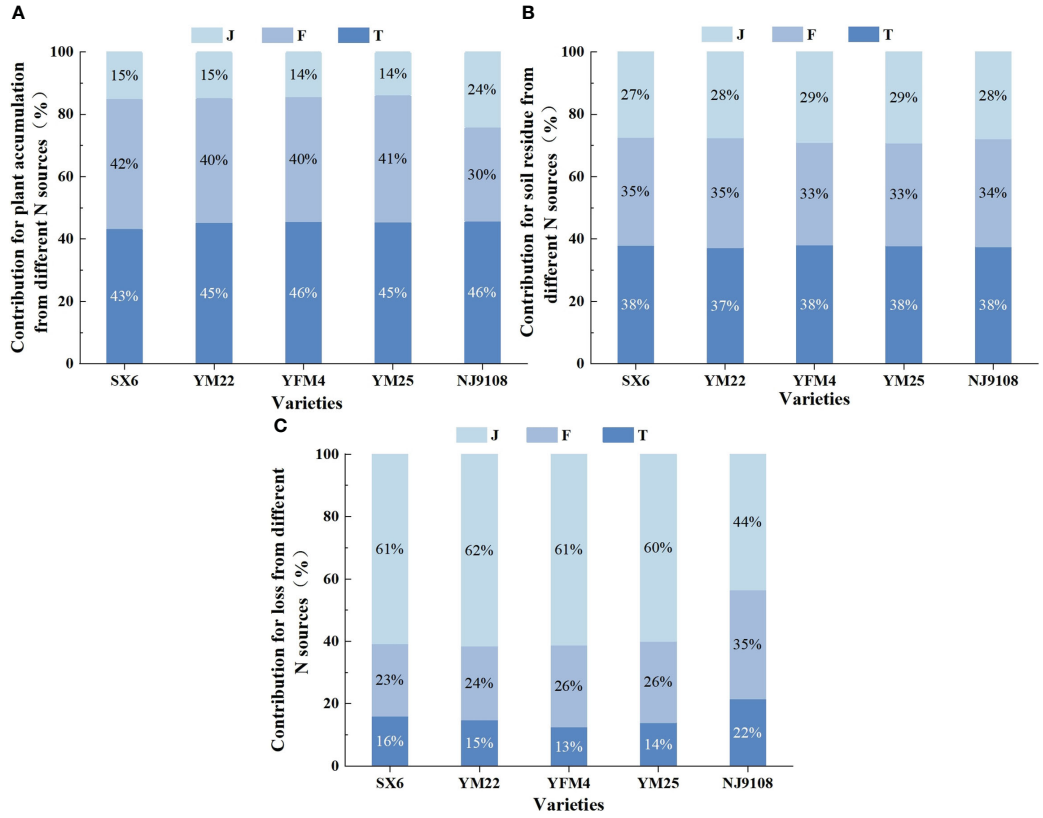

FIGURE 6
Effects of different nitrogen sources on plant nitrogen accumulation, soil nitrogen residue, and nitrogen loss in wheat and rice at maturity. **(A–C)** Represent the contribution rate of the three treatments to different transport directions.

straw in the later stage of utilization, which also depended on the mineralization ability of straw nitrogen. The decrease in loss rate was most significant under F and least significant under J. There was no significant difference in the decreasing trend of soil residual rate among them, only a slight decrease in J. The most significant decrease or increase in plant utilization rate was in F, while the smallest change was still in J. Differences between these trends were mainly caused by changes in crop characteristics, soil fertility, and even environmental conditions (temperature and humidity). The results also indicated that the seasonal performance of fertilizer nitrogen was the most unstable, of which soil nitrogen and straw nitrogen were more controllable in use. In addition, straw nitrogen had the greatest potential in the early operation of the rice-wheat rotation system.

TABLE 4 Multivariate variance analysis of the contribution of the interaction between cultivars and nitrogen sources to the three nitrogen utilization indicators.

	NPU	NSR	NLO
V	**	**	**
S	**	**	**
V × S	**	**	**

** indicate a significant difference at the 1 % level (P<= 0.01). V and S refer to varieties and nitrogen sources, respectively.

4 Discussion

4.1 The contribution of different N sources to nitrogen transport in the crop-soil system

Crops maintain growth and development by absorbing nutrient elements from nitrogen fertilizers (Guo et al., 2022). The contribution ability of different nitrogen sources in the rice-wheat rotation multiple cropping systems was different, and there were commonalities and individuality among them. Soil nitrogen was composed of the primary nitrogen pool (soil native nitrogen) that was continuously exhausted without fertilizer nitrogen input and the self-fixed supplementary nitrogen pool (residual fertilizer nitrogen and straw nitrogen) after input of urea. It was generally divided into residual inorganic nitrogen and soil mineral nitrogen, which together determined the profit and loss of the soil nitrogen pool (Ye et al., 2022). Previous studies showed that 70.20%~79.27% of the nitrogen absorbed by crops at anthesis came from soil nitrogen, accounting for 45.0%~66.0% at maturity (Jia et al., 2011). It indicated that plants were most dependent on soil nitrogen when it was at a stable fertility level. In this paper, the statistics (43.28%~45.70% at maturity) were basically consistent with the previous results (Figure 6). The grain nitrogen accumulation also showed the rule, of which nitrogen translocation (73.1%~87.9%) before anthesis was much larger than

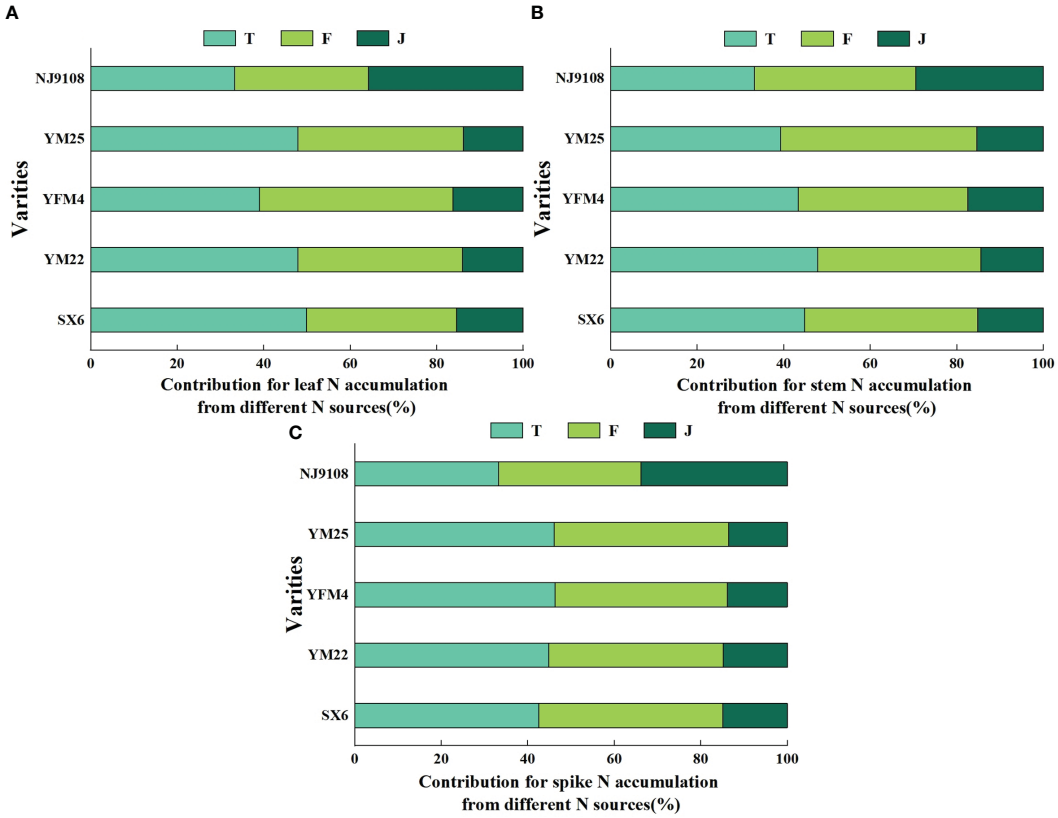

FIGURE 7
Effects of different nitrogen sources on leaf, stem, and spike in wheat and rice at maturity. **(A–C)** Represent the contribution rate of the three treatments to different organs.

nitrogen assimilation (12.1%~26.9%) after anthesis (Liu et al., 2020). Most of the pre-anthesis nitrogen translocation came from soil nitrogen, which also confirmed the physiological mechanism of soil nitrogen regulation crop response to nitrogen. In addition to the direct contributions, soil nitrogen also played an indirect role in nitrogen flow (Fang et al., 2022). The nitrogen absorbed from fertilizer nitrogen and straw residues was mineralized into organic nitrogen, thereby replenishing the endogenous supply of the soil nitrogen pool.

Fertilizer nitrogen had a legacy effect, changing the balance of the soil nitrogen pool directly or indirectly (crop residues) (Wytse et al., 2022). It showed a strong seasonal effect on nitrogen utilization, and the results in this study were basically consistent with other research. Fertilizer nitrogen that was not absorbed and stored by crops appeared as organic nitrogen in the soil, and then entered a depth of 0~100 cm in the soil with straw nitrogen, especially in the 0~40 cm soil layer in the form of mineralizable nitrogen (Chen et al., 2020). The high permeability of the 0~30 cm soil profile could lead to the high activity of straw and fertilizer nitrogen remaining in the surface layer (Hu et al., 2017). Also, the available amount could increase, which contributed greatly to the promotion of organic nitrogen mineralization in the soil and the supplement of the soil nitrogen pool. In this study, the soil residual rate of fertilizer nitrogen was approximately 37.64%~49.49% (0~20 cm soil layer) (Figures 2B, 5B), which was higher than that in previous findings (24.5%~44.0% in 0~80 cm soil layer) (Jia et al., 2011; Shi et al., 2012). It was possible to calculate the crop type (wheat varieties with different nitrogen response efficiency), or the soil type (sandy loam, clay, etc.) could also be a major factor affecting the ability of nitrogen retention and remineralization of fertilizers, but the indirect effect of fertilizer nitrogen in the soil was still unconfirmed.

The effectiveness and contribution rate of straw throughout the entire growth period of plants seemed to be very low, while it has been proved that straw incorporation could increase crop yield (Bai et al., 2023). The sudden incorporation of crop straw into soil could lead to seasonal nitrogen deficiency in crops (Chen et al., 2016). It is possibly due to the modification of straw decomposition on soil physical properties, which encouraged the breakdown and reproduction of microorganisms, and then induced nitrogen fixation in the process (Huang et al., 2021; Sun et al., 2022). Therefore, straw nitrogen played an indispensable role in increasing the soil organic nitrogen pool, which was usually mineralized or immobilized when supplying crops (Zhang J. T. et al., 2017). The conclusion that the direction of ^{15}N-labeled straw was soil residual rate > plant utilization efficiency also supported this viewpoint (Figures 2A, 5A). Xu et al. (2021) found that the nitrogen utilization rate and loss rate of straw incorporation increased by 52.5% and decreased by 12.8%, respectively, compared with the control treatment. This situation also had an obvious influence on improving the harvest index and crop yields, which was consistent with our findings (Figures 2A, 5A). Straw nitrogen has potential utilization value, reducing carbon footprint and increasing crop

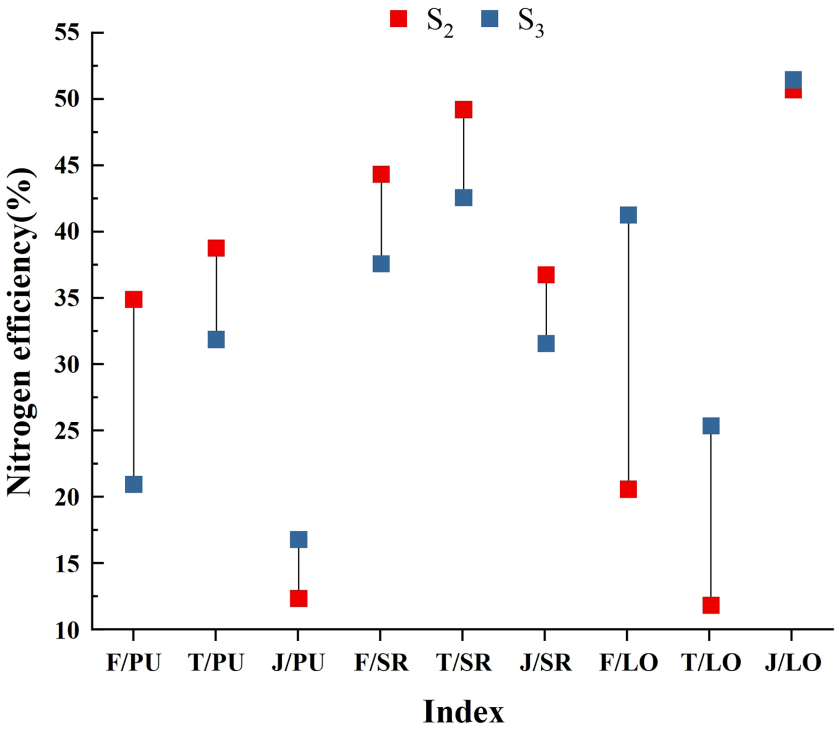

FIGURE 8
The figure shows the trend of nitrogen transport under different nitrogen sources. S_2 and S_3 represent the second and third quarters, respectively. The red square represents S_2, the blue square represents S_3, and the vertical line represents the difference in nitrogen efficiency between the two quarters under different treatments. Each indicator was named after 'treatment/ratio'. The left side of the slash represents three treatments, namely, ^{15}N-labeled fertilizer (F), ^{15}N-labeled soil (T), and ^{15}N-labeled straw (J). The right side of the slash represents nitrogen efficiency, namely, plant utilization efficiency (PU), soil residual rate (SR), and seasonal loss rate (LO).

production (Dachraoui and Sombrero, 2020). Therefore, the efficient use of soil nitrogen was conducive to improving soil nitrogen supply capacity and promoting the effective implementation of nitrogen-saving goals, and it was of great significance in improving soil fertility.

In summary, fertilizer nitrogen and straw nitrogen maintained the balance of the soil nitrogen pool synchronously by directly converting it into organic nitrogen (Bai et al., 2023). Soil nitrogen and straw nitrogen simultaneously reduced gas emissions and promoted the implementation of nitrogen conservation and emission reduction (Liang et al., 2017; Li et al., 2021; Yang et al., 2022). Fertilizer nitrogen and soil nitrogen played a dominant role in plant nitrogen accumulation and transport at the same time. The three different sources of nitrogen synergistically reduced nitrogen loss, which was beneficial to improve nitrogen utilization efficiency under optimal nitrogen fertilizer management, and ultimately achieved the two goals of optimizing nitrogen fertilizer supply pathways and improving soil fertility.

4.2 Effects of different N sources on the availability of nitrogen in the current season and the sustainability in the following season

Some studies indicated that residual nitrogen in soil profiles (0~40 cm) had great potential (Chen et al., 2020). If not utilized by plants, most residual nitrogen would leach into soil layers of 1.2 m or even deeper in the form of nitrate (NO_3^-), greatly exacerbating losses (Richter and Roelcke, 2000). From the viewpoint of soil, nitrogen efficiency was regulated by soil depth and soil nitrogen residue to a great degree, as well as the strength of inherent soil productivity (Ren et al., 2023). Consistent with our findings, combined with a loss rate of ^{15}N-labeled soil, the two seasons were 11.95% and 25.45%, respectively (Figures 2C, 5C). The elaborate pot experiment design reduced the occurrence of losses, avoiding the effects of excessive irrigation or heavy rainfall (downward leaching or surface runoff) through closed barrels and concomitant rain shelters. This measure retained more effective nitrogen for subsequent crops and reduced the possibility of deep soil pollution (Zhang J. T. et al., 2017). When the fertilizer nitrogen was applied to the soil, although some of the nitrogen derived from fertilizer could enter the residual rice straw, it could return to the soil in a later stage (Wytse et al., 2022). This study confirmed the interpretation that the soil residual rate of wheat in the second season was in the order of T > F > J (Figure 2).

The initial application of fertilizer nitrogen was beneficial to ensure the nitrogen recycling efficiency of rice/wheat over several years while maintaining the stability of nitrogen transfer in the plant-soil system. In this experiment, ^{15}N was applied in the first season of rice before transplanting, and then the residual fertilizer was retained and detected in the second season, confirming the effectiveness of nitrogen recovery in the later season (Yu and Shi,

2015). The plant utilization rate of F in the first season was 45.44% (Figure 1), while the rates in the second and third seasons were approximately 34.95% and 21.05% (Figures 2B, 5B), which align well with the discovery by Smith and Chalk (2018), that the recovery rate decreased by 10% year by year in their study. According to their conclusions, the recovery rate of fertilizer nitrogen remaining in the soil in the first season was between 20% and 30%, which was slightly lower than our study. Water conditions and low soil nitrogen leaching rates were considered to be the reasons for this result (Figure 2B). In addition, there were some hypotheses that have been proved by previous studies that fertilizer nitrogen contributed more to nitrogen uptake by crops in the first few years after application (Wytse et al., 2022). Although the utilization rate showed a decreasing trend, there was no significant change in the soil residual rate (basically maintained at 40%); it seemed likely that there was still a potential for fertilizer nitrogen to be recovered in the later stage.

Other aspects that support the above views were that the ^{15}N-labeled straw was designed in our experiment. It has been proved that the straw can be effectively used and recycled by crops for multiple seasons. The utilization rates of the two seasons were 12.45% and 16.91% (Figures 2A, 5A), respectively, and the numerical gap under the ^{15}N-labeled fertilizer was gradually narrowed (Xu et al., 2021). The loss rate of straw nitrogen in the last two seasons was 50.73% and 51.46% (Figures 2A, 5A), respectively. There could exist two reasons for the higher results. The unrecovered straw nitrogen remained in the crop residue and was not decomposed, or was discharged in the form of gas (N_2O or NH_3) (Liu et al., 2021). In terms of nitrogen loss, it was possible that the undecomposed organic nitrogen was more than the emitted gaseous nitrogen (Yan et al., 2019). By comparing the lower loss rates of ^{15}N-labeled soil and ^{15}N-labeled fertilizer under the same nitrogen application management, as well as the increase of straw nitrogen in the utilization efficiency of two crops, this inference could be drawn (Figures 2, 5).

Soil nitrogen and straw nitrogen could synergistically play a huge advantage in lowering production costs (mainly by cutting artificial nitrogen application) and reducing environmental pollution when it comes to economic and ecological benefits (Sun et al., 2022). However, we have not conducted thorough research on the standard measurement of environmental pollution indicators (the value of greenhouse gas emissions under different treatments and whether there are differences) (Huang et al., 2022; Zhang A. F. et al., 2017). Also, fertilizer nitrogen belonged to inorganic nitrogen, straw nitrogen belonged to organic nitrogen, and soil nitrogen belonged to organic and inorganic nitrogen. The high-efficiency utilization rate of soil nitrogen also relatively confirmed the significance of organic-inorganic fertilization in the nitrogen fertilizer model in the promotion of the agricultural industry nowadays (Choudhary et al., 2021).

5 Conclusion and prospect

Through the study of different sources of nitrogen, the proportion of different fates was considered; soil nitrogen had the largest contribution ratio to plant utilization and soil residue, followed by fertilizer nitrogen and straw nitrogen. According to the plant utilization rate, it could be judged that the after-effects of straw nitrogen and seasonal availability of soil nitrogen were both the strongest, while the stability of fertilizer nitrogen was the worst. Nitrogen accumulation and distribution ratio in shoots of rice and wheat both showed the most in grains and the least in leaves, regardless of the differences in nitrogen efficiency of crops. In summary, three nitrogen sources tested showed intensive characteristics and determined the necessity of nitrogen saving, quantified emission reduction, and multi-season recovery in crop production.

In the future, the practical application of this study will focus on the cultivation of soil fertility under the combination of straw returning and ^{15}N stable isotope tracer technology. We hope that the need for fertilizer could be declined by making full utilization of straw nitrogen and soil nitrogen from the previous crops, as well as reducing production costs and reducing N_2O emissions in the field. During this period, different straw returning methods (carbonized returning, total direct returning, adding decomposing agent returning, etc.) will also be used as a direction to extend the consideration of straw nitrogen. Through the optimization of management mode (reasonable C/N ratio and stable nitrogen recovery rate), high-yield and high-quality crop cultivation and sustainable development of ecological environment on the basis of nitrogen reduction will be achieved.

Data availability statement

The original contributions presented in the study are included in the article/supplementary material. Further inquiries can be directed to the corresponding author.

Author contributions

WJ: Data curation, Formal Analysis, Investigation, Methodology, Writing – original draft. QM: Investigation, Writing – review & editing. LL: Investigation, Writing – review & editing. CD: Investigation, Writing – review & editing. MZ: Project administration, Supervision, Writing – review & editing. CL: Conceptualization, Resources, Writing – review & editing. JD: Conceptualization, Resources, Writing – review & editing. WG: Conceptualization, Resources, Writing – review & editing. XZ: Project administration, Supervision, Writing – review & editing.

Funding

The author(s) declare financial support was received for the research, authorship, and/or publication of this article. This work was financially supported by the Special Technology Innovation Fund of Carbon Peak and Carbon Neutrality in Jiangsu Province (BE2022312); the earmarked fund for Jiangsu Agricultural Industry Technology System (JATS [2022] 502); the Vice President of Science and Technology Project in Jiangsu Province (FZ20211404); the construction project of advantageous disciplines in universities in

Jiangsu Province; and the Famous Teacher Studio in Yangzhou, Jiangsu Province.

Conflict of interest

The authors declare that the research was conducted in the absence of any commercial or financial relationships that could be construed as a potential conflict of interest.

Publisher's note

References

(2020). Available at: http://www.fao.org/sustainability/background/en/.

Bai, J. Z., Song, J. J., Chen, D. Y., Zhang, Z. H., Yu, Q., Ren, G. X., et al. (2023). Biochar combined with N fertilization and straw return in wheat-maize agroecosystem: Key practices to enhance crop yields and minimize carbon and nitrogen footprints. *Agric. Ecosyst. Environ.* 357, 108366. doi: 10.1016/j.agee.2023.108366

Benincasa, P., Reale, L., and Tedeschini, E. (2017). The relationship between grain and ovary size in wheat: An analysis of contrasting grain weight cultivars under different growing conditions. *Field Crops Res.* 210, 175–182. doi: 10.1016/j.fcr.2017.05.019

Bhattacharya, A. (2019). *Changing climate And Resource Use Efficiency In Plants* (Cambridge, MA: Academic Press).

Bhattarai, D., Abagandura, G. O., Nleya, T., and Kumar, S. (2021). Responses of soil surface greenhouse gas emissions to nitrogen and sulfur fertilizer rates to *Brassica carinata* grown as a bio-jet fuel. *GCB Bioenergy* 13, 627–639. doi: 10.1111/GCBB.12784

Chen, N., Li, X., Imnek, J., Shi, H., and Zhang, Y. (2020). The effects of biodegradable and plastic film mulching on nitrogen uptake, distribution, and leaching in a drip-irrigated sandy field. *Agric. Ecosyst. Environ.* 292, e6817. doi: 10.1016/j.agee.2020.106817

Chen, Z. M., Wang, H. Y., Liu, X. W., Lu, D. J., and Zhou, J. M. (2016). The fates of ^{15}N-labeled fertilizer in a wheat-soil system as influenced by fertilization practice in a loamy soil. *Sci. Rep.* 6, 34754. doi: 10.1038/srep34754

Choudhary, M., Meena, V. S., Panday, S. C., Mondal, T., Yadav, R. P., Mishra, P. K., et al. (2021). Long-term effects of organic manure and inorganic fertilization on biological soil quality indicators of soybean-wheat rotation in the Indian mid-Himalaya. *Appl. Soil Ecol.* 157, 103754. doi: 10.1016/j.apsoil.2020.103754

Cui, H. X., Luo, Y. L., Li, C. H., Chang, Y. L., Jin, M., Li, Y., et al. (2023). Effects of nitrogen forms on nitrogen utilization, yield, and quality of two wheat varieties with different gluten characteristics. *Eur. J. Agron.* 149, 126919. doi: 10.1016/j.eja.2023.126919

Dachraoui, M., and Sombrero, A. (2020). Effect of tillage systems and different rates of nitrogen fertilisation on the carbon footprint of irrigated maize in a semiarid area of castile and leon, Spain. *Soil Tillage Res.* 196, 104472. doi: 10.1016/j.still.2019.104472

Ding, Y. G., Zhang, X. B., Ma, Q., Li, F. J., Tao, R. R., Zhu, M., et al. (2022). Tiller fertility is critical for improving grain yield,photosynthesis,and nitrogen efficiency in wheat. *J. Inter. Agr.* 22, 2054–2066. doi: 10.1016/j.jia.2022.10.005

Falcinelli, B., Galieni, A., Tosti, G., Stagnari, F., Trasmundi, F., Oliva, E., et al. (2022). Effect of wheat crop nitrogen fertilization schedule on the phenolic content and antioxidant activity of sprouts and wheatgrass obtained from offspring grains. *Plants (Basel)* 11, e2042. doi: 10.3390/plants11152042

Fang, H., Liu, F., Gu, X., Chen, P., Li, Y., and Li, Y. (2022). The effect of source-sink on yield and water use of winter wheat under ridge-furrow with film mulching and nitrogen fertilization. *Agr. Water Manage.* 267, e7616. doi: 10.1016/j.agwat.2022.107616

González-Cencerrado, A., Ranz, J. P., Jiménez, M., and Gajardo, B. R. (2020). Assessing the environmental benefit of a new fertilizer based on activated biochar applied to cereal crops. *Sci. Total Environ.* 711, e4668. doi: 10.1016/j.scitolenv.2019.134668

Guo, J. B., Li, C., Xu, X. B., Sun, M. X., and Zhang, L. X. (2022). Farmland scale and chemical fertilizer use in rural China: New evidence from the perspective of nutrient elements. *J. Clean. Prod.* 376, e134278. doi: 10.1016/J.JCLEPRO.2022.134278

Guo, R., Miao, W., Fan, C., Li, X., Shi, X., Li, F., et al. (2021). Exploring optimal nitrogen management for high yielding maize in arid areas *via* ^{15}N-labeled technique. *Geoderma* 382, e114711. doi: 10.1016/j.geoderma.2020.114711

Hu, J. J., Zhu, L. F., Hu, Z. H., Zhong, C., Lin, Y. J., Zhang, J. H., et al. (2017). Effects of soil aeration methods on soil nitrogen transformation, rice nitrogen utilization and yield. *Trans. Chin. Soc Agric. Eng.* 33, 167–174. doi: 10.11975/j.issn.1002-6819.2017.01.023

Huang, Q., Zhang, G. B., Ma, J., Song, K. F., Zhu, X. L., Shen, W. Y., et al. (2022). Dynamic interactions of nitrogen fertilizer and straw application on greenhouse gas emissions and sequestration of soil carbon and nitrogen: a 13-year field study. *Agric. Ecosyst. Environ.* 325, 107753. doi: 10.11975/j.agee.2021.107753

Huang, S. H., Ding, W. C., Jia, L. L., Hou, Y. P., Zhang, J. J., Xu, X. P., et al. (2021). Cutting environmental footprints of maize systems in China through Nutrient Expert management. *J. Environ. Manage.* 282, 111956. doi: 10.1016/j.envman.2021.111956

Huddell, A., Ernfors, M., Crews, M., Vico, G., and Menge, N. L. (2023). Nitrate leaching losses and the fate of ^{15}N fertilizer in perennial intermediate wheatgrass and annual wheat-A field study. *Sci. Total Environ.* J857, e159255. doi: 10.1016/j.scitotenv.2022.159255

Jia, S. L., Wang, X. B., Yang, Y. M., Dai, K., Meng, C. X., Zhao, Q. S., et al. (2011). Fate of labeled urea-^{15}N as basal and topdressing applications in an irrigated wheat maize rotation system in North China Plain: I winter wheat. *Nutr. Cycl. Agroecosys.* 90, 331–340. doi: 10.1007/s10705-011-9433-5

Kaur, R., Kaur, S., Deol, J. S., Sharma, R., Kaur, T., Brar, J. S., et al. (2021). Soil properties and weed dynamics in wheat as affected by rice residue management in the rice-wheat cropping system in South Asia: A review. *Plants (Basel)* 10, e953. doi: 10.3390/plants10050953

Li, S. H., Guo, L. J., Cao, C. G., and Li, C. F. (2021). Effects of straw returning levels on carbon footprint and net ecosystem economic benefits from rice-wheat rotation in central China. Environ. *Sci. pollut. Res. Int.* 28, 5742–5754. doi: 10.1007/s11356-020-10914-w

Liang, K., Zhong, X., Huang, N., Lampayan, R. M., Liu, Y., Pan, J., et al. (2017). Nitrogen losses and greenhouse gas emissions under different N and water management in a subtropical double-season rice cropping system. *Sci. Total Environ.* 609, 46–57. doi: 10.1016/j.scitotenv.2017.07.118

Liu, X., Dong, W. Y., Jia, S. H., Liu, Q., Li, Y. Z., Hossain, M. E., et al. (2021). Transformations of N derived from straw under long-term conventional and no-tillage soils: A ^{15}N labeling study. *Sci. Total Environ.* 786, e147428. doi: 10.1016/j.scitotenv.2021.147428

Liu, Z., Gao, J., Gao, F., Dong, S., Liu, P., Zhao, B., et al. (2018). Integrated agronomic practices management improve yield and nitrogen balance in double cropping of winter wheat-summermaize. *Field Crop Res.* 221, 196–206. doi: 10.1016/j.fcr.2018.03.001

Liu, M., Wu, X. L., Li, C. S., Li, M., Xiong, T., and Tang, Y. L. (2020). Dry matter and nitrogen accumulation, partitioning, and translocation in synthetic-derived wheat cultivars under nitrogen deficiency at the post-jointing stage. *Field Crop Res.* 248, e107720. doi: 10.1016/j.fcr.2020.107720

Mahmood, H., Cai, J., Zhou, Q., Wang, X., Samo, A., Huang, M., et al. (2022). Optimizing nitrogen and seed rate combination for improving grain yield and nitrogen uptake efficiency in winter wheat. *Plants (Basel)* 11, e1745. doi: 10.3390/plants11131745

Pareja-Sánchez, E., Cantero-Martínez, C., Álvaro-Fuentes, J., and Plaza-Bonilla, D. (2020). Impact of tillage and N fertilization rate on soil N_2O emissions in irrigated maize in a Mediterranean agroecosystem. *Agric. Ecosyst. Environ.* 287, e106687. doi: 10.1016/j.agee.2019.106687

Ren, K. Y., Xu, M. G., Li, R., Zheng, L., Wang, H. Y., Liu, S. G., et al. (2023). Achieving high yield and nitrogen agronomic efficiency by coupling wheat varieties with soil fertility. *Sci. Total Environ.* 881, e3531. doi: 10.1016/j.scitolenv.2023.163531

Rhymes, J., Jones, L., Wallace, H., Jones, T. G., Dunn, C., and Fenner, N. (2016). Small changes in water levels and groundwater nutrients alter nitrogen and carbon processing in dune slack soils. *Soil Biol. Biochem.* 99, 28–35. doi: 10.1016/j.soilbio.2016.04.018

Richter, J., and Roelcke, M. (2000). The N-cycle as determined by intensive agriculture-examples from Central Europe and China. *Nutr. Cycl. Agroecosyst.* 57, 33–46. doi: 10.1023/A:1009802225307

Rivera-Amado, C., Trujillo-Negrellos, E., Molero, G., Reynolds, M. P., Sylvester-Bradley, R., and Foulkes, M. J. (2019). Optimizing dry-matter partitioning for increased spike growth, grain number and harvest index in spring wheat. *Field Crops Res.* 240, 154–167. doi: 10.1016/j.fcr.2019.04.016

Sharma, L. K., and Bali, S. K. (2018). A review of methods to improve nitrogen use efficiency in agriculture. *Sustainability* 10, e51. doi: 10.3390/su10010051

Sharma, S., Kaur, G., Singh, P., Alamri, S., Kumar, R., and Siddiqui, M. H. (2022). Nitrogen and potassium application effects on productivity, profitability and nutrient use efficiency of irrigated wheat (*Triticum aestivum* L.). *PloS One* 17, e0264210. doi: 10.1371/journal.pone.0264210

Shi, Z. L., Jing, Q., Cai, J., Jiang, D., Cao, W. X., and Dai, T. B. (2012). The fates of ^{15}N fertilizer in relation to root distributions of winter wheat under different N splits. *Eur. J. Agron.* 40, 86–93. doi: 10.1016/j.eja.2012.01.006

Smith, C. J., and Chalk, P. M. (2018). The residual value of fertiliser N in crop sequences: An appraisal of 60 years of research using ^{15}N tracer. *Field Crops Res.* 217, 66–74. doi: 10.1016/j.fcr.2017.12.006

Sun, G. L., Zhang, Z. G., Xiong, S. W., Guo, X. Y., Han, Y. C., Wang, G. P., et al. (2022). Mitigating greenhouse gas emissions and ammonia volatilization from cotton fields by integrating cover crops with reduced use of nitrogen fertilizer. *Agric. Ecosyst. Environ.* 332, e7946. doi: 10.1016/j.agee.2022.107946

Tan, Y., Chai, Q., Li, G., Zhao, C., Yu, A., Fan, Z., et al. (2021). Improving wheat grain yield *via* promotion of water and nitrogen utilization in arid areas. *Sci. Rep.* 11, e13821. doi: 10.1038/s41598-021-92894-6

Tan, Z., and Liu, S. (2015). Corn belt soil carbon and macronutrient budgets with projected sustainable stover harvest. *Agric. Ecosyst. Environ.* 212, 119–216. doi: 10.1016/j.agee.2015.06.022

Wan, X., Wu, W., and Shah, F. (2021). Nitrogen fertilizer management for mitigating ammonia emission and increasing nitrogen use efficiencies by ^{15}N stable isotopes in winter wheat. *Sci. Total Environ.* 790, e147587. doi: 10.1016/j.scitotenv.2021.147587

Wang, L., Yuan, X., Liu, C., Li, Z., Chen, F., Li, S., et al. (2019). Soil C and N dynamics and hydrological processes in a maize-wheat rotation field subjected to different tillage and straw management practices. *Agric. Ecosyst. Environ.* 285, e106616. doi: 10.1016/j.agee.2019.106616

Wytse, J.V., Renske, H., Glendining, M. J., Powlson, D. S., Bhogal, A., Merbach, I., et al. (2022). The legacy effect of synthetic N fertiliser. *Eur. J. Soil Sci.* 73, e13238. doi: 10.1111/EJSS.13238

Xu, C., Han, X., Zhuge, Y., Xiao, G., Ni, G., Xu, X., et al. (2021). Crop straw incorporation alleviates overall fertilizer-N losses and mitigates N_2O emissions per unit applied N from intensively farmed soils: An in *situ* ^{15}N tracing study. *Sci. Total Environ.* 764, e142884. doi: 10.1016/j.scitotenv.2020.142884

Yan, F., Yan, S. S., Jia, S. S., Dong, S. K., Ma, C., and Gong, Z. P. (2019). Decomposition characteristics of rice straw returned to the soil in northeast China. *Nutr. Cycl. Agroecosys.* 114, 211–224. doi: 10.1007/s10705-019-09999-8

Yang, H. K., Li, J. G., Wu, G., Huang, X. L., and Fan, G. Q. (2023). Maize straw mulching with no-tillage increases fertile spike and grain yield of dryland wheat by regulating root-soil interaction and nitrogen nutrition. *Soil Tillage Res.* 228, 105652. doi: 10.1016/j.still.2023.105652

Yang, L., Muhammad, I., Chi, Y. X., Liu, Y. X., Wang, G. Y., Wang, Y., et al. (2022). Straw return and nitrogen fertilization regulate soil greenhouse gas emissions and global warming potential in dual maize cropping system. *Sci. Total Environ.* 853, e158370. doi: 10.1016/j.scitotenv.2022.158370

Ye, T. Y., Liu, B., Wang, X. L., Zhou, J., Liu, L. L., Tang, L., et al. (2022). Effects of water-nitrogen interactions on the fate of nitrogen fertilizer in a wheat-soil system. *Eur. J. Agron.* 136, e126507. doi: 10.1016/J.eja.2022.126507

Yu, F., and Shi, W. M. (2015). Nitrogen use efficiencies of major grain crops in China in recent 10 years. *Acta Pedologica Sinica*. 52, 1311–1324. doi: 10.11766/trxb201501270058

Zhang, A. F., Cheng, G., Hussain, Q., Zhang, M., Feng, H., Dyck, M., et al. (2017). Contrasting effects of straw and straw–derived biochar application on net global warming potential in the loess plateau of China. *Field Crops Res.* 205, 45–54. doi: 10.1016/J.fcr.2017.02.006

Zhang, J. T., Wang, Z. M., Liang, S. B., Zhang, Y. H., Zhou, S. L., Lu, L. Q., et al. (2017). Quantitative study on the fate of residual soil nitrate in winter wheat based on a ^{15}N-labeling method. *PloS One* 12, e0171014. doi: 10.1371/journal.pone.0171014

Zörb, C., Ludewig, U., and Hawkesford, M. J. (2018). Perspective on wheat yield and quality with reduced nitrogen supply. *Trends Plant Sci.* 23, 1029–1037. doi: 10.1016/j.tplants.2018.08.012

frontiers | Frontiers in Plant Science

TYPE Original Research
PUBLISHED 20 October 2023
DOI 10.3389/fpls.2023.1281670

OPEN ACCESS

EDITED BY
Sumera Anwar,
Durham University, United Kingdom

REVIEWED BY
Hanuman Singh Jatav,
Sri Karan Narendra
Agriculture University, India
Farinaz Vafadar,
Isfahan University of Technology, Iran
Zafar Siddiq,
Government College University,
Lahore, Pakistan

*CORRESPONDENCE
Thiago Assis Rodrigues Nogueira
tar.nogueira@unesp.br

RECEIVED 22 August 2023
ACCEPTED 02 October 2023
PUBLISHED 20 October 2023

CITATION
Silva MB, Camargos LS, Teixeira Filho MCM, Souza LA, Coscione AR, Lavres J, Abreu-Junior CH, He Z, Zhao F, Jani AD, Capra GF and Nogueira TAR (2023) Residual effects of composted sewage sludge on nitrogen cycling and plant metabolism in a no-till common bean-palisade grass-soybean rotation. *Front. Plant Sci.* 14:1281670. doi: 10.3389/fpls.2023.1281670

Residual effects of composted sewage sludge on nitrogen cycling and plant metabolism in a no-till common bean-palisade grass-soybean rotation

Mariana Bocchi da Silva[1], Liliane Santos de Camargos[1], Marcelo Carvalho Minhoto Teixeira Filho[1], Lucas Anjos Souza[2], Aline Renée Coscione[3], José Lavres[4], Cassio Hamilton Abreu-Junior[4], Zhenli He[5], Fengliang Zhao[6], Arun Dilipkumar Jani[7], Gian Franco Capra[8,9] and Thiago Assis Rodrigues Nogueira[1,10]*

[1]Department of Plant Protection, Rural Engineering, and Soils, São Paulo State University, Ilha Solteira, SP, Brazil, [2]Instituto Federal de Educação, Ciência e Tecnologia Goiano, Rio Verde, GO, Brazil, [3]Center of Soils and Environmental Resources of the Campinas Agronomic Institute, Campinas, SP, Brazil, [4]Center for Nuclear Energy in Agriculture, Universidade de São Paulo, Piracicaba, SP, Brazil, [5]Indian River Research and Education Center, Institute of Food and Agricultural Sciences, University of Florida, Fort Pierce, FL, United States, [6]Environment and Plant Protection Institute, Chinese Academy of Tropical Agricultural Sciences, Haikou, China, [7]Department of Biology and Chemistry, California State University, Monterey Bay, Seaside, CA, United States, [8]Dipartimento di Architettura, Design e Urbanistica, Università Degli Studi di Sassari, Sassari, Italy, [9]Desertification Research Centre, Università Degli Studi di Sassari, Sassari, Italy, [10]Department of Agricultural Sciences, School of Agricultural and Veterinarian Sciences, São Paulo State University, Jaboticabal, SP, Brazil

Introduction and aims: In the context of increasing population and decreasing soil fertility, food security is one of humanity's greatest challenges. Large amounts of waste, such as sewage sludge, are produced annually, with their final disposal causing environmental pollution and hazards to human health. Sludge has high amounts of nitrogen (N), and, when safely recycled by applying it into the soil as composted sewage sludge (CSS), its residual effect may provide gradual N release to crops. A field study was conducted in the Brazilian *Cerrado*. The aims were to investigate the residual effect of successive applications of CSS as a source of N in the common bean (*Phaseolus vulgaris* L. cv. BRS Estilo)-palisade grass (*Urochloa brizantha* (A.Rich.) R.D. Webster)-soybean (*Glycine max* L.) rotation under no-tillage. Additionally, N cycling was monitored through changes in N metabolism; the efficiency of biological N_2 fixation (BNF) and its implications for plant nutrition, development, and productivity, was also assessed.

Methods: The experiment consisted of a randomized complete block design comparing four CSS rates (10, 15, 20, and 25 Mg ha^{-1}, wet basis) to a control treatment (without adding mineral or organic fertilizer) over two crop years. Multiple plant and soil analyses (plant development and crop yield, Falker chlorophyll index (FCI), enzymatic, biochemical, ^{15}N natural abundance, was evaluated, root and shoot N accumulation, etc.) were evaluated.

Results and discussion: Results showed that CSS: *i*) maintained adequate N levels for all crops, increasing their productivity; *ii*) promoted efficient BNF, due to the stability of ureide metabolism in plants and increased protein content; *iii*) increased the nitrate content and the nitrate reductase activity in soybean; *iv*) affected urease activity and ammonium content due to changes in the plant's urea metabolism; *v*) increased N accumulation in the aerial part of palisade grass. Composted sewage sludge can be used as an alternative source to meet crops' N requirements, promoting productivity gains and N cycling through forage and improving N metabolism.

KEYWORDS

biological N_2 fixation, organic fertilizer, cover crops, urban waste, no-till

1 Introduction

The use of sewage sludge in agriculture is a viable option for some producers because of the low operating cost associated with its disposal by sewage treatment plants (STPs). It is used as organic fertilizer and/or soil conditioner (Brasil, 2020a), whereas composting sewage sludge has a cost of 49% lower than the cost of disposal in landfills and a profitability of 61% in Brazil (D'avila et al., 2019; Martins et al., 2021). This practice is considered environmentally sustainable and economically viable compared to landfill disposal (Kacprzak et al., 2017). In addition, it provides organic matter and nutrients such as nitrogen, phosphorus, and micronutrients (Nascimento et al., 2020), improving soil fertility (Ferraz et al., 2016) and consequently the productivity of agricultural and forestry crops (Nogueira et al., 2013; Zuba Junio et al., 2019; Abreu-Junior et al., 2020; Elsalam et al., 2021). However, SS may contain heavy metals (Nascimento et al., 2020), organic compounds (Alvarenga et al., 2017), and pathogenic organisms (Murray et al., 2019). In Brazil, the National Council for the Environment (CONAMA) regulated Resolution No. 498, which sets out criteria and procedures for using SS and treatment methods to reduce contaminants in this byproduct (Brasil, 2020a).

Composting has been used to stabilize organic matter and reduce the risks of heavy metals and pathogens, mainly aiming for continuous agricultural sludge recycling (Hargreaves et al., 2008; Wang et al., 2017a). Composted sewage sludge (CSS) as organic fertilizer can improve the chemical, physical, and biological properties of soil, in addition to preventing the contamination and degradation of water resources (Jakubus and Graczyk, 2020; Prates et al., 2020; Prates et al., 2022; Silva et al., 2022a, Silva et al., 2022b). Unlike SS, CSS is already considered a safe product for use in agriculture as it complies with Brazilian standards for registration of organic fertilizers (Brasil, 2020b), which establish maximum limits for heavy metals and pathogenic organisms in CCS. Thus, CSS can be used to fertilize different crops without risks to the environment and human health.

Taking the nitrogen (N) nutrition of the crops into consideration, the amounts of sludge to be applied must meet the N needs of the crop and avoid the generation of nitrate in excessive amounts that will leach in the soil profile to groundwater (Gangbazo et al., 1995). Additionally, SS application provides other nutrients (Boeira et al., 2002). Biological N_2 fixation (BNF) plays an important role in plant cultivation and mineral fertilization management because it is the most productive and economical N acquisition process and is environmentally viable (Biswas and Gresshoff, 2014).

The supply of CSS as organic fertilizer may at least partially replace the amounts of nutrients applied via mineral fertilizer because the slow and gradual release of the nutrients contained in the compost may result in better use of these nutrients by the plants. The increase in organic matter through the application of CSS may also be highly favorable to the maintenance and improvement of soil quality (e.g., C stock, increased biota, greater moisture retention). In addition, there are still no studies related to the residual effect of CSS on N availability in the soil and on N metabolism through changes in the nodulation, BNF, physiology, and development of soybean and common bean cultivated under a no-tillage system (NTS) in the *Cerrado* region. It is essential to evaluate these aspects to understand the effects caused by the supply of N via CSS and to reduce the use of N fertilizers. Such aspects are reflected in a lower production cost for farmers in addition to reducing the environmental impacts of producing such inputs and the surplus of mineral fertilizers that can be transferred to water bodies and the atmosphere.

In this scenario, which lacks experimental results on the effects of CSS supply on the development and productivity of these crops, the following hypotheses were tested: *i*) the residual effect of CSS applications in *Cerrado* soil may meet the N demand of common bean, forage, and soybean in rotation under an NTS in the *Cerrado*; *ii*) Palisade grass used as a cover crop promotes greater N cycling and an increase in grain yield; and *iii*) CSS supplies N in the system, decreasing the C/N ratio of palisade grass, which favors N mineralization, and providing greater N availability in the soil, which interferes with the efficiency of the BNF process and consequently with N metabolism in common bean and soybean. The objective of this study was to evaluate the residual effect of

successive applications of CSS as an N source in a common bean-palisade grass-soybean rotation under NTS in the *Cerrado*, monitoring N cycling through changes in N metabolism (with emphasis on the efficiency of the BNF process), and examining its implications on nutrition, development, and productivity of crops.

2 Materials and methods

2.1 Experimental area

The study was conducted under field conditions in the municipality of Selvíria, MS (20°20'35" S and 51°24'04" W, with an altitude of 358 m, Figure 1). The region has an annual average rainfall of 1,370 mm, an annual average temperature of 24.5°C, and an average annual relative humidity of 75% (Climate Change Knowledge Portal, 2021). The climate type of the region is Aw, according to the Köppen classification, characterized by rainy summers and dry winters (Lombardi Neto and Drugowich, 1994). During the entire experiment, daily data on temperature, relative air humidity, and rainfall were collected (Figure 2).

After a detailed survey, the soil at the site was classified as Rhodic Hapludox, a typical dystrophic sandy clay (Soil Survey Staff, 2014). Before the experiment, samples were collected in the 0–0.2 m layer to evaluate physical (Teixeira et al., 2017) and chemical (Raij et al., 2001) attributes and the following values were obtained: pH ($CaCl_2$) = 4.5 ± 0.1; organic matter (OM) = 19.0 ± 1.2 g dm^{-3}; phosphorus (P) (resin) = 16 ± 0.6. mg dm^{-3}; potassium (K) = 1.7 ± 0.2 $mmol_c$ dm^{-3}; calcium (Ca) = 13 ± 0.6 $mmol_c$ dm^{-3}; magnesium (Mg) = 12 ± 1.0 $mmol_c$ dm^{-3}; potential acidity [hydrogen (H) + aluminum (Al)] = 37 ± 2.3 $mmol_c$ dm^{-3}; sum of bases (SB) = 27.0 ± 1.7 $mmol_c$ dm^{-3}; cation exchange capacity (CEC) at pH 7.0 = 63.7 ± 0.9 $mmol_c$ dm^{-3}; base saturation (V) = 42 ± 3.0%; boron (B) = 0.22 ± 0.04 mg dm^{-3}; copper (Cu) = 1.8 ± 0.1 mg dm^{-3}; iron (Fe) = 15 ± 0.6 mg dm^{-3}; manganese (Mn) = 18.8 ± 0.6 mg dm^{-3}; zinc (Zn) = 0.6 ± 0.1 mg dm^{-3}; aluminum (Al) = 4.0 ± 0.0 $mmol_c$ dm^{-3}; clay = 370 ± 19 g kg^{-1}, silt = 80 ± 3 g kg^{-1}, and sand = 550 ± 13 g kg^{-1}.

2.2 Experimental design and treatments

A randomized complete block design was adopted, with five treatments and four replications, totaling 20 experimental units. The treatments consisted of the residual effect of four rates of composted sewage sludge - CSS (10, 15, 20, and 25 Mg ha^{-1}, wet basis), accumulated from two consecutive applications during the 2017/18 and 2018/19 seasons, and one control treatment (without the application of CSS and mineral fertilizers). To evaluate the residual effect of the two applications of CSS as the N source, no fertilization (mineral or organic) was included during the 2019/20 and 2020/21 seasons.

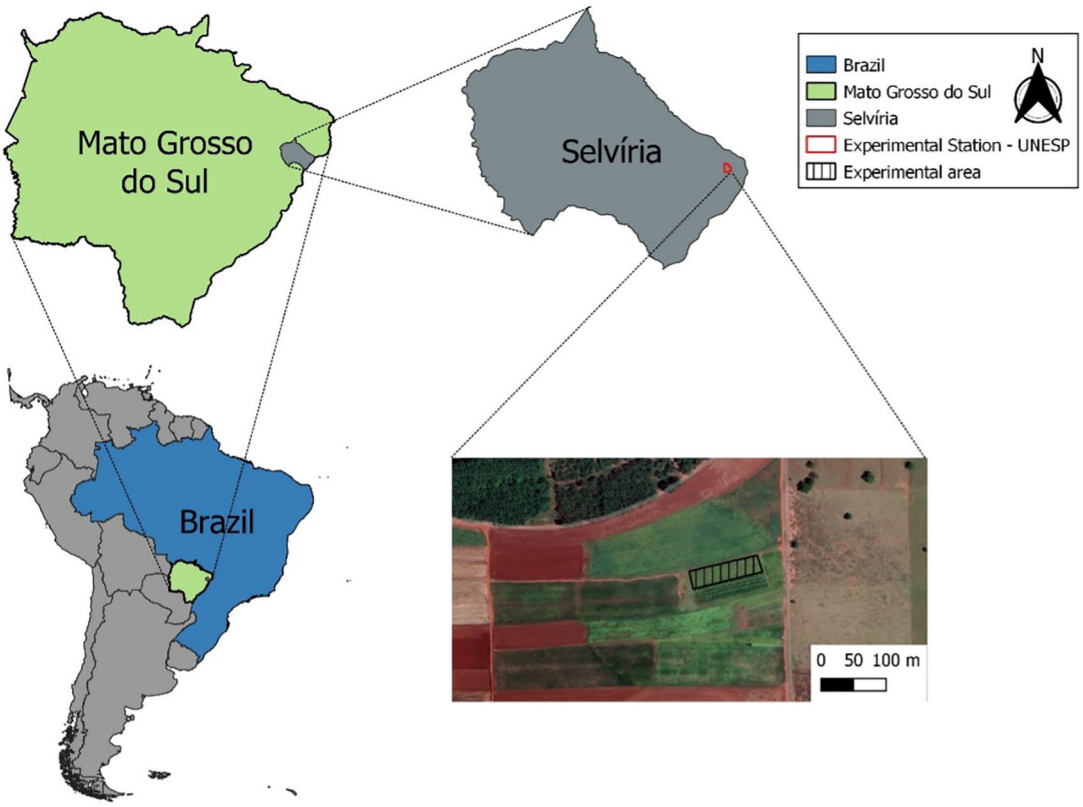

FIGURE 1
Study location: Selvíria municipality, Mato Grosso do Sul, Brazil.

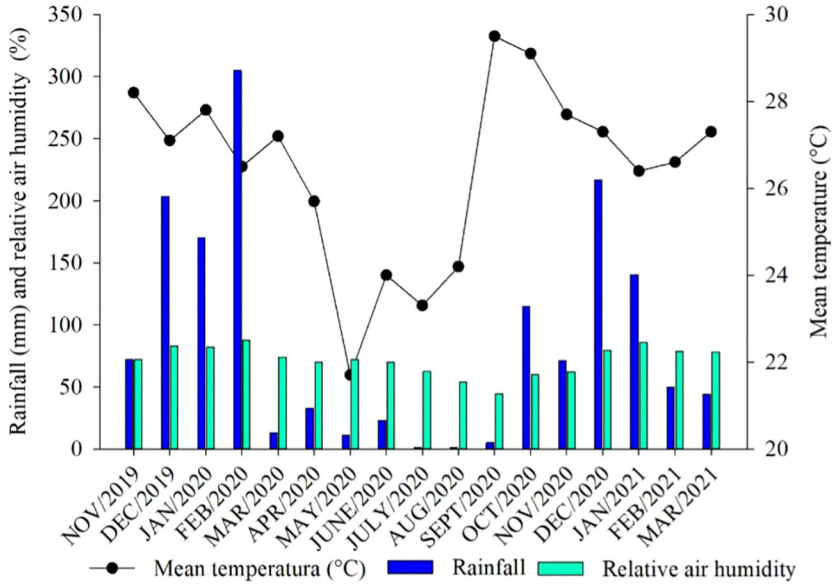

FIGURE 2
Mean temperature, rainfall, and relative air humidity during the experiment. Data were collected from the weather station of the School of Engineering of Ilha Solteira, São Paulo, Brazil.

2.3 CSS source and characterization

The CSS used is classified as a Class B organic fertilizer (Brasil, 2020b) and is derived from thermophilic composting of urban organic wastes. In addition to sewage sludge, sludge from wastewater treatment systems generated in agroindustries, such as breweries and various food industries, fruit and vegetable processing, and the remains of industrialized and unserviceable food products make up the sewage sludge. The CSS was characterized according to Conama Resolution No 498 (Table 1).

According to the total N present in the CSS and the rates used in the experiment, the total amounts of N added to the soil after the two CSS applications were calculated (dry basis): 10 Mg ha^{-1} = 91 kg of N; 15 Mg ha^{-1} = 130 kg of N; 20 Mg ha^{-1} = 173 kg of N; and 25 Mg ha^{-1} = 216 kg of N.

2.4 Experiment installation and development

The experimental area was chisel plowed in September 2017 to 0.3 m depth. Lime was incorporated at 2.2 Mg ha^{-1} followed by surface application gypsum at 1.8 Mg ha^{-1} based on recommendations by Raij et al. (1997). One week before soybean planting (November 2017 and 2018), CSS was manually spread out on the soil surface within each plot but not incorporated, considering the moisture content of the material (45% for the first season and 36% for the second season). To evaluate the residual effect of CSS on the development of common bean (2019/20) and soybean (2020/21), no other fertilizer was used for these crops.

As test plants, in the 2017/18 and 2018/19 crop years, soybean in the first crop and corn (*Zea mays* L.) in the second crop were cultivated in succession. In the 2019/20 crop year, a no-tillage system was implemented to cultivate marandu palisadegrass (*Urochloa brizantha* (A.Rich.) R.D. Webster) (as a cover crop). Soon after, the common bean was cultivated (*Phaseolus vulgaris* L. cv. BRS Estilo). In the 2020/21 crop year, marandu palisadegrass was used again as a cover crop, followed by soybean (*Glycine max* L. cv TMG 7063 Ipro).

Each experimental unit consisted of ten rows for marandu palisadegrass (spaced 0.34 m apart) and seven rows of beans and soybeans (spaced 0.45 m apart), with a length of 10 meters, totaling 35 m^2 per plot and 700 m^2 of total area. The area of the plot for data collection consisted of three central rows, with 2.5 m from each end eliminated as border.

Marandu palisadegrass was planted in November 2019, with 140 days of cultivation, and then in August 2020, with another 60 days of cultivation. Before the cultivation of each main crop, the marandu palisadegrass was desiccated by glyphosate (1,800 g ha^{-1} of the a.i.) and 2,4-D (670 g ha^{-1} of the a.i.). Common bean and soybean seed were treated with the fungicides, thiophanate methyl + pyraclostrobin (45 g + 5 g a.i. per 100 kg of seed) and fipronil insecticide (50 g a.i. per 100 kg of seed) and with CoMo (200 mL ha^{-1}).

Common bean seed was inoculated with *Rhizobium tropici* (Semia 4080, 100 g per 25 kg of seeds). Soybean seed was inoculated with *Bradyrhizobium elkanii* (CEPA SEMIA 5019) and *Bradyrhizobium japonicum* (CEPA SEMIA 5079), following the manufacturer's recommendations (100 mL for 50 kg of seeds - Masterfix L. Stoller inoculant). Common bean was planted in April 2020, and soybean was sown in November 2020. Irrigation ranging from 10–14 mm per event was applied via a central pivot.

TABLE 1 Chemical and microbiological composition of composted sewage sludge samples.

Characteristic	Unit	2017/18	2018/19	Allowed value [1]
Chemistry		Dry basis		
pH $_{(CaCl2)}$	–	7.0 ± 0.1	7.3 ± 0.1	–[2]
Moisture (60-65 °C)	%	41.0 ± 0.3	34.4 ± 0.5	–
Total moisture	%	45.5 ± 0.2	35.8 ± 0.6	–
Total OM (combustion)	g kg^{-1}	308.7 ± 10.0	255.0 ± 7.4	–
CEC	mmol$_c$ dm $^{-3}$	520 ± 20.00	–	–
C/N	–	12.0 ± 0.8	9.0 ± 0.6	–
Total N	g kg^{-1}	13.9 ± 0.3	15.3 ± 1.5	–
Total P	g kg^{-1}	12.3 ± 1.4	14.1 ± 0.0	–
Total S	g kg^{-1}	4.8 ± 0.3	8.4 ± 1.4	–
Na	mg kg^{-1}	3930.0 ± 32.0	3915.0 ± 32.0	–
K	g kg^{-1}	6.0 ± 2.2	8.2 ± 0.4	–
Ca	g kg^{-1}	19.4 ± 4.4	31.1 ± 1.1	–
Mg	g kg^{-1}	5.2 ± 0.5	9.9 ± 0.2	–
As	mg kg^{-1}	3.2 ± 1.8	–	20.0
B	mg kg^{-1}	94.0 ± 4.5	94.0 ± 4.6	–
Cd	mg kg^{-1}	1.0 ± 0.1	–	3.0
Cu	mg kg^{-1}	237.0 ± 16.5	191.2 ± 5.8	–
Pb	mg kg^{-1}	18.1 ± 1.6	–	150.0
Cr	mg kg^{-1}	54.3 ± 1.8	–	2.0
Fe	mg kg^{-1}	16,400 ± 1300	14,708 ± 249	–
Mn	mg kg^{-1}	246.0 ± 37.0	310.0 ± 15.0	–
Hg	mg kg^{-1}	0.22 ± 0.1	–	1.0
Mo	mg kg^{-1}	5.26 ± 0.2	–	–
Ni	mg kg^{-1}	26.5 ± 0.5	–	70.0
Zn	mg kg^{-1}	456 ± 8	684 ± 7	–
Microbiological				
Salmonella sp.	MPN 10 g^{-1}	Absent	Absent	
Thermotolerant coliforms	MPN g^{-1}	0	<103 MPN g^{-1} on dry weight	
Viable helminth eggs	Eggs g^{-1} on dry weight	0.12	<10 Eggs g^{-1} on dry weight	

[1]Limits to organic fertilizers use established by the Ministry of Agriculture, Livestock and Food Supply in Brazil (MAPA, 2016). [2]Not determined. MPN, Most probable number; CEC, cation exchange capacity.
(mean ± standard deviation; n = 3).

2.5 Soil-plant analysis and evaluated parameters

2.5.1 Plants' nutritional status

Common bean and soybean nutritional analyses were conducted according to the recommendations described by Ambrosano et al. (1997). During common bean's full flowering period, the third leaf with petiole was randomly collected from the middle third of 10 plants per plot. For soybean, also at full flowering, the third fully developed leaf with petiole was randomly collected from the apex to the base, from 30 plants per plot. The samples were dried in an oven with forced air circulation at 65°C for 72 h, crushed in a Wiley-type mill, and stored until the time of analysis. Leaf N concentration was extracted by sulfuric digestion and determined by the Kjeldahl method (Malavolta et al., 1997).

2.5.2 Falker chlorophyll index (FCI)

The FCI was evaluated at the R6 bean stage, the relative chlorophyll content was evaluated in 10 leaves per plot, with readings performed next to the midrib of the fully expanded leaves (Barbiere Junior et al., 2012). In soybean, at the R2 stage, the readings were taken on the third fully developed trifoliate leaf from the plant's apex, with an average of 10 readings per leaflet, in five plants per plot. ClorofiLOG portable equipment, model CFL 1030, Falker brand, was used.

2.5.3 Biological N_2 fixation

Biological N_2 fixation was evaluated using the ^{15}N natural abundance method. Briefly, N_2 from air contains about 0.3663% ^{15}N and the rest (99.6337%) is ^{14}N (Boddey et al., 2001). Each unit of delta ^{15}N is considered to have natural abundance divided by one thousand, i.e., 0.0003663 atom % excess ^{15}N (Cadisch et al., 2000; Lavres et al., 2016). Species capable of obtaining most of the N needed for their nutrition will have $\delta^{15}N$ values very close to zero, because most of the N will come from the air, which is the standard of the technique and contains 0.3663% ^{15}N, meaning zero excess units of $\delta^{15}N$ (Cadisch et al., 2000; Boddey et al., 2001; Lavres et al., 2016). Conversely, non-N-fixing species (control plants) grown in the same soil will have higher $\delta^{15}N$ values, close to those of the soil, because all or most of the N required for their development will be derived from the soil. Like other isotopic techniques, this one depends on the basic assumption that fixing and non-fixing plants, grown in the same soil, take up N with the same isotopic labeling from the very close soil volume by both roots (Boddey et al., 2001; Guimaraes et al., 2008; Lavres et al., 2016). Sub-samples of dried and ground material from diagnostic leaf and grain of common bean and soybean were analyzed for % N and $\delta^{15}N$ on an automated mass spectrometer coupled to an ANCA-GSL N analyzer (Sercon Co., UK). The proportion of N in plants that can fix N_2 from the air by the BNF process was calculated by the equation of Shearer and Kohl (1986):

$$\%\,BNF = 100 \times (\delta^{15}N\ reference - \delta^{15}N\ fixing\ plant)/\delta^{15}N\ reference - B \quad (1)$$

where:

% BNF = percentage of N obtained from BNF in the fixing plants;

δ^{15} N reference = natural abundance of ^{15}N in the reference (non-N-fixing) plant;

δ^{15} N fixing plant = natural abundance of ^{15}N in common bean and soybean plants;

B = fractional contribution of ^{15}N relative to ^{14}N by the fixing plants in soil N uptake. For common bean, the 'B' value used in the present study was -1.2 ‰ determined for the common bean cultivars grown on an N-free hydroaeroponic culture fully dependent on BNF (Pacheco et al., 2017), and -1.17‰ for soybean (Guimaraes et al., 2008).

2.5.4 Total soil N and C

Soil sampling (0-0.1 m and 0.1-0.2 m depth) was performed at the end of each crop cycle, within the useful area of each plot. Five sub-samples were randomly collected per plot to compose a sample. These samples were taken with the help of a soil sampler and, afterwards, air dried, crushed and passed through a sieve with 2 mm of mesh opening, packed in polyethylene bags, identified, and stored in a dry chamber until the moment of the analyses. The total C and total N contents were determined using an automatic elemental analyzer (Swift, 1996). The N-organic content was calculated from the difference between total N and N-mineral (NO_3^- + NH_4^+).

2.5.5 Dry matter and nodulation

At the R5 stage of common bean and at the R2 stage of soybean, six plants were collected within each experimental plot with the aid of a cutting shovel. The plants were separated into shoots and roots. All excess soil from the roots was removed with water and a sieve to avoid losses. The nodules were removed from the roots, counted, and then passed through a 2 mm sieve, and those larger than 2 mm were cut in half to observe their viability (nodules of normal appearance with the presence of leghemoglobin, with a characteristic reddish color). After this last stage, the nodules, roots, and shoots were packed in paper bags and placed in a forced air oven at 65°C for 72 h. The following were evaluated: root and shoot dry matter, the number of total nodules, the number of viable nodules, and the nodule dry matter (Matoso and Kusdra, 2014).

2.5.6 Root and shoot N accumulation

After drying and weighing, the roots and shoots from the previous stage were ground in a Wiley-type mill with a 40-mesh sieve and subjected to sulfuric digestion and steam distillation to determine the N concentrations (Malavolta et al., 1997). The accumulated amounts of N were calculated based on the N concentrations and dry matter production.

2.5.7 Plant development and crop yield

At physiological maturity of common bean (R9; ~ 80 DAE) and soybean (R8; 100 DAE), 10 random plants were collected from the useful area of each plot to analyze yield parameters. The following were analyzed for common bean: 100-grain weight, number of grains per plant, number of grains per pod, number of pods per plant, and pod length. For soybeans, the following were analyzed: 100-grain weight, number of pods per plant, number of grains per pod, plant height, and first pod insertion height. At the end of each crop cycle, all plants in the useful area were harvested and manually threshed to avoid losses. After these procedures, the calculations were performed with extrapolation to kg ha^{-1} and corrected for 13% moisture (wet basis) to estimate crop yield (Sabundjian et al., 2016).

2.5.8 Enzymatic analyses

For the enzymatic analyses, five leaves were collected from each plot at the R6 bean and R2 soybean stages, following the recommendations for the analysis of nutritional contents (Ambrosano et al., 1997). The leaves were placed on ice in a thermal box to preserve enzymatic activity until the time of analysis.

- Urease activity: The *in vivo* samples were prepared by adapting the methodology described by Hogan et al.

(1983). The leaf tissue (200 mg of green leaves, cut into "strips" with a width of 1 mm) was placed in a medium containing 8 mL of NaH_2PO_4 buffer with urea (12.61 g L^{-1}), pH 7.4, and incubated for 3 h at 30°C under constant agitation. In a test tube containing 0.5 mL of the extract obtained after incubation, 2.5 mL of reagent I (1.25 mL of crystal phenol, 12.5 mg of sodium nitroprusside, and 250 mL of distilled water) and 2.5 mL of reagent II (1.25 g of NaOH, 13.4 g of $Na_2HPO_4.12H_2O$, 2.5 mL of NaOCl, and 250 mL of distilled water) were added. The tubes were incubated in a water bath at 37°C for 35 min. After incubation, the reaction was measured by colorimetry in a spectrophotometer at 625 nm. Urease activity was measured through the production of N-NH_4, according to the method by McCullough (1967);

- Nitrate reductase activity: Leaf samples were collected in the morning, and 0.5 g of fresh leaf tissue was cut into thin strips, placed into a test tube containing 5 mL of NaH_2PO_4 buffer, pH 7.5, with KNO_3 and incubated in a water bath at 30°C for 60 min in the dark. Then, 1 mL of the extraction solution, 0.5 mL of 1% sulfanilamide, and 0.5 mL of 0.02% naphthylethylenediamine were added. After this step, the reaction was measured by colorimetry in a spectrophotometer at 540 nm. The assay and the determination of NR activity followed the recommendations described in Radin (1974).

2.5.9 Biochemical analyses

For the biochemical analyses, five leaves were collected from each plot at stage R6 of common bean and R2 of soybean, according to the recommendations for the analysis of nutritional contents (Ambrosano et al., 1997). Initially, soluble compounds were extracted (Bieleski and Turner, 1966), in which 0.5 g of plant material was ground in 5 mL of MCW (600 mL of methanol, 250 mL of chloroform, and 150 mL of distilled water) and homogenized in a centrifuge at 8500 rpm for 15 min. After centrifugation, the supernatant was added to another tube, and the precipitate was used for the protein assay. For every 4 mL of supernatant, 1 mL of chloroform and 1.5 mL of distilled water were added, and the samples were allowed to rest for 24 h in the refrigerator. After this period, the fat-soluble phase was discarded, and the volume of the water-soluble phase was recorded and stored until the time of analysis. After extraction, the following physiological analyses were performed:

- *Protein* quantification: 5 mL of 0.1 M NaOH was added to the precipitate resulting from the extraction of soluble compounds and placed in a centrifuge at 8500 rpm for 15 min. After this period, 5 mL of Bradford reagent was added to 100 µl of supernatant and incubated for 3 min. The reaction was measured by colorimetry in a spectrophotometer at 595 nm (Bradford, 1976).
- Quantification of *amino acids*: The reaction sample consisted of 25 µL of the water-soluble phase + 975 µL of distilled water, 500 µL of pH 5.0 citrate buffer, 200 µL of 5% methyl glycol ninhydrin, and 1 mL of 0.0002 mol L^{-1} KCN and was incubated in a water bath at 100° C for 20 min. Then, the mixture was incubated for 10 min at room temperature, after which 1 mL of 60% ethanol was added. The reaction was measured by colorimetry in a spectrophotometer at 570 nm (Yemm and Cocking, 1955).
- Quantification of *nitrate*: Following the methodology described by Cataldo et al. (1975), we used 50 µL of the water-soluble phase together with 200 µL of 5% salicylic acid in H_2SO_4 and waited 20 min at room temperature. Then, 4.75 mL of NaOH 2N was added, and the mixture was cooled to room temperature until the reaction stabilized. Afterward, the assay was measured by colorimetry in a spectrophotometer at 410 nm.
- Quantification of *ammonium*: For the ammonium assay, 100 µL of the water-soluble phase was used, and 500 µL of reagent I (1.25 mL of crystal phenol, 12.5 mg of sodium nitroprusside, and 250 mL of distilled water) and 500 µl of reagent II (1.25 g of NaOH, 13.4 g of Na_2 $HPO_4.12H_2O$, 2.5 mL of NaOCl and 250 mL of distilled water) were added; the samples were then placed in a water bath at 37°C for 1 h. After this period, the reading was continued by colorimetry in a spectrophotometer at 630 nm (McCullough, 1967).
- Quantification of *ureides*, *allantoic acid*, and *allantoin*: according to the method proposed by Vogels and van der Drift (1970), the assay consists of four stages. Step I: 250 µL of the water-soluble phase was diluted in 500 µL of distilled water, 250 µL of NaOH 0.5N and 1 drop of 0.33% phenylhydrazine were added, and the samples were heated in a water bath at 100°C for 8 min and then cooled to room temperature. Step II: 250 µL of HCl 0.65N was added, and the samples were heated in a water bath at 100°C for 4 min and then cooled to room temperature. Step III: 250 µL of phosphate buffer pH 7.0 and 250 µL of phenylhydrazine were added and left to stand for 5 min at room temperature and 5 min on ice. Step IV: While still on ice, 1.25 mL of 37% HCl (which must be kept in the freezer for analysis) was added; the samples were then removed from the ice, and 250 µL of $K_3Fe(CN)_6$ was added; the tubes were shaken and incubated for 15 min at room temperature prior to reading by colorimetry in a spectrophotometer at 535 nm. To quantify total ureides, we followed the four steps described above. To quantify allantoic acid, we diluted 250 µL of the water-soluble phase in 500 µL of distilled water and followed the assay beginning with step II. To quantify allantoin, we subtracted the value obtained for total ureides from that obtained for allantoic acid.

2.5.10 Marandu palisadegrass phytomass production and N accumulation

To evaluate the biomass production of marandu palisadegrass in the 2019/20 crop, two cuts were performed at 70 and 140 days after emergence (DAE), and in the 2020/21 crop, a cutoff was performed at 60 DAE. The cuts were performed randomly at four

points per plot as close to the soil as possible using a 0.25 m^2 square. After the first cut (crop 2019/20), Triton was applied to uniform the area, and the plants sprouted again to form a new straw on the soil. In the second cut of the 2019/20 crop and in the only cut of the 2020/21 crop, after completion, the grass was desiccated with glyphosate herbicide (1,800 g ha^{-1} of the a.i.) and 2,4-D (670 g ha^{-1} of the a.i.) for crop sowing in succession (beans followed by soybeans). The collected samples were dried in a forced circulation oven at 65°C for 72 h, and the plant material was weighed to obtain the total amount of straw formed (kg ha^{-1}) in each season evaluated.

Nitrogen accumulation was evaluated by analyzing the shoot samples of marandu palisadegrass from each crop. In particular, shoots were weighed and then ground in a Wiley-type mill with a 40-mesh sieve and homogenized, then N concentration was obtained using sulfuric digestion and steam distillation (Malavolta et al., 1997). Based on the N concentration and dry matter production, the accumulated amounts of N were calculated and extrapolated to kg ha^{-1}.

2.6 Statistical analysis

Statistical analysis was performed using R software (R Core Team, 2019) and AgroEstat software (Barbosa and Maldonado, 2015). The results were subjected to the Shapiro–Wilk normality test and the O'Neill and Mathews test of homogeneity of variances at 5%. After meeting the hypotheses of normality, the results were subjected to analysis of variance, and the means were compared using the HSD-Tukey test ($P < 0.05$) in cases in which the F test was significant.

3 Results

3.1 The FCI, foliar N, dry matter, and N uptake

The residual effect of CSS influenced the Falker chlorophyll index (FCI) of common bean, with a difference between the studied rates; the highest value of FCI was obtained at the 10 Mg ha^{-1} CSS rate (Figure 3A). For soybean, there was no residual effect of CSS on the FCI (Figure 3B).

There was no effect of CSS application on N levels in the leaves of common bean and soybean (Figures 3C, D, respectively). For common bean, in the control treatment and in the plots that received 10 Mg ha^{-1} CSS, the leaf N concentration of common bean remained within the sufficiency range (30–50 g kg^{-1}) established by Ambrosano et al. (1997). However, where the highest rates of CSS were applied, the N levels in the leaves were above the maximum level of N (Figure 3C). In soybean, leaf N concentration remained within the range of adequate N concentration (40–54 g kg^{-1}) described by Ambrosano et al. (1997), (Figure 3D).

Shoot dry matter (SDM), shoot N accumulation (SNA), and the root dry matter (RDM) of common bean were not affected by the residual effect of successive CSS applications (Figures 3E, G, I). However, there was greater root N accumulation (RNA) of the common bean plants grown in the plots that received 10 and 15 Mg ha^{-1} of CSS, with accumulated amounts of 1.8 and 2.3 mg per plant, respectively (Figure 3K).

In soybean, successive CSS applications had a residual effect on SDM, SNA, RDM, and RNA (Figures 3F, H, J, L). The CSS 25 Mg ha^{-1} rate greatly increased SDM, RDM and RNA, i.e., 19.95 g, 0.43 g, and 1.09 mg, respectively. For SNA, the 15 Mg ha^{-1} rate promoted the largest N increase, 146.72 mg per plant.

3.2 Biological N fixation (BNF) and total N and C soil

There was a significant influence of the residual effect of CSS on BNF by common bean. The rate of 10 Mg ha^{-1} of CSS and control treatment indicated, respectively, that 97% and 96% of the accumulated N was from BNF, and the rate of 20 Mg ha^{-1} of SSC showed the lowest % of BNF, 91% (Figure 4A). There was no difference between the treatments evaluated for soybean, with values varying between 86% and 97%, in the treatments with 0 and 15 Mg ha^{-1} of CSS, respectively (Figure 4B).

In grain (phenological stage R9), it was observed that there was no influence of the residual effect of CSS for common bean, where there was a variation of 86% to 90% in the rate of 25 and 20 Mg ha^{-1} of CSS, respectively (Figure 4C). For soybeans, on the other hand, the influence of the residual effect of CSS on the grains was noted. The control treatment and the 10 Mg ha^{-1} CSS rate presented the highest % BNF averages, 100 and 98%, respectively, and were similar to each other, while the other rates evaluated (15, 20 and 25 Mg ha^{-1} CSS) the BNF values were, respectively, of 97%, 96% and 95% (Figure 4D).

Total soil N and C were evaluated at two depths (0–0.1 m and 0.1–0.2 m) after the cultivation of each crop studied. It was possible to note that both total N and total C at each depth were not influenced by the residual effect of CSS for common bean and soybean (Figure 5). For common bean, total N at the 0-0.1 m depth ranged from 0.09 to 0.08% for the 10 Mg ha^{-1} CSS rate and for the control treatment, respectively (Figure 5A). At the depth of 0.1-0.2 m, the values were similar in all treatments, 0.07% (Figure 5C). Total C ranged from 1.04 to 0.92% at the 0–0.1 m depth, in the control treatment and at the 15 Mg ha^{-1} CSS rate, respectively (Figure 5E) and 0.91 to 0.81% at the 0.1–0.2 m depth, at the 10 and 15 Mg ha^{-1} CSS rates (Figure 5G).

In soybean, total soil N at the depth 0-0.1 m was similar in all treatments, with a value of 0.09% (Figure 5B). The same was observed for the 0.1–0.2 m depth (Figure 5D). The total C in the depth of 0–0.1 m varied from 1 to 0.95%, in the control treatment and in the rate of 20 Mg ha^{-1} CSS rate, respectively (Figure 5F). In the depth 0.1-0.2 m, the values found were similar in all treatments, 0.9% (Figure 5H).

3.3 Nodulation, enzymes, nitrate, and ammonium

To evaluate the nodulation efficiency in common bean and soybean plants, the number of nodules per plant (NNP), the

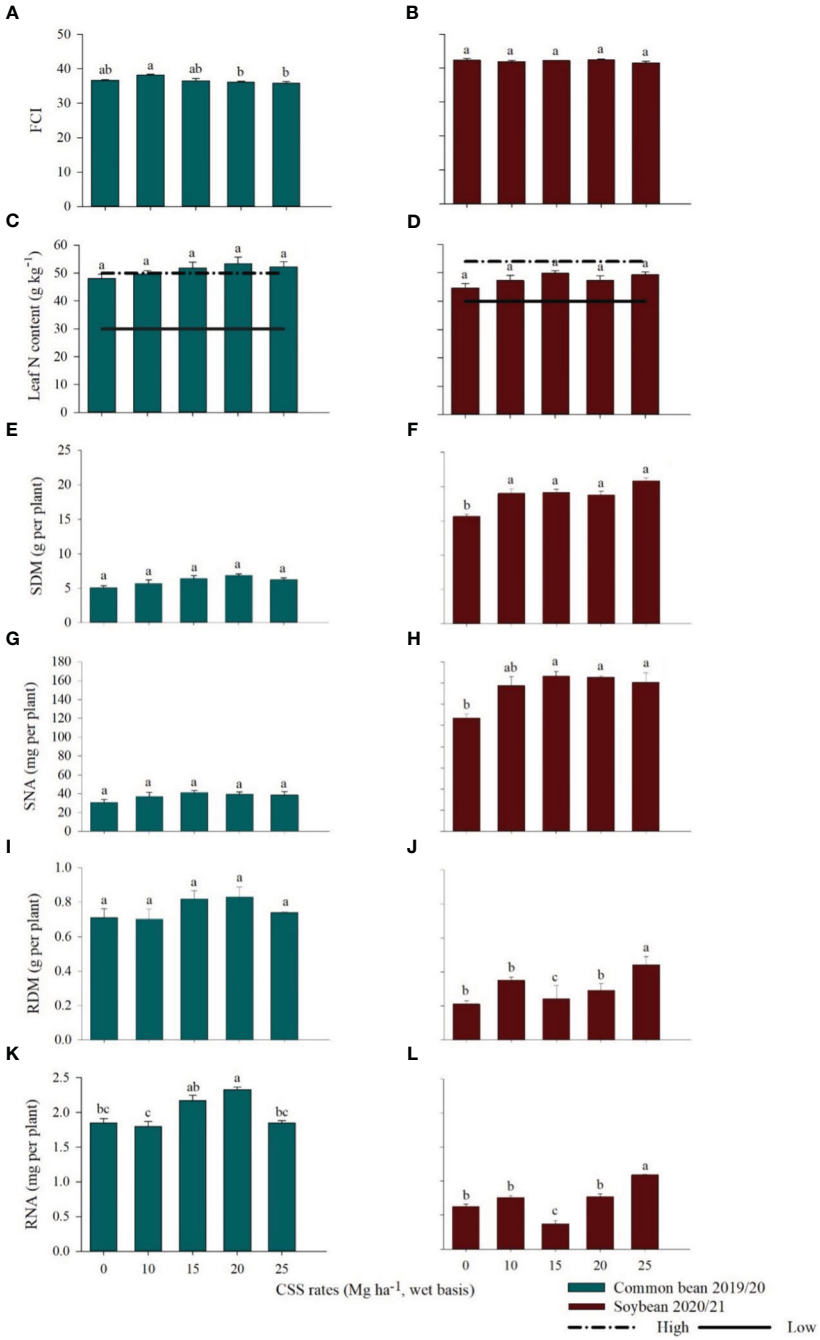

FIGURE 3
Falker chlorophyll index (FCI) **(A, B)**, leaf N content **(C, D)**, shoot dry matter (SDM) **(E, F)**, shoot N accumulation (SNA) **(G, H)**, root dry matter (RDM) **(I, J)**, and root N accumulation (RNA) **(K, L)** in common bean and soybean plants cultivated under the residual effect of the application of rates of composted sewage sludge (CSS). Means ± standard errors followed by the same letter did not differ from each other by Tukey's test at 5% probability. The horizontal lines on graph bars represent range of interpretation of N concentrations established by Ambrosano et al. (1997).

number of viable nodules per plant (NVNP), and the nodule dry matter (NDM) were determined (Figure 6). The NNP and NVNP in common bean (Figures 6A, C) and NNP and NDM in soybean (Figures 6B, F) did not differ between treatments as a function of the residual effect of the CSS rates evaluated. However, the values of NDM in common bean differed between the rates evaluated: control treatment and the 20 and 25 Mg ha^{-1} CSS rates presented the highest values, i.e., 0.24, 0.22, and 0.23 g per plant, respectively (Figure 6E). In soybean, the NVNP values differed between the rates evaluated: the residual of the highest rate of CSS (25 Mg ha^{-1} CSS) provided the largest number of viable nodules, with an average of 26 nodules per plant (Figure 6D).

The residual effect of CSS application affected the activity of nitrate reductase (NR) and the nitrate (NT) content in soybean

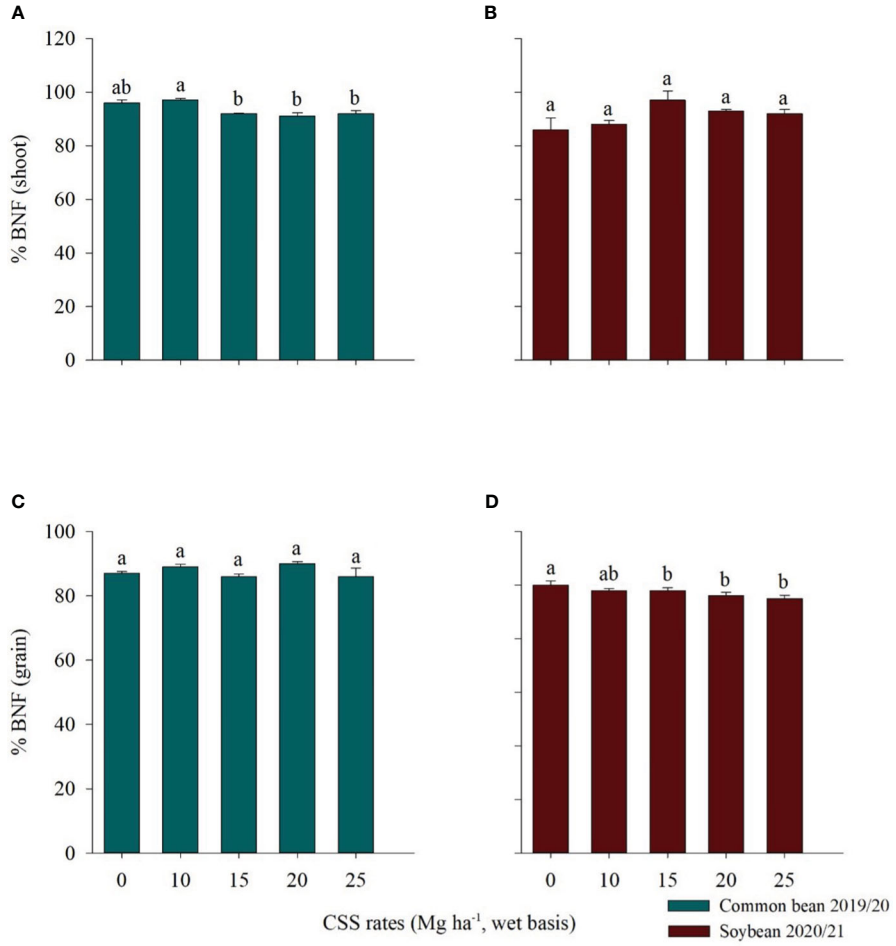

FIGURE 4
Percentage of BNF (biological nitrogen fixation) in the shoot **(A, B)** and in the grains **(C, D)** of common bean and soybean plants cultivated under the residual effect of the application of rates of composted sewage sludge (CSS). Means ± standard error followed by the same letter do not differ by the Tukey test at 5% probability.

(Figures 7B, D) and the urease activity (UR) and ammonium (AM) content in beans and soybeans (Figures 7E–H), respectively. In common bean, the highest values of UR activity were observed in the treatments that received 15 and 20 Mg ha^{-1} CSS (range 0.02 to 0.03 µmol $N\text{-}NH_4^+$ g^{-1} FM h^{-1}) (Figure 7E). Consecutive application of the highest rate (25 Mg ha^{-1}) of CSS promoted the greatest gains in AM (0.19 µmol g FM^{-1}) (Figure 7G). There was no difference between the treatments tested in relation to the activity of the NR enzyme and the NT content in the common bean (Figures 7A, C).

In soybean, the 20 and 25 Mg ha^{-1} CSS rates increased NR activity, with values between 24.39 and 22.36 µmol $N\text{-}NO_2^-$ g^{-1} FM h^{-1}, respectively (Figure 7B). Soybean NT content increased as the CSS rate increased compared to the control treatment, reaching the highest value at 20 Mg ha^{-1} (13.23 µmol g FM^{-1}) (Figure 7D). In soybean, UR activity was also influenced by CSS, with an increase in activity in the presence of CSS (Figure 7F). The AM content was also affected by the residual effect of CSS: the highest value was found for the 20 Mg ha^{-1} CSS rate (0.20 µmol g FM^{-1}) and the lowest for the of 25 Mg ha^{-1} CSS rate (0.09 µmol g FM^{-1}) (Figure 7H).

3.4 Ureides, amino acids, and protein

There was no difference in ureides, allantoic acid, and allantoin among treatments in common bean and soybean experiments (Figures 8A–F). There was also no difference in total soluble amino acids (TSA) content among the treatments evaluated in bean and soybean experiments (Figures 8G, H). There was a difference regarding the proteins in the two crops. In common bean, the highest protein value (5.35 µmol g FM^{-1}) was observed in the treatment of largest amount of CSS (25 Mg ha^{-1}) (Figure 8I). The same behavior was observed in soybean, where the highest PROT content was found for the 25 Mg ha^{-1} CSS rate, i.e., 5.78 µmol g FM^{-1}, which was different only from the treatment with 10 Mg ha^{-1} CSS (Figure 8J).

3.5 Production and productivity components

For common bean, the 100-grain weight (WG), number of grains per plant (NGP), number of grains per pod (GP), number of pods per plant (NPP), pod length (PL), and yield were evaluated. There was no

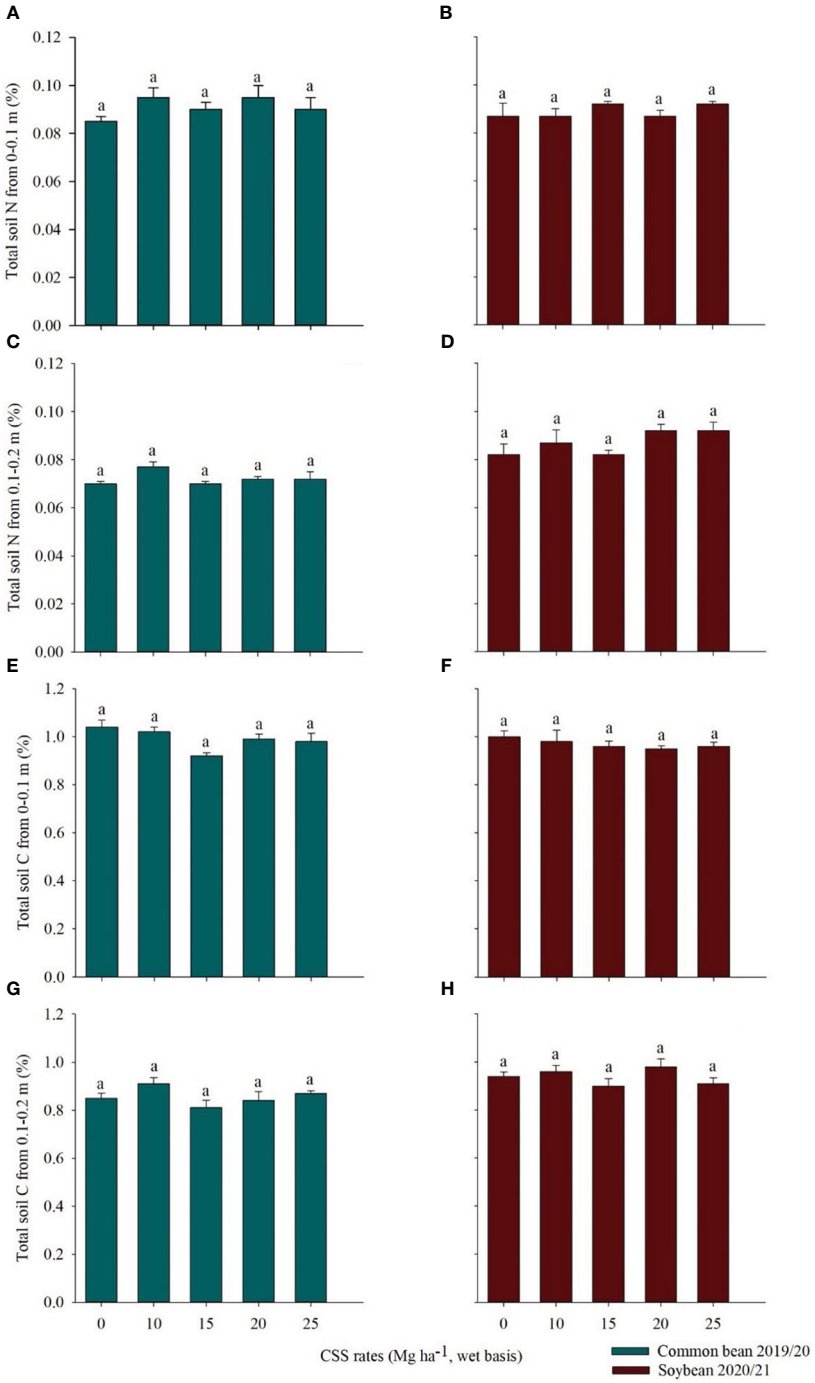

FIGURE 5
Total soil N from 0–0.1 m **(A, B)** and 0.1–0.2 m **(C, D)**, total soil C from 0–0.1 m **(E, F)** and 0.1–0.2 m **(G, H)** after common bean and soybean cultivation under the residual effect of the application of rates of composted sewage sludge (CSS). Means ± standard error followed by the same letter do not differ by Tukey test at 5% probability.

influence of the residual effect of CSS application for WG, NGP, GP, NPP and PL (Figures 9A–E). A difference in productivity was observed between the studied treatments in which there was a variation from 1945.27 kg ha^{-1} to 2515.72 kg ha^{-1}, with the highest values found from the 15 Mg ha^{-1} CSS rate (Figure 9F).

For soybean, NGP, NPP and FPIH were not affected by the residual effect of CSS application (Figures 10B, C, E), while WG, PH and yield were influenced by the residual effect of CSS application (Figures 10A, D, F). The two highest rates (20 and 25 Mg ha^{-1} CSS) yielded 19.32 g and 18.97 g WG, respectively (Figure 10A), which implies that these grains had greater accumulation of photoassimilates. For PH, the three highest rates (15, 20, and 25 Mg ha^{-1} CSS) presented the highest values, with heights of 103.93, 103.51, and 105.52 cm, respectively (Figure 10D). In terms of productivity, the 20 Mg ha^{-1} CSS

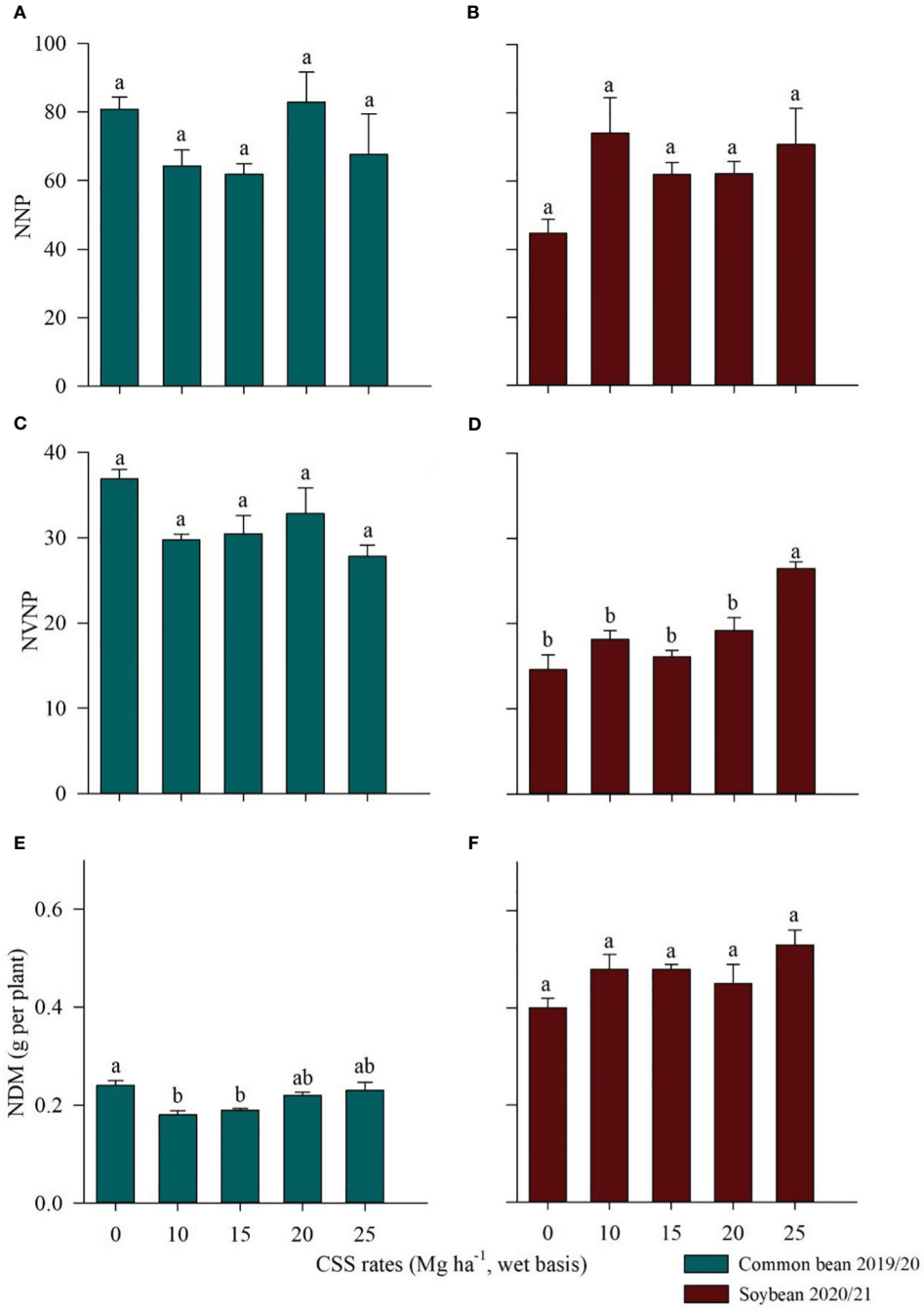

FIGURE 6
Number of nodules per plant (NNP) **(A, B)**, number of viable nodules per plant (NVNP) **(C, D)**, and nodule dry matter (NDM) **(E, F)** in common bean and soybean plants cultivated under the residual effect of the application of rates of composted sewage sludge (CSS). Means ± standard errors followed by the same letter did not differ from each other by Tukey's test at 5% probability.

rate showed the highest productivity gain, with a value of 4574.51 kg ha^{-1}, followed by 10 Mg ha^{-1} (4184.43 kg ha^{-1}) and 25 Mg ha^{-1} (4162.63 kg ha^{-1}) (Figure 10F).

3.6 Phytomass production and N accumulation in marandu palisadegrass

Figure 11 shows the total dry matter (TDM) and total N accumulation (TNA) in marandu grass after two cuts (70 and 140 DAE) in the 2019/20 crop year. The residual effect of CSS did not affect the TDM of marandu palisadegrass (Figure 11A), and the values ranged from 7090 kg ha^{-1} to 8947 kg ha^{-1}, showing a 26% gain in TDM. On the other hand, TNA was influenced by the residual effect of successive applications of CSS, in which the control treatment differed from the treatments that received the highest rates of CSS (Figure 11B). CSS rates also increased N accumulation in marandu palisadegrass.

There was no effect of residual CSS application on dry matter (DM) and nitrogen accumulation (NA) in marandu

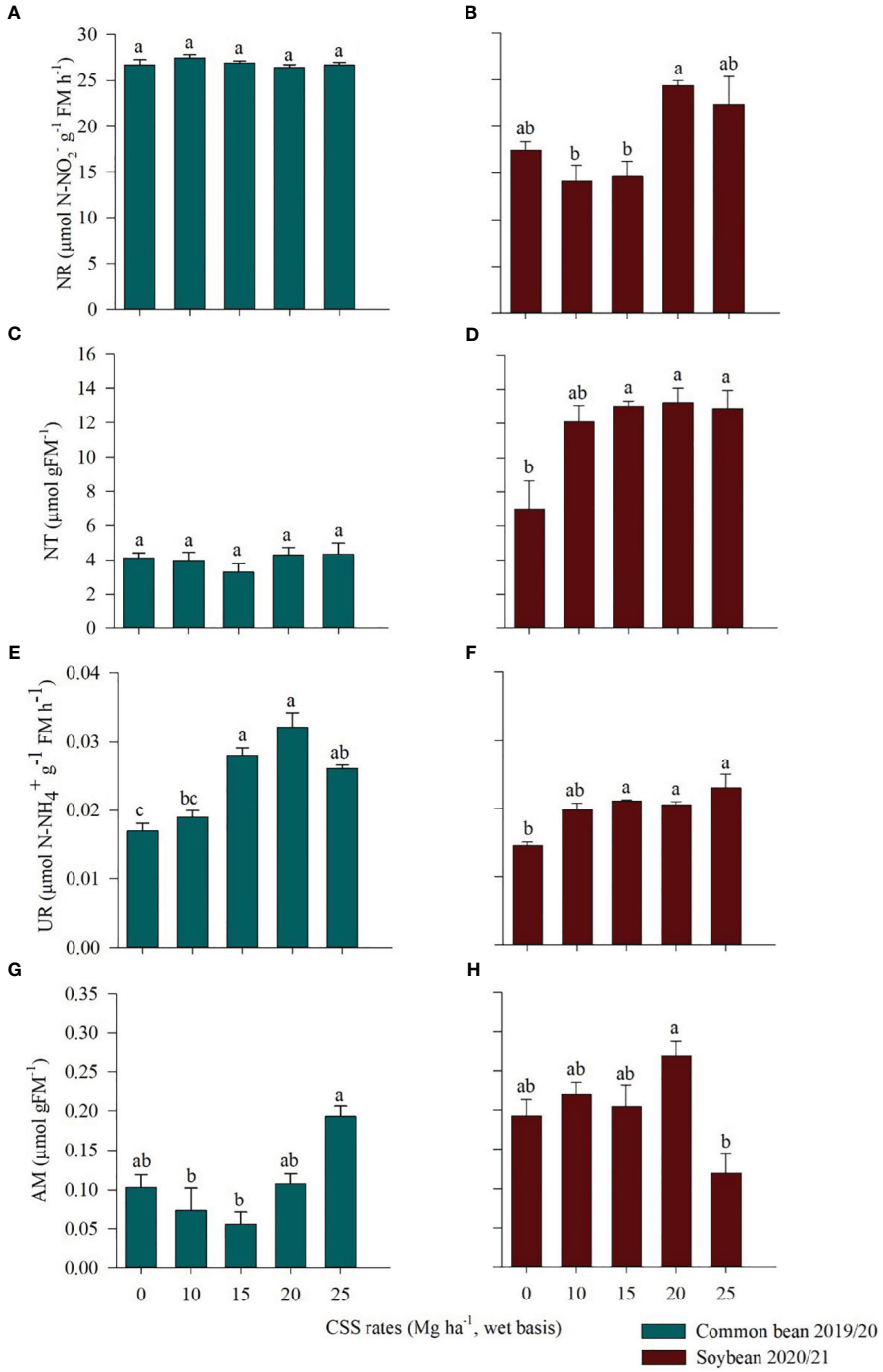

FIGURE 7
Nitrate reductase (NR) **(A, B)**, nitrate (NT) **(C, D)**, urease (UR) **(E, F)**, and ammonium (AM) **(G, H)** in common bean and soybean plants cultivated under the residual effect of the application of composted sewage sludge (CSS). Means ± standard errors followed by the same letter did not differ from each other by Tukey's test at 5% probability.

palisadegrass at 60 DAE in crop year 2020/21 (Figures 12A, B). The values for DM ranged from 1118 kg ha^{-1} to 1567 kg ha^{-1}, representing a 40% gain in DM. (Figure 12A). The accumulated amounts of N ranged from 13 kg ha^{-1} to 22 kg ha^{-1} of N per plant (Figure 12B).

4 Discussion

The FCI is an important parameter to indirectly evaluate the chlorophyll content and correlate it with the N levels in leaf tissue, since N is part of the molecular structure of chlorophyll (Filla et al.,

10.3389/fpls.2023.1281670

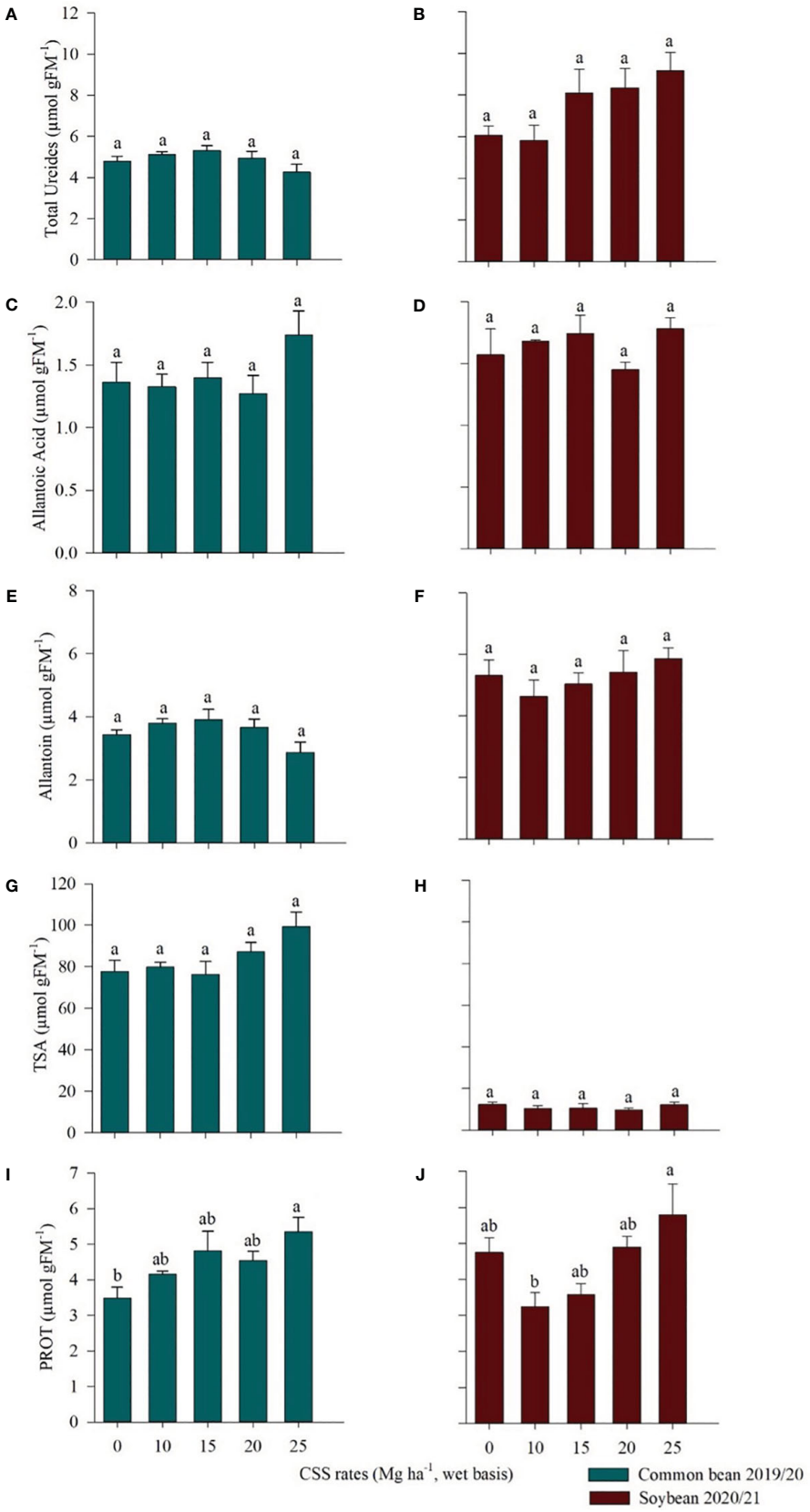

FIGURE 8
Total ureides **(A, B)**, allantoic acid **(C, D)**, allantoin **(E, F)**, total soluble amino acids (TSA) **(G, H)**, and protein (PROT) **(I, J)** in common bean and soybean cultivated under the residual effect of the application of rates of composted sewage sludge (CSS). Means ± standard errors followed by the same letter did not differ from each other by Tukey's test at 5% probability.

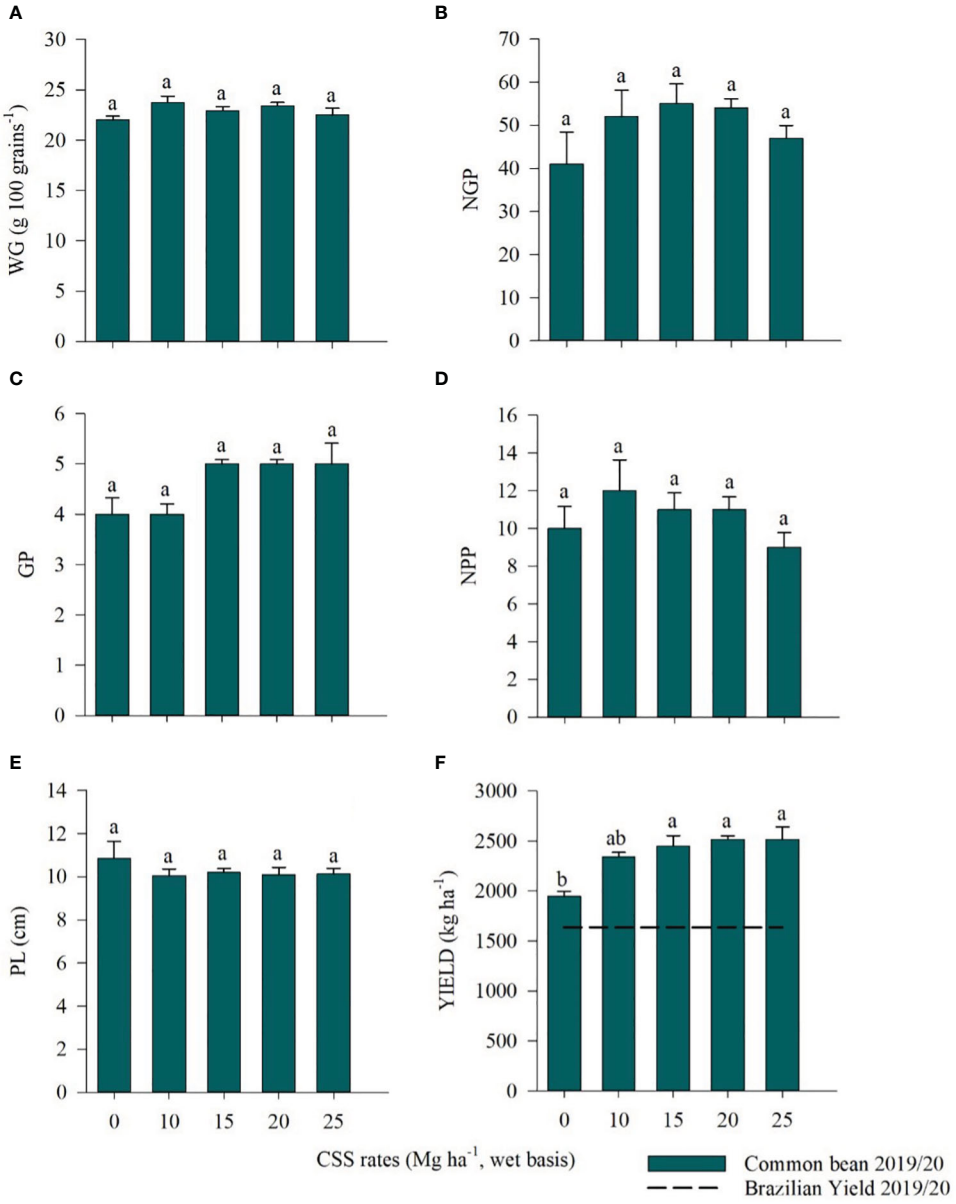

FIGURE 9
100-grain weight (WG) **(A)**, number of grains per plant (NGP) **(B)**, number of grains per pod (GP) **(C)**, number of pods per plant (NPP) **(D)**, pod length (PL) **(E)**, and yield **(F)** of common bean plants cultivated under the residual effect of the application of rates of composted sewage sludge (CSS). Means ± standard errors followed by the same letter did not differ from each other by Tukey's test at 5% probability. Average productivity in Brazil (Conab, 2020).

2020). In common bean, there was an influence of the residual effect of the CSS rates, with the highest FCI value (38.18) found for the 10 Mg ha^{-1} CSS rate. These results differ from those found by Nakao (2015), who observed no influence of fertilization with organic compost on FCI of common bean, where the values ranged between 38.17 and 41.17. In soybean, there was no influence of the residual effect of CSS application, contrary to the study by Ragagnin et al. (2013), who tested different rates (1.0, 2.0, 4.0, and 8.0 Mg ha^{-1}) using organic material from chicken litter and found higher chlorophyll contents compared to the control treatment.

The residual effect of successive CSS applications did not increase the leaf N content in common bean and soybean. However, these parameters remained within the appropriate range for both crops (30–50 g kg^{-1} for bean and 40–54 g kg^{-1} for soybean). This finding may be related to the higher content of potentially mineralizable N in the soil, which allows its release and use by crops throughout their development cycle, as occurs with common bean (Bettiol and Ghini, 2011). Boeira and Maximiliano (2009) reported that there is an effect of previous sludge applications on the N mineralization potential and that higher rates lead to the accumulation of NO_3^- in the soil. It is known that soil nitrate can be easily lost by leaching. Therefore, adequate rates of CSS should always be applied to maintain crop nutrition and avoid possible environmental risks (Moretti et al., 2015; Rigby et al.,

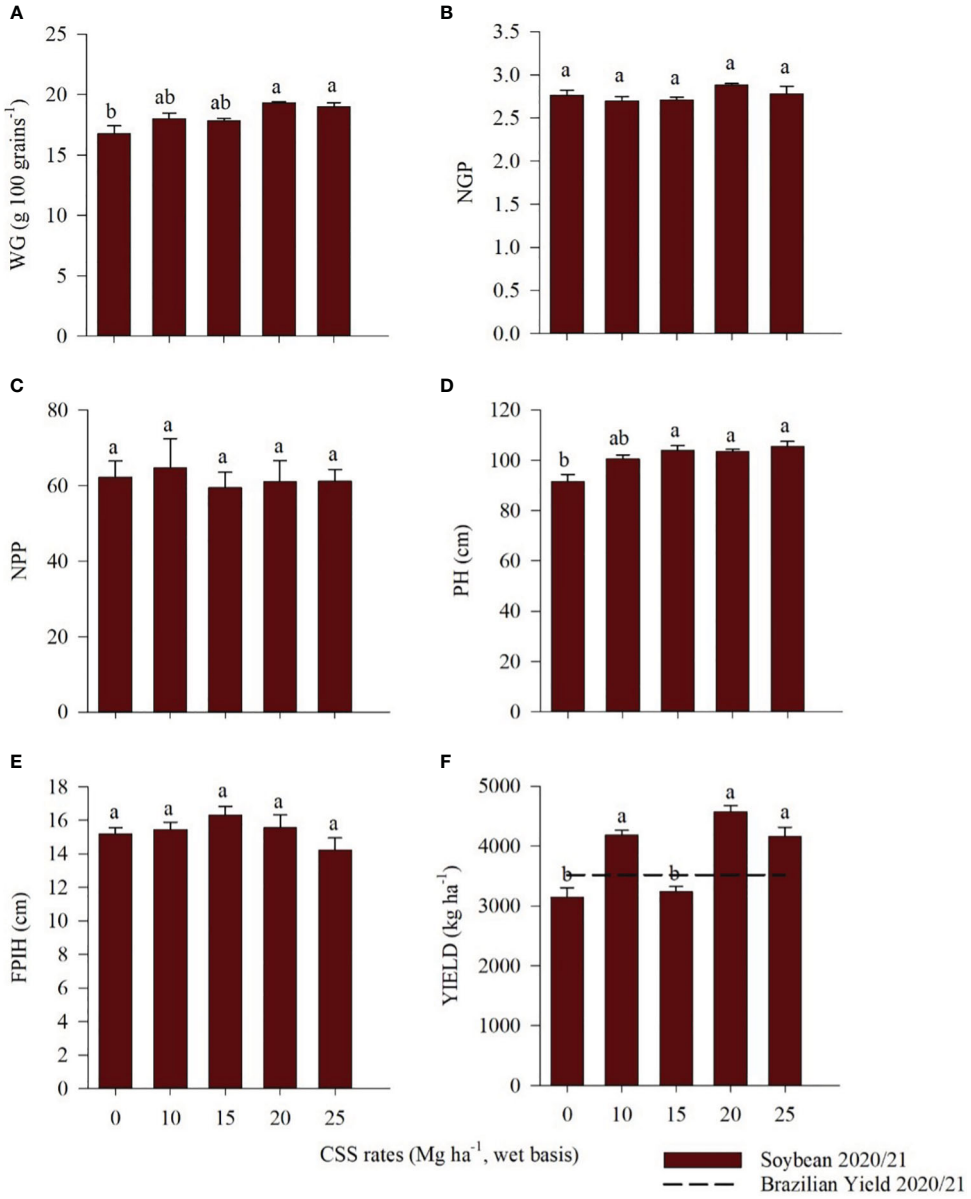

FIGURE 10
100-grain weight (WG) **(A)**, number of grains per pod (NGP) **(B)**, number of pods per plant (NPP) **(C)**, plant height (PH) **(D)**, first pod insertion height (FPIH) **(E)**, and yield **(F)** of soybean plants cultivated under the residual effect of the application of rates of composted sewage sludge (CSS). Means ± standard errors followed by the same letter did not differ from each other by Tukey's test at 5% probability. Average productivity in Brazil (Conab, 2021).

2016). In addition, crop rotation and the use of cover crops are essential so that part of leachable N is recovered through N-cycling (Borges et al., 2014).

The SDM, RDM, SNA, and RNA of soybean increased with the residual application of CSS. These results agree with other studies reporting that the residual effect of SS application provided the slow release of nutrients, in which the success of SS depends on the conditions of the production process, the rates used, the type of soil, and the crop cultivated (Melo et al., 2018). Yuruk and Bozkurt (2006) reported that SS treatments increased the grain yield and biomass of common bean and chickpeas (*Cicer arietinum* L.) and did not cause any nutrition imbalance of these plants.

Some studies have already shown that SS may favor nodulation in legume plants, such as soybeans and fava beans (Rebah et al., 2007; Eid et al., 2018). Furthermore, Rebah et al. (2007) indicated that several components of SS are essential to increase the activity of N-fixing bacteria, with nodulation notably favored when SS was used. In our study, CSS altered the dry matter of common bean nodules and increased the number of viable nodules in soybean with increasing rates of CSS. Several studies have shown that total nodule number and nodule dry matter analyses (Ferreira and Castro, 1995; Martins et al., 2022) are efficient for estimating BNF. Thus, in a study performed to evaluate BNF with the use of composted SS, there was an increase in the number of nodules up to a rate of 19 Mg

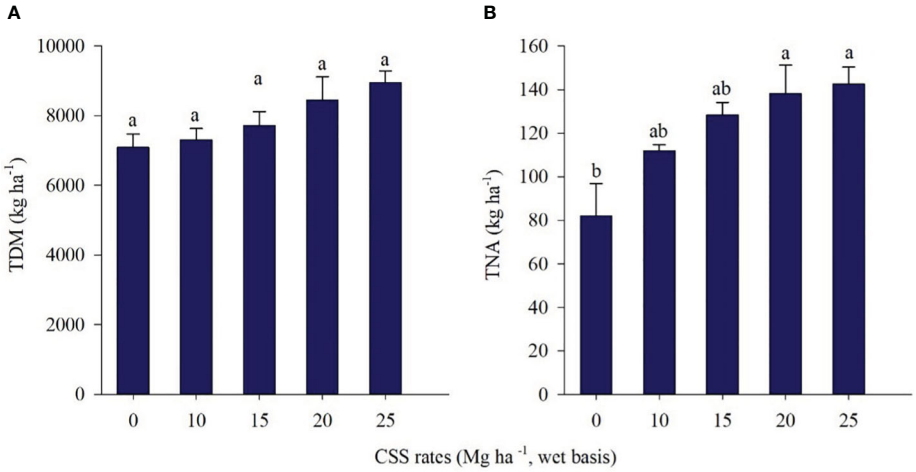

FIGURE 11
Total dry matter (TDM) **(A)** and total nitrogen accumulation (TNA) **(B)** in two cuts of marandu palisadegrass in the 2019/20 crop, cultivated under the residual effect of composted sewage sludge (CSS) application. Means ± standard errors followed by the same letter did not differ from each other by Tukey's test at 5% probability.

ha^{-1} SS and an increase in dry matter at rates of 30 and 40 Mg ha^{-1} associated with seed inoculation (Lobo et al., 2012). In addition, the ^{15}N natural abundance technique used in our study to accurately estimate how much of the fixed N comes from BNF, showed that values from 90 to 97% of the common bean N in the CSS treatments comes from BNF and the difference with the control treatment may have been due to the transformations of the N present in the compost in the soil.

It is noteworthy that the increase in viable soybean nodules and the stability of % BNF during the soybean reproductive stage in our study indicates an efficient BNF in the soybean crop that was not negatively affected by CSS, as already concluded by Souza et al. (2009), who found that SS application at rates of up to 6 Mg ha^{-1} does not negatively affect soybean nodulation in a two-year period. In an experiment carried out under field conditions, Currie et al. (2003) demonstrated that applying SS can increase the BNF rates in soybean. Although we observed that the % BNF in soybean (calculated at R8 grains phenological stage) receiving CSS decreased compared to the control, about 95% (on average) of the fixed N was from BNF in the CSS treatments.

The concentration of cellular nitrate is the main factor controlling the expression of NR because this enzyme reduces nitrate in the cellular environment. If the concentration of NO_3^- decreases, the NR activity will consequently decrease or, with the addition of N-NO_3^-, a higher concentration of nitrate and NR activity is expected (Hirel and Krapp, 2020). In the present study,

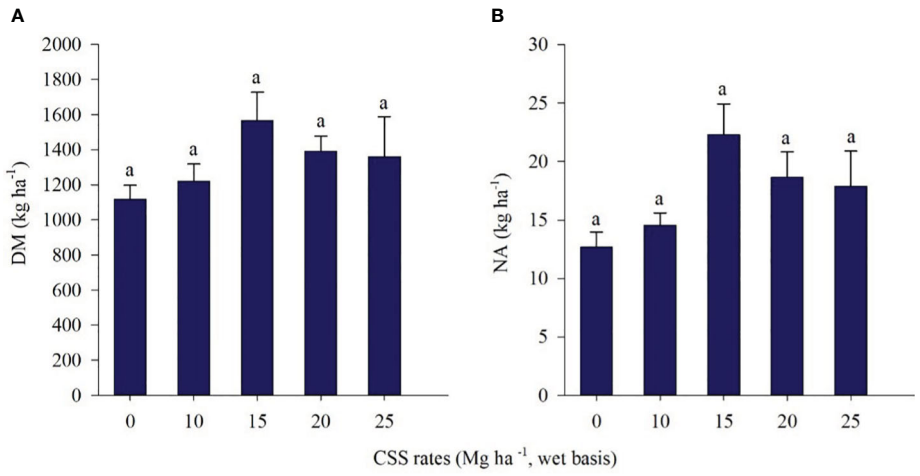

FIGURE 12
Dry matter (DM) **(A)** and nitrogen accumulation (NA) **(B)** of marandu palisadegrass in the 2020/21 crop year under the residual effect of composted sewage sludge (CSS) application. Means ± standard errors followed by the same letter did not differ from each other by Tukey's test at 5% probability.

for common bean, this relationship remained stable and was not affected by CSS application. For soybean, this relationship was true because CSS influenced the nitrate content and consequently the NR activity in soybean leaves, where the highest rates of CSS showed higher means for these two parameters.

The CSS altered urease activity and consequently the ammonium content in common bean and soybean leaves. However, in soybean, the highest rate of CSS (25 Mg ha^{-1}) showed the lowest mean ammonium content. Urease activity is greatly influenced according to the type of nitrogen fertilization used, since the plant can uptake N as urea due to specific transporters (Witte, 2011). In addition, urea is also generated within plants through arginine catabolism (protein degradation) and photorespiration, which generates NH_4^+ that will be incorporated by glutamine synthetase (Rennenberg et al., 2010; Witte, 2011). Urea in the plant cytosol is hydrolyzed by urease and releases ammonia/ammonium that is used for amino acids biosynthesis (Carter et al., 2009; Witte, 2011). As in our study, we did not use any source of urea, the increase in urease activity, the decrease in NH_4^+ concentration and the increase in soluble proteins are linked to urea biosynthesis in the plant, promoting a rapid cycling of these metabolites and without causing damage to the plant, as they indicate an efficient assimilation of N generated in the form of NH_4^+.

Moreover, the materials involved in sludge composting may influence this characteristic of urease and ammonium because N-containing substances such as proteins, amino acids, and nucleic acids present in the sludge can release N as ammonium in the soil (Sharma et al., 2017; Raheem et al., 2018). The process of protein decomposition occurs in several steps and releases several amino acids. These amino acids undergo a deamination process, releasing the amine group as ammonia, which in the soil reacts quickly with water to form ammonium, which plants can uptaken (Vieira, 2017). Thus, all these metabolic processes involving urease and ammonium seem to have been influenced by CSS, but studies demonstrating these effects are still scarce.

The residual effect of CSS application positively influenced the protein content of beans and soybeans. The increase in protein content may be the compensation found in this study to maintain N-fixation; we did not observe changes in ureide metabolism, as they are the main N-containing molecules used for N transportation from nodules in bean and soybean to other plant tissues for use in protein biosynthesis (Díaz-Leal et al., 2012; Hirel and Krapp, 2020).

The consecutive CSS applications increased the plant height and the weight of 100 soybean grains, with the highest values found at the highest rates applied (20 and 25 Mg ha^{-1} of CSS). The same was observed in a study that tested organic fertilization through chicken litter at 3, 6, and 9 Mg ha-1 rates in a Cambisol. For the development and production components of soybean, there was an increase in plant height and 1,000-grain weight, in addition to the first pod insertion height, the number of pods per plant, and the soybean grain yield (Carvalho et al., 2011).

Fertilizers based on biosolids improve crop productivity and increase the availability of ammonium (NH_4^+) and nitrate (NO_3^-) in the soil due to organic N mineralization (Price et al., 2015; Wang et al., 2017b; Wijesekara et al., 2017). The use of CSS in this study affected common bean and soybean yields and maintained N levels within the recommended ranges for the crops. For common beans, plants that received CSS showed higher yields than those cultivated in the control treatment, with 2515 kg ha^{-1} production at the highest compost rate. Only the 10 Mg ha^{-1} CSS rate yielded production similar to that of the control, but all the studied treatments obtained a yield above the national average (1636 kg ha^{-1}) for the 2019/20 crop of the third bean crop, according to a survey from CONAB (2020). For soybean, the averages obtained for the 10, 20, and 25 Mg ha^{-1} CSS rates remained above the national average (3527 kg ha^{-1}) for the 2020/21 crop, confirming the CONAB survey findings (2021).

Such responses were already evidenced by Santos et al. (2011), who observed a 65% increase in common bean yield using CSS derived from the treatment of effluents of the beverage and paper industry compared to control treatment (without compost). One study that aimed to evaluate changes in organic matter contents and N forms in sludge-corrected soils and in the growth of maize (*Zea mays* L.) and fava beans (*Vicia faba* L.) also showed that the residual effect of CSS promoted a greater response in the grain yield of fava beans (Elsalam et al., 2021). In addition, our soybean yield values are similar to those found (3222 kg ha^{-1}) in a study in which soybean was fertilized with mineral N by applying a rate of 300 kg ha^{-1} of N in the form of urea (Kubar et al., 2021). In the present study, with the rates of CSS applied, soybean yielding ranged from 3240 to 4574 kg ha^{-1}.

In the first evaluation season (2019/20) of marandu palisadegrass, CSS rates led to an increase in N, especially at the highest rates (138.19 and 142.6 kg ha^{-1}). In the second crop evaluated (2020/21), there was no increase in dry matter and N in marandu palisadegrass. Long-term CSS application can promote the increase in available N levels in the soil by increasing the amounts uptake by marandu palisadegrass, since there is a greater accumulation of this nutrient, especially at the highest rates of CSS supplied. The higher availability of N is also associated with the residual effect of CSS in the soil, which acts as a source of organic matter, improving fertility and providing N to the system, as has already been demonstrated for fescue forage (*Festuca arundinacea* Schreb.) for 19 years through the application of biosolids (Cogger et al., 2013).

Vendruscolo et al. (2016) showed that residual SS application in the recovery of a degraded area and the management with brachiaria (*Urochloa decumbens*) influenced the chemical attributes, especially the P and K contents, of the soil over nine years of evaluation.

In addition, cropping systems with forages preceding the main crop showed positive effects on the physicochemical characteristics of the soil, culminating in increased bean productivity on *U. ruziziensis* straw (Sabundjian et al., 2013; Amaral et al., 2016) and higher soybean grain yield and nutrient cycling on *Urochloa brizantha* straw (Moraes et al., 2014; Tanaka et al., 2019). Another important effect of these grasses is the high release and cycling of nutrients, especially N (Borges et al., 2014), P, and K (Pacheco et al., 2011).

It is believed that in the second crop evaluated, the absence of a CSS residual effect on marandu palisadegrass may have occurred due to its shorter cultivation time in the soil compared to the previous crop and to the immobilization-mineralization relationship of N in the soil. The type of straw on the soil surface, such as that with a high C/N ratio, promotes an increase in the rate of N immobilization by soil microorganisms and influences crop management, especially nitrogen fertilization (Amaral et al., 2016). At the beginning of the NTS, as is the case in the present study, the immobilization of nutrients and organic matter in the soil tends to be greater than the mineralization; however, mineralization changes with time, which increases the mineralization rate (Torres et al., 2008). Regardless, the consolidation of NTS leads to a balance between the mineralization and immobilization processes (Teixeira et al., 2011), in addition to mitigating N losses from the system through cycling and immobilization in its phytomass (Lara Cabezas et al., 2004).

5 Conclusions

The residual effect of successive CSS applications as a source of N in the bean-palisade grass-soybean rotation under no-tillage in the *Cerrado* may meet the N needs of the crops studied, especially at the highest applied rates (20 and 25 Mg ha^{-1} of CSS, wet basis). Through the two CSS applications in highly weathered tropical soil, a residual effect of this fertilizer was observed as increases in common bean and soybean grain yield and adequate foliar N concentration in the crops. The percent of nitrogen derived from BNF in the shoot of beans and grains of soybean decreased with increasing CSS rates but remained stable with increasing nodule dry matter in beans and increasing viable nodules in soybean. The protein content increased with the residual effect of CSS. The mineralization of N present in the CSS influenced the nitrate content and the activity of nitrate reductase and urease in soybean. The urease activity and the ammonium content in the crops were affected by the residual effect of the compost, which may have occurred due to urea metabolism in leaves. The residual effect of CSS application in *Cerrado* soil may meet the long-term nutritional N demand of marandu palisadegrass under NTS and promote greater N cycling to subsequent crops, leading to a balance between the immobilization and mineralization rates of N. In terms of sustainable agriculture, the use of sewage sludge as composted organic fertilizer (i.e., CSS) can help in mitigating problems (e.g., food insecurity) due to the lack of both: *i*) mineral fertilizers, available for commercialization in Brazilian agriculture; *ii*) decreasing fertile lands, in addition to; *iii*) reducing the difficulties in using mineral fertilizers, especially in the State of São Paulo. Furthermore, it is an appropriate final destination for sewage sludge, which continues to be produced on a large scale in Brazil.

Data availability statement

The raw data supporting the conclusions of this article will be made available by the authors, without undue reservation.

Author contributions

MB: Conceptualization, Methodology, Software, Writing – original draft. LS: Data curation, Investigation, Writing – review & editing. MT: Data curation, Investigation, Validation, Visualization, Writing – review & editing. LS: Formal Analysis, Investigation, Methodology, Writing – review & editing. AC: Data curation, Formal Analysis, Validation, Writing – review & editing. JL: Data curation, Formal Analysis, Validation, Writing – review & editing. CA: Validation, Writing – review & editing. ZH: Data curation, Writing – review & editing. FZ: Visualization, Writing – review & editing. AJ: Validation, Writing – original draft. GC: Validation, Writing – review & editing. TN: Conceptualization, Funding acquisition, Project administration, Supervision, Visualization, Writing – review & editing.

Funding

The authors declare financial support was received for the research, authorship, and/or publication of this article. This research was funded by the National Council for Scientific and Technological Development (CNPq) (grant # 404815/2021-9). This study was financed in part by the Coordenação de Aperfeiçoamento de Pessoal de Nível Superior—Brasil (PROAP Program - AUXPE no. 2671/ 2022).

Acknowledgments

We thank the Coordination for the Improvement of Higher Education Personnel (CAPES 88887.463840/2019-00), for the master's scholarship granted to the first author and for funding the translation of the article (PROAP Program - AUXPE no. 2671/ 2022). Also, the authors thank the National Council for Scientific and Technological Development for the fellowship provided (CNPq PQ2 grant # 308374/2021-5), to GENAFERT (Study Group on Nutrition, Fertilization, and Soil Fertility) for the technical support, and to Biossolo Agricultura e Ambiente Ltda. and Tera Ambiental for supplying compost.

Conflict of interest

The authors declare that the research was conducted in the absence of any commercial or financial relationships that could be construed as a potential conflict of interest.

Publisher's note

References

Abreu-Junior, C. H., Oliveira, M. G., Cardoso, P. H. S., Mandu, T. S., Florentino, A. L., Oiveira, F. C., et al. (2020). Sewage sludge application in *Eucalyptus urograndis* plantation: availability of phosphorus in soil and wood production. *Front. Environ. Sci.* 8. doi: 10.3389/fenvs.2020.00116

Alvarenga, A. C., Sampaio, R. A., Pinho, G. P., Cardoso, P. H., Sousa, I. P., and Barbosa, M. H. (2017). Phytoremediation of chlorobenzenes in sewage sludge cultivated with Pennisetum purpureum at different times. *Rev. Bras. Eng.* 21, 573–578. doi: 10.1590/1807-1929/agriambi.v21n8p573-578

Amaral, C. A., Pinto, C. C., Flôres, J. A., Mingotte, F. L. C., Lemos, L. B., and Filho, D. F. (2016). Produtividade e qualidade do feijoeiro cultivado sobre palhadas de gramíneas e adubado com nitrogênio em plantio direto. *Pesquisa Agropecuária Bras.* 51, 1602–1609. doi: 10.1590/S0100-204X2016000900060

Ambrosano, E. J., Tanaka, R. T., Mascarenhas, H. A. A., Raij Van, B., Quaggio, J. A., and Cantarella, H. (1997). "Leguminosas e oleaginosas," in *Recomendações de Adubação e Calagem Para o Estado de São Paulo*, *2 ed* (Campinas: Instituto Agronômico de Campinas), 189–191.

Barbiere Junior, E., Rossiello, R. O. P., Silva, R. V. M. M., Ribeiro, R. C., and Morenz, M. J. F. (2012). Um novo clorofilômetro para estimar teores de clorofila em folhas de capim Tifton 85. *Ciec. Rural* 42, 2242–2245. doi: 10.1590/S0103-84782012005000109

Barbosa, J. C., and Maldonado, Junior W. (2015). *AgroEstat- Sistema para Análises Estatísticas de Ensaios Agronômicos* (Jaboticabal: FCAV- UNESP).

Bettiol, W., and Ghini, R. (2011). Impacts of sewage sludge in tropical soil: a case study in Brazil. *Appl. Environ. Soil Sci.* 2011, 1–11. doi: 10.1155/2011/212807

Bieleski, R. L., and Turner, N. A. (1966). Separation and estimation of amino acids in crude plant extracts by thin-layer electrophoresis and chromatography. *Anal. Biochem.* 17, 278–293. doi: 10.1016/0003-2697(66)90206-5

Biswas, B., and Gresshoff, P. (2014). The role of symbiotic nitrogen fixation in sustainable production of biofuels. *Int. J. Mol. Sci.* 15, 7380–7397. doi: 10.3390/ijms15057380

Boddey, R. M., Polidoro, J. C., Resende, A. S., Alves, B. J. R., and Uurquiaga, S. (2001). Use of the ^{15}N natural abundance technique for the quantification of the contribution of N_2 fixation to grasses and cereals. *Aust. J. Plant Physiol.* 28, 889–895. doi: 10.1071/PP01058

Boeira, R. C., Ligo, M. A. V., and Dynia, J. F. (2002). Mineralização de nitrogênio em solo tropical tratado com lodos de esgoto. *Pesqui. Agropecu. Bras.* 37, 1639–1647. doi: 10.1590/S0100-204X2002001100016

Boeira, R. C., and Maximiliano, V. C. B. (2009). Mineralização de compostos nitrogenados de lodos de esgoto na quinta aplicação em Latossolo. *Rev. Bras. Cienc. Solo* 33, 711–722. doi: 10.1590/S0100-06832009000300023

Borges, W. L. B., Freitas, R. S., Mateus, G. P., Sá, M. E., and Alves, M. C. (2014). Absorção de nutrientes e alterações químicas em Latossolos cultivados com plantas de cobertura em rotação com soja e milho. *Rev. Bras. Cienc. Solo* 38, 252–261. doi: 10.1590/S0100-06832014000100025

Bradford, M. M. (1976). A rapid and sensitive method for the quantitation of microgram quantities of protein utilizing the principle of protein-dye binding. *Analytical Biochem.* 72, 248–254. doi: 10.1006/abio.1976.9999

Brasil (2020a). *Resolução n° 498, de 19 de agosto de 2020. Define critérios e procedimentos para produção e aplicação de biossólido em solos, e dá outras providências* Vol. 161. Ed. D. F. Brasilia (Brasília: Diário Oficial da União), 265. 21 ago. 2020. Seção 1.

Brasil (2020b). *Instrução normativa n° 61, de 8 de julho de 2020. Estabelece as regras sobre definições, exigências, especificações, garantias, tolerâncias, registro, embalagem e rotulagem dos fertilizantes orgânicos e dos biofertilizantes, destinados à agricultura* Vol. 134 5. Ed. D. F. Brasília (Brasília: Diário Oficial da União). 15 jul. 2020. Seção 1.

Cadisch, G., Hairiah, K., and Giller, K. E. (2000). Applicability of the natural ^{15}N abundance technique to measure N_2 fixation in *Arachis hypogaea* grown on an Ultisol. *Net. J. Agric. Sci.* 48, 31–45. doi: 10.1016/S1573-5214(00)80003-2

Carter, E. L., Flugga, N., Boer, J. L., Mulrooney, S. B., and Hausinger, R. P. (2009). Interplay of metal ions and urease. *Metallomics* 1, 207–221. doi: 10.1039/b903311d

Carvalho, E. R., Rezende, P. M., Andrade, M. J. B., Passos, A. M. A., and Oliveira, J. Á. (2011). Fertilizante mineral e resíduo orgânico sobre características agronômicas da soja e nutrientes no solo. *Rev. Cienc. Agron.* 42, 930–939. doi: 10.1590/S1806-66902011000400015

Cataldo, D. A., Haroon, M., Schrader, L. E., and Youngs, V. L. (1975). Rapid colorimetric determination of nitrate in plant-tissue by nitration of salicylic-acid. *Commun. Soil Sci. Plant Anal.* 6, 71–80. doi: 10.1080/00103627509366547

Climate Change Knowledge Portal (2021) *Current Climate "Climatology"*. Available at: https://climateknowledgeportal.worldbank.org/country/Brazil/climate-data-historical (Accessed 04 Sept 2023).

Cogger, C. G., Bary, A. I., Myhre, E. A., and Fortuna, A. M. (2013). Biosolids applications to tall fescue have long-term influence on soil nitrogen, carbon, and phosphorus. *J. Environ. Qual.* 42, 516–522. doi: 10.2134/jeq2012.0269

Companhia Nacional de Abastecimento – CONAB (2020) *Observatório agrícola – Acompanhamento da safra brasileira: grãos*. Available at: http://conab.gov.br/ (Accessed 20 July 2023).

Companhia Nacional de Abastecimento – CONAB (2021) *Acompanhamento da Safra Brasileira de Grãos*. Available at: http://conab.gov.br/ (Accessed 20 July 2023). safra 2020/21, n. 12, décimo segundo levantamento, setembro. 2021.

Currie, V. C., Angle, J. S., and Hill, R. L. (2003). Biosolids application to soybeans and effects on input and output of nitrogen. *Agric. Ecosyst. Environ.* 97, 345–351. doi: 10.1016/S0167-8809(03)00134-8

D'avila, J. V., Chaves, M. C. C., Santos, F. S., and Peres, A. A. C. (2019). Análise da viabilidade econômico-financeira de sistemas de disposição final de lodo de esgoto. *Rev. Agro. Amb.* 12, 541–555. doi: 10.17765/2176-9168.2019v12n2p541-555

Díaz-Leal, J. L., Gálvez-Valsivieso, G., Fernández, J., Pineda, M., and Alamillo, J. M. (2012). Developmental effects on ureide levels are mediated by tissue-specific regulation of allantoinase in *Phaseolus vulgaris* L. *J. Exp. Bot.* 63, 4095–4106. doi: 10.1093/jxb/ers090

Eid, E. M., Alrumman, S. A., El-Bebany, A. F., Fawy, K. F., Taher, M. A., Hesham, A. L., et al. (2018). The evaluation of sewage sludge application as a fertilizer for broad bean (*Faba sativa* Bernh.) crops. *Food Energy Secur.* 7, 1–13. doi: 10.1002/fes3.142

Elsalam, H. E. A., El-Sharnouby, M. E., Mohamed, A. E., Raafat, B. M., and El-Gamal, E. H. (2021). Effect of sewage sludge sompost usage on corn and faba bean growth, carbon and nitrogen forms in plants and soil. *Agronomy* 11, 1–20. doi: 10.3390/agronomy11040628

Ferraz, A., Momentel, L. T., and Poggiani, F. (2016). Soil fertility, growth and mineral nutrition in *Eucalyptus grandis* plantation fertilized with different kinds of sewage sludge. *New For.* 47, 861–876. doi: 10.1007/s11056-016-9549-1

Ferreira, E. M., and Castro, I. V. (1995). Nodulation and growth of subterranean clover (*Trifolium subterraneum* L.) in soils previously treated with sewage sludge. *Soil Biol. Biochem.* 27, 1177–1183. doi: 10.1016/0038-0717(95)00029-E

Filla, V. A., Coelho, A. P., Leal, F. T., Bettiol, J. V. T., and Lemos, L. B. (2020). Portable chlorophyll mater in monitoring and management of nitrogen in common bean cultivars. *Rev. la Facultad Cienc. Agrar.* 52, 64–77.

Gangbazo, G., Pesant, A. R., Barnett, G. M., Charuest, J. P., and Cluis, D. (1995). Water contamination by ammonium nitrogen following the spreading of hog manure and mineral fertilizers. *J. Environ. Qual.* 24, 420–425. doi: 10.2134/jeq1995.00472425002400030004x

Guimaraes, A. P., Morais, R. F., Urquiaga, S., Boddey, R. M., and Alves, B. J. R. (2008). Bradyrhizobium strainand the ^{15}N natural abundance quantification of biological N_2 fixation in soybean. *Sci. Agric.* 65, 516–524. doi: 10.1590/S0103-90162008000500011

Hargreaves, J. C., Adl, M. S., and Warman, P. R. (2008). A review of the use of composted municipal solid waste in agriculture. *Agric. Ecosyst. Environ.* 123, 1–14. doi: 10.1016/j.agee.2007.07.004

Hirel, B., and Krapp, A. (2020). *Nitrogen Utilization in Plants I, Biological and Agronomic Importance. 3th ed* (Paris: Degrutyer).

Hogan, M. E., Swift, I. E., and Done, H. J. (1983). Urease assay and ammonia release from tissue. *Phytochemistry* 22, 663–667. doi: 10.1016/S0031-9422(00)86958-7

Jakubus, M., and Graczyk, M. (2020). Microelement variability in plants as an effect of sewage sludge compost application assessed by different statistical methods. *Agronomy* 10, 642. doi: 10.3390/agronomy10050642

Kacprzak, M., Neczaj, E., Fijałkowski, K., Grobelak, A., Grosser, A., Worwag, M., et al. (2017). Sewage sludge disposal strategies for sustainable development. *Environ. Res.* 156, 39–46. doi: 10.1016/j.envres.2017.03.010

Kubar, M. S., Shar, A. H., Kubar, K. A., Rind, N. A., Ullah, H., Kalhoro, S. A., et al. (2021). Optimizing nitrogen supply promotes biomass, physiological characteristics and yield components of soybean (*Glycine max* L. Merr.). *Saudi J. Biol. Sci.* 28, 6209–6217. doi: 10.1016/j.sjbs.2021.06.073

Lara Cabezas, W. A. R., Alves, B. J. R., Urquiaga, S., and Santana, D. G. (2004). Influência da cultura antecessora e da adubação nitrogenada na produtividade de milho em sistema plantio direto e solo preparado. *Ciênc. Rural* 34, 1005–1013. doi: 10.1590/S0103-84782004000400006

Lavres, J., Franco, G. C., and Câmara, G. M. S. (2016). Soybean seed treatment with nickel improves biological nitrogen fixation and urease activity. *Front. Environ. Sci.* 4. doi: 10.3389/fenvs.2016.00037

Lobo, T. F., Grassi Filho, H., Cardoso, E. J. B. N., Almeida, L. S., and Nomiyama Junior, N. (2012). Crescimento e fixação biológica de nitrogênio em soja cutivada com rates de lodo de esgoto compostado. *Semina: Ciênc. Agrár.* 33, 1333–1342. doi: 10.5433/1679-0359.2012v33n4p1333

Lombardi Neto, F., and Drugowich, M. (1994). *Manual Técnico de Manejo e Conservação de Solo e Água* (Campinas: CATI).

Malavolta, E. A., Vitti, G. C., and Oliveira, S. A. (1997). *Avaliação do Estado Nutricional das Plantas: Princípios e Aplicações* (Piracicaba: Potafós).

Martins, S. F., Esperancini, M. S. T., Quintana, N. R. G., and Barbosa, F. S. (2021). Análise econômica da produção de lodo de esgoto compostado para fins agrícolas na estação de tratamento de esgoto de Botucatu-SP. *Energ. Agric.* 36, 218–229. doi: 10.17224/EnergAgric.2021v36n2p218-229

Martins, J. T., Rasmussem, J., Eriksen, J., Arf, O., Notaris, C., and Moretti, L. G. (2022). Biological N fixation activity in soybean can be estimated based on nodule dry

weight and is increased by additional inoculation. *Rhizosphere* 24, 1–6. doi: 10.1016/j.rhisph.2022.100589

Matoso, S. C. G., and Kusdra, J. F. (2014). Nodulação e crescimento do feijoeiro em resposta à aplicação de molibdênio e inoculante rizobiano. *Rev. Bras. Eng. Agricola e Ambient.* 18, 567–573. doi: 10.1590/S1415-43662014000600001

McCullough, H. (1967). The determination of ammonia in whole blood by a direct colormetric method. *Clin. Chim. Acta* 17, 297–304. doi: 10.1016/0009-8981(67)90133-7

Melo, T. M., Bottlinger, M., Schulz, E., Leandro, W. M., Aguiar Filho, A. M., Wang, H., et al. (2018). Plant and soil responses to hydrothermally converted sewage sludge (sewchar). *Chemosphere* 206, 338–348. doi: 10.1016/j.chemosphere.2018.04.178

Moraes, A., Carvalho, P. C. F., Anghinoni, I., Lustosa, S. B. C., Costa, S. E. V. G. A., and Kunrath, T. R. (2014). Integrated crop–livestock systems in the Brazilian subtropics. *Eur. J. Agron.* 57, 4–9. doi: 10.1016/j.eja.2013.10.004

Moretti, S. M. L., Bertoncini, E. I., and Abreu-Junior, C. H. (2015). Decomposição de lodo de esgoto e composto de lodo de esgoto em nitossolo háplico. *Rev. Bras. Cienc. Solo* 39, 1796–1805. doi: 10.1590/01000683rbcs20150082

Murray, R., Tien, Y.-C., Scott, A., and Topp, E. (2019). The impact of municipal sewage sludge stabilization processes on the abundance, field persistence, and transmission of antibiotic resistant bacteria and antibiotic resistance genes to vegetables at harvest. *Sci. Total Environ.* 651, 1680–1687. doi: 10.1016/j.scitotenv.2018.10.030

Nakao, A. H. (2015). *Composto orgânico de agroindústrias na produção de feijão de inverno e milho no sistema plantio direto* (Ilha Solteira: [Universidade Estadual Paulista]: Faculdade de Engenharia de Ilha Solteira).

Nascimento, A. L., Souza, A. J., Oliveira, F. C., Coscione, A. R., Viana, D. G., and Regitano, J. B. (2020). Chemical attributes of sewage sludges: Relationships to sources and treatments, and implications for sludge usage in agriculture. *J. Clean. Prod.* 258, 120746. doi: 10.1016/j.jclepro.2020.120746

Nogueira, T. A. R., Franco, A., He, Z., Braga, V. S., Firme, L. P., and Abreu-Junior, C. H. (2013). Short-term usage of sewage sludge as organic fertilizer to sugarcane in a tropical soil bears little threat of heavy metal contamination. *J. Environ. Manage.* 114, 168–177. doi: 10.1016/j.jenvman.2012.09.012

Pacheco, L. P., Barbosa, J. M., Leandro, W. M., MaChado, P. L. O. A., Assis, R. L., Madari, B. E., et al. (2011). Produção e ciclagem de nutrientes por plantas de cobertura nas culturas de arroz de terras altas e de soja. *Rev. Bras. Cienc. Solo* 35, 1787–1799. doi: 10.1590/S0100-06832011000500033

Pacheco, R. S., Boddey, R. M., Alves, B. J. R., Straliotto, R., and Araújo, A. P. (2017). Growth patterns of common bean cultivars affect the'B'value required to quantify biological N_2 fixation using the ^{15}N natural abundance technique. *Plant Soil* 419, 293–304. doi: 10.1007/s11104-017-3331-9

Prates, A. R., Coscione, A. R., Teixeira Filho, M. C. M., Miranda, B. G., Arf, O., Abreu-Junior, C. H., et al. (2020). Composted sewage sludge enhances soybean production and agronomic performance in naturally infertile soils (*Cerrado* Region, Brazil). *Agronomy* 10, 1677. doi: 10.3390/agronomy10111677

Prates, A. R., Kawakami, K. C., Coscione, A. R., Teixeira Filho, M. C. M., Arf, O., Abreu-Junior, C. H., et al. (2022). Composted sewage sludge sustains high maize productivity on an infertile Oxisol in the Brazilian Cerrado. *Land* 11, 1–13. doi: 10.3390/land11081246

Price, G. W., Astatkie, T., Gillis, J. D., and Liu, K. (2015). Long-term influences on nitrogen dynamics and pH in an acidic sandy soil after single and multi-year applications of alkaline treated biosolids. *Agric. Ecosyst. Environ.* 208, 1–11. doi: 10.1016/j.agee.2015.04.010

Radin, J. W. (1974). Distribution and development of nitrate reductase activity in germinating cotton seedlings. *Plant Physiol.* 53, 458–463. doi: 10.1104/pp.53.3.458

Ragagnin, V. A., Júnior, S., Dias, D. S., Braga, W. F., and Nogueira, P. D. M. (2013). Growth and nodulation of soybean plants fertilized with poultry litter. *Ciênc. e Agrotecnologia* 37, 17–24. doi: 10.1590/S1413-70542013000100002

Raheem, A., Sikarwar, V. S., He, J., Dastyar, W., Dionysiou, D. D., Wang, W., et al. (2018). Opportunities and challenges in sustainable treatment and resource reuse of sewage sludge: A review. *Chem. Eng. J.* 337, 616–641. doi: 10.1016/j.cej.2017.12.149

Raij, B., Andrande, J. C., Cantarella, H., and Guaggio, J. A. (2001). *Análise Química para Avaliação da Fertilidade de Solos Tropicais. 1st ed* (Campinas: Instituto Agronômico de Campinas).

Raij, B., Cantarella, H., Quaggio, J. A., and Furlani, A. M. C. (1997). *Recomendações de Adubação e Calagem Para o Estado de São Paulo. 2nd ed* (Campinas: Instituto Agronômico de Campinas).

R Core Team (2019) *R: A language and environment for statistical computing* (Vienna: R Foundation for Statistical Computing). Available at: https://www.R-project.org/ (Accessed 20 July 2023).

Rebah, F. B., Prévost, D., Yezza, A., and Tyagi, R. D. (2007). Agroindustrial waste materials and wastewater sludge for rhizobial inoculant production: A review. *Biores. Technol.* 98, 3535–3546. doi: 10.1016/j.biortech.2006.11.066

Rennenberg, H., Wildhagen, H., and Ehlting, B. (2010). Nitrogen nutrition of poplar trees. *Plant Biol.* 12, 275–291. doi: 10.1111/j.1438-8677.2009.00309.x

Rigby, H., Clarke, B. O., Pritchard, D. L., Meehan, B., Beshah, F., Smith, S. R., et al. (2016). A critical review of nitrogen mineralization in biosolids-amended soil, the associated fertilizer value for crop production and potencial for emissions to the environment. *Sci Tot. Environ.* 541, 1310–1338. doi: 10.1016/j.scitotenv.2015.08.089

Sabundjian, M. T., Arf, O., Meirelles, F. C., Nascimento, V., Kaneko, F. H., and Tarumoto, M. B. (2016). Fertilização nitrogenada no desempenho agronômico do feijoeiro de inverno em sucessão a gramíneas de verão. *Rev. Ciências Agrárias* 59, 152–161. doi: 10.4322/rca.2203

Sabundjian, M. T., Arf, O., Kaneko, F. H., and Ferreira, J. P. (2013). Nitrogen fertilization on bean plants in succession to single and intercropped cultivation of corn and Urochloa ruziziensis. *Research Agropec. Trop.* 43, 292–299. doi: 10.1590/S1983-40632013000300007

Santos, L. Z. H., Myrna, S. O., Wenndy, L. W., Andrea, V. R., and Manuel, G. P. J. (2011). Effects of compost made with sludge and organic residues on bean (*Phaseolus vulgaris* L.) crop and arbuscular mycorrhizal fungi density. *Afr. J. Agric. Res.* 6, 1580–1585. doi: 10.5897/AJAR10.1132

Sharma, B., Sarkar, A., Singh, P., and Singh, R. P. (2017). Agricultural utilization of biosolids: A review on potential effects on soil and plant grown. *Waste Manage* 64, 117–132. doi: 10.1016/j.wasman.2017.03.002

Shearer, G., and Kohl, D. H. (1986). N_2 -fixation in field settings: estimations based on natural ^{15}N abundance. *Aust. J. Plant Physiol.* 13, 699–756. doi: 10.1071/PP9860699

Silva, R. D. S., Jalal, A., Nascimento, R. E. N., Elias, N. C., Kawakami, K. C., Abreu-Junior, C. H., et al. (2022a). Composted sewage sludge application reduces mineral fertilization requirements and improves soil fertility in sugarcane seedling nurseries. *Sustainability* 14, 4684. doi: 10.3390/su14084684

Silva, R. D. S., Jalal, A., Nascimento, R. E., Elias, N. C., Kawakami, K. C., Abreu-Junior, C. H., et al. (2022b). Composted sewage sludge application in a sugarcane seedling nursery: crop nutritional status, productivity, and technological quality implications. *Sustainability* 14, 4682. doi: 10.3390/su14084682

Soil Survey Staff (2014). "Keys to soil taxonomy," in *USDA, twelfth ed* (Washington, DC: Natural Resources Conservation Service).

Souza, C. A., Reis Junior, F. B., Mendes, I. C., Lemainski, J., and Silva, J. E. (2009). Lodo de esgoto em atributos biológicos do solo e na nodulação e produção de soja. Pesqui. *Agropecu. Bras.* 44, 1319–1327. doi: 10.1590/S0100-204X2009001000016

Swift, R. S. (1996). "Organic matter characterization, in: Soil Sciense Society of America and American Society of Agronomy," in *Methods of Soil Analysis* (Madison), 1011–1069.

Tanaka, K. S., Crusciol, C. A. C., Soratto, R. P., Momesso, L., Costa, C. H. M., Franzluebbers, A. J., et al. (2019). Nutrients released by *Urochloa* cover crops prior to soybean. *Nutr. Cycling Agroecosyst* 113, 267–281. doi: 10.1007/s10705-019-09980-5

Teixeira, P. C., Donagemma, G. K., Fontana, A., and Teixeira, W. G. (2017). *Manual de Métodos de Análise de Solo. 3rd ed* (Brasília: Embrapa Informação Tecnológica).

Teixeira, M. B., Loss, A., Pereira, M. G., and Pimentel, C. (2011). Decomposição e liberação de nutrientes da parte aérea de plantas de milheto e sorgo. *Rev. Bras. Cienc. Solo* 35, 867–876. doi: 10.1590/S0100-06832011000300021

Torres, J. L. R., Pereira, M. G., and Fabian, A. J. (2008). Produção de fitomassa por plantas de cobertura e mineralização de sues resíduos em plantio direto. *Pesq. Agropec. Bras.* 43, 421–428. doi: 10.1590/S0100-204X2008000300018

Vendruscolo, E. P., Leal, A. J. F., Souza, E. J., and Souto Filho, S. N. (2016). Atributos químicos de solo degradado em função da adoção de biochar, culturas de cobertura e residual da aplicação de lodo de esgoto. *Rev. Cienc. Agrar.* 59, 235–242. doi: 10.4322/rca.2161ARTIGO

Vieira, R. F. (2017). *Ciclo do Nitrogênio em Sistemas Agrícolas* (Embrapa: Brasília).

Vogels, G. D., and van der Drift, C. (1970). Differential analysis of glyphosate derivatives. *Analytical Biochem.* 33, 143–157. doi: 10.1016/0003-2697(70)90448-3

Wang, M., Awasthi, M., Wang, Q., Chem, H., Ren, X., Zhao, J., et al. (2017a). Comparison of additives amendment for mitigation of greenhouse gases and ammonia emission during sewage sludge co-composting based on correlation analysis. *Biores. Technol.* 243, 520–527. doi: 10.1016/j.biortech.2017.06.158

Wang, Y., Lu, J., Ren, T., Hussain, S., Guo, C., Wang, S., et al. (2017b). Effects of nitrogen and tiller type on grain yield and physiological responses in rice. *AoB Plants* 9, 1–14. doi: 10.1093/aobpla/plx012

Wijesekara, H., Bolan, N. S., Thangavel, R., Seshadri, B., Surapaneni, A., Saint, C., et al. (2017). The impact of biosolids application on organic carbon and carbon dioxide fluxes in soil. *Chemosphere* 189, 565–573. doi: 10.1016/j.chemosphere.2017.09.090

Witte, C. P. (2011). Urea metabolism in plants. *Plant Sci.* 180, 431–438. doi: 10.1016/j.plantsci.2010.11.010

Yemm, E. W., and Cocking, E. C. (1955). The determination of amino acids by ninhydrin. *Analyst* 80, 209–213. doi: 10.1039/an9558000209

Yuruk, A., and Bozkurt, M. A. (2006). Heavy metal accumulation in different organs of plants grown under high sewage sludge rates. *Fresen. Environ. Bull.* 15, 107–112.

Zuba Junio, G. R., Sampaio, R. A., Fernandes, L. A., Pegoraro, R. F., Maia, V. M., Cardoso, P. H. S., et al. (2019). Content of heavy metals in soil and in pineapple fertilized with sewage sludge. *J. Agric. Sci.* 11, 281–292. doi: 10.5539/jas.v11n9p281

frontiers | Frontiers in Plant Science

TYPE Review
PUBLISHED 27 October 2023
DOI 10.3389/fpls.2023.1277510

OPEN ACCESS

EDITED BY
Fahad Shafiq,
Government College University, Lahore, Pakistan

REVIEWED BY
Rishikesh Singh,
Panjab University, India
Milan Skalicky,
Czech University of Life Sciences Prague, Czechia
Mir Muhammad Nizamani,
Guizhou University, China

*CORRESPONDENCE
Hailong Shen
shenhl-cf@nefu.edu.cn
Peng Zhang
zhangpeng@nefu.edu.cn

RECEIVED 14 August 2023
ACCEPTED 16 October 2023
PUBLISHED 27 October 2023

CITATION
Saha S, Huang L, Khoso MA, Wu H, Han D, Ma X, Poudel TR, Li B, Zhu M, Lan Q, Sakib N, Wei R, Islam MZ, Zhang P and Shen H (2023) Fine root decomposition in forest ecosystems: an ecological perspective.
Front. Plant Sci. 14:1277510.
doi: 10.3389/fpls.2023.1277510

Fine root decomposition in forest ecosystems: an ecological perspective

Sudipta Saha[1], Lei Huang[1], Muneer Ahmed Khoso[2], Haibo Wu[1,3], Donghui Han[1], Xiao Ma[1], Tika Ram Poudel[4], Bei Li[1], Meiru Zhu[1], Qiurui Lan[1], Nazmus Sakib[1], Ruxiao Wei[1], Md. Zahirul Islam[3], Peng Zhang[1,3]* and Hailong Shen[1,5]*

[1]College of Forestry, Northeast Forestry University, Harbin, China, [2]Key Laboratory of Saline-Alkali Vegetation Ecology Restoration, Ministry of Education, Department of Life Science, Northeast Forestry University, Harbin, China, [3]Key Laboratory of Sustainable Forest Ecosystem Management, Ministry of Education, Northeast Forestry University, Harbin, China, [4]Feline Research Center of National Forestry and Grassland Administration, College of Wildlife and Protected Area, Northeast Forestry University, Harbin, China, [5]State Forestry and Grassland Administration Engineering Technology Research Center of Korean Pine, Harbin, China

Fine root decomposition is a physio-biochemical activity that is critical to the global carbon cycle (C) in forest ecosystems. It is crucial to investigate the mechanisms and factors that control fine root decomposition in forest ecosystems to understand their system-level carbon balance. This process can be influenced by several abiotic (e.g., mean annual temperature, mean annual precipitation, site elevation, stand age, salinity, soil pH) and biotic (e.g., microorganism, substrate quality) variables. Comparing decomposition rates within sites reveals positive impacts of nitrogen and phosphorus concentrations and negative effects of lignin concentration. Nevertheless, estimating the actual fine root breakdown is difficult due to inadequate methods, anthropogenic activities, and the impact of climate change. Herein, we propose that how fine root substrate and soil physiochemical characteristics interact with soil microorganisms to influence fine root decomposition. This review summarized the elements that influence this process, as well as the research methods used to investigate it. There is also need to study the influence of annual and seasonal changes affecting fine root decomposition. This cumulative evidence will provide information on temporal and spatial dynamics of forest ecosystems, and will determine how logging and reforestation affect fine root decomposition.

KEYWORDS

climatic factors, decomposition, forest ecosystem, fine root, microorganism, physio-biochemical activity

1 Introduction

While plant litter decomposition in terrestrial systems is one of the largest annual fluxes in global carbon (C) and nutrient cycling, the role of fine root traits relative to above-ground litter is inadequately understood (See et al., 2019). Every year, a massive amount of organic matter enters the decomposition cycle, mostly in the form of dead plant matter. When a plant loses its leaves, branches, or small roots, organic debris builds up on the forest floor, where these materials becomes a vital resource for soil organisms (Findlay, 2021). Because of foliar litters abundance and its relatively high nutrient content, it has received disproportionate attention in forest litter decomposition studies (Zhou et al., 2020).

In contrast, while researchers initially paid little attention to fine roots (which make most underground litter), research is now clarifying the important of these roots to terrestrial ecosystems (Cheng et al., 2022). Fine roots are essential to the below-ground forest biomass and contribute substantially to the soils organic matter (Hayashi et al., 2023). Understanding fine root characteristics is necessary to describe forest ecosystem C and nitrogen (N) cycles (Zhu et al., 2021). Responses by a terrestrial ecosystem to changes in its surrounding environment can be seen in the decay dynamics of fine roots, which also carry water and nutrients and perform tasks below the ground level (Cheng et al., 2022). However, in fine root decomposition research, their chemical makeup, turnover rates, and interactions with decomposer species have not been fully examined.

Fine root turnover contributes from 14-27% of net primary production (NPP) globally (Mccormack et al., 2015) and is thought to account for 33% of annual forest litter inputs and 48% of the inputs in grasslands (Freschet et al., 2017). Historically, root diameter has been used to categorize it as 'fine' or 'coarse,', with the former having a diameter of ≤2mm and the latter having a diameter >2mm (Berg and Mcclaugherty, 2020). Root litter input is highly variable across ecosystems, but in at least some it contributes the same amount of organic matter and nutrients to the soil as does foliar litter (Prescott and Grayston, 2023). Rine root death and decomposition represent a major C cost to plants, and is a potential soil C sink (Chou et al., 2022).

Fine root biomass, and its nutrient contents and rate of decomposition, can be influenced by a number of abiotic and biotic variables (Zhang et al., 2021). When organic matter is decomposed by biotic microorganisms like bacteria and fungi, more complex molecules are converted into simpler forms (Islam et al., 2022). Due to their recalcitrant character, roots with high levels of lignin (L) and secondary chemicals degrade more slowly (Phillips et al., 2023). By decomposing root tissues and promoting microbial activity in the microenvironment they create, mycorrhizal fungi and soil-dwelling biota also have an impact on decomposition (Wu et al., 2023). Microbial activity, enzyme function, and decomposition rates are affected by abiotic factors such as temperature, moisture, oxygen, N, phosphorus (P), and soil texture (Lull et al., 2023). While nutrient-rich soils promote faster decomposition due to higher biomass, well-aerated soils promote effective decomposition (Abdul Rahman et al., 2021). Understanding these factors is essential for forecasting how land use and environmental changes will affect C and nutrients cycles in terrestrial ecosystems.

In forests, tree species and functional groups differ greatly in their root characteristics (Herzog et al., 2019). The fine root biomass of boreal forests has an inverse relation with soil fertility, but has a positive association with mean annual temperature (MAT) and mean annual precipitation (MAP), and stand age (Peng and Chen, 2021). The fine root biomass of temperate forests increases with site elevation, and with higher MAT (Gao et al., 2021). Climate and soil nutrients are also linked to nutrient concentrations and fine roots contents in forest ecosystems (Pandey et al., 2023). Sometimes, the nutrient amounts released by fine roots decays exceeds that released by the decomposition of leaf residue, and a significant portion of the net primary productivity is allocated to fine roots (Yuan and Chen, 2010).

Mycorrhizal associations, which improve tree nutrition, stress tolerance, and disease protection, also occur on the network formed by fine roots (Tedersoo et al., 2020). Recent research on the function and nutrition of saprophytic fungi has led to several breakthroughs. However, how and why saprophytic fungi help break down fine roots has been infrequently addressed (Gray and Kernaghan, 2020). Recent research has revealed that, in addition to substrate quality, soil microorganisms have a significant impact on fine root decomposition (Fu et al., 2021). Additionally, the nutrient quality of litter substrate affects the growth status of saprophytic fungi, which in turn affects their abundance and diversity (Dai et al., 2021).

Moreover, the most important factor in determining how fine roots decompose depends on the root's initial chemical characteristics (Jing et al., 2019). Thinner fine roots (0.5-1.0 mm diameter) decompose more quickly than thicker fine roots (1.0 mm diameter), possibly because the former have higher N concentration and lower C to N (C/N) ratio, which are favorable for microorganism decomposition and utilization (Lin et al., 2011). The rate of fine root breakdown may also depend on the concentrations of structural carbohydrates and non-structural carbohydrates (Zhai et al., 2023). Small molecules like glucose and starch are easy for microorganisms to break down, while macromolecules like L and cellulose can only be broken down by certain types of bacteria (Hemati et al., 2022).

For instance, microorganisms like white rot fungi (WRF) and brown rot fungi (BRF) produce ligninolytic enzymes that break down L (Theradimani and Ramamoorthy, 2022). Additionally, by altering plant histochemistry, the effect of soil nutrient availability on decomposition is more likely to indirectly (rather than directly) affect root decomposition rate (Jiang and Liang, 2022). Fertilizers applied only for a short periods can boost root detritus decomposition (thereby encouraging N release in soils for plant uptake) and contribute to long-term soil C accumulation through either additional C inputs from manures or N-induced effects on microbial activity (Fornara et al., 2020).

Furthermore, fine roots turnovers is a significant route for the transport of C and nutrients from plants to soils (Wang et al., 2020a). However, current difficulties with measuring fine root decomposition rate prevents us from precisely quantifying the scale of this activity (Sun et al., 2021). The most common

approaches to assessing fine root decomposition rates use litterbags or intact cores, through their methodological efficacies have not been critically assessed (Li et al., 2022a). Litterbags and soil cores may affect the rate of decomposition and microbial activity because they separate litter from its ecosystem and may thus give misleading results about decomposition dynamics (Dornbush et al., 2002; Wu et al., 2022). Accurate total fine root decomposition measurements provide insight into subsurface C cycling processes and reduces uncertainty in soil C flux estimates. Specifically in global budgets and climate change mitigation efforts, fine root decomposition processes offer a comprehensive perspective of below-ground C dynamics, boosting soil C flow projections and enhancing C cycle management in terrestrial ecosystems (Huang et al., 2022).

Fine roots, which make up the vast majority of underground litter, are essential to terrestrial ecosystems due to their roles in redistributing water and nutrients, performing important below-ground functions, and making considerable contributions to forest ecosystem C and N cycles. Understanding fine root properties is crucial to describing forest environment C and N cycles. The biomass, nutritional content, and decomposition rate of fine roots are influenced by a variety of abiotic and biotic variables. Forecasting how changes in land use and the environment will affect cycling of C and nutrients in terrestrial ecosystems requires understanding these factors. The availability of soil nutrients can indirectly influence decomposition rates, and sparingly supplied fertilizers may hasten root debris decomposition and increase soil C levels. Accurate measurements of total fine root decomposition reduce uncertainty in soil C flux estimations and shed light on subsurface C cycling processes. Herein, we highlight the fine root decomposition process and the elements influencing that process reference for below-ground C cycle research.

2 Fine roots

Fine roots (≤2 mm diameter) are the plants major water and nutrient uptake channels (Finér et al., 2019). They actively interface with the environment play key roles in terrestrial ecosystem processes, and make up 33% of the world's annual NPP (Li et al., 2019). Fine roots components can be divided into long-lived transport fine roots (TFRs) and short-lived absorptive fine roots (AFRs) (Figure 1) (Huang et al., 2023). TFRs (root orders 4 and 5) help with long-distance transport and hydraulic conductivity by moving water and nutrients from the soil to above-ground plant components. The surface area for nutrient absorption and nutrient uptake efficiency are increased by AFRs (root orders 1-3), which are finely branched and coated in root hairs (Mccormack et al., 2015; Kou et al., 2018). Plant growth and survival are guaranteed by this division of labor, which enables plants to efficiently acquire nutrients and water while preserving structural integrity (Kou et al., 2018).

Fine root activity has the potential to alter soil physical, chemical, and biological characteristics, which can impact both individual plants and entire ecosystems (Mccormack et al., 2015). For example, as fine roots grow and proliferate, they create macropores and pathways that improve the soil's structure and ability to hold air. These changes facilitate soil microbial mobility, enhance water infiltration, and reduce soil compaction (Wendel et al., 2022). Exudation of organic substances by fine roots (e.g., sugars, organic acids) also affects soil pH, availability of nutrients, and microbial activity. These modifications can improve N cycle processes and provide a more favorable environment for helpful soil bacteria (Keiluweit et al., 2015).

In addition, fine roots are essential to the soil C sequestration process and play crucial roles in nutrient cycling (Pandey et al., 2023). Because of the high turnover rate, the quantity of C and nutrients that are returned to the soil through fine roots is comparable to or even greater than, that which is returned through litter (Hu et al., 2020). Fine roots create a matrix that captures and stabilizes organic matter, lowering its susceptibility to quick decomposition, and thus offering physical protection for soil organic C (Waring et al., 2020).

Forest succession is likely to influence fine root decomposition, which is an important process for nutrient intake and C exchange in terrestrial ecosystems (Fu et al., 2021). Lower L contents and nutrient concentrations in early forest successional phases leads to increased decomposition rates (Morffi-Mestre et al., 2023). Slower decomposition rates are caused by changes in the fine root characteristics of old forests. Rapid decomposition releases nutrients for ecosystem productivity, but also alters nutrient cycle dynamics. Slower decomposition in mature forests helps retain nutrients, fostering conservation and long-term stability (Bhattarai et al., 2022). The world's fine root P pool is 4.4×10^7 Mg and its fine root N pool is one-seventh of the total terrestrial vegetation (Jackson et al., 1997). Thus, as a significant source of root bioenergy, small, quickly decomposing plant fine roots (<2 mm diameter) are crucial to forest nutrients cycling (Rodtassana and Tanner, 2018). Understanding these processes is crucial for sustaining and restoring forest health, while controlling nutrient cycling in shifting landscapes, through ecosystem management (Rai, 2022).

3 Fine root decomposition

Fine-root decomposition is a material exchange process with the environment that involves soil biological metabolism and the absorption and release of chemical elements as a result of soil leaching and breakdown (He et al., 2019). Fine root decomposition regulates nutrient release, carbon dioxide (CO_2) emission, and soil organic matter (SOM) synthesis in forest ecosystems (Jacobs et al., 2018; Babur and Dindarolu, 2020). In the initial phase of decomposition, environmental factors, such as soil temperature, soil moisture content, and substrate breakdown cause rapid eluviation of carbohydrates and other soluble compounds (He et al., 2019).

Later, biological action dominates the decomposition process, breaking down the soluble components and leaving insoluble molecules (such as L and cellulose) for sluggish microbiological degradation (He et al., 2019). Both bacteria and fungi, which carry out distinct tasks within their respective groups, are microorganisms engaged in the breakdown process (Zhao et al.,

2021a). As early decomposers, bacteria use enzymatic activities to reduce complex organic matter to simpler molecules. In the initial decomposition stages, they serve a crucial role in making organic matter accessible to other organisms. Later decomposition phases are aided by fungi, which are effective at dissolving complex substances like L and cellulose (Bonfante and Genre, 2010). Decomposition dynamics are further influenced by mycorrhizal fungi, which create symbiotic connections with plants and aid nutrient intake (Schädler et al., 2010).

Fine root decomposition may differ at the species level depending on traits related to aspects of the plant economics spectrum like growth form (e.g., woody vs. herbaceous, broadleaf vs. conifer), nutrient acquisition strategy (i.e. mycorrhizal association), leaf lifespan of woody plants (i.e. deciduous vs. evergreen), and herbaceous life cycle (i.e. annual vs. perennial) (See et al., 2019). The main factors affecting fine root decomposition include substrate quality and soil environmental parameters, including soil temperature, humidity, pH, bulk density, and soil microorganisms (Zhang et al., 2019a; Zhang et al., 2019b; Tanikawa et al., 2023). The dynamic structure and function of the microbial community will adapt to the degradation process (Yan et al., 2022). Indeed, through underground root decomposition and nutrient humidification, soil microbial communities enzyme systems contributes to about 90% of forest ecosystem biological cycle (Finzi et al., 2006).

However, significant variation remains unexplained, both worldwide and regionally, as plant tissue breakdown rates are positively associated with MAT and MAP (Santos and Herndon, 2023). Higher precipitation provides moisture, while warmer temperatures increases microbial activity (Wahid et al., 2020). These correlations might differ among environments due to variables like soil quality and litter quality (Hermans et al., 2020). Understanding these relations emphasizes the significance of considering MAT and MAP as significant drivers in C and nutrient cycling, and may aids forecasting fine root decomposition's responses to climate and environmental changes.

In temperate and boreal woodlands, changes in fine root biomass have a considerable impact on N cycling and ecosystem function (Cornejo et al., 2023). Fine root biomass is inversely associated with soil fertility in boreal forests, but positively correlated with MAT, MAP, and stand age (Yuan and Chen, 2010). Fine root biomass increased with site elevation in temperate forests, but declines with MAT (Esser et al., 2012). Fine root biomass changes impact both the ability of boreal forests to store C, and nutrient cycling and availability in temperate woodlands (Meena et al., 2023). Higher fine root biomass can make it easier for plants to get the nutrients they need, which can help them grow and produce more (Gao et al., 2021). However, too much biomass can cause nutrients to become immobile, which can slow plant growth and production (Li et al., 2021). To maintain ecosystem function and nutrient cycling in these forest types, it is essential to understand and manage fine root biomass changes. Fine root degradation processes are shown in Figure 2.

4 Factors affecting fine root decomposition

Terrestrial environments nutrient cycles rely heavily on fine root decomposition (Zhao et al., 2023b). The two primary variables affecting decomposition are climate (Table 1) and fine root chemical properties (Guo et al., 2021). Root decomposition rate is positively associated with both global MAT and MAP (See et al., 2019). How roots' chemical properties affect the decomposition rate also depends, in turn, on root factors. Increases in root N and decreases in root L concentrations both enhance the fine root decomposition rate (Bonanomi et al., 2021). Mycorrhizal symbioses can be formed between more than 90% of all woody

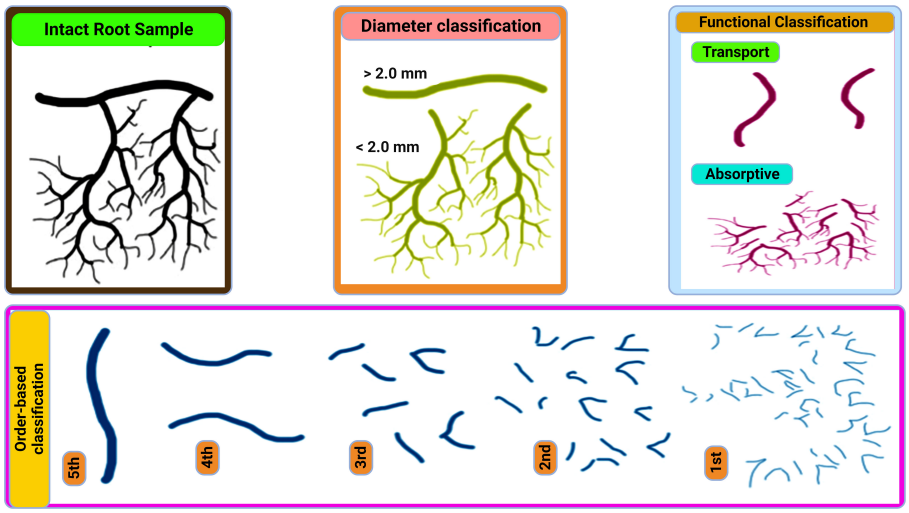

FIGURE 1
Overview of fine-root classification according to McCormack et al. (2015).

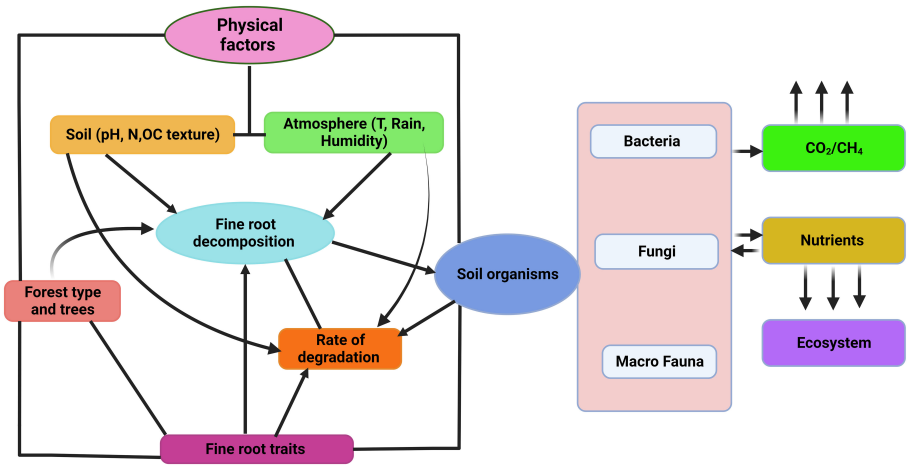

FIGURE 2
Diagrammatic representation of factors affecting fine root decomposition in forest ecosystem.

plants (Chen et al., 2016). Root morphological features and chemical composition may influence the pace of fine root degradation in trees that have either arbuscular mycorrhizal (AM) or ectomycorrhizal (ECM) relations (Chen et al., 2018).

4.1 Climatic factors

Given that temperature and precipitation are key influences of plant growth and decomposer activity, root decomposition is likely to be highly responsive to variations in these two parameters (Bonato et al., 2023; Semeraro et al., 2023). In addition, the availability of nutrients and C sources influences the response of microorganisms to climate change (Sullivan et al., 2019). It is important to consider the general reactions of C stocks in terrestrial ecosystems to changes in climatic condition changes, especially temperature and precipitation, as well as the consequences of synergies of these factors (Fanin et al., 2022b). If the nutrients and effective C sources required for microbial activity are lacking, microorganisms will not sensitive to temperature changes, and their effect on decomposition will be weak (Baldrian et al., 2023). Soil temperature and humidity can alter microbial activities such as fungal hyphae expansion, fruiting body formation, spore germination, and release, and subsurface ecological processes such as root decomposition (Kvasko et al., 2022). However, annual air temperature is also linked to the root decomposition rate globally (Guo et al., 2021). At all sites assessed, the rate of C mineralization decreases with soil depth and time, and increases with temperature (Jia et al., 2022). Fine roots vitality's is reduced by 90% for every 10°C increase in annual average temperature (Eissenstat and Yanai, 2002). The primary causes of this phenomenon are: (1) As temperature rises, root respiration increases (Wang et al., 2021a); (2) Soil N mineralization speeds up (Lakshmi et al., 2020); and (3) Bacterial activity is improved in warm soil (Nottingham et al., 2019).

A primary causes of fine roots concentrations in the surface layer is thought to be the quick decrease in soil temperature of descending layers; the higher surface layer temperature also encourages decomposition and increases soil nutrients, favoring fine root growth (Sihui et al., 2022). Higher soil temperatures not only increases fine root biomass, it leads to their distribution in deeper soil (Jarvi and Burton, 2020). With decreased or increased precipitation, fine root biomass, production, and decomposition increase, decrease, or remain unaltered across plant types and soil depths (Wang et al., 2020b). A plant's capacity for water absorption and transmission is influenced by its fine root diameter and length. Reduced precipitation slows root growth due to nutrient deficits (Yan et al., 2019).

TABLE 1 A comparative table on root decomposition in different climatic zones.

Climatic Zone	Average Temperature (°C)	Moisture Levels	Decomposition Rate	Main Factors	Reference
Tropical	25-30	High	Rapid	Warm temperature, Enough rainfall, Abundant litter input, Microbial diversity, and mycorrhizal association	(Powers et al., 2009; Guerrero-Ramírez et al., 2016; Zhao et al., 2023b)
Temperate	5-20	Moderate to High	Moderate	Seasonal climatic conditions, Coniferous litter, mycorrhizal fungi, Soil invertebrates	(Solly et al., 2014; Zhao et al., 2023a; Zhao et al., 2023b)
Mediterranean	15-25	Moderate to low	Moderate to slow	Dry summer, Mild winter, Root chemistry, and Root order, Specific microbial community	(Zhang and Wang, 2015; Sun et al., 2016; Bonanomi et al., 2021)

According to resource economics theory, fine roots may display a strategy that increases resource acquisition in areas with ample precipitation by lengthening their total root length, specific root length, and specific root area (Weemstra et al., 2017). Reduced precipitation greatly boosts fine root decomposition but has no impact on root production (Zhang et al., 2018b). Additionally, pulse precipitation mechanics encourage microbes to rapidly decompose SOM over short periods, causing significant CO_2 release into the atmosphere (Xu et al., 2020).

After precipitation, the rate of microbial mineralization might rise by a factor of several to 10, leading to increased ecosystem nutrient availability and enhanced microbial activity (Sponseller, 2007). Soil microbial activity peaks as rainwater enters the ground, and because it remains elevated for a longer time, more CO_2 is produced. After reaching peak activity levels, soil bacteria quickly degrade abundant organic substrates, releasing CO_2 in much greater quantities compared with that of tropical forests (Zhaoxia et al., 2021). Increase CO_2 emissions brought on by rainfall is responsible for about 20% of total annual soil CO_2 emissions (Austin et al., 2004). This occurs rainwater introducing new organic matter (e.g., plant remains, litter) to soil, effectively promoting microorganisms activity's (Javed et al., 2022). This increased microbe metabolic activity following entry of fresh organic material increases, the rate at which organic matter decomposes; thus increased microbial activity causes emission of more CO_2 from the soil into the atmosphere (Mehmood et al., 2020). The precipitation-induced priming effect, which also emphasizes how transient environmental events like rainfall can significantly impact annual C emissions from terrestrial settings, demonstrates the dynamic, interrelated nature of ecosystem C cycles.

4.2 Substrate quality

Root substrate quality is among the most important factors of root nutrient cycling (Jing et al., 2019). Different root diameter sizes exhibit notable variations in morphology, physical-chemical characteristics, and stoichiometric ratios as a result of the root branching hierarchy (Han et al., 2019). The rate of element release or immobilization during the root decomposition process may therefore be mediated by diameter-associated variations in root substrate chemistry (Wang et al., 2014). However, previous studies have demonstrated that initial quality primarily mediates root decomposition (See et al., 2019). While fine roots are often nonwoody and ephemeral absorptive roots, coarser roots function as conduits, storage sites, and physical anchors for nutrients. Thus, the breakdown patterns may change based on their functional differences (Guo et al., 2008). Furthermore, fine root decomposition is typically largely slowed by high L concentrations (Da et al., 2017). Early studies comparing root and leaf chemical features showed that roots have higher concentrations of L, and the lower L content in leaves is frequently cited as the main factor for their rapid decomposition (Fujimaki et al., 2008).

Other initial litter substrate qualities, such as N, P, calcium (Ca), and L/N ratios, have been identified as regulators of mass loss and nutrient cycling rates in comparisons of composition among various tree species (e.g., broadleaves vs. conifers, N-fixing vs. non-fixing) (Aponte et al., 2012; Li et al., 2014). These initial traits support the theory, expressed in multiple studies of various ecosystems, that the L: N ratio control litter decomposition alone or in combination with other factors (Berg, 2014). Leaf litter with a low initial L: N ratio produces a higher fraction of slowly dissolving organic matter in late decomposition stages, while N is negatively linked with species-specific decomposition limit values (Berg, 2014; Hobbie, 2015). Thus, higher decomposition rates can be expected from plant litter with lower C/N or L/N ratios.

4.3 Roles of soil properties

Roots can die and disintegrate at any time of year, continually supplying soil nutrients and playing an important role in the biogeochemical cycle (Sardar et al., 2023). Root exudation, mortality, and shedding are other important contributors to soil C pool replenishment (Liu and Liao, 2022). Root decay thus becomes a primary source of subterranean nutrients and organic materials. Root decomposition releases significant volumes of organic matter and nutrients into the soil, where they serve an essential part in reviving and boosting soil fertility, enhancing forest productivity, and ensuring continued, sustainable growth of forest ecosystems (Gulati and Kaur, 2023). Root activities significantly impact both the rate at which organic C is accumulated in the soil and overall C circulation throughout the biosphere (Kowalska et al., 2020). Through interpenetration, entanglement, and cementation, roots can effectively enhance soil structure and stabilize organic C in soils (Dijkstra et al., 2021). The initial phase of fine root decomposition is rapid due to high root quantities of soluble carbohydrates, which are easily lost by leaching and then used by soil microbes, which further speed up root decomposition (Ahmed et al., 2022). Furthermore, accumulation of L and other difficult-to-decompose compounds in fine roots during the late decomposition stage results in a lower root decomposition rate (Wambsganss et al., 2021; Li et al., 2022b). Soil pH also impacts plant enzyme activity's, with mean soil acidity reducing soil microorganism numbers, which slows the organic matter decomposition rate, and thus prevents litter decomposition (Fu et al., 2021; Fanin et al., 2022a; Li et al., 2022b).

The root N-release technique is more complicated. The various stages of root decomposition either release N into the soil or increase its availability. After plant decomposition, soil N concentration increases to 120–150% of its original value (Zhao et al., 2021b). There is also an enrichment-release pattern of soil nutrients, with total soil N concentration lower in the summer and higher in autumn, during fine root decomposition periods (Jiang and Liang, 2022). Others have asserted that during plant litter breakdown, dynamics of N, P, and heavy metal elements (e.g., Fe, Al, Mn, Pb, Cu, and Zn) typically demonstrated enrichment-release mechanisms (Gong et al., 2020; Alon et al., 2021; Bhattarai et al., 2022). N is released during the initial root decomposition stage, slightly increasing soil nitrate nitrogen levels. However, rises in warmth and rainfall have led to more modest increase in ammonium nitrogen content. Temperature and moisture

variations across seasons have major impact on organic N mineralization, nitrification, and denitrification processes, as well as accessible N quantities (Dong et al., 2020; Jiang and Liang, 2022). Application of N or P fertilizer has been shown to increase and develop decomposition rates of fine roots at longer-term treatment sites, whereas the rates of thin roots at the shortest-term sites did not respond significantly; this may be related to soil microbial activity after fertilization, in which N and P limit C sources rather than the opposite (Table 2) (Titus and Malcolm, 1987).

Moreover, Ca^{2+} plays a unique role in the decomposition process. It is not only an essential metabolic component for microorganism growth, Ca^{2+} in the root can also be used by fungi and heterotrophic bacteria to form oxalate, which provides nutrients for microorganism metabolisms in conditions that would be otherwise unfavorable (Grabovich et al., 1995). Although Ca^{2+} concentration influences how quickly root decompose, its role in how quickly fine roots decompose remain unclear.

4.4 Mycorrhizal association

Mycorrhiza plays a significant part in soil C and N cycle, and in root formation in the plant-soil system (Hawkins et al., 2023). AMF colonization is thought to improve aboveground litter decomposition but has little influence on root litter (Figure 3) (Schädler et al., 2010). N is regarded as a key component in the mycorrhizal influence on breakdown processes. Through the effective utilization of decomposition byproducts, AMF can accelerate the pace of litter decomposition and acquire inorganic N produced from the litter during its breakdown (Urcelay et al., 2011).

However, by altering the proportions of soil ammonium-N and nitrate-N, AMF can speed up the process of litter decomposition (Liu et al., 2021). Conifer fine roots deteriorate more slowly than those of broadleaved plants, whereas the fine roots of non-woody plants decay more slowly than those of woody plants (Phillips et al., 2023). In addition, the discovery that fine root of woody ECM and

TABLE 2 Effects of nitrogen deposition on fine root decomposition in forest ecosystems.

Fine root	Research sites	Nitrogen deposition	Nitrogen application frequency (a)	Major finding	Reference
Decomposition	Northern hardwood forest stands, Michigan, USA	N deposition (n = 3); ambient N + 30 kg N ha^{-1} $year^{-1}$ as $NaNO_3$ pellets in six equal applications	20	Decomposition of fine root litter is impeded by N deposition, and SOM contributions from lignin-derived fine root chemicals are raised.	(Argiroff et al., 2019)
	Erguna River Basin, in the northeastern part of Inner Mongolia, China	Control, 10: 0, 7: 3, 5: 5, 3: 7, and 0: 10 (IN: NH_4NO_3, ON:CO $(NH_2)_2$, and $C_2H_5NO_2$)	2	Decomposition rates for fine roots of all species were increased after being exposed to exogenous N in either IN or ON forms.	(Dong et al., 2020)
	In Heilongjiang Province, Northeast China, National nature reserve called Liangshui.	Control, Low-N, Medium-N, and High-N (0, 20, 40, 80 $kgNha^{-1}yr^{-1}$)	3	Root decomposition was slowed down by nitrogen deposition, which also improved soil retention of nutrients and carbon.	(Geng and Jin, 2022)
	Shaanxi Tielongwan Forest Farm Oil pine	0, 30, 60, 90 $kg{\cdot}hm^{-2}{\cdot}a^{-1}$ $(CO(NH_2)_2)$	3	It has a certain stage, and the rate size presents the characteristics of first fast and then slow.	(Gu and Wang, 2017)
Decomposition	Songyugou watershed in the Loess Plateau region, Shaanxi Province, China	0, 3, 6, and 9 g N m^{-2} y^{-1} (NH_4NO_3)	2	The decomposition of fine roots, which is influenced by N deposition, alters the biogeochemical processes of forest ecosystems.	(Jing et al., 2019)
	Jiangxi Tropical Wetland Pine Forest	0, 40, 120 $kg{\cdot}hm^{-2}{\cdot}a^{-1}$ (NH_4Cl and $NaNO_3$)	6	It promotes the absorption of fine root turnover rate but does not accelerate the transport of fine root turnover rate.	(Kou et al., 2018)
	Heilongjiang temperate typical forest ecological system	0, 100 $kg{\cdot}hm^{-2}{\cdot}a^{-1}$ (NH_4NO_3)	9	The quality loss of fine roots reached 30% ~ 50% on day 516, and then the change in mass residue rate was relatively flat.	(Li et al., 2017)
	Northeast Laoshan temperate forest	0, 100 (NH_4NO_3)	4	The initial decomposition rate of tertiary and quaternary roots was increased, but it had an inhibitory effect on primary and secondary roots.	(Sun et al., 2015)
	Northeast Daxing'an Ridge deciduous pine forest	0, 25, 50, 75 $kg{\cdot}hm^{-2}{\cdot}a^{-1}$ (NH_4NO_3)	5	The fine root turnover rate tends to decrease, possibly due to slower subsurface C cycling due to nitrogen deposition.	(Yan et al., 2017)

ericoid species degrade more slowly than those of AM species adds to the growing list of biogeochemical variations between these forest types (Craig et al., 2018; Zhang et al., 2018a). Several isolates of ECM fungi decompose much faster than fine root (*P. resinosa*) seedlings. Depending on the fungus isolate, ECM colonization either does not affect root decomposition or significantly sped root breakdown. Tested isolates include *Srobilomyces floccupus* (SC111), *Cladophialophora* sp. (SC052), *Lactarius oculatus* (SC076), *Amanita rubescens* (SC009), *Suillus intermedius* (SC065), *Amanita pantherina* (SC004), *Amanita citrina* (SC070), *Russula* sp. (SC079), *Amanita muscaria* var. *formosa* (SC059), *Tylopilus felleus* (SC121), and *Amanita brunnescens* (SC007 and SC040) (Koide et al., 2011).

The primary cause of root decomposition is difference in soil water and temperature differences during the initial decomposition stage. Although there are slight differences between fine root decomposition rates of *A. halodendron* at different starting times, other factors, such as variability in soil moisture and its interaction with soil temperature, are likely to have a greater impact on the root decomposition process overall (Luo et al., 2016; Luo et al., 2020). Consistent with those findings, the presence of mycelia hastens fine root decomposition (Pritsch and Garbaye, 2011). Mycelia can increase the activity of soil bacteria by providing them with fresh C, speeding up the breakdown of soil organic carbon (SOC), especially the pool of inert C (Zhang et al., 2018b). Root exudates are thought to play a significant role in litter decomposition and the soil N cycle, with their secondary metabolites inhibiting soil microbes to prevent SOC decomposition (Yin et al., 2014; Zwetsloot et al., 2018).

Additionally, plant-soil feedback processes can impact ecosystem performance because primary metabolite exudation processes are linked to plant nutrition strategies and have substantial effects on SOM decomposition by soil microorganisms (Canarini et al., 2019). Thus, a mechanistic understanding of the function that roots exudation of metabolites and plant-microbe interactions play in nutrient intake and plant community dynamics is essential for developing more efficient root decomposition dynamics in forest ecosystems.

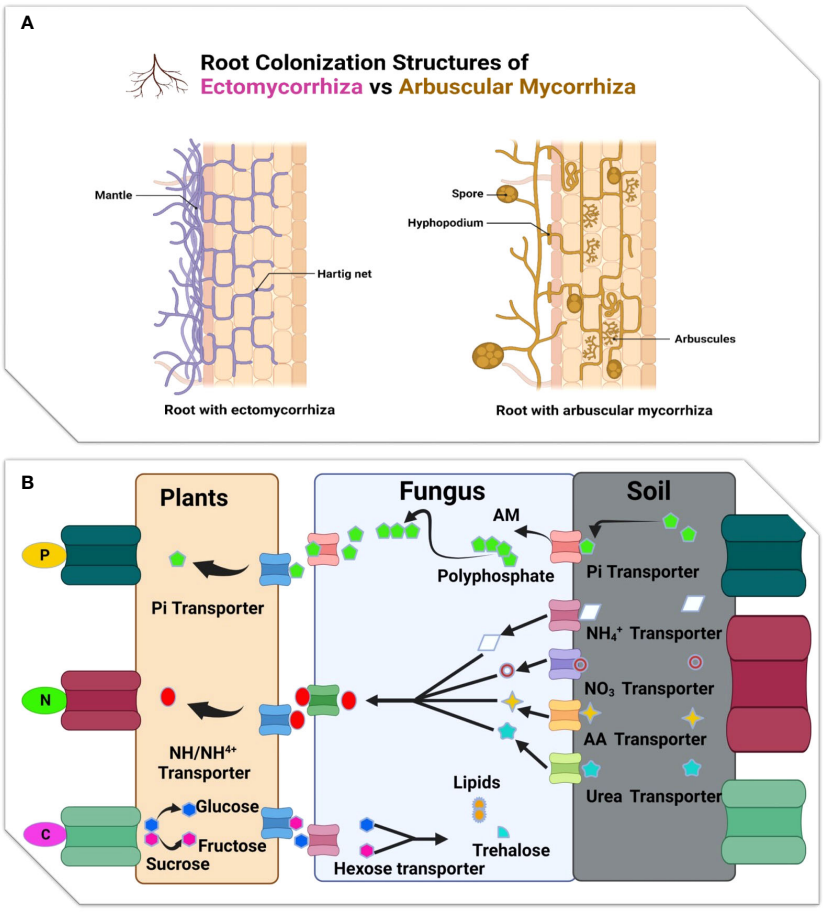

FIGURE 3
(A) Illustration root colonization structure of Ectomycorrhizal and Arbuscular mycorrhiza: While the Hartig net grows around epidermal cells (green), the ectomycorrhizal fungus surrounds the root tip with a thick mantle of tightly packed hyphae. The root tip is often not colonised by arbuscular mycorrhizas. A hyphopodium is produced on the root epidermis by the growth of hyphae from a spore. The formation of arbuscules, or tiny fungal trees, inside inner cortical cells, is the result of intraradical colonisation, which takes place both intracellularly and intercellularly. **(B)** Diagram showing the primary nutrient transfer pathways that take place during the EM and AM symbiosis.

4.4.1 Saprophytic fungi in fine root decomposition

Saprophytic fungi are a crucial component of soil ecosystems; as the primary litter decomposers, they play a key role in nutrient cycling and plant community health (Sudharsan et al., 2023). Roots in forests are primarily decomposed by saprophytic fungi (Purahong et al., 2016; Baldrian, 2017), some of which (i.e., primarily basidiomycetes) have genes encoding enzymes (Riley et al., 2014), which can disrupt plant cell walls during the decomposition of forest fine roots and subsequently affect organic matter breakdown, C fixation, and N/P conversion.

Extracellular oxidative reductionase-laccase, a peroxidase is actively secreted by WRF, allowing it to degrade L (Kellner et al., 2014). Manganese peroxidase (MnP) is the only peroxidase that requires manganese (Mn^{2+}) as a substrate; however, other peroxidases, such as versatile peroxidase (VP), are also applicable. Though Mn^{2+} is oxidized, it is not required for enzymatic activity, such as L peroxylase, and general oxidase. The function of additional peroxidases is unknown, however, MnP, V), and LiPs are L breakdown enzymes (Lundell et al., 2010; Hatakka and Hammel, 2011; Riley et al., 2014); the enzyme system responsible for breaking down cellulose in decomposition is shared by Apiforma and WRF. Soft rot fungi (SRF) don't have LiPs, which helps break down L by releasing laccase. BRF extracellular carboxyl radicals break down the woody cell wall first, releasing small molecular weight oxidants through a Fenton-type chemical reaction called 'random attack', which breaks down substrates and speeds L breakdown (Leonhardt et al., 2019; Venkatesagowda, 2019).

During litter decomposition, WRF and BRF release many organic acids to make an ideal environment for L decomposition (Leonhardt et al., 2019). Copper-ion-dependent polysaccharide monooxygenase can increase the ability of glycoside hydrolases to break down cellulose by oxidative cleavage, increasing other cellulases activities (Long et al., 2022).

5 Degradation patterns of biomass materials in fine root

5.1 Cellulose and hemicellulose

In the forest subsurface, fungi play a crucial role in litter decomposition. To prevent polysaccharides from being degraded by microorganisms, deciduous cell walls are rich in cellulose and hemicellulose (Liers et al., 2010), and only basidiomycetes and a few ascomycetes fungi are capable of decomposing their cell wall structure (Stokland et al., 2012) to separate organic materials. Cellulose is a biopolymer polymer generated by β -1,4 glycosidic linkages linked to glucose that is difficult to disintegrate spontaneously (Klemm et al., 2005). To obtain the energy and nutrients required for mycelium growth and respiratory metabolism, saprophytic fungi 'attack' the cellulose microfibril structure by releasing endoglucanase, which breaks down particular macromolecules into small molecules and makes them soluble substances (Edwards et al., 2008).

The polymer known as hemicellulose is made up of xylan, xylogcan, galactosylmannan, and other similar substances (Edwards et al., 2008). Saprophytic fungi are most active in the early decomposition of hemicellulose; xyloglucan decomposition requires enzymes similar to cellulose cleavage activity, as well as xyloglucan-specific endoglucanases and exoglucanases (Master et al., 2008); Galactomannan is abundant in the cell wall of coniferous plants, the skeleton of which consists of D-mannose residues linked by β-1,4 bonds (Edwards et al., 2008). Fungi can also secrete endomannanase, β-mannosinoside enzymes such as enzymes achieve complete decomposition of them (Master et al., 2008).

5.2 Lignin

The secondary cell wall is coated with L, the second-most ubiquitous biopolymer after cellulose, which gives the wall its structural stability and hydrophobicity (Sreejaya et al., 2022). Syringyl (S), vanillyl, guaiacyl (G), and p-hydroxyphenyl are the three monomeric units making up L. Ls are rich in G-units that form branching Ls, which are more resistant than linear S-rich Ls, and the L matrix in plants is a function of the proportionate abundance of monomers (Jiang et al., 2023). Degradation of L is considered a process that varies among the three primary categories of decomposers, or fungi that cause white rot, soft rot, and brown rot (Floudas, 2021). Although organisms use a wide variety of enzyme pathways for L breakdown, only a subset has been thoroughly characterized. Only the WRF *Phanerochaete chrysosporium* currently has a well-described mechanism for L breakdown (Pandharikar et al., 2022). Several physiological phenomena, including synthesis of the ligninolytic enzyme *P. chrysosporium* system, appear to be induced by N deprivation (Reineke and Schlömann, 2023). Almost all WRF produce MnP, which may lead to the formation of an ecological niche based on Mn as a limiting nutrient (Baker et al., 2019). Although our understanding of *P. chrysosporium's* ligninolytic system exceeds that of most other white-rots, it appears that the systems are species-specific (Hatakka, 2001). In WRF *Ganoderma lucidum* generates MnP in a medium containing poplar wood but not one containing pine wood (D'souza et al., 1999).

Additionally, BRF can drastically alter the L molecule but cannot fully mineralize substance; rather, they primarily degrade the cellulose and hemicellulose components of wood (Devi et al., 2023). Residual L after cellulose decomposition by BRF can resist further breakdown, forming humus, and has been associated with soil C pools, and play an important role in terrestrial C sequestration (Bonner et al., 2019). WRF and BRF are thought to have similar break-down methods. In both cases, it is important for hydroxyl radicals to form and attack wood parts, a process aided by high-oxygen tensions (Hatakka, 2001). Radicals generated by BRF can remove methoxyl groups from L and produce methanol, leaving primarily modified L as residues (Venkatesagowda and Dekker, 2021). Brown-rotted Ls are structurally different from the native version in that they have more phenolic hydroxyl groups and fewer methoxyl groups (Wei et al., 2023). Instead of breaking down L, SRF seek to soften wood

by dissolving the cell walls central lamella. Ascomycetes and deuteromycetes, which make up the majority of SRF, flourish in wood with high moisture content (Philippe et al., 2022).

6 Analytical methods to study fine root decomposition

Our current understanding of elemental fluxes through decaying fine roots has been gleaned from the litterbag technique, which is by far the most widely used method for monitoring fine-root decay (Silver and Miya, 2001). However, whether fine roots are appropriate for litterbags use has not been confirmed (Wu et al., 2022). Fine-root decay rates recorded using litterbags appear to be too low to account for fine-root turnover rates measured with minirhizotrons and other *in situ* methods (Wu et al., 2022). The process of preparing litterbags often includes removing roots from soil and rhizosphere communities, washing and drying them, and frequently incorporating living root material (Li et al., 2022a). It follows that the rates of mass loss and nutrient turnover estimated from litterbag data may be inaccurate.

Additionally, in several significant aspects, the intact-core technique differs from litterbag research. To begin, the initial mass of roots that are included within each core is unknown. This is due to the fact that cores are taken from field soils and are preserved as whole units. Consequently mass loss estimates from undamaged cores are derived from shifts in population means over time, rather than from variations in individual samples, as is possible with litterbags (Li et al., 2022a). Although fine roots naturally senesce, the intact cores that contain both living and dead roots represent the relative decomposition rates of freshly removed live and dead roots (Li et al., 2022a).

Two novel 'balanced hybrid' modeling methods may provide better approach to determining how much fine root decomposition takes place in forests. In this approach, minirhizotrons and sequential soil coring procedures are used to determine how fine root dynamics are affected by the absence of any soil modification. Insights into the dynamic nature of fine root systems were gained through the use of minirhizotrons to estimate fine root turnover and mortality rates. To obtain a more complete picture of the distribution and makeup of fine roots, sequential soil coring was also used to measure the standing biomass and necromass of those roots. A mass balance model was used to calculate the overall amount of fine root decomposition, accounting for important factors like the fine root turnover rate, mortality rate, observed fine root biomass, and necromass. This method enabled a more complete assessment of belowground C cycling and nutrient dynamics in the studied ecosystem by integrating data from minirhizotrons and soil coring, providing a more holistic understanding of fine root dynamics such as growth, mortality, and decomposition (Kou et al., 2018; Li et al., 2020).

7 Future research perspectives

For hundreds of years, partial above ground litter has been the research subject. In contrast, fine roots researches has a recent history, and early studies tended to concentrate on fine root yield and growth distribution rather than their decomposition rate. To fully appreciate the importance of forest ecosystems, we must understand the function of fine roots in nutrient cycling, SOM dynamics, and C sequestration (Wang et al., 2021b). For synthesis, we must also collect extensive data on the variables that control fine root breakdown at different scales. While many studies have examined the role of biotic and abiotic factors in fine root decomposition (Zhang et al., 2021), comparing their results is challenging due to problems with inconsistent research methods (Solly, 2015), like use of net bags with varying pore sizes (Table 3). Few studies have addressed fine root decomposition around the world (Freschet et al., 2021), though not nearly enough to construct regional or global models and even less is known about how root decomposition reacts to global change and anthropogenic activities like forest conversion and forestry management.

There are differences in decomposition patterns and factors controlling fine roots buried underground, despite the chemical composition of fine roots being identical to that of aboveground litter (Wang et al., 2021c). This fact makes improves our ability to study novel research methods and research directions of aboveground litter decomposition. We submit that future studies should priorities the following areas: 1) Investigating fine root decomposition in various ecosystem types to reveal their dynamic changes and the factors influencing their decomposition (Bonanomi et al., 2021); 2) Root decomposition pattern under anthropogenic disturbances and global climate changes and their effects on C sequestration (Panchal et al., 2022); 3) Function of soil organisms in fine root decomposition, as revealed by isotope tracking of fine root decomposition products and the fine root portions consumed by soil microorganisms (Prescott and Vesterdal, 2021); 4) Innovative techniques, such as solid-state 13C nuclear magnetic resonance spectroscopy (13C-NMR spectroscopy), to study fine root decomposition at the molecular level (Chu, 2020); 5) Model development to characterize decomposition processes and forecast decomposition rates based on suitable data sets, and 6) Assess how the diverse community structure of saprophytic fungi breaks down organic matter and recycles nutrients in the forest ecosystem (Zhao et al., 2020). To these ends, the General Unified Nametagging for Fungi (GUNGuild), GeoChip, Network, and other technologies can be leveraged to investigate the ecological functions and driving factors of microbial communities in forest ecosystems, as well as nutritional strategies, functional selections, and interspecific relations of saprophytic fungi.

8 Conclusions

Understanding how fine roots breakdown is important, toward explaining both how C and nutrients cycle, and ecosystem health and sustainable management practices as a whole. The quantities of C and N that are recycled through the development of fine roots and their subsequent decomposition is comparable to or even larger than, the aboveground plants component. Decomposition rate is correlated with the residence period of soil C and, consequently, fine root decomposition is a significant contributor to the global C budget. The production and death of fine roots, and the factors that affect them are important for energy flow and nutrient cycling in forest

TABLE 3 Advantages and Limitation of different root litter decomposition methods.

Methods	Advantages	Limitation	Reference
Litterbags	It is simple and inexpensive to use, can determine the decomposition rate of specific species, and may be used for all forest types.	Decomposer community composition, substrate unrepresentation, and the living root effect are affected by the experimental duration, length, and sampling regime.	(Bonanomi et al., 2021; Li et al., 2022a)
Intact core	Capable of preserving the rhizosphere's integrity.	Limited to monodominant plantation forests, unrepresentative substrates, altered decomposer community composition, no living roots, low temporal precision, and labor-intensive.	(Freschet et al., 2021; Li et al., 2022a)
Mass balance model	Fine root decomposition can be estimated in detail with the help of the mass balance model, which takes into account variables such as turnover, mortality, biomass, and necromass. It compares ecosystems and treatment conditions using long-term breakdown trends and quantitative estimations. It provides a more detailed view of the process by factoring in microbial activity, ambient variables, and root quality. This adaptable model may be used in a wide range of environments to better understand ecological processes.	A mass balance model is intricate and data-intensive, needing precise measurements of elements like biomass and root turnover. In dynamic ecosystems, it may be misleading to rely on assumptions like constant turnover rates and steady-state conditions. For successful modeling, especially in remote or less-researched locations, precise parameter data is essential.	(Li and Lange, 2015; Li et al., 2020)

ecosystems. Yet they are still not well understood largely because the methods used to study them are limited. It is also difficult to summarize this complex process because the rate of fine root decomposition is impacted by a wide variety of variables. Climate (such as MAT, MAP, and altitude), substrate quality, microorganisms (such as saprophytic fungus), and soil features are all important in affecting the rates of litter decomposition. Researchers have yet to establishe a system that simultaneously accounts for all these variables. However, considering the increasing anthropogenic impacts on biogeochemical cycles, research into fine root decomposition is essential. This research examines the elements that contribute to fine root degradation, the degradation pattern of biomass materials, and the techniques used to investigate fine root degradation. Knowledge from this area of inquiry will help us plan for sustainable land use and forestry, and will contribute to our environments long-term productivity and wellness for coming generations.

Author contributions

SS: Conceptualization, Writing – original draft, Writing – review & editing. LH: Writing – original draft. MK: Writing – original draft, Writing – review & editing. HW: Writing – original draft, Writing – review & editing. DH: Writing – original draft, Writing – review & editing. XM: Writing – original draft, Writing – review & editing. TP: Writing – original draft, Writing – review & editing. BL: Writing – original draft, Writing – review & editing. MZ: Writing – original draft, Writing – review & editing. QL: Writing – original draft, Writing – review & editing. NS: Writing – original draft. RW: Writing – original draft. MI: Writing – original draft. PZ: Conceptualization, Writing – original draft, Writing – review & editing. HS: Conceptualization, Supervision, Writing – original draft, Writing – review & editing.

Funding

This work was funded by the National Nature Science Foundation of China (Grant No. 31972950) and the Heilongjiang Touyan Innovation Team Program (Technology Development Team for High-efficient Silviculture of Forest Resources).

Acknowledgments

The authors are grateful to the reviewers, Rishikesh Singh, Milan Skalicky, and Mir Muhammad Nizamani, and an editor, Fahad Shafiq, whose substantiative comments helped to polish the manuscript. We are thankful to Nathan James Roberts, Feline Research Center of National Forestry and Grassland Administration, College of Wildlife and Protected Area, Northeast Forestry University, Harbin, 150040, China, who participated in initial English editing and provided comments on final manuscripts, which were helpful in polishing the final manuscript.

Conflict of interest

The authors declare that the research was conducted in the absence of any commercial or financial relationships that could be construed as a potential conflict of interest.

Publisher's note

References

Abdul Rahman, N. S. N., Abdul Hamid, N. W., and Nadarajah, K. (2021). Effects of abiotic stress on soil microbiome. *Int. J. Mol. Sci.* 22 (16), 9036. doi: 10.3390/ijms22169036

Ahmed, M., Aslam, M. A., Fayyaz-Ul-Hassan,, Hayat, R., and Ahmad, S. (2022). Nutrient dynamics and the role of modeling. *Building Climate Resilience Agric.* 297–316 doi: 10.1007/978-3-030-79408-8_19

Alon, M., Dovrat, G., Masci, T., and Sheffer, E. (2021). Soil nitrogen regulates symbiotic nitrogen fixation in a legume shrub but does not accumulate under it. *Ecosphere.* 12 (12), e03843. doi: 10.1002/ecs2.3843

Aponte, C., García, L. V., and Maraón, T. (2012). Tree species effect on litter decomposition and nutrient release in mediterranean oak forests changes over time. *Ecosystems* 15, 1204–1218. doi: 10.1007/s10021-012-9577-4

Argiroff, W. A., Zak, D. R., Upchurch, R. A., Salley, S. O., and Grandy, A. S. (2019). Anthropogenic N deposition alters soil organic matter biochemistry and microbial communities on decaying fine roots. *Global Change Biol.* 25 (12), 4369–4382. doi: 10.1111/gcb.14770

Austin, A. T., Yahdjian, L., Stark, J. M., Belnap, J., Porporato, A., Norton, U., et al. (2004). Water pulses and biogeochemical cycles in arid and semiarid ecosystems. *Oecologia*. 141, 221–235. doi: 10.1007/s00442-004-1519-1

Babur, E., and Dindarolu, T. (2020). *Seasonal changes of soil organic carbon and microbial biomass carbon in different forest ecosystems*. Environmental factors affecting human health, 1, 1–21.

Baker, P., Tiroumalechetty, A., and Mohan, R. (2019). "Fungal enzymes for bioremediation of xenobiotic compounds," in *Recent advancement in white biotechnology through fungi: volume 3: perspective for sustainable environments*. Eds. A. N. Yadav, S. Singh, S. Mishra and A. Gupta (Cham: Springer International Publishing), 463–489.

Baldrian, P. (2017). Forest microbiome: diversity, complexity and dynamics. *FEMS Microbiol. Rev.* 41 (2), 109–130. doi: 10.1093/femsre/fuw040

Baldrian, P., López-Mondéjar, R., and Kohout, P. (2023). Forest microbiome and global change. *Nat. Rev. Microbiol.* 1–15. doi: 10.1038/s41579-023-00876-4

Berg, B. (2014). Decomposition patterns for foliar litter–a theory for influencing factors. *Soil Biol. Biochem.* 78, 222–232. doi: 10.1016/j.soilbio.2014.08.005

Berg, B., and Mcclaugherty, C. (2020). "Decomposition of root tips, fine roots, and coarse roots," in *Plant litter: decomposition, humus formation, carbon sequestration* (Cham: Springer International Publishing), 189–208.

Bhattarai, K. P., Mandal, T. N., and Gautam, T. P. (2022). Fine root decomposition and nutrient release in two tropical forests of Central Himalaya: a comparative and factor controlling approach. *Trop. Ecol.* 63 (3), 440–452. doi: 10.1007/s42965-022-00231-3

Bonanomi, G., Idbella, M., Zotti, M., Santorufo, L., Motti, R., Maisto, G., et al. (2021). Decomposition and temperature sensitivity of fine root and leaf litter of 43 mediterranean species. *Plant Soil* 464 (1-2), 453–465. doi: 10.1007/s11104-021-04974-1

Bonato, A., Wirth, C., Eisenhauer, N., and Hines, J. (2023). On the phenology of soil organisms: Current knowledge and future steps. *Ecol. Evol.* 13 (4), e10022. doi: 10.1002/ece3.10022

Bonfante, P., and Genre, A. (2010). Mechanisms underlying beneficial plant–fungus interactions in mycorrhizal symbiosis. *Nat. Commun.* 1 (1), 48. doi: 10.1038/ncomms1046

Bonner, M. T. L., Castro, D., Schneider, A. N., Sundstrom, G., Hurry, V., Street, N. R., et al. (2019). Why does nitrogen addition to forest soils inhibit decomposition. *Soil Biol. Biochem.* 137, 107570. doi: 10.1016/j.soilbio.2019.107570

Canarini, A., Kaiser, C., Merchant, A., Richter, A., and Wanek, W. (2019). Root exudation of primary metabolites: mechanisms and their roles in plant responses to environmental stimuli. *Front. Plant Sci.* 10, 157. doi: 10.3389/fpls.2019.00157

Chen, W., Koide, R. T., Adams, T. S., Deforest, J. L., Cheng, L., and Eissenstat, D. M. (2016). Root morphology and mycorrhizal symbioses together shape nutrient foraging strategies of temperate trees. *Proc. Natl. Acad. Sci. United States America* 113 (31), 8741. doi: 10.1073/pnas.1601006113

Chen, W., Koide, R. T., and Eissenstat, D. M. (2018). Nutrient foraging by mycorrhizas: From species functional traits to ecosystem processes. *Funct. Ecol.* 32 (4), 858–869. doi: 10.1111/1365-2435.13041

Cheng, T., Hussain, Z., Li, Y., Yao, C., Li, M., and Huang, Z. (2022). Fine root densities of grasses and perennial sugarcane significantly reduce stream channel erosion in southern China. *J. Environ. Manage.* 316, 115279. doi: 10.1016/j.jenvman.2022.115279

Chou, M.-Q., Lin, W.-J., Lin, C.-W., Wu, H.-H., and Lin, H.-J. (2022). Allometric equations may underestimate the contribution of fine roots to mangrove carbon sequestration. *Sci. Total Environ.* 833, 155032. doi: 10.1016/j.scitotenv.2022.155032

Chu, W. (2020). *Structural characterization of organic matter in oil shales using multiple nuclear magnetic resonance spectroscopic techniques* (Doctoral dissertation, Old Dominion University. ProQuest Dissertations Publishing).

Cornejo, N. S., Becker, J. N., Hemp, A., and Hertel, D. (2023). Effects of land-use change and disturbance on the fine root biomass, dynamics, morphology, and related C and N fluxes to the soil of forest ecosystems at different elevations at Mt. Kilimanjaro (Tanzania). *Oecologia* 201 (4), 1089–1107. doi: 10.1007/s00442-023-05353-6

Craig, M. E., Turner, B. L., Liang, C., Clay, K., Johnson, D. J., and Phillips, R. P. (2018). Tree mycorrhizal type predicts within-site variability in the storage and distribution of soil organic matter. *Global Change Biol.* 24 (8), 3317–3330. doi: 10.1111/gcb.14132

Da, L., Ruimei, C., Zuomin, S., and Weixia, W. (2017). Decomposition of leaves and fine roots in three subtropical plantations in China affected by litter substrate quality and soil microbial community. *Forests* 8 (11), 412–412. doi: 10.3390/f8110412

Dai, Z., Xiong, X., Zhu, H., Xu, H., and Xu, J. (2021). Association of biochar properties with changes in soil bacterial, fungal and fauna communities and nutrient cycling processes. *Biochar* 3, 239–254. doi: 10.1007/s42773-021-00099-x

Devi, K. B., Malakar, R., Kumar, A., Sarma, N., and Jha, D. K. (2023). "Chapter 17 - Ecofriendly utilization of lignocellulosic wastes: mushroom cultivation and value addition," in *Value-addition in agri-food industry waste through enzyme technology*. Eds. M. Kuddus and P. Ramteke (Academic Press), 237–254. doi: 10.1016/B978-0-323-89928-4.00016-X

Dijkstra, F. A., Zhu, B., and Cheng, W. (2021). Root effects on soil organic carbon: a double-edged sword. *New Phytologist.* 230 (1), 60–65. doi: 10.1111/nph.17082

Dong, L., Berg, B., Sun, T., Wang, Z., and Han, X. (2020). Response of fine root decomposition to different forms of N deposition in a temperate grassland. *Soil Biol. Biochem.* 147, 107845. doi: 10.1016/j.soilbio.2020.107845

Dornbush, M. E., Isenhart, T. M., and Raich, J. W. (2002). Quantifying fine-root decomposition: An alternative to buried litterbags. *Ecology* 83 (11), 2985–2990. doi: 10.1890/0012-9658(2002)083[2985:QFRDAA]2.0.CO;2

D'souza, T. M., Merritt, C. S., and Reddy, C. A. (1999). Lignin-modifying enzymes of the white rot basidiomycete Ganoderma lucidum. *Appl. Environ. Microbiol.* 65 (12), 5307–5313. doi: 10.1128/AEM.65.12.5307-5313.1999

Edwards, I. P., Upchurch, R. A., and Zak, D. R. (2008). Isolation of fungal cellobiohydrolase I genes from sporocarps and forest soils by PCR. *Appl. Environ. Microbiol.* 74 (11), 3481–3489. doi: 10.1128/AEM.02893-07

Eissenstat, D. M., and Yanai, R. D. (2002). "Root life span, efficiency, and turnover," in *Plant roots* (CRC Press) 3, 221–238. doi: 10.1201/9780203909423.ch13

Esser, K., Lüttge, U., Beyschlag, W., and Hellwig, F. (2012). "Genetics physiology systematics ecology," in *Progress in botany*, vol. 64. (Springer Science & Business Media). doi: 10.1007/978-3-642-57203-6

Fanin, N., Maxwell, T. L., Altinalmazis-Kondylis, A., Bon, L., Meredieu, C., Jactel, H., et al. (2022a). Effects of mixing tree species and water availability on soil organic carbon stocks are depth dependent in a temperate podzol. *Eur. J. Soil Sci.* 73 (1), e13133. doi: 10.1111/ejss.13133

Fanin, N., Mooshammer, M., Sauvadet, M., Meng, C., Alvarez, G., Bernard, L., et al. (2022b). Soil enzymes in response to climate warming: Mechanisms and feedbacks. *Funct. Ecol.* 36 (6), 1378–1395. doi: 10.1111/1365-2435.14027

Findlay, S. E. (2021). "Organic matter decomposition," in *Fundamentals of ecosystem science* (Elsevier, Academic Press), 81–102. doi: 10.1016/B978-0-12-812762-9.00004-6

Finér, L., Zverev, V., Palviainen, M., Romanis, T., and Kozlov, M. V. (2019). Variation in fine root biomass along a 1000 km long latitudinal climatic gradient in mixed boreal forests of North-East Europe. *For. Ecol. Manage.* 432, 649–655. doi: 10.1016/j.foreco.2018.09.060

Finzi, A. C., Sinsabaugh, R. L., Long, T. M., and Osgood, M. P. (2006). Microbial community responses to atmospheric carbon dioxide enrichment in a warm-temperate forest. *Ecosystems* 9 (2), 215–226. doi: 10.1007/s10021-005-0078-6

Floudas, D. (2021). Evolution of lignin decomposition systems in fungi - ScienceDirect. *Adv. Botanical Res.* 99, 37–76. doi: 10.1016/bs.abr.2021.05.003

Fornara, D. A., Flynn, D., and Caruso, T. (2020). Effects of nutrient fertilization on root decomposition and carbon accumulation in intensively managed grassland soils. *Ecosphere* 11 (4), e03103. doi: 10.1002/ecs2.3103

Freschet, G. T., Pagès, L., Iversen, C., Comas, L., and Mccormack, M. L. (2021). A starting guide to root ecology: strengthening ecological concepts and standardizing root classification, sampling, processing and trait measurements. *New Phytologist* 232 (3), 973–1122. doi: 10.1111/nph.17572

Freschet, G. T., Valverde-Barrantes, O. J., Tucker, C. M., Craine, J. M., Mccormack, M. L., Violle, C., et al. (2017). Climate, soil and plant functional types as drivers of global fine-root trait variation. *J. Ecology.* 105 (5), 1182–1196. doi: 10.1111/1365-2745.12769

Fu, Y., Feng, F., Zhang, X., and Qi, D. (2021). Changes in fine root decomposition of primary Pinus koraiensis forest after clear cutting and restoration succession into secondary broad-leaved forest. *Appl. Soil Ecol.* 158, 103785. doi: 10.1016/j.apsoil.2020.103785

Fujimaki, R., Takeda, H., and Wiwatiwitaya, D. (2008). Fine root decomposition in tropical dry evergreen and dry deciduous forests in Thailand. *J. For. Res.* 13 (6), 338–346. doi: 10.1007/s10310-008-0087-3

Gao, G., Liu, Z., Wang, Y., Wang, S., Ju, C., and Gu, J. (2021). Tamm review: Fine root biomass in the organic (O) horizon in forest ecosystems: Global patterns and controlling factors. *For. Ecol. Manage.* 491, 119208. doi: 10.1016/j.foreco.2021.119208

Geng, P., and Jin, G. (2022). Fine root morphology and chemical responses to N addition depend on root function and soil depth in a Korean pine plantation in Northeast China. *For. Ecol. Manage.* 520, 120407. doi: 10.1016/j.foreco.2022.120407

Gong, X. W., Guo, J. J., Jiang, D. M., Li, X. H., Scholz, F. G., Bucci, S. J., et al. (2020). Contrasts in xylem hydraulics and water use underlie the sorting of different sand-fixing shrub species to early and late stages of dune stabilization. *For. Ecol. Manage.*, 457, 117705. doi: 10.1016/j.foreco.2019.117705

Grabovich, M., Dubinina, G., Churikova, V., Churikov, S., and Korovina, T. (1995). Mechanisms of synthesis and utilization of oxalate inclusions in the colorless sulfur bacterium Macromonas bipunctata. *Microbiol. (New York NY)* 64 (5), 536–542.

Gray, L., and Kernaghan, G. (2020). Fungal succession during the decomposition of ectomycorrhizal fine roots. *Microbial Ecol.* 79 (2), 271–284. doi: 10.1007/s00248-019-01418-3

Gu, L.-C., and Wang, G.-L. (2017). Effects of N addition on carbohydrate contents in different diameter fine roots of Pinus tabuliformis seedlings. *Chin. J. Ecol.* 36 (8), 2184. doi: 10.13292/j.1000-4890.201708.033

Guerrero-Ramírez, N. R., Craven, D., Messier, C., Potvin, C., Turner, B. L., and Handa, I. T. (2016). Root quality and decomposition environment, but not tree species richness, drive root decomposition in tropical forests. *Plant Soil* 404, 125–139. doi: 10.1007/s11104-016-2828-y

Gulati, S., and Kaur, J. (2023). Potential of decomposing leaf litter of Leucaena leucocephala in influencing mycoflora of the soil and its role in increasing soil fertility. *Vegetos*, 1–17. doi: 10.1007/s42535-023-00654-w

Guo, L., Deng, M., Yang, S., Liu, W., Wang, X., Wang, J., et al. (2021). The coordination between leaf and fine root litter decomposition and the difference in their controlling factors. *Global Ecology and Biogeography* 30, 2286–2296. doi: 10.1111/geb.13384

Guo, D., Xia, M., Wei, X., Chang, W., Liu, Y., and Wang, Z. (2008). Anatomical traits associated with absorption and mycorrhizal colonization are linked to root branch order in twenty-three Chinese temperate tree species. *New Phytol.* 180 (3), 673–683. doi: 10.1111/j.1469-8137.2008.02573.x

Han, S. H., Kim, S., Chang, H., Kim, H.-J., Khamzina, A., and Son, Y. (2019). Soil depth- and root diameter-related variations affect root decomposition in temperate pine and oak forests. *J. Plant Ecol.* 12 (5), 871–881. doi: 10.1093/jpe/rtz023

Hatakka, A. (2001). "Biodegradation of lignin," in *humic substances and coal*, vol. 1., 129–180.

Hatakka, A., and Hammel, K. E. (2011). "Fungal biodegradation of lignocelluloses," in *Industrial applications*. Ed. M. Hofrichter (Berlin, Heidelberg: Springer Berlin Heidelberg), 319–340.

Hawkins, H.-J., Cargill, R. I., Van Nuland, M. E., Hagen, S. C., Field, K. J., Sheldrake, M., et al. (2023). Mycorrhizal mycelium as a global carbon pool. *Curr. Biol.* 33 (11), R560–R573. doi: 10.1016/j.cub.2023.02.027

Hayashi, R., Maie, N., Wagai, R., Hirano, Y., Matsuda, Y., Makita, N., et al. (2023). An increase of fine-root biomass in nutrient-poor soils increases soil organic matter but not soil cation exchange capacity. *Plant and Soil.* 482 (1-2), 89–110. doi: 10.1007/s11104-022-05675-z

He, L. X., Jia, Z. Q., Li, Q. X., Feng, L. L., and Yang, K. Y. (2019). Fine-root decomposition characteristics of four typical shrubs in sandy areas of an arid and semiarid alpine region in western China. *Ecol. Evol.* 9 (9), 5407–5419. doi: 10.1002/ece3.5133

Hemati, A., Nazari, M., Asgari Lajayer, B., Smith, D. L., and Astatkie, T. (2022). Lignocellulosics in plant cell wall and their potential biological degradation. *Folia Microbiologica* 67 (5), 671–681. doi: 10.1007/s12223-022-00974-5

Hermans, S. M., Buckley, H. L., Case, B. S., Curran-Cournane, F., Taylor, M., and Lear, G. (2020). Using soil bacterial communities to predict physico-chemical variables and soil quality. *Microbiome* 8, 1–13. doi: 10.1186/s40168-020-00858-1

Herzog, C., Hartmann, M., Frey, B., Stierli, B., Rumpel, C., Buchmann, N., et al. (2019). Microbial succession on decomposing root litter in a drought-prone Scots pine forest. *ISME J.* 13 (9), 2346–2362. doi: 10.1038/s41396-019-0436-6

Hobbie, S. E. (2015). Plant species effects on nutrient cycling: revisiting litter feedbacks. *Trends Ecol. Evol.* 30 (6), 357–363. doi: 10.1016/j.tree.2015.03.015

Hu, Q., Sheng, M., Bai, Y., Jie, Y., and Xiao, H. (2020). Response of C, N, and P stoichiometry characteristics of Broussonetia papyrifera to altitude gradients and soil nutrients in the karst rocky ecosystem, SW China. *Plant Soil* 14), 1–14. doi: 10.1007/s11104-020-04742-7

Huang, C., Weishu, G., and Yong, P. (2022). Remote sensing and forest carbon monitoring—a review of recent progress, challenges and opportunities. *J. Geodesy Geoinformation Sci.* 5 (2), 124–147. doi: 10.11947/j.JGGS.2022.0212

Huang, L., Zhao, R., Zhao, X., Tian, Q., Yue, P., and Liu, F. (2023). Effects of stand condition and root density on fine-root dynamics across root functional groups in a subtropical montane forest. *J. forestry Res.* 34 (3), 665–675. doi: 10.1007/s11676-022-01514-0

Islam, M. R., Singh, B., and Dijkstra, F. A. (2022). Stabilisation of soil organic matter: Interactions between clay and microbes. *Biogeochemistry* 160 (2), 145–158. doi: 10.1007/s10533-022-00956-2

Jackson, R. B., Mooney, H. A., and Schulze, E.-D. (1997). A global budget for fine root biomass, surface area, and nutrient contents. *Proc. Natl. Acad. Sci.* 94 (14), 7362–7366. doi: 10.1073/pnas.94.14.7362

Jacobs, L. M., Sulman, B. N., Brzostek, E. R., Feighery, J. J., and Phillips, R. P. (2018). Interactions among decaying leaf litter, root litter and soil organic matter vary with mycorrhizal type. *J. Ecol.* 106 (2), 502–513. doi: 10.1111/1365-2745.12921

Jarvi, M. P. B., and Burton, A. J. (2020). Root respiration and biomass responses to experimental soil warming vary with root diameter and soil depth. *Plant Soil* 451 (1a2), 435–446. doi: 10.1007/s11104-020-04540-1

Javed, A., Ali, E., Afzal, K. B., Osman, A., and Riaz, S. (2022). Soil fertility: Factors affecting soil fertility, and biodiversity responsible for soil fertility. *Int. J. Plant Anim. Environ. Sci.* 12 (1), 21–33. doi: 10.26502/ijpaes.202129

Jia, B., Jia, L., Mou, X. M., Chen, J., Li, F.-C., Ma, Q.-J., et al. (2022). Shrubification decreases soil organic carbon mineralization and its temperature sensitivity in alpine meadow soils. *Soil Biol. Biochem.* 168, 108651. doi: 10.1016/j.soilbio.2022.108651

Jiang, H., and Liang, Q. (2022). Effects of plant and tree roots decomposition on soil nutrients in an abandoned pyrite mining area in China. *Polish J. Environ. Stud.* 31 (5). doi: 10.15244/pjoes/150423

Jiang, L., Wang, C.-G., Chee, P. L., Qu, C., Fok, A. Z., Yong, F. H., et al. (2023). Strategies for lignin depolymerization and reconstruction towards functional polymers. *Sustain. Energy Fuels* 7 (13), 2953–2973. doi: 10.1039/D3SE00173C

Jing, H., Zhang, P., Li, J., Yao, X., Liu, G., and Wang, G. (2019). Effect of nitrogen addition on the decomposition and release of compounds from fine roots with different diameters: the importance of initial substrate chemistry. *Plant Soil* 438 (1a2), 281–296. doi: 10.1007/s11104-019-04017-w

Keiluweit, M., Bougoure, J. J., Nico, P. S., Pett-Ridge, J., Weber, P. K., and Kleber, M. (2015). Mineral protection of soil carbon counteracted by root exudates. *Nat. Climate Change* 5 (6), 588–595. doi: 10.1038/nclimate2580

Kellner, H., Luis, P., Pecyna, M. J., Barbi, F., Kapturska, D., Krüger, D., et al. (2014). Widespread occurrence of expressed fungal secretory peroxidases in forest soils. *PloS One* 9 (4), e95557. doi: 10.1371/journal.pone.0095557

Klemm, D., Heublein, B., Fink, H. P., and Bohn, A. (2005). Cellulose: fascinating biopolymer and sustainable raw material. *Angewandte Chemie Int. Edition* 44 (22), 3358–3393. doi: 10.1002/anie.200460587

Koide, R. T., Fernandez, C. W., and Peoples, M. S. (2011). Can ectomycorrhizal colonization of Pinus resinosa roots affect their decomposition? *New Phytol.* 191 (2), 508–514. doi: 10.1111/j.1469-8137.2011.03694.x

Kou, L., Jiang, L., Fu, X., Dai, X., Wang, H., and Li, S. (2018). Nitrogen deposition increases root production and turnover but slows root decomposition in Pinus elliottii plantations. *New Phytol.* 218 (4), 1450–1461. doi: 10.1111/nph.15066

Kowalska, A., Pawlewicz, A., Dusza, M., Jaskulak, M., and Grobelak, A. (2020). Plant–soil interactions in soil organic carbon sequestration as a restoration tool - ScienceDirect. *Climate Change Soil Interact.*, 663–688. doi: 10.1016/B978-0-12-818032-7.00023-0

Kvasko, O., Kolomiiets, Y., Buziashvili, A., and Yemets, A. (2022). Biotechnological approaches to increase the bacterial and fungal disease resistance in potato. *Open Agric. J.* 16 (1). doi: 10.2174/18743315-v16-e2210070

Lakshmi, G., Okafor, B. N., and Visconti, D. (2020). "Soil microarthropods and nutrient cycling," in *Environment, climate, plant and vegetation growth*. Eds. S. Fahad, M. Hasanuzzaman, M. Alam, H. Ullah, M. Saeed, I. Ali Khan and M. Adnan (Cham: Springer International Publishing), 453–472.

Leonhardt, S., Hoppe, B., Stengel, E., Noll, L., Moll, J., Bässler, C., et al. (2019). Molecular fungal community and its decomposition activity in sapwood and heartwood of 13 temperate European tree species. *PloS One* 14 (2), e0212120. doi: 10.1371/journal.pone.0212120

Li, Y., Gong, J., Zhang, Z., Shi, J., Zhang, W., and Song, L. (2022b). Grazing directly or indirectly affect shoot and root litter decomposition in different decomposition stage by changing soil properties. *Catena* 209, 105803. doi: 10.1016/j.catena.2021.105803

Li, M., Huang, C., Yang, T., Drosos, M., and Hu, Z. (2019). Role of plant species and soil phosphorus concentrations in determining phosphorus: nutrient stoichiometry in leaves and fine roots. *Plant Soil.* 445, 231–242. doi: 10.1007/s11104-019-04288-3

Li, X., and Lange, H. (2015). A modified soil coring method for measuring fine root production, mortality and decomposition in forests. *Soil Biol. Biochem.* 91, 192–199. doi: 10.1016/j.soilbio.2015.08.015

Li, S., Liu, W. Y., Li, D. W., Li, Z. X., Song, L., Chen, K., et al. (2014). Slower rates of litter decomposition of dominant epiphytes in the canopy than on the forest floor in a subtropical montane forest, southwest China. *Soil Biol. Biochem.* 70, 211–220. doi: 10.1016/j.soilbio.2013.12.031

Li, X., Minick, K. J., Li, T., Williamson, J. C., Gavazzi, M., Mcnulty, S., et al. (2020). An improved method for quantifying total fine root decomposition in plantation forests combining measurements of soil coring and minirhizotrons with a mass balance model. *Tree Physiol.* 40 (10), 1466–1473. doi: 10.1093/treephys/tpaa074

Li, Y., Wang, Z., and Sun, T. (2017). Response of fine root decomposition to long-term nitrogen addition in the temperate forest. *Bull. Botanical Res.* 37 (6), 848–854. doi: 10.7525/j.issn.1673-5102.2017.06.007

Li, X., Zhang, C., Zhang, B., Wu, D., Shi, Y., Zhang, W., et al. (2021). Canopy and understory nitrogen addition have different effects on fine root dynamics in a temperate forest: implications for soil carbon storage. *New Phytol.* 231 (4), 1377–1386. doi: 10.1111/nph.17460

Li, X., Zheng, X., Zhou, Q., Mcnulty, S., and King, J. S. (2022a). Measurements of fine root decomposition rate: Method matters. *Soil Biol. Biochem.* 164, 108482. doi: 10.1016/j.soilbio.2021.108482

Liers, C., Bobeth, C., Pecyna, M., Ullrich, R., and Hofrichter, M. (2010). DyP-like peroxidases of the jelly fungus Auricularia auricula-judae oxidize nonphenolic lignin model compounds and high-redox potential dyes. *Appl. Microbiol. Biotechnol.* 85 (6), 1869–1879. doi: 10.1007/s00253-009-2173-7

Lin, C., Yang, Y., Guo, J., Chen, G., and Xie, J. (2011). Fine root decomposition of evergreen broadleaved and coniferous tree species in mid-subtropical China:dynamics of dry mass, nutrient and organic fractions. *Plant Soil* 338 (1-2), 311–327. doi: 10.1007/s11104-010-0547-3

Liu, C., and Liao, W. (2022). Potassium signaling in plant abiotic responses: Crosstalk with calcium and reactive oxygen species/reactive nitrogen species. *Plant Physiol. Biochem.* 173-), 173. doi: 10.1016/j.plaphy.2022.01.016

Liu, X., Luo, Y., Cheng, L., Hu, H., Wang, Y., and Du, Z. (2021). Effect of root and mycelia on fine root decomposition and release of carbon and nitrogen under Artemisia halodendron in a semi-arid sandy grassland in China. *Front. Plant Sci.* 12, 698054. doi: 10.3389/fpls.2021.698054

Long, L., Hu, Y., Sun, F., Gao, W., Hao, Z., and Yin, H. (2022). Advances in lytic polysaccharide monooxygenases with the cellulose-degrading auxiliary activity family 9 to facilitate cellulose degradation for biorefinery. *Int. J. Biol. Macromolecules.* 219 (68-83). doi: 10.1016/j.ijbiomac.2022.07.240

Lull, C., Gil-Ortiz, R., Bautista, I., and Lidón, A. (2023). Seasonal variation and soil texture-related thinning effects on soil microbial and enzymatic properties in a semi-arid pine forest. *Forests* 14 (8), 1674. doi: 10.3390/f14081674

Lundell, T. K., Mkel, M. R., and Hildén, K. (2010). Lignin-modifying enzymes in filamentous basidiomycetes – ecological, functional and phylogenetic review. *J. Basic Microbiol.* 50 (1), 5–20. doi: 10.1002/jobm.200900338

Luo, Y., Ding, J., Zhao, X., Li, Y., Lian, J., and Wang, T. (2020). Grazing exclusion altered the effect of plant root diameter on decomposition rates in a semiarid grassland ecosystem, northeastern China. *Ecol. Res.* 35 (2), 405–415. doi: 10.1111/1440-1703.12089

Luo, Y., Zhao, X., Ding, J., and Wang, T. (2016). Vertical distribution of Artemisia halodendron root system in relation to soil properties in Horqin Sandy Land, NE China. *Sci. Cold Arid Regions* 8 (5), 411–418.

Master, E. R., Zheng, Y., Storms, R., Tsang, A., and Powlowski, J. (2008). A xyloglucan-specific family 12 glycosyl hydrolase from Aspergillus Niger: recombinant expression, purification and characterization. *Biochem. J.* 411 (1), 161–170. doi: 10.1042/BJ20070819

Mccormack, M. L., Dickie, I. A., Eissenstat, D. M., Fahey, T. J., Fernandez, C. W., Guo, D., et al. (2015). Redefining fine roots improves understanding of below-ground contributions to terrestrial biosphere processes. *New Phytol.* 207 (3), 505–518. doi: 10.1111/nph.13363

Meena, M., Yadav, G., Sonigra, P., Nagda, A., Mehta, T., Swapnil, P., et al. (2023). Multifarious responses of forest soil microbial community toward climate change. *Microbial Ecol.* 86 (1), 49–74. doi: 10.1007/s00248-022-02051-3

Mehmood, I., Bari, A., Irshad, S., Khalid, F., Liaqat, S., Anjum, H., et al. (2020). Carbon cycle in response to global warming. *Environment climate Plant vegetation Growth*, 1–15. doi: 10.1007/978-3-030-49732-3_1

Morffi-Mestre, H., Ángeles-Pérez, G., Powers, J. S., Andrade, J. L., Feldman, R. E., May-Pat, F., et al. (2023). Leaf litter decomposition rates: influence of successional age, topography and microenvironment on six dominant tree species in a tropical dry forest. *Front. Forests Global Change* 6, 1082233. doi: 10.3389/ffgc.2023.1082233

Nottingham, A. T., Bth, E., Reischke, S., Salinas, N., and Meir, P. (2019). Adaptation of soil microbial growth to temperature: Using a tropical elevation gradient to predict future changes. *Global Change Biol.* 25 (3), 827–838. doi: 10.1111/gcb.14502

Panchal, P., Preece, C., Peñuelas, J., and Giri, J. (2022). Soil carbon sequestration by root exudates. *Trends Plant Sci.* 27 (8), 749–757. doi: 10.1016/j.tplants.2022.04.009

Pandey, R., Bargali, S. S., Bargali, K., Karki, H., Kumar, M., and Sahoo, U. (2023). Fine root dynamics and associated nutrient flux in Sal dominated forest ecosystems of Central Himalaya, India. *Front. Forests Global Change* 5, 1064502. doi: 10.3389/ffgc.2022.1064502

Pandharikar, G., Claudien, K., Rose, C., Billet, D., Pollier, B., Deveau, A., et al. (2022). Comparative Copper Resistance Strategies of Rhodonia placenta and Phanerochaete chrysosporium in a Copper/Azole-Treated Wood Microcosm. *J. Fungi* 8 (7), 706. doi: 10.3390/jof8070706

Peng, S., and Chen, H. Y. (2021). Global responses of fine root biomass and traits to plant species mixtures in terrestrial ecosystems. *Global Ecol. Biogeography* 30 (1), 289–304. doi: 10.1111/geb.13205

Philippe, M., Mcloughlin, S., Strullu-Derrien, C., Bamford, M., Kiel, S., Nel, A., et al. (2022). Life in the woods: Taphonomic evolution of a diverse saproxylic community within fossil woods from Upper Cretaceous submarine mass flow deposits (Mzamba Formation, southeast Africa). *Gondwana Res.* 109, 113–133. doi: 10.1016/j.gr.2022.04.008

Phillips, C., Bloomberg, M., Marden, M., and Lambie, S. (2023). Tree root research in New Zealand: a retrospective 'review'with emphasis on soil reinforcement for soil conservation and wind firmness. *New Z. J. Forestry Sci.* 53, 6. doi: 10.33494/nzjfs532023x177x

Powers, J. S., Montgomery, R. A., Adair, E. C., Brearley, F. Q., Dewalt, S. J., Castanho, C. T., et al. (2009). Decomposition in tropical forests: a pan-tropical study of the effects of litter type, litter placement and mesofaunal exclusion across a precipitation gradient. *J. Ecol.* 97 (4), 801–811. doi: 10.1111/j.1365-2745.2009.01515.x

Prescott, C. E., and Grayston, S. J. (2023). TAMM review: Continuous root forestry—Living roots sustain the belowground ecosystem and soil carbon in managed forests. *For. Ecol. Manage.* 532, 120848. doi: 10.1016/j.foreco.2023.120848

Prescott, C. E., and Vesterdal, L. (2021). Decomposition and transformations along the continuum from litter to soil organic matter in forest soils. *For. Ecol. Management.* 498, 119522. doi: 10.1016/j.foreco.2021.119522

Pritsch, K., and Garbaye, J. (2011). Enzyme secretion by ECM fungi and exploitation of mineral nutrients from soil organic matter. *Ann. For. Sci.* 68 (1), 25–32. doi: 10.1007/s13595-010-0004-8

Purahong, W., Wubet, T., Lentendu, G., Schloter, M., Pecyna, M. J., Kapturska, D., et al. (2016). Life in leaf litter: novel insights into community dynamics of bacteria and fungi during litter decomposition. *Mol. Ecology.* 25 (16), 4059–4074. doi: 10.1111/mec.13739

Rai, P. K. (2022). Environmental degradation by invasive alien plants in the anthropocene: challenges and prospects for sustainable restoration. *Anthropocene Sci.* 1 (1), 5–28. doi: 10.1007/s44177-021-00004-y

Reineke, W., and Schlömann, M. (2023). "Microbial degradation of pollutants," in *Environmental microbiology* (Berlin, Heidelberg: Berlin Heidelberg), 161–290. doi: 10.1007/978-3-662-66547-3_6

Riley, R., Salamov, A. A., Brown, D. W., Nagy, L. G., Floudas, D., Held, B. W., et al. (2014). Extensive sampling of basidiomycete genomes demonstrates inadequacy of the white-rot/brown-rot paradigm for wood decay fungi. *Proc. Natl. Acad. Sci. United States America* 111 (27), 9923–9928. doi: 10.1073/pnas.1400592111

Rodtassana, C., and Tanner, E. V. J. (2018). Litter removal in a tropical rain forest reduces fine root biomass and production but litter addition has few effects. *Ecology* 99 (3), 735–742. doi: 10.1002/ecy.2143

Santos, F., and Herndon, E. (2023). Plant-soil relationships influence observed trends between manganese and carbon across biomes. *Global Biogeochemical Cycles* 37 (1), e2022GB007412. doi: 10.1029/2022GB007412

Sardar, M. F., Younas, F., Farooqi, Z. U. R., and Li, Y. (2023). Soil nitrogen dynamics in natural forest ecosystem: a review. *Front. Forests Global Change* 6, 1144930. doi: 10.3389/ffgc.2023.1144930

Schädler, M., Brandl, R., and Kempel, A. (2010). "Afterlife" effects of mycorrhization on the decomposition of plant residues. *Soil Biol. Biochem.* 42 (3), 521–523. doi: 10.1016/j.soilbio.2009.11.031

See, C. R., Luke Mccormack, M., Hobbie, S. E., Flores-Moreno, H., Silver, W. L., and Kennedy, P. G. (2019). Global patterns in fine root decomposition: climate, chemistry, mycorrhizal association and woodiness. *Ecol. Lett.* 22 (6), 946–953. doi: 10.1111/ele.13248

Semeraro, S., Kipf, P., Le Bayon, R.-C., and Rasmann, S. (2023). Solar radiation explains litter degradation along alpine elevation gradients better than other climatic or edaphic parameters. *Front. Microbiol.* 14. doi: 10.3389/fmicb.2023.1152187

Sihui, T., Xin, L., Baocheng, J., and Xuechun, Z. (2022). Contribution of fine roots to soil organic carbon accumulation in different desert communities in the sangong river basin. *International Journal of Environmental Research and Public Health* 19, 17, 10936. doi: 10.3390/ijerph191710936

Silver, W. L., and Miya, R. K. (2001). Global patterns in root decomposition: comparisons of climate and litter quality effects. *Oecologia* 129 (3), 407–419. doi: 10.1007/s004420100740

Solly, E. F. (2015). No depth-dependence of fine root litter decomposition in temperate beech forest soils. *Plant Soil* 393 (1-2), 273–282. doi: 10.1007/s11104-015-2492-7

Solly, E. F., Schöning, I., Boch, S., Kandeler, E., Marhan, S., Michalzik, B., et al. (2014). Factors controlling decomposition rates of fine root litter in temperate forests and grasslands. *Plant Soil 382*, 203–218. doi: 10.1007/s11104-014-2151-4

Sponseller, R. A. (2007). Precipitation pulses and soil CO2 flux in a Sonoran Desert ecosystem. *Global Change Biol.* 13 (2), 426–436. doi: 10.1111/j.1365-2486.2006.01307.x

Sreejaya, M. M., Sankar, R. J., Ramanunni, K., Pillai, N. P., Ramkumar, K., Anuvinda, P., et al. (2022). Lignin-based organic coatings and their applications: A review. *Materials Today: Proceedings* 60, 494–501. doi: 10.1016/j.matpr.2022.01.325

Stokland, J. N., Siitonen, J., and Jonsson, B. G. (2012). *Biodiversity in Dead Wood (Ecology, Biodiversity and Conservation)* (Cambridge: Cambridge university press). doi: 10.1017/CBO9781139025843

Sudharsan, M. S., Rajagopal, K., and Banu, N. (2023). "An insight into fungi in forest ecosystems," in *Plant mycobiome: diversity, interactions and uses* (Cham: Springer International Publishing), 291–318. doi: 10.1007/978-3-031-28307-9_12

Sullivan, M. B., Cavicchioli, R., Timmis, K. N., Bakken, L. R., Baylis, M., Boetius, A., et al. (2019). Scientists' warning to humanity: microorganisms and climate change. *Nat. Rev. Microbiol.* 17 (9), 569–586. doi: 10.1038/s41579-019-0222-5

Sun, L., Ataka, M., Han, M., Han, Y., Gan, D., Xu, T., et al. (2021). Root exudation as a major competitive fine-root functional trait of 18 coexisting species in a subtropical forest. *New Phytol.* 229 (1), 259–271. doi: 10.1111/nph.16865

Sun, T., Dong, L., and Mao, Z. (2015). Simulated atmospheric nitrogen deposition alters decomposition of ephemeral roots. *Ecosystems* 18, 1240–1252. doi: 10.1007/s10021-015-9895-4

Sun, T., Dong, L., Zhang, L., Wu, Z., Wang, Q., Li, Y., et al. (2016). Early stage fine-root decomposition and its relationship with root order and soil depth in a Larix gmelinii plantation. *Forests* 7 (10), 234. doi: 10.3390/f7100234

Tanikawa, T., Maie, N., Fujii, S., Sun, L., Hirano, Y., Mizoguchi, T., et al. (2023). Contrasting patterns of nitrogen release from fine roots and leaves driven by microbial communities during decomposition. *Sci. Total Environ.* 855, 158809. doi: 10.1016/j.scitotenv.2022.158809

Tedersoo, L., Bahram, M., and Zobel, M. (2020). How mycorrhizal associations drive plant population and community biology. *Science* 367 (6480), eaba1223. doi: 10.1126/science.aba1223

Theradimani, M., and Ramamoorthy, V. (2022). "Advances in microbial management of soil," in *Biological approaches to controlling pollutants* (Elsevier: Woodhead Publishing), 15–27. doi: 10.1016/B978-0-12-824316-9.00018-5

Titus, B. D., and Malcolm, D. C. (1987). The effect of fertilization on litter decomposition in clearfelled spruce stands. *Plant Soil* 100 (1), 297–322. doi: 10.1007/BF02370947

Urcelay, C., Vaieretti, M. V., Perez, M., and Diaz, S. (2011). Effects of arbuscular mycorrhizal colonisation on shoot and root decomposition of different plant species and species mixtures. *Soil Biol. Biochem.* 43 (2), 466–468. doi: 10.1016/j.soilbio.2010.11.006

Venkatesagowda, B. (2019). Enzymatic demethylation of lignin for potential biobased polymer applications. *Fungal Biol. Rev.* 33 (3-4), 190–224. doi: 10.1016/j.fbr.2019.06.002

Venkatesagowda, B., and Dekker, R. F. H. (2021). Microbial demethylation of lignin: Evidence of enzymes participating in the removal of methyl/methoxyl groups. *Enzyme Microbial Technol.* 147, 109780. doi: 10.1016/j.enzmictec.2021.109780

Wahid, F., Sharif, M., Ali, A., Fahad, S., Adnan, M., Noor, M., et al. (2020). Plant-microbes interactions and functions in changing climate. *Environment climate Plant vegetation Growth*, 397–419. doi: 10.1007/978-3-030-49732-3_16

Wambsganss, J., Freschet, G. T., Beyer, F., Bauhus, J., and Scherer-Lorenzen, M. (2021). Tree diversity, initial litter quality, and site conditions drive early-stage fine-root decomposition in european forests. *Ecosystems.* 25 (7), 1493–1509. doi: 10.1007/s10021-021-00728-3

Wang, X., Dai, W., Filley, T. R., Wang, C., and Bai, E. (2021c). Aboveground litter addition for five years changes the chemical composition of soil organic matter in a temperate deciduous forest. *Soil Biol. Biochem.* 161, 108381. doi: 10.1016/j.soilbio.2021.108381

Wang, J., Defrenne, C., Mccormack, M. L., Yang, L., Tian, D., Luo, Y., et al. (2021a). Fine-root functional trait responses to experimental warming: a global meta-analysis. *New Phytologist.* 230 (5), 1856–1867. doi: 10.1111/nph.17279

Wang, P., Huang, K., and Hu, S. (2020b). Distinct fine-root responses to precipitation changes in herbaceous and woody plants: a meta-analysis. *New Phytol.* 225 (4), 1491–1499 doi: 10.1111/nph.16266

Wang, N., Wang, C., and Quan, X. (2020a). Variations in fine root dynamics and turnover rates in five forest types in northeastern China. *J. forestry Res.* 31 (3), 871–884. doi: 10.1007/s11676-019-01065-x

Wang, Q., Zhang, Z., Guo, W., Zhu, X., Xiao, J., Liu, Q., et al. (2021b). Absorptive and transport roots differ in terms of their impacts on rhizosphere soil carbon storage and stability in alpine forests. *Soil Biol. Biochem.* 161, 108379. doi: 10.1016/j.soilbio.2021.108379

Wang, W., Zhang, X., Tao, N., Ao, D., and Zeng, H. (2014). Effects of litter types, microsite and root diameters on litter decomposition in Pinus sylvestris plantations of northern China. *Plant Soil* 374 (1-2), 677–688. doi: 10.1007/s11104-013-1902-y

Waring, B. G., Sulman, B. N., Reed, S., Smith, A. P., Averill, C., Creamer, C. A., et al. (2020). From pools to flow: The PROMISE framework for new insights on soil carbon cycling in a changing world. *Global Change Biol.* 26 (12), 6631–6643. doi: 10.1111/gcb.15365

Weemstra, M., Sterck, F. J., Visser, E. J. W., Kuyper, T. W., Goudzwaard, L., and Mommer, L. (2017). Fine-root trait plasticity of beech (Fagus sylvatica) and spruce (Picea abies) forests on two contrasting soils. *Plant Soil.* 415, 175–188. doi: 10.1007/s11104-016-3148-y

Wei, L., Hao, S., Guanhua, W., Wenjie, S., Lin, D., and Chuanling, S. (2023). Lignin as a green and multifunctional alternative of phenol for resin synthesis. *Green Chem*. 25, 2241–2261. doi: 10.1039/D2GC04319J

Wendel, A. S., Bauke, S. L., Amelung, W., and Knief, C. (2022). Root-rhizosphere-soil interactions in biopores. *Plant Soil* 475 (1-2), 253–277. doi: 10.1007/s11104-022-05406-4

Wu, S., Fu, W., Rillig, M. C., Chen, B., Zhu, Y. G., and Huang, L. (2023). Soil organic matter dynamics mediated by arbuscular mycorrhizal fungi–an updated conceptual framework. *New Phytologist.* doi: 10.1111/nph.19178

Wu, Y., Zhang, M., Cheng, Z., Wang, F., and Cui, X. (2022). Root-order-associated variations in fine-root decomposition and their effects on soil in a subtropical evergreen forest. *Ecol. Processes* 11 (1), 48. doi: 10.1186/s13717-022-00393-x

Xu, M., Wu, S., Jiang, Z., Xu, L., and He, N. (2020). Effect of pulse precipitation on soil CO2 release in different grassland types on the Tibetan Plateau. *Eur. J. Soil Biol.* 101, 103250. doi: 10.1016/j.ejsobi.2020.103250

Yan, L., Chen, W., Wang, C., Liu, S., Liu, C., Yu, L., et al. (2022). Tetracycline removal in granulation: Influence of extracellular polymers substances, structure, and metabolic function of microbial community. *Chemosphere* 288, 132510. doi: 10.1016/j.chemosphere.2021.132510

Yan, Z., Qi, Y., Peng, Q., Dong, Y., Guo, S., He, Y., et al. (2017). Effects of increased precipitation and nitrogen deposition on soil enzyme activities. *Acta Ecologica Sin.* 37, 3019–3027.

Yan, G., Xhou, M., Wang, M., Han, S., Liu, G., Zhang, X., et al. (2019). Nitrogen deposition and decreased precipitation altered nutrient foraging strategies of three temperate trees by affecting root and mycorrhizal traits. *Catena: Interdiscip. J. Soil Sci. Hydrology-Geomorphology Focusing Geoecology Landscape Evol.* 181, 104094. doi: 10.1016/j.catena.2019.104094

Yin, H., Wheeler, E., and Phillips, R. P. (2014). Root-induced changes in nutrient cycling in forests depend on exudation rates. *Soil Biol. Biochem.* 78 (78), 213–221. doi: 10.1016/j.soilbio.2014.07.022

Yuan, Z. Y., and Chen, H. (2010). Fine root biomass, production, turnover rates, and nutrient contents in boreal forest ecosystems in relation to species, climate, fertility, and stand age: literature review and meta-analyses. *Crit. Rev. Plant Sci.* 29 (4), 204–221. doi: 10.1080/07352689.2010.483579

Zhai, Z., Fang, Y., Cheng, J., Tian, Y., Liu, L., and Cao, X. (2023). Intrinsic morphology and spatial distribution of non-structural carbohydrates contribute to drought resistance of two mulberry cultivars. *Plant Biol.* doi: 10.1111/plb.13533

Zhang, Y., Li, C., and Wang, M. (2019b). Linkages of C: N: P stoichiometry between soil and leaf and their response to climatic factors along altitudinal gradients. *J. Soils Sediments.* 19, 1820–1829. doi: 10.1007/s11368-018-2173-2

Zhang, H. Y., Lü, X.-T., Hartmann, H., Keller, A., Han, X. G., Trumbore, S., et al. (2018a). Foliar nutrient resorption differs between arbuscular mycorrhizal and ectomycorrhizal trees at local and global scales. *Global Ecol. Biogeography* 27 (7), 875–885. doi: 10.1111/geb.12738

Zhang, X., and Wang, W. (2015). The decomposition of fine and coarse roots: their global patterns and controlling factors. *Sci. Rep.* 5 (1), 9940. doi: 10.1038/srep09940

Zhang, X., Wang, B., and Liu, Z. (2019a). Mutual effects between Pinus armandii and broadleaf litter during mixed decomposition. *History*. 88 (3), 3629. doi: 10.5586/asbp.3629

Zhang, Y., Xiao, L., Guan, D., Chen, Y., Motelica-Heino, M., Peng, Y., et al. (2021). The role of mangrove fine root production and decomposition on soil organic carbon component ratios. *Ecol. Indic.* 125, 107525. doi: 10.1016/j.ecolind.2021.107525

Zhang, Z., Xiao, J., Yuan, Y., Zhao, C., and Yin, H. (2018b). Mycelium- and root-derived C inputs differ in their impacts on soil organic C pools and decomposition in forests. *Soil Biol. Biochem.* 123, 257–265. doi: 10.1016/j.soilbio.2018.05.015

Zhao, P. S., Guo, M. S., Gao, G. L., Zhang, Y., Ding, G. D., Ren, Y., et al. (2020). Community structure and functional group of root-associated Fungi of Pinus sylvestris var. mongolica across stand ages in the Mu Us Desert. *Ecol. Evolution.* 10 (6), 3032–3042. doi: 10.1002/ece3.6119

Zhao, M., Luo, Y., Chen, Y., Shen, H., and Hu, H. (2021b). Varied nitrogen versus phosphorus scaling exponents among shrub organs across eastern China. *Ecol. Indic.* 121 (1), 107024. doi: 10.1016/j.ecolind.2020.107024

Zhao, X., Tian, Q., Michelsen, A., Lin, Q., Zhao, R., Yuan, X., et al. (2023b). The effects of mycorrhizal associations on fine root decomposition in temperate and (sub) tropical forests. *Plant Soil*, 1–12. doi: 10.1007/s11104-023-05925-8

Zhao, B., Xing, P., and Wu, Q. L. (2021a). Interactions between bacteria and fungi in macrophyte leaf litter decomposition. *Environ. Microbiol.* 23 (2), 1130–1144. doi: 10.1111/1462-2920.15261

Zhao, R., Zhu, Y., Mao, Z., Gu, W., Zhang, H., Long, F., et al. (2023a). Predicting fine root decomposition from functional traits in 10 temperate tree species. *Forests* 14 (2), 372. doi: 10.3390/f14020372

Zhaoxia, J., Hongfeng, B., Li, X., Mingxu, L., and Nianpeng, H. (2021). Effects of pulse precipitation on soil organic matter mineralization in forests: spatial variation and controlling factors. *J. Plant Ecology.* 14 (5), 970–980. doi: 10.1093/jpe/rtab057

Zhou, S., Butenschoen, O., Barantal, S., Handa, I. T., Makkonen, M., Vos, V., et al. (2020). Decomposition of leaf litter mixtures across biomes: The role of litter identity, diversity and soil fauna. *J. Ecol.* 6), 108. doi: 10.1111/1365-2745.13452

Zhu, H., Zhao, J., and Gong, L. (2021). The morphological and chemical properties of fine roots respond to nitrogen addition in a temperate Schrenk's spruce (Picea schrenkiana) forest. *Sci. Rep.* 11 (1), 3839. doi: 10.1038/s41598-021-83151-x

Zwetsloot, M. J., Kessler, A., and Bauerle, T. L. (2018). Phenolic root exudate and tissue compounds vary widely among temperate forest tree species and have contrasting effects on soil microbial respiration. *New Phytol* 218 (2), 530–541. doi: 10.1111/nph.15041

frontiers | Frontiers in Plant Science

TYPE Original Research
PUBLISHED 08 December 2023
DOI 10.3389/fpls.2023.1291662

OPEN ACCESS

EDITED BY
Fahad Shafiq,
Government College University, Lahore, Pakistan

REVIEWED BY
Baobao Pan,
The University of Melbourne, Australia
Markus Weinmann,
University of Hohenheim, Germany

*CORRESPONDENCE
Douglas Guelfi
douglasguelfi@ufla.br

RECEIVED 09 September 2023
ACCEPTED 07 November 2023
PUBLISHED 08 December 2023

CITATION
Sarkis LF, Dutra MP, Oliveira DP, Fernandes TJ, de Souza TR, Builes VR and Guelfi D (2023) Ammonia volatization from conventional and stabilized fertilizers, agronomic aspects and microbiological attributes in a Brazilian coffee crop system. *Front. Plant Sci.* 14:1291662. doi: 10.3389/fpls.2023.1291662

Ammonia volatization from conventional and stabilized fertilizers, agronomic aspects and microbiological attributes in a Brazilian coffee crop system

Leonardo Fernandes Sarkis[1], Mateus Portes Dutra[1], Damiany Pádua Oliveira[1], Tales Jesus Fernandes[2], Thaís Regina de Souza[3], Victor Ramirez Builes[3] and Douglas Guelfi[1]*

[1]Department of Soil Science, Federal University of Lavras, Lavras, MG, Brazil, [2]Department of Statistics, Federal University of Lavras, Lavras, MG, Brazil, [3]Yara International, Berlin, Germany

We aimed to quantify the N losses through volatilization of the main conventional and stabilized N fertilizers applied in coffee plantations. Additionally, we also assessed microbiological attributes of the soil (microbial biomass carbon (MBC); microbial biomass nitrogen (MBN); microbial basal respiration (MBR); metabolic quotient (qCO_2); urease, β-glucosidase, acid phosphatase, and arylsulfatase activities) and agronomic aspects of the crop (N content in the leaves and beans, yield, and N exportation by the beans). Treatments consisted of the combination of three fertilizers (ammonium nitrate - AN, conventional urea - U, and urea with N- (n-butyl) thiophosphoric triamide (NBPT) - U_{NBPT}, and five doses of N (0, 150, 275, 400, and 525 kg ha^{-1} $year^{-1}$ of N), with four replicates, totalling 60 experimental plots. In the two crop seasons evaluated, daily and cumulative losses of N-NH_3 from the split fertilizer applications were influenced by the N fertilizer technologies. The application of U resulted in losses of 22.0% and 22.8% for the doses of 150 and 400 kg ha^{-1} $year^{-1}$ of N. This means that 66 and 182 kg ha^{-1} of N-NH_3 were lost, respectively, at the end of six fertilizations with U. U_{NBPT} reduced urease activity and N-NH_3 losses compared to conventional urea, avoiding the volatilization of 15.9 and 24.3 kg ha^{-1} of N. As for AN, N-NH_3 losses did not exceed 1% of the applied dose, regardless of the weather conditions during the fertilization. Urease activity was higher on days of maximum NH_3 volatilization. There was an effect of the N sources (NS), soil sampling time (ST), and their interaction (NS × ST) on the MBN and arylsulfatase activity. The N sources also influenced the MBC and the qCO_2. A substantial amount of N was removed from the system by the beans and husks of the harvested fruits. Our study showed that N fertilizer technologies are interesting options to reduce N-NH_3 losses by volatilization, increase N retention in the soil,

10.3389/fpls.2023.1291662

and improve microbiological attributes and the sustainability of coffee production systems.

KEYWORDS

nitrogen fertilizers, urease inhibitor, coffea arabica, basal respiration, enzymatic activity, soil health

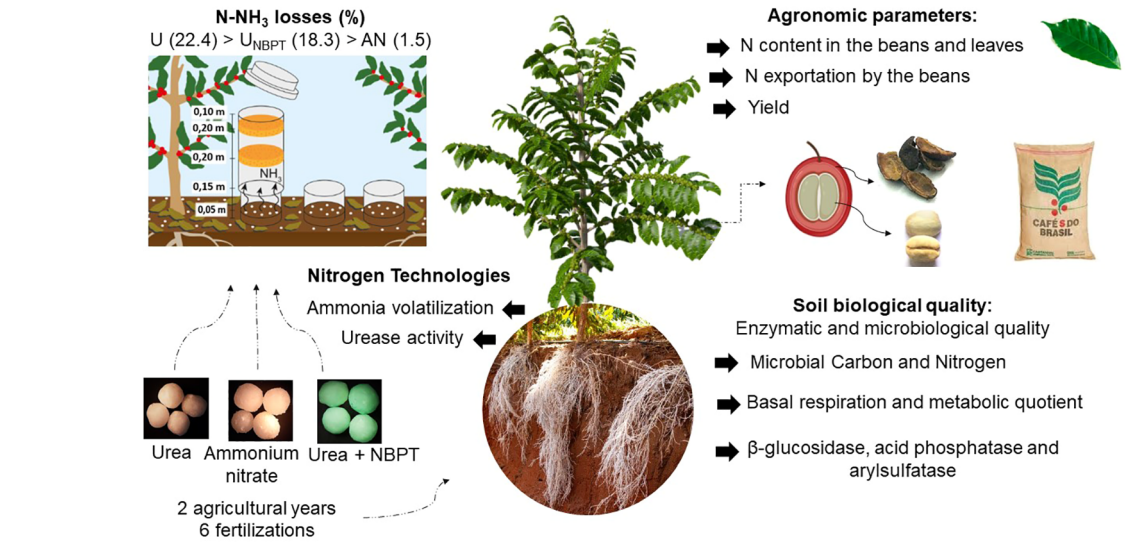

GRAPHICAL ABSTRACT

Highlights

- Microbiological indicators reflect long-term soil coffee management.
- N-fertilization increases the carbon input and the microbiological activity of the system.
- U_{NBPT} reduces urease activity and N-NH_3 losses.
- N-NH_3 losses by ammonium nitrate do not exceed 1%, regardless of weather conditions.
- The high soil biological quality depends on the correct management of fertilization.

1 Introduction

Brazil is the world's largest producer and exporter of coffee (*Coffea arabica* L.). Increasing fertilizer use efficiency through innovative technologies reduces costs of production, improves the quality of the beverage, and makes farming activity more sustainable and competitive, especially in times of high input prices. The application of nitrogen (N) fertilizers is essential for the productivity of this high-value crop. Brazilian agriculture consumed 9.2 million tonnes of N fertilizers in 2020 (FAOSTAT, 2021), in which coffee production alone was estimated do consume 10-15% of the country's N (1.4 million tonnes per year).

The intense dynamics of the N transformations in the soil and the diverse pathways it can be lost in coffee production systems result in low N fertilizer use efficiency (NUE) (Salamanca-Jimenez et al., 2017). Studies using ^{15}N demonstrated that coffee plants recover less than 25% of the N fertilizer when conventional urea is used (Cannavo et al., 2013; Salamanca-Jimenez et al., 2017), a complex scenario considering that approximately 50% of the global N fertilizer production is represented by urea (Heffer and Prud'homme, 2016; FAOSTAT, 2021).

Ammonia (NH_3) volatilization is the main process of N loss in coffee cultivation areas in Brazil, especially when conventional urea

Abbreviations: N, Nitrogen; NUE, N fertilizer use efficiency; NH_3Ammonia; GHG, Greenhouse gases; EEFs, enhanced-efficiency fertilizers; NBPT. N-(n-butyl)thiophosphoric triamide; CPL, Critical period of losses; U, Urea, AN, Ammonium nitrate, U_{NBPT}, urea + NBPT; MBC, Microbial biomass carbon; MBN Microbial biomass nitrogen; SBR, Soil basal respiration; qCO_2, Metabolic quotient; MDL, Maximum daily loss.

is applied without the incorporation and in the presence of plant residues (Martins et al., 2021; Freitas et al., 2022; de Souza et al., 2023), common practices in perennial crops such as coffee. Generally, for every three nitrogen applications with conventional urea in coffee systems, one is lost due to volatilization (Chagas et al., 2016; Dominghetti et al., 2016; Freitas et al., 2022; de Souza et al., 2023), configuring the most important agronomic loss.

The enhanced-efficiency fertilizers (EEFs) encompass many technologies for fertilizers and its one of the most studied strategies to increase NUE (Chien et al., 2009; Azeem et al., 2014; Timilsena et al., 2015) and mitigate greenhouse gas emissions in agriculture. For N fertilizers, these technologies are divided in the following main categories: conventional fertilizers, stabilized fertilizers, slow-release fertilizers, controlled-release fertilizers, and their blends (Guelfi, 2017). The proper use of EEFs is an interesting option to reduce N losses, carbon footprint, and climate change, in addition to increasing N retention in the soil (Snyder, 2017; Zhang et al., 2021; Freitas et al., 2022).

Stabilized fertilizers have additives, such as urease inhibitors (NBPT, NPPT, 2-NPT, and Duromide) and nitrification inhibitors (DCD, DMPP, and DMPSA), that inhibit or delay a determined stage of the N transformation process in the soil (Guelfi, 2017; Byrne et al., 2020). In Brazilian coffee cultivation, urease inhibitors are already widely used, while nitrification inhibitors or the combination of these two subgroups are still not significant in the national market. Currently, some authors have highlighted the need to evaluate the possible negative impacts of some additives on human health in future studies (Cai and Akiyama, 2017), which may be related to the persistence of some molecules in the environment.

The N-(n-butyl)thiophosphoric triamide (NBPT) is currently the most widely used molecule as a urease inhibitor (Sanz-Cobena et al., 2011). NBPT is reported to effectively reduce N-NH_3 losses through volatilization when added to urea (Adotey et al., 2017; Santos et al., 2020). The reduction of NH_3 losses is related to the maintenance of the N in the form of amide through a temporary inhibition of the urease activity, the enzyme which catalyzes the hydrolysis of urea (Santos et al., 2021; Freitas et al., 2022). This is due to the ability of the NBPT to oxidize into its analog, NBPTO, which forms stable complexes with the enzyme, causing its inactivation (Sanz-Cobena et al., 2011). The potential inhibition of the additive depends on the concentration and stability of the inhibitor in the fertilizer, which can vary depending on its compatibility with physical mixtures, time, and storage temperature.

The use of stabilized fertilizers may not be the most suitable technology among the strategies to reduce N-NH_3 losses in a brazilian coffee crop system, as they depend on the occurrence of rain to incorporate the N fertilizer. The highest N losses through volatilization for conventional urea occur in the first 7 days after fertilization (Costa et al., 2003; Afshar et al., 2018), which is a critical period of losses (CPL). NBPT typically delays the CPL to increase the chance of incorporation of the N fertilizer into the soil by the precipitation. However, relying solely on weather conditions represents a high risk of inefficiency in N fertilizer incorporation, as it also depends on both the volume and intensity of rainfall (Dawar et al., 2011). In addition, the architecture of the coffee plants creates a barrier that reduces the rainfall under the canopy and the direct incidence on the N fertilizer applied in that location.

Currently, microbiological attributes have been used and disseminated as a tool to ensure ecosystem sustainability and monitoring the health of soil studies. The attributes most used as "microbiological indicators of soil quality" are microbial biomass carbon, microbial biomass nitrogen, microbial basal respiration, and enzymatic activities (Doran and Parkin 1994; Dick et al., 1996). The enzymes most used for this purpose are related to the C, N, P, and S cycles (Gil-Sotres et al., 2005; Moreira and Siqueira, 2006; Bastida et al., 2008).

Our hypothesis was that the technologies for nitrogen fertilizers can help mitigate N losses and improve agronomic efficiency and microbiological attributes in coffee fields. Therefore, the aims of this study were: i) quantify N-NH_3 losses from two conventional sources of N and from urea stabilized with NBPT at two doses of N (150 and 400 kg ha^{-1}); ii) determine the effect of nitrogen fertilizer technologies and doses of N (0, 150, 275, 400, and 525 kg ha^{-1} crop $season^{-1}$, divided into three applications) for improvement in the nutrition and yield of coffee plants; iii) update the numbers of N exportation by the beans of recent coffee cultivars and understand the real N demand to avoid nitrate losses by leaching; iv) evaluate the effect of nitrogen fertilization on soil microbiological attributes (microbial biomass carbon, microbial biomass nitrogen, microbial basal respiration, metabolic quotient, urease, β-glucosidase, acid phosphatase and arylsulfatase enzyme activities; and, finally, v) support researchers, commercial farmers and fertilizer industries with a new insight and inedited results of N fertilizer technologies as interesting options for reducing N-NH_3 losses by volatilization and increasing the sustainability of coffee production systems.

2 Materials and methods

2.1 Characterization of the experimental area

The experiment was conducted during the 2019/2020 and 2020/2021 crop seasons with coffee plants under field conditions. The commercial plantation belongs to the Lagoa Coffee Plantation, owned by the NKG/Fazendas Brasileiras group, located in the municipality of Santo Antônio do Amparo, in the state of Minas Gerais, Brazil (Figure 1).

This municipality is located in a traditional coffee-producing region in Brazil within the Campos das Vertentes geographical indication, at 1,100 meters of altitude, latitude 20°53'26.04" S, and longitude 44°52'04.14" W. According to the Köppen classification, the climate is Cwa, with a humid tropical climate with a dry winter and a temperate summer. The mean annual precipitation is approximately 1,493 mm and the mean annual temperature is 19.6°C.

The soil was classified as an Oxisol according to United States Department of Agriculture (USDA) Soil Taxonomy (Soil Survey Staff, 2018). Before the experiment, soil samples were collected at 0 to 20 cm depth to identify the texture as 32%, 8%, and 60% of sand,

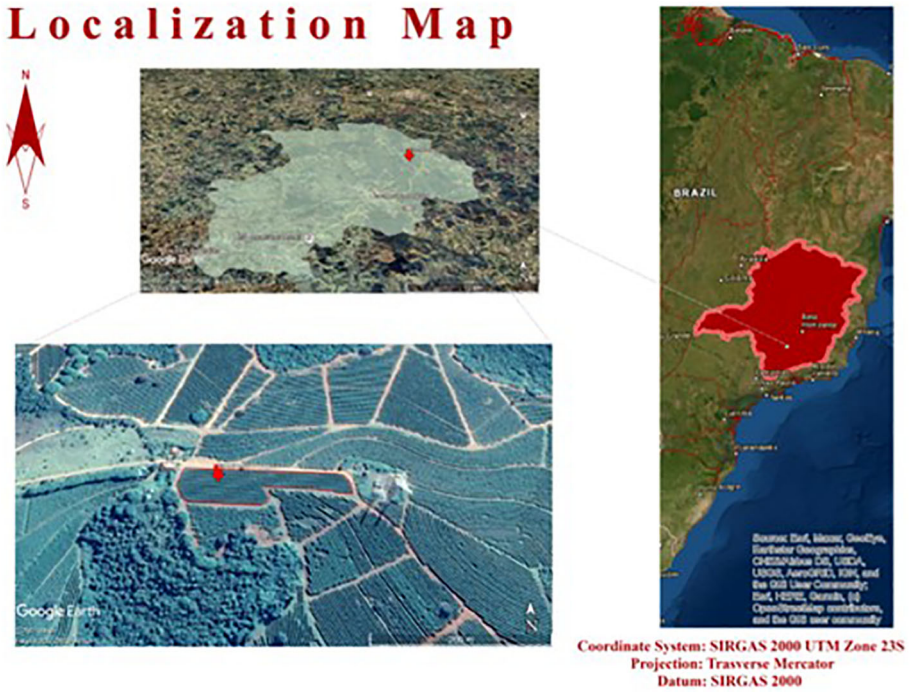

FIGURE 1
Location of the experimental areas in the municipality of Santo Antônio do Amparo, Minas Gerais state, Brazil.

silt, and clay, respectively, using the Bouyoucos method (Bouyoucos, 1951).

The five years old plantation in the production phase was planted with *Coffea arabica* L., Catuaí Vermelho – IAC 99 cultivar. Plants were spaced by 3.40 m between rows and 0.6 m between plants, resulting in 4,902 plants ha^{-1}.

2.2 Fertilizer characterization

The fertilizers used in this study were chosen from the main technologies currently used in Brazilian coffee production. These fertilizers belong to two major technology groups: conventional and stabilized. All fertilizers were photographed using an Olympus microscope, SZ60 Japan model (S.1). For the conventional group, U (46% N) (S.1a) and AN (33% N) (S.1b) were used. For the stabilized group, U_{NBPT} (46% N) (S.1c) was used.

The concentration of NBPT in the fertilizers was analyzed by liquid chromatography (HP1100 Agilent model) with a diode array detector, according to the method described by the European Committee for Standardization (2008). This procedure was done to verify if the concentration of the additive in U_{NBPT} was the same as the manufacturer's specification (530 mg kg^{-1} of NBPT). However, at the time of application, the NBPT concentration was

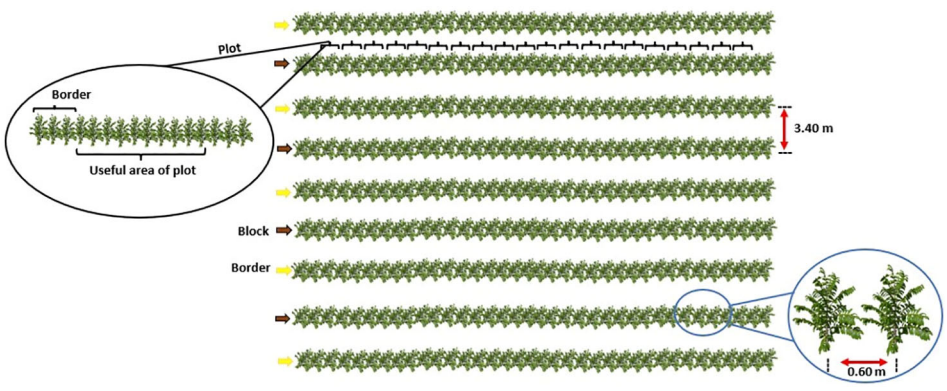

FIGURE 2
Illustration of the experimental design.

110 mg kg^{-1}, indicating that there was degradation of the molecule between the manufacturing and commercialization. Some conditions such as storage time and temperature (Cantarella et al., 2018) and contact with phosphate fertilizers and ammonium sulfate that contain free acidity (Sha et al., 2020) accelerate the degradation of this additive and, consequently, reduce the potential for enzyme inhibition.

The treatment of urea with this additive consists of spraying 2.5 to 3 L of a 20% NBPT solution per t^{-1} of fertilizer. This solution is composed of the NBPT molecule, organic solvent, and dye used to distinguish the stabilized from the conventional fertilizers.

2.3 Experimental design

A randomized block design was used in a 3 × 5 factorial scheme, composed of three fertilizers and five doses with four replications, totaling 60 experimental units. Each experimental unit was composed of 16 coffee plants. The area comprising the central 10 plants was used as the useful area for data collection. An entire row on each site was left as border between blocks (Figure 2).

The treatments were composed of U, AN, and U_{NBPT}, applied at doses of 0, 150, 275, 400, and 525 kg ha^{-1} $year^{-1}$ of N. The fertilization was split into three equal parts applied 30 to 40 days after the previous fertilization, starting in November, at the beginning of the rainy season. All fertilizers were applied as topdressing and under the projection of the canopy of the coffee plants.

2.4 Complementary fertilization management

Liming was done 60 days before the application of the treatments to increase soil base saturation to 60%. Each treatment plot received 1.1 t ha^{-1} of limestone (90% ENP 16% MgO), 1.5 t ha^{-1} of gypsum, and 400 kg ha^{-1} of magnesium oxide (70% MgO). Additional fertilization was done with KCl (60% K_2O) at 260 kg ha^{-1} $year^{-1}$ of K_2O divided into three applications and triple superphosphate (TSP – 46% P_2O_5) at 100 kg P_2O_5 ha^{-1} $year^{-1}$ applied in a single application. Both KCl and TSP were applied in the projection of the coffee tree canopy.

Micronutrients were applied via foliar fertilization along with the plant disease control treatments during the formation and management of the plantation. A commercial product with the following composition was applied at 5 kg ha^{-1} in 300 L ha^{-1} of solution: 6.0% of zinc ($ZnSO_4$), 3.0% of boron (H_3BO_3), 2.0% of manganese ($MnSO_4$), 10% of copper ($Cu(OH)_2$), 10% of sulfur (SO_4), 1.0% of magnesium ($MgSO_4$) and 10% of potassium (KCl). This fertilization was divided into three applications per year at intervals of 45 days between November and February. The soil was also fertilized with 3 kg ha^{-1} of B as H_3BO_4 and 5 kg ha^{-1} of Zn as $ZnSO_4$ along with the first application of the maintenance fertilization.

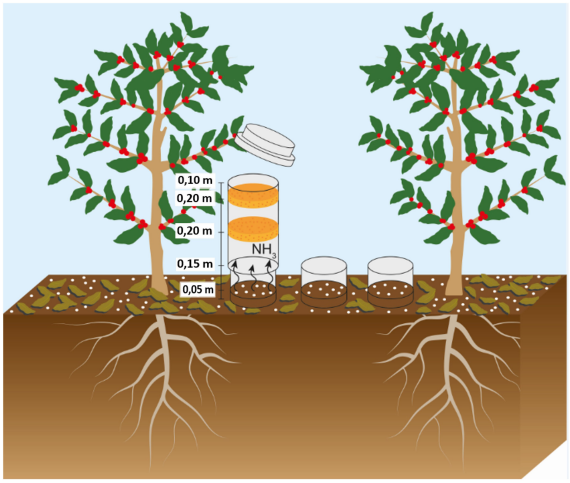

FIGURE 3
Illustration of the collectors used for the quantification of ammonia emissions.

2.5 Monitoring of climatic conditions

A climatological station set up near the experimental area was used for daily monitoring of rainfall, temperature (maximum and minimum), and relative humidity throughout the period of conducting the trials in the four agricultural crop seasons. Rain collectors were also installed beneath the coffee tree canopy to assess how much these plants reduce the direct incidence of rain where limestone and fertilizer are applied.

2.6 Quantification of the N-NH_3 losses

A 3 × 2 factorial arrangement was adopted involving the same plots with the N sources of experimental design (described above) and two of those doses of N (150 and 400 kg N ha^{-1} crop $season^{-1}$) were selected. The losses of N through NH_3 volatilization resulting from soil N fertilization were quantified using the semi-open collector, adapted from Lara-Cabezas et al. (1999) method for capturing N-NH_3. In each experimental plot that received 150 and 400 kg ha^{-1} of N, three 200 mm diameter bases made of PVC, with 20 cm height, were installed at 5 cm depth in the soil under the projection of the canopies (Figure 3).

PVC chambers similar to the bases but measuring 50 cm height were used to collect the emissions. Specifications are presented in Figure 3. Within each base (0.2 linear meters), the amount of fertilizer corresponding to the dose applied per hectare was added.

Immediately after fertilization, collection chambers were added over the bases in all plots. Within each chamber, two laminated foam disks with 0.02 g cm^{-3} density and 2 cm thickness, cut to the same diameter as the tube, were inserted. The disks were positioned 30 and 40 cm above the soil. The lower sponge was previously soaked with 80 ml of a solution composed of H_3PO_4 (60 ml L^{-1}) and glycerin (50 ml L^{-1}) to retain the volatilized ammonia. The upper sponge served to protect against possible environmental contamination.

The lower sponges were collected on the 1st, 2nd, 3rd, 4th, 5th, 6th, 8th, 10th, 13th, 16th, 20th, 24th, 28th, and 32nd day after each fertilizer application. After replacing the sponges, the chamber was switched to the other base to reduce the spatial variability of the ammonia emissions. This rotation allowed a greater influence of climatic variations, such as temperature and precipitation.

The solution contained in the sponge was then extracted by filtration through a Buchner funnel and a vacuum pump, along with five consecutive washes with 80 mL of distilled water. From the extract, 20 mL were taken to determine the N content by distillation using the Kjeldahl (1883) method. The N content in the sample was calculated according to Equation 1:

$$NT = [(Va - Vb) \times F \times 0.1 \times 0.014 \times 100]/P1$$

in which TN: Total nitrogen concentration in the sample (%); Va: Volume of hydrochloric acid solution used for titration of the sample (mL); Vb: Volume of hydrochloric acid solution used for titration of the blank (mL); F: Correction factor for 0.01 M hydrochloric acid; P1: mass of the sample (g).

The N concentration in the samples collected in the area of the chambers was extrapolated to the percentage of $N\text{-}NH_3$ loss per hectare. To calculate the accumulated losses during the evaluation days, the losses from the 1st and 2nd day were added, then the sum of these was added to the 3rd day, and so on until the last day of sampling.

2.7 Microbiological analyses

2.7.1 Soil sampling

To quantification of urease activity, soil samples were collected at 2 cm depth from the line of the N fertilizer application on the same dates that the sponges used to capture $N\text{-}NH_3$ were collected. A split-plot design with repeated measures over time was adopted with four replications. The soil, with the same field moisture, was sieved through a 2 mm mesh to remove plant debris, and then stored at 4°C until analysis.

To evaluate the effects of the N sources on microbial C and N, basal respiration and metabolic quotient, β-glucosidase, acid phosphatase, and arylsulfatase, a split-plot design with repeated measures over time was also adopted with four replications. The design consisted of two sampling times in plots with no N (dose 0) and in plots with 400 kg ha^{-1} of N of AN, U, and U_{NBPT} sources to assess the impact of this dose, often used by farmers, on microbiological attributes in productive and high-investment coffee plantation. Soil samples from the 0-0.10 m layer were collected in the 2021/2022 crop season, both in the projection of the coffee tree canopy and in the fertilization line of each plot. The samples were collected two times: immediately before the start of the N fertilization and after 2/3 (267 kg N ha^{-1}) of the N application to evaluate the influence of treatments that have been applied for consecutive years. The samples (2000 g each) were sieved through a 2 mm mesh and stored at 4°C for the following analyses. Other fertilization and management practices were kept constants for all plots, following the same detailed procedure as previously described.

2.7.2 Microbial C and N

Microbial biomass carbon (MBC) and microbial biomass nitrogen (MBN) in the soil were determined in triplicate by the irradiation/extraction method (Islam and Weil, 1998) using 20 g of soil and 50 mL of potassium sulfate (0.5 mol L^{-1}). The determination of MBC was carried out through oxidation with potassium dichromate (0.066 mol L^{-1}) and subsequent addition of H_2SO_4 and H_3PO_4. The resulting mixture was heated on a hot plate until ebullition. After cooling, the solution was titrated with ammonium ferrous sulfate (0.033 mol L^{-1}) and 1% diphenylamine as an indicator (Vance et al., 1987). MBN was determined by the Kjeldahl method.

2.7.3 Basal respiration and metabolic quotient

The soil basal respiration (SBR) was quantified by incubating 20 g of soil in a hermetically closed container with NaOH solution (0.5 mol L^{-1}) for three days at 28°C. The reaction was stopped by adding $BaCl_2.2H_2O$ (0.5 mol L^{-1}) and the solution was titrated with HCl (0.5 mol L^{-1}) (Anderson and Domsch, 1993). The metabolic quotient (qCO_2) was calculated by the division SBR/MBC (Anderson and Domsch, 1993).

2.7.4 β-glucosidase, acid phosphatase, and arylsulfatase

Samples of 1 g of soil, containing 1 mL of substrates (ρ-nitrophenyl-β-D-glucoside for β-glucosidase, ρ-nitrophenyl-phosphate for acid phosphatase and ρ-nitrophenyl-sulfate for arylsulfatase) were incubated for one hour at 37°C in the presence of toluene and standard solution at specific pH for each activity (pH 6.0 for β-glucosidase, 6.5 for acid phosphatase and 5.8 for arylsulfatase). After the incubation period, the reaction was stopped with the addition of $CaCl_2$ (0.5 mol L^{-1}) and NaOH (0.5 mol L^{-1}). The supernatant was filtered and readings were taken in a spectrophotometer at 410 nm by the colorimetric determination of the ρ-nitrophenol using 4-nitrophenyl β-D-glucopyranoside, potassium 4-nitrophenyl sulfate, and disodium 4-nitrophenyl orthophosphate as substrates, respectively (Dick et al., 1996; Aragão et al., 2020). The values of each activity were expressed in μg PNP g^{-1} soil h^{-1}.

2.7.5 Urease activity

The quantification of the urease activity was based on the determination of the $N\text{-}NH_4^+$ released after soil incubation with urea solution (Tabatabai and Bremner, 1972). For each treatment, a 5 g soil sample was mixed with 0.2 mL of toluene, 9.0 mL of buffer solution (pH 9.0), and 1.0 mL of a 0.2 mol L^{-1} urea solution, and then incubated for 2 hours at 25 °C in a temperature and humidity controlled chamber (model TE-371 TECNAL). After incubation, 35 mL of a 100 ppm solution composed of 2 mol L^{-1} KCl and 2 mol L^{-1} Ag_2SO_4 were added to stop the reaction. After shaking, the solution was left to rest for 5 minutes at room temperature, and the volume was then completed to 50 mL with KCl and Ag_2SO_4, of which 20 mL were distilled with 0.2 g of magnesium oxide. The distillate was collected in flasks containing boric acid and the indicators methyl

red and bromocresol green, and then titrated with a standard 0.005 mol L^{-1} H_2SO_4 solution. The control followed the same procedures described above, but the urea was added after the addition of the KCl and Ag_2SO_4 solution.

2.8 N content in the beans, N content in the leaves, and N exportation by the beans

The N content in the beans and leaves were determined by the Kjeldhal method (Kjeldahl, 1883) after sulfuric digestion (Bremner, 1996). Samples of coffee beans were also collected from nearby commercial farms of the same age as the experimental area. These samples belonged to 8 different cultivars, commonly planted in the region. The beans were dried and processed to quantify the bean/husk ratio and the respective N content, according to the international NIST standard. This procedure allowed the comparison between the proportion of beans/husks and the exported amount of N of the main coffee cultivars, which is a piece of information currently unavailable in the literature.

2.9 Yield

The yield of the coffee plants was also evaluated in both crop seasons by manually harvesting the fruits when approximately 70% of them were mature (cherry stage). The harvested volume was measured, and a 5 L sample was sun-dried until reach 11.5% humidity. After drying, the sample was processed, weighed, and subsequently converted into 60 kg bags of processed coffee per hectare.

2.10 Calculations and statistical analyses

Data were subjected to a non-linear regression analysis using a logistic model (Equation 2) to evaluate the variable ammonia loss through volatilization. This model is already well-used for estimating plant growth, but it has been recently used to estimate the accumulated N-NH_3 loss (Soares et al., 2012; Silva et al., 2017; Minato et al., 2020).

$$Yi = [\alpha/\{1 + e^{\wedge} k(b - daai)\}] + Ei \quad \text{Equation 2}$$

Where Yi is the i-th observation of the cumulative loss of N-NH_3 in %, being i = 1, 2… n; daai is the i-th day after fertilization; α is the asymptotic value that can be interpreted as the maximum cumulative amount of N-NH_3 loss; b is the abscissa of the inflection point and indicates the day when the maximum loss due to volatilization occurs; k is the value that indicates the precocity index and the higher its value, the lower time needed to reach the maximum loss by volatilization (α); Ei is the random error associated with the i-th observation, which is assumed to be independent and identically distributed according to a normal distribution with mean zero and constant variance, $E \sim N(0, I\,\sigma^2)$.

To estimate the maximum daily loss (day of the maximum loss of N-NH_3), that is, to determine the inflection point of the curve, the following equation was used:

$$MDL = k \times (\alpha/4) \quad \text{Equation 3}$$

Where k is a relative index used to obtain the maximum daily loss (MDL), and α would be the asymptotic value that can be interpreted as the maximum cumulative loss of N-NH_3.

After checking for normality (Shapiro-Wilk's test) and homogeneity of variances (Bartlett's test), an analysis of variance was applied to test the influence of the N sources applied on the variables of N-NH_3 loss by volatilization, urease activity, N concentration in the leaves, and yield. The significance of the differences was evaluated at $P \leq 0.05$, and after validation of the statistical model, means were grouped by the Scott-Knott's algorithm using R software 3.3.1 (R Development Core Team, 2018).

3 Results

3.1 Weather conditions

The accumulated precipitation on the 1st, 2nd, and 3rd applications of the N fertilizer in the 2019/2020 crop season were 289, 457, and 336 mm, respectively, totalling 1082 mm. In the first seven days after each fertilization, the precipitation corresponded to 0 mm (0%), 63 mm (14%), and 159 mm (47%).

In the 2020/2021 crop season, the accumulated precipitation on the 1st, 2nd, and 3rd fertilization were 291, 280, and 336 mm, respectively, totalling 907 mm. In the first seven days after each fertilization, the precipitation corresponded to 14 mm (15%), 28 mm (10%), and 0.2 mm (0.05%). The precipitation influenced the processes related to N-NH_3 losses and we observed that lower rainfall in the first seven days after fertilization resulted in lower N-NH_3 losses.

The area under the coffee canopy, where liming and fertilizers are applied, received 30 to 40% less precipitation compared to the inter-row area, depending on the rainfall volume and intensity, plant architecture, leaf area, and development stage.

The relative air humidity was above 70% for most of the period following the N fertilization in both crop seasons. The average temperature during the same period was 22 °C, with a minimum of 18.3 °C and a maximum of 36.6 °C.

3.2 N volatilization and urease activity

3.2.1 Daily and cumulative losses of N-NH_3

Daily and cumulative losses of N-NH_3 from the three fertilizer applications in each crop year were influenced ($P \leq 0.05$) by the N fertilizer technologies. The volatilization of N-NH_3 was similar for the doses of 150 and 400 kg ha^{-1} of N. The application of U resulted in losses of 22.0% and 22.8% for these respective doses, considering the average of the two evaluated crop seasons. This means that 66 and 182 kg ha^{-1} of N were lost, respectively, at the end of six fertilizations with conventional urea (Table 1).

10.3389/fpls.2023.1291662

TABLE 1 Mean Cumulative losses of ammonia (% of the applied N), for conventional and stabilized N fertilizers, in three fertilizations in the coffee plantation, during the 2019/2020 and 2020/2021 crop seasons.

Treatment	Dose (kg ha^{-1})	Ammonia Loss (%)								Mean*	LRCCU**	N-NH_3 Loss	Avoided N-NH_3 Loss
		2019/2020 Season				2020/2021 Season							
		1[a]	2[a]	3[a]	Mean	1[a]	2[a]	3[a]	Mean	(%)		kg ha^{-1}	
Urea	150	19.8	12.6	14.6	15.7	20.2	29.4	35.4	28.3	22.0	–	66.1	–
Urea + NBPT		14.3	8.7	9.9	11.0	12.3	27.7	28.4	22.8	16.9	23.3	50.7	15.4
Ammonium nitrate		0.6	1.3	0.7	0.8	3.6	3.1	2.8	3.2	2.0	90.9	6.0	60.0
Urea	400	19.16	13.6	12.58	15.1	21.98	36.49	33.01	30.5	22.8	–	182.4	–
Urea + NBPT		17.17	10.17	7.49	11.6	18.08	31.63	34.08	27.9	19.8	13.3	158.2	24.3
Ammonium nitrate		0.74	0.28	0.25	0.4	1.19	1.51	1.73	1.5	1.0	95.8	7.6	174.8

NBPT, N-(n butyl) thiophosphoric triamide. In each crop season, 150 or 400 kg N ha^{-1} per year were split into three equal applications for conventional and stabilized N fertilizers, totaling 300 or 800 kg N ha^{-1} for both crop seasons, respectively. *Means followed by the same lowercase letter in the column do not differ by the Scott-Knott's test ($P \leq 0.05$). Mean of the six fertilization sources performed between November and February during both seasons. ** (LRCCU) Loss reduction compared to conventional urea.

TABLE 2 Adjusted regression parameters for the accumulated and maximum daily losses of N-NH_3 from conventional and stabilized N fertilizers in the 2020/2021 crop season.

Treatment	Split Fertilization	Crop season	Parameters				MDL
			α	b	k	R^2	
			Maximum NH_3 Loss	Day of the Maximum Loss			(kg)
–		2020/2021	**150 kg ha^{-1} of N**				
Urea	1		19.14	2.76	0.62	0.96	2.97
	2		28.79	1.91	1.23	0.99	8.85
	3		33.60	1.77	1.15	0.97	9.66
Ammonium Nitrate	1		3.52	9.49	0.45	0.99	0.40
	2		2.93	8.75	0.19	0.94	0.14
	3		2.64	8.24	0.21	0.97	0.14
Urea + NBPT	1		13.15	6.86	0.40	0.99	1.32
	2		25.62	3.48	0.71	0.97	4.55
	3		27.09	3.28	0.67	0.98	4.54
–			**400 kg ha^{-1} of N**				
Urea	1		21.48	4.07	0.58	0.99	3.11
	2		35.66	2.49	0.89	0.99	7.93
	3		32.26	3.08	0.73	0.99	5.89
Ammonium Nitrate	1		1.26	11.40	0.22	0.97	0.07
	2		1.29	4.30	0.23	0.89	0.07
	3		1.77	12.90	0.16	0.98	0.07
Urea + NBPT	1		17.83	5.08	0.57	0.99	2.54
	2		30.31	2.82	0.84	0.99	6.37
	3		33.09	4.14	0.50	0.98	4.14

α: Asymptotic value (percentage of the estimated maximum accumulated loss); b: Day when the maximum ammonia loss occurs; k: relative index; MDL (maximum daily loss of ammonia); and NBPT, N-(n butyl) thiophosphoric triamide.

10.3389/fpls.2023.1291662

TABLE 3 Adjusted regression parameters for the cumulative and maximum daily losses of N-NH_3 from conventional and stabilized N fertilizers in the 2019/2020 crop season.

Treatment	Split Fertilization	Crop season	Parameters				MDL
			α	b	k	R^2	
			Maximum NH_3 Loss	Day of the Maximum Loss			(kg)
–		2019/2020	**150 kg ha^{-1} of N**				
Conventional Urea	1		19.66	3.87	0.57	0.99	2.80
	2		12.14	1.79	1.22	0.98	3.70
	3		14.29	1.40	2.06	0.99	7.36
Ammonium Nitrate	1		0.55	7.31	0.35	0.98	0.05
	2		1.28	4.59	0.15	0.97	0.05
	3		0.61	7.20	0.19	0.96	0.03
Urea + NBPT	1		14.15	5.64	0.62	0.99	2.19
	2		8.29	3.07	1.06	0.99	2.20
	3		9.57	1.90	1.81	0.99	4.33
–			**400 kg ha^{-1} of N**				
Conventional Urea	1		18.82	4.07	0.60	0.99	2.82
	2		13.16	2.55	1.00	0.98	3.29
	3		12.32	1.88	1.66	0.99	5.11
Ammonium Nitrate	1		0.73	5.76	0.51	0.98	0.09
	2		0.26	8.28	0.18	0.96	0.01
	3		0.23	6.90	0.21	0.96	0.01
Urea + NBPT	1		16.84	6.15	0.49	0.99	2.06
	2		9.81	3.46	0.78	0.98	1.91
	3		7.28	2.04	1.31	0.98	2.38

α: Asymptotic value (percentage of the estimated maximum accumulated loss); b: Day when the maximum ammonia loss occurs; k: relative index; MDL (maximum daily loss of ammonia); and NBPT, N-(n butyl) thiophosphoric triamide.

U_{NBPT} reduced N-NH_3 losses compared to U. Average losses of 16.9% and 19.8% were observed for doses of 150 and 400 kg ha^{-1} of N supplied by this stabilized source with a urease inhibitor additive. This reduction in volatilization prevented the loss of 15.9 and 24.3 kg ha^{-1} of N, respectively, compared to U (Table 2). As for AN, N-NH_3 losses did not exceed 1% of the applied dose, regardless of the weather conditions at the time of the fertilization. This reduction in volatilization was 90.9 and 95.8% lower, respectively, preventing losses of 60 and 174.8 kg ha^{-1} of N compared to conventional urea (Table 1).

In the 2019/2020 crop season, the maximum daily N-NH_3 volatilization for U occurred 1.4 (7.36 kg ha^{-1} of N) and 1.88 (5.11 kg ha^{-1} of N) days after the application of 150 and 400 kg ha^{-1} of N. For AN, the maximum daily losses of 0.05 and 0.09 kg ha^{-1} of N occurred 7.31 and 5.76 days after the fertilization, respectively. For urea stabilized with NBPT, the maximum daily losses of 4.33 and 2.38 kg ha^{-1} of N occurred at 1.9 and 2.04 days after fertilization, respectively (Table 3).

In the 2020/2021 crop season, the maximum daily loss for U occurred 1.77 and 3.11 days after the N fertilization, with 9.66 and 4.07 kg ha^{-1} of N, respectively. For AN, the maximum daily loss occurred 9.49 and 12.90 days after fertilization, with similar volatilization to the first season (less than 0.5 kg ha^{-1} of N). U_{NBPT} presented maximum losses at 3.48 and 2.82 days, with the volatilization of 4.55 and 6.37 kg ha^{-1} of N, respectively (Table 2).

The average cumulative loss of N-NH_3 in the 2019/2020 and 2020/2021 crop seasons (considering the divided application of the N fertilizer) for the dose of 150 kg ha^{-1} of N decreased as follows: U (15.7%) > U_{NBPT} (11%) > AN (0.8%); and U (28.3%) > U_{NBPT} (22.8%) > AN (3.2%), respectively (Table 1).

Considering the dose of 400 kg ha^{-1} of N, the losses decreased as follows: U (15.1%) > U_{NBPT} (11.6%) > AN (0.4%); U (30.5%) > U_{NBPT} (27.9%) > AN (1.5%), respectively for the two crop seasons (Table 1).

During the first seven days, losses for the 150 kg ha^{-1} of N dose were: 14.4% > 9.08% > 0.48% (2019/2020) and 25.74% > 17.50% > 1.10% (2020/2021). For the 400 kg ha^{-1} N dose, these losses were 13.35% > 8.69% > 0.27% (2019/2020) and 26.96% > 22.42% > 0.61% (2020/2021). That is, for U, 88 to 92% of the cumulative N-NH_3 losses occurred in the first week after fertilizer application in both crop seasons, while for U_{NBPT} accumulated losses ranged from 75 to 82%. For AN, on average, 50% of the cumulative volatilized N occurred in the first week, not exceeding 0.6% of the applied fertilizer dose (Tables 3, 2).

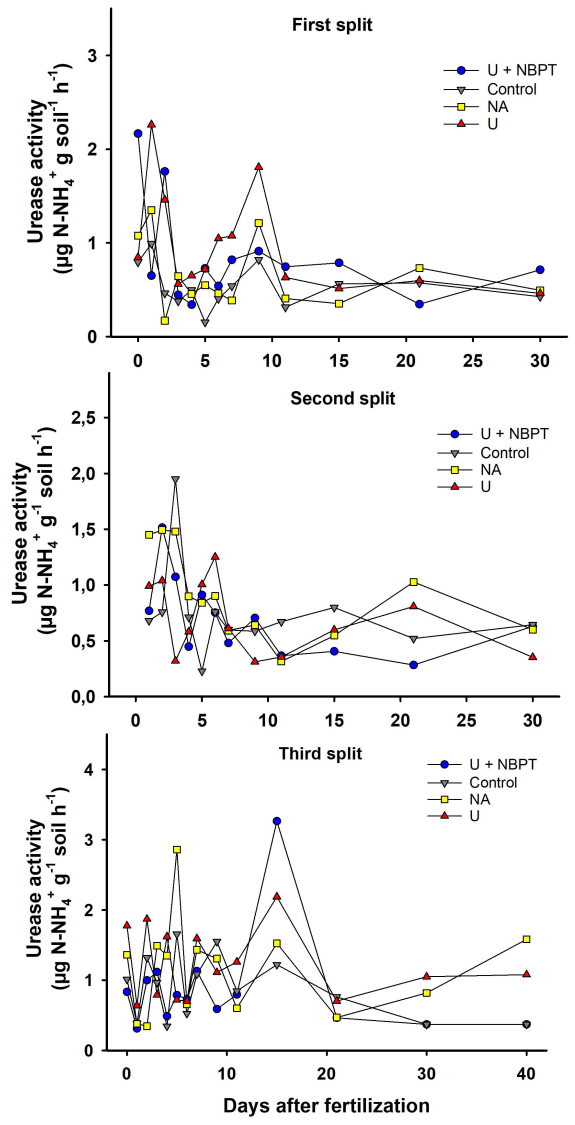

FIGURE 4
Soil urease activity after N fertilizer application with split fertilization (0 and 400 kg ha^{-1} of N) in coffee plantation.

3.2.2 Urease activity

Urease activity was higher on days of maximum NH_3 volatilization. In general, the following sequence for the treatments was observed: U > U_{NBPT} > AN, despite some variations that are common for these factors (Figure 4). U_{NBPT} reduced the urease activity, proving that the additive associated with the fertilizer prolonged the urea hydrolysis due to the enzymatic inhibition that resulted in a decrease in N-NH_3 losses presented in item 3.2.

3.3 Microbiological attributes

There was an effect of the N sources (NS), soil sampling time (ST), and their interaction (NS × ST) on the MBN and arylsulfatase activity. The N sources also influenced the MBC and the metabolic quotient (qCO_2).

In general, the soil showed high biological quality. The average content of N in the soil microbial biomass was higher after the N fertilization (average MBN = 644 µg N g^{-1} of dry soil), and the U_{NBPT} stood out (1681 µg N g^{-1} of dry soil) (Figure 5A). The MBN of this treatment before the fertilization (45 µg N g^{-1} of dry soil) was lower than the control without N fertilization (216 µg N g^{-1} of dry soil) and in the soil fertilized with conventional urea (354 µg N g^{-1} of dry soil). Soil microbial C content varied significantly with the N sources only before the fertilization (48 to 430 µg C g^{-1} of dry soil), where it decreased in the following order: U_{NBPT} = control > ammonium nitrate > conventional urea (Figure 5B). The sampling time did not interfere with the MBC in the control and urea + NBPT treatments.

The average SBR was 12 mg C-CO_2 kg^{-1} dry soil h^{-1}. The results of basal respiration of the N fertilizers remained equivalent to the control treatment in both sampling times (Figure 5C). Conversely, the soil fertilized with conventional urea had the highest qCO_2 before the fertilization (Figure 5D). This result is directly related to the low microbial carbon identified in the initial sampling (48 µg C g^{-1} dry soil). The high qCO_2 with conventional urea (321 µg h^{-1} C-CO_2 µg^{-1} C-mic) represents about seven times the average of the other treatments for the same sampling time. However, this effect was not observed in the qCO_2 after fertilization, where the result with conventional urea was statistically similar to the other treatments (Figure 5D), thus indicating the variability of these parameters.

The activities of β-glucosidase and acid phosphatase were not influenced by the addition of the N fertilizers in either of the soil sampling. High levels of p-nitrophenol (PNP), which reflect the enzymatic activity, were observed in both sampling times. For β-glucosidase (Figure 6A), PNP activity ranged from 3780 to 4970 µg PNP g^{-1} of dry soil before the fertilization and from 2260 to 4550 µg PNP g^{-1} of dry soil after the fertilization. For acid phosphatase (Figure 6B), PNP activity ranged from 660 to 1538 µg PNP g^{-1} of dry soil before fertilization and from 620 to 1405 µg PNP g^{-1} of dry soil after fertilization.

The arylsulfatase activity before fertilization was higher in the soil with NBPT, while the other N sources did not differ significantly in the first sampling time (Figure 6C). After fertilization, the control results were superior, especially compared to the conventional urea, which represented only 18% of the total activity of the treatment without N fertilization. There was a significant decrease in arylsulfatase activity between the samplings, with reductions of 45%, 69%, and 77% in the levels of p-nitrophenol (PNP) immediately after fertilization with ammonium nitrate, urea + NBPT, and conventional urea, respectively.

3.4 N content in the beans and leaves

The total N content in the beans of the 2019/2020 and 2020/2021 crop seasons were not influenced ($P \leq 0.05$) by the isolated effect of the N doses and sources, and there was no significance ($P \leq 0.05$) for the interaction between these factors (Table 4). The average N content was 2.6% in the beans and 1.6% in the husk,

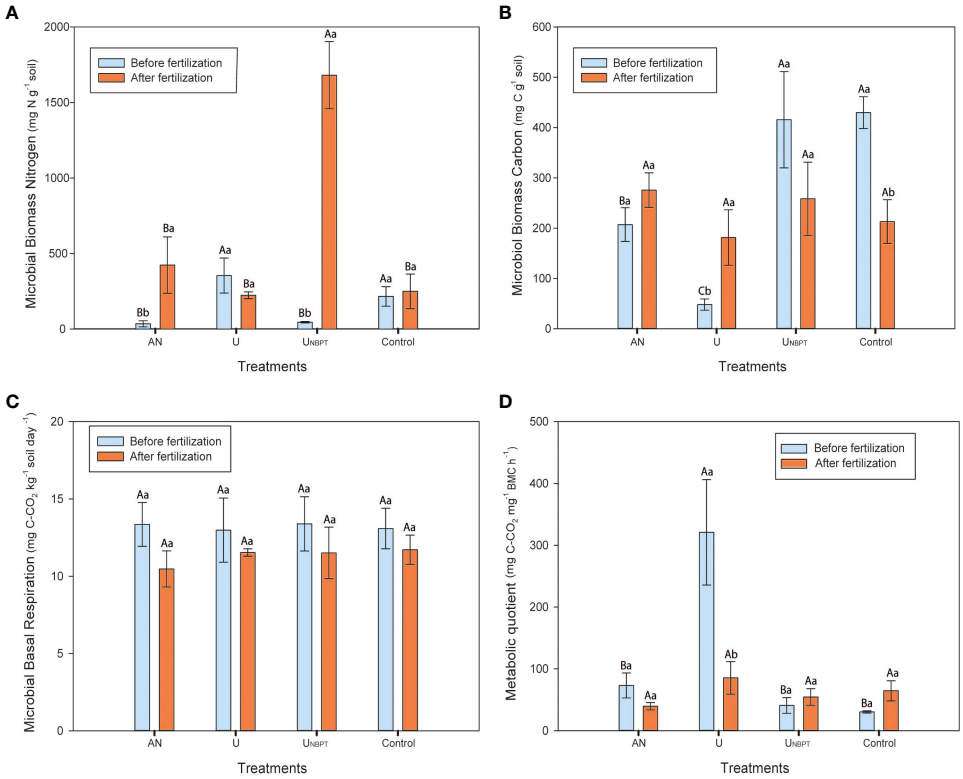

FIGURE 5
Microbial biomass nitrogen **(A)** and carbon **(B)**; soil basal respiration **(C)**; and metabolic quotient **(D)** as a function of the N sources (ammonium nitrate, conventional urea, urea + N-(n-butyl) thiophosphoric triamide (NBPT), and control without mineral N fertilization for six years), for the doses 0 and 400 kg ha^{-1} of N, and soil sampling time (samples 1 and 2). Means followed by the same uppercase letter between N sources and lowercase letter between soil sampling time do not differ statistically by Scott-Knott's and F tests ($P \leq 0.05$), respectively. Standard error bar; mean of four replicates.

while the average bean/husks ratio is 1:1, despite the cultivar or productive load.

The average N content in the leaves (30 mg kg^{-1}) of the samples collected during the green cherry stage was not influenced ($P \leq 0.05$) by the isolated effect of the N doses and sources. There was also no significance ($P \leq 0.05$) for the interaction between these factors (Table 5), which is explained by the high levels of N present in the soil.

The extraction and export of N by coffee plants depends on the crop's productivity and vegetation intensity, which vary in accordance with the biennial nature of the crop and annual soil and climate conditions.

3.5 Yield

Treatments did not lead to different yields ($P \leq 0.05$) in the 2019/2020 crop season. For the 2020/2021 crop season, there was a significant effect ($P \leq 0.05$) of the N sources within the dose of 525 kg ha^{-1}, with AN being higher than U and U_{NBPT} (Table 6).

In both seasons, no relationship was observed between the amount of N lost by volatilization and yield, meaning that yield was not affected even in the treatments that showed higher losses by volatilization (Table 6).

4 Discussion

4.1 Weather conditions, N-NH_3 volatilization and urease activity

In this study, the climatic conditions, especially precipitation and temperature, directly influenced the losses of N-NH_3 by volatilization. In both coffee seasons, most of the N-NH_3 losses occurred during the first seven days after the split application of the N fertilizers. The precipitation during these first days was essential to incorporate the fertilizer into the soil and reduce the N-NH_3.

Rainfall, depending on the volume and intensity, enables the incorporation of the N fertilizer into the soil (Dawar et al., 2011). Higher rainfall volume and intensity are usually associated with better fertilizer incorporation and, consequently, lower losses by volatilization. The lower precipitation volume immediately after the application of the fertilizers on the soil hindered the incorporation of the N and favored N-NH_3 losses. Thus, our results indicated that relying solely on environmental conditions for fertilizer incorporation increases the risk of N losses and, consequently, lead to the low efficiency of the fertilization.

Moreover, the architecture of the coffee plant obstructs the direct incidence of rainfall that would incorporate the N fertilizer applied under the canopy. Additionally, the presence of plant residues on the soil also acts as a barrier to fertilizer

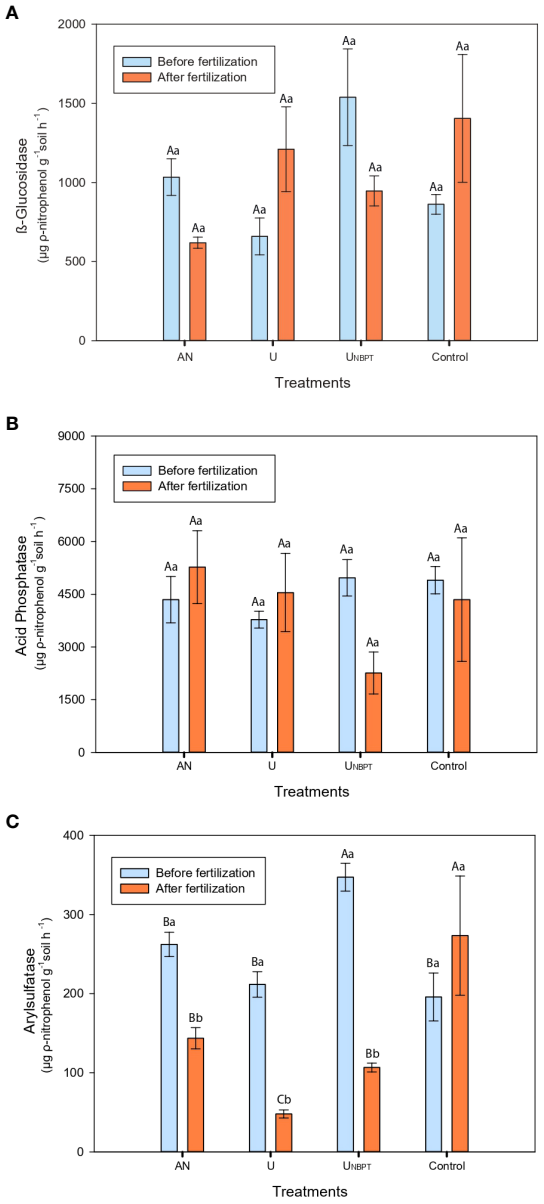

FIGURE 6
Enzymatic activity of β-glucosidase **(A)**, acid phosphatase **(B)**, and arylsulfatase **(C)** as a function of N sources (ammonium nitrate, conventional urea, urea + N-(n-butyl) thiophosphoric triamide (NBPT), and control with no mineral N-fertilization for six years), for the doses 0 and 400 kg ha^{-1} of N, and soil sampling time (sampling 1 and 2). Means followed by the same uppercase letter among nitrogen sources and lowercase letter among soil sampling time do not differ statistically by Scott-Knott's and F tests ($P \leq 0.05$), respectively. Standard error bars; mean of four replicates. PNP = ρ-nitrophenol.

incorporation and creates a favorable environment for volatilization due to the high concentration of urease. The low concentration of NBPT demonstrated by chromatography analysis, as mentioned, may often not be sufficient to inhibit urease activity, resulting in daily N-NH_3 losses similar to those observed for conventional urea.

Ammonium nitrate is a widely used N fertilizer in Brazilian coffee cultivation. In this study, the use of this fertilizer reduced over 90% of the N-NH_3 losses in both crop seasons. The insignificant loss of N-NH_3 for this N source is related to its acid to neutral reaction in the soil, especially at pH< 7. Another positive aspect is that these fertilizers do not depend on weather conditions at the time of application (Freitas et al., 2022; de Souza et al., 2023). Therefore, ammonium nitrate can be a strategic option for N fertilization in coffee cultivation systems. Conversely, amidic N is reported as the most susceptible to N-NH_3 losses and represents an average of 30% of the N applied in coffee cultivation areas in Brazil (Chagas et al., 2016; Dominghetti et al., 2016; Silva et al., 2017). This means that for every three fertilizer applications, approximately one is lost due to volatilization. For an average annual fertilization of 845 kg of urea per hectare (380 kg of N ha^{-1}), 254 kg of urea per hectare (114 kg of N ha^{-1}) are lost. This currently corresponds to a financial loss of US$ 228 per hectare (FL= average annual loss of N-NH_3 x average value per kg N-fertilizer), considering US$897 as the recent average value per ton of fertilizer. For ammonium nitrate, these losses rarely exceed 1%, an amount that is probably emitted by the soil, which justifies the greater retention and storage of N in soil fertilized in the correct dose, time, and location.

4.2 Microbial and enzymatic activity

The soil microbiological attributes indicated high biological quality for this adequately fertilized scenario of productive coffee farming. The results demonstrate that soil sampling over time (before or after fertilization) can identify different levels of microbial activity, highlighting spatial and temporal variability for soil quality indicators. These indicators are not always related to the fertilization carried out in that crop season, but to the fertility management adopted over several years that favor microbial resilience and sustainability of the productive system.

These enzymes are related to the carbon (β-glucosidase) and phosphorus (phosphatases) biocycles and are an indicator of soil quality (Gil-Sotres et al., 2005; Moreira and Siqueira, 2006; Bastida et al., 2008).

The abundance of this enzyme in the soil is an indicator of a high rate of organic sulfur mineralization and high fungal biomass, which is the main producer of soil sulfate esters (Dick et al., 1996).

Some factors such as soil texture, organic matter, moisture, and oxygen affect the survival of microorganisms (Zantua and Bremner, 1977; Burns, 1982; Flores-Rentería et al., 2020) and, consequently, the level of microbial and enzymatic activity. Thus, soil biological quality indicators have little contribution to decision-making regarding short-term agronomic management of coffee crops, and the results reflect the management adopted for several years, necessary for significant changes to occur in C stocks (Sarkis et al., 2021), soil profile building for adequate plant development, organic residue input, and physical, chemical, and biological balance of the soil.

4.3 N content in the beans, N content in the leaves, and N exportation by the beans

The N content in coffee beans is a physiological characteristic of the plants themselves, independent of the cultivar (Table 5). The

green cherry stage is the time of highest plant demand (Prieto Martinez et al., 2003) and this plants redistributes the stored N to the fruits, maintaining these levels almost constant, regardless of the productive load. In addition to the N exported by the processed coffee and the absorption necessary for plant growth (Table 4), a large amount of N is removed from the system by the husk of the harvested fruits, which represents approximately 50% of the harvested fruit weight (Tables 4, 5). Is emphasized that the exceeding doses of N applied in coffee plantations results in a $N_{mineral}$ movement from the surface to the subsurface (N loss by leaching) despite the source of the fertilizer (Sarkis et al., 2023). Cannavo et al. (2013) also observed that the addition of large amounts of N fertilizer every year in this system led to a soil N saturation and a high potential of N losses through NO_3^-.

4.4 Yield

In the experiment, the reduction in ammonia volatilization did not influence crop yield. Other authors reported that N volatilization, in the form of NH_3, does not limit production (Chagas et al., 2016). This may be explained by the amount of N applied as fertilizer being more than sufficient for plant growth. The biennial cycle of coffee, with one year being more productive than the following, can make difficult the observation of the effects of treatments on yield. Furthermore, the N stock in the soil organic matter should be taken into account, as it can compensate for the N lost through volatilization in conventional fertilizers, providing a good short-term productivity for the crop. However, over time, there may be a reduction in the N stocks due to lower N retention in the soil. The lower N-NH_3 losses from the use of AN can increase the average mineral N content by 50% when compared to urea and U_{NBPT} (Sarkis et al., 2021).

5 Conclusions

Our study showed that N fertilizer technologies are interesting options for reducing N-NH_3 losses by volatilization, increasing N retention in the soil, and the sustainability of coffee production systems. U_{NBPT} inhibited urease activity in the soil and reduced N-NH_3 losses compared to conventional urea, but it is not the most strategic option in the context of coffee farming because it depends on the volume and intensity of rain to incorporate the fertilizer after the fertilization. Regardless of the weather conditions, AN lost less than 1% of N by volatilization, being the safest option for N fertilization efficiency in coffee production. This characteristic is especially advantageous considering the specific microclimate in the projection of plant canopies that hinders the incorporation of the fertilizers by the direct incidence of rainfall. Thus, AN is the source that contributes the most to increasing soil N stocks and supplying the demands of the vegetative and reproductive stages of the coffee plants. Soil microbial and enzymatic activity indicated high biological quality for this appropriately fertilized productive coffee farming.

TABLE 4 N content in the beans (%) and N export per bag of processed coffee (kg N bag^{-1}) for conventional and stabilized N fertilizers in a coffee plantation, during the 2019/2020 and 2020/2021 crop seasons.

Source	Dose	*N content in the bean (%)		Ept (kg N ha^{-1})		Ept (kg N bag^{-1})	
		2019/2020	2020/2021	2019/2020	2020/2021	2019/2020	2020/2021
AN	0	1.4	2.1	35.6	9.6	0.8	1.3
	150	2.3	2.6	87.6	21.8	1.4	1.6
	275	2.4	2.7	118.7	24.1	1.4	1.6
	400	2.6	2.5	148.2	20.5	1.6	1.5
	525	2.6	2.6	132.9	61.6	1.6	1.6
U	0	1.4	2.1	35.6	9.6	0.8	1.3
	150	2.4	2.4	78.5	26.1	1.4	1.4
	275	2.4	2.5	114.0	18.1	1.4	1.5
	400	2.6	2.4	135.6	22.7	1.6	1.4
	525	2.6	2.4	126.8	36.7	1.6	1.4
U_{NBPT}	0	1.4	2.1	35.6	9.6	0.8	1.3
	150	2.3	2.5	108.2	19.0	1.4	1.5
	275	2.5	2.5	121.7	19.3	1.5	1.5
	400	2.5	2.6	118.1	25.3	1.5	1.6
	525	2.6	2.6	116.2	26.2	1.6	1.6

NBPT, N-(n butyl) thiophosphoric triamide; Ept: N export per bag of processed coffee. In each crop season, 150 or 400 kg N ha^{-1} per year were split into three equal applications for conventional and stabilized N fertilizers, totaling 300 or 800 kg N ha^{-1} for both crop seasons, respectively. *Means did not differ by the Scott-Knott's test ($P \leq 0.05$).

10.3389/fpls.2023.1291662

TABLE 5 Percentage of beans and husks, and N content in the beans of different coffee cultivars at full productive potential, harvested during the 2020/2021 crop seasons.

	Coffee fruits		N content	
	Beans	Husks	Beans	Husks
Cultivar	%		%	
Bourbom Amarelo	53	47	2.6	1.6
Catiguá-MG2	44	56	2.5	1.4
Topázio Amarelo	50	50	2.4	1.4
Acaiá	43	57	2.7	1.9
Arara	47	53	2.6	1.8
Mundo Novo	49	51	2.8	1.6
Catuaí Amarelo	48	52	2.7	1.5
Catuaí 99	50	50	2.5	1.5
NIST standard	–	–	100	100

NIST, International standard for validation of foliar analysis.

TABLE 6 Coffee bean yield (bags ha^{-1}) according to the interaction between the N sources and N doses during the 2019/2020 and 2020/2021 crop seasons.

Sources	Crop season/Doses (kg N ha^{-1})				
	0	150	275	400	525
	2020				
AN	42.4 A	63.5 A	82.4 A	95.0 A	85.2 A
U	42.4 A	54.5 A	79.2 A	86.9 A	81.3 A
U_{NBPT}	42.4 A	78.4 A	81.1 A	78.7 A	74.5 A
	2021				
AN	7.65 A	14.00 A	14.87 A	13.64 A	39.47 A
U	7.65 A	18.10 A	12.08 A	15.75 A	25.46 B
U_{NBPT}	7.65 A	12.64 A	12.88 A	16.19 A	16.82 B

AN, Ammonium nitrate; U_{NBPT}, urea + N-(n-butyl) thiophosphoric triamide (NBPT). Uppercase letters cluster sources (with four replications each of each one of the doses) according to the Scott-Knott's test.

Although indicators of soil biological quality have been widely discussed in recent scientific publications, our results indicated that these guidelines have done little to aid decision-making regarding agronomic management of coffee crop, reflecting the management practices adopted for several years that have resulted in the accumulation of organic carbon, development of soil profile for adequate plant growth, organic residue input and maintenance of physical, chemical, and biological balance of the soil.

Data availability statement

The original contributions presented in the study are included in the article/Supplementary Materials. Further inquiries can be directed to the corresponding author.

Author contributions

LS: Conceptualization, Data curation, Formal analysis, Investigation, Methodology, Writing – original draft, Writing – review & editing. MD: Conceptualization, Data curation, Formal analysis, Investigation, Methodology, Writing – original draft. DO: Conceptualization, Data curation, Formal analysis, Investigation, Methodology, Writing – original draft. TF: Conceptualization, Data curation, Formal analysis, Methodology, Writing – original draft. TS: Writing – review & editing, Conceptualization, Validation, Investigation, Resources. VRB: Writing – review & editing, Conceptualization, Validation, Investigation, Resources. DG: Conceptualization, Data curation, Funding acquisition, Investigation, Methodology, Project administration, Supervision, Visualization, Writing – original draft, Writing – review & editing.

Funding

The author(s) declare financial support was received for the research, authorship, and/or publication of this article. This work was supported by the Yara International, National Council for Scientific Development and Technology, the Agency for Improvement of Higher-Level Personnel and Minas Gerais Research Foundation.

Conflict of interest

The authors declare that the research was conducted in the absence of any commercial or financial relationships that could be construed as a potential conflict of interest.

Publisher's note

Supplementary material

The Supplementary Material for this article can be found online at: https://www.frontiersin.org/articles/10.3389/fpls.2023.1291662/full#supplementary-material

SUPPLEMENTARY FIGURE 1
Photographs of the conventional fertilizers: urea **(A)**; ammonium nitrate **(B)**, and NBPT stabilized urea **(C)**.

References

Adotey, N., Kongchum, M., Li, J., Whitehurst, G. B., Sucre, E., and Harrell, D. L. (2017). Ammonia volatilization of zinc sulfate-coated and NBPT-treated urea fertilizers. *Agron. J.* 109, 2918–2926. doi: 10.2134/agronj2017.03.0153

Afshar, R. K., Lin, R., Assen, Y. M., and Chen, C. (2018). Agronomic effects of urease and nitrification inhibitors on ammonia volatilization and nitrogen utilization in a dryland farming system: Field and laboratory investigation. *J. Clean. Prod* 172, 4130–4139. doi: 10.1016/j.jclepro.2017.01.105

Anderson, T. H., and Domsch, K. H. (1993). The metabolic quotient for CO2 (qCO2) as a specific activity parameter to assess the effects of environmental conditions, such as pH, on the microbial biomass of forest soils. *Soil Biol. Biochem.* 25, 393–395. doi: 10.1016/0038-0717(93)90140-7

Aragão, O. O. S., Oliveira-Longatti, S. M., Caputo, P. S. C., Rufini, M., Carvalho, G. R., Carvalho, T. S., et al. (2020). Microbiological indicators of soil quality are related to greater coffee yield in the Brazilian Cerrado region Ecol. *Indic* 113, 106205. doi: 10.1016/j.ecolind.2020.106205

Azeem, B., Kushaari, K., Man, Z. B., Basit, A., and Thanh, T. H. (2014). Review on materials & methods to produce controlled release coated urea fertilizer. *J. Control Release.* 181, 11–21. doi: 10.1016/j.jconrel.2014.02.020

Bastida, F., Zsolnay, A., Hernandez, T., and Garcia, C. (2008). Past, present and future of soil quality indices: a biological perspective. *Geoderma* 147, 159–171. doi: 10.1016/j.geoderma.2008.08.007

Bouyoucos, G. J. (1951). A recalibration of the hydrometer method for making mechanical analysis of soils. *Agron. J.* 43, 434–438. doi: 10.2134/agronj1951.00021962004300090005x

Bremner, J. M. (1996). "Nitrogen total," in *Methods of Soil Analysis. Part 3*. Ed. D. L. Sparks (Madison: ASA), 1085e1121.

Burns, R. (1982). Enzyme activity in soil: location and a possible role in microbial ecology. *Soil Biol. Biochem.* 14, 423–427. doi: 10.1016/0038-0717(82)90099-2

Byrne, M. P., Tobin, J. T., Forrestal, P. J., Danaher, M., Nkwonta, C. G., Richards, K., et al. (2020). Urease and nitrification inhibitors—As mitigation tools for greenhouse gas emissions in sustainable dairy systems: A review. *Sustainability* 12 (15), 6018. doi: 10.3390/su12156018

Cai, H., and Akiyama, Y. (2017). Effects of inhibitors and biochar on nitrous oxide emissions, nitrate leaching, and plant nitrogen uptake from urine patches of grazing animals on grasslands: a meta-analysis. *Soil Sci. Plant Nutr.* 4, 405–414. doi: 10.1080/00380768.2017.1367627

Cannavo, P., Harmand, J.-M., Zeller, B., Vaast, P., Ramírez, J. E., and Dambrine, E. (2013). Low nitrogen use efficiency and high nitrate leaching in a highly fertilized Coffea arabica–Inga densiflora agroforestry system: a 15N labeled fertilizer study. *Nutrient Cycling Agroecosys.* 95, 377–394. doi: 10.1007/s10705-013-9571-z

Cantarella, H., Otto, R., Soares, J., and Silva, A. G. B. (2018). Agronomic efficiency of NBPT as a urease inhibitor: A review. *J. Adv. Res.* 13, 19–27. doi: 10.1016/j.jare.2018.05.008

Chagas, W. F. T., Guelfi, D. R., Caputo, A. L. C., Souza, T. L., Andrade, A. B., and Faquin, V. (2016). Ammonia volatilization from blends with stabilized and controlled-released urea in the coffee system. *Ciênc. Agrotec.* 40, 497–509. doi: 10.1590/1413-70542016405008916

Chien, S. H., Prochnow, L. I., and Cantarella, H. (2009). Recent developments of fertilizer production and use to improve nutrient efficiency and minimize environmental impacts. *Adv. Agron.* 102, 267–322. doi: 10.1016/S0065-2113(09)01008-6

Costa, M. C. G., Vitti, G. C., and Cantarella, H. (2003). N-NH_3 losses from nitrogen sources applied over unburned sugarcane straw. *Rev. Bras. Cienc. Solo* 27, 631–637. doi: 10.1590/S0100-06832003000400007

Dawar, K., Zaman, M., Rowarth, J. S., Blennerhassett, J., and Turnbull, M. H. (2011). Urea hydrolysis and lateral and vertical movement in the soil: Effects of urease inhibitor and irrigation. *Biol. Fertil. Soils* 47, 139–146. doi: 10.1007/s00374-010-0515-3

Development Core Team R (2018). *R: a language and environment for statistical computing* (Vienna, Austria: R Found. Stat. Comput).

Dick, R. P., Breakwell, D. P., and Turco, R. F. (1996). "Soil enzyme activities and biodiversity measurements as integrative microbiological indicators," in *Methods for Assessing Soil Quality*, Eds. J. W. Doran and A. J. Jones (Madison: Soil Science Society of America), 247–272.

Dominghetti, A. W., Silva, D. R. G., Guimarães, R. J., Caputo, A. L. C., Spehar, C. R., and Faquin, V. (2016). Nitrogen loss by volatilization of nitrogen fertilizers applied to coffee orchard. *Cienc. e Agrotecnol.* 40, 1–11. doi: 10.1590/1413-70542016402029615

Doran, J. W., and Parkin, T. B. (1994). Defining and assessing soil quality," In: Doran, J. W., Coleman, D. C., Bezdicek, D. F., and Stewart, B. A. (eds). *Defining soil quality for a sustainable environment*, vol 35. (Madison, WI: Soil Science Society of America), pp 3–21. doi: 10.2136/sssaspecpub35.c1

European Committee for Standardization (2008) *Fertilizers-Determination of urease inhibitor N-(n-butyl) thiophosphoric triamide (NBPT) using high performance liquid chromatography (HPLC)*. Available at: https://infostore.saiglobal.com/preview/is/en/2015/i.s.en1665.12015.pdf (Accessed August 2021).

FAOSTAT. (2021). *Food and Agricultural Organization of the United Nations. Fertilizer by nutrients*. Available at: http://www.fao.org/faostat/en/#data/RFN (Accessed 1 mar. 2022).

Flores-Rentería, D., Sánchez-Gallén, I., Morales-Rojas, D., Larsen, J., and Álvarez-Sánchez, J. (2020). Changes in the abundance and composition of a microbial community associated with land use change in a Mexican tropical rain forest. *J. Soil Sci. Plant Nutr* 20, 1144–1155. doi: 10.1007/s42729-020-00200-6

Freitas, T., Bartelega, L., Santos, C., Dutra, M. P., Sarkis, L. F., Guimarães, R. J., et al. (2022). Technologies for fertilizers and management strategies of N-fertilization in coffee cropping systems to reduce ammonia losses by volatilization. *Plants* 11, 3323. doi: 10.3390/plants11233323

Gil-Sotres, F., Trasar-Cepeda, C., Leirós, M. C., and Seoane, S. (2005). Different approaches to evaluating soil quality using biochemical properties. *Soil Biol. Biochem.* 37, 877–887. doi: 10.1016/j.soilbio.2004.10.003

Guelfi, D. (2017). Fertilizantes nitrogenados estabilizados, de liberação lenta ou controlada. *Informações Agronômicas IPNI* 157, 1–14.

Heffer, P., and Prud'homme, M. (2016). "Fertilizer outlook 2016–2020," in *International Fertilizer Association (ed.) 84th IFA Annual Conference*, Fertilizer Outlook 2016-2020. (IFA: Moscow). 1–5.

Islam, K. R., and Weil, R. R. (1998). Microwave irradiation of soil for routine measurement of microbial biomass carbon. *Biol. Fert. Soils* 27, 408–416. doi: 10.1007/s003740050

Kjeldahl, J. (1883). Neue methode zur bestimmung des stickstoffs in organischen Körpern. *Z. F. Anal. Chemie.* 22, 366–382. doi: 10.1007/BF01338151

Lara-Cabezas, A. R., Trivelin, P. C. O., Bendassolli, J. A., Santana, D. G., and Gascho, G. J. (1999). Calibration of a semi-open static collector for determination of ammonia volatilization from nitrogen fertilizers. *Commun. Soil Sci. Plant Analysis.* 30 (3-4), 389–406. doi: 10.1080/00103629909370211

Martins, M. R., Sarkis, L. F., Sant'Anna, S. A. C., Santos, C. A., Araujo, K. E., Santos, R. C., et al. (2021). Optimizing the use of open chambers to measure ammonia volatilization in field plots amended with urea. *Pedosphere* 31, 243–254. doi: 10.1016/S1002-0160(20)60078-9

Minato, E. A., Cassim, B. M. A. R., Besen, M. R., Mazzi, F. L., Inoue, T. T., and Batista, M. A. (2020). Controlled-release nitrogen fertilizers: characterization, ammonia volatilization, and effects on second-season corn. *Rev. Bras. Ciênc. Solo*. 44, 190108. doi: 10.36783/18069657rbcs20190108

Moreira, F. M. S., and Siqueira, J. O. (2006). *Microbiologia e Bioquimica do Solo. 2nd ed.* (Lavras: Editora UFLA).

Prieto Martinez, H. E., Scherrer Menezes, J. F., Bartolomeu De Souza, R., Alvarez Venegas, V. H., and Gontijo Guimaraes, P. T. (2003). Critical nutrient ranges and evaluation of nutritional status in coffee-tree plantations of Minas Gerais. *Pesqui. Agropecu. Bras.* 38, 703–713. doi: 10.1590/s0100-204x2003000600006

Salamanca-Jimenez, A., Doane, T. A., and Horwath, W. R. (2017). Coffee response to nitrogen and soil water content during the early growth stage. *J. Plant Nutr. Soil Sci.* 180, 614–623. doi: 10.1002/jpln.201600601

Santos, C. F., Aragão, O. O. S., Silva, D. R. G., Jesus, E. C., Chagas, W. F. T., Correia, O. S., et al. (2020). Environmentally friendly urea produced from the association of N-(nbutyl) thiophosphoric triamide with biodegradable polymer coating obtained from a soybean processing byproduct. *J. Clean. Prod.* 276, 1–13. doi: 10.1016/j.jclepro.2020.123014

Santos, C. F., Nunes, A. P. P., Aragão, O. O. S., Guelfi, D., Souza, A. A., Abreu, L. B., et al. (2021). Dual functional coatings for urea to reduce ammonia volatilization and improve nutrients use efficiency in a Brazilian corn crop system. *J. Soil Sci. Plant Nutr.* 21, 1591–1609. doi: 10.1007/s42729-021-00464-6

Sanz-Cobena, A., Misselbrook, T., Camp, V., and Vallejo, A. (2011). Effect of water addition and the urease inhibitor NBPT on the abatement of ammonia emission from surface applied urea. *Atmos. Environ.* 45, 1517–1524. doi: 10.1016/j.atmosenv.2010.12.051

Sarkis, L. F., Andrade, A. B., Guelfi, D., Chagas, W. F. T., Faquin, V., and Guareschi, R. F. (2021). Carbon dioxide flux of conventional and slow or controlled release nitrogen fertilizers in coffee crop. *Commun. Soil Sci. Plant Anal.* 52, 2884–2897. doi: 10.1080/00103624.2021.1971690

Sarkis, L. F., Dutra, M. P., Santos, C. A., Alves, B. J. R., Urquiaga, S., and Guelfi, D. (2023). Nitrogen fertilizers technologies as a smart strategy to mitigate nitrous oxide emissions and preserve carbon and nitrogen soil stocks in a coffee crop system. *Atmosph. environ.: X Anal.* 20, 100224. doi: 10.1016/j.aeaoa.2023.100224

Sha, Z., Lv, T., Staal, M., Ma, X., Wen, Z., Li, Q., et al. (2020). Effect of combining urea fertilizer with P and K fertilizers on the efficacy of urease inhibitors under different storage conditions. *J. Soils Sediments.* 20, 2130–2140. doi: 10.1007/s11368-019-02534-w

Silva, A. G. B., Sequeira, C. H., Sermarini, R. A., and Otto, R. (2017). Urease inhibitor NBPT on ammonia volatilization and crop productivity: a meta-analysis. *Agron. J.* 109, 1–13. doi: 10.2134/agronj2016.04.0200

Snyder, C. S. (2017). Enhanced nitrogen fertiliser technologies support the '4R' concept to optimise crop production and minimise environmental losses. *Soil Res.* 55, 463–472. doi: 10.1071/SR16335

Soares, J. R., Cantarella, H., and Menegale, M. L. C. (2012). Ammonia volatilization losses from surface-applied urea with urease and nitrification inhibitors. *Soil Biol. Biochem.* 52, 82–89. doi: 10.1016/j.soilbio.2012.04.019

Soil Survey Staff (2018). *Official Soil Series Descriptions* (Washington, D.C: USDA-NRCS).

de Souza, T. L., de Oliveira, D. P., Santos, C. F., Reis, T. H. P., Cabral, J. P. C., da Silva Resende, É. R., et al. (2023). Nitrogen fertilizer technologies: Opportunities to improve nutrient use efficiency towards sustainable coffee production systems. *Agric. Ecosyst. Environ.* 345, 108317. doi: 10.1016/j.agee.2022.108317

Tabatabai, M. A., and Bremner, J. M. (1972). Assay of urease activity in soils. *Soil Biol. Biochem.* 4, 479e487. doi: 10.1016/0038-0717(72)90064-8

Timilsena, Y. P., Adhikari, R., Casey, P., Muster, T., Gill, H., and Adhikari, B. (2015). Enhanced efficiency fertilisers: a review of formulation and nutrient release patterns. *J. Sci. Food Agric.* 95, 1131–1142. doi: 10.1002/jsfa.6812

Vance, E. D., Brooks, P. C., and Jenkinson, D. S. (1987). An extraction method for measuring soil microbial biomass C. *Soil Biol. Biochem.* 19, 703–707. doi: 10.1016/0038-0717(87)90052-6

Zantua, M. I., and Bremner, J. M. (1977). Stability of urease in soils. *Soil Biol. Biochem.* 9, 135–140. doi: 10.1016/0038-0717(77)90050-5

Zhang, X., Zou, T., Lassaletta, L., Mueller, N. D., Tubiello, F. N., Lisk, M. D., et al. (2021). Quantification of global and national nitrogen budgets for crop production. *Nat. Food* 2, 529–540. doi: 10.1038/s43016-021-00318-5

frontiers | Frontiers in Plant Science

TYPE Original Research
PUBLISHED 11 December 2023
DOI 10.3389/fpls.2023.1309219

OPEN ACCESS

EDITED BY
Sumera Anwar,
Durham University, United Kingdom

REVIEWED BY
Farinaz Vafadar,
Isfahan University of Technology, Iran
Kailou Liu,
Jiangxi Institute of Red Soil, China
Muhammad Zahid Mumtaz,
The University of Lahore, Pakistan

*CORRESPONDENCE
Guangping Qi
qigp@gsau.edu.cn

RECEIVED 08 October 2023
ACCEPTED 23 November 2023
PUBLISHED 11 December 2023

CITATION
Tian R, Qi G, Kang Y, Jia Q, Wang J, Xiao F, Gao Y, Wang C, Lu Q and Chen Q (2023) Effects of irrigation and nitrogen application on soil water and nitrogen distribution and water-nitrogen utilization of wolfberry in the Yellow River Irrigation Region of Gansu Province, China. *Front. Plant Sci.* 14:1309219. doi: 10.3389/fpls.2023.1309219

Effects of irrigation and nitrogen application on soil water and nitrogen distribution and water-nitrogen utilization of wolfberry in the Yellow River Irrigation Region of Gansu Province, China

Rongrong Tian[1], Guangping Qi[1]*, Yanxia Kang[1], Qiong Jia[1], Jinghai Wang[1], Feng Xiao[1], Yalin Gao[1], Chen Wang[1], Qiang Lu[1] and Qidong Chen[2]

[1]College of Water Conservancy and Hydropower Engineering, Gansu Agricultural University, Lanzhou, China, [2]Jingtaichuan Electric Power Irrigation Water Resource Utilization Center in Gansu Province, Baiyin, China

To address the problems of extensive field management, low productivity, and inefficient water and fertilizer utilization in wolfberry (*Lycium barbarum* L.) production, an appropriate water and nitrogen regulation model was explored to promote the healthy and sustainable development of the wolfberry industry. Based on a field experiment conducted from 2021 to 2022, this study compared and analyzed the effects of four irrigation levels [75%–85% θ_f (W0, full irrigation), 65%–75% θ_f (W1, slight water deficit), 55%–65% θ_f (W2, moderate water deficit), and 45%–55% θ_f (W3, severe water deficit)] and four nitrogen application levels [0 kg·ha^{-1} (N0, no nitrogen application), 150 kg·ha^{-1} (N1, low nitrogen application), 300 kg·ha^{-1} (N2, medium nitrogen application), and 450 kg·ha^{-1} (N3, high nitrogen application)] on soil water distribution, soil nitrate nitrogen (NO_3^-–N) migration, yield, and water-nitrogen use efficiency of wolfberry. The soil moisture content of the 40–80 cm soil layer was higher than those of 0-40 cm and 80-120 cm soil layer. The average soil moisture content followed the order of W0 > W1 > W2 > W3 and N3 > N2 > N1 > N0. The NO_3^-–N content in the 0–80 cm soil layer was more sensitive to water and nitrogen regulation, and the cumulative amount of NO_3^-–N in the soil followed the order of W0 > W1> W2 > W3 and N3 > N2 > N1 > N0 during the vegetative growth period. There was no evidently change in soil NO_3^-–N accumulation between different treatments during the autumn fruit. The yield of wolfberry under the W1N2 treatment was the highest (2623.09 kg·ha^{-1}), which was 18.04% higher than that under the W0N3 treatment. The average water consumption during each growth period of wolfberry was the highest during the full flowering period, followed by the vegetative growth and full fruit periods, and the lowest during the autumn fruit period. The water use efficiency reached a peak value of 6.83 kg·ha^{-1}·mm^{-1} under the W1N2 treatment. The nitrogen uptake of fruit and nitrogen fertilizer recovery efficiency of fruit first increased and then decreased with increasing irrigation and nitrogen application. The treatment of W1N2 obtained the highest nitrogen uptake of fruit and nitrogen recovery efficiency of fruit, which were

63.56 kg·ha^{-1} and 8.17%, respectively. Regression analysis showed that the yield and water-nitrogen use efficiency of wolfberry improved when the irrigation amount ranged from 315.4 to 374.3 mm, combined with nitrogen application amounts of 300.0 to 308.3 kg·ha^{-1}. Additionally, the soil NO_3^-–N residue was reduced, making it an optimal water and nitrogen management model for wolfberry planting. The present findings contribute novel insights into the production of wolfberry with saving water and reducing nitrogen, which helps to improve the level of wolfberry productivity in the Yellow River irrigation region of Gansu Province and other areas with similar climate.

KEYWORDS

water and nitrogen regulation, soil moisture content, soil NO_3^-–N, yield, water-nitrogen use efficiency, wolfberry

1 Introduction

Wolfberry (*Lycium barbarum* L.) is a perennial deciduous shrub belonging to the Solanaceae family (Kulczyński and Gramza-Michałowska, 2016). It thrives in cold and cool climates and exhibits strong resistance to cold temperatures (Yao et al., 2018). It plays an important role in medical health care, water and soil conservation, and saline-alkali soil improvement (Wozniak et al., 2012; Danial et al., 2022). Wolfberry is mainly distributed in China, the United States, France, and other places, among which China is the main producer of wolfberry in the world, and the planting area accounts for approximately 95% of the total global planting area (Anastasia et al., 2014; Huang and Zhang, 2021). Since the "14th Five-Year Plan", under the background of structural reform on the agricultural supply side and characteristic agricultural products driving local economic development, wolfberry has become an advantageous industry in northwest China. By 2020, the planting area of wolfberry will reach 148,300 ha, and the output of dried fruit will be approximately 428,500 tons (Ma et al., 2021; Hao, 2022). The rapid development of the wolfberry industry is of great significance for alleviating the problems of the "three rural areas", consolidating the achievements of poverty alleviation, and promoting rural revitalization (Jing and Han, 2018; Ren and Wang, 2019; Wang et al., 2021). However, the northwest of China is short of water resources and poor in soil (Zhang et al., 2015). The extensive management of water and fertilizer in the cultivation of wolfberry not only reduces crop productivity and utilization of water and fertilizer resources, but also increases greenhouse gas emissions in farmland, and aggravates greenhouse effect (Lu et al., 2022). At the same time, the excessive irrigation and fertilization will also leading to soil aeration and water permeability, affecting crop nutrient absorption and normal growth (Zhou and Bai, 2015), raising the groundwater level, increasing the salt content of soil solution and the decomposition of soil organic matter, causing groundwater pollution, soil salinization and soil acidification (Li et al., 2015a; Niu et al., 2022), and accompanied by problems of soil desertification and desertification (Chen and Tian, 2011). Therefore, exploring the development potential of appropriate water and fertilizer management modes in the wolfberry industry is very important. It will not only contribute to alleviate the problems of water and fertilizer resource waste and ecological environment pollution, but also contribute to improve the productivity of wolfberry and ensure the green and sustainable development of the wolfberry industry in northwest China and even the global.

Water and nitrogen are important factors that limit crop growth and yield (Gonzalez-Dugo et al., 2010; Darren et al., 2020; Tan et al., 2021). As a good solvent and carrier, water not only accelerates the dissolution and mineralization of nitrogen in soil but also transports it to crop roots in the form of diffusion or mass flow (Crevoisier et al., 2010), which affects the availability of soil nitrogen and changes the absorption, transport, and assimilation of nitrogen by crops (Guan et al., 2015). Nitrogen is a macronutrient in crops that significantly affects the accumulation and distribution of dry matter (Sun et al., 2014). The supply of water and nitrogen, either too high or too low, is detrimental to crop growth. The lack of soil water and nitrogen limits the potential for crop production. However, excessive soil water and nitrogen reduce soil permeability, accelerate nitrogen migration and leaching, and lead to problems such as reduced water and nitrogen utilization rates and groundwater pollution (Mokhele et al., 2012; Cameron et al., 2013). Appropriate water and nitrogen supply can produce synergistic and complementary effects, showing the effect of 1 + 1>2 (Fan et al., 2014; Kumar et al., 2016), which can promote crop yield and efficiency while effectively avoiding resource waste and ecological environment problems (Li et al., 2015b; Bai et al., 2018). Cong et al. (2021) conducted a study on the North China Plain and reported that compared with high water and high nitrogen (irrigation of 495 mm and nitrogen application of 330 kg·ha^{-1}), the optimal water nitrogen reduction mode (irrigation of 370 mm and nitrogen application of 255 kg·ha^{-1}) could improve the soil water storage capacity and soil water content of wheat. NO_3^-–N leaching was reduced by 15.87%. Armin et al. (2022) found in a study conducted in Arizona that corn grain yield significantly increased with 90%–100% field capacity (θ_f) coupled with a

nitrogen application of 180 kg·ha^{-1}. Rakesh et al. (2022) found in a study conducted in India that the nitrogen uptake of cotton bolls was highest with 600 mm of irrigation and a nitrogen application of 225 kg·ha^{-1}, whereas the nitrogen recovery efficiency of cotton reached its peak with 600 mm of irrigation and a nitrogen application of 150 kg·ha^{-1}. Cabello et al. (2008) found in a study conducted in Spain that the water use efficiency of melon with 90% crop evapotranspiration combined with 90 kg·ha^{-1} of nitrogen was the highest.

In summary, existing research has focused on water and nitrogen regulation in crops such as wheat, corn, cotton, and other food and cash crops (Zhang et al., 2017; Si et al., 2020; Ishfaq et al., 2018; Emile et al., 2023). Few studies have systematically analyzed the comprehensive effects of water and nitrogen regulation on the production of economic forests and wolfberry, particularly those that consider both production and ecological effects. Gansu Province is the second-largest wolfberry-producing area after the Ningxia Hui Autonomous Region. The Yellow River irrigation region is an important comprehensive agricultural commodity production base in Gansu Province (Yang et al., 2019). Currently, the cultivation area for wolfberry is 36,700 ha, with a production of 20,000 tons of dried fruit. The total output value amounts to two billion yuan, making it an important agricultural industry in the region (Ren and Bai, 2022). However, the characteristics of resource endowment and traditional cultivation practices in the irrigation area of Gansu Province severely hinder the sustainable and healthy development of the wolfberry industry. In view of this, this study used wolfberry as the object aiming to (1) analyze the effects of water and nitrogen regulation on soil water and nitrogen distribution, yield and water-nitrogen use efficiency of wolfberry; (2) clarify the functional relationship between wolfberry productivity and water and nitrogen regulation; (3) correct the wrong cognition of farmers on the water and nitrogen demand law of wolfberry production; (4) obtain the water and nitrogen regulation model for increasing yield and improving efficiency of wolfberry in the Yellow River irrigation region of Gansu Province and other similar climate areas.

2 Materials and methods

2.1 Description of the experimental site

The experiment was conducted at the Irrigation Experimental station (37° 23′ N, 104° 08′ E, altitude 2028 m) of Jingtaichuan Electric Power Irrigation Water Resource Utilization Center in Gansu Province from May to September 2021 and 2022. This region has a temperate continental arid climate, with strong sunshine, rare rainfall, and a dry climate. The annual average sunshine duration, frost-free period, radiation amount, temperature, precipitation, and evaporation are 2652 hours, 191 days, 6.18×10^5 J·cm^{-2}, 8.6 °C, 201.6 mm, and 3028 mm, respectively. The groundwater depth was greater than 40 m. The soil texture of the experimental site was loam, the dry bulk weight of soil was 1.63 g·cm^{-3}, and the field water capacity was 24.1% (mass water content). The initial soil properties of the study site was organic matter 6.09 g·kg^{-1}, total nitrogen 1.62 g·kg^{-1}, total phosphorus 1.32 g·kg^{-1}, total potassium 34.03 g·kg^{-1}, available nitrogen 74.51 mg·kg^{-1}, available phosphorus 26.31 mg·kg^{-1}, available potassium 173 mg·kg^{-1}, and alkali-hydrolyzed nitrogen 55.2 mg·kg^{-1} in the 0-60 cm soil layer. Meteorological data (precipitation and daily mean temperature) were measured during the experiment using a small intelligent agricultural weather station installed at the test station (Figure 1).

2.2 Experimental design and field management

The experiment adopted a completely randomized block design, with irrigation and nitrogen application levels as two factors. Among them, the irrigation level (the upper and lower limits of irrigation were set to control the percentage of soil volumetric moisture content to field water capacity θ_f, and the planned depth of humid layer was 60 cm) included 75%–85% θ_f (W0, full irrigation),

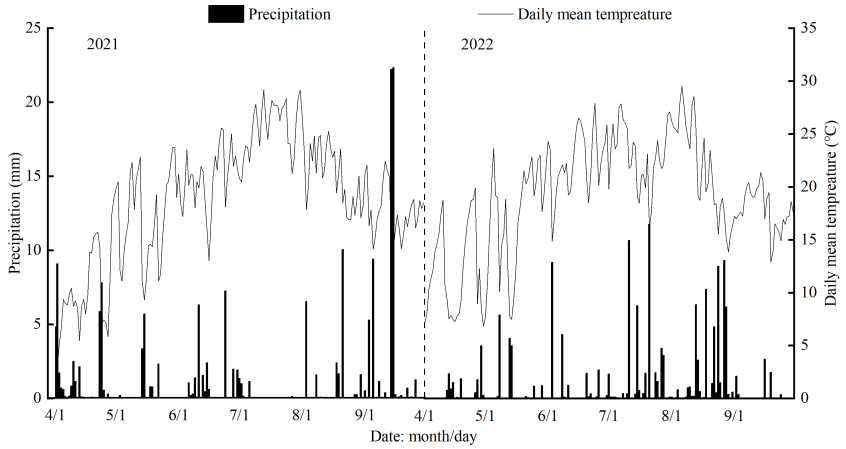

FIGURE 1
Distribution of precipitation and daily mean temperature during the experiment.

65%–75% θ_f (W1, slight water deficit), 55%–65% θ_f (W2, moderate water deficit) and 45%–55% θ_f (W3, severe water deficit); nitrogen application (pure nitrogen) levels included 0 kg·ha^{-1} (N0, no nitrogen application), 150 kg·ha^{-1} (N1, low nitrogen application), 300 kg·ha^{-1} (N2, medium nitrogen application), and 450 kg·ha^{-1} (N3, high nitrogen application) in 16 treatments (Table 1). Each treatment was repeated three times for a total of 48 plots. The residential area was 76.5 m^2 (10.2 m × 7.5 m). The test wolfberry (Ningqi No.5) was a two-year-old seedling transplanted on April 12, 2021, with a plant spacing of 1.5 m and row spacing of 3.0 m. Drip irrigation was then performed. Valves and water meters (accuracy 0.0001 m^3) were independently installed in the water-delivery pipes of each district to effectively regulate the amount of irrigation (Table 1). The spacing of the drip irrigation belt layout was 0.3 m, the design flow rate of the drip head was 2.0 L·h^{-1}, and the spacing of the drip head was 0.3 m. In each growing season, nitrogen fertilizer (urea and nitrogen content 46%) according to 6:2:2 was applied during the vegetative growth period (May 16 and 21), the full flowering period (June 4 and 7), and the full fruit period (July 7 and 4). Phosphate (superphosphate, 12% phosphorus content) and potassium (potassium chloride, 60% potassium content) at 130 kg·ha^{-1} were applied as the base fertilizer in a single application during the vegetative growth period (May 16 and 21). The remainder of the field management and pest control were consistent with that of local growers.

2.3 Indicators and methods for measurement

2.3.1 Soil moisture content (%)

A portable time-domain reflectometer (TDR; PICO–BT, IMKO, Germany) was used to determine the soil moisture content, irrigation time, and irrigation quota. The TDR tube was placed 0.3 m away from the trunk of the wolfberry in the center of the plot. The observation depth was 120 cm and the measurements were taken every 20 cm. The measurements were performed before and after precipitation and irrigation.

2.3.2 Soil nitrate-nitrogen content (NO_3^-–N, mg·kg^{-1})

During the vegetative growth and autumn fruit periods of wolfberry, soil samples were collected using the soil drilling method. Samples were taken from a depth of 0–100 cm at intervals of 10 cm. The collection point was located 0.3 m away from the trunk of the wolfberry in the center of the plot, ensuring a distance from the TDR measuring tube. After air-drying, the soil sample was sieved through a 2 mm screen and extracted with a 2 mol·L^{-1} KCl solution (using a mass ratio of 1:10 for 5 g of dry soil to liquid). The concentration of NO_3^-–N in the soil was subsequently measured using a UV-visible spectrophotometer (Beijing Puxi General Instrument Co., Ltd., T6 New Century) (Guo et al., 2022).

TABLE 1 Experimental design.

Treatment	Irrigation level (%)		Nitrogen application level (kg·ha^{-1})	Irrigation quota (mm)	
				2021	2022
W0N0	Full irrigation	75–85	0	316.23	452.84
W0N1			150	360.15	414.34
W0N2			300	324.00	372.16
W0N3			450	302.89	392.60
W1N0	Slight water deficit	65–75	0	286.09	384.91
W1N1			150	312.01	391.40
W1N2			300	279.38	315.41
W1N3			450	278.33	333.27
W2N0	Moderate water deficit	55–65	0	229.70	316.98
W2N1			150	255.67	290.04
W2N2			300	239.30	260.51
W2N3			450	206.89	274.46
W3N0	Severe water deficit	45–55	0	187.28	249.06
W3N1			150	207.54	227.89
W3N2			300	169.31	204.69
W3N3			450	194.62	316.98

(1) Soil-nitrate nitrogen accumulation (NR, kg·ha^{-1}) (Cambouris et al., 2008).

$$NR = \rho_i h_i N_i / 10 \quad (1)$$

Where is the bulk density of soil of layer i, g·cm^{-3}; h_i is the soil thickness of layer i, cm; N_i is the nitrate nitrogen content of the soil in layer i, mg·kg^{-1}.

2.3.3 Wolfberry yield (Y, kg·ha^{-1})

Wolfberry was planted in the year in 2021, and there was no yield. This study only analyzed the yield of wolfberry in 2022. From the end of July to the end of August 2022, wolfberry fruits were harvested every 7 days. The weight of the fresh fruit was measured during each harvest, and the sum of the fresh fruit weights represented the total fruit yield for the year. Dried fruits were obtained by natural sun-drying of fresh fruits.

2.3.4 Total nitrogen content of wolfberry fruit ($N_{\%}$, %)

During the harvest period, three representative wolfberry trees were selected from each plot to pick fresh fruits, which were naturally dried and then baked to a constant quality at 45 °C, crushed, and sifted over 0.5 mm, and then cooked with H_2SO_4-H_2O_2. The total nitrogen content of the wolfberry fruits was measured using the Kelley nitrogen determination method (Jiang et al., 2022).

2.3.5 Water-nitrogen use efficiency

(1) Water consumption (ET, mm) (Nie et al., 2019).

Water consumption during the growth period of the wolfberry was calculated using the water balance method.

$$ET = P + I + \Delta S - U - R - D \quad (2)$$

Where P is the effective rainfall, mm; I is the irrigation amount, mm; ΔS the change of soil water, mm; U is groundwater recharge, mm; R is the runoff, mm; D is the deep leakage, mm.

Because the groundwater in the test area was buried deep (> 40 m), the terrain was flat, the single rainfall was low, the depth of the wet layer planned by drip irrigation was shallow, and the U, R, and D parameters were ignored.

(1) Water use efficiency (WUE, kg·ha^{-1}·mm^{-1}) (Nie et al., 2019).

$$WUE = Y / ET \quad (3)$$

Where Y is the yield of wolfberry, kg·ha^{-1}; ET is the water consumption in 2022, mm.

(2) Nitrogen uptake of fruit (N_g, kg·ha^{-1}) (Ding et al., 2023).

$$N_g = N_{\%} \times Y \quad (4)$$

Where $N_{\%}$ is total nitrogen content of wolfberry fruit, %.

(3) Nitrogen fertilizer recovery efficiency of fruit (NRE_g, %) (Ding et al., 2023).

$$NRE_g = (N_{gl} - N_{g0}) / F \times 100\,\% \quad (5)$$

Where N_{gl} is the nitrogen uptake of fruit in nitrogen application zone, kg·ha^{-1}; N_{g0} is the nitrogen uptake of fruit in no nitrogen application zone, kg·ha^{-1}; F is the amount of nitrogen applied, kg·ha^{-1}.

2.4 Data analysis

Microsoft Excel 2010 was used to organize and calculate the data. IBM SPSS Statistics software (version 25.0) was used for statistical analysis of the data, and one-way ANOVA and Duncan method were used for variance analysis and multiple comparison of indicators in different treatments. Two-factor ANOVA was used to examine irrigation, nitrogen application and their interaction effects, and the significance level α=0.05. Origin 2021 software was used for the drawing.

3 Results

3.1 Effects of water and nitrogen regulation on temporal and spatial distribution of soil water

The soil moisture content of the 0–120 cm soil layer first increased and then decreased with the advance of time (growth period) and increase in soil depth (Figure 2). In the two-year growing season, the soil moisture content of the 0–40 cm layer changed most obviously with time (growth period), and the overall trend first increased and then decreased. Under the same irrigation level, the soil moisture content followed the order N3 (16.60%–22.93%) > N2 (15.86%–21.49%) > N1 (15.82%–21.39%) > N0 (15.93%–20.45%). Under the same nitrogen application level, the soil moisture content followed the order W0 (18.41%–22.93%) > W1 (16.26%–22.71%) > W2 (16.41%–20.13%) > W3 (15.82%–18.74%). The soil moisture content in the 60–80 cm soil layer decreased significantly with increasing soil depth, and this change was inconsistent with time (growth period). The soil moisture content from June to August (full flowering to full fruit period) was higher than that from May to June (vegetative growth-full flowering period) and from August to September (full fruit-autumn fruit period). The temporal and spatial changes in soil water content were similar in the 40–60 cm and 80–120 cm soil layers, and both first increased and then decreased with the increase in soil depth and advancement of the growth period.

3.2 Effects of water and nitrogen regulation on NO_3^-–N migration in soil

3.2.1 Distribution of NO_3^-–N in soil

Vegetative and autumn fruit growth periods are crucial for the overall development and reproductive growth of wolfberry. Taking the vegetative growth and autumn fruit periods as examples, the

10.3389/fpls.2023.1309219

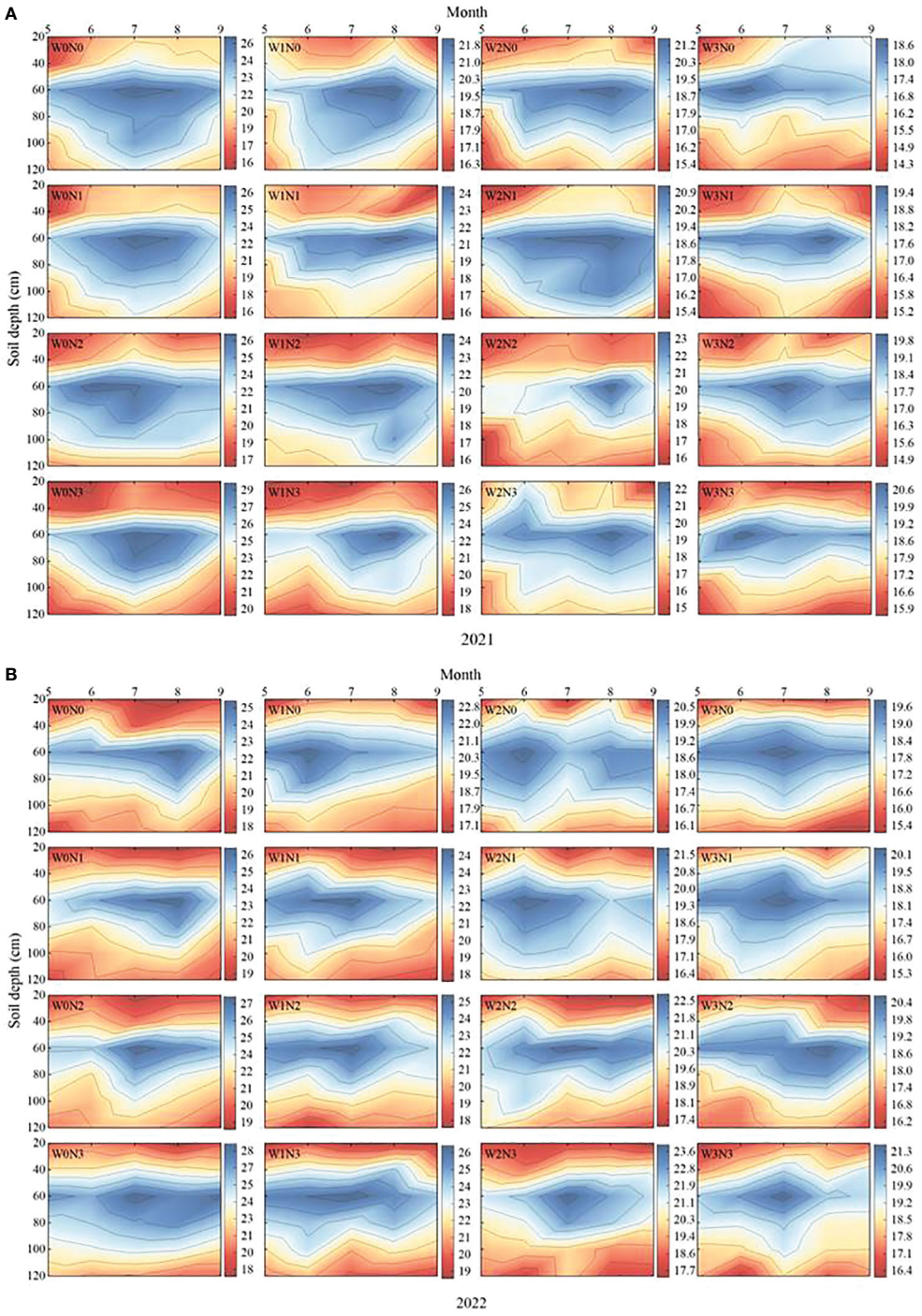

FIGURE 2
Effects of water-nitrogen regulation on the temporal and spatial distributions of soil water of wolfberry. **(A, B)** represent the temporal and spatial distributions of soil water of wolfberry in 2021 and 2022, respectively. The legends on the right of the figure represents the soil moisture content (%). W0, W1, W2 and W3 refers to full irrigation (75%–85%θ_f), slight water deficit (65%–75%θ_f), moderate water deficit (55%–65%θ_f) and severe water deficit (45%–55%θ_f), respectively. N0, N1, N2 and N3 refers to the nitrogen application level is 0 kg·ha^{-1}, 150 kg·ha^{-1}, 300 kg·ha^{-1} and 450 kg·ha^{-1}, respectively.

effects of water and nitrogen regulation on the vertical distribution of soil NO_3^-–N were analyzed (Figure 3). In the two-year growing season, the NO_3^-–N content in the 0–100 cm soil layer in each vegetative growth period first increased and then decreased with increasing soil depth. Under the same irrigation level, the NO_3^-–N content in the 0–30 cm soil layer (shallow layer) followed the order N3 > N2 > N1 > N0 with increasing nitrogen application rate. The average NO_3^-–N content in N3 was significantly increased by 13.09%–27.66% compared with N0. The NO_3^-–N content in the 30–40 cm soil layer showed a leaching peak, and the average NO_3^-–N content of N1, N2, and N3 increased by 2.48%–15.92%, 5.48%–26.65%, and 16.64%–33.42%, respectively, compared with N0. The

10.3389/fpls.2023.1309219

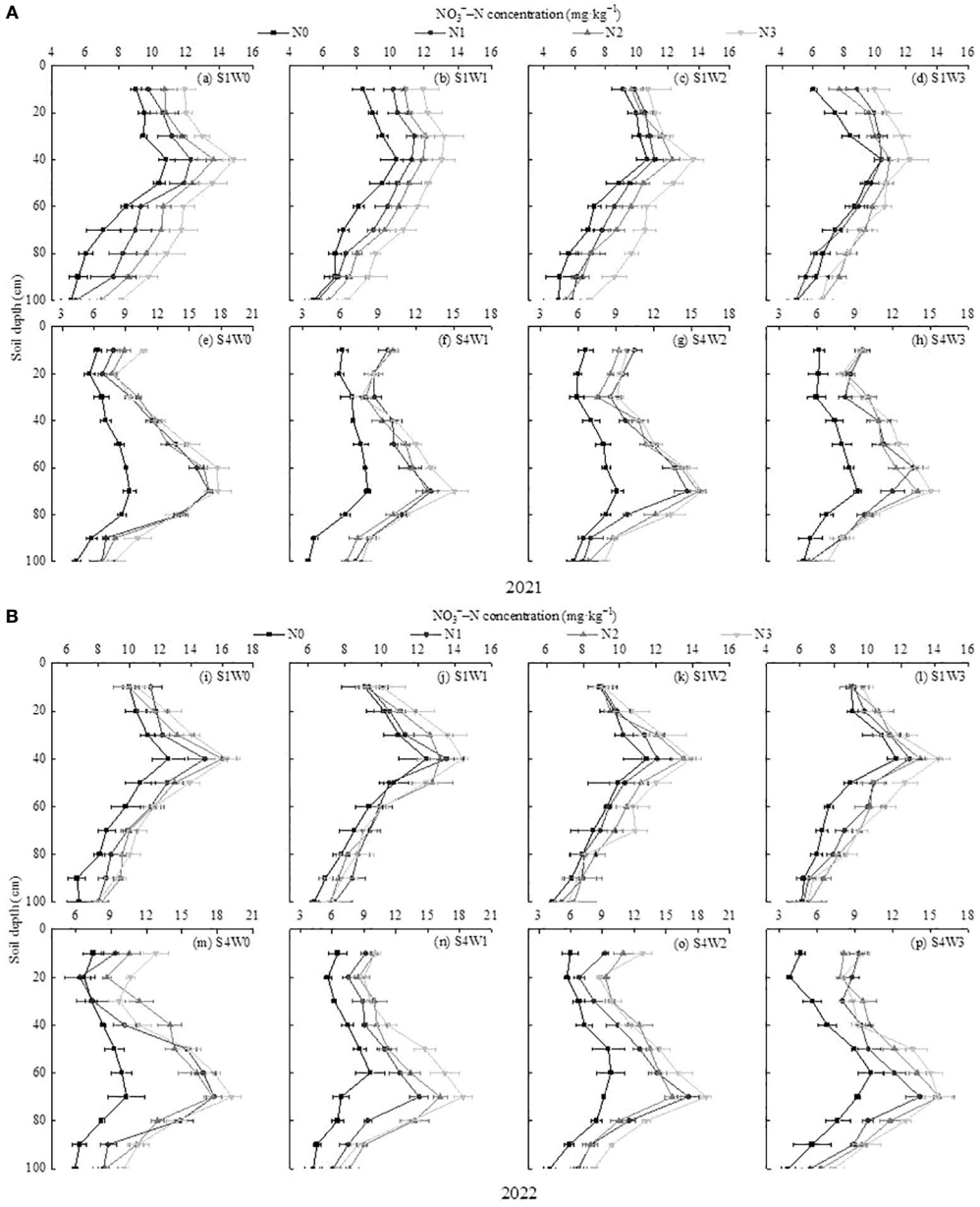

FIGURE 3
Effects of water and nitrogen regulation on the spatial and temporal distribution of NO_3^-–N in the 0–100 cm soil layer. **(A, B)** represent soil NO_3^-–N distribution for four irrigation levels in 2021 and 2022, respectively. S1 and S4 correspond to the vegetative growth and autumn fruit periods of wolfberry, respectively.

NO_3^-–N content in the 40–100 cm soil layer increased with an increase in the nitrogen application rate, and N3 was significantly increased by 22.45%–37.27% compared with N0. Under the same nitrogen application level, the average NO_3^-–N content in the 0–100 cm soil layer was W0 > W1 > W2 > W3. W0 increased by 1.92%–21.39%, 4.80%–25.14%, and 10.34%–31.51% compared with W1, W2, and W3, respectively.

In contrast to the vegetative growth period, the NO_3^-–N content in the 0–100 cm soil layer in each treatment during the autumn fruit period showed a trend of first decreasing (20–30 cm), increasing (60–70 cm), and then decreasing with increasing soil depth. In the 20–30 cm soil layer, the NO_3^-–N content of N0 was significantly lower than that of N1, N2, and N3. The NO_3^-–N in the 0–10 cm and 30–100 cm soil layers was in the order N3 > N2 > N1 > N0. The average NO_3^-–N content in the 0–100 cm soil layer was N3 > N2 > N1> N0, and N0 decreased by 30.41%–40.42%, 32.97%–42.70%, and 37.36%–47.04% compared with N1, N2, and N3, respectively. Under the same nitrogen application level, the average NO_3^-–N content in the 0–100 cm soil layer was W0 > W1 > W2 and W3, and W0 increased by 14.71%–24.40% compared with W1.

3.2.2 Soil NO_3^-–N accumulation

Irrigation and nitrogen application had significant effects on NO_3^-–N accumulation in the soil during the vegetative growth and autumn fruit periods ($P < 0.01$), and their interaction effects only

had significant effects on NO_3^-–N accumulation during the autumn fruit period ($P < 0.01$, Table 2). During the vegetative growth period, the average accumulation of NO_3^-–N in the soil followed the order N3 > N2 > N1 > N0, at the same irrigation level, in which N3 showed an increase of 21.23%–33.47%, 12.21%–16.45%, and 5.86%–9.77% compared with N0, N1, and N2, respectively. At the same nitrogen application level, the average soil NO_3^-–N accumulation followed the order W0 > W1 > W2 > W3, and there was no significant difference between W1 and W2 at the N0 and N1 levels.

During the autumn fruit period, the average soil NO_3^-–N accumulation at the same irrigation level was in the order N3 > N2 > N1 > N0 (except W1). At the W1 level, the cumulative amount of NO_3^-–N in the soil during the 2021 growing season was N3 > N1 > N2 > N0, in which N3 increased by 64.02%, 5.99%, and 9.04% compared with N0, N1, and N2, respectively, whereas the cumulative amount of NO_3^-–N in the soil during the 2022 growing season followed the order N3 > N2 > N1 > N0. The variation in NO_3^-–N accumulation at the same nitrogen application level over the two years was inconsistent, and the growth season in 2021 was in the order W0 > W2 > W3 > W1 (except N1). In the 2022 growing season, the NO_3^-–N accumulation was W0 > W2 > W3 > W1 at the N0 and N1 levels, and W0 > W2 > W1 > W3 at the N2 and N3 levels.

3.3 Effects of water and nitrogen regulation on the yield of wolfberry

Irrigation, nitrogen application, and their interaction significantly affected wolfberry yield ($P < 0.05$, Figure 4A). Under the same irrigation level, the yield of wolfberry first increased and then decreased with increasing nitrogen application and reached its peak under N2 conditions. The yield of wolfberry significantly increased by 20.38%–41.37%, 16.67%–22.36%, and 5.42%–11.48% compared with N0, N1, and N3, respectively. Under the same

TABLE 2 Effects of water and nitrogen regulation on soil NO_3^-–N accumulation (kg·ha^{-1}).

Treatment	2021		Treatment	2022	
	Vegetative growth period	Autumn fruit period		Vegetative growth period	Autumn fruit period
W0N0	133.16 ± 6.65dA	116.33 ± 5.17cA	W0N0	154.56 ± 8.57bA	130.64 ± 5.85cA
W0N1	155.44 ± 10.57cA	178.84 ± 9.09bA	W0N1	178.08 ± 7.40aA	186.73 ± 5.73bA
W0N2	172.24 ± 4.97bA	185.51 ± 6.60bA	W0N2	183.33 ± 5.97aA	203.33 ± 8.32aA
W0N3	191.80 ± 6.77aA	199.06 ± 11.73aA	W0N3	189.96 ± 3.96aA	215.27 ± 4.29aA
W1N0	131.75 ± 6.47cA	103.98 ± 4.13cAB	W1N0	150.38 ± 11.41bAB	107.74 ± 7.04dAB
W1N1	150.53 ± 5.79bA	160.91 ± 7.51bB	W1N1	161.04 ± 3.50abB	154.84 ± 10.37cB
W1N2	161.45 ± 6.81bB	156.41 ± 3.81abB	W1N2	164.83 ± 9.49abB	179.12 ± 4.43bB
W1N3	179.54 ± 9.06aAB	170.55 ± 3.55aB	W1N3	171.31 ± 1.80aB	192.21 ± 3.46aB
W2N0	128.13 ± 10.54cA	115.21 ± 7.06cAB	W2N0	146.26 ± 2.32cAB	117.51 ± 4.87dB
W2N1	142.22 ± 6.67bcAB	165.48 ± 9.17bB	W2N1	152.70 ± 4.81bcBC	170.38 ± 8.11cBC
W2N2	149.16 ± 2.75bC	170.40 ± 3.13aC	W2N2	162.01 ± 9.02abB	181.24 ± 2.56bB
W2N3	172.80 ± 9.14aBC	182.23 ± 4.57aC	W2N3	167.22 ± 7.51aB	201.40 ± 3.92aC
W3N0	123.47 ± 7.49cA	111.95 ± 6.78bB	W3N0	136.99 ± 4.35cB	108.31 ± 8.87cB
W3N1	134.46 ± 5.92bcC	159.06 ± 8.73bB	W3N1	150.91 ± 3.89bC	157.12 ± 4.86bC
W3N2	147.50 ± 2.39abC	162.64 ± 1.84bC	W3N2	157.21 ± 6.22abB	171.61 ± 1.74aB
W3N3	157.87 ± 11.57aC	172.10 ± 5.99aC	W3N3	164.56 ± 5.12aB	179.84 ± 6.23aD
Test of variance of significance					
Irrigation (W)	**	**	Irrigation (W)	**	**
Nitrogen (N)	**	**	Nitrogen (N)	**	**
W×N	ns	**	W×N	ns	**

Different lowercase letters indicate the difference between different nitrogen application levels under the same irrigation level, and different capital letters indicate the difference between different irrigation levels under the same nitrogen application level ($P < 0.05$). W and N refer to irrigation and nitrogen application levels, respectively; N × W refers to interaction effect between the two. ** indicates an extremely significant difference ($P < 0.01$); ns indicates no significant difference ($P > 0.05$).

10.3389/fpls.2023.1309219

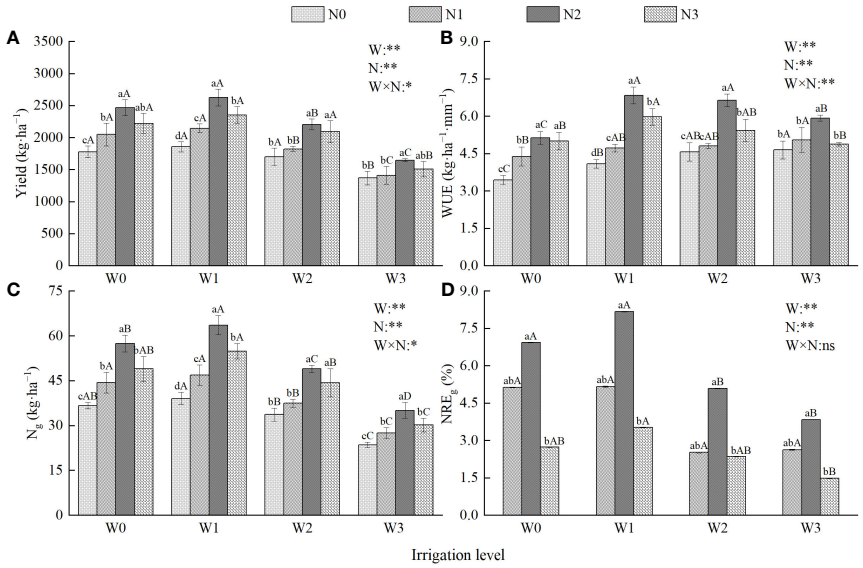

FIGURE 4
Effects of water and nitrogen regulation on the yield and water-nitrogen use efficiency of wolfberry. **(A–D)** represents yield, water use efficiency, nitrogen uptake and nitrogen recovery efficiency of fruit, respectively. Different lowercase letters indicate the difference between different nitrogen application levels under the same irrigation level, and different capital letters indicate the difference between different irrigation levels under the same nitrogen application level ($P < 0.05$). W and N refer to irrigation and nitrogen application levels, respectively; N × W refers to interaction effect between the two. ** indicates an extremely significant difference ($P < 0.01$); * indicates a significant difference ($P < 0.05$); ns indicates no significant difference ($P > 0.05$).

nitrogen application level, the yield of wolfberry first increased and then decreased with increasing irrigation amount and reached its peak under W1 conditions; the yield was significantly increased by 4.41%–6.36%, 9.23%–18.97%, and 35.67%–59.26% compared with W0, W2, and W3, respectively. Among all treatments, W1N2 had the highest yield of wolfberry (2623.09 kg·ha^{-1}).

Regression analysis was conducted with the irrigation amount (W) and nitrogen application amount (N) as independent variables and yield (Y) as the dependent variable (Table 3 and Figure 5A), and the fitting equation was obtained: Y=-0.037W^2-0.006N^2-0.004WN +28.164W+5.155N-3439.08, $P < 0.01$, and R^2 = 0.878. This shows that the regression equation has a good fit and a high prediction reliability. The coefficient of the primary term of the equation was positive, and the coefficient of the secondary term was negative, indicating that the yield of wolfberry first increased and then decreased with an increase in the irrigation and nitrogen application, whereas the coefficient of the interaction term of water and nitrogen was negative, and the interaction between the two was significant (Figure 4A), indicating that there was a significant coupling effect between water and nitrogen yield. When the yield of wolfberry was the highest, and the corresponding amounts of irrigation and nitrogen application amount were 363.93 mm and 308.27 kg·ha^{-1}, respectively.

3.4 Effects of water and nitrogen regulation on water-nitrogen use efficiency of wolfberry

3.4.1 Water consumption characteristic

As shown in Figure 6, under different water and nitrogen treatments in the 2021 growing season, the water consumption and the proportion of water consumption in the vegetative growth period, full flowering period, full fruit period, and autumn fruit period were 66.68–129.74 mm and 24.49%–28.16%, 88.12–170.42 mm and 22.05%–24.66%, 60.16–115.98 mm and 30.60%–33.85%, and 46.90–88.91 mm and 16.57%–18.62%, respectively; the total water consumption was the highest in W0N1 treatment (503.42 mm) and the lowest in W3N0 treatment (263.27 mm). Compared with the growing season in 2021, the water consumption during the vegetative growth, full flowering, and full fruit periods of the growing season in 2022 under different water and nitrogen

TABLE 3 Regression equations of yield and water-nitrogen use efficiency of wolfberry under different water and nitrogen treatments.

Dependent variable	Regression equation	R^2	P
Yield (Y)	Y= –0.037W^2–0.006N^2–0.004WN+28.164W+5.155N–3439.08	0.878	< 0.01
Water use efficiency (WUE)	WUE= –0.000061W^2–0.000014N^2 + 0.000002WN+0.036W+0.009N+0.678	0.731	< 0.01
Nitrogen uptake of fruit (N_g)	N_g= –0.001W^2–0.00018N^2–0.00015WN+0.794W+0.165N–111.696	0.854	< 0.01
Nitrogen fertilizer recovery efficiency of fruit (NRE_g)	NRE_g= –0.000097W^2–0.000085N^2–0.000005WN+0.073W+0.047N–13.333	0.745	< 0.01

10.3389/fpls.2023.1309219

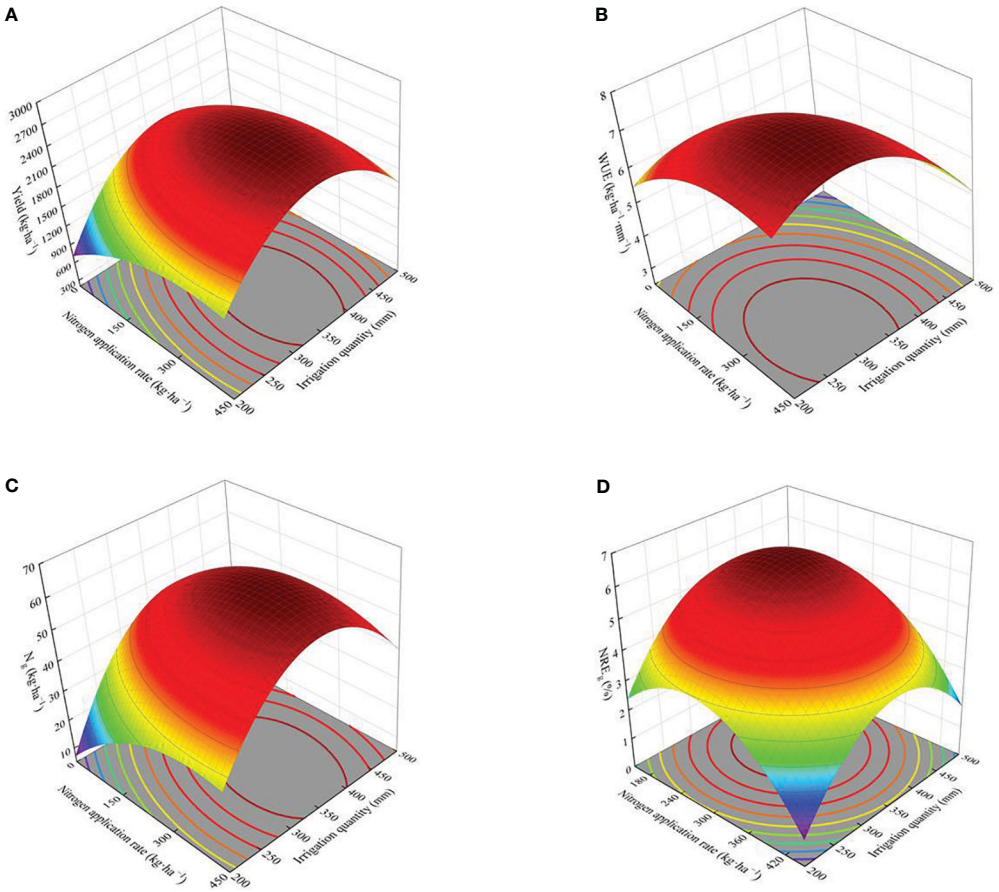

FIGURE 5
Regression models of wolfberry yield and water-nitrogen use efficiency under different water and nitrogen regulations. **(A–D)** represents yield, water use efficiency, nitrogen uptake and nitrogen recovery efficiency of fruit, respectively.

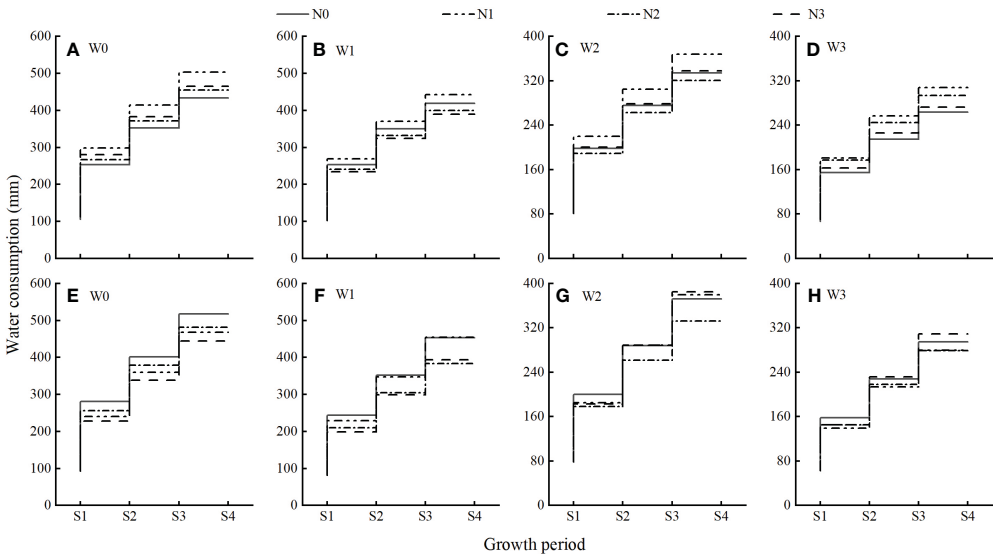

FIGURE 6
Water consumption during different growth periods of wolfberry under different water and nitrogen treatments. (S1) – (S4) correspond to the vegetative growth, full flowering, full fruit, and autumn fruit periods, respectively. **(A–D)** is the water consumption for each growth period in 2021, and **(E–H)** is the water consumption for each growth period in 2022.

treatments decreased by 1.28%, 2.16%, and 6.36%, respectively, whereas the water consumption in the autumn fruit period increased by 30.85%. The total water consumption was highest (517.17 mm) in the W0N0 treatment and lowest (278.57 mm) in the W3N2 treatment.

3.4.2 Water use efficiency

The water use efficiency of wolfberry was significantly affected by irrigation, nitrogen application, and their interaction ($P < 0.01$, Figure 4B). Under the same irrigation level, the water use efficiency of wolfberry was in the order N2 > N1 > N3 > N0, in which N2 was significantly increased by 27.31%–66.99%, 16.86%–44.70% and 2.60%–22.28% compared with N0, N1, and N3, respectively. Under the same nitrogen application level, the water use efficiency of wolfberry showed different trends with increasing irrigation amount. At the N0 and N1 levels, the water use efficiency of wolfberry decreased with an increase in irrigation amount, and the difference between W0 and W3 was significant. Under N2 and N3 levels, the water use efficiency of wolfberry first increased and then decreased with increasing irrigation amount. Among all treatments, W1N2 had the highest water use efficiency (6.83 $kg{\cdot}ha^{-1}{\cdot}mm^{-1}$).

The determination coefficient of the fitting equation for the water use efficiency of wolfberry was 0.731 ($P < 0.01$, Table 3 and Figure 5B), indicating that irrigation and nitrogen application had significant effects on the water use efficiency of wolfberry (Figure 4B). In the model, the coefficients of the primary and secondary terms of irrigation water quantity were positive and negative, respectively, indicating that water use efficiency first increased and then decreased with the increase in irrigation water quantity, which was inconsistent with the change rule of water use efficiency decreasing with the increase in irrigation water quantity under N0 and N1 levels (Figure 4B); therefore, the optimization of the model failed.

3.4.3 Nitrogen use efficiency

3.4.3.1 Nitrogen uptake of fruit

Irrigation, nitrogen application, and their interaction significantly affected the nitrogen uptake of wolfberry fruits ($P < 0.05$, Figure 4C). Under the same irrigation level, the nitrogen absorption of wolfberry fruit was N2 > N1 > N3 > N0, and N2 was significantly increased by 45.37%–62.77%, 27.59%–35.70%, and 10.62%–17.40% compared with N0, N1, and N3, respectively. Under the same nitrogen application level, the nitrogen absorption of wolfberry fruit was W1 > W0 > W2 > W3, and W1 significantly increased by 5.64%–12.16%, 15.94%–29.82%, and 65.96%–81.81% compared with W0, W2, and W3, respectively. In all treatments, the nitrogen uptake of W1N2 fruits reached a peak of 63.56 $kg{\cdot}ha^{-1}$.

3.4.3.2 Nitrogen fertilizer recovery efficiency of fruit

Irrigation and nitrogen application had significant effects on the nitrogen recovery efficiency of fruits ($P < 0.01$), but their interaction had no significant effect on the nitrogen recovery efficiency of fruits ($P > 0.05$, Figure 4D). Under the same irrigation level, the nitrogen recovery efficiency of fruit was higher than that of N1 and N3, and N2 was significantly increased by 35.09%–101.98% and 116.60%–159.46% compared with N1 and N3, respectively. Under the same nitrogen application level, the nitrogen recovery efficiency of fruit was in the order W1 > W0 > W2 > W3, and W1 significantly increased by 0.58%–28.94%, 49.79%–104.76%, and 96.20%–137.84% compared with W0, W2, and W3, respectively. In all treatments, the nitrogen recovery efficiency of W1N2 fruit peaked at 8.17%.

The coefficient of the primary term of nitrogen uptake (Table 3 and Figure 5C) and fruit nitrogen recovery efficiency model (Table 3 and Figure 5D) were positive, whereas that of the secondary term was negative, indicating that both first increased and then decreased with increasing irrigation and nitrogen application. The interaction coefficient was negative, indicating a significant interaction between fruit nitrogen uptake (Figure 4C). These results indicate that there is a certain coupling between water-nitrogen and nitrogen uptake and the nitrogen recovery efficiency of the fruit. However, this is inconsistent with the result that the interaction between the nitrogen recovery efficiency of fruit is not significant (Figure 4D), and the model of nitrogen recovery efficiency of fruit cannot be optimized; therefore, only the regression model fort fruit nitrogen uptake is optimized. The results showed that when the irrigation amount was 374.31 mm and the nitrogen application amount was 302.37 $kg{\cdot}ha^{-1}$, the results of the optimization were as follows: the wolfberry fruit had the highest nitrogen absorption (61.84 $kg{\cdot}ha^{-1}$).

4 Discussion

4.1 Effects of water and nitrogen regulation on temporal and spatial distribution of soil moisture in wolfberry

Soil moisture is a key factor constraining agroforestry production, which is closely related to plant physiological growth and yield accumulation, and its influence is particularly pronounced in arid and semi-arid regions where water resources are scarce (Liu et al., 2020a). On the one hand, irrigation and nitrogen application are two interconnected factors that influence the soil moisture status. Moisture can mobilize the enthusiasm of cell turgor, promote the division and extension of plant cells and affect the growth and redistribution of plant roots (Tang et al., 2022). After the irrigation satisfies the normal water demand and evapotranspiration of the plants, excessive moisture will directly affect the spatial and temporal distribution of soil moisture by altering the soil structure, water-holding and water-conducting capacity (Hu et al., 2011). On the other hand, by participating in plant cell metabolism to enhance the water absorption capacity of plant roots, and increase soil water potential and activating deep soil water, nitrogen can indirectly affect the spatial and temporal distribution of soil water (Hu et al., 2011; Wu et al., 2018). At the same time, appropriate water and nitrogen regulation can effectively increase soil available nitrogen content, promote plant organic synthesis, and make up for the negative effects of external factors on crop growth. In this study, it was found that the soil water

content of wolfberry was maintained at 14.08%–29.03% throughout the reproductive period under different water and nitrogen regulations. The 0–40 cm soil layer exhibited the most active soil water content, with an overall performance of W0 > W1 > W2 > W3 and N3 > N2 > N1 > N0. This finding was similar to those reported by Zheng et al. (2012) and Zhan et al. (2016). The active layer of the wolfberry root system is primarily concentrated at a depth of 0–40 cm (Zhan et al., 2016). The soil water content is significantly affected by irrigation and crop root activities, and the root system of wolfberry within this soil layer is well-developed and exhibits a strong water absorption capacity (Hupet and Vanclooster, 2002). However, Yin et al. (2021) found that the soil water content of the 0-60 cm soil layer of wolfberry varied significantly under different irrigation rates in the gray-calcium soil area of Ningxia. This may be related to the soil texture in the test area, which is characterized by a low-water holding capacity in the field and a high infiltration coefficient in the profile (Jin and Ma, 2000), which is prone to deep soil seepage. Consistent with the findings of Zhao et al. (2021) regarding various sand-resistant vegetation in the Mu Us Sandy area, this study also observed an "S-shaped" change in the soil water content in the 0-100 cm soil layer. This is mainly because crop growth relies primarily on the consumption of shallow soil moisture. Compared with shallow soil, deep soil is less disturbed by tillage and is more stable (Kang et al., 2023), and the water not absorbed by the crop root system will naturally infiltrate under the influence of gravity (Jia et al., 2013), causing water to accumulate in a specific soil layer.

4.2 Effects of water and nitrogen regulation on soil NO_3^-–N distribution in wolfberry

The soil NO_3^-–N content, the main inorganic form of nitrogen that is easily absorbed and utilized by crops, represents the ability of soil to supply nitrogen to a certain extent, which is of decisive significance for the improvement of soil fertility, promotion of crop growth, and enhancement of economic output (Darren et al., 2020). In this study, the average NO_3^-–N content in the 0–100 cm soil layer during the nutrient growth period of wolfberry was in the order of W0 > W1 > W2 > W3 and N3 > N2 > N1 > N0, suggesting that soil NO_3^-–N transport and crop nitrogen uptake are susceptible to the effects of irrigation and nitrogen application (Emile et al., 2023). Meanwhile, excessive irrigation and nitrogen application cannot be sufficiently absorbed and utilized by crop roots, which may cause soil nitrogen leaching loss, reduce nitrogen use efficiency, and increase the risk of soil compaction and secondary salinization (Luo et al., 2020). Guo et al. (2022) concluded that soil NO_3^-–N content in the 0–200 cm soil layer of vineyards showed a gradual increase from top to bottom in sandy loam soil in the Taihang Mountain region of Hebei Province. However, in this study, conducted on loam soil in the Yellow Irrigation Area of Gansu Province, it was observed that the NO_3^-–N content in the 0–100 cm soil layer of wolfberry showed an increase followed by a decrease during the nutrient growth period and a decrease followed by an increase followed by a subsequent decrease during the fall fruiting period. Sandy loam has larger particles, extreme water permeability, very poor water and fertilizer retention capacity, and is prone to oxidize NH_4^+ to NO_3^-, increasing the risk of nitrogen leaching. Gao et al. (2005) observed no significant correlation between spring corn soil NO_3^-–N accumulation and irrigation volume in Yongshou County, Shaanxi Province. However, we found that the average soil NO_3^-–N accumulation during the nutritive growth and fall fruiting periods of wolfberry was W0 > W1 > W2 > W3 and W0 > W2 > W1 and W3, respectively. The results showed that compared with adequate irrigation, proper control of irrigation amount was conducive to reducing the accumulation of soil inorganic nitrogen, reducing the risk of NO_3^-–N leaching (Lv et al., 2018), increasing the rate of soil mineralization, promoting soil ecological balance and organic matter decomposition, and improving soil fertility and crop nutrient supply (Zheng et al., 2020). At the same time, the soil NO_3^-–N accumulation of W0N1, W0N2 and W0N3 treatments showed a trend of increasing gradually with the increase of nitrogen application. The result indicates that under the condition of high nitrogen application rate, excessive irrigation can easily cause NO_3^-–N leaching in soil, increase the concentration of soil solution, enhance the nitrification and denitrification of soil microorganisms, and lead to soil acidification and greenhouse gas emissions (Chen et al., 2019). In addition, this study found that under different water and nitrogen regulations (except N0), soil NO_3^-–N accumulation was higher during the autumn fruit period of wolfberry than during the vegetative growth period. Compared with the pre-reproductive stage, wolfberry had a lower demand for water and nitrogen during the late reproductive growth period. Excessive nitrogen content in the soil increases the substrate concentration of nitrification and promotes nitrification fluxes, and excessive soil moisture exacerbates the migration and leaching of residual nitrogen (Liu et al., 2020b), which increases the risk of groundwater contamination.

4.3 Effects of water and nitrogen regulation on the yield of wolfberry

Crop yield is one of the most intuitive indexes to evaluate planting efficiency, and it is closely related to soil water and fertilizer status. Excessive irrigation and fertilization application may cause the phenomena of "futile growth" and "low flowering and low yield", which may produce deep soil leakage and reduce the utilization rate of water and fertilizer resources (Haefele et al., 2008; Min et al., 2011). Reasonable water and fertilizer supply can achieve the effect of "regulating fertilizer with water and promoting water with fertilizer" to realize a synergistic effect on crop yield (Er et al., 2022). In this study, the yield of wolfberry was W1 > W0 > W2 > W3 and N2 > N3 > N1 > N0. This is consistent with the findings of Liu et al. (2018a) in the Inner Mongolia Autonomous Region and Ma et al. (2023) in the central arid region of Ningxia on wolfberry. The result showed that when irrigation and nitrogen supply are coordinated, it can maintain appropriate soil moisture and nutrient concentrations, increase the reproduction of soil ammonia bacteria and soil ammonium nitrogen content, and

ultimately promote the accumulation of crop dry matter and yield formation (Ihsan et al., 2022). The study revealed that the water and nitrogen inputs required to achieve the highest wolfberry yield varied by region. Specifically, the Yellow Irrigation Area of Gansu Province demonstrated the highest yield (2623.09 kg·ha^{-1}) when the irrigation-applied nitrogen levels were 315.41 mm and 300 kg·ha^{-1}, respectively. The highest yield (5547.22 kg·ha^{-1}) was obtained in the Inner Mongolia Autonomous Region when the nitrogen applied by irrigation was 750 kg·ha^{-1} and 285.00 mm, respectively. Similarly, the highest yield (2356.34 kg·ha^{-1}) was obtained in the central arid area of Ningxia when the nitrogen applied by irrigation was 225 kg·ha^{-1} and 256.50 mm, respectively. In addition, we found that the wolfberry yield first increased and then decreased when the lower limit of irrigation was reached. This is inconsistent with the results of Wang et al. (2015), who concluded that the yield of wolfberry significantly increased with an increase in the irrigation lower limit in their study conducted in Qinghai. This may stem from the following two factors: one is related to the age of the wolfberry (2–3 years and 3–4 years, respectively); as the wolfberry plants grow, their growth increases, leading to an increased demand for water. The other factor is related to the climate of the test site, which can be either a temperate continental arid climate or a plateau continental climate. Compared with the temperate continental arid climate, the plateau continental climate has stronger solar radiation and higher soil evaporation. As a result, wolfberry growth is more dependent on irrigation.

4.4 Effects of water and nitrogen regulation on water-nitrogen use efficiency of wolfberry

Water and nitrogen utilization efficiency not only reflects the energy conversion in the crop production process but also measures the suitability of crop growth and yield-to-input ratio (Qin et al., 2021). Studies have shown that the water use efficiency of corn and wheat tends to increase and then decrease with an increase in irrigation and nitrogen application, whereas the nitrogen fertilizer recovery efficiency tends to increase and then decrease with an increase in irrigation (Liu et al., 2018b; Wang et al., 2022). However, in this study, we found that the water use efficiency of wolfberry decreased with increasing irrigation at the N0 and N1 levels, and the nitrogen fertilizer recovery efficiency of fruits decreased, then increased, and then decreased with increasing irrigation at the N1 level. Excessive irrigation leads to soil nutrient leaching, reduces soil fertility, and simultaneously changes crop cell expansion pressure, weakening the ability of crops to absorb nitrogen and resulting in crop yield reduction, thus affecting water use efficiency and fruit nitrogen fertilizer recovery efficiency. This study showed that the nitrogen uptake of wolfberry fruits first increased and then decreased with increasing nitrogen application. This is inconsistent with the findings of Luo et al. (2020) in the Shaanxi area, who showed that the nitrogen uptake of 100 kg of winter wheat grain increased with an increase in nitrogen application. This may be related to the nitrogen application gradient settings. Wheat is a gramineous grain that is significantly affected by exogenous nitrogen (Lv et al., 2023). Although herbaceous wolfberry plants obtain inherent nitrogen from the soil, their roots can absorb a large amount of exogenous nitrogen, which promotes the transfer of nitrogen stored in the vegetative organs to the fruits and increases the total nitrogen content of the fruits, thereby increasing their nitrogen uptake. In addition, in this study, the change in water use efficiency of wolfberry and the amount of irrigation water (Figure 4B) was inconsistent with the constructed model (Table 3). Similarly, the change in fruit nitrogen fertilizer recycling efficiency with the amount of irrigation water and the response to water and nitrogen (Figure 4D) was inconsistent with the constructed model (Table 3). This phenomenon may be because the irrigation and nitrogen application levels set in this experiment did not reach the threshold for water-use efficiency. Compared with N1, the increase in fruit nitrogen uptake in N2 was lower than that in nitrogen application, which led to an inconsistency between the change rule of fruit nitrogen fertilizer recycling efficiency with the amount of irrigation in the model and the experimental results. As a result, the model failed to achieve optimal success. Therefore, in production practice, comprehensive consideration should be given to crop dry matter accumulation as well as water and nitrogen utilization efficiency. Therefore, it is important to adopt reasonable water and nitrogen management modes.

5 Conclusions

During the two-year wolfberry growing season, the average soil moisture content followed the order W0 > W1 > W2 > W3 and N3 > N2 > N1 > N0, depending on the nitrogen application and irrigation amount. The average water consumption during the full flowering period accounted for 24.36%–27.46% of the total water consumption. During the vegetative growth period, the soil NO_3^-–N content of different water-nitrogen combinations increased and then decreased with increasing soil depth, with average NO_3^-–N accumulation ranging from 130.23–190.88 kg·ha^{-1}. During the autumn fruiting period, there was a decrease, followed by an increase and then a decrease, with the average accumulation ranging from 123.49–207.17 kg·ha^{-1}. The wolfberry yield followed the order W1 > W0 > W2 > W3 and N2 > N3 > N1 > N0. The wolfberry yield was obtained when treated with W1N2, which was 18.04%, 18.97%, and 85.80% higher than those treated with W0N3, W2N2, and W3N1, respectively. The water use efficiency, fruit nitrogen uptake, and fruit nitrogen recovery efficiency first increased and then decreased with increasing nitrogen application. The results of the regression analysis revealed that the optimal combined effects of wolfberry yield, water use efficiency, and nitrogen use efficiency were within the range of 315.4–374.3 mm, and the nitrogen application rate ranged from 300.0–308.3 kg·ha^{-1} in the Yellow River Irrigation Region of Gansu Province. The present findings contribute novel insights and theoretical bases for water and nitrogen management of wolfberry in the Yellow River Irrigation Region. However, climatic factors (such as rainfall) and soil conditions (such as field water capacity, soil texture) vary in different region. Therefore, the mechanisms of climate change and soil conditions in different regions influencing the effects of water

and nitrogen regulation on soil water and nitrogen distribution, yield and water and nitrogen use efficiency of wolfberry require further investigation.

Data availability statement

The original contributions presented in the study are included in the article/supplementary material. Further inquiries can be directed to the corresponding author.

Author contributions

RT: Conceptualization, Data curation, Formal Analysis, Investigation, Methodology, Writing – original draft. GQ: Conceptualization, Formal Analysis, Funding acquisition, Writing – review & editing. YK: Data curation, Formal Analysis, Project administration, Writing – review & editing. QJ: Funding acquisition, Writing – review & editing. JW: Supervision, Writing – review & editing. FX: Writing – review & editing. YG: Investigation, Writing – review & editing. CW: Methodology, Writing – review & editing. QL: Project administration, Writing – review & editing. QC: Project administration, Writing – review & editing.

Funding

The author(s) declare financial support was received for the research, authorship, and/or publication of this article. This study was funded by the National Natural Science Regional Foundation Project, China (Grant Nos. 51969003 and 52069001); the Key research and development project of Gansu Province, China (Grant No. 22YF7NA110); the Sheng Tongsheng Innovation Funds of Gansu Agricultural University (Grant No. GSAU-STS-2021-18); the Gansu Agricultural University youth mentor support fund project (Grant No. GAU-QDFC-2022-22); the "Northwest arid region Collaborative Utilization of water and soil resources innovation team" of Gansu Agricultural University discipline team construction project; Gansu Provincial Universities Young Doctor Fund Project (Grant No. 22QB-08); Research Team Construction Project of College of Water Conservancy and Hydropower Engineering, Gansu Agricultural University, China (Grant No. Gaucwky-01); Gansu Water Science Experimental Research and Technology Extension Program (Grant No. 22GSLK023).

Acknowledgments

The authors would like to thank the Jingtai Wolfberry Science and Technology Academy of Gansu Province and the Harmless Wolfberry Cultivation Engineering Research Center of Gansu Province for their support of this study. We also gratefully acknowledge the editors and reviewers who put forward constructive comments on this article.

Conflict of interest

The authors declare that the research was conducted in the absence of any commercial or financial relationships that could be construed as a potential conflict of interest.

Publisher's note

References

Anastasia, K., Camilla, M. B., Vincieri, F. F., and Rita, B. A. (2014). Validated method for the analysis of goji berry, a rich source of zeaxanthin dipalmitate. *J. Agric. Food Chem.* 62 (52), 12529–12535. doi: 10.1021/jf503769s

Armin, M. S., Mohammad, P., Akbar, A. M., Abbas, R., Peyman, F., Amir, T., et al. (2022). Modeling and determining the best combination of nitrogen and irrigation levels for achieving high yield in sweet corn. *J. Plant Nutr.* 45 (18), 2748–2757. doi: 10.1080/01904167.2022.2067063

Bai, Z. H., Lu, J., Zhao, H., Velthof, G. L., Oenema, O., Chadwick, D., et al. (2018). Designing vulnerable zones of nitrogen and phosphorus transfers to control water pollution in China. *Environ. Sci. Technol.* 52 (16), 8987–8988. doi: 10.1021/acs.est.8b02651

Cabello, M., Castellanos, M., Romojaro, F., Martínez-Madrid, C., and Ribas, F. (2008). Yield and quality of melon grown under different irrigation and nitrogen rates. *Agric. Water Manage.* 96 (5), 866–874. doi: 10.1016/j.agwat.2008.11.006

Cambouris, N. A., Zebarth, J. B., Nolin, C. M., and Laverdière, R. M. (2008). Apparent fertilizer nitrogen recovery and residual soil nitrate under continuous potato cropping: Effect of N fertilization rate and timing. *Can. J. Plant Sci.* 88 (5), 813–815. doi: 10.4141/CJSS07107

Cameron, K. C., Di, H. J., and Moir, J. L. (2013). Nitrogen losses from the soil/plant system: a review. *Ann. Appl. Biol.* 162 (2), 145–173. doi: 10.1111/aab.12014

Chen, L., Song, S. H., Yun, P., Zhou, L., Gao, X., Lu, C. A., et al. (2019). Effects of reduced nitrogen fertilizer for three consecutive years on maize growth and rhizosphere nitrogen supply in fluvo-aquic soil. *Plant Nutr. Fert. Sci.* 25 (09), 1482–1494. doi: 10.11674/zwyf.18362

Chen, R. Y., and Tian, W. H. (2011). Study on security system of developing water-saving agriculture in arid area of northwest China. *Resour. Dev. Mark.* 27 (05), 467–463. doi: 10.3969/j.issn.1005-8141.2011.05.024

Cong, X., Pang, G. B., Zhang, L. Z., Xu, Z. H., Yang, J. L., and Mou, X. Y. (2021). Effects of nitrogen-reducing and suitable wateron photosynthetic characteristics of winter wheat and distribution of soil water and nitrogen. *Trans. Chin. Soc Agric. Mach.* 52 (06), 324–332. doi: 10.6041/j.issn.1000-1298.2021.06.034

Crevoisier, D., Popova, Z., Mailhol, J. C., and Ruelle, P. (2010). Assessment and simulation of water and nitrogen transfer under furrow irrigation. *Agric. Water Manage.* 95, 354–366. doi: 10.1016/j.agwat.2007.10.021

Danial, F., Luisa, M. A., and Giancarlo, C. (2022). Quality of Goji Berry fruit (*Lycium barbarum* L.) stored at different temperatures. *Foods* 11 (22), 3700. doi: 10.3390/FOODS11223700

Darren, C. P., Kosala, R., Melino, J. V., Noriyuki, K., Yusaku, U., and Kronzucker, J. H. (2020). The intersection of nitrogen nutrition and water use in plants: new paths toward improved crop productivity. *J. Exp. Bot.* 71 (15), 4452–4468. doi: 10.1093/jxb/eraa049

Ding, J. F., Xu, D. Y., Ding, Y. G., Zhu, M., Li, C. Y., Zhu, X. K., et al. (2023). Effects of cultivation patterns on grain yield, nitrogen uptake and utilization, and population quality of wheat under rice-wheat rotation. *Sci. Agric. Sin.* 56 (04), 619–634. doi: 10.3864/j.issn.0578-1752.2023.04.003

Emile, I. R., Wang, W. M., Li, Y. T., and Li, X. J. (2023). Translocation of nitrate in rice rhizosphere and total nitrogen uptake improvement under interactive effect of water and nitrogen supply. *Commun. Soil Sci. Plant Anal.* 54 (3), 378–391. doi: 10.1080/00103624.2022.2115059

Er, C., Lin, T., Xia, W., Zhang, H., Xu, G. Y., and Tang, Q. X. (2022). Coupling effects of irrigation and nitrogen levels on yield, water distribution and nitrate nitrogen residue of machine-harvested cotton. *Acta Agron. Sinica.* 48 (02), 497–510. doi: 10.3724/SP.J.1006.2022.04277

Fan, Z. B., Lin, S., Zhang, X. M., Jiang, Z. M., Yang, K. C., Jian, D. D., et al. (2014). Conventional flooding irrigation causes an overuse of nitrogen fertilizer and low nitrogen use efficiency in intensively used solar greenhouse vegetable production. *Agric. Water Manage.* 144, 11–19. doi: 10.1016/j.agwat.2014.05.010

Gao, Y. J., Li, S. X., Li, S. Q., Tian, X. H., Wang, C. H., Zheng, X. F., et al. (2005). Effect of fertilization and irrigation on residual nitrate N in soil. *J. Soil Water Conserv.* 19 (06), 63–66. doi: 10.13870/j.cnki.stbcxb.2005.06.016

Gonzalez-Dugo, V., Durand, J. L., and Gastal, F. (2010). Water deficit and nitrogen nutrition of crops. A review. *Agron. Sustain Dev.* 30 (3), 529–544. doi: 10.1051/agro/2009059

Guan, D. H., Zhang, Y. S., Al-kaisi, M. M., Wang, Q. Y., Zhang, M. C., and Li, Z. H. (2015). Tillage practices effect on root distribution and water use efficiency of winter wheat under rain-fed condition in the North China Plain. *Soil Tillage Res.* 146, 286–295. doi: 10.1016/j.still.2014.09.016

Guo, L. H., Wang, H. P., Li, Y., Xu, A., Li, W. C., Sun, Z. M., et al. (2022). Accumulation characteristics and influencing factors of soil nitrogen in vineyard in piedmont plain of Taihang mountain, Hebei Province. *J. Soil Water Conserv.* 36 (03), 280–285. doi: 10.13870/j.cnki.stbcxb.2022.03.040

Haefele, S. M., Jabbar, S. M. A., Siopongco, J. D. L. C., Tirol-Padre, A., Amarante, S. T., Sta Cruz, P. C., et al. (2008). Nitrogen use efficiency in selected rice (*Oryza sativa* L.) genotypes under different water regimes and nitrogen levels. *Field Crops Res.* 107 (2), 137–146. doi: 10.1016/j.fcr.2008.01.007

Hao, Z. H. (2022). Reflections and countermeasures on promoting the high quality development of modern Chinese wolfberry industry in Ningxia. *Sci. Tech. Ningxia Agric. For* 63 (Z1), 84–87+102. doi: 10.3969/j.issn.1002-204x.2022.h10.022

Hu, B. H., Liao, Y. C., Wang, K. Q., and Chen, Q. B. (2011). Spatiotemporal patterns of soil water variations in farmlands of Mu Us Sandland. *Bull. Soil Water Conserv.* 31 (05), 144–148. doi: 10.13961/j.cnki.stbctb.2011.05.041

Huang, L. Q., and Zhang, X. B. (2021). *Statistical report of Chinese medicinal materials production in China, (2020)* (Shanghai, China: Shanghai Science Technology Press), 171–174.

Hupet, F., and Vanclooster, M. (2002). Intraseasonal dynamics of soil moisture variability within a small agricultural maize cropped field. *J. Hydrol.* 261 (1), 86–101. doi: 10.1016/S0022-1694(02)00016-1

Ihsan, M., Li, Y., Shakeel, A., Saqib, F., Ahmed, A. A., Ahmad, K., et al. (2022). Nitrogen fertilizer modulates plant growth, chlorophyll pigments and enzymatic activities under different irrigation regimes. *Agronomy* 12 (4), 845. doi: 10.3390/AGRONOMY12040845

Ishfaq, A., Aftab, S. W., Ashfaq, A., Masud, C. M. J., and Jasmeet, J. (2018). Optimizing irrigation and nitrogen requirements for maize through empirical modeling in semi-arid environment. *Environ. Sci. pollut. Res. Int.* 26 (2), 1227–1237. doi: 10.1007/s11356-018-2772-x

Jia, Y., Shao, M., and Jia, X. (2013). Spatial pattern of soil moisture and its temporal stability within profiles on a loessial slope in Northwestern China. *J. Hydrol.* 495, 150–161. doi: 10.1016/j.jhydrol.2013.05.001

Jiang, Y. B., Qi, G. P., Yin, M. H., Kang, Y. X., Ma, Y. L., Wang, J. H., et al. (2022). Effects of water regulation and planting patterns on soil moisture, yield and quality in artificial grassland. *J. Soil Water Conserv.* 36 (6), 260–270. doi: 10.13870/j.cnki.stbcxb.2022.06.032

Jin, G. Z., and Ma, Y. L. (2000). Development and utilization of light sierozem in Ningxia. *Arid Zone Res.* 17 (03), 59–63. doi: 10.13866/j.azr.2000.03.011

Jing, Y., and Han, D. Z. (2018). Comprehensive evaluation of the industrial competitiveness of five major production areas of Chinese *Lycium Barbarum*. *Iss. For Economics.* 38 (03), 86–91+111. doi: 10.16832/j.cnki.1005–9709.2018.03.015

Kang, Y. X., Yin, M. H., Ma, Y. L., Tang, Z. X., Jia, Q., Qi, G. P., et al. (2023). Response of water-nitrogen distribution and use to water deficit under different applied nitrogen fertilizer rates in *Bromus inermis* Grassland. *Agronomy* 13 (3), 745. doi: 10.3390/AGRONOMY13030745

Kulczyński, B., and Gramza-Michałowska, A. (2016). Goji Berry (*Lycium barbarum*): Composition and health effects–a review. *Pol. J. Food Nutr. Sci.* 66 (2), 67–75. doi: 10.1515/pjfns-2015-0040

Kumar, M., Rajput, T., Kumar, R., and Patel, N. (2016). Water and nitrate dynamics in baby corn (*Zea mays* L.) under different fertigation frequencies and operating pressures in semi-arid region of India. *Agric. Water Manage.* 163, 263–274. doi: 10.1016/j.agwat.2015.10.002

Li, Q. Q., Bian, C. Y., Liu, X. H., Ma, C. J., and Liu, Q. R. (2015b). Winter wheat grain yield and water use efficiency in wide-precision planting pattern under deficit irrigation in North China Plain. *Agric. Water Manage.* 153, 71–76. doi: 10.1016/j.agwat.2015.02.004

Li, Y. K., Ma, Q. L., Wang, Y. L., Sun, T., Jin, H. J., Song, D. W., et al. (2015a). Soil characteristics of medlar wood growing on secondary salinization land in Jingdian irrigation zone. *Acta Pratac. Sin.* 24 (05), 66–74. doi: 10.11686/cyxb20150508

Liu, M., Yang, S. Q., Fu, X., and Wan, H. (2018a). Effects of water nitrogen interaction on growth and yield of *Lycium Barbarum* under brackish water drip irrigation. *Sav. Irrig.* 01, 33–37. doi: 10.3969/j.issn.1007-4929.2018.01.008

Liu, M., Zhang, Z. X., Zheng,, E. N., Chen, P., Chen, S. H., and Shang, W. B. (2018b). Photosynthesis, water and nitrogen use efficiency of maize as impacted by different combinations of water and nitrogen applications. *J. Irrig. Drainage.* 37 (12), 27–34. doi: 10.13522/j.cnki.ggps.20180197

Liu, X. H., Guo, C. C., He, S. S., Zhu, H. Y., Li, J. Y., Yu, Z. Y., et al. (2020b). Divergent gross nitrogen transformation paths in the topsoil and subsoil between abandoned and agricultural cultivation land in irrigated areas. *Sci. Total Environ.* 716 (C), 137148. doi: 10.1016/j.scitotenv.2020.137148

Liu, X. L., Ma, L. H., Yan, X. Y., Yang, R. H., and Zi, H. (2020a). Effect of different irrigation method on sandy soil moisture and yield of wolfberry. *J. Irrig. Drainage.* 39 (02), 10–15. doi: 10.13522/j.cnki.ggps.2019234

Lu, J. J., Nie, Y. F., Wei, J. J., Sheng, H. Y., Hua, M. X., Xu, M. C., et al. (2022). Effects of different nitrogen application measures on NH_3 volatilization and N_2O emissions in a wolfberry orchard. *J. Agro-Environ. Sci.* 41 (1), 210–220. doi: 10.11654/jaes.2021-0702

Luo, W. H., Shi, Z. J., Wang, X. M., Li, J., and Wang, R. (2020). Effects of water saving and nitrogen reduction on soil nitrate nitrogen distribution, water and nitrogen use efficiencies of winter wheat. *Acta Agron. Sin.* 46 (06), 924–936. doi: 10.3724/SP.J.1006.2020.91060

Lv, H. F., Lin, S., Wang, Y. F., Lian, X. J., Zhao, Y. M., Li, Y. J., et al. (2018). Drip fertigation significantly reduces nitrogen leaching in solar greenhouse vegetable production system. *Environ. pollut.* 245 (01), 694–701. doi: 10.1016/j.envpol.2018.11.042

Lv, Y. R., Wang, J. H., Yin, M. H., Kang, Y. X., Ma, Y. L., Jia, Q., et al. (2023). Effects of planting and nitrogen application patterns on alfalfa yield, quality, water–nitrogen use efficiency, and economic benefits in the Yellow River Irrigation Region of Gansu Province, China. *Water* 15 (2), 251. doi: 10.3390/W15020251

Ma, P. S., Zhu, R. Y., Bai, C. C., and Yu, J. Q. (2021). Survey on the plant resources and industrial development of wolfberry in Ningxia China. *Chin. Tradit Patent Med.* 43, 171–174. doi: 10.3969/j.issn.1001-1528.2021.11.061

Ma, Z. H., Yin, J., Yang, Y. P., Sun, F. B., and Yang, Z. (2023). Effect of water and nitrogen coupling regulation on the growth, physiology, yield, and quality attributes and comprehensive evaluation of wolfberry (*Lycium barbarum* L.). *Front. Plant Sci.* 14. doi: 10.3389/FPLS.2023.1130109

Min, J., Zhao, X., Shi, W. M., Xing, G. X., and Zhu, Z. L. (2011). Nitrogen balance and loss in a greenhouse vegetable system in Southeastern China. *Pedosphere* 21, 464–472. doi: 10.1016/S1002-0160(11)60148-3

Mokhele, B., Zhan, X. J., Yang, G. Z., and Zhang, X. L. (2012). Review: Nitrogen assimilation in crop plants and its affecting factors. *Can. J. Plant Sci.* 92 (3), 399–405. doi: 10.4141/cjps2011-135

Nie, T., Chen, P., Zhang, Z., Qi, Z. J., Lin, Y. Y., and Xu, D. (2019). Effects of different types of water and nitrogen fertilizer management on greenhouse gas emissions, yield, and water consumption of paddy fields in cold region of China. *Int. J. Environ. Res. Public Health* 16 (9), 1639. doi: 10.3390/ijerph16091639

Niu, X. Q., Jia, X. X., Yang, X. F., Wang, J., Wei, X. R., Wu, L. H., et al. (2022). Tracing the sources and fate of NO_3^- in the vadose zone-groundwater system of a thousand-year-cultivated region. *Environ. Sci. Technol.* 56, 9335–9345. doi: 10.1021/acs.est.1c06289

Qin, Z. Y., Zhang, Z. X., Sun, D., Song, J., Sun, Z. H., and Li, T. C. (2021). Effect of water and nitrogen coupling on rice yield and nitrogen absorption and utilization in black Soil. *Trans. Chin. Soc Agric. Mach.* 52 (12), 324–335. doi: 10.6041/j.issn.1000-1298.2021.12.034

Rakesh, K., Kumar, P. N., Uttam, K., Talha, J., Al-Huqail, A. A., Singh, R. V., et al. (2022). Coupling effects of nitrogen and irrigation levels on growth attributes, nitrogen use efficiency, and economics of cotton. *Front. Plant Sci.* 13. doi: 10.3389/FPLS.2022.890181

Ren, H., and Bai, H. L. (2022). Study on the development status, dilemmas and countermeasures of wolfberry industry in Ningxia. *Gansu Agric. Sci. Tech.* 53 (09), 10–14. doi: 10.3969/j.issn.1001-1463.2022.09.003

Ren, H., and Wang, J. L. (2019). The Development status and improving path of *Lycium Barbarum* L. Industry in China. *Sci. Tech Dev.* 15 (03), 310–317. doi: 10.11842/chips.2019.03.011

Si, Z. Y., Zain, M., Mehmood, F., Wang, G. S., Gao, Y., and Duan, A. W. (2020). Effects of nitrogen application rate and irrigation regime on growth, yield, and water-nitrogen use efficiency of drip-irrigated winter wheat in the North China Plain. *Agric. Water Manage.* 231, 106002. doi: 10.1016/j.agwat.2020.106002

Sun, P. Y., Li, X. Z., Gong, X. L., Liu, Y., Zhang, X. Y., and Wang, L. (2014). Carbon, nitrogen and phosphorus ecological stoichiometry of Lateolabrax macultus and Acanthogobius ommaturus in the estuary of Yangtze River, China. *Acta Ecologica Sinica.* 34 (4), 196–203. doi: 10.1016/j.chnaes.2013.06.009

Tan, J., Liu, F., Xu, T., and Xiao, T. (2021). Exploration of water-nitrogen coupling effects in paddy field based on ORYZA (v3) model. *J. Sci. Food Agric.* 102, 396–406. doi: 10.1002/jsfa.11369

Tang, Z. X., Yin, M. H., Qi, G. P., Kang, Y. X., Ma, Y. L., Wang, J. H., et al. (2022). Effects of optimal irrigation and nitrogen coupling on *Bromus inermis* yield, nitrogen, phosphorus, and potassium stoichiometric characteristics. *J. Plant Nutr. Fert.* 28 (03), 32–545. doi: 10.11674/zwyf.2021460

Wang, Y. L., Cheng, J., Xu, J. J., Lei, X., Guo, J. X., He, Z. H., et al. (2021). High-quality development suggestions and quality safety status of wolfberry in Gansu-Based on the quality safety status of wolfberry in Jingyuan County, Gansu Province. *For. By-Prod Spec.* 175 (06), 87–91. doi: 10.13268/j.cnki.fbsic.2021.06.033

Wang, L., Pan, Q. L., Li, R. J., and Guo, K. X. (2015). The application of fertigation in Qaidam wolfberry production. *J. Qinghai Univ. (Nat. Sci.)* 33, 24–28. doi: 10.13901/j.cnki.qhwxxbzk.2015.02.005

Wang, H., Su, W. P., Zhao, X. L., Kuerban, A., Sun, S. R., Xue, L. H., et al. (2022). Effect of different irrigation and nitrogen application on yield, water and nitrogen use efficiency of spring wheat sown in winter. *J. Triticeae Crops.* 42 (11), 1381–1390. doi: 10.7606/j.issn.1009-1041.2022.11.09

Wozniak, J. R., Swannack, M. T., Butzler, R., Llewellyn, C., and Davis, S. E. (2012). River inflow, estuarine salinity, and Carolina wolfberry fruit abundance: linking abiotic drivers to whooping crane food. *J. Coast. Conserv.* 16 (3), 345–354. doi: 10.1007/s11852-012-0205-4

Wu, J. N., Wei, X. D., Li, X., Zhang, J. F., and Xie, Y. F. (2018). Research progress in nitrogen use efficiency in plants. *Plant Physiol.* 54 (09), 1401–1408. doi: 10.13592/j.cnki.ppj.2018.0071

Yang, S. C., Wang, C. B., Huo, L., Jiang, W. L., and Wen, M. J. (2019). Effects of different tillage practices on soil organic carbon of cultivated land in Gansu Yellow River irrigation district. *Trans. Chin. Soc Agric. Eng.* 35 (02), 114–121. doi: 10.11975/j.issn.1002-6819.2019.02.015

Yao, R., Heinrich, M., and Weckerle, C. S. (2018). The genus *Lycium* as food and medicine: A botanical, ethnobotanical and historical review. *Ethnopharmacol* 212, 50–66. doi: 10.1016/j.jep.2017.10.010

Yin, Z. R., Lei, J. Y., Zhao, Y., Gui, L. G., and Huang, J. C. (2021). Effect of drip irrigation amounts on characteristics of moisture and nutrient transfer in soil in the *Lycium barbarum* Field. *Res. Soil Water Conserv.* 28 (04), 62–69. doi: 10.13869/j.cnki.rswc.2021.04.009

Zhan, Y. F., Lu, Y. F., Zhen, W. L., and Da, S. C. (2016). Spatial distribution characteristics of root system of *Lycium barbarum* L. @ in Hexi Irrigation Area. *Res. Soil Water Conserv.* 23 (04), 133–137. doi: 10.13869/j.cnki.rswc.2016.04.017

Zhang, H. Z., Khan, A., Tan, D. K.Y., and Luo, H. H. (2017). Rational water and nitrogen management improves root growth, increases yield and maintains water use efficiency of cotton under mulch drip irrigation. *Front. Plant Sci.* 8. doi: 10.3389/fpls.2017.00912

Zhang, Y., Wang, P., Wang, L., Sun, G. Q., Zhao, J. Y., Zhang, H., et al. (2015). The influence of facility agriculture production on phthalate esters distribution in black soils of northeast China. *Sci. Total Environ.* 506, 118–125. doi: 10.1016/j.scitotenv.2014.10.075

Zhao, X., Xin, Y. F., Zhang, Y. L., Zhu, C., Zheng, Y. Z., Tian, X. F., et al. (2021). Effect of different vegetation types on temporal and spatial variation of soil moisture on leeward slope of Mu Us Sandy Land. *J. Northwest For Univ.* 36 (03), 36–43. doi: 10.3969/j.issn.1001-7461.2021.03.06

Zheng, H. Y., Cao, X. S., Chang, L. M., and Hao, Y. X. (2020). Research on optimized irrigation schedule of winter wheat indifferent saline soils in Hetao Irrigation Area. *J. Water Resour. Water Eng.* 31 (4), 152–156. doi: 10.11705/j.issn.1672-643X.2020.04.22

Zheng, G. B., Zhang, Y. P., Kong, D. J., and Zhu, J. X. (2012). Effect on changes of soil water dynamics of *Lycium barbarum* by different irrigation. *Acta Agric. Bor-Occid Sin.* 21 (02), 117–120. doi: 10.7606/j.issn.1004-1389.2012.2.024

Zhou, C. Y., and Bai, G. S. (2015). Formation cause and control methods about soil salinization in Hetao lrrigation Area. *Yellow River* 37 (09), 143–148. doi: 10.3969/j.issn.1000-1379.2015.09.038

frontiers | Frontiers in Plant Science

TYPE Original Research
PUBLISHED 24 January 2024
DOI 10.3389/fpls.2024.1298249

OPEN ACCESS

EDITED BY
Shahbaz Khan,
Huazhong Agricultural University, China

REVIEWED BY
Mir Muhammad Nizamani,
Guizhou University, China
Anyong Hu,
Nantong University, China
Li Jing,
Chinese Academy of Sciences (CAS), China

*CORRESPONDENCE
Bozhi Wu
bozhiwu@outlook.com
Feng Zhou
2015061@ynau.edu.cn

†These authors have contributed equally to this work

RECEIVED 26 October 2023
ACCEPTED 10 January 2024
PUBLISHED 24 January 2024

CITATION
Zhou S, Xia P, Chen J, Xiong Q, Li G, Tian J, Wu B and Zhou F (2024) Optimizing nitrogen application position to change root distribution in soil and regulate maize growth and yield formation in a wide–narrow row cropping system: pot and field experiments. *Front. Plant Sci.* 15:1298249. doi: 10.3389/fpls.2024.1298249

Optimizing nitrogen application position to change root distribution in soil and regulate maize growth and yield formation in a wide–narrow row cropping system: pot and field experiments

Shiyong Zhou†, Pan Xia†, Junping Chen, Qijiao Xiong, Guanhan Li, Jingyi Tian, Bozhi Wu* and Feng Zhou*

Faculty of Agronomy and Biotechnology, Yunnan Agricultural University, Kunming, Yunnan, China

The wide-and narrow-row cropping technology used for maize has the advantages of protecting cultivated soil and improving the population structure in maize fields. However, the relationship between nitrogen application position and root interactions has not been determined. Through pot and field experiments, we evaluated the effects of two nitrogen application positions ((narrow row nitrogen application (RC) and wide row nitrogen application (RN)) and two nitrogen application regimens ((high nitrogen(HN) and low nitrogen(LN)) on root growth and yield composition of wide-narrow row maize during the flowering and harvest stages. In field experiments, RC increased the biomass, length and surface area of competing roots (narrow-row roots, CR) at the flowering stage. The yield and agronomic efficiency of N(AEN) and partial factor productivity of N(PFPN) were increased by RN compared to RC under HN, However, the AEN under LN was significantly lower; There was no significant effect on maize growth and biomass allocation at the same level of application of N. At the flowering stage, the results of CR and non-competing roots (wide-row roots, NCR) was consistent under pot experiments and the field experiments, and the yield under RN was also higher than that under RC, although the difference was not significant. Furthermore, according to the principal component analysis and correlation analysis, the competing roots were the main factor influencing yield and AEN. In conclusion, our study showed that RN is a useful fertilization method to improve overall productivity. All in all, how roots coordinate neighbors and nitrogen spatial heterogeneity is a complex ecological process, and its trophic behavior deserves further study.

KEYWORDS

wide-and narrow-row cropping system, maize, yield, foraging behavior, nitrogen

1 Introduction

The achievement of efficient nutrient utilization, the improvement of crop productivity, and the reduction of competition among individuals in the population are the primary goals of optimizing fertilization methods, as well as the requirements of achieving intensive agricultural development (Liu et al., 2022; Wu et al., 2022a). Strip fertilizer has been widely discussed as a method for improving fertilizer utilization efficiency in modern agricultural production. Strip tillage and deep strip application of nitrogen have been reported to significantly improve maize growth, nutrient absorption, and grain yield (Nash et al., 2013; Jia et al., 2018). It has also been reported that applying a single nutrient belt or a combined nutrient belt near the maize planting ditch at planting can improve nutrient absorption and utilization efficiency in the early stage and promote plant growth under humid soil conditions (Rutan and Steinke, 2018; Quinn et al., 2020). This is not only due to the heterogeneity of soil nutrients created by strip fertilization, which leads to local nutrient concentrations, stimulates lateral root development, and establishes an ideal root configuration, thus increasing nutrient absorption and crop yield, but also due to the concentration of soil nutrient resources by strip fertilization, which regulates root morphology and physiology to respond to changes in environmental conditions, enhancing the ability of the plant to obtain resources. In addition, strip fertilization can also reduce ammonia volatilization in the soil, reduce the fixation and adsorption of phosphorus and potassium by soil particles, and improve the effectiveness of phosphorus and potassium. For example, in the no-tillage mode, the application of urea strips significantly reduces ammonia volatilization by 52% compared to spraying (Trapeznikov et al., 2003; Rochette et al., 2009).

The depth of strip fertilization is also an important factor that affects fertilizer of efficiency. Many studies have shown that increasing the depth of fertilization to an appropriate level can increase the nitrogen content of nitrate in the soil, improve the photosynthetic characteristics of the leaves, increase the rate of fertilizer utilization, and indirectly improve the nutritional status of maize plants (Aluoch et al., 2022; Wu et al., 2022b). For example, the seed yield, oil yield, and fertilizer use efficiency of rapeseed fertilized at a depth of 10 cm were significantly greater than those at 5 and 15 cm (Chen et al., 2023). In the maize–wheat rotation system, a strip fertilization depth of 15 cm can effectively increase the root length density, root surface area density, nitrogen absorption, leaf area index, dry matter accumulation, and radiation interception ability of maize and, at the same time, increase the yield of subsequent crops (wheat) (Chen et al., 2022). In monoculture maize, compared to conventional nitrogen application, increasing the fertilization depth to 12 cm and reducing the amount of slow-release fertilizer applied by 20% still maintained a higher maize yield (Hu et al., 2023). In summary, although strip fertilization is superior to conventional hole fertilization and scatter fertilization in fertilizer utilization rate and yield, the above research does not consider the influence of the interaction between crop roots under intensive planting conditions. In the wide-and narrow-rows of the maize planting systems, the roots between the narrow-rows are highly overlapped, which has a competitive effect on nutrients. We changed the position of strip application (fertilization between narrow-rows: fertilizer and roots interaction; wide interrow fertilization: root communication but no fertilizer effect) to change the complex communication between crop roots and to explore how crop roots respond to the strip application position in an intensive planting system according to the interaction between roots and fertilizers.

We hypothesized that changing the fertilization position (nitrogen application in overlapping areas or nonoverlapping areas) could change the heterogeneity of soil nitrogen distribution and then change the distribution of inter-plant roots, reduce the competition of inter-plant roots for nutrients in the population, and improve the spatial matching degree between maize roots and soil nutrients, and improve the utilization rate of nutrient resources and crop productivity to realize sustainable agricultural development. Here, a pot experiment using the 'root splitting' method and a field validation experiment were used to evaluate the strip application of nitrogen fertilizer in different positions. The purpose of this study was: (1) to determine the effects of nitrogen application at different locations on the spatial distribution and growth of maize roots; (2) to determine the effects of nitrogen fertilizer application at different positions on root cultivation behavior and fertilizer utilization rate; (3) to study the effects of nitrogen fertilization on maize growth, biomass distribution, and yield. Through this study, we hope to better understand the effects of nitrogen application at different locations on root distribution and growth, as well as its effects on crop nutrient utilization and yield. This approach will help provide sustainable agricultural development solutions, promote soil health, and ensure the sustainability of crop production.

2 Materials and methods

2.1 Field experiment

2.1.1 Experiment site

This experiment was carried out at the Daheqiao Experimental Station (103°16′41"E, 25°31′07"N), Xundian County, Yunnan Agricultural University, from April to August 2023. The altitude of this area is 1850 m, and precipitation is concentrated from June to September. The average annual precipitation is 1180 mm, and the average annual evaporation is 2384 mm. This area belongs to the north subtropical monsoon climate, with an annual average temperature of 15.3 C. The soil was yellow brown soil (GB/T 17296-2009, 17% sand (0.05–2 mm), 38% silt (0.002-0.05 mm), and 45% clay (< 0.002 mm)). The pH of the 0–20 cm soil layer was 6.92, and the contents of total nitrogen, phosphorus, and potassium contents were 1.16, 0.79, and 11.82 g kg^{-1}, respectively. The available N, P, and K were 45.26, 20.34, and 83.62 mg kg^{-1}, respectively, and the content of organic matter in the soil was 16.88 g kg^{-1}.

2.2.2 Experimental design

There were two experimental factors: nitrogen position and nitrogen level. The nitrogen application position included

competitive root side nitrogen application(RC) (i.e., narrow-row side nitrogen application, as shown in Figure 1B) and non-competitive root side nitrogen application (RN) (i.e., wide-row side nitrogen application, as shown in Figure 1A). The nitrogen level was established with two nitrogen levels: high nitrogen (HN, 9 g/plant) and low nitrogen (LN, 4.5 g/plant). There were four treatments in total, namely a narrow-row with high nitrogen (RCHN), narrow row with low nitrogen (RCLN), wide row with high nitrogen (RNHN), and wide row with low nitrogen (RNLN), which were arranged in a randomized block design. Each treatment was repeated three times, with a plot area of 5 m × 7 m = 35 m^2 and an interval of 1 m between the plots. Planting specifications were based on wide-and narrow-rows, with wide-rows of 80 cm, narrow-rows of 20 cm, and a plant spacing of 30 cm. The treatments are shown in Figures 1A, B, and the plant density was 66,667 plants/ha. The maize was sown on April 3, 2023. Before sowing, 150 kg ha^{-1} calcium superphosphate (P_2O_5 < 16%) and 100 kg ha^{-1} potassium sulfate (K_2O < 52%) were applied uniformly to the 20 cm soil layer at one time. N fertilizer (Urea, N = 46%) was applied in 50%:50% furrow strips at the seedling stage (April 28, 2020) and the booting stage (May 20, 2023), with a depth of 10 cm. Experimental management was carried out as necessary for artificial weeding and pest control.

2.2 Pot experiment

2.2.1 Experimental design

The pot experiment was conducted in a greenhouse at the same position as the field experiment, treatments were the same as in the field experiment: location of nitrogen (no competitive side nitrogen application (Figure 2A) and competitive root side nitrogen application (Figure 2B) and nitrogen level (high nitrogen and low nitrogen). The tested soils were taken from the field experiment. In this experiment, the 'root splitting' technology was used to explore the feeding behavior of the maize roots with different nitrogen application positions, which was an effective way to separate underground parts to prevent the diffusion of soil nutrients between nutrient pots (Yu et al., 2013; in 't Zandt et al., 2015). we bundled three plastic bottles with a size of 18 cm × 17 cm × 41 cm (length × width × height) together, put a layer of nylon mesh (0.1 mm aperture) on the bottom to prevent the roots from sticking and to facilitate water penetration, and then cut off a groove with a height of 5 cm from the upper joint to facilitate seedling transplantation. Specific test devices are shown in Figures 2A, B. The completely random arrangement was repeated in the greenhouse to prevent uneven illumination. In three conjoined containers, 2.5 g of superphosphate (P_2O_5 < 16%) and 4 g of

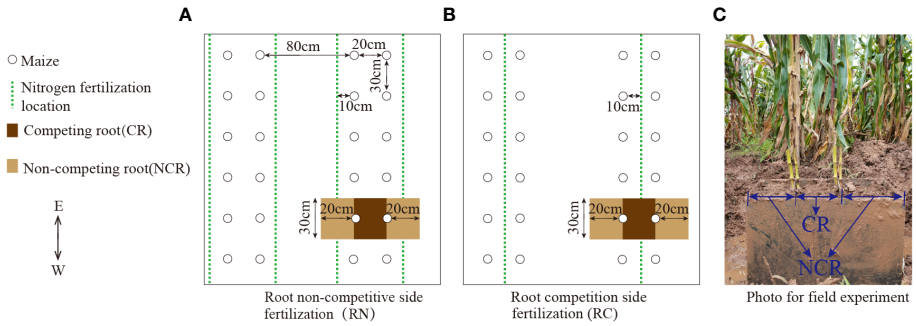

FIGURE 1
Planting diagram of the field experiment and sampling diagram of the roots. **(A)** Root non-competitive side fertilization (RN). **(B)** Root competition side fertilization (RC). **(C)** Photo of the field experiment. CR, Competing root; NCR, Non-competing root.

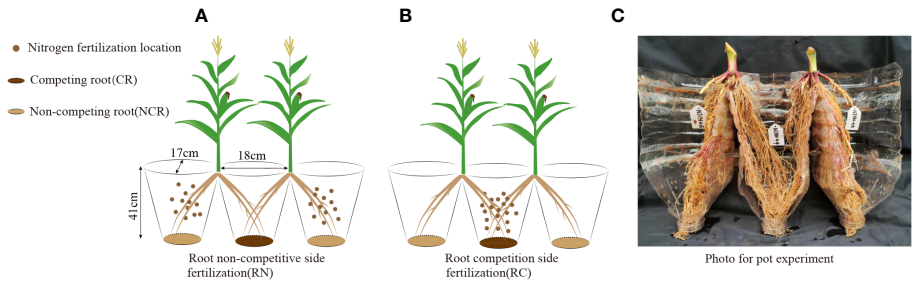

FIGURE 2
(A) Root non-competitive side fertilization (RN), **(B)** Root competition side fertilization (RC), **(C)** Photo of the pot experiment. CR, Competing root; NCR, Non-competing root.

potassium sulfate (K_2O < 52%) were mixed with sifted dry soil as base fertilizer and applied uniformly in three conjoined containers (approximately 10 kg per containers) at one time. The nitrogen application rate was the same as that in the field experiment, and was applied at 50%:50% of the total fertilizer amount two weeks after maize transplant and at the big bell mouth stage. The weeds were manually removed from the nutrient pots during growth.

2.2.2 Seedling preparation

The seeds of 'Qiaodan-6' of the same size and plumpness were soaked in warm water at 45°C for 24 hours and then placed on a wet filter paper seedbed to germinate. After the roots grew, they were cut with sterilized scissors, and the seeds were placed in a nutrition cup (8 cm × 10 cm, cylindrical) to germinate. Seven days after the seeds germinated in the nutrition cup, seedlings of the same size were selected for transplantation on March 20, 2023. After planting, seedlings that died or suffered serious diseases within one week were replaced with new plants, and plants were watered every 5 days to control the intensity of watering to ensure that no leakage occurred at the bottom.

2.3 Sampling and observation

In the field experiment, 12 plants were selected for each treatment at the flowering stage (July 6, 2023) and harvest stage (August 20, 2023). For the pot experiment, 16 plants were selected for each treatment at the flowering stage (June 20, 2023) and harvest stage (August 1, 2023), respectively. The leaf area was measured by the length–width coefficient method (maximum leaf length × maximum leaf width × 0.75) and then divided into vegetative and reproductive organs (mature stage). After the enzymes were deactivated at 105°C for 30 min and drying at 70°C until constant weight, the weight of dry matter was measured. In the mature stage under the field experiment, two rows of maize were selected in the middle of each plot for harvesting and yield measurement, and the yield was calculated using a 14% standard water content, which was converted into yield per unit area according to the measured yield area.

Root sampling: In the field experiment, because the roots of two adjacent maize plants between narrow-rows were interlaced with each other, it was impossible to distinguish a complete single root system between narrow-rows, so we considered two plants as a sampling unit. Before sampling, two maize roots were cut into two-halves from the center of the stem along the planting row with two self-made knives (thin steel plate with a thickness of 15 mm, cut to a length of 29 cm, and a width of 40 cm, and one side was polished to make it sharp for root cutting), and then the steel plate (with a thickness of 15 mm) was welded into a cuboid with a length, width, and height of 60 × 30 × 40 cm. The two maize roots were divided into three parts by hammering them into the soil, as shown in Figure 1C, and the surrounding soil was digged out. A steel plate with a length of 60 cm and a width of 30 cm was hammered into the bottom of the cuboid to remove the whole cuboid clod, and a nylon mesh cloth was placed on the bottom, and the roots were then brought back to the laboratory for further cleaning, which included the middle competitive roots and the noncompetitive roots on both sides. After being scanned with a root scanner (Shanghai Zhongjing Technology Co., Ltd., China, Shanghai, China, ScanMaker i800 Plus) at the flowering stage, root length, root surface area, and average root diameter were analyzed by WinRHIZO 2019b (Regent Instruments Canada lnc., Quebec City, QB, Canada) and then dried to a constant weight at 70°C, which was recorded as dry matter.

Root sampling in the pot experiment was performed after withholding water for one week. When sampling, the nutrient pot was tapped to scatter the soil, and a cut was made around the nutrient pot at the original position during the maize flowering and harvest periods. They were then rinsed under flowing water, and all collected roots were brought back to the laboratory for further cleaning. After cleaning, the roots were divided into middle pot roots and two pot roots, which were recorded as competitive roots (RC) and noncompetitive roots (NCR), respectively (Figures 2A, B). Root scanning was carried out at the flowering stage (same as the field experiment) and then dried to a constant weight at 70°C, which was recorded as the dry matter of the root system. This sampling method maintained the integrity of the root system and allowed comparative analysis of competitive roots and noncompetitive roots.

2.4 Data analysis

To clarify the effect of plant resource acquisition ability and allocation strategy, we used the root: shoot ratio to evaluate the competitiveness of plants under the nitrogen application position and nitrogen level and the biomass investment ratio of roots and shoots. In the analysis of the accuracy of roots, we used the ratio of root biomass between high nitrogen patches and low nitrogen patches to measure the adaptive response of plants to heterogeneous nutrients; the higher the ratio, the higher the accuracy of root cultivation (Wu et al., 2012). In this study, CR/NCR biomass under narrow row nitrogen application, and NCR/CR biomass was used under wide row nitrogen application. Moreover, agronomic nitrogen efficiency (AEN) and partial nitrogen productivity (PFPN) were used to evaluate nitrogen efficiency, and the calculation formula was as follows: AEN (kg kg^{-1}) = (maize grain yield in the nitrogen application area − maize grain yield in the non-nitrogen application area)/nitrogen application rate; PFPN (kg kg^{-1}) = grain yield/nitrogen application rate in the nitrogen application area (Zhang et al., 2020; Liang et al., 2022).

Using SPSS 24.0 as a fixed factor, the yield, harvest index, total root biomass, total root surface area, average root diameter, root: shoot ratio, and nitrogen use efficiency of maize in the field and pot experiments were analyzed by two-factor variance analysis with nitrogen application position and nitrogen level as fixed factors. After analysis, multiple comparisons were made using the least significant difference (LSD) method. The biomass, surface area, length, and average diameter of competitive and noncompetitive roots in field and pot experiments were analyzed using Student's t-test. Based on PCA and correlation analysis (data were processed standardized with a double-tailed test), the key factors influencing competitive and non-competitive roots on the yield and agronomic efficiency of nitrogen fertilizer were explored. Significance was considered as $P < 0.05$.

3 Results

3.1 Field experiment

3.1.1 Yield, biomass allocation, and agronomic characteristics

Under high nitrogen conditions, the maize yield in the RN treatment was significantly higher than that of the RC treatment (F = 5.45, P = 0.02), while the difference in yield was not significant under low nitrogen conditions. However, RC was higher than RN, and the yield increased by 3.63% (Figure 3A), indicating that the wide-row application of high nitrogen had obvious advantages in increasing the yield, while low nitrogen had slight disadvantages. There were no significant differences in the harvest index between treatments (F = 1.39, P = 0.25), showing the trend: RNHN > RCLN > RNLN > RCLN (Figure 3B). Although there was no significant statistical difference between treatments (F = 1.72, P = 0.19), the root: shoot ratio was higher for RC than for RN (Figure 3C), indicating that the RC treatments had greater investment in the root system, which was not conducive to growth and an increase in the yield of the aboveground parts. Under RN, the root:shoot ratio was lower under high nitrogen conditions than under low nitrogen conditions, indicating that an adequate nitrogen fertilizer supply could reduce the root:shoot ratio, which reduces the distribution of dry matter to the underground roots.

The leaf area index (LAI) reflects the total area of the plant leaves, which is closely related to the photosynthesis ability of the plants. Under RC, there were no significant differences between high and low nitrogen levels. Under RN, the LAI of high nitrogen was significantly greater than that of low nitrogen (F = 6.13, P < 0.01), indicating that treatment with RN could better regulate leaf growth (Figure 3F). A higher plant height and stem diameter of crops can help them occupy a higher position in the population, better competition for light and other resources needed for growth, and improve their competitiveness. As shown in Figures 3D, E, in RC, the plant height was significantly higher under high nitrogen conditions than under low nitrogen conditions (F = 5.24, P < 0.01). There was no significant difference in the stem diameter (F = 0.95, P = 0.33), but under wide-rows, the opposite was true for nitrogen application. These results indicate that the nitrogen application rate significantly affected the leaf area index, plant height, and stem diameter of crops and that a higher nitrogen application rate could achieve greater production potential.

3.1.2 Root growth and cultivation behavior

For total root biomass, RCLN was significantly higher than RCHN at the flowering stage (Figure 4A), while RN was the opposite (F = 4.02, P = 0.02). Moreover,CR biomass was significantly higher than that of NCR biomass in RC (high nitrogen: F = 0. 35, P = 0. 02; low nitrogen: F = 0.52, P = 0.03). The biomass of CR was significantly less than that of NCR biomass in RN (high nitrogen: F = 0.70, P = 0.02, low nitrogen: F = 1.27, P = 0.001). At maturity, there was no significant difference neither in total biomass of CR nor NCR biomass between treatments, but in the trend of total biomass, CR and NCR biomass was consistent during the flowering period for narrow row nitrogen application. However, in wide-row nitrogen application, the CR and NCR biomass exhibited opposite trends during the flowering period (Figure 4B), indicating that after the flowering period, the field nitrogen was exhausted and that the root system grew toward the

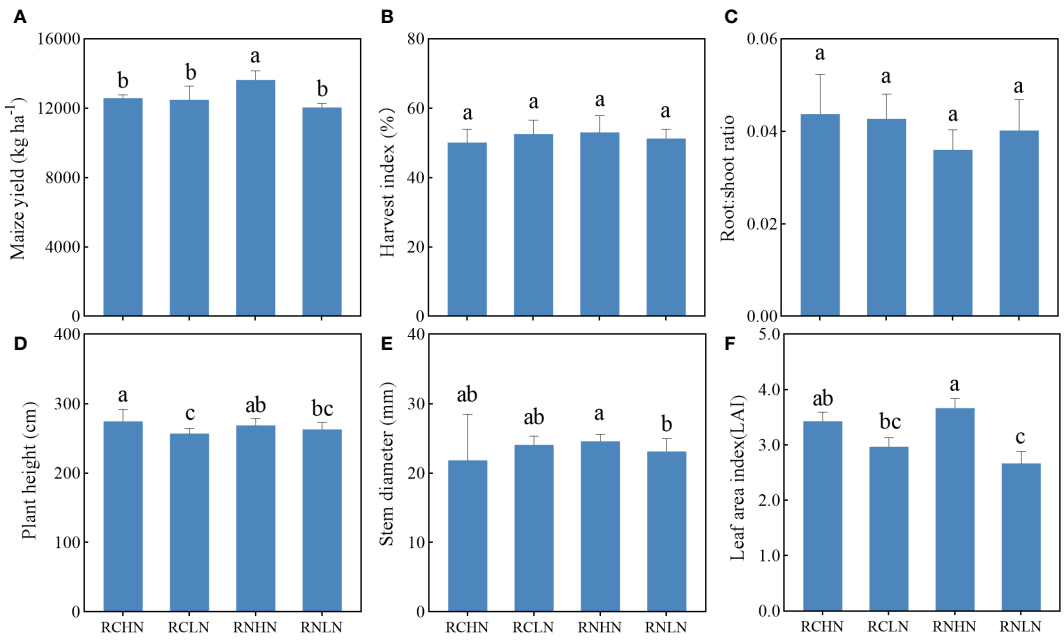

FIGURE 3
Effects of nitrogen application location and nitrogen level on yield, biomass allocation and agronomic traits in the field experiment. **(A)** Yield. **(B)** Harvest index. **(C)** Root : shoot ratio. **(D)** Plant height. **(E)** Stem diameter and **(F)** Leaf area index. Different lowercase letters indicate a significant difference between treatments (P < 0.05).

10.3389/fpls.2024.1298249

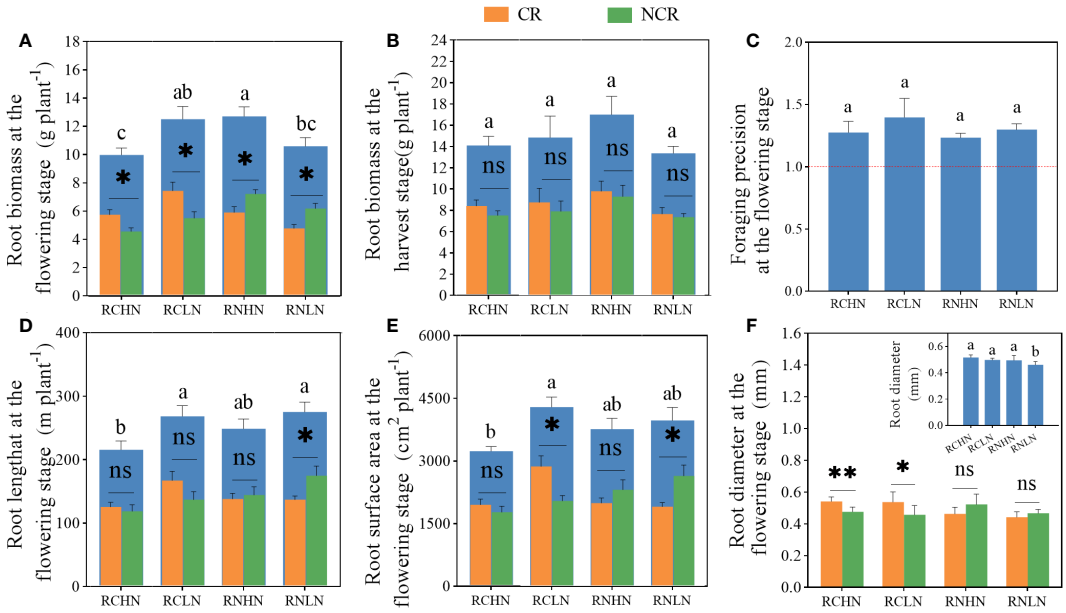

FIGURE 4
Effects of nitrogen application location and nitrogen level on root traits and foraging precision in the field experiment. **(A)** Root biomass at the flowering stage. **(B)** Root biomass at the harvest stage. **(C)** Foraging precision at the flowering stage. **(D)** Root length at the flowering stage. **(E)** Root surface area at the flowering stage. **(F)** Root diameter at the flowering stage; CR, Competitive root; NCR, Non-competiting root. Different lowercase letters indicate significant differences between treatments (P< 0.05). ns,* and ** indicate significance between the CR and NCR (P>0.05, P<0.05, and P<0.01), respectively.

roots of neighboring plants to absorb nutrients. Moreover, there was no significant difference in the foraging precision ($F = 0.55$,$P = 0.65$) (Figure 4C), which were greater than 1, indicated that the greater degree to which the plant was heterogeneous in terms of root adaptation to nitrogen, the greater degree to which the plant was seeking culture.

The root length and root surface area exhibited the same trend (Figures 4D, E), showing that under the narrow-row nitrogen application, these values were significantly greater under low nitrogen application than under high nitrogen application (root length: $F = 5.25$, $P = 0.008$; surface area: $F = 3.40$, $P = 0.038$). In the wide-row nitrogen application, there was no significant difference between the high nitrogen and low nitrogen application. Compared with the root length and surface area of CR and NCR, only was NCR significantly higher than CR under the application of wide-row nitrogen with low nitrogen (root length: $F = 3.34$, $P = 0.045$; surface area: $F = 3.60$, $P = 0.039$). When comparing the root length and surface area ratios of different diameters, the total root length ratio of high nitrogen application was higher than that of low nitrogen application, and the root length of RCHN, RCLN, RNHN, and RNLN with diameters less than 2.5 mm accounted for 96.45, 97.59, 97.67 and 97.95%, respectively, of the total root length, which was 81.09, 82.26, 81.92 and 83.96% of the total surface area. The length and surface area of roots larger than 4 mm in diameter under RNHN treatment were significantly higher than those in the RNLN treatment, indicating that the roots were sensitive to nitrogen under low nitrogen application (Supplementary Tables 1, 2). Root diameter is closely related to the ability of plants to absorb water and nutrients. The application of high nitrogen was significantly higher than the application of low nitrogen when nitrogen was applied in wide-rows ($F = 5.08$, $P = 0.009$), but there was no significant difference when nitrogen was applied in narrow-rows. Specifically, the diameter of the competitive roots was significantly higher than that of non-competitive roots when nitrogen was applied in narrow-rows because thicker roots provide a larger absorption area and help plants absorb more water and nutrients. There was no significant difference in diameter between CR and NCR when nitrogen was applied to wide-rows (Figure 4F). Combined with root biomass, root growth showed great spread and adaptability (growth toward nitrogen enrichment) despite the interaction of root systems among plants.

3.2 Pot experiment

3.2.1 Yield, biomass allocation, and agronomic characteristics

The yield was basically consistent with the trend of the field experiment and the yield under high nitrogen application was significantly greater than that under low nitrogen application in wide- rows ($F = 6.53$, $P < 0.01$), while the difference of yield in narrow-rows was not significant (Figure 5A). The harvest index of the wide-rows with high nitrogen had greater productivity, which was significantly higher than that of the wide-rows with low nitrogen, the narrow-rows with high nitrogen, and narrow-rows with low nitrogen ($F = 7.20$, $P < 0.01$), indicating that the crops could convert light energy into yield more effectively (Figure 5B). The root:shoot ratio of high nitrogen in narrow-rows was

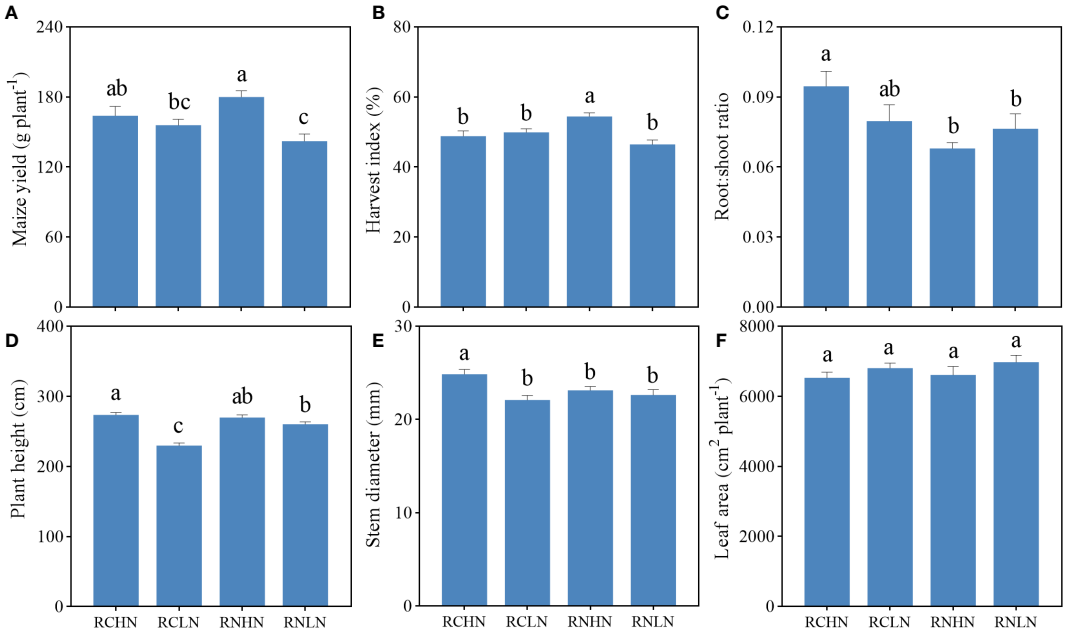

FIGURE 5
Effects of nitrogen application location and nitrogen level on yield, biomass allocation and agronomic traits in the pot experiment. **(A)** Yield. **(B)** Harvest index. **(C)** Root : shoot ratio. **(D)** Plant height. **(E)** Stem diameter, **(F)** Leaf area index. Different lowercase letters indicate significant difference between treatments ($P < 0.05$).

significantly higher than that in wide-rows ($F = 3.55$, $P = 0.02$), indicating that narrow-rows of roots were more sensitive to competition. There was no significant difference from application in wide-rows, but high nitrogen application in wide-rows was still the lowest (Figure 5C). These results indicate that crop biomass allocation was affected by nitrogen application position and nitrogen level, and it may be that nitrogen application position regulates the interaction between crop roots.

The trends in plant height and stem diameter were consistent with those observed in the field experiment (Figures 5D, E). Under narrow-row nitrogen application, the plant height and stem diameter were significantly greater in response to high nitrogen application than in response to low nitrogen application (plant height: $F = 30.97$, $P < 0.01$; stem diameter: $F = 5.88$, $P = 0.001$); There was no significant difference from the wide-row nitrogen application. There was no significant difference in leaf area of per plant (Figure 5F), but the general trend showed that the leaf area of per plant was higher under low nitrogen application than under high nitrogen application.

3.2.2 Root growth and cultivation behavior

Unlike the field experiment, there was no significant difference in root biomass in the pot culture ($F = 1.84$, $P = 0.062$), but the CR and NCR biomass exhibited the same trend as those in the field experiment. Except under RNLN, CR and NCR reached a significant levels in the other treatments (RCHN: $F = 0.053$, $P = 0.035$); RCLN: $F = 1.49$, $P = 0.048$, RNHN: $F = 1.41$, $P = 0.026$; Figure 6A). The root biomass in response to narrow-row nitrogen application was greater than that in response to wide-row nitrogen application at maturity and reached a significant level at a high nitrogen level ($F = 3.069$, $F = 0.044$). The biomass was lower in CR than in NCR (Figure 6B), indicating that under pot conditions, the application of narrow-row nitrogen promoted root biomass and the CR roots competed more for nitrogen, which was consistent with the accuracy of the root cultivation (Figure 6C).

The length (Figure 6D) and surface area (Figure 6E) of the roots were greater in the narrow- rows than in the wide-rows (root length: $F = 9.745$, $P < 0.01$, surface area: $F = 6.111$, $P = 0.002$), while the effects of nitrogen application position and nitrogen application rate were different between the CR and NCR. Under narrow-rows and low nitrogen conditions, the length and surface area of the NCR roots were significantly greater than those of the CR roots(root length: $F = 0.888$, $P = 0.045$, surface area: $F = 1.056$, $P = 0.048$). Under wide-rows, these traits were significantly greater in the NCR than in the CR (root length: $F = 0.904$, $P = 0.006$, surface area: $F = 0.674$, $P = 0.003$). Furthermore, under narrow-row nitrogen application, the proportion of roots length of different diameters accounted for the total length of root, except for those of 0 to 0.5 mm diameter, was significantly greater than that under low nitrogen application, while the difference in wide-row nitrogen application was mainly between 0.5 to 2.5 mm (Figure 6F). The 0 to 2.5 mm root length in RCHN, RCLN, RNHN and RNLN accounted for 96.67, 97.99, 97.38 and 97.20% of the total root length, respectively. Under wide-row nitrogen application, the proportion of root surface area with different diameters was not affected by the nitrogen application rate, while under the narrow-row nitrogen application, low nitrogen significantly affected the root surface area with 0 to 1 mm diameter, and low nitrogen promoted the root surface area with a small diameter to promoted the roots to obtain more nutrients and water in a deeper space. The proportion

10.3389/fpls.2024.1298249

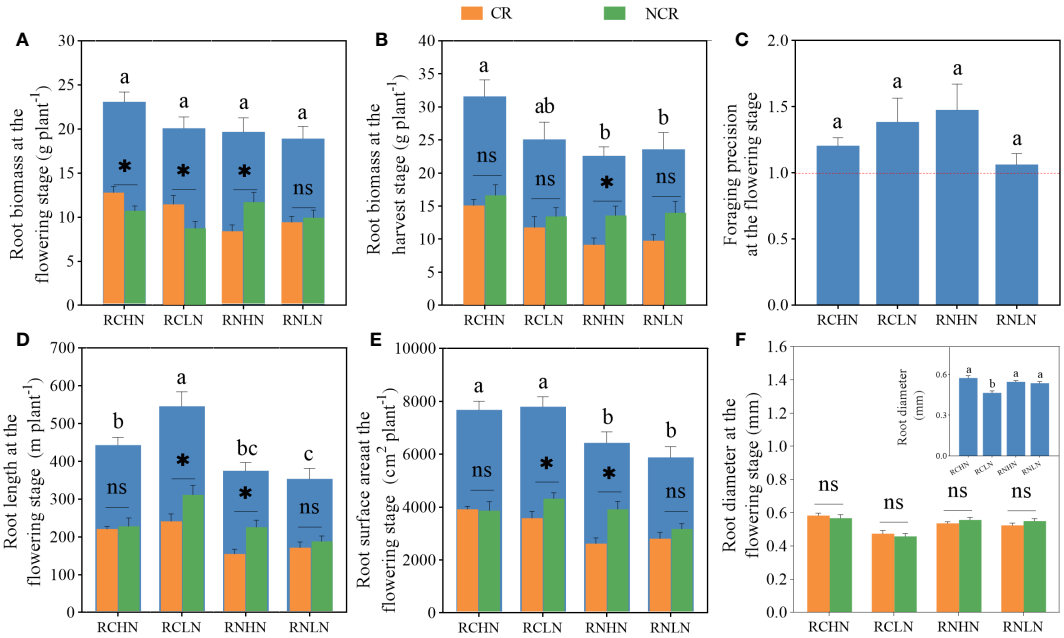

FIGURE 6
Effects of nitrogen application location and nitrogen level on root traits and foraging behavior in the pot experiment. **(A)** Root biomass at the flowering stage. **(B)** Root biomass at the harvest stage. **(C)** Foraging precision at the flowering stage. **(D)** Root length at the flowering stage. **(E)** Root surface area at the flowering stage. **(F)** Root diameter at the flowering stage; CR: Competitive root, NCR: Non-competiting root. Different lowercase letters indicate significant differences between treatments ($P < 0.05$). ns,* indicates a significant difference between the CR and NCR ($P > 0.05$, $P < 0.05$), respectively.

of the root surface area with 0 to 2.5 mm diameter in RCHN, RCLN, RNHN and RNLN to the total root surface area were 77.01, 83.95, 79.73 and 80.45%, respectively (Supplementary Tables 3, 4). The root diameter of high nitrogen was significantly higher than that of low nitrogen in the application of narrow-row nitrogen application ($F = 12.566$, $P < 0.01$), but the root diameter of CR and NCR were not significantly different under the wide-row nitrogen application. CR was greater than NCR in the narrow-row nitrogen application but was the opposite in response to wide-row nitrogen application, which was consistent with the results of the field experiment. The results indicate that the roots were more sensitive to low nitrogen application under the narrow-rows and that low nitrogen promoted root competition among CR, but this competition decreased with wide-row nitrogen application.

3.3 Nitrogen use efficiency

In the field experiment, by comparing different nitrogen levels, the AEN and PFPN were significantly greater at a low nitrogen level than at a high nitrogen level (AEN: $F = 76.68$, $P < 0.01$, PFPN: $F = 518.15$, $P < 0.01$; Table 1), indicating that plants generally adjust their physiological and metabolic processes to improve the efficiency of limited nitrogen use and achieve high nitrogen use efficiency under low nitrogen levels. Under a low nitrogen application rate, RC was significantly higher than RN, indicating that nitrogen uptake and utilization by roots could be stimulated by physical contact, chemical signals or shared resources and that the nitrogen uptake capacity of plants would be saturated under a high nitrogen application rate, leading to the inability to use some nitrogen effectively. The above data indicate that plants can limit nitrogen uptake by regulating the root architecture and the nitrogen uptake pathway or may reduce root growth and development and the nitrogen uptake area to avoid the negative impact of nitrogen surplus on plants, which can be confirmed by the root surface area and the root length of CR and NCR. In the pot experiment, under narrow-row nitrogen application, the agronomic efficiency of high nitrogen and the partial productivity of nitrogen were significantly reduced, which was consistent with the field experiment. With wide-row nitrogen application, high nitrogen reduced the partial productivity of nitrogen but improved the agronomic efficiency of nitrogen, and the interaction between the position of N application and the level of N was caused by root reinforcement.

3.4 Analysis of key factors of yield and nitrogen use efficiency of CR and NCR in field and pot experiments

According to the PCA results, PC1 and PC2 together explained 61.3% of the yield (Figure 7A) and 64.2% of AEN in the field experiment, (Figure 7C). The diameter, biomass, and surface area of competitive roots were important factors that affected yield, and the biomass and diameter of competitive roots were significantly positively correlated with yield (Figure 7B). The length, surface area, and biomass of competitive roots were important factors affecting the agronomic efficiency of nitrogen fertilizer. The competitive surface area ($r = 0.52$, $P = 0.009$) and length ($r =$

10.3389/fpls.2024.1298249

TABLE 1 Effects of nitrogen application location and nitrogen level on nitrogen use efficiency in the field and pot experiments.

Factor		Field Experiment		Pot Experiment	
NAP	NL	AEN (kg kg^{-1})	PFPN (kg kg^{-1})	AEN (kg kg^{-1})	PFPN (kg kg^{-1})
RC	HN	12.39±1.23c	21.76±3.61c	4.73±2.14b	18.21±2.07c
	LN	23.33±3.01a	42.08±5.81a	7.66±1.71a	34.62±1.71a
RN	HN	13.31±1.05c	22.68±2.56c	6.51±1.03a	19.99±2.31c
	LN	17.16±1.69b	35.91±6.33b	4.64±2.46b	31.61±1.09b
NAP (F-value)		0.02	0.01	1.60	0.37
NL (F-value)		76.68**	518.15**	1.18	189.66**
NAP*NL (F-value)		4.41	3.76	24.02**	5.57*

NAP, Nitrogen application position; NL, Nitrogen level; NAP*NL: Interaction effect. * and **indicates significance between treatments (P< 0.05, P < 0.01), respectively. AEN, Agronomic efficiency of N; PFPN, Partial factor productivity of N.

0.62, P = 0.001) were significantly positively correlated with AEN (Figure 7D). In the pot experiment, PC1 and PC2 explained 63.9% of the yield (Figure 7E) and 62.5% of the AEN (Figure 7G). The biomass and surface area of competitive roots and non-competitive roots were the key factors affecting the yield, and the non-competitive root biomass was positively correlated with the yield (r = 0.45, P = 0.01; Figure 7F), while the length of competitive roots and the surface area of noncompetitive roots were the key indicators affecting AEN (Figure 7H). In summary, the increase in competitive root length, surface area, and biomass were beneficial for yield, while the surface area of non-competitive roots was more strongly correlated with AEN. These findings demonstrate the effects of competitive roots and non-competitive roots on yield and AEN on different nitrogen application positions.

4 Discussion

4.1 Importance of the position of nitrogen application to root seeking behavior and productivity

In agroecosystems, root length, root surface area, root biomass, and other indicators are widely considered important factors that determine nitrogen absorption and utilization in the soil by crops. With the continuous development of intensive and diversified planting, the interactions between roots have become increasingly complex (Ma et al., 2022). In wide-and narrow-row cropping systems, changing the position of nitrogen application is particularly prominent in regulating plant growth and root distribution patterns, affecting the dynamic changes and competitive relationships of the plant population (Li et al., 2021). In this study, field experiments showed that, in a wide- and narrow-row planting system, the application of wide-row nitrogen had obvious positive effects on increasing total root biomass, total root surface area, and root length compared to those in narrow-row planting systems, especially under high nitrogen conditions (Figures 4A, D, E). This may be due to the excessive absorption of a small amount of nutrient resources by two adjacent maize roots in narrow-rows, which reduces the concentration of nutrients, thus causing the competition of root with each other, avoiding the space and nutrients occupied by adjacent plant roots, and showing asymmetric growth in space for adjacent plant roots (i.e., the growth of noncompetitive roots is better than that of competitive roots) (Kroon et al., 2009; Wang et al., 2016; Zhang et al., 2022). The application of nitrogen in a wide-row is equivalent to a 'resource pull', which promotes root growth on the non-competitive side, and this 'resource pull' becomes larger with increasing nitrogen application rate (Kembel and Cahill, 2005), increasing the root surface area and length ratio of 0 to2.5 mm in diameter to obtain more nutrients (Supplementary Tables 1, 2).

However, in narrow-row nitrogen application, although it is generally believed that nitrogen is more concentrated in the soil (compared to wide-row nitrogen application, the degree of heterogeneous soil resources is smaller), it is easier for roots to actively forage resources (roots consume less energy in the process of foraging resources, and roots are easier to proliferate in large quantities between narrow-rows). From this perspective, the application of narrow-row nitrogen is beneficial to plant growth. However, this kind of root proliferation weakens the ability of non-competitive roots to actively forage resources (reducing the biomass allocation of non-competitive roots). Furthermore, root competition for nitrogen between narrow-rows shows that plants generally increase their investment in roots, according to the theory of 'competition-induced root growth' (Chen et al., 2021; Pretzsch, 2022), and for plants, root growth tends to occupy the growth resources (space and nutrients) of neighboring plants rather than increase the cost of investing in themselves (Ljubotina and Cahill, 2019; Cabal, 2022). The nutrient acquisition capacity of roots has become a limiting factor for growth. Additionally, from the discovery of the proportion of root length and surface area of 0 to 2.5 mm (Supplementary Tables 3, 4), under narrow-row nitrogen application, the proportion of fine roots was less than in wide-row nitrogen application, which is more unfavorable for plants nutrients absorption. From this perspective, this easy foraging process between narrow-rows is unfavorable for plant growth. Will plants have this beneficial and unfavorable effect under narrow-row nitrogen application? This may depend on which roots between two adjacent plants has foraging ability first, thus occupying a favorable niche because the competitive effect of individuals has a

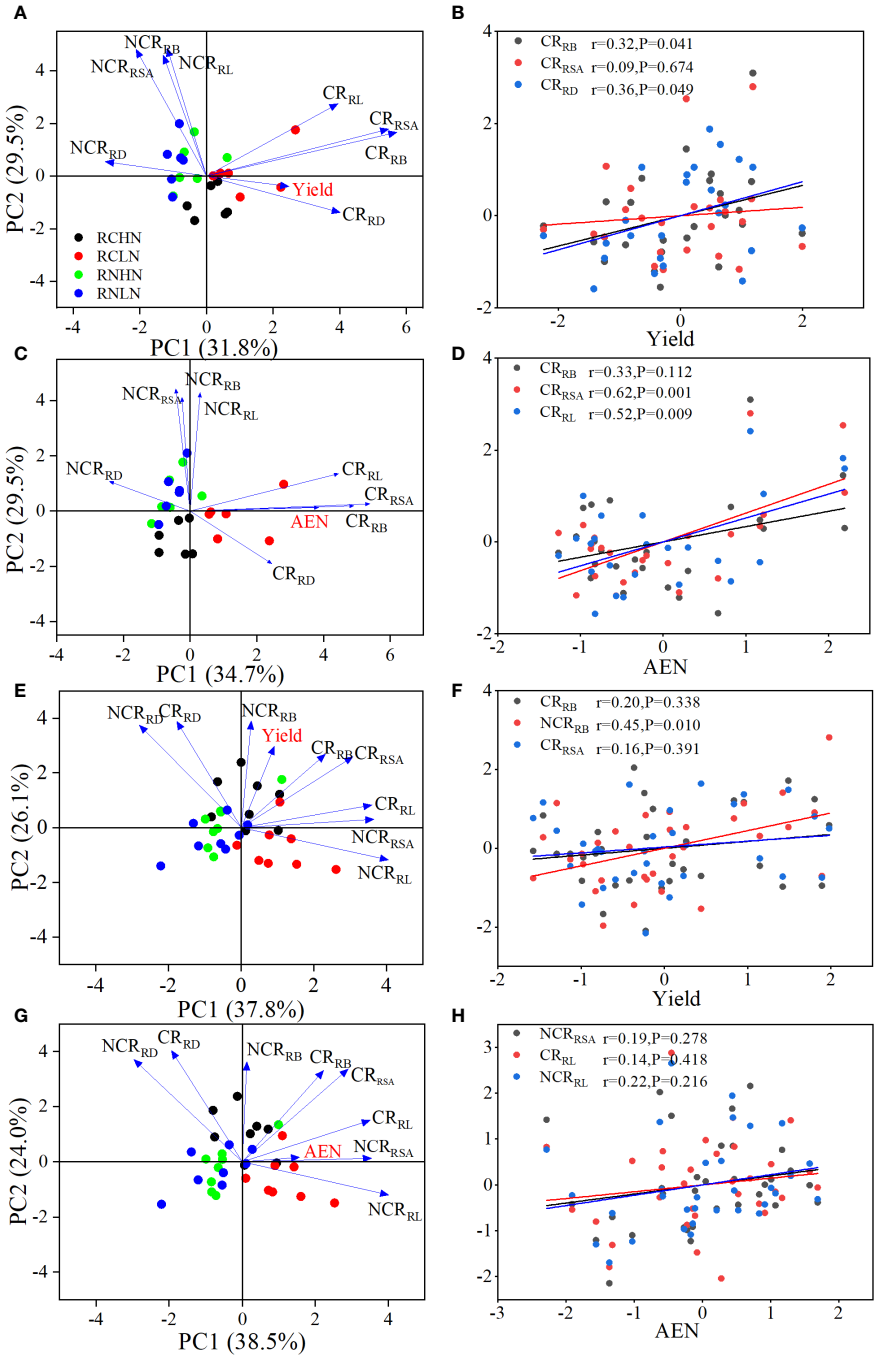

FIGURE 7
Key factors and correlation analysis of CR and NCR on yield and AEN. **(A)** PCA of yield in the field experiment. **(B)** Correlation analysis of yield in the field experiment. **(C)** PCA of AEN in the field experiment. **(D)** Correlation analysis of AEN in the field experiment. **(E)** PCA of yield in the pot experiment. **(F)** Correlation analysis of yield in the pot experiment. **(G)** PCA of AEN in the pot experiment. **(H)** Correlation analysis of AEN in the pot experiment. CR_{RB}: Root biomass of competing root, NCR_{RB}: Root biomass of noncompeting root, CR_{RSA}: Root surface area of competing root, NCR_{RSA}: Root surface area of non-competing roots, CR_{RL}: Root length of competing roots, NCR_{RL}: Root length of non-competing roots, CR_{RD}: Root diameter of competing roots, NCR_{RD}: Root diameter of non-competing roots.

certain correlation with the root foraging scale (root biomass) and the root foraging rate (time required to reach the patch) (Dell et al., 2014). Generally, the interaction between the heterogeneous nitrogen supplication and the existence of adjacent plants increased the input of maize foraging resources into nitrogen-rich areas.

The nitrogen availability is also an important factor that affects the root cultivation process. Previous studies have also shown that only when the nitrogen concentration in the soil is at a low level can the root system fully exploit the biological potential of 'fertilizer displacement', and this effect is obviously inhibited under conditions of excessive nitrogen supplication (Broadbent et al.,

2018; Dybzinski et al., 2019). This was consistent with the results of narrow-row nitrogen application in a field experiment, but the effect was the opposite under the wide-row nitrogen application. Therefore, when there is root interaction, changing the nitrogen application position can adjust root growth and change root distribution to improve overall root-seeking behavior. In addition, unlike the field experiment, the process and behavior of root cultivation in pot culture differ. Under narrow-row nitrogen application, the length and surface area of competitive roots and non-competitive roots were opposite those in the field experiment, while those under wide-row nitrogen application were consistent. It may be that the space resources occupied by competitive roots in potted plants are smaller than those in large fields, and the volume of potted plants (especially the nutrient pots where competitive roots are located) may limit the growth of plant roots and strengthen contact between plants (Figure 2C), and there is no exchange of nutrients (Chen et al., 2012).

Increased foraging precision usually the performance of the adaptability of the plant to environmental resources, which is helpful for the absorption of plant nutrients and enhances the competitive advantage of the plant. However, in field studies, although the precision of finding nutrients during narrow-row nitrogen application was improved compared to wide-row nitrogen application (at the same nitrogen level), the comparative yield of maize did not increase, especially in the case of greater nitrogen application (Figures 3A, C). According to the "competitor–stress-tolerant–disturbance-tolerant" theory (Grime, 1974), in an environment with high productivity (under high nitrogen conditions), the intensity of competition among plants will increase because the biomass of adjacent plants aboveground is positively linearly correlated with the intensity of competition, and biomass of plant increases with the improvement of soil fertility. However, the further expansion of the root absorption area, the fiercer the competition in fertile soil. This may be an important reason why the yield under wide-row nitrogen application is significantly higher than that of a narrow-row nitrogen application under a high nitrogen application rate (Zhai et al., 2017; Monson et al., 2022). Furthermore, when the nutrient patch is in the middle of two maize plants, many roots grow coincidently in the nutrient patch area greatly improving the intensity of competition between plants. However, when nitrogen is applied in wide-rows, non-competitive roots show a pattern of mutual avoidance distribution in biomass, surface area, and length compared to the competitive roots, reducing the competition of roots for common resources. Our results have been verified in related studies, involving woody, grassland, and food crops (Cahill et al., 2010; Lorts and Lasky, 2020; Shen et al., 2020).

4.2 Relationship between root seeking behavior and nitrogen use efficiency

The spatial distribution of plant roots directly determines their uptake and utilization of nutrients and ultimately manifests itself in the uptake of aboveground nutrients and the accumulation of biomass. In the field experiment, the AEN and PFPN under wide-row nitrogen application were greater than those under narrow-row nitrogen application under a high nitrogen application rate, while that of the narrow-row nitrogen application were significantly greater than that of the wide-row nitrogen application under low nitrogen, which indicated that the spatial heterogeneity of nutrients could have specificity for the absorption of shoot nutrients based on the nitrogen position. The reason may be that although narrow-row nitrogen application can promote root proliferations in patches under high nitrogen application. Root proliferation is related to its type. Generally, we think that roots with a small diameter (0 to 2.5 mm) have a greater absorption capacity (Jackson, 2000). According to Figure 4F, the diameter of the competitive roots was significantly higher than that of the non-competitive roots under nitrogen application in narrow-row. Although a larger root diameter has a larger root surface area, this root proliferation is not necessarily beneficial in absorbing more nutrients. Stimulation of root proliferation in nutrient-rich areas may not be the only reason for improving plant 'income'. According to the hypothesis of 'ineffective proliferation', there may be a trade-off between long-lived coarse absorber roots and fast-foraging fine absorber roots (Hodge et al., 2010; Mommer et al., 2012; Zhu et al., 2022).

Most studies have shown that during competition, the amount of nutrients obtained by plants is positively related to the size of their roots, which can improve the efficiency of nutrient utilization of plants in nutrient patches in a short time and have a positive promotional effect on the growth of above-ground parts (Jansen et al., 2006; Jing et al., 2012). However, in the field experiments, nutrients can be consumed rapidly and flow through the nature rainfall, making this advantage last for a short time. Eventually, fine roots with a short life expectancy will cause a large amount of energy loss. Additionally, the reason for the low nitrogen utilization rate of narrow-row nitrogen application under high nitrogen may be that when there are nutrient patches, the different times and degrees of utilization of two maize roots contacting the nutrient patches do not lead to a linear correlation between nutrient absorption by the roots and root size, demonstrating that heterogeneous nutrients lead to asymmetric competition between two maize roots. Plants that arrive first at the local supply of nutrients will occupy this part of the nutrient patch, 'neutralizing' nitrogen utilization efficiency between the two maize plants (Raynaud and Leadley, 2005; Weiner and Damgaard, 2006; Rasmussen et al., 2019). Obviously, the local supply of nutrients has different effects on root behavior and root foraging. However, in addition to nutrient attributes, the sensitivity of plant roots to nutrients, the length of the plant growth cycle, the occurrence of interactions between roots, and the occurrence of interactions between competition and reciprocity strongly influence plant nutrient absorption and root plasticity. In the future, the ecological functions of nutrient patches in root foraging behavior should be systematically evaluated on different time scales to explain the quantitative regulation of root foraging behavior.

4.3 Regulation of nitrogen application position on above-ground and underground parts

The allocation between the roots and crowns of plants is determined by the minimum access to resources and balanced growth among adjacent roots (Yuan et al., 2021). In wide-row nitrogen applications, the sharing of resources among roots is more balanced than that in narrow-row nitrogen applications. The growth environment of whole plant is mild, while competition among above-ground, underground, and whole plants is weak (Venterink and Güsewell, 2010). Therefore, in this case, neighboring plants in the underground part will experience less competition than other plants, and plants may change from underground to above-ground competition for light resources when weighing the competition relationship. However, the overall intensity of competition does not change with the change in productivity. Therefore, plants increase their height and leaf area, to improve the productivity of the upper part, and to reduce the root:shoot ratio. During narrow-row nitrogen application, for two maize plants, and the resource supply is concentrated, the interaction between plants and roots increase the competition between the aboveground and underground, and the total effect of competition increases. According to the hypothesis of balanced growth of roots and shoots, plant growth is limited by constant light resources, and the competition between soil resources and roots decreases with increasing resource availability, which may be a potential mechanism to explain the spatial heterogeneity of resources and the coordination of biomass allocation by root competition (Meziane, 2010; Poorter and Sack, 2012). In other words, the response of plants to the spatial heterogeneity of soil nutrients and root interactions and the mechanism of searching for nutrients has become one of the hot spots in ecological research. Clarifying its mechanism can not only improve our understanding of plant ecosystems, but also help optimize the application of farmland planting, ecological restoration, and plant protection.

5 Conclusions

Field and pot experiments showed that narrow-and wide-row nitrogen applications improved the precision of foraging precision. Wide-row nitrogen application reduced the sensitivity of underground roots to soil resources, improved the overall productivity of the crops, optimized the investment ratio of the crops to the above-ground and underground parts, and reduced the efficiency of nitrogen use under low nitrogen application. To better understand the relationships among resource availability, root interactions, and nitrogen spatial heterogeneity, it is necessary to clarify the influence of aboveground light resources on this process. Specifically, it is necessary to clarify whether aboveground resources coordinate root interactions and nitrogen spatial heterogeneity in this process. Therefore, to improve the sustainability of crop production and promote healthy soil development, this process deserves further study.

Data availability statement

The original contributions presented in the study are included in the article/Supplementary Material. Further inquiries can be directed to the corresponding authors.

Author contributions

SZ: Data curation, Investigation, Validation, Writing – original draft. PX: Data curation, Investigation, Methodology, Writing – original draft. JC: Data curation, Investigation, Methodology, Writing – original draft. QX: Data curation, Methodology, Writing – original draft. GL: Investigation, Writing – original draft. JT: Data curation, Investigation, Writing – original draft. BW: Conceptualization, Funding acquisition, Project administration, Supervision, Writing – review & editing. FZ: Conceptualization, Funding acquisition, Project administration, Supervision, Visualization, Writing – review & editing.

Funding

The author(s) declare financial support was received for the research, authorship, and/or publication of this article. This study was financially supported by the Major Science and Technology Special Project of Yunnan Province (2019ZG00902), Fundamental Research Project of Science and Technology Department of Yunnan Province (202201AT070270), Major Science and Technology Project of Yunnan Province (202202AE090034) and National key research and development plan project (2022YFD1901504).

Conflict of interest

The authors declare that the research was conducted in the absence of any commercial or financial relationships that could be construed as a potential conflict of interest.

Publisher's note

Supplementary material

The Supplementary Material for this article can be found online at: https://www.frontiersin.org/articles/10.3389/fpls.2024.1298249/full#supplementary-material

References

Aluoch, S. O., Li, Z., Li, X., Hu, C., Mburu, D. M., Yang, J., et al. (2022). Effect of mineral N fertilizer and organic input on maize yield and soil water content for assessing optimal N and irrigation rates in Central Kenya. *Field Crops Res.* 277, 108420. doi: 10.1016/j.fcr.2021.108420

Broadbent, A., Stevens, C. J., Peltzer, D. A., Ostle, N. J., and Orwin, K. H. (2018). Belowground competition drives invasive plant impact on native species regardless of nitrogen availability. *Oecologia* 186 (2), 577–587. doi: 10.1007/s00442-017-4039-5

Cabal, C. (2022). Root tragedy of the commons: Revisiting the mechanisms of a misunderstood theory. *Front. Plant Sci.* 13. doi: 10.3389/fpls.2022.960942

Cahill, J. F. Jr., McNickle, G., Haag, J. J., Lamb, E. G., Nyanumba, S. M., and St Clair, C. C. (2010). Plants integrate information about nutrients and neighbors. *Science* 328 (5986), 1657–1657. doi: 10.1126/science.1189736

Chen, G., Cai, T., Wang, J., Wang, Y., Ren, L., Wu, P., et al. (2022). Suitable fertilizer application depth enhances the efficient utilization of key resources and improves crop productivity in rainfed farmland on the loess plateau, China. *Front. Plant Sci.* 13. doi: 10.3389/fpls.2022.900352

Chen, B. J., During, H. J., and Anten, N. P. (2012). Detect thy neighbor: identity recognition at the root level in plants. *Plant Sci.* 195, 157–167. doi: 10.1016/j.plantsci.2012.07.006

Chen, H., Gao, L., Li, M., Liao, Y., and Liao, Q. (2023). Fertilization depth effect on mechanized direct-seeded winter rapeseed yield and fertilizer use efficiency. *J. Scie. Food Agric.* 103 (5), 2574–2584. doi: 10.1002/jsfa.12261

Chen, B. J. W., Huang, L., During, H. J., Wang, X., Wei, J., and Anten, N. P. R. (2021). No neighbour-induced increase in root growth of soybean and sunflower in mesh-divider experiments after controlling for nutrient concentration and soil volume. *AoB Plants* 13 (3), plab020. doi: 10.1093/aobpla/plab020

Dell, A. I., Pawar, S., and Savage, V. M. (2014). Temperature dependence of trophic interactions are driven by asymmetry of species responses and foraging strategy. *J. Of Anim. Ecol.* 83 (1), 70–84. doi: 10.1111/1365-2656.12081

Dybzinski, R., Kelvakis, A., McCabe, J., Panock, S., Anuchitlertchon, K., Vasarhelyi, L., et al. (2019). How are nitrogen availability, fine-root mass, and nitrogen uptake related empirically? Implications for models and theory. *Global Change Biol.* 25 (3), 885–899. doi: 10.1111/gcb.14541

Grime, J. P. (1974). Vegetation classification by reference to strategies. *Nature* 250 (5461), 26–31. doi: 10.1038/250026a0

Hodge, A., Robinson, D., Griffiths, B. S., and Fitter, A. H. (2010). Why plants bother: root proliferation results in increased nitrogen capture from an organic patch when two grasses compete. *Plant Cell Environ.* 22 (7), 811–820. doi: 10.1046/j.1365-3040.1999.00454.x

Hu, K., Zhao, P., Wu, K., Yang, H., Yang, Q., Fan, M., et al. (2023). Reduced and deep application of controlled-release urea maintained yield and improved nitrogen-use efficiency. *Field Crops Res.* 295, 108876. doi: 10.1016/j.fcr.2023.108876

in 't Zandt, D., Le Marié, C., Kirchgessner, N., Visser, E. J. W., and Hund, A. (2015). High-resolution quantification of root dynamics in split-nutrient rhizoslides reveals rapid and strong proliferation of maize roots in response to local high nitrogen. *J. Exp. Bot.* 66 (18), 5507–5517. doi: 10.1093/jxb/erv307

Jackson, G. R. B. (2000). NUTRIENT CONCENTRATIONS IN FINE ROOTS. *Ecology* 81 (1), 275–280. doi: 10.2307/177151

Jansen, C., Kempen, M. M. L. V., Bögemann, G. M., Bouma, T. J., and Kroon, H. D. (2006). Limited costs of wrong root placement in Rumex palustris in heterogeneous soils. *New Phytol.* 171), 117–126. doi: 10.1111/j.1469-8137.2006.01733.x

Jia, Q., Xu, Y., Ali, S., Sun, L., Ding, R., Ren, X., et al. (2018). Strategies of supplemental irrigation and modified planting densities to improve the root growth and lodging resistance of maize (Zea mays L.) under the ridge-furrow rainfall harvesting system. *Field Crops Res.* 224, 48–59. doi: 10.1016/j.fcr.2018.04.011

Jing, J., Zhang, F., Rengel, Z., and Shen, J. (2012). Localized fertilization with P plus N elicits an ammonium-dependent enhancement of maize root growth and nutrient uptake - ScienceDirect. *Field Crops Res.* 133 (4), 176–185. doi: 10.1016/j.fcr.2012.04.009

Kembel, S. W., and Cahill, J. F. (2005). Plant phenotypic plasticity belowground: a phylogenetic perspective on root foraging trade-offs. *Am. Nat.* 166 (2), 216–230. doi: 10.1086/431287

Kroon, H. D., Visser, E. J. W., Huber, H., Mommer, L., and Hutchings, M. J. (2009). A modular concept of plant foraging behaviour: The interplay between local responses and systemic control. *Plant Cell Environ.* 32 (6), 704–712. doi: 10.1111/j.1365-3040.2009.01936.x

Li, L., Zheng, Z., Hua, T., Ashraf, U., and Shenggang, P. (2021). Nitrogen deep placement combined with straw mulch cultivation enhances physiological traits, grain yield and nitrogen use efficiency in mechanical pot-seedling transplanting rice. *Rice Sci.* 28, 89–100. doi: 10.1016/j.rsci.2021.12.00

Liang, G., Sun, P., and Waring, B. G. (2022). Nitrogen agronomic efficiency under nitrogen fertilization does not change over time in the long term: Evidence from 477 global studies. *Soil Tillage Res.* 223, 105648. doi: 10.1016/j.still.2022.105468

Liu, P., Yan, H., Xu, S., Lin, X., Wang, W., and Wang, D. (2022). Moderately deep banding of phosphorus enhanced winter wheat yield by improving phosphorus availability, root spatial distribution, and growth. *Soil Tillage Res.* 220, 105388. doi: 10.1016/j.still.2022.105388

Ljubotina, M. K., and Cahill, J. F.Jr. (2019). Effects of neighbour location and nutrient distributions on root foraging behaviour of the common sunflower. *Proc. Biol. Sci.* 286 (1911), 20190955. doi: 10.1098/rspb.2019.0955

Lorts, C. M., and Lasky, J. R. (2020). Competition×drought interactions change phenotypic plasticity and the direction of selection on Arabidopsis traits. *New Phytol.* 227 (4), 1060–1072. doi: 10.1111/nph.16593

Ma, Z., Ren, B., Zhao, B., Liu, P., and Zhang, J. (2022). Optimising the root traits of summer maize to improve nutrient uptake and utilisation through rational application of urea ammonium nitrate solution. *Plant Soil Environ.* 2), 98–107. doi: 10.17221/335/2021-PSE

Meziane, B. S. (2010). The balanced-growth hypothesis and the allometry of leaf and root biomass allocation. *Funct. Ecol.* 16 (3), 326–331. doi: 10.1046/j.1365-2435.2002.00626.x

Mommer, L., Ruijven, J. V., Jansen, C., Steeg, H. M. V. D., and Kroon, H. D. (2012). Interactive effects of nutrient heterogeneity and competition: implications for root foraging theory? *Funct. Ecol.* 26 (1), 66–73. doi: 10.1111/j.1365-2435.2011.01916.x

Monson, R. K., Trowbridge, A. M., Lindroth, R. L., and Lerdau, M. T. (2022). Coordinated resource allocation to plant growth-defense tradeoffs. *New Phytol.* 233 (3), 1051–1066. doi: 10.1111/nph.17773

Nash, P. R., Nelson, K. A., and Motavalli, P. P. (2013). Corn yield response to timing of strip-tillage and nitrogen source applications. *Agron. J.* 105 (3), 623–630. doi: 10.2134/agronj2012.0338

Poorter, H., and Sack, L. (2012). Pitfalls and possibilities in the analysis of biomass allocation patterns in plants. *Front. Plant Sci.* 3 (259). doi: 10.3389/fpls.2012.00259

Pretzsch, H. (2022). Facilitation and competition reduction in tree species mixtures in Central Europe: Consequences for growth modeling and forest management. *Ecol. Model.* 464, 109812. doi: 10.1016/j.ecolmodel.2021.109812

Quinn, D. J., Lee, C. D., and Poffenbarger, H. J. (2020). Corn yield response to sub-surface banded starter fertilizer in the U.S.: A meta-analysis. *Field Crops Res.* 254, 107834. doi: 10.1016/j.fcr.2020.107834

Rasmussen, C. R., Weisbach, A. N., Thorup-Kristensen, K., and Weiner, J. (2019). Size-asymmetric root competition in deep, nutrient-poor soil. *J. Plant Ecol.* 12 (1), 78–88. doi: 10.1093/jpe/rtx064

Raynaud, X., and Leadley, P. W. (2005). Symmetry of belowground competition in a spatially explicit model of nutrient competition. *Ecol. Model.* 189 (3-4), 447–453. doi: 10.1016/j.ecolmodel.2005.03.008

Rochette, P., Angers, D. A., Chantigny, M. H., MacDonald, J. D., Gasser, M.-O., and Bertrand, N. (2009). Reducing ammonia volatilization in a no-till soil by incorporating urea and pig slurry in shallow bands. *Nutrient Cycling Agroecosyst.* 84 (1), 71–80. doi: 10.1007/s10705-008-9227-6

Rutan, J., and Steinke, K. (2018). Pre-plant and in-season nitrogen combinations for the northern corn belt. *Agron. J.* 110 (5), 2059–2069. doi: 10.2134/agronj2018.03.0153

Shen, N., Liu, C., Yu, H., and Qu, J. (2020). Effects of resource heterogeneity and environmental disturbance on the growth performance and interspecific competition of wetland clonal plants. *Global Ecol. Conserv.* 22, e00914. doi: 10.1016/j.gecco.2020.e00914

Trapeznikov, V. K., Ivanov, I. I., and Kudoyarova, G. R. (2003). Effect of heterogeneous distribution of nutrients on root growth, ABA content and drought resistance of wheat plants. *Plant Soil* 252 (2), 207–214. doi: 10.1023/A:1024734310214

Venterink, H. O., and Güsewell, S. (2010). Competitive interactions between two meadow grasses under nitrogen and phosphorus limitation. *Funct. Ecol.* 24 (4), 877–886. doi: 10.1111/j.1365-2435.2010.01692.x

Wang, Y. J., Shi, X. P., Meng, X. F., Wu, X. J., Luo, F. L., and Yu, F. H. (2016). Effects of spatial patch arrangement and scale of covarying resources on growth and intraspecific competition of a clonal plant. *Front. Plant Sci.* 7. doi: 10.3389/fpls.2016.00753

Weiner, J., and Damgaard, C. (2006). Size-asymmetric competition and size-asymmetric growth in a spatially explicit zone-of-influence model of plant competition. *Ecol. Res.* 21 (5), 707–712. doi: 10.1007/s11284-006-0178-6

Wu, K., Fullen, M. A., An, T., Fan, Z., Zhou, F., Xue, G., et al. (2012). Above- and below-ground interspecific interaction in intercropped maize and potato: A field study using the 'target' technique. *Field Crops Res.* 139, 63–70. doi: 10.1016/j.fcr.2012.10.002

Wu, P., Liu, F., Chen, G., Wang, J., Huang, F., Cai, T., et al. (2022a). Can deep fertilizer application enhance maize productivity by delaying leaf senescence and decreasing nitrate residue levels? *Field Crops Res.* 277, 108417. doi: 10.1016/j.fcr.2021.108417

Wu, P., Liu, F., Wang, J., Liu, Y., Gao, Y., Zhang, X., et al. (2022b). Suitable fertilization depth can improve the water productivity and maize yield by regulating development of the root system. *Agric. Water Manage.* 271, 107784. doi: 10.1016/j.agwat.2022.107784

Yu, P., Li, X., Yuan, L., and Li, C. (2013). A novel morphological response of maize (Zea mays) adult roots to heterogeneous nitrate supply revealed by a splitroot experiment. *Physiol. Plant.* 150 (1), 133–144. doi: 10.1111/ppl.12075

Yuan, Y., Kleunen, M. V., and Li, J. (2021). A parasite indirectly affects nutrient distribution by common mycorrhizal networks between host and neighboring plants. *Ecology* 102, e03339. doi: 10.1002/ecy.3339

Zhai, L., Xie, R., Li, S., and Zhang, Z. (2017). Effects of nitrogen and plant density on competition between two maize hybrids released in different eras. *Agron. J.* 109 (6), 2670. doi: 10.2134/agronj2017.03.0176

Zhang, M., Geng, Y., Cao, G., Zou, X., and Stephano, M. F. (2020). Effect of magnesium fertilizer combined with straw return on grain yield and nitrogen use efficiency. *Agron. J.* 113 (1), 345–357. doi: 10.1002/AGJ2.20483

Zhang, G., Hou, Y., Zhang, H., Fan, H., Wen, X., Han, J., et al. (2022). Optimizing planting pattern and nitrogen application rate improves grain yield and water use efficiency for rain-fed spring maize by promoting root growth and reducing redundant root growth. *Soil Tillage Res.* 220, 105385. doi: 10.1016/j.still.2022.105385

Zhu, Y. H., Weiner, J., Jin, Y., Yu, M. X., and Li, F. M. (2022). Biomass allocation responses to root interactions in wheat cultivars support predictions of crop evolutionary ecology theory. *Front. Plant Sci.* 13. doi: 10.3389/fpls.2022.858636

Frontiers in
Plant Science

Cultivates the science of plant biology and its applications

The most cited plant science journal, which advances our understanding of plant biology for sustainable food security, functional ecosystems and human health.

Discover the latest Research Topics

See more →

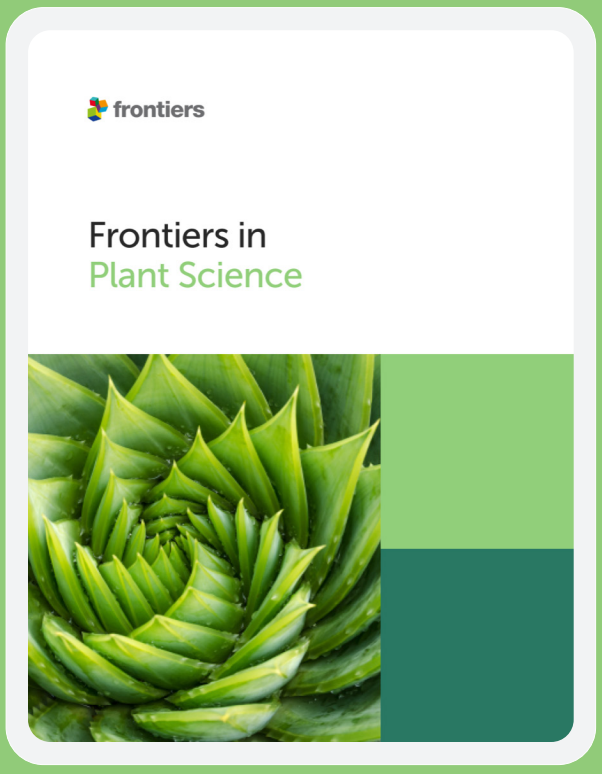

Frontiers

Avenue du Tribunal-Fédéral 34
1005 Lausanne, Switzerland
frontiersin.org

Contact us

+41 (0)21 510 17 00
frontiersin.org/about/contact